Konstantin K. Likharev

Essential Graduate Physics

Lecture Notes and Problems

Open online access at mirror sites

http://commons.library.stonybrook.edu/egp/

https://essentialgraduatephysics.org/

https://sites.google.com/site/likharevegp/

under the Creative Commons http://creativecommons.org/licenses/by-nc-sa/4.0/ license

Part CM:
Classical Mechanics

Last edit: July 1, 2025

B/W paperback copies of this volume are also available on *Amazon.com*:
https://www.amazon.com/dp/B0D82C8Z7L

About the author:
https://you.stonybrook.edu/likharev/

© K. Likharev

Table of Contents

* * *

Supplemental file **Exercise Problems with Model Solutions** (202 problems, 304 pp.)
is available online:
https://essentialgraduatephysics.org/Files/CM%20exercises.pdf .

B/W paperback copies of these materials are available on *Amazon.com*:
https://www.amazon.com/gp/product/B0D7ZC7CVX .

Additional file **Test Problems with Model Solutions** (45 problems, 42 pp.)
is available for course instructors from the author upon request – see *Front Matter*.

* * *

Introductory Remarks

This course mostly follows the well-established traditions of teaching classical mechanics to physics graduate students. Its most distinguishing feature is substantial attention to the mechanics of physical continua, including the discussions of 1D waves in Chapter 6, deformations and elasticity (including 3D waves) in Chapter 7, and fluid dynamics in Chapter 8. A natural extension of the discussion of turbulence in the last of these chapters becomes possible after a brief introduction to deterministic chaos in Chapter 9.

Another not-quite-standard feature of this course is that the introduction to analytical mechanics, starting with the Lagrangian formalism in Chapter 2, is based on the experiment-based Newton's laws rather than general concepts such as the Hamilton principle, which is discussed only at the end of the course (Sec. 10.3). I feel that this route emphasizes better the experimental roots of physics, and the secondary nature of any general principles – regardless of their aesthetic and heuristic value.

Chapter 1. Review of Fundamentals

After a brief discussion of the title and contents of the course, this introductory chapter reviews the basic notions and facts of the non-relativistic classical mechanics, that are supposed to be known to the reader from their undergraduate studies.[1] *Due to this reason, the discussion is very short.*

1.0. Terminology: Mechanics and dynamics

A more fair title for this course would be *Classical Mechanics and Dynamics*, because the notions of mechanics and dynamics, though much intertwined, are still somewhat different. The term *mechanics*, in its narrow sense, means the derivation of equations of motion of point-like particles and their systems (including solids and fluids), the solution of these equations, and an interpretation of the results. *Dynamics* is a more ambiguous term; it may mean, in particular:

(i) the part of physics that deals with motion (in contrast to *statics*);

(ii) the part of physics that deals with reasons for motion (in contrast to *kinematics*);

(iii) the part of mechanics that focuses on its two last tasks, i.e. the solution of the equations of motion and discussion of the results.[2]

Because of this ambiguity, after some hesitation, I have opted to use the traditional name *Classical Mechanics*, with the word *Mechanics* in its broad sense that includes (similarly to *Quantum Mechanics* and *Statistical Mechanics*) studies of dynamics of some non-mechanical systems as well.

1.1. Kinematics: Basic notions

The basic notions of kinematics may be defined in various ways, and some mathematicians pay much attention to alternative systems of axioms and the relations between them. In physics, we typically stick to less rigorous ways (in order to proceed faster to solving particular problems) and end debating any definition as soon as "everybody in the room" agrees that we are all speaking about the same thing – at least in the context in which they are being discussed. Let me hope that the following notions used in classical mechanics do satisfy this criterion in our "room":

---

[1] The reader is advised to perform (perhaps after reading this chapter as a reminder) a self-check by solving a few problems of those listed in Sec. 1.6. If the results are not satisfactory, it may make sense to start with some remedial reading. For that, I could recommend, e.g., J. Marion and S. Thornton, *Classical Dynamics of Particles and Systems,* 5th ed., Saunders, 2003; and D. Morin, *Introduction to Classical Mechanics*, Cambridge U., 2008.

[2] The reader may have noticed that the last definition of dynamics is suspiciously close to the part of mathematics devoted to differential equation analysis; what is the difference? An important bit of philosophy: physics may be defined as an art (and a bit of science :-) of describing Mother Nature by mathematical means; hence in many cases the approaches of a mathematician and a physicist to a problem are very similar. The main difference between them is that physicists try to express the results of their analyses in terms of the properties of the *systems* under study, rather than the *functions* describing them, and as a result develop a sort of intuition ("gut feeling") about how other similar systems may behave, even if their exact equations of motion are somewhat different – or not known at all. The intuition so developed has enormous heuristic power, and most discoveries in physics have been made through gut-feeling-based insights rather than by plugging one formula into another one.

© K. Likharev

(i) All the *Euclidean geometry* notions, including the *point*, the *straight line*, the *plane*, etc.[3]

(ii) *Reference frames*: platforms for observation and mathematical description of physical phenomena. A reference frame includes a *coordinate system* used for measuring the point's position (namely, its *radius vector* **r** that connects the coordinate origin to the point – see Fig. 1) and a clock that measures *time t*. A coordinate system may be understood as a certain method of expressing the radius vector **r** of a point as a set of its *scalar coordinates*. The most important of such systems (but by no means the only one) are the *Cartesian* (orthogonal, linear) *coordinates*[4] r_j of a point, in which its radius vector may be represented as the following sum:

$$\mathbf{r} = \sum_{j=1}^{3} \mathbf{n}_j r_j \,, \tag{1.1}$$

Cartesian coordinates

where $\mathbf{n}_1$, $\mathbf{n}_2$, and $\mathbf{n}_3$ are unit vectors directed along the coordinate axis – see Fig. 1.[5]

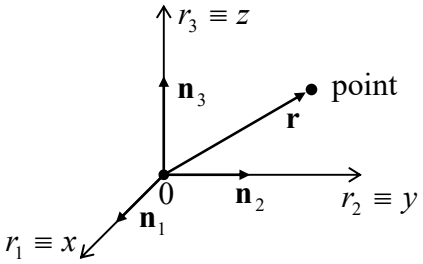

Fig. 1.1. Cartesian coordinates of a point.

(iii) The *absolute* ("Newtonian") *space/time*,[6] which does not depend on the matter distribution. The space is assumed to have the *Euclidean metric*, which may be expressed as the following relation between the length *r* of any radius vector **r** and its Cartesian coordinates:

$$r^2 \equiv |\mathbf{r}|^2 = \sum_{j=1}^{3} r_j^2 \,, \tag{1.2}$$

Euclidean metric

while time *t* is assumed to run similarly in all reference frames. These assumptions are critically revised in the relativity theory (which, in this series, is discussed only starting from EM Chapter 9.)

---

[3] All these notions are of course abstractions: *simplified models* of the real objects existing in Nature. But please always remember that *any* quantitative statement made in physics (e.g., a formula) may be strictly valid only for an approximate model of a physical system. (The reader should not be disheartened too much by this fact: experiments show that many models make extremely precise predictions of the behavior of the real systems.)

[4] In this series, the Cartesian coordinates (introduced in 1637 by René Descartes, a.k.a. Cartesius) are denoted either as either $\{r_1, r_2, r_3\}$ or $\{x, y, z\}$, depending on convenience in each particular case. Note that axis numbering is important for operations like the vector ("cross") product; the "correct" (meaning generally accepted) numbering order is such that the rotation $\mathbf{n}_1 \to \mathbf{n}_2 \to \mathbf{n}_3 \to \mathbf{n}_1 \ldots$ looks counterclockwise if watched from a point with all $r_j > 0$ – like the one shown in Fig. 1.

[5] Note that representation (1) is also possible for locally orthogonal but *curvilinear* (for example, polar/cylindrical and spherical) coordinates, which will be extensively used in this series. However, such coordinates are not Cartesian, and for them some of the relations given below are invalid – see, e.g., MA Sec. 10.

[6] These notions were formally introduced by Sir Isaac Newton in his main work, the three-volume *Philosophiae Naturalis Principia Mathematica* published in 1686-1687, but are rooted in earlier ideas by Galileo Galilei, published in 1632.

(iv) The (instant) *velocity* of the point,

Velocity

$$\mathbf{v}(t) \equiv \frac{d\mathbf{r}}{dt} \equiv \dot{\mathbf{r}}\,, \tag{1.3}$$

and its *acceleration*:

Acceleration

$$\mathbf{a}(t) \equiv \frac{d\mathbf{v}}{dt} \equiv \dot{\mathbf{v}} = \ddot{\mathbf{r}}\,. \tag{1.4}$$

(v) *Transfer between reference frames*. The above definitions of vectors **r**, **v**, and **a** depend on the chosen reference frame (are "reference-frame-specific"), and we frequently need to relate those vectors as observed in different frames. Within Euclidean geometry, the relation between the radius vectors in two frames with the corresponding axes parallel at the moment of interest (Fig. 2), is very simple:

Radius vector's transformation

$$\mathbf{r}\big|_{\text{in } 0'} = \mathbf{r}\big|_{\text{in } 0} + \mathbf{r}_0\big|_{\text{in } 0'}\,. \tag{1.5}$$

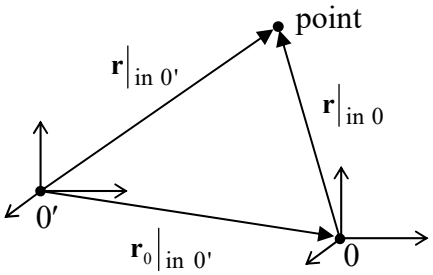

Fig. 1.2. Transfer between two reference frames.

If the frames move versus each other by *translation* only (no mutual rotation!), similar relations are valid for the velocities and accelerations as well:

$$\mathbf{v}\big|_{\text{in } 0'} = \mathbf{v}\big|_{\text{in } 0} + \mathbf{v}_0\big|_{\text{in } 0'}\,, \tag{1.6}$$

$$\mathbf{a}\big|_{\text{in } 0'} = \mathbf{a}\big|_{\text{in } 0} + \mathbf{a}_0\big|_{\text{in } 0'}\,. \tag{1.7}$$

Note that in the case of mutual rotation of the reference frames, the transfer laws for velocities and accelerations are more complex than those given by Eqs. (6) and (7). Indeed, in this case, notions like $\mathbf{v}_0\big|_{\text{in } 0'}$ are not well defined: different points of an imaginary rigid body connected to frame 0 may have different velocities when observed in frame 0'. It will be more natural for me to discuss these more general relations at the end of Chapter 4 devoted to rigid body motion.

(vi) A *particle* (or "point particle"): a localized physical object whose size is negligible, and whose shape is irrelevant *to the given problem*. Note that the last qualification is extremely important. For example, the size and shape of a spaceship are not too important for the discussion of its orbital motion but are paramount when its landing procedures are being developed. Since classical mechanics neglects the quantum mechanical uncertainties,[7] in it, the position of a particle at any particular instant t may be identified with a single geometrical point, i.e. with a single radius vector $\mathbf{r}(t)$. The formal final goal of classical mechanics is finding the *laws of motion* $\mathbf{r}(t)$ of all particles in the given problem.

[7] This approximation is legitimate when the product of the coordinate and momentum scales of the particle motion is much larger than Planck's constant $\hbar \sim 10^{-34}$ J·s. More detailed conditions of the classical mechanics' applicability depend on a particular system – see, e.g., the QM part of this series.

1.2. Dynamics: Newton's laws

Generally, the classical dynamics is fully described (in addition to the kinematic relations discussed above) by three *Newton's laws*. In contrast to the impression some textbooks on theoretical physics try to create, these laws are experimental in nature, and cannot be derived from *purely* theoretical arguments.

I am confident that the reader of these notes is already familiar with Newton's laws,[8] in some formulation. Let me note only that in some formulations, the *1st Newton's law* looks just like a particular case of the 2nd law – when the net force acting on a particle equals zero. To avoid this duplication, the 1st law may be formulated as the following postulate:

> There exists at least one reference frame, called *inertial*, in which any *free particle* (i.e. a particle fully isolated from the rest of the Universe) moves with $\mathbf{v} = \text{const}$, i.e. with $\mathbf{a} = 0$.

1st Newton's law

Note that according to Eq. (7), this postulate immediately means that there is also an infinite number of inertial reference frames – because all frames 0' moving without rotation or acceleration relative to the postulated inertial frame 0 (i.e. having $\mathbf{a}_0\big|_{\text{in } 0'} = 0$) are also inertial.

On the other hand, the 2nd and 3rd Newton's laws may be postulated *together* in the following elegant way. Each particle, say number k, may be characterized by a scalar constant (called *mass* m_k), such that at any interaction of N particles (isolated from the rest of the Universe), in any inertial system,

$$\mathbf{P} \equiv \sum_{k=1}^{N} \mathbf{p}_k \equiv \sum_{k=1}^{N} m_k \mathbf{v}_k = \text{const}. \tag{1.8}$$

Total momentum and its conservation

(Each component of this sum,

$$\mathbf{p}_k \equiv m_k \mathbf{v}_k, \tag{1.9}$$

Particle's momentum

is called the *mechanical momentum*[9] of the corresponding particle, while the sum $\mathbf{P}$, the *total momentum* of the system.)

Let us apply this postulate to just two interacting particles. Differentiating Eq. (8) written for this case, over time, we get

$$\dot{\mathbf{p}}_1 = -\dot{\mathbf{p}}_2. \tag{1.10}$$

Let us give the derivative $\dot{\mathbf{p}}_1$ (which is a vector) the name of the *force* $\mathbf{F}$ exerted on particle 1. In our current case, when the only possible source of the force is particle 2, it may be denoted as $\mathbf{F}_{12}$: $\dot{\mathbf{p}}_1 \equiv \mathbf{F}_{12}$. Similarly, $\mathbf{F}_{21} \equiv \dot{\mathbf{p}}_2$, so Eq. (10) becomes the *3rd Newton's law*

$$\mathbf{F}_{12} = -\mathbf{F}_{21}. \tag{1.11}$$

3rd Newton's law

Plugging Eq. (1.9) into these force definitions, and differentiating the products $m_k\mathbf{v}_k$, taking into account that particle masses are constants,[10] we get that for the k and k' taking any of values 1, 2,

---

[8] Due to the genius of Sir Isaac, these laws were formulated in the same *Principia* (1687), well ahead of the physics of his time.

[9] The more extended term *linear momentum* is typically used only in cases when there is a chance of confusion with the *angular momentum* of the same particle/system – see below. The present-day definition of linear momentum and the term itself belong to John Wallis (1670), but the concept may be traced back to more vague notions of several previous scientists – all the way back to at least a 570 AD work by John Philoponus.

$$m_k \dot{\mathbf{v}}_k \equiv m_k \mathbf{a}_k = \mathbf{F}_{kk'}, \qquad \text{where } k' \neq k.. \tag{1.12}$$

Now, returning to the general case of several interacting particles, and making an additional (but very natural) assumption that all partial forces $\mathbf{F}_{kk'}$ acting on particle k add up as vectors, we may generalize Eq. (12) into the *2nd Newton's law*

2nd Newton's law

$$\boxed{m_k \mathbf{a}_k \equiv \dot{\mathbf{p}}_k = \sum_{k' \neq k} \mathbf{F}_{kk'} \equiv \mathbf{F}_k,} \tag{1.13}$$

that allows a clear interpretation of the mass as a measure of a particle's *inertia*.

As a matter of principle, if the dependence of all pair forces $\mathbf{F}_{kk'}$ of particle positions (and generally of time as well) is known, Eq. (13) augmented with the kinematic relations (2) and (3) allows calculation of the laws of motion $\mathbf{r}_k(t)$ of all particles of the system. For example, for one particle the 2nd law (13) gives an ordinary differential equation of the second order:

$$m\ddot{\mathbf{r}} = \mathbf{F}(\mathbf{r}, t), \tag{1.14}$$

which may be integrated – either analytically or numerically.

In certain cases, this is very simple. As an elementary example, for local motions with $\Delta r << r$, Newton's gravity force[11]

Newton's gravity law

$$\boxed{\mathbf{F} = -G\frac{mm'}{R^3}\mathbf{R}} \tag{1.15}$$

(where $\mathbf{R} \equiv \mathbf{r} - \mathbf{r}'$ is the distance between particles of masses m and m')[12] may be approximated as

Uniform gravity field

$$\boxed{\mathbf{F} = m\mathbf{g},} \tag{1.16}$$

with the vector $\mathbf{g} \equiv -(Gm'/R^3)\mathbf{R}$ being constant.[13] As a result, m in Eq. (13) cancels, it is reduced to just $\ddot{\mathbf{r}} = \mathbf{g} = \text{const}$, and may be easily integrated twice:

$$\dot{\mathbf{r}}(t) \equiv \mathbf{v}(t) = \int_0^t \mathbf{g}\, dt' + \mathbf{v}(0) = \mathbf{g}t + \mathbf{v}(0), \qquad \mathbf{r}(t) = \int_0^t \mathbf{v}(t')dt' + \mathbf{r}(0) = \mathbf{g}\frac{t^2}{2} + \mathbf{v}(0)t + \mathbf{r}(0), \tag{1.17}$$

thus giving the generic solution to all those undergraduate problems on the projectile motion, which should be so familiar to the reader.

---

[10] Note that this may not be true for composite bodies of varying total mass M (e.g., rockets emitting jets, see Problem 11), in these cases the momentum's derivative may differ from $M\mathbf{a}$.

[11] Introduced in the same famous *Principia*!

[12] The fact that the masses participating in Eqs. (14) and (16) are equal, the so-called *weak equivalence principle*, is actually highly nontrivial, but has been repeatedly verified with gradually improved relative accuracy, starting from $\sim 10^{-3}$ in Isaac Newton's own experimentation and all the way down to 1.5×10^{-15} from recent satellite experiments – see P. Touboul *et al.*, *Phys. Rev. Lett.* **129**, 121102 (2022).

[13] Of course, the most important particular case of Eq. (16) is the gravity field near the Earth's surface. In this case, using the fact that Eq. (15) remains valid for the gravity field created by a spherically uniform sphere, we get $g = GM_E/R_E^2$, where M_E and R_E are the Earth's mass and radius. Plugging in their values, $M_E \approx 5.97\times10^{24}$ kg and $R_E \approx 6.37\times10^6$ m, we get $g \approx 9.82$ m/s^2. The experimental value of g varies from 9.78 to 9.83 m/s^2 at various locations on the surface (due to the deviations of Earth's shape from a sphere, and the location-dependent effect of the centrifugal "inertial force" – see Sec. 4.5 below), with an average value of approximately 9.807 m/s^2.

All this looks (and indeed is) very simple, but in most other cases, Eq. (13) leads to more complex calculations. As an example, let us think about how would we use it to solve another simple problem: a bead of mass m sliding, without friction, along a round ring of radius R in a gravity field obeying Eq. (16) – see Fig. 3. (This system is equivalent to the usual *point pendulum*, i.e. a point mass suspended from point 0 on a light rod or string, and constrained to move in one vertical plane.)

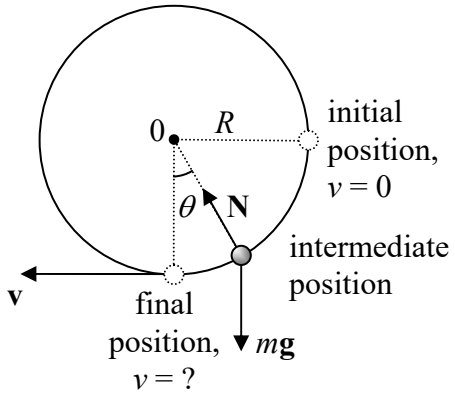

Fig. 1.3. A bead sliding along a vertical ring.

Suppose we are only interested in the bead's velocity v at the lowest point after it has been dropped from the rest at the rightmost position. If we want to solve this problem using only the Newton laws, we have to take the following steps:

(i) consider the bead in an arbitrary intermediate position on a ring, described, for example by the angle θ shown in Fig. 3;

(ii) draw all the forces acting on the particle – in our current case, the gravity force $m\mathbf{g}$ and the reaction force $\mathbf{N}$ exerted by the ring – see Fig. 3 above

(iii) write the Cartesian components of the 2nd Newton's law (14) for the bead acceleration: $ma_x = N_x$, $ma_y = N_y - mg$,

(iv) recognize that in the absence of friction, the force $\mathbf{N}$ should be normal to the ring, so that we can use two additional equations, $N_x = -N\sin\theta$ and $N_y = N\cos\theta$;

(v) eliminate unknown variables N, N_x, and N_y from the resulting system of four equations, thus getting a single second-order differential equation for one variable, for example, θ:

$$mR\ddot{\theta} = -mg\sin\theta; \tag{1.18}$$

(vi) use the mathematical identity $\ddot{\theta} \equiv d\left(\dot{\theta}^2/2\right)/d\theta$ to integrate this equation over θ once to get an expression relating the velocity $\dot{\theta}$ and the angle θ; and, finally,

(vii) using our specific initial condition ($\dot{\theta} = 0$ at $\theta = \pi/2$), find the final velocity as $v = R\dot{\theta}$ at $\theta = 0$.

All this is very much doable, but please agree that the procedure it too cumbersome for such a simple problem. Moreover, in many other cases even writing equations of motion along relevant coordinates is very complex, and any help the general theory may provide is highly valuable. In many cases, such help is given by *conservation laws*; let us review the most general of them.

1.3. Conservation laws

(i) *Energy* conservation is arguably the most general law of physics, but in mechanics, it takes a more humble form of *mechanical energy conservation*, which has limited applicability. To derive it, we first have to define the *kinetic energy* of a particle as[14]

Kinetic energy

$$T \equiv \frac{m}{2} v^2 , \tag{1.19}$$

and then recast its differential as[15]

$$dT \equiv d\left(\frac{m}{2} v^2\right) \equiv d\left(\frac{m}{2} \mathbf{v}\cdot\mathbf{v}\right) = m\mathbf{v}\cdot d\mathbf{v} = m\frac{d\mathbf{r}\cdot d\mathbf{v}}{dt} = d\mathbf{r}\cdot\frac{d\mathbf{p}}{dt}. \tag{1.20}$$

Now plugging in the momentum's derivative from the 2nd Newton's law, $d\mathbf{p}/dt = \mathbf{F}$, where $\mathbf{F}$ is the full force acting on the particle, we get $dT = \mathbf{F}\cdot d\mathbf{r}$. The integration of this equality along the particle's trajectory connecting some points A and B gives the formula that is sometimes called the *work-energy principle*:

Work-energy principle

$$\Delta T \equiv T(\mathbf{r}_B) - T(\mathbf{r}_A) = \int_A^B \mathbf{F}\cdot d\mathbf{r} , \tag{1.21}$$

where the integral on the right-hand side is called the *work* of the force $\mathbf{F}$ on the path from A to B.

The next step may be made only for a *potential* (also called "conservative") force that may be represented as the (minus) gradient of some scalar function $U(\mathbf{r})$, called the *potential energy*.[16] The vector operator ∇ (called either *del* or *nabla*) of spatial differentiation[17] allows a very compact expression of this fact:

Force vs potential energy

$$\mathbf{F} = -\nabla U . \tag{1.22}$$

For example, for the uniform gravity field (16),

$$U = mgh + \text{const}, \tag{1.23}$$

where h is the vertical coordinate directed "up" – opposite to the direction of the vector $\mathbf{g}$.

Integrating the tangential component F_τ of the vector $\mathbf{F}$ given by Eq. (22), along an arbitrary path connecting the points A and ***B***, we get

$$\int_A^B F_\tau dr \equiv \int_A^B \mathbf{F}\cdot d\mathbf{r} = U(\mathbf{r}_A) - U(\mathbf{r}_B) , \tag{1.24}$$

---

[14] In such quantitative form, the kinetic energy was introduced (under the name "living force") by Gottfried Leibniz and Johann Bernoulli (circa 1700), though its main properties (21) and (27) had not been clearly revealed until an 1829 work by Gaspard-Gustave de Coriolis. The modern term "kinetic energy" was coined only in 1849-1851 by Lord Kelvin (born William Thomson).

[15] In these notes, $\mathbf{a}\cdot\mathbf{b}$ denotes the scalar (or "dot-") product of vectors $\mathbf{a}$ and $\mathbf{b}$ – see, e.g., MA Eq. (7.1).

[16] Note that because of its definition via the gradient, the potential energy is only defined up to an arbitrary additive constant. This notion had been used already by G. Leibniz, though the term we are using for it nowadays was introduced much later (in the mid-19th century) by William Rankine.

[17] Its basic properties are listed in MA Sec. 8.

i.e. work of potential forces may be represented as the difference of values of the function $U(\mathbf{r})$ in the initial and final points of the path. (Note that according to Eq. (24), the work of a potential force on any closed path, with $\mathbf{r}_A = \mathbf{r}_B$, is zero.)

Now returning to Eq. (21) and comparing it with Eq. (24), we see that

$$T(\mathbf{r}_B) - T(\mathbf{r}_A) = U(\mathbf{r}_A) - U(\mathbf{r}_B), \quad \text{i.e. } T(\mathbf{r}_A) + U(\mathbf{r}_A) = T(\mathbf{r}_A) + U(\mathbf{r}_A), \tag{1.25}$$

so the *total mechanical energy* E, defined as

$$E \equiv T + U, \tag{1.26}$$

Total mechanical energy

is indeed conserved:

$$E(\mathbf{r}_A) \equiv E(\mathbf{r}_B), \tag{1.27}$$

Mechanical energy: conservation

but for conservative forces only. (Non-conservative forces may change E by either transferring energy from its mechanical form to another form, e.g., to heat in the case of friction, or by pumping the energy into the system under consideration from another, "external" system.)

Mechanical energy conservation allows us to return for just a second to the problem shown in Fig. 3 and solve it in one shot by writing Eq. (27) for the initial and final points:[18]

$$0 + mgR = \frac{m}{2}v^2 + 0. \tag{1.28}$$

The (elementary) solution of Eq. (28) for v immediately gives us the desired answer. Let me hope that the reader agrees that this way of problem's solution is much simpler, and I have earned their attention to discuss other conservation laws – which may be equally effective.

(ii) *Linear momentum*. The conservation of the full linear momentum of any system of particles isolated from the rest of the world was already discussed in the previous section, and may serve as the basic postulate of classical dynamics – see Eq. (8). In the case of one free particle, the law is reduced to the trivial result $\mathbf{p}$ = const, i.e. $\mathbf{v}$ = const. If a system of N particles *is* affected by external forces $\mathbf{F}^{(\text{ext})}$, we may write

$$\mathbf{F}_k = \mathbf{F}_k^{(\text{ext})} + \sum_{k=1}^{N} \mathbf{F}_{kk'}. \tag{1.29}$$

If we sum up the resulting Eqs. (13) for all particles of the system then, due to the 3rd Newton's law (11) valid for any indices $k \neq k'$, the contributions of all internal forces $\mathbf{F}_{kk'}$ to the resulting double sum on the right-hand side cancel, and we get the following equation:

$$\dot{\mathbf{P}} = \mathbf{F}^{(\text{ext})}, \quad \text{where } \mathbf{F}^{(\text{ext})} \equiv \sum_{k=1}^{N} \mathbf{F}_k^{(\text{ext})}. \tag{1.30}$$

System's momentum evolution

It tells us that the translational motion of the system as a whole is similar to that of a single particle, under the effect of the *net external force* $\mathbf{F}^{(\text{ext})}$. As a simple sanity check, if the external forces have a zero sum, we return to the postulate (8). Just one reminder: Eq. (30), as its precursor Eq. (13), is only valid in an inertial reference frame.

[18] Here the arbitrary constant in Eq. (23) is chosen so that the potential energy is zero at the final point.

I hope that the reader knows numerous examples of the application of the linear momentum's conservation law, including all these undergraduate problems on car collisions, where the large collision forces are typically not known so the direct application of Eq. (13) to each car is impracticable.

(iii) The *angular momentum* of a particle[19] is defined as the following vector:[20]

Angular momentum: definition

$$\mathbf{L} \equiv \mathbf{r} \times \mathbf{p}, \tag{1.31}$$

where $\mathbf{a}\times\mathbf{b}$ means the vector (or "cross-") product of the vector operands.[21] Differentiating Eq. (31) over time, we get

$$\dot{\mathbf{L}} = \dot{\mathbf{r}} \times \mathbf{p} + \mathbf{r} \times \dot{\mathbf{p}}. \tag{1.32}$$

In the first product, $\dot{\mathbf{r}}$ is just the velocity vector $\mathbf{v}$, parallel to the particle momentum $\mathbf{p} = m\mathbf{v}$, so this term vanishes since the vector product of any two parallel vectors equals zero. In the second product, $\dot{\mathbf{p}}$ is equal to the full force $\mathbf{F}$ acting on the particle, so Eq. (32) is reduced to

Angular momentum: evolution

$$\dot{\mathbf{L}} = \boldsymbol{\tau}, \tag{1.33}$$

where the vector

Torque

$$\boldsymbol{\tau} \equiv \mathbf{r} \times \mathbf{F}, \tag{1.34}$$

is called the *torque* exerted by force $\mathbf{F}$.[22] (Note that the torque is reference-frame specific – and again, the frame has to be inertial for Eq. (33) to be valid, because we have used Eq. (13) for its derivation.) For an important particular case of a *central* force $\mathbf{F}$ that is directed along the radius vector $\mathbf{r}$ of a particle, the torque vanishes, so (in that particular reference frame only!) the angular momentum is conserved:

Angular momentum: conservation

$$\mathbf{L} = \text{const}. \tag{1.35}$$

For a system of N particles, the total angular momentum is naturally defined as

System's angular momentum: definition

$$\mathbf{L} \equiv \sum_{k=1}^{N} \mathbf{L}_k. \tag{1.36}$$

Differentiating this equation over time, using Eq. (33) for each $\dot{\mathbf{L}}_k$, and again partitioning each force per Eq. (29), we get

$$\dot{\mathbf{L}} = \sum_{\substack{k,k'=1 \\ k'\neq k}}^{N} \mathbf{r}_k \times \mathbf{F}_{kk'} + \boldsymbol{\tau}^{(\text{ext})}, \quad \text{where } \boldsymbol{\tau}^{(\text{ext})} \equiv \sum_{k=1}^{N} \mathbf{r}_k \times \mathbf{F}_k^{(\text{ext})}. \tag{1.37}$$

The first (double) sum may be always divided into pairs of the type $(\mathbf{r}_k \times \mathbf{F}_{kk'} + \mathbf{r}_{k'} \times \mathbf{F}_{k'k})$. With a natural assumption of the central forces, $\mathbf{F}_{kk'} \parallel (\mathbf{r}_k - \mathbf{r}_{k'})$, each of these pairs equals zero. Indeed, in this case,

---

[19] Here we imply that the internal motions of the particle, including its rotation about its axis, are negligible. (Otherwise, it could not be represented by a point, as was postulated in Sec. 1.)

[20] This explicit definition of angular momentum (in different mathematical forms, and under the name of "moment of rotational motion") appeared in scientific publications only in the 1740s, though the fact of its conservation (35) in the field of central forces, in the form of the 2nd Kepler law (see Fig. 3.4 below), had been proved already by I. Newton in his *Principia*.

[21] See, e.g., MA Eq. (7.3).

[22] Alternatively, especially in mechanical engineering, torque is called the *force moment*. This notion may be traced all the way back to Archimedes' theory of levers developed in the 3rd century BC.

each component of the pair is a vector perpendicular to the plane containing the positions of both particles and the reference frame origin, i.e. to the plane of the drawing in Fig. 4.

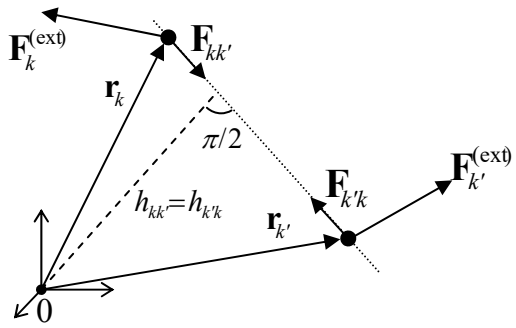

Fig. 1.4. Internal and external forces, and the internal torque cancellation in a system of two particles.

Also, due to the 3rd Newton's law (11), these two forces are equal and opposite, and the magnitude of each term in the sum may be represented as $|F_{kk'}|\,h_{kk'}$, with equal "lever arms" $h_{kk'} = h_{k'k}$. As a result, each sum $(\mathbf{r}_k \times \mathbf{F}_{kk'} + \mathbf{r}_{k'} \times \mathbf{F}_{k'k})$, and hence the whole double sum in Eq. (37) vanish, and it is reduced to a very simple result,

$$\dot{\mathbf{L}} = \boldsymbol{\tau}^{(ext)}, \tag{1.38}$$

System's angular momentum: evolution

which is similar to Eq. (33) for a single particle, and is the angular analog of Eq. (30).

In particular, Eq. (38) shows that if the full external torque $\boldsymbol{\tau}^{(ext)}$ vanishes for some reason (e.g. if the system of particles is isolated from the rest of the Universe), the conservation law (35) is valid for the full angular momentum $\mathbf{L}$ even if its individual components $\mathbf{L}_k$ are not conserved due to inter-particle interactions.

Please note again that since the conservation laws may be derived from Newton's laws (as was done above), they do not introduce anything new to the dynamics of any system. Indeed, from the mathematical point of view, the conservation laws discussed above are just the first integrals of the second-order differential equations of motion following from Newton's laws. However, for a physicist, thinking about particular systems in terms of the conserved (or potentially conserved) quantities frequently provides decisive clues on their dynamics.

1.4. Potential energy and equilibrium

Another important role of the potential energy U, especially for dissipative systems whose total mechanical energy E is *not* conserved because it may be drained to the environment, is finding the positions of equilibrium (sometimes called the *fixed points*) of the system and analyzing their stability with respect to small perturbations. For a single particle, this is very simple: the force (22) vanishes at each extremum (either minimum or maximum) of the potential energy.[23] (Of those fixed points, only the minimums of $U(\mathbf{r})$ are stable – see Sec. 3.2 below for a discussion of this point.)

A slightly more subtle case is a particle with an internal potential energy $U(\mathbf{r})$, subjected to an *additional* external force $\mathbf{F}^{(ext)}(\mathbf{r})$. In this case, the stable equilibrium is reached at the minimum of not the function $U(\mathbf{r})$, but of what is sometimes called the *Gibbs potential energy*

[23] Assuming that the additional, non-conservative forces (such as viscosity) responsible for the mechanical energy drain, vanish at equilibrium – as they typically do. (The static friction is one counter-example.)

Gibbs' potential energy

$$U_G(\mathbf{r}) \equiv U(\mathbf{r}) - \int^{\mathbf{r}} \mathbf{F}^{(ext)}(\mathbf{r}') \cdot d\mathbf{r}', \tag{1.39}$$

which is defined, just as $U(\mathbf{r})$ is, to an arbitrary additive constant.[24] The proof of Eq. (39) is very simple: in an extremum of this function, the total force acting on the particle,

$$\mathbf{F}^{(tot)} = \mathbf{F} + \mathbf{F}^{(ext)} \equiv -\nabla U + \nabla \int^{\mathbf{r}} \mathbf{F}^{(ext)}(\mathbf{r}') \cdot d\mathbf{r}' \equiv -\nabla U_G \tag{1.40}$$

vanishes, as it is necessary for equilibrium.

Physically, the difference $U_G - U$ specified by Eq. (39) is the $\mathbf{r}$-dependent part of the potential energy $U^{(ext)}$ of the external system responsible for the force $\mathbf{F}^{(ext)}$, so U_G is just the total potential energy $U + U^{(ext)}$, excluding its part that does not depend on $\mathbf{r}$ and hence is irrelevant for the analysis. According to the 3rd Newton's law, the force exerted by the particle on the external system equals $(-\mathbf{F}^{(ext)})$, so its work (and hence the change of $U^{(ext)}$ due to the change of $\mathbf{r}$) is given by the second term on the right-hand side of Eq. (39). Thus the condition of equilibrium, $\nabla U_G = 0$, is just the condition of an extremum of the total potential energy, $U + U^{(ext)} + \text{const}$, of the two interacting systems.

For the simplest (and very frequent) case when the applied force is independent of the particle's position, the Gibbs potential energy (39) is just[25]

$$U_G(\mathbf{r}) \equiv U(\mathbf{r}) - \mathbf{F}^{(ext)} \cdot \mathbf{r} + \text{const}. \tag{1.41}$$

As the simplest example, consider a 1D deformation of the usual elastic spring providing the returning force $(-\kappa x)$, where x is the deviation from its equilibrium. As follows from Eq. (22), its potential energy is $U = \kappa x^2/2 + \text{const}$, so its minimum corresponds to $x = 0$. Now let us apply an additional external force F, say independent of x. Then the equilibrium deformation of the spring, $x_0 = F/\kappa$, corresponds to the minimum of not U, but rather of the Gibbs potential energy (41), in our particular case taking the form

$$U_G \equiv U - Fx = \frac{\kappa x^2}{2} - Fx. \tag{1.42}$$

1.5. OK, we've got it – can we go home now?

Sorry, not yet. In many cases, the conservation laws discussed above provide little help, even in systems without dissipation. As a simple example, consider a generalization of the bead-on-the-ring problem shown in Fig. 3, in which the ring is rotated by external forces, with a constant angular velocity ω, about its vertical diameter.[26] In this problem (to which I will repeatedly return below, using it as an

[24] Unfortunately, in most textbooks, the association of the (unavoidably used) notion of U_G with the glorious name of Josiah Willard Gibbs is postponed until a course of statistical mechanics and/or thermodynamics, where U_G is a part of the *Gibbs free energy*, in contrast to U, which is a part of the *Helmholtz free energy* – see, e.g., SM Sec. 1.4. I use this notion throughout my series, because the difference between U_G and U, and hence that between the Gibbs and Helmholtz free energies, has nothing to do with statistics or thermal motion, and belongs to the whole physics, including not only mechanics but also electrodynamics and quantum mechanics.

[25] Eq. (41) is a particular case of what mathematicians call the *Legendre transformations*.

[26] This is essentially a simplified model of the mechanical control device called the *centrifugal* (or "flyball", or "centrifugal flyball") *governor* – see, e.g., http://en.wikipedia.org/wiki/Centrifugal_governor. (Sometimes the device is called the "Watt's governor", after the famous James Watts who used it in 1788 in one of his first steam

analytical mechanics "testbed"), none of the three conservation laws listed in the last section, holds. In particular, the bead's energy,

$$E = \frac{m}{2}v^2 + mgh\,, \tag{1.43}$$

is *not* constant, because the external forces rotating the ring may change it. Of course, we still can solve the problem using Newton's laws, but this is even more complex than for the above case of the ring at rest, in particular because the force **N** exerted on the bead by the ring now may have three rather than two Cartesian components, which are not simply related. On the other hand, it is clear that the bead still has just one degree of freedom (say, the angle θ), so its dynamics should not be too complicated.

This case gives us a clue on how situations like this one can be simplified: if we only could exclude the so-called *reaction forces* such as **N**, that take into account *external constraints* imposed on the particle motion, in advance, that should help a lot. Such a constraint exclusion may be provided by analytical mechanics, in particular its Lagrangian formulation, to which we will now proceed.

Of course, the value of the Lagrangian approach goes far beyond simple systems such as the bead on a rotating ring. Indeed, this system has just two externally imposed constrains: the fixed distance of the bead from the center of the ring, and the instant angle of rotation of the ring about its vertical diameter. Now let us consider the motion of a rigid body. It is essentially a system of a very large number, $N >> 1$, of particles ($\sim 10^{23}$ of them if we think about atoms in a 1-cm-scale body). If the only way to analyze its motion would be to write Newton's laws for each of the particles, the situation would be completely hopeless. Fortunately, the number of constraints imposed on its motion is almost similarly huge. (At negligible deformations of the body, the distances between each pair of its particles should be constant.) As a result, the number of actual degrees of freedom of such a body is small (at negligible deformations, just six – see Sec. 4.1), so with the kind help from analytical mechanics, the motion of the body may be, in many important cases, analyzed even without numerical calculations.

One more important motivation for analytical mechanics is given by the dynamics of "non-mechanical" systems, for example, of the electromagnetic field – possibly interacting with charged particles, conducting bodies, etc. In many such systems, the easiest (and sometimes the only practicable) way to find the equations of motion is to derive them from either the Lagrangian or Hamiltonian function of the system. Moreover, the Hamiltonian formulation of the analytical mechanics (to be reviewed in Chapter 10 below) offers a direct pathway to deriving quantum-mechanical Hamiltonian operators of various systems, which are necessary for the analysis of their quantum properties.

1.6. Self-test problems

1.1. A bicycle, ridden with velocity v on wet pavement, has no mudguards on its wheels. How far behind should the following biker ride to avoid being splashed over? Neglect the air resistance effects.

---

engines, though it had been used in European windmills at least since the early 1600s.) Just as a curiosity: the now-ubiquitous term *cybernetics* was coined by Norbert Wiener in 1948 from the word "governor" (or rather from its Ancient-Greek original κυβερνήτης) exactly in this meaning because the centrifugal governor had been the first well-studied control device.

1.2. Two round disks of radius R are firmly connected with a coaxial cylinder of a smaller radius r, and a thread is wound on the resulting spool. The spool is placed on a horizontal surface, and the thread's end is being pooled out at angle φ – see the figure on the right. Assuming that the spool does not slip on the surface, what direction would it roll?

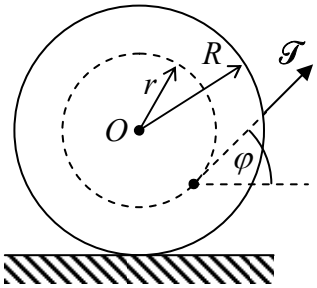

1.3.* Calculate the equilibrium shape of a flexible heavy rope of length l, with a constant mass μ per unit length, if it is hung in a uniform gravity field between two points separated by a horizontal distance d – see the figure on the right.

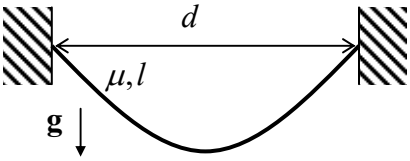

1.4. A uniform, long, thin bar is placed horizontally on two similar round cylinders rotating toward each other with the same angular velocity ω and displaced by distance d – see the figure on the right. Calculate the laws of relatively slow horizontal motion of the bar within the plane of the drawing, for both possible directions of cylinder rotation, assuming that the kinetic friction force between the slipping surfaces of the bar and each cylinder obeys the simple *Coulomb approximation*[27] $|F| = \mu N$, where N is the normal pressure force between them, and μ is a constant (velocity-independent) coefficient. Formulate the condition of validity of your result.

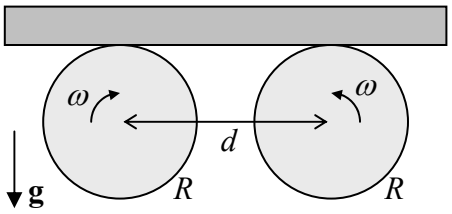

1.5. A small block slides, without friction, down a smooth slide that ends with a round loop of radius R – see the figure on the right. What smallest initial height h allows the block to make its way around the loop without dropping from the slide if it is launched with negligible initial velocity?

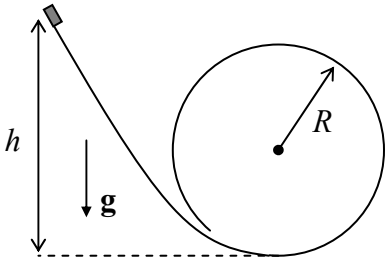

1.6. A satellite of mass m is being launched from height H over the surface of a spherical planet with radius R and mass $M >> m$ – see the figure on the right. Find the range of initial velocities $\mathbf{v}_0$ (normal to the radius) providing closed orbits above the planet's surface.

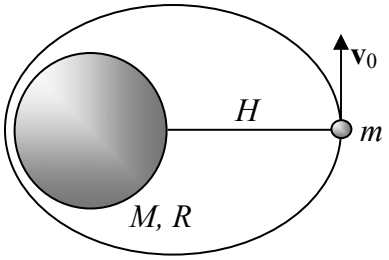

1.7. Prove that the thin-uniform-disk model of a galaxy allows for small sinusoidal ("harmonic") oscillations of stars inside it, along the direction normal to the disk, and calculate the frequency of these oscillations in terms of Newton's gravitational constant G and the average density ρ of the disk's matter.

[27] It was suggested in 1785 by the same Charles-Augustin de Coulomb who discovered the famous *Coulomb law* of electrostatics, and hence pioneered the whole quantitative science of electricity – see EM Ch. 1.

1.8. Derive differential equations of motion for small oscillations of two similar pendula coupled with a spring (see the figure on the right), within their common vertical plane. Assume that at the vertical position of both pendula, the spring is not stretched ($\Delta d = 0$).

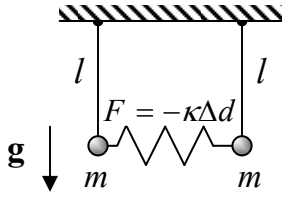

1.9. One of the popular futuristic concepts of travel is digging a straight railway tunnel through the Earth and letting a train go through it, without initial velocity – driven only by gravity. Calculate the train's travel time through such a tunnel, assuming that the Earth's density ρ is constant, and neglecting the friction and planet-rotation effects.

1.10. A small bead of mass m may slide, without friction, along a light string stretched with force $\mathcal{T} >> mg$, between two points separated by a horizontal distance $2d$ – see the figure on the right. Calculate the frequency of oscillations of the bead about its equilibrium position, within the vertical plane.

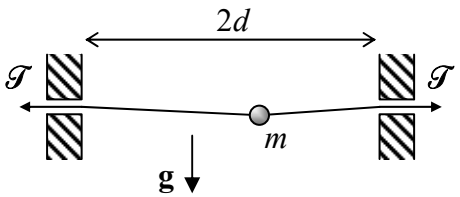

1.11. For a rocket accelerating (in free space) due to its working jet motor (and hence spending the jet fuel), calculate the relation between its velocity and the remaining mass.

Hint: For the sake of simplicity, consider the 1D motion.

1.12. Prove the following *virial theorem*:[28] for a set of N particles performing a periodic motion,

$$\overline{T} = -\frac{1}{2}\sum_{k=1}^{N}\overline{\mathbf{F}_k \cdot \mathbf{r}_k},$$

where the top bar means averaging over time – in this case over the motion period. What does the virial theorem say about:

(i) a 1D motion of a particle in the confining potential[29] $U(x) = ax^{2s}$, with $a > 0$ and $s > 0$, and
(ii) an orbital motion of a particle in the central potential $U(r) = -C/r$?

Hint: Explore the time derivative of the following scalar function of time: $G(t) \equiv \sum_{k=1}^{N}\mathbf{p}_k \cdot \mathbf{r}_k$.

1.13. As will be discussed in Chapter 8, if a solid body moves through a fluid with a sufficiently high velocity v, the fluid's drag force is approximately proportional to v^2. Use this approximation (introduced by Sir Isaac Newton himself) to find the velocity as a function of time during the body's vertical fall in the air near the Earth's surface.

1.14. A particle of mass m, moving with velocity u, collides head-on with a particle of mass M, initially at rest, increasing its internal energy by ΔE. Calculate the velocities of both particles after the collision, if u is barely sufficient for such an internal energy increase.

---

[28] It was first stated by Rudolf Clausius in 1870.

[29] Here and below I am following the (regretful) custom of using the single word "potential" for the potential energy of the particle – just for brevity. This custom is also common in quantum mechanics, but in electrodynamics, these two notions should be clearly distinguished – as they are in the EM part of this series.

Chapter 2. Lagrangian Analytical Mechanics

The goal of this chapter is to describe the Lagrangian formalism of analytical mechanics, which is extremely useful for obtaining the differential equations of motion (*and sometimes their first integrals*) *not only for mechanical systems with holonomic constraints but also for some other dynamic systems.*

2.1. Lagrange equations

In many cases, the constraints imposed on the 3D motion of a system of N particles may be described by N vector (i.e. $3N$ scalar) algebraic equations

$$\mathbf{r}_k = \mathbf{r}_k(q_1, q_2, ..., q_j, ..., q_J, t), \qquad \text{with } 1 \le k \le N, \tag{2.1}$$

where q_j are certain *generalized coordinates* that (together with constraints) completely define the system position. Their number $J \le 3N$ is called the number of the actual *degrees of freedom* of the system. The constraints that allow such a description are called *holonomic*.[1]

For example, for the problem already mentioned in Section 1.5, namely, the bead sliding along a rotating ring (Fig. 1), $J = 1$, because with the constraints imposed by the ring, the bead's position is uniquely determined by just one generalized coordinate – for example, its polar angle θ.

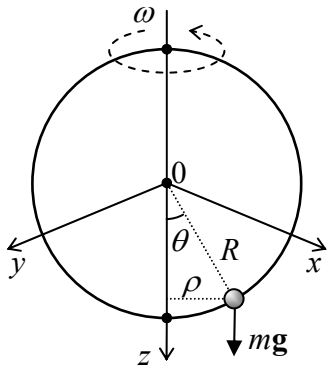

Fig. 2.1. A bead on a rotating ring as an example of a system with just one degree of freedom ($J = 1$).

Indeed, selecting the reference frame as shown in Fig. 1 and using the well-known formulas for the spherical coordinates,[2] we see that in this case, Eq. (1) has the form

$$\mathbf{r} \equiv \{x, y, z\} = \{R\sin\theta\cos\varphi,\ R\sin\theta\sin\varphi,\ R\cos\theta\}, \qquad \text{where } \varphi = \omega t + \text{const}, \tag{2.2}$$

with the last constant depending on the exact selection of the axes x and y and the time origin. Since the angle φ, in this case, is a fixed function of time, and R is a fixed constant, the particle's position in space

[1] Possibly, the simplest counter-example of a *non-holonomic* constraint is a set of inequalities describing the hard walls confining the motion of particles in a closed volume. Non-holonomic constraints are better dealt with by other methods, e.g., by imposing proper boundary conditions on the (otherwise unconstrained) motion.

[2] See, e.g., MA Eq. (10.7).

© K. Likharev

at any instant t is completely determined by the value of its only generalized coordinate θ. (Note that its dimensionality is different from that of Cartesian coordinates!)

Now returning to the general case of J degrees of freedom, let us consider a set of small *variations* (alternatively called "virtual displacements") δq_j allowed by the constraints. Virtual displacements differ from the actual small displacements (described by *differentials* dq_j proportional to time variation dt) in that δq_j describes not the system's motion as such, but rather its possible variation – see Fig. 1.

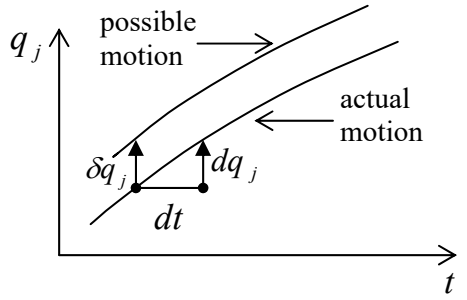

Fig. 2.2. Actual displacement dq_j vs. the virtual one (i.e. variation) δq_j.

Generally, operations with variations are the subject of a special field of mathematics, the calculus of variations.[3] However, the only math background necessary for our current purposes is the understanding that operations with variations are similar to those with the usual differentials, though we need to watch carefully what each variable is a function of. For example, if we consider the variation of the radius vectors (1), at a fixed time t, as functions of independent variations δq_j, we may use the usual formula for the differentiation of a function of several arguments:[4]

$$\delta \mathbf{r}_k = \sum_j \frac{\partial \mathbf{r}_k}{\partial q_j} \delta q_j . \tag{2.3}$$

Now let us break the force acting upon the k^{th} particle into two parts: the frictionless, constraining part $\mathbf{N}_k$ of the reaction force and the remaining part $\mathbf{F}_k$ – including the forces from other sources and possibly the frictional part of the reaction force. Then the 2nd Newton's law for the k^{th} particle of the system may be rewritten as

$$m_k \dot{\mathbf{v}}_k - \mathbf{F}_k = \mathbf{N}_k . \tag{2.4}$$

Since any variation of the motion has to be allowed by the constraints, its $3N$-dimensional vector with N 3D-vector components $\delta \mathbf{r}_k$ has to be perpendicular to the $3N$-dimensional vector of the constraining forces, also having N 3D-vector components $\mathbf{N}_k$. (For example, for the problem shown in Fig. 1, the virtual displacement vector $\delta \mathbf{r}_k$ may be directed only along the ring, while the constraining force $\mathbf{N}$ exerted by the ring, has to be perpendicular to that direction.) This condition may be expressed as

[3] For a concise introduction to the field see, e.g., either I. Gelfand and S. Fomin, *Calculus of Variations*, Dover, 2000, or L. Elsgolc, *Calculus of Variations*, Dover, 2007. An even shorter review may be found in Chapter 17 of Arfken and Weber – see MA Sec. 16. For a more detailed discussion, using many examples from physics, see R. Weinstock, *Calculus of Variations*, Dover, 2007.

[4] See, e.g., MA Eq. (4.2). Also, in all formulas of this section, summations over j are from 1 to J, while those over the particle number k are from 1 to N, so for the sake of brevity, these limits are not explicitly specified.

$$\sum_k \mathbf{N}_k \cdot \delta\mathbf{r}_k = 0, \tag{2.5}$$

where the scalar product of $3N$-dimensional vectors is defined exactly like that of 3D vectors, i.e. as the sum of the products of the corresponding components of the operands. The substitution of Eq. (4) into Eq. (5) results in the so-called *D'Alembert principle*:[5]

D'Alembert principle

$$\boxed{\sum_k (m_k \dot{\mathbf{v}}_k - \mathbf{F}_k) \cdot \delta\mathbf{r}_k = 0.} \tag{2.6}$$

Plugging Eq. (3) into Eq. (6), we get

$$\sum_j \left\{ \sum_k m_k \dot{\mathbf{v}}_k \cdot \frac{\partial \mathbf{r}_k}{\partial q_j} - \mathscr{F}_j \right\} \delta q_j = 0, \tag{2.7}$$

where the scalars $\mathscr{F}_j$, called the *generalized forces*, are defined as follows:[6]

Generalized force

$$\boxed{\mathscr{F}_j \equiv \sum_k \mathbf{F}_k \cdot \frac{\partial \mathbf{r}_k}{\partial q_j}.} \tag{2.8}$$

Now we may use the standard argument of the calculus of variations: for the left-hand side of Eq. (7) to be zero for an arbitrary selection of independent variations δq_j, the expression in the curly brackets, for every j, should equal zero. This gives us the desired set of $J \le 3N$ equations

$$\sum_k m_k \dot{\mathbf{v}}_k \cdot \frac{\partial \mathbf{r}_k}{\partial q_j} - \mathscr{F}_j = 0; \tag{2.9}$$

what remains is just to recast them in a more convenient form.

First, using the differentiation by parts to calculate the following time derivative:

$$\frac{d}{dt}\left(\mathbf{v}_k \cdot \frac{\partial \mathbf{r}_k}{\partial q_j} \right) = \dot{\mathbf{v}}_k \cdot \frac{\partial \mathbf{r}_k}{\partial q_j} + \mathbf{v}_k \cdot \frac{d}{dt}\left(\frac{\partial \mathbf{r}_k}{\partial q_j} \right), \tag{2.10}$$

we may notice that the first term on the right-hand side is exactly the scalar product in the first term of Eq. (9).

Second, let us use another key fact of the calculus of variations (which is, essentially, evident from Fig. 3): the differentiation of a variable over time and over the generalized coordinate variation (at a fixed time) are interchangeable operations. As a result, in the second term on the right-hand side of Eq. (10), we may write

$$\frac{d}{dt}\left(\frac{\partial \mathbf{r}_k}{\partial q_j} \right) = \frac{\partial}{\partial q_j}\left(\frac{d\mathbf{r}_k}{dt} \right) \equiv \frac{\partial \mathbf{v}_k}{\partial q_j}. \tag{2.11}$$

[5] It was spelled out in a 1743 work by Jean le Rond d'Alembert, though the core of this result has been traced to an earlier work by Jacob (Jean) Bernoulli (1667 – 1748) – not to be confused with his son Daniel Bernoulli (1700-1782) who is credited, in particular, for the *Bernoulli equation* for ideal fluids, to be discussed in Sec. 8.4 below.

[6] Note that since the dimensionality of generalized coordinates may be arbitrary, that of generalized forces may also differ from the newton.

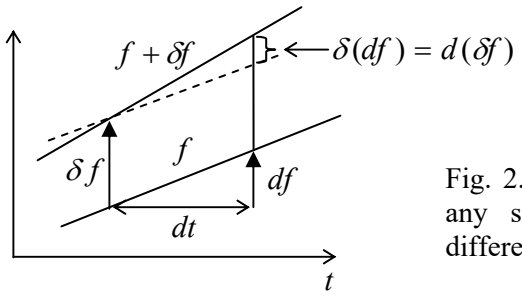

Fig. 2.3. The variation of the differential (of any smooth function *f*) is equal to the differential of its variation.

Finally, let us differentiate Eq. (1) over time:

$$\mathbf{v}_k \equiv \frac{d\mathbf{r}_k}{dt} = \sum_j \frac{\partial \mathbf{r}_k}{\partial q_j}\dot{q}_j + \frac{\partial \mathbf{r}_k}{\partial t}. \tag{2.12}$$

This equation shows that particle velocities $\mathbf{v}_k$ may be considered to be linear functions of the generalized velocities $\dot{q}_j$ *considered as independent variables*, with proportionality coefficients

$$\frac{\partial \mathbf{v}_k}{\partial \dot{q}_j} = \frac{\partial \mathbf{r}_k}{\partial q_j}. \tag{2.13}$$

With the account of Eqs. (10), (11), and (13), Eq. (9) turns into

$$\frac{d}{dt}\sum_k m_k \mathbf{v}_k \cdot \frac{\partial \mathbf{v}_k}{\partial \dot{q}_j} - \sum_k m_k \mathbf{v}_k \cdot \frac{\partial \mathbf{v}_k}{\partial q_j} - \mathscr{F}_j = 0. \tag{2.14}$$

This result may be further simplified by making, for the total kinetic energy of the system,

$$T \equiv \sum_k \frac{m_k}{2} v_k^2 = \frac{1}{2}\sum_k m_k \mathbf{v}_k \cdot \mathbf{v}_k, \tag{2.15}$$

the same commitment as for $\mathbf{v}_k$, i.e. considering T a function of not only the generalized coordinates q_j and time t but also of the generalized velocities $\dot{q}_i$ – as variables *independent* of q_j and t. Then we may calculate the partial derivatives of T as

$$\frac{\partial T}{\partial q_j} = \sum_k m_k \mathbf{v}_k \cdot \frac{\partial \mathbf{v}_k}{\partial q_j}, \qquad \frac{\partial T}{\partial \dot{q}_j} = \sum_k m_k \mathbf{v}_k \cdot \frac{\partial \mathbf{v}_k}{\partial \dot{q}_j}, \tag{2.16}$$

and notice that they are exactly the two sums participating in Eq. (14). As a result, we get a system of J *Lagrange equations*,[7]

$$\frac{d}{dt}\frac{\partial T}{\partial \dot{q}_j} - \frac{\partial T}{\partial q_j} - \mathscr{F}_j = 0, \quad \text{for } j = 1, 2, ..., J. \tag{2.17}$$

General Lagrange equations

Their big advantage over the initial Newton's-law equations (4) is that the Lagrange equations do not include the constraining forces $\mathbf{N}_k$, and thus there are only J of them – typically much fewer than $3N$.

[7] They were derived in 1788 by Joseph-Louis Lagrange, who pioneered the whole field of analytical mechanics – not to mention his key contributions to number theory and celestial mechanics.

This is as far as we can go for arbitrary forces. However, if all the forces may be expressed in a form similar to, but somewhat more general than Eq. (1.22): $\mathbf{F}_k = -\nabla_k U(\mathbf{r}_1, \mathbf{r}_2, \ldots, \mathbf{r}_N, t)$, where U is the effective potential energy of the system,[8] and ∇_k denotes the spatial differentiation over coordinates of the k^{th} particle, we may recast Eq. (8) into a simpler form:

$$\mathcal{F}_j \equiv \sum_k \mathbf{F}_k \cdot \frac{\partial \mathbf{r}_k}{\partial q_j} = -\sum_k \left(\frac{\partial U}{\partial x_k}\frac{\partial x_k}{\partial q_j} + \frac{\partial U}{\partial y_k}\frac{\partial y_k}{\partial q_j} + \frac{\partial U}{\partial z_i}\frac{\partial z_i}{\partial q_j} \right) \equiv -\frac{\partial U}{\partial q_j}. \tag{2.18}$$

Since we assume that U depends only on particle coordinates (and possibly time), but not velocities: $\partial U / \partial \dot{q}_j = 0$, with the substitution of Eq. (18), the Lagrange equation (17) may be represented in the so-called *canonical form*:

Canonical Lagrange equations

$$\boxed{\frac{d}{dt}\frac{\partial L}{\partial \dot{q}_j} - \frac{\partial L}{\partial q_j} = 0,} \tag{2.19a}$$

where L is the *Lagrangian function* (sometimes called just the "Lagrangian"), defined as

Lagrangian function

$$\boxed{L \equiv T - U\ .} \tag{2.19b}$$

(It is crucial to distinguish this function from the mechanical energy (1.26), $E = T + U$.)

Note also that according to Eq. (2.18), for a system under the effect of an additional generalized external force $\mathcal{F}_j(t)$ we have to use, in all these relations, not the internal potential energy $U^{(\text{int})}$ of the system, but its Gibbs potential energy $U \equiv U^{(\text{int})} - \mathcal{F}_j q_j$ – see the discussion in Sec. 1.4.

Using the Lagrangian approach in practice, the reader should always remember, first, that each system has only *one* Lagrange function (19b), but is described by $J \geq 1$ Lagrange equations (19a), with j taking values 1, 2,…, J, and second, that differentiating the function L, we have to consider the generalized velocities as its independent arguments, ignoring the fact they are actually the time derivatives of the generalized coordinates.

2.2. Three simple examples

As the first, simplest example, consider a particle constrained to move along one axis (say, x):

$$T = \frac{m}{2}\dot{x}^2, \qquad U = U(x,t). \tag{2.20}$$

In this case, it is natural to consider x as the (only) generalized coordinate, and $\dot{x}$ as the generalized velocity, so

$$L \equiv T - U = \frac{m}{2}\dot{x}^2 - U(x,t). \tag{2.21}$$

Considering $\dot{x}$ and x as independent variables, we get $\partial L / \partial \dot{x} = m\dot{x}$, and $\partial L / \partial x = -\partial U / \partial x$, so Eq. (19) (the only Lagrange equation in this case of the single degree of freedom!) yields

[8] Note that due to the possible time dependence of U, Eq. (17) does not mean that the forces $\mathbf{F}_k$ have to be conservative – see the next section for more discussion. With this understanding, I will still use for function U the convenient name of "potential energy".

$$\frac{d}{dt}(m\dot{x}) - \left(-\frac{\partial U}{\partial x}\right) = 0, \tag{2.22}$$

evidently the same result as the x-component of the 2nd Newton's law with $F_x = -\partial U/\partial x$. This example is a good sanity check, but it also shows that the Lagrange formalism does not provide too much advantage in this particular case.

Such an advantage is, however, evident in our testbed problem – see Fig. 1. Indeed, taking the polar angle θ for the (only) generalized coordinate, we see that in this case, the kinetic energy depends not only on the generalized velocity but also on the generalized coordinate:[9]

$$\begin{aligned} T &= \frac{m}{2}R^2\left(\dot{\theta}^2 + \omega^2 \sin^2\theta\right), \qquad U = -mgz + \text{const} \equiv -mgR\cos\theta + \text{const}, \\ L &\equiv T - U = \frac{m}{2}R^2\left(\dot{\theta}^2 + \omega^2 \sin^2\theta\right) + mgR\cos\theta + \text{const}. \end{aligned} \tag{2.23}$$

Here it is especially important to remember that at substantiating the Lagrange equation, θ and $\dot{\theta}$ have to be treated as independent arguments of L, so

$$\frac{\partial L}{\partial \dot{\theta}} = mR^2\dot{\theta}, \qquad \frac{\partial L}{\partial \theta} = mR^2\omega^2 \sin\theta\cos\theta - mgR\sin\theta, \tag{2.24}$$

giving us the following equation of motion:

$$\frac{d}{dt}\left(mR^2\dot{\theta}\right) - \left(mR^2\omega^2 \sin\theta\cos\theta - mgR\sin\theta\right) = 0. \tag{2.25}$$

As a sanity check, at $\omega = 0$, Eq. (25) is reduced to the equation (1.18) of the usual pendulum:

$$\ddot{\theta} + \Omega^2 \sin\theta = 0, \quad \text{where } \Omega \equiv \left(\frac{g}{R}\right)^{1/2}. \tag{2.26}$$

We will explore Eq. (25) in more detail later, but please note how simple its derivation was – in comparison with writing the 3D Newton's law and then excluding the reaction force.

Next, though the Lagrangian formalism was derived from Newton's law for mechanical systems, the resulting equations (19) are applicable to other dynamic systems, especially those for which the kinetic and potential energies may be readily expressed via some generalized coordinates. As the simplest example, consider the well-known connection of a capacitor with capacitance C to an inductive coil with self-inductance $\mathscr{L}$[10] (Electrical engineers frequently call it the *LC tank circuit*.)

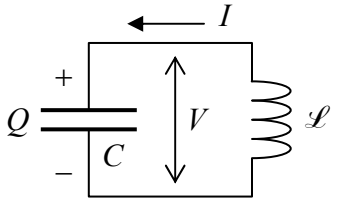

Fig. 2.4. *LC* tank circuit.

[9] The above expression for $T \equiv (m/2)(\dot{x}^2 + \dot{y}^2 + \dot{z}^2)$ may be readily obtained either by the formal differentiation of Eq. (2) over time, or just by noticing that the velocity vector has two perpendicular components: one (of magnitude $R\dot{\theta}$) along the ring, and another one (of magnitude $\omega\rho = \omega R\sin\theta$) normal to the ring's plane.

[10] A fancy font is used here to avoid any chance of confusion between the inductance and the Lagrange function.

As the reader (hopefully :-) knows from their undergraduate studies, at relatively low frequencies we may use the so-called lumped-circuit approximation, in which the total energy of this system is the sum of two components, the electric energy E_e localized inside the capacitor, and the magnetic energy E_m localized inside the inductance coil:

$$E_e = \frac{Q^2}{2C}, \qquad E_m = \frac{\mathscr{L} I^2}{2}. \tag{2.27}$$

Since the electric current I through the coil and the electric charge Q on the capacitor are related by the charge continuity equation $dQ/dt = I$ (evident from Fig. 4), it is natural to declare Q the generalized coordinate of the system, and the current, its generalized velocity. With this choice, the electrostatic energy $E_e(Q)$ may be treated as the potential energy U of the system, and the magnetic energy $E_m(I)$, as its kinetic energy T. With this attribution, we get

$$\frac{\partial T}{\partial \dot{q}} \equiv \frac{\partial E_m}{\partial I} = \mathscr{L} I \equiv \mathscr{L} \dot{Q}, \qquad \frac{\partial T}{\partial q} \equiv \frac{\partial E_m}{\partial Q} = 0, \qquad \frac{\partial U}{\partial q} \equiv \frac{\partial E_e}{\partial Q} = \frac{Q}{C}, \tag{2.28}$$

so the Lagrange equation (19) becomes

$$\frac{d}{dt}\left(\mathscr{L}\dot{Q}\right) - \left(-\frac{Q}{C}\right) = 0, \qquad \text{i.e. } \ddot{Q} + \frac{1}{\mathscr{L}C} Q = 0. \tag{2.29}$$

Note, however, that the above choice of the generalized coordinate and velocity is not unique. Instead, one can use, as the generalized coordinate, the magnetic flux Φ through the inductive coil, related to the common voltage V across the circuit (Fig. 4) by Faraday's induction law $V = -d\Phi/dt$. With this choice, $(-V)$ becomes the generalized velocity, $E_m = \Phi^2/2\mathscr{L}$ should be understood as the *potential* energy, and $E_e = CV^2/2$ treated as the *kinetic* energy. For this choice, the resulting Lagrange equation of motion is equivalent to Eq. (29). If both parameters of the circuit, $\mathscr{L}$ and C, are constant in time, Eq. (29) describes sinusoidal oscillations with the frequency

$$\omega_0 = \frac{1}{\left(\mathscr{L}C\right)^{1/2}}. \tag{2.30}$$

This is of course a well-known result, which may be derived in a more standard way – by equating the voltage drops across the capacitor ($V = Q/C$) and the inductor ($V = -\mathscr{L}dI/dt \equiv -\mathscr{L}d^2Q/dt^2$). However, the Lagrangian approach is much more convenient for more complex systems – for example, for the general description of the electromagnetic field and its interaction with charged particles.[11]

2.3. Hamiltonian function and energy

The canonical form (19) of the Lagrange equation has been derived using Eq. (18), which is formally similar to Eq. (1.22) for a potential force. Does this mean that the system described by Eq. (19) always conserves energy? Not necessarily, because the "potential energy" U that participates in Eq. (18), may depend not only on the generalized coordinates but on time as well. Let us start the analysis of this issue with the introduction of two new (and very important!) notions: the *generalized momentum* corresponding to each generalized coordinate q_j,

[11] See, e.g., EM Secs. 9.7 and 9.8.

$$p_j \equiv \frac{\partial L}{\partial \dot{q}_j}, \tag{2.31}$$

Generalized momentum

and the *Hamiltonian function*[12]

$$H \equiv \sum_j \frac{\partial L}{\partial \dot{q}_j}\dot{q}_j - L \equiv \sum_j p_j \dot{q}_j - L\,. \tag{2.32}$$

Hamiltonian function: definition

To see whether the Hamiltonian function is conserved during the motion, let us differentiate both sides of its definition (32) over time:

$$\frac{dH}{dt} = \sum_j \left[\frac{d}{dt}\left(\frac{\partial L}{\partial \dot{q}_j} \right)\dot{q}_j + \frac{\partial L}{\partial \dot{q}_j}\ddot{q}_j \right] - \frac{dL}{dt}. \tag{2.33}$$

If we want to make use of the Lagrange equation (19), the last derivative has to be calculated considering L as a function of independent arguments q_j, $\dot{q}_j$, and t, so

$$\frac{dL}{dt} = \sum_j \left(\frac{\partial L}{\partial q_j}\dot{q}_j + \frac{\partial L}{\partial \dot{q}_j}\ddot{q}_j \right) + \frac{\partial L}{\partial t}, \tag{2.34}$$

where the last term is the derivative of L as an *explicit* function of time. We see that the last term in the square brackets of Eq. (33) immediately cancels with the last term in the parentheses of Eq. (34). Moreover, using the Lagrange equation (19a) for the first term in the square brackets of Eq. (33), we see that it cancels with the first term in the parentheses of Eq. (34). As a result, we arrive at a very simple and important result:

$$\frac{dH}{dt} = -\frac{\partial L}{\partial t}. \tag{2.35}$$

Hamiltonian function: time evolution

The most important corollary of this formula is that if the Lagrangian function does not depend on time explicitly ($\partial L / \partial t = 0$), the Hamiltonian function is an integral of motion:

$$H = \text{const}. \tag{2.36}$$

Let us see how this works, using the first two examples discussed in the previous section. For a 1D particle, the definition (31) of the generalized momentum yields

$$p_x \equiv \frac{\partial L}{\partial v} = mv\,, \tag{2.37}$$

so it coincides with the usual linear momentum – or rather with its x-component. According to Eq. (32), the Hamiltonian function for this case (with just one degree of freedom) is

$$H \equiv p_x v - L = p_x \frac{p_x}{m} - \left(\frac{m}{2}\dot{x}^2 - U \right) = \frac{p_x^2}{2m} + U\,, \tag{2.38}$$

[12] It is named after Sir William Rowan Hamilton, who developed his approach to analytical mechanics in 1833, on the basis of the Lagrangian mechanics. This function is sometimes called just the "Hamiltonian", but it is advisable to use the full term "Hamiltonian function" in classical mechanics, to distinguish it from the *Hamiltonian operator* used in quantum mechanics, whose abbreviation to *Hamiltonian* is extremely common. (The relation of these two notions will be discussed in Sec. 10.1 below.)

i.e. coincides with the particle's mechanical energy $E = T + U$. Since the Lagrangian does not depend on time explicitly, both H and E are conserved.

However, it is not always that simple! Indeed, let us return again to our testbed problem (Fig. 1). In this case, the generalized momentum corresponding to the generalized coordinate θ is

$$p_\theta \equiv \frac{\partial L}{\partial \dot{\theta}} = mR^2\dot{\theta}, \tag{2.39}$$

and Eq. (32) yields:

$$\begin{aligned} H \equiv p_\theta\dot{\theta} - L &= mR^2\dot{\theta}^2 - \left[\frac{m}{2}R^2\left(\dot{\theta}^2 + \omega^2\sin^2\theta\right) + mgR\cos\theta\right] + \text{const} \\ &\equiv \frac{m}{2}R^2\left(\dot{\theta}^2 - \omega^2\sin^2\theta\right) - mgR\cos\theta + \text{const}. \end{aligned} \tag{2.40}$$

This means that (as soon as $\omega \neq 0$), the Hamiltonian function *differs* from the mechanical energy

$$E \equiv T + U = \frac{m}{2}R^2\left(\dot{\theta}^2 + \omega^2\sin^2\theta\right) - mgR\cos\theta + \text{const}. \tag{2.41}$$

The difference, $E - H = mR^2\omega^2\sin^2\theta$ (besides an inconsequential constant), may change at the bead's motion along the ring, so although H *is* an integral of motion (since $\partial L/\partial t = 0$), the energy is generally *not* conserved.

In this context, let us find out when these two functions, E and H, do coincide. In mathematics, there is a notion of a *homogeneous function* $f(x_1, x_2,\ldots)$ *of degree* λ, defined in the following way: for an arbitrary constant a,

$$f(ax_1, ax_2,...) = a^\lambda f(x_1, x_2,...). \tag{2.42}$$

Such functions obey the following *Euler theorem*:[13]

$$\sum_j \frac{\partial f}{\partial x_j}x_j = \lambda f, \tag{2.43}$$

which may be simply proved by differentiating both parts of Eq. (42) over a and then setting this parameter to the particular value $a = 1$. Now, consider the case when the kinetic energy is a quadratic form of all generalized velocities $\dot{q}_j$:

$$T = \sum_{j,j'} t_{jj'}(q_1, q_2,...,t)\,\dot{q}_j\dot{q}_{j'}, \tag{2.44}$$

with no other terms. It is evident that such T satisfies the definition (42) of a homogeneous function of the velocities with $\lambda = 2$,[14] so the Euler theorem (43) gives

$$\sum_j \frac{\partial T}{\partial \dot{q}_j}\dot{q}_j = 2T. \tag{2.45}$$

[13] This is just one of many theorems bearing the name of their author – the genius mathematician Leonhard Euler (1707-1783).

[14] Such functions are called *quadratic-homogeneous*.

But since U is independent of the generalized velocities, $\partial L/\partial \dot{q}_j = \partial T/\partial \dot{q}_j$, and the left-hand side of Eq. (45) is exactly the first term in the definition (32) of the Hamiltonian function, so in this case

$$H = 2T - L = 2T - (T - U) = T + U = E. \tag{2.46}$$

So, for a system with a kinetic energy of the type (44), for example, a free particle with T considered as a function of its Cartesian velocities,

$$T = \frac{m}{2}\left(v_x^2 + v_y^2 + v_z^2\right), \tag{2.47}$$

the notions of the Hamiltonian function and mechanical energy are identical. Indeed, some textbooks, very regrettably, do not distinguish these notions at all! However, as we have seen from our bead-on-the-rotating-ring example, these variables do not always coincide. For that problem, the kinetic energy, in addition to the term proportional to $\dot{\theta}^2$, has another, velocity-independent term – see the first of Eqs. (23) – and hence is *not* a quadratic-homogeneous function of the angular velocity, giving $E \neq H$.

Thus, Eq. (36) expresses a new conservation law, generally different from that of mechanical energy conservation.

2.4. Other conservation laws

Looking at the Lagrange equation (19), we immediately see that if $L \equiv T - U$ is independent of some generalized coordinate q_j, $\partial L/\partial q_j = 0$,[15] then the corresponding generalized momentum is an integral of motion:[16]

$$p_j \equiv \frac{\partial L}{\partial \dot{q}_j} = \text{const}. \tag{2.48}$$

For example, for a 1D particle with the Lagrangian (21), the momentum p_x is conserved if the potential energy is constant (and hence the x-component of force is zero) – of course. As a less obvious example, let us consider a 2D motion of a particle in the field of central forces. If we use polar coordinates r and φ in the role of generalized coordinates, then the Lagrangian function[17]

$$L \equiv T - U = \frac{m}{2}\left(\dot{r}^2 + r^2\dot{\varphi}^2\right) - U(r) \tag{2.49}$$

is independent of φ, and hence the corresponding generalized momentum,

$$p_\varphi \equiv \frac{\partial L}{\partial \dot{\varphi}} = mr^2\dot{\varphi}, \tag{2.50}$$

[15] Such coordinates are frequently called *cyclic*, because in some cases (like φ in Eq. (49) below) they represent periodic coordinates such as angles. However, this terminology is somewhat misleading, because some "cyclic" coordinates (e.g., x in our first example) have nothing to do with rotation.

[16] This fact may be considered a particular case of a more general mathematical statement called the *Noether theorem* – named after its author, Emmy Nöther, sometimes called the "greatest woman mathematician ever lived". Unfortunately, because of time/space restrictions, for its discussion I have to refer the interested reader elsewhere – for example to Sec. 13.7 in H. Goldstein *et al*., *Classical Mechanics*, 3rd ed. Addison Wesley, 2002.

[17] Note that here $\dot{r}^2$ is the square of the scalar derivative $\dot{r}$, rather than the square of the vector $\dot{\mathbf{r}} = \mathbf{v}$.

is conserved. This is just a particular (2D) case of the angular momentum conservation – see Eq. (1.24). Indeed, for the 2D motion within the [*x, y*] plane, the angular momentum vector,

$$\mathbf{L} \equiv \mathbf{r} \times \mathbf{p} = \begin{vmatrix} \mathbf{n}_x & \mathbf{n}_y & \mathbf{n}_z \\ x & y & z \\ m\dot{x} & m\dot{y} & m\dot{z} \end{vmatrix}, \tag{2.51}$$

has only one component different from zero, namely the component normal to the motion plane:

$$L_z = x(m\dot{y}) - y(m\dot{x}). \tag{2.52}$$

Differentiating the well-known relations between the polar and Cartesian coordinates,

$$x = r\cos\varphi, \qquad y = r\sin\varphi, \tag{2.53}$$

over time, and plugging the result into Eq. (52), we see that

$$L_z = mr^2\dot{\varphi} \equiv p_\varphi. \tag{2.54}$$

Thus the Lagrangian formalism provides a powerful way of searching for non-evident integrals of motion. On the other hand, if such a conserved quantity is obvious or known *a priori*, it is helpful for the selection of the most appropriate generalized coordinates, giving the simplest Lagrange equations. For example, in the last problem, if we knew in advance that p_φ had to be conserved, this could provide sufficient motivation for using the angle φ as one of the generalized coordinates.

2.5. Exercise problems

In each of Problems 1-11, for the given system:

(i) introduce a convenient set of generalized coordinates q_j,
(ii) write down the Lagrangian L as a function of $q_j, \dot{q}_j$, and (if appropriate) time,
(iii) write down the Lagrange equation(s) of motion,
(iv) calculate the Hamiltonian function H; find out whether it is conserved,
(v) calculate the mechanical energy E; is $E = H$?; is the energy conserved?
(vi) any other evident integrals of motion?

2.1. A double pendulum – see the figure on the right. Consider only the motion within the vertical plane containing the suspension point.

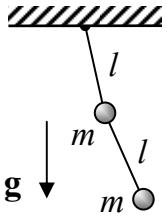

2.2. A stretchable pendulum (i.e. a massive particle hung on an elastic cord that exerts force $F = -\kappa(l - l_0)$, where κ and l_0 are positive constants), also confined to the vertical plane:

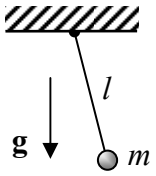

2.3. A fixed-length pendulum hanging from a point whose motion law $x_0(t)$ in the horizontal direction is fixed. (No vertical plane constraint here.)

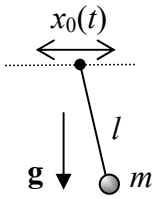

2.4. A pendulum of mass m, hung on another point mass m' that may slide, without friction, along a straight horizontal rail – see the figure on the right. The motion is confined to the vertical plane that contains the rail.

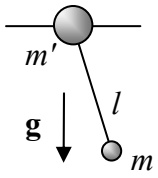

2.5. A point-mass pendulum of length l, attached to the rim of a disk of radius R, which is rotated in a vertical plane with a constant angular velocity ω – see the figure on the right. (Consider only the motion within the disk's plane.)

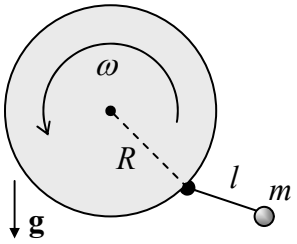

2.6. A bead of mass m, sliding without friction along a light string with a fixed tension $\mathcal{T}$, hung between two horizontally displaced supports – see the figure on the right. Here, in contrast to the similar Problem 1.10, the tension $\mathcal{T}$ may be comparable with the bead's weight mg, and the motion is *not* restricted to the vertical plane.

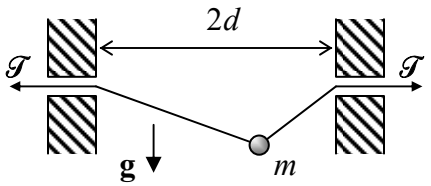

2.7. A bead of mass m, sliding without friction along a light string of a fixed length $2l$, that is hung between two support points displaced horizontally by distance $2d < 2l$ – see the figure on the right. As in the previous problem, the motion is not restricted to the vertical plane.

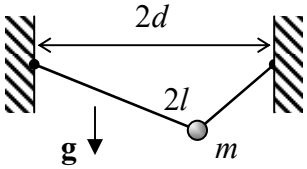

2.8. A block of mass m that can slide, without friction, along the inclined plane surface of a heavy wedge with mass m'. The wedge is free to move, also without friction, along a horizontal surface – see the figure on the right. (Both motions are within the vertical plane containing the steepest slope line.)

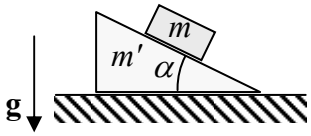

2.9. The two-pendula system that was the subject of Problem 1.8 – see the figure on the right.

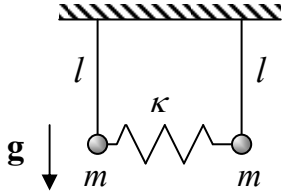

2.10. A system of two similar, inductively coupled *LC* circuits – see the figure on the right.

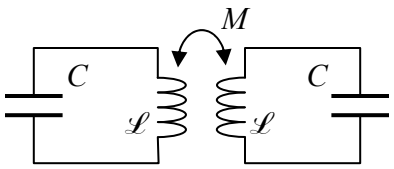

2.11.* A small *Josephson junction* – the system consisting of two superconductors (S) weakly coupled by Cooper-pair tunneling through a thin insulating layer (I) that separates them – see the figure on the right.

Hints:

(i) At not very high frequencies (whose quantum $\hbar\omega$ is lower than the binding energy 2Δ of the Cooper pairs), the Josephson effect in a sufficiently small junction may be described by the following coupling energy:

$$U(\varphi) = -E_J \cos\varphi + \text{const},$$

where the constant E_J describes the coupling strength, while the variable φ (called the *Josephson phase difference*) is connected to the voltage V across the junction by the famous *frequency-to-voltage relation*

$$\frac{d\varphi}{dt} = \frac{2e}{\hbar}V,$$

where $e \approx 1.602\times10^{-19}$ C is the fundamental electric charge and $\hbar \approx 1.054\times10^{-34}$ J·s is the Planck constant.[18]

(ii) The junction (as any system of two close conductors) has a substantial electric capacitance C.

[18] More discussion of the Josephson effect and the physical sense of the variable φ may be found, for example, in EM Sec. 6.5 and QM Secs. 1.6 and 2.8, but the given problem may be solved without that additional information.

This page is intentionally left blank

Chapter 3. A Few Simple Problems

The objective of this chapter is to solve a few simple but very important particle dynamics problems that may be reduced to 1D motion. They notably include the famous "planetary" problem of two particles interacting via a spherically symmetric potential, and the classical particle scattering problem. In the process of solution, several methods that will be very essential for the analysis of more complex systems are also discussed.

3.1. One-dimensional and 1D-reducible systems

If a particle is confined to motion along a straight line (say, axis x), its position is completely determined by this coordinate. In this case, as we already know, the particle's Lagrangian function is given by Eq. (2.21):

$$L = T(\dot{x}) - U(x,t), \quad T(\dot{x}) = \frac{m}{2}\dot{x}^2, \tag{3.1}$$

so the Lagrange equation of motion given by Eq. (2.22),

$$m\ddot{x} = -\frac{\partial U(x,t)}{\partial x} \tag{3.2}$$

is just the x-component of the 2nd Newton's law.

It is convenient to discuss the dynamics of such *really-1D systems* as a part of a more general class of *effectively-1D systems*. This is a system whose position, due to either holonomic constraints and/or conservation laws, is also fully determined by one generalized coordinate q, and whose Lagrangian may be represented in a form similar to Eq. (1):

Effectively-1D system

$$L = T_{\text{ef}}(\dot{q}) - U_{\text{ef}}(q,t), \qquad T_{\text{ef}} = \frac{m_{\text{ef}}}{2}\dot{q}^2, \tag{3.3}$$

where m_{ef} is some constant which may be considered as the *effective mass* of the system, and the function U_{ef}, its *effective potential energy*. In this case, the Lagrange equation (2.19), describing the system's dynamics, has a form similar to Eq. (2):

$$m_{\text{ef}}\ddot{q} = -\frac{\partial U_{\text{ef}}(q,t)}{\partial q}. \tag{3.4}$$

As an example, let us return to our testbed system shown in Fig. 2.1. We have already seen that for this system, having one degree of freedom, the genuine kinetic energy T, expressed by the first of Eqs. (2.23), is *not* a quadratically-homogeneous function of the generalized velocity. However, the system's Lagrangian function (2.23) still may be represented in the form (3),

$$L = \frac{m}{2}R^2\dot{\theta}^2 + \frac{m}{2}R^2\omega^2\sin^2\theta + mgR\cos\theta + \text{const} \equiv T_{\text{ef}} - U_{\text{ef}}, \tag{3.5}$$

provided that we take

$$T_{\rm ef} \equiv \frac{m}{2} R^2 \dot{\theta}^2, \qquad U_{\rm ef} \equiv -\frac{m}{2} R^2 \omega^2 \sin^2\theta - mgR\cos\theta + \text{const}. \tag{3.6}$$

In this new partitioning of the function L, which is legitimate because $U_{\rm ef}$ depends only on the generalized coordinate θ, but not on the corresponding generalized velocity, $T_{\rm ef}$ includes only a part of the genuine kinetic energy T of the bead, while $U_{\rm ef}$ includes not only its real potential energy U in the gravity field but also an additional term related to ring rotation. (As we will see in Sec. 4.6, this term may be interpreted as the effective potential energy due to the inertial centrifugal "force" arising at the problem's solution in the non-inertial reference frame rotating with the ring.)

Returning to the general case of effectively-1D systems with Lagrangians of the type (3), let us calculate their Hamiltonian function, using its definition (2.32):

$$H = \frac{\partial L}{\partial \dot{q}}\dot{q} - L = m_{\rm ef}\dot{q}^2 - (T_{\rm ef} - U_{\rm ef}) = T_{\rm ef} + U_{\rm ef}. \tag{3.7}$$

So, H is expressed via $T_{\rm ef}$ and $U_{\rm ef}$ exactly as the energy E is expressed via genuine T and U.

3.2. Equilibrium and stability

Autonomous systems are defined as dynamic systems whose equations of motion do not depend on time explicitly. For the effectively-1D (and in particular the really-1D) systems obeying Eq. (4), this means that their function $U_{\rm ef}$, and hence the Lagrangian function (3) should not depend on time explicitly. According to Eqs. (2.35), in such systems, the Hamiltonian function (7), i.e. the sum $T_{\rm ef} + U_{\rm ef}$, is an integral of motion. However, be careful! Generally, this conclusion is not valid for the genuine mechanical energy E of such a system; for example, as we already know from Sec. 2.2, for our testbed problem, with the generalized coordinate $q = \theta$ (Fig. 2.1), E is not conserved.

According to Eq. (4), an autonomous system, at appropriate initial conditions, may stay in equilibrium at one or several *stationary* (alternatively called *fixed*) *points* q_n, corresponding to either the minimum or a maximum of the effective potential energy (see Fig. 1):

$$\frac{dU_{\rm ef}}{dq}(q_n) = 0. \tag{3.8}$$

Fixed-point condition

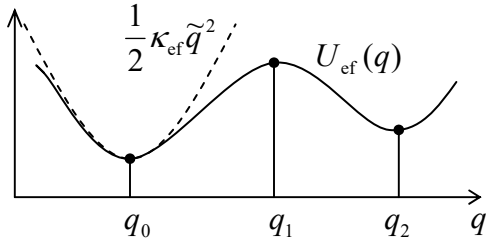

Fig. 3.1. An example of the effective potential energy profile near stable (q_0, q_2) and unstable (q_1) fixed points, and its quadratic approximation (10) near point q_0.

In order to explore the *stability* of such fixed points, let us analyze the dynamics of small deviations

$$\tilde{q}(t) \equiv q(t) - q_n \tag{3.9}$$

from one of such points. For that, let us expand the function $U_{\rm ef}(q)$ in the Taylor series at q_n:

$$U_{\text{ef}}(q) = U_{\text{ef}}(q_n) + \frac{dU_{\text{ef}}}{dq}(q_n)\,\tilde{q} + \frac{1}{2}\frac{d^2U_{\text{ef}}}{dq^2}(q_n)\,\tilde{q}^2 + \dots . \tag{3.10}$$

The first term on the right-hand side, $U_{\text{ef}}(q_n)$, is an arbitrary constant and does not affect motion. The next term, linear in the deviation $\tilde{q}$, equals zero – see the fixed point's definition (8). Hence the fixed point's stability is determined by the next term, quadratic in $\tilde{q}$, more exactly by its coefficient,

$$\kappa_{\text{ef}} \equiv \frac{d^2U_{\text{ef}}}{dq^2}(q_n), \tag{3.11}$$

which is frequently called the *effective spring constant*. Indeed, neglecting the higher terms of the Taylor expansion (10),[1] we see that Eq. (4) takes the familiar form:

$$m_{\text{ef}}\ddot{\tilde{q}} + \kappa_{\text{ef}}\tilde{q} = 0. \tag{3.12}$$

I am confident that the reader of these notes knows everything about this equation, but since we will soon run into similar but more complex equations, let us review the formal procedure of its solution. From the mathematical standpoint, Eq. (12) is an ordinary linear differential equation of the second order, with constant coefficients. The general theory of such equations tells us that its general solution (for any initial conditions) may be represented as

$$\tilde{q}(t) = c_+ e^{\lambda_+ t} + c_- e^{\lambda_- t}, \tag{3.13}$$

where the constants $c_\pm$ are determined by initial conditions, while the so-called *characteristic exponents* $\lambda_\pm$ are completely defined by the equation itself. To calculate these exponents, it is sufficient to plug just one partial solution, $e^{\lambda t}$, into the equation. In our simple case (12), this yields the following *characteristic equation*:

$$m_{\text{ef}}\lambda^2 + \kappa_{\text{ef}} = 0. \tag{3.14}$$

If the ratio $k_{\text{ef}}/m_{\text{ef}}$ is positive, i.e. the fixed point corresponds to the minimum of potential energy (e.g., see points q_0 and q_2 in Fig. 1), the characteristic equation yields

$$\lambda_\pm = \pm i\omega_0, \qquad \text{with } \omega_0 \equiv \left(\frac{\kappa_{\text{ef}}}{m_{\text{ef}}}\right)^{1/2}, \tag{3.15}$$

(where i is the imaginary unit, $i^2 = -1$), so Eq. (13) describes *harmonic* (sinusoidal) oscillations of the system,[2]

$$\tilde{q}(t) = c_+ e^{+i\omega_0 t} + c_- e^{-i\omega_0 t} \equiv c_c \cos\omega_0 t + c_s \sin\omega_0 t, \tag{3.16}$$

[1] Those terms may be important only in very special cases when κ_{ef} is exactly zero, i.e. when a fixed point is also an *inflection point* of the function $U_{\text{ef}}(q)$.

[2] The reader should not be scared of the first form of (16), i.e. of the representation of a real variable (the deviation from equilibrium) via a sum of two complex functions. Indeed, any real initial conditions give $c_-^* = c_+$, so the sum is real for any t. An even simpler way to deal with such complex representations of real functions will be discussed in the beginning of Chapter 5, and then used throughout this series.

with the frequency ω_0, about the fixed point – which is thereby *stable*.[3] On the other hand, at the potential energy maximum ($k_{ef} < 0$, e.g., at point q_1 in Fig. 1), we get

$$\lambda_{\pm} = \pm\lambda, \quad \text{where } \lambda \equiv \left(\frac{|\kappa_{ef}|}{m_{ef}}\right)^{1/2}, \quad \text{so that } \tilde{q}(t) = c_+ e^{+\lambda t} + c_- e^{-\lambda t}. \tag{3.17}$$

Since the solution has an exponentially growing part,[4] the fixed point is *unstable*.

Note that the *quadratic* expansion of function $U_{ef}(q)$, given by the truncation of Eq. (10) to the three displayed terms, is equivalent to a *linear* Taylor expansion of the effective force:

$$F_{ef} \equiv -\frac{dU_{ef}}{dq} \approx -\kappa_{ef}\tilde{q}, \tag{3.18}$$

immediately resulting in the linear equation (12). Hence, to analyze the stability of a fixed point q_n, it is sufficient to *linearize* the equation of motion with respect to small deviations from the point, and study possible solutions of the resulting linear equation. This linearization procedure is typically simpler to carry out than the quadratic expansion (10).

As an example, let us return to our testbed problem (Fig. 2.1) whose function U_{ef} we already know – see the second of Eqs. (6). With it, the equation of motion (4) becomes

$$mR^2\ddot{\theta} = -\frac{dU_{ef}}{d\theta} = mR^2\left(\omega^2\cos\theta - \Omega^2\right)\sin\theta, \quad \text{i.e. } \ddot{\theta} = \left(\omega^2\cos\theta - \Omega^2\right)\sin\theta, \tag{3.19}$$

where $\Omega \equiv (g/R)^{1/2}$ is the frequency of small oscillations of the system at $\omega = 0$ – see Eq. (2.26).[5] From Eq. (8), we see that on any 2π-long segment of the angle θ,[6] the system may have four fixed points; for example, on the half-open segment $(-\pi, +\pi]$ these points are

$$\theta_0 = 0, \qquad \theta_1 = \pi, \qquad \theta_{2,3} = \pm\cos^{-1}\frac{\Omega^2}{\omega^2}. \tag{3.20}$$

The last two fixed points, corresponding to the bead shifted to either side of the rotating ring, exist only if the angular velocity ω of the rotation exceeds Ω. (In the limit of very fast rotation, $\omega >> \Omega$, Eq. (20) yields $\theta_{2,3} \to \pm\pi/2$, i.e. the stationary positions approach the horizontal diameter of the ring – in accordance with our physical intuition.)

To analyze the fixed point stability, we may again use Eq. (9), in the form $\theta = \theta_n + \tilde{\theta}$, plug it into Eq. (19), and Taylor-expand both trigonometric functions of θ up to the term linear in $\tilde{\theta}$:

$$\ddot{\tilde{\theta}} = \left[\omega^2\left(\cos\theta_n - \sin\theta_n\,\tilde{\theta}\right) - \Omega^2\right]\left(\sin\theta_n + \cos\theta_n\,\tilde{\theta}\right). \tag{3.21}$$

[3] This particular type of stability, when the deviation from the equilibrium oscillates with a constant amplitude, neither growing nor decreasing in time, is called either *orbital*, or "neutral", or "indifferent" *stability*.

[4] Mathematically, the growing part vanishes at some special (exact) initial conditions which give $c_+ = 0$. However, the futility of this argument for real physical systems should be obvious to anybody who has ever tried to balance a pencil on its sharp point.

[5] Note that Eq. (19) coincides with Eq. (2.25). This is a good sanity check illustrating that the procedure (5)-(6) of moving a term from the potential to the kinetic energy within the Lagrangian function is indeed legitimate.

[6] For this particular problem, the values of θ that differ by a multiple of 2π, are physically equivalent.

Generally, this equation may be linearized further by purging its right-hand side of the term proportional to $\tilde{\theta}^2$; however in this simple case, Eq. (21) is already convenient for analysis. In particular, for the fixed point $\theta_0 = 0$ (corresponding to the bead's position at the bottom of the ring), we have $\cos\theta_0 = 1$ and $\sin\theta_0 = 0$, so Eq. (21) is reduced to a linear differential equation

$$\ddot{\tilde{\theta}} = \left(\omega^2 - \Omega^2\right)\tilde{\theta}\,, \tag{3.22}$$

whose characteristic equation is similar to Eq. (14) and yields

$$\lambda^2 = \omega^2 - \Omega^2, \quad \text{for } \theta \approx \theta_0\,. \tag{3.23a}$$

This result shows that if $\omega^2 < \Omega^2$, both roots λ are imaginary, so this fixed point is orbitally stable. However, if the rotation speed is increased so that $\Omega^2 < \omega^2$, the roots become real: $\lambda_\pm = \pm(\omega^2 - \Omega^2)^{1/2}$, with one of them positive, so the fixed point becomes unstable beyond this threshold, i.e. as soon as fixed points $\theta_{2,3}$ exist. Absolutely similar calculations for other fixed points yield

$$\lambda^2 = \begin{cases} \Omega^2 + \omega^2 > 0, & \text{for } \theta \approx \theta_1, \\ \Omega^2 - \omega^2, & \text{for } \theta \approx \theta_{2,3}\,. \end{cases} \tag{3.23b}$$

These results show that the fixed point θ_1 (the bead on the top of the ring) is always unstable – just as we could foresee, while the side fixed points $\theta_{2,3}$ are orbitally stable as soon as they exist – at $\Omega^2 < \omega^2$.

Thus, our fixed-point analysis may be summarized very simply: an increase of the ring rotation speed ω beyond a certain threshold value, equal to Ω given by Eq. (2.26), causes the bead to move to one of the ring sides, oscillating about one of the fixed points $\theta_{2,3}$. Together with the rotation about the vertical axis, this motion yields quite a complex (generally, open) spatial trajectory as observed from a lab frame, so it is fascinating that we could analyze it quantitatively in such a simple way.

Later in this course, we will repeatedly use the linearization of the equations of motion for the analysis of the stability of more complex dynamic systems, including those with energy dissipation.

3.3. Hamiltonian 1D systems

Autonomous systems that are described by time-independent Lagrangians are frequently called *Hamiltonian* ones because their Hamiltonian function H (again, not necessarily equal to the genuine mechanical energy E!) is conserved. In our current 1D case, described by Eq. (3),

$$H = \frac{m_{\text{ef}}}{2}\dot{q}^2 + U_{\text{ef}}(q) = \text{const}\,. \tag{3.24}$$

From a mathematical standpoint, this conservation law is just the first integral of motion. Solving Eq. (24) for $\dot{q}$, we get the first-order differential equation,

$$\frac{dq}{dt} = \pm\left\{\frac{2}{m_{\text{ef}}}\left[H - U_{\text{ef}}(q)\right]\right\}^{1/2}, \qquad \text{i.e. } \pm\left(\frac{m_{\text{ef}}}{2}\right)^{1/2}\frac{dq}{\left[H - U_{\text{ef}}(q)\right]^{1/2}} = dt\,, \tag{3.25}$$

which may be readily integrated:

$$\pm\left(\frac{m_{\rm ef}}{2}\right)^{1/2}\int_{q(t_0)}^{q(t)}\frac{dq'}{\left[H-U_{\rm ef}(q')\right]^{1/2}}=t-t_0\,. \tag{3.26}$$

Since the constant H (as well as the proper sign before the integral – see below) is fixed by initial conditions, Eq. (26) gives the reciprocal form, $t = t(q)$, of the desired law of system motion, $q(t)$. Of course, for any particular problem, the integral in Eq. (26) still has to be worked out, either analytically or numerically, but even the latter procedure is typically much easier than the numerical integration of the initial, second-order differential equation of motion, because at the addition of many values (to which any numerical integration is reduced[7]) the rounding errors are effectively averaged out.

Moreover, Eq. (25) also allows a general classification of 1D system motion. Indeed:

(i) If $H > U_{\rm ef}(q)$ in the whole range of our interest, the effective kinetic energy $T_{\rm ef}$ (3) is always positive. Hence the derivative dq/dt cannot change its sign, so this effective velocity retains the sign it had initially. This is an unbound motion in one direction (Fig. 2a).

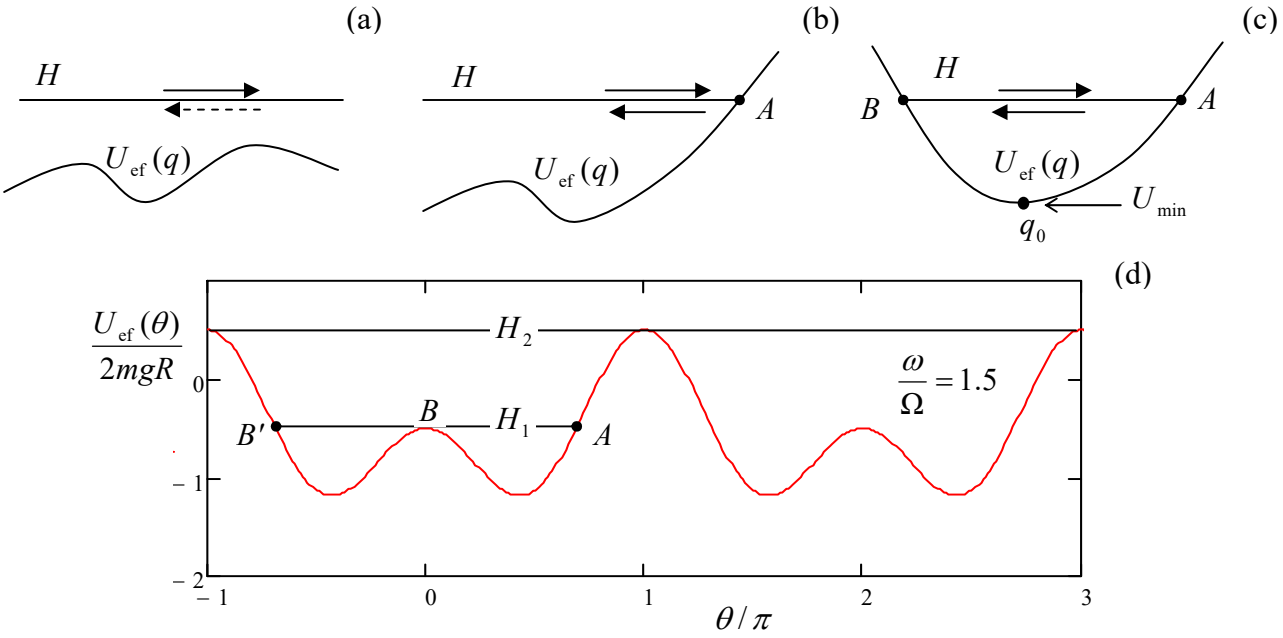

Fig. 3.2. Graphical representations of Eq. (25) for three different cases: (a) an unbound motion, with the velocity sign conserved, (b) a reflection from a "classical turning point", accompanied by the velocity sign change, and (c) bound, periodic motion between two turning points – schematically. (d) The effective potential energy (6) of the bead on the rotating ring (Fig. 2.1) for a particular case with $\Omega^2 < \omega^2$.

(ii) Now let the particle approach a *classical turning point A* where $H = U_{\rm ef}(q)$ – see Fig. 2b.[8] According to Eq. (25), at that point, the particle velocity vanishes, while its acceleration, according to Eq. (4), is still finite. This means that the particle's velocity sign changes its sign at this point, i.e. it is *reflected* from it.

[7] See, e.g., MA Eqs. (5.2) and (5.3).

[8] This terminology comes from quantum mechanics, which shows that a particle (or rather its wavefunction) actually can, to a certain extent, penetrate "classically forbidden" regions where $H < U_{\rm ef}(q)$.

(iii) If, after the reflection from some point A, the particle runs into another classical turning point B (Fig. 2c), the reflection process is repeated again and again, so the particle is bound to a periodic motion between two turning points.

The last case of *periodic oscillations* presents a large conceptual and practical interest, and the whole of Chapter 5 will be devoted to a detailed analysis of this phenomenon and numerous associated effects. Here I will only note that for an autonomous Hamiltonian system described by Eq. (4), Eq. (26) immediately enables the calculation of the oscillation period:

Oscillation period

$$\mathcal{T} = 2\left(\frac{m_{\rm ef}}{2}\right)^{1/2} \int_B^A \frac{dq}{[H - U_{\rm ef}(q)]^{1/2}}, \tag{3.27}$$

where the additional front factor 2 accounts for two time intervals: of the motion from B to A and back – see Fig. 2c. Indeed, according to Eq. (25), at each classically allowed point q, the velocity's magnitude is the same, so these time intervals are equal to each other.

(Note that the dependence of points A and B on H is not necessarily continuous. For example, for our testbed problem, whose effective potential energy is plotted in Fig. 2d for a particular value of $\omega > \Omega$, a gradual increase of H leads to a sudden jump, at $H = H_1$, of the point B to a new position B', corresponding to a sudden switch from oscillations about one fixed point $\theta_{2,3}$ to oscillations about two adjacent fixed points – before the beginning of a persistent rotation around the ring at $H > H_2$.)

Now let us consider a particular, but a very important limit of Eq. (27). As Fig. 2c shows, if H is reduced to approach $U_{\rm min}$, the periodic oscillations take place at the very bottom of this *potential well*, about a stable fixed point q_0. Hence, if the potential energy profile is smooth enough, we may limit the Taylor expansion (10) to the displayed quadratic term. Plugging it into Eq. (27), and using the mirror symmetry of this particular problem about the fixed point q_0, we get

$$\mathcal{T} = 4\left(\frac{m_{\rm ef}}{2}\right)^{1/2} \int_0^A \frac{d\tilde{q}}{\left[H - \left(U_{\rm min} + \kappa_{\rm ef}\tilde{q}^2/2\right)\right]^{1/2}} = \frac{4}{\omega_0} I, \qquad \text{with } I \equiv \int_0^1 \frac{d\xi}{\left(1-\xi^2\right)^{1/2}}, \tag{3.28}$$

where $\xi \equiv \tilde{q}/A$, with $A \equiv (2/\kappa_{\rm ef})^{1/2}(H - U_{\rm min})^{1/2}$ being the classical turning point, i.e. the oscillation amplitude, and ω_0 the frequency given by Eq. (15). Taking into account that the elementary integral I in that equation equals $\pi/2$,[9] we finally get

$$\mathcal{T} = \frac{2\pi}{\omega_0}, \tag{3.29}$$

as it should be for the harmonic oscillations (16). Note that the oscillation period does not depend on the oscillation amplitude A, i.e. on the difference $(H - U_{\rm min})$ – while it is sufficiently small.

3.4. Planetary problems

Leaving a more detailed study of oscillations for Chapter 5, let us now discuss the so-called *planetary systems*[10] whose description, somewhat surprisingly, may be also reduced to an effectively 1D

[9] Indeed, introducing a new variable ζ as $\xi \equiv \sin\zeta$, we get $d\xi = \cos\zeta\, d\zeta = (1-\xi^2)^{1/2}\, d\zeta$, so that the function under the integral is just $d\zeta$, and its limits are $\zeta = 0$ and $\zeta = \pi/2$.

problem. Indeed, consider two particles that interact via a conservative central force $\mathbf{F}_{21} = -\mathbf{F}_{12} = \mathbf{n}_r F(r)$, where r and $\mathbf{n}_r$ are, respectively, the magnitude and the direction of the *distance vector* $\mathbf{r} \equiv \mathbf{r}_1 - \mathbf{r}_2$ connecting the two particles (Fig. 3).

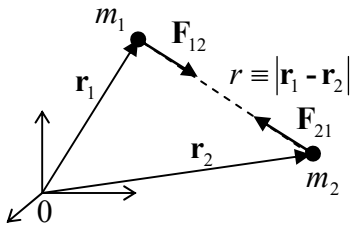

Fig. 3.3. Vectors in the planetary problem.

Generally, two particles moving without constraints in 3D space, have 3 + 3 = 6 degrees of freedom, which may be described, e.g., by their Cartesian coordinates $\{x_1, y_1, z_1, x_2, y_2, z_2\}$ However, for this particular form of interaction, the following series of tricks allows the number of essential degrees of freedom to be reduced to just one.

First, the conservative force of particle interaction may be described by a time-independent potential energy $U(r)$, such that $F(r) = -\partial U(r)/\partial r$.[11] Hence the Lagrangian function of the system is

$$L \equiv T - U(r) = \frac{m_1}{2}\dot{\mathbf{r}}_1^2 + \frac{m_2}{2}\dot{\mathbf{r}}_2^2 - U(r). \tag{3.30}$$

Let us perform the transfer from the initial six scalar coordinates of the particles to the following six generalized coordinates: three Cartesian components of the distance vector

$$\mathbf{r} \equiv \mathbf{r}_1 - \mathbf{r}_2, \tag{3.31}$$

and three scalar components of the following vector:

$$\mathbf{R} \equiv \frac{m_1\mathbf{r}_1 + m_2\mathbf{r}_2}{M}, \quad \text{with } M \equiv m_1 + m_2, \tag{3.32}$$

Center of mass

which defines the position of the *center of mass* of the system, with the total mass M. Solving the system of two linear equations (31) and (32) for $\mathbf{r}_1$ and $\mathbf{r}_2$, we get

$$\mathbf{r}_1 = \mathbf{R} + \frac{m_2}{M}\mathbf{r}, \qquad \mathbf{r}_2 = \mathbf{R} - \frac{m_1}{M}\mathbf{r}. \tag{3.33}$$

Plugging these relations into Eq. (30), we see that it is reduced to

$$L = \frac{M}{2}\dot{\mathbf{R}}^2 + \frac{m}{2}\dot{\mathbf{r}}^2 - U(r), \tag{3.34}$$

where m is the so-called *reduced mass*:

$$m \equiv \frac{m_1 m_2}{M}, \quad \text{so that } \frac{1}{m} \equiv \frac{1}{m_1} + \frac{1}{m_2}. \tag{3.35}$$

Reduced mass

[10] This name is very conditional, because this group of problems includes, for example, charged particle scattering (see Sec. 3.7 below).

[11] See, e.g., MA Eq. (10.8) with $\partial/\partial\theta = \partial/\partial\varphi = 0$.

Note that according to Eq. (35), the reduced mass is lower than that of the lightest component of the two-body system. If one of $m_{1,2}$ is *much* less than its counterpart (like it is in most star-planet or planet-satellite systems), then with a good precision $m \approx \min[m_1, m_2]$.

Since the Lagrangian function (34) depends only on $\dot{\mathbf{R}}$ rather than $\mathbf{R}$ itself, according to our discussion in Sec. 2.4, all Cartesian components of R are cyclic coordinates, and the corresponding generalized momenta are conserved:

$$P_j \equiv \frac{\partial L}{\partial \dot{R}_j} \equiv M\dot{R}_j = \text{const}, \quad j = 1, 2, 3. \tag{3.36}$$

Physically, this is just the conservation law for the full momentum $\mathbf{P} \equiv M\mathbf{R}$ of our system, due to the absence of external forces. Actually, in the axiomatics used in Sec. 1.3 this law is postulated – see Eq. (1.10) – but now we may attribute the momentum $\mathbf{P}$ to a certain geometric point, with the center-of-mass radius vector $\mathbf{R}$. In particular, since according to Eq. (36) the center moves with a constant velocity in the inertial reference frame used to write Eq. (30), we may consider a new inertial frame with the origin at point $\mathbf{R}$. In this new frame, $\mathbf{R} \equiv 0$, so the vector $\mathbf{r}$ (and hence the scalar r) remain the same as in the old frame (because the frame transfer vector adds equally to $\mathbf{r}_1$ and $\mathbf{r}_2$, and cancels in $\mathbf{r} = \mathbf{r}_1 - \mathbf{r}_2$), and the Lagrangian (34) is now reduced to

$$L = \frac{m}{2}\dot{\mathbf{r}}^2 - U(r). \tag{3.37}$$

Thus our initial problem has been reduced to just three degrees of freedom – three scalar components of the vector $\mathbf{r}$. In other words, Eq. (37) shows that the dynamics of the vector $\mathbf{r}$ of our initial, two-particle system is identical to that of the radius vector of a *single particle* with the effective mass m, moving in the central potential field $U(r)$.

Two more degrees of freedom may be excluded from the planetary problem by noticing that according to Eq. (1.35), the angular momentum $\mathbf{L} = \mathbf{r}\times\mathbf{p}$ of our effective single particle of mass m is also conserved, both in magnitude and direction. Since the direction of $\mathbf{L}$ is, by its definition, perpendicular to both $\mathbf{r}$ and $\mathbf{v} = \mathbf{p}/m$, this means that the particle's motion is confined to the plane whose orientation is determined by the initial directions of the vectors $\mathbf{r}$ and $\mathbf{v}$. Hence we can completely describe the particle's position by just two coordinates in that plane, for example by the distance r to the origin, and the polar angle φ. In these coordinates, Eq. (37) takes the form identical to Eq. (2.49):

$$L = \frac{m}{2}\left(\dot{r}^2 + r^2\dot{\varphi}^2\right) - U(r). \tag{3.38}$$

Moreover, the latter coordinate, polar angle φ, may be also eliminated by using the conservation of angular momentum's magnitude, in the form of Eq. (2.50): [12]

$$L_z = mr^2\dot{\varphi} = \text{const}. \tag{3.39}$$

A direct corollary of this conservation is the so-called *2nd Kepler's law*:[13] the radius vector $\mathbf{r}$ sweeps equal areas A in equal time periods. Indeed, in the linear approximation in $dA << A$, the area

[12] Here index z stands for the coordinate perpendicular to the motion plane. Since other components of the angular momentum equal zero, this index is not really necessary, but I will still use it – just to make a clear distinction between the angular momentum L_z and the Lagrangian function L.

differential dA is equal to the area of a narrow right triangle with the base being the arc differential $rd\varphi$, and the height equal to r – see Fig. 4. As a result, according to Eq. (39), the time derivative of the area,

$$\frac{dA}{dt} = \frac{r(rd\varphi)/2}{dt} \equiv \frac{1}{2}r^2\dot{\varphi} = \frac{L_z}{2m}, \tag{3.40}$$

remains constant. Since the factor $L_z/2m$ is constant, integration of this equation over an arbitrary (not necessarily small!) time interval Δt proves the 2nd Kepler's law: $A \propto \Delta t$.

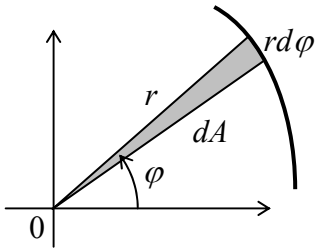

Fig. 3.4. The area differential dA in the polar coordinates.

Now note that since $\partial L/\partial t = 0$, the Hamiltonian function H is also conserved, and since, according to Eq. (38), the kinetic energy of the system is a quadratic-homogeneous function of the generalized velocities $\dot{r}$ and $\dot{\varphi}$, we have $H = E$, so the system's energy E,

$$E = \frac{m}{2}\dot{r}^2 + \frac{m}{2}r^2\dot{\varphi}^2 + U(r), \tag{3.41}$$

is also the first integral of motion.[14] However, according to Eq. (39), the second term on the right-hand side of Eq. (41) may be represented as

$$\frac{m}{2}r^2\dot{\varphi}^2 = \frac{L_z^2}{2mr^2}, \tag{3.42}$$

so the energy (41) may be expressed as that of a 1D particle moving along axis r,

$$E = \frac{m}{2}\dot{r}^2 + U_{\text{ef}}(r), \tag{3.43}$$

in the following effective potential:

$$U_{\text{ef}}(r) \equiv U(r) + \frac{L_z^2}{2mr^2}. \tag{3.44}$$

Effective potential energy

So the planetary motion problem has been reduced to the study of an effectively-1D system.[15]

[13] This is one of the three laws deduced, from the extremely detailed astronomical data collected by Tycho Brahe (1546-1601), by Johannes Kepler in the early 17th century. In turn, the three Kepler's laws have become the main basis for Newton's discovery, a few decades later, of the gravity law (1.15). That relentless march of physics…

[14] One may argue that this fact should have been evident earlier because the effective particle of mass m moves in a potential field $U(r)$, which conserves energy.

[15] Note that this reduction has been done in a way different from that used for our testbed problem (Fig. 2.1) in Sec. 2 above. (The reader is encouraged to analyze this difference.) To emphasize this fact, I will keep writing E instead of H here, though for the planetary problem we are discussing now, these two notions coincide.

Now we may proceed just like we did in Sec. 3, with due respect to the very specific effective potential (44) which, in particular, diverges at $r \to 0$ – besides the very special case of an exactly radial motion, $L_z = 0$. In particular, we may solve Eq. (43) for dr/dt to get

$$dt = \left(\frac{m}{2}\right)^{1/2} \frac{dr}{[E - U_{\text{ef}}(r)]^{1/2}}. \tag{3.45}$$

This equation enables us not only to get a direct relation between time t and distance r, similarly to Eq. (26),

$$t = \pm\left(\frac{m}{2}\right)^{1/2} \int \frac{dr}{[E - U_{\text{ef}}(r)]^{1/2}} = \pm\left(\frac{m}{2}\right)^{1/2} \int \frac{dr}{[E - U(r) - L_z^2/2mr^2]^{1/2}}, \tag{3.46}$$

but also do a similar calculation of the angle φ of the effective particle. Indeed, integrating Eq. (39),

$$\varphi \equiv \int \dot{\varphi}\, dt = \frac{L_z}{m} \int \frac{dt}{r^2}, \tag{3.47}$$

and plugging dt from Eq. (45), we get an explicit expression for the particle's trajectory $\varphi(r)$:

$$\varphi = \pm \frac{L_z}{(2m)^{1/2}} \int \frac{dr}{r^2 [E - U_{\text{ef}}(r)]^{1/2}} = \pm \frac{L_z}{(2m)^{1/2}} \int \frac{dr}{r^2 [E - U(r) - L_z^2/2mr^2]^{1/2}}. \tag{3.48}$$

Note that according to Eq. (39), the derivative $d\varphi/dt$ does *not* change sign at the reflection from any classical turning point $r \neq 0$, so, in contrast to Eq. (46), the sign on the right-hand side of Eq. (48) is uniquely determined by the initial conditions and cannot change during the motion.

Let us use these results, valid for any interaction law $U(r)$, for the planetary motion's classification. (Following a good tradition, in what follows I will select the arbitrary constant in the potential energy in the way to provide $U \to 0$ and hence $U_{\text{ef}} \to 0$, at $r \to \infty$.) The following cases should be distinguished.

If $U(r) < 0$, i.e. the particle interaction is *attractive* (as it always is in the case of gravity), and the divergence of the attractive potential at $r \to 0$ is faster than $1/r^2$, then $U_{\text{ef}}(r) \to -\infty$ at $r \to 0$, so at appropriate initial conditions the particle may drop on the center even if $L_z \neq 0$ – the event called the *capture*.[16] On the other hand, with $U(r)$ either converging or diverging slower than $1/r^2$, at $r \to 0$, the effective energy profile $U_{\text{ef}}(r)$ has the shape shown schematically in Fig. 5. This is true, in particular, for the very important case

Attractive Coulomb potential

$$U(r) = -\frac{\alpha}{r}, \quad \text{with } \alpha > 0, \tag{3.49}$$

which describes, in particular, the *Coulomb* (electrostatic) *interaction* of two particles with electric charges of opposite signs, and Newton's gravity law (1.15). This particular case will be analyzed in detail below, but for now, let us return to the analysis of an arbitrary attractive potential $U(r) < 0$ leading to the effective potential shown in Fig. 5 when the angular-momentum term in Eq. (44) dominates at small distances r.

[16] In order to analyze what exactly happens at the capture, i.e. at $r = 0$, we would need a model more specific than Eq. (30).

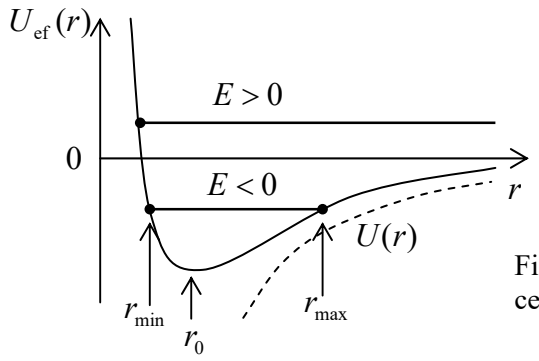

Fig. 3.5. Effective potential profile of an attractive central field, and two types of motion in it.

According to the analysis in Sec. 3, such potential profile, with a minimum at some distance r_0, may sustain two types of motion, depending on the energy E (determined by initial conditions):

(i) If $E > 0$, there is only one classical turning point where $E = U_{ef}$, so the distance r either grows with time from the very beginning or (if the initial value of $\dot{r}$ was negative) first decreases and then, after the reflection from the increasing potential U_{ef}, starts to grow indefinitely. The latter case, of course, describes the *scattering* of the effective particle by the attractive center.[17]

(ii) On the opposite, if the energy is within the range

$$U_{ef}(r_0) \le E < 0, \tag{3.50}$$

the system moves periodically between two classical turning points r_{min} and r_{max} – see Fig. 5. These oscillations of the distance r correspond to the bound orbital motion of our effective particle about the attracting center.

Let us start with the discussion of the bound motion, with the energy within the range (50). If the energy has its minimal possible value,

$$E = U_{ef}(r_0) \equiv \min[U_{ef}(r)], \tag{3.51}$$

the distance cannot change, $r = r_0 = \text{const}$, so the particle's orbit is circular, with the radius r_0 satisfying the condition $dU_{ef}/dr = 0$. Using Eq. (44), we see that the condition for r_0 may be written as

$$\frac{L_z^2}{mr_0^3} = \left.\frac{dU}{dr}\right|_{r=r_0}. \tag{3.52}$$

Since at circular motion, the velocity $\mathbf{v}$ is perpendicular to the radius vector $\mathbf{r}$, L_z is just mr_0v, the left-hand side of Eq. (52) equals mv^2/r_0, while its right-hand side is just the magnitude of the attractive force, so this equality expresses the well-known 2nd Newton's law for the circular motion. Plugging this result into Eq. (47), we get a linear law of angle change, $\varphi = \omega t + \text{const}$, with the angular velocity

$$\omega = \frac{L_z}{mr_0^2} = \frac{v}{r_0}, \tag{3.53}$$

and hence the rotation period $\mathcal{T}_\varphi \equiv 2\pi/\omega$ obeys the elementary relation

[17] In the opposite case when the interaction is *repulsive*, $U(r) > 0$, the addition of the positive angular energy term only increases the trend, and the scattering scenario is the only one possible.

$$\mathcal{T}_\varphi = \frac{2\pi r_0}{v}. \tag{3.54}$$

Now let the energy be above its minimum value (but still negative). Using Eq. (46) just as in Sec. 3, we see that the distance r oscillates with the period

$$\mathcal{T}_r = 2\left(\frac{m}{2}\right)^{1/2} \int_{r_{\min}}^{r_{\max}} \frac{dr}{[E - U(r) - L_z^2/2mr^2]^{1/2}}. \tag{3.55}$$

This period is not necessarily equal to another period, $\mathcal{T}_\varphi$, that corresponds to the 2π-change of the angle. Indeed, according to Eq. (48), the change of the angle φ between two sequential points of the nearest approach,

$$|\Delta\varphi| = 2\frac{L_z}{(2m)^{1/2}} \int_{r_{\min}}^{r_{\max}} \frac{dr}{r^2\left[E - U(r) - L_z^2/2mr^2\right]^{1/2}}, \tag{3.56}$$

is generally different from 2π. Hence, the general trajectory of the bound motion has a spiral shape – see, e.g., an illustration in Fig. 6.

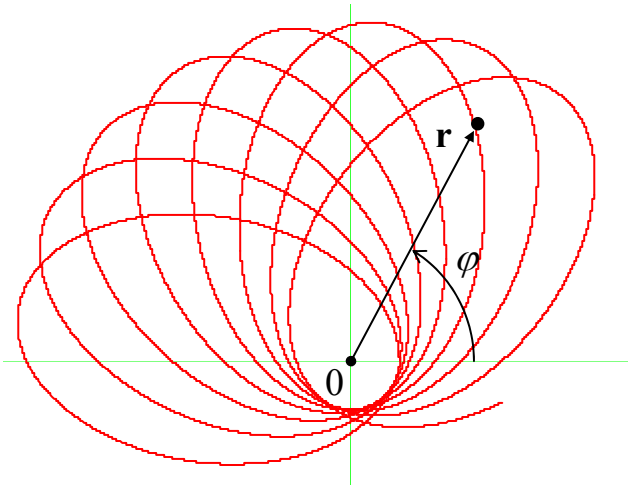

Fig. 3.6. A typical open orbit of a particle moving in a non-Coulomb central field.

The situation is special, however, for a very important particular case, namely that of the Coulomb potential described by Eq. (49).[18] Indeed, plugging this potential into Eq. (48), we get

$$\varphi = \pm\frac{L_z}{(2m)^{1/2}} \int \frac{dr}{r^2\left(E + \alpha/r - L_z^2/2mr^2\right)^{1/2}}. \tag{3.57}$$

This is a table integral,[19] giving

$$\varphi = \pm\cos^{-1}\frac{L_z^2/m\alpha r - 1}{\left(1 + 2EL_z^2/m\alpha^2\right)^{1/2}} + \text{const}. \tag{3.58}$$

[18] For the power-law interaction, $U \propto r^\nu$, the orbits are closed curves only if either $\nu = -1$ (the Coulomb potential) or $\nu = +2$ (the 3D harmonic oscillator) – the so-called *Bertrand theorem*, proved by J. Bertrand only in 1873.

[19] See, e.g., MA Eq. (6.3a).

Hence the reciprocal function, $r(\varphi)$, is 2π-periodic:

$$r = \frac{p}{1 + e\cos(\varphi + \text{const})}, \tag{3.59}$$

Elliptic orbit and its parameters

so at $E < 0$, the orbit is a closed line characterized by the following parameters:[20]

$$p \equiv \frac{L_z^2}{m\alpha}, \qquad e \equiv \left(1 + \frac{2EL_z^2}{m\alpha^2}\right)^{1/2}. \tag{3.60}$$

The physical meaning of these parameters is very simple. Indeed, the general Eq. (52), in the Coulomb potential for which $dU/dr = \alpha/r^2$, shows that p is just the circular orbit radius[21] for the given L_z: $r_0 = L_z^2/m\alpha \equiv p$, so

$$\min\left[U_{\text{ef}}(r)\right] \equiv U_{\text{ef}}(r_0) = -\frac{\alpha^2 m}{2L_z^2}. \tag{3.61}$$

Using this equality together with the second of Eqs. (60), we see that the parameter e (called the *eccentricity*) may be represented just as

$$e = \left\{1 - \frac{E}{\min[U_{\text{ef}}(r)]}\right\}^{1/2}. \tag{3.62}$$

Analytical geometry tells us that Eq. (59), with $e < 1$, is one of the canonical representations of an *ellipse,* with one of its two focuses located at the origin. The fact that planets have such trajectories is known as the *1st Kepler's law*. Figure 7 shows the relations between the dimensions of the ellipse and the parameters p and e.[22]

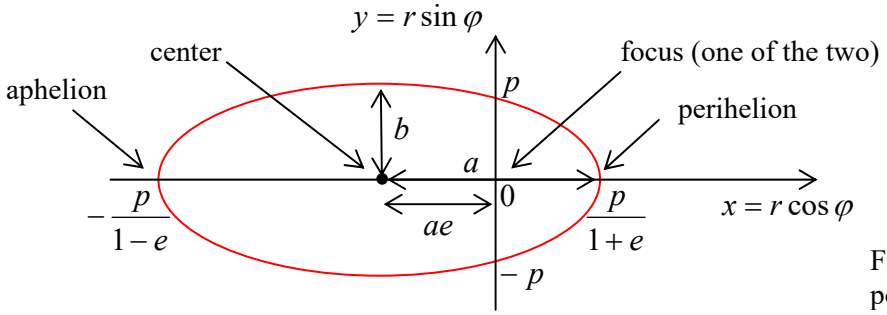

Fig. 3.7. Ellipse, and its special points and dimensions.

In particular, the *major semi-axis a* and the *minor semi-axis b* are simply related to p and e and hence, via Eqs. (60), to the motion integrals E and L_z:

$$a = \frac{p}{1-e^2} = \frac{\alpha}{2|E|}, \qquad b = \frac{p}{(1-e^2)^{1/2}} = \frac{L_z}{(2m|E|)^{1/2}}. \tag{3.63}$$

[20] Let me hope that the difference between the parameter p and the particle momentum's magnitude is absolutely clear from the context, so using the same (traditional) notation for both notions cannot lead to confusion.

[21] Mathematicians prefer a more solemn terminology: the parameter $2p$ is called the *latus rectum* of the ellipse.

[22] In this figure, the constant participating in Eqs. (58)-(59) is assumed to be zero. A different choice of the constant corresponds just to a different origin of φ, i.e. a constant turn of the ellipse about the origin.

As was mentioned above, at $E \to \min [U_{\text{eff}}(r)]$ the orbit is almost circular, with $r(\varphi) \cong r_0 \approx p$. On the contrary, as E is increased to approach zero (its maximum value for the closed orbit), then $e \to 1$, so that the aphelion point $r_{\max} = p/(1 - e)$ tends to infinity, i.e. the orbit becomes extremely extended – see the magenta lines in Fig. 8.

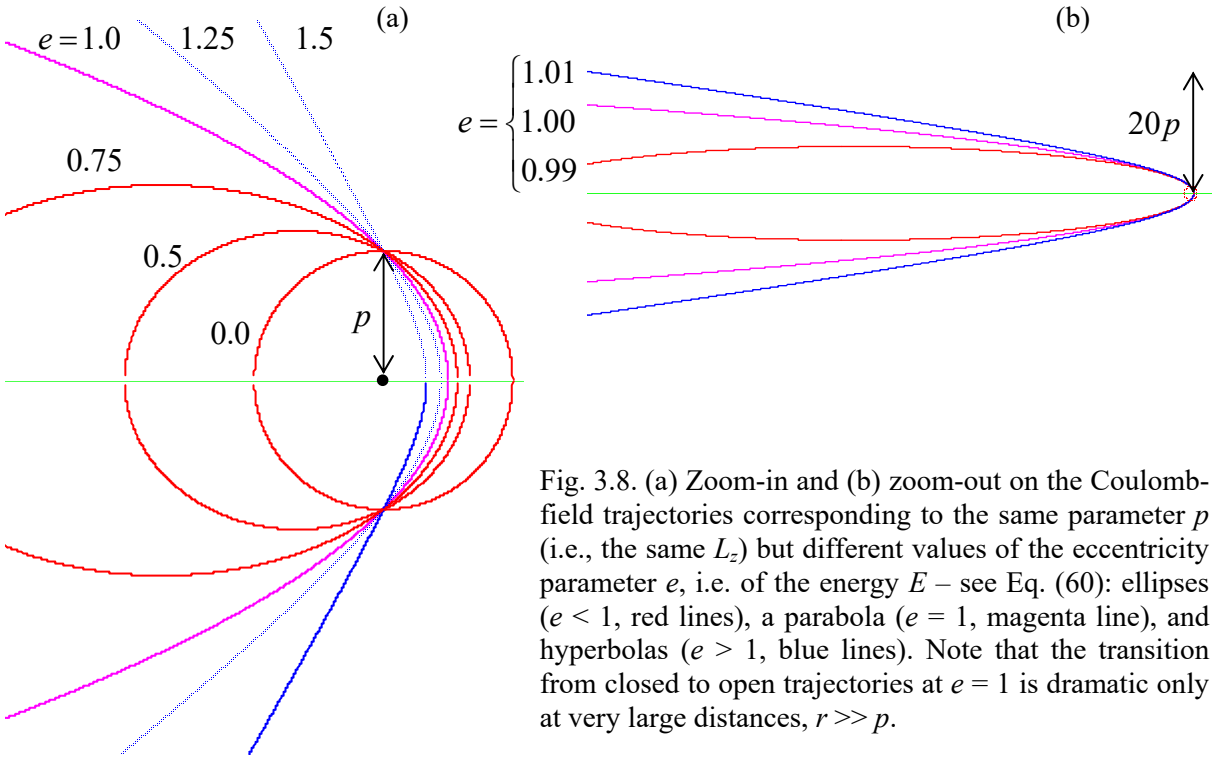

Fig. 3.8. (a) Zoom-in and (b) zoom-out on the Coulomb-field trajectories corresponding to the same parameter p (i.e., the same L_z) but different values of the eccentricity parameter e, i.e. of the energy E – see Eq. (60): ellipses ($e < 1$, red lines), a parabola ($e = 1$, magenta line), and hyperbolas ($e > 1$, blue lines). Note that the transition from closed to open trajectories at $e = 1$ is dramatic only at very large distances, $r >> p$.

The above relations enable, in particular, a ready calculation of the rotation period $\mathcal{T} \equiv \mathcal{T}_r = \mathcal{T}_\varphi$. (In the case of a closed trajectory, $\mathcal{T}_r$ and $\mathcal{T}_\varphi$ coincide.) Indeed, it is well known that the ellipse's area $A = \pi ab$. But according to the 2nd Kepler's law (40), $dA/dt = L_z/2m = \text{const}$. Hence

$$\mathcal{T} = \frac{A}{dA/dt} = \frac{\pi ab}{L_z/2m}. \tag{3.64a}$$

Using Eqs. (60) and (63), this important result may be represented in several other forms:

$$\mathcal{T} = \frac{\pi p^2}{(1-e^2)^{3/2}(L_z/2m)} = \pi\alpha\left(\frac{m}{2|E|^3}\right)^{1/2} = 2\pi a^{3/2}\left(\frac{m}{\alpha}\right)^{1/2}. \tag{3.64b}$$

Since for the Newtonian gravity (1.15), $\alpha = Gm_1m_2 = GmM$, at $m_1 << m_2$ (i.e. $m << M$), this constant is proportional to m, and the last form of Eq. (64b) yields the *3rd Kepler's law*: the periods of motion of different planets in the same central field, say that of our Sun, scale as $\mathcal{T} \propto a^{3/2}$. Note that in contrast to the 2nd Kepler's law (which is valid for any central field), the 1st and the 3rd Kepler's laws are potential-specific.

Now reviewing the above derivation of Eqs. (59)-(60), we see that they are also valid in the case of $E \geq 0$ – see the top horizontal line in Fig. 5 and its discussion above, if we limit the results to the

physically meaningful range $r \geq 0$. This means that if the energy is exactly zero, Eq. (59) (with $e = 1$) is still valid for all values of φ (except for one special point $\varphi = \pi$ where r becomes infinite) and describes a *parabolic* (i.e. open) trajectory – see the magenta lines in Fig. 8.

Moreover, if $E > 0$, Eq. (59) is still valid within a certain sector of angles φ,

$$\Delta\varphi = 2\cos^{-1}\frac{1}{e} \equiv 2\cos^{-1}\left(1+\frac{2EL_z^2}{m\alpha^2}\right)^{-1/2} < \pi, \qquad \text{for } E > 0, \tag{3.65}$$

and describes an open, *hyperbolic* trajectory (see the blue lines in Fig. 8). As was mentioned earlier, such trajectories are typical, in particular, for particle scattering.

3.5. Elastic scattering

If $E > 0$, the motion is unbound for any realistic interaction potential. In this case, the two most important parameters of the particle trajectory are the *impact parameter b* and the *scattering angle* θ (Fig. 9), and the main task of the theory is to find the relation between them in the given potential $U(r)$.

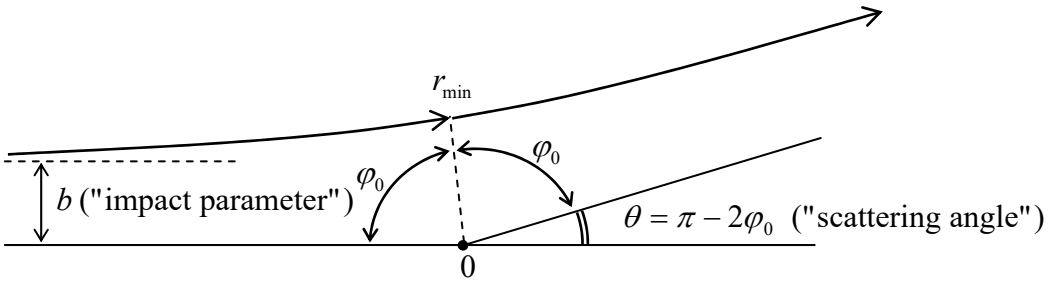

Fig. 3.9. Main geometric parameters of the scattering problem.

For that, it is convenient to note that b is related to the two conserved quantities, the particle's energy[23] E and its angular momentum L_z, in a simple way. Indeed, at $r >> b$, the definition $\mathbf{L} = \mathbf{r}\times(m\mathbf{v})$ yields $L_z = bmv_\infty$, where $v_\infty = (2E/m)^{1/2}$ is the initial (and hence the final) speed of the particle, so

$$L_z = b(2mE)^{1/2}. \tag{3.66}$$

Hence the angular contribution to the effective potential (44) may be represented as

$$\frac{L_z^2}{2mr^2} = E\frac{b^2}{r^2}. \tag{3.67}$$

Next, according to Eq. (48), the trajectory sections going from infinity to the nearest approach point ($r = r_{min}$) and from that point to infinity, have to be similar, and hence correspond to equal angle changes φ_0 – see Fig. 9. Hence we may apply the general Eq. (48) to just one of the sections, say [r_{min}, ∞], to find the scattering angle:

[23] The energy conservation law is frequently emphasized by calling such process *elastic scattering*.

$$\theta = \pi - 2\varphi_0 = \pi - 2\frac{L_z}{(2m)^{1/2}}\int_{r_{\min}}^{\infty}\frac{dr}{r^2\left[E - U(r) - L_z^2/2mr^2\right]^{1/2}} \equiv \pi - 2\int_{r_{\min}}^{\infty}\frac{bdr}{r^2\left[1 - U(r)/E - b^2/r^2\right]^{1/2}}. \quad (3.68)$$

In particular, for the Coulomb potential (49), now with an arbitrary sign of α, we can use the same table integral as in the previous section to get[24]

$$|\theta| = \left|\pi - 2\cos^{-1}\frac{\alpha/2Eb}{\left[1+(\alpha/2Eb)^2\right]^{1/2}}\right|. \quad (3.69a)$$

This result may be more conveniently rewritten as

$$\tan\frac{|\theta|}{2} = \frac{|\alpha|}{2Eb}. \quad (3.69b)$$

Very clearly, the scattering angle's magnitude increases with the potential strength α, and decreases as either the particle energy or the impact parameter (or both) are increased.

The general result (68) and the Coulomb-specific relations (69) represent a formally complete solution of the scattering problem. However, in a typical experiment on elementary particle scattering, the impact parameter b of a single particle is unknown. In this case, our results may be used to obtain the statistics of the scattering angle θ, in particular, the so-called *differential cross-section*[25]

Differential cross-section

$$\boxed{\frac{d\sigma}{d\Omega} \equiv \frac{1}{n}\frac{dN}{d\Omega},} \quad (3.70)$$

where n is the average number of the *incident* particles per unit area, and dN is the average number of the particles *scattered* into a small solid angle interval $d\Omega$. For a uniform beam of initial particles, $d\sigma/d\Omega$ may be calculated by counting the average number of incident particles that have the impact parameters within a small range db:

$$dN = n\,2\pi b db. \quad (3.71)$$

Scattered by a spherically-symmetric center, which provides an axially-symmetric scattering pattern, these particles are scattered into the corresponding small solid angle interval $d\Omega = 2\pi|\sin\theta\, d\theta|$. Plugging these two equalities into Eq. (70), we get the following general geometric relation:

$$\frac{d\sigma}{d\Omega} = b\left|\frac{db}{\sin\theta d\theta}\right|. \quad (3.72)$$

In particular, for the Coulomb potential (49), a straightforward differentiation of Eq. (69) yields the so-called *Rutherford scattering formula* (reportedly, derived by R. H. Fowler):

Rutherford scattering formula

$$\boxed{\frac{d\sigma}{d\Omega} = \left(\frac{\alpha}{4E}\right)^2\frac{1}{\sin^4(\theta/2)}.} \quad (3.73)$$

[24] Alternatively, this result may be recovered directly from the first form of Eq. (65), with the eccentricity e expressed via the same dimensionless parameter $(2Eb/\alpha)$: $e = [1 + (2Eb/\alpha)^2]^{1/2} > 1$.

[25] This terminology stems from the fact that an integral (74) of $d\sigma/d\Omega$ over the full solid angle, called the *total cross-section* σ, has the dimension of the area: $\sigma = N/n$, where N is the total number of scattered particles.

This result, which shows very strong scattering to small angles (so strong that the integral that expresses the total cross-section

$$\sigma \equiv \oint_{4\pi} \frac{d\sigma}{d\Omega} d\Omega \qquad (3.74)$$

Total cross-section

is diverging at $\theta \to 0$)[26] and very weak *backscattering* (to angles $\theta \approx \pi$), was historically extremely significant: in the early 1910s, its good agreement with α-particle scattering experiments carried out by Ernest Rutherford's group gave a strong justification for his introduction of the *planetary model* of atoms, with electrons moving around very small nuclei – just as planets move around stars.

Note that elementary particle scattering is frequently accompanied by electromagnetic radiation and/or other processes leading to the loss of the initial mechanical energy of the system. Such *inelastic scattering* may give significantly different results. (In particular, the capture of an incoming particle becomes possible even for a Coulomb attracting center.) Also, quantum-mechanical effects may be important at the scattering of light particles with relatively low energies,[27] so the above results should be used with caution.

3.6. Exercise problems

3.1. For the system considered in Problem 2.6 (a bead sliding along a string with fixed tension $\mathcal{T}$, see the figure on the right), analyze small oscillations of the bead near the equilibrium.

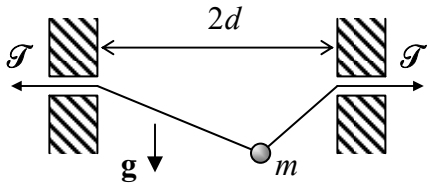

3.2. For the system considered in Problem 2.7 (a bead sliding along a string of a fixed length $2l$, see the figure on the right), analyze small oscillations near the equilibrium.

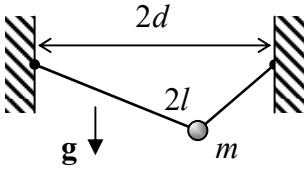

3.3. A bead is allowed to slide, without friction, along an inverted cycloid in a vertical plane – see the figure on the right. Calculate the frequency of its free oscillations as a function of their amplitude.

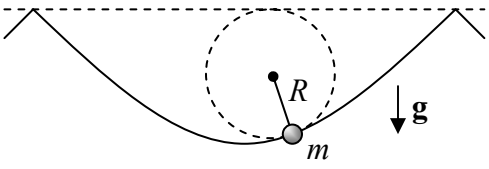

Hint: The simplest way to describe a cycloid is to express the Cartesian coordinates of its arbitrary point as functions of some parameter φ.[28] For the inverted cycloid shown in the figure on the right, such *parametric representation* is

$$x = R(\varphi + \sin\varphi), \qquad y = -R(1 + \cos\varphi).$$

[26] This divergence, which persists at the quantum-mechanical treatment of the problem (see, e.g., QM Chapter 3), is due to particles with very large values of b, and disappears at an account, for example, of any non-zero concentration of the scattering centers.

[27] Their discussion may be found in QM Secs. 3.3 and 3.8.

[28] This parameter may be understood as the angle of rotation of a circle of the radius R, rolled along a horizontal rail with $y = 0$ (see the dashed lines in the figure above), whose point moves along the cycloid..

3.4. Illustrate the changes of the fixed point set of our testbed system (Fig. 2.1), which was analyzed at the end of Sec. 3.2 of the lecture notes, on the so-called *phase plane* $[\theta, \dot{\theta}]$.

3.5. For a 1D particle of mass m, placed into the potential well $U(q) = \alpha q^{2n}$ (where $\alpha > 0$, and n is a positive integer), calculate the functional dependence of the particle's oscillation period $\mathcal{T}$ on its energy E. Explore the limit $n \to \infty$.

3.6. Two small masses m_1 and $m_2 \le m_1$ may slide without friction over a horizontal surface. They are connected with a spring with an equilibrium length l and an elastic constant κ, and at $t < 0$ are at rest. At $t = 0$, the mass m1 gets a very short kick with impulse $\mathbf{P} \equiv \int \mathbf{F}(t)dt$ in a direction different from the spring's line. Calculate the largest and smallest magnitude of its velocity at $t > 0$.

3.7. Explain why the term $mr^2\dot{\varphi}^2/2$, recast in accordance with Eq. (42), cannot be merged with $U(r)$ in Eq. (38), to form an effective 1D potential energy $U(r) - L_z^2/2mr^2$, with the second term's sign opposite to that given by Eq. (44). We have done an apparently similar thing for our testbed bead-on-rotating-ring problem at the very end of Sec. 1 – see Eq. (6); why cannot the same trick work for the planetary problem? Besides a formal explanation, discuss the physics behind this difference.

3.8. A system of two equal masses m on a light rod of a fixed length l (frequently called a *dumbbell*) can slide without friction along a vertical ring of radius R, rotated about its vertical diameter with a constant angular velocity ω – see the figure on the right. Derive the condition of stability of the lower horizontal position of the dumbbell.

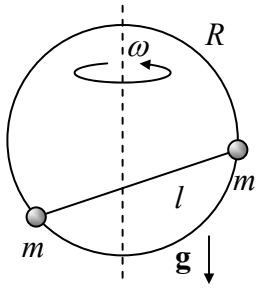

3.9. Analyze the dynamics of the so-called *spherical pendulum* – a point mass hung, in a uniform gravity field $\mathbf{g}$, on a light cord of length l, with no motion's confinement to a vertical plane. In particular:

(i) find the integrals of motion and reduce the problem to a 1D one,
(ii) calculate the time period of the possible circular motion around the vertical axis, and
(iii) explore small deviations from the circular motion. (Are the pendulum's orbits closed?)[29]

3.10. If our planet Earth was suddenly stopped in its orbit around the Sun, how long would it take it to fall on our star? Solve this problem using two different approaches, neglecting the Earth's orbit eccentricity and the Sun's size.

3.11. The orbits of Mars and Earth around the Sun may be well approximated as coplanar circles,[30] with a radii ratio of 3/2. Use this fact, and the Earth's year duration, to calculate the time of travel to Mars when spending the least energy on the spacecraft's launch. Neglect the planets' size and the effects of their own gravitational fields.

[29] Solving this problem is very good preparation for the analysis of the symmetric top's rotation in Sec. 4.5.
[30] Indeed, their eccentricities are close to, respectively, 0.093 and 0.0167.

3.12. Derive first-order and second-order differential equations for the reciprocal distance $u \equiv 1/r$ as a function of φ, describing the trajectory of a particle's motion in a central potential $U(r)$. Spell out the latter equation for the particular case of the Coulomb potential (49) and discuss the result.

3.13. For the motion of a particle in the Coulomb attractive field ($U(r) = -\alpha/r$, with $\alpha > 0$), calculate and sketch the so-called *hodograph*[31] – the trajectory followed by the head of the velocity vector **v**, provided that its tail is kept at the origin.

3.14. Prove that for an arbitrary motion of a particle of mass m in the Coulomb field $U = -\alpha/r$, the vector $\mathbf{A} \equiv \mathbf{p}\times\mathbf{L} - m\alpha\mathbf{n}_r$ (where $\mathbf{n}_r \equiv \mathbf{r}/r$) is conserved.[32] After that:

(i) spell out the scalar product $\mathbf{r}\cdot\mathbf{A}$ and use the result for an alternative derivation of Eq. (59), and for a geometric interpretation of the vector **A**;

(ii) spell out $(\mathbf{A} - \mathbf{p}\times\mathbf{L})^2$ and use the result for an alternative derivation of the hodograph diagram discussed in the previous problem.

3.15. For a particle moving in the following central potential:

$$U(r) = -\frac{\alpha}{r} + \frac{\beta}{r^2},$$

(i) for positive α and β, and all possible ranges of energy E, calculate the orbit $r(\varphi)$;

(ii) prove that in the limit $\beta \to 0$, for energy $E < 0$, the orbit may be represented as a slowly rotating ellipse;

(iii) express the angular velocity of this slow rotation via the parameters α and β, the particle's mass m, its energy E, and the angular momentum L_z.

3.16. A star system contains a much lighter planet and an even much smaller mass of dust. Assuming that the attractive gravitational potential of the dust is spherically symmetric and proportional to the square of the distance from the star,[33] calculate the slow precession it gives to a circular orbit of the planet.

3.17. A particle is moving in the field of an attractive central force with the potential

$$U(r) = -\frac{\alpha}{r^n}, \qquad \text{where } \alpha n > 0.$$

For what values of n, the circular orbits are stable?

3.18. Determine the condition for a particle of mass m, moving under the effect of a central attractive force

[31] The use of this notion for the characterization of motion may be traced back at least to an 1846 treatise by W. Hamilton. Nowadays, it is most often used in applied fluid mechanics, in particular meteorology.

[32] This fact, first proved in 1710 by Jacob Hermann, was repeatedly rediscovered during the next two centuries. As a result, the most common name of **A** is, rather unfairly, the *Runge-Lenz vector*.

[33] As may be readily shown from the gravitation version of the Gauss law (see, e.g., the model solution of Problem 1.7), this approximation is exact if the dust density is constant between the star and the planet.

$$\mathbf{F} = -\alpha \frac{\mathbf{r}}{r^3} \exp\left\{-\frac{r}{R}\right\},$$

where α and R are positive constants, to have a stable circular orbit.

3.19. A particle of mass m, with an angular momentum L_z, moves in the field of an attractive central force with a distance-independent magnitude F. If the particle's energy E is slightly higher than the value $E_{\min}$ corresponding to its circular orbit, what is the time period of its radial oscillations? Compare the period with that of the circular orbit at $E = E_{\min}$.

3.20. A particle may move without friction, in the uniform gravity field $\mathbf{g} = -g\mathbf{n}_z$, over an axially-symmetric surface that is described, in the cylindrical coordinates $\{\rho, \varphi, z\}$, by a smooth function $Z(\rho)$ – see the figure on the right. Derive the condition of stability of circular orbits of the particle around the symmetry axis z, with respect to small perturbations. For the cases when the condition is fulfilled, find out whether the weakly perturbed orbits are open or closed. Spell out your results for the following particular cases:

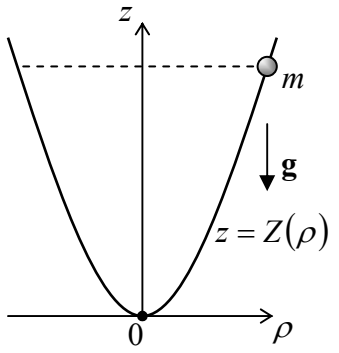

(i) a conical surface with $Z = \alpha\rho$,
(ii) a paraboloid with $Z = \kappa\rho^2/2$, and
(iii) a spherical surface with $Z^2 + \rho^2 = R^2$, for $\rho < R$.

3.21. The gravitational potential (i.e. the gravitational energy of a unit probe mass) of our Milky Way galaxy, averaged over interstellar distances, is reasonably well approximated by the following axially symmetric function:

$$\phi(r,z) = \frac{V^2}{2} \ln\left(r^2 + \alpha z^2\right),$$

where r is the distance from the galaxy's symmetry axis and z is the distance from its central plane, while V and $\alpha > 0$ are constants.[34] Prove that circular orbits of stars in this gravity field are stable, and calculate the frequencies of their small oscillations near such orbits, in the r- and z-directions.

3.22. For particle scattering by a repulsive Coulomb field, calculate the minimum approach distance $r_{\min}$ and the velocity $v_{\min}$ at that point, and analyze their dependence on the impact parameter b (see Fig. 9) and on the initial velocity v_∞ of the particle.

3.23. A particle is launched from afar, with an impact parameter b, toward an attracting center creating the potential

$$U(r) = -\frac{\alpha}{r^n}, \quad \text{with } n > 2 \text{ and } \alpha > 0.$$

(i) For the case when the initial kinetic energy E of the particle is barely sufficient for escaping its capture by this attracting center, express the minimum approach distance via b and n.

(ii) Calculate the capture's total cross-section and explore its limit at $n \to 2$.

[34] Just for the reader's reference, these constants are close to, respectively, 2.2×10^5 m/s and 6.

3.24. A small body with an initial velocity v_∞ approaches an atmosphere-free planet of mass M and radius R.

(i) Find the condition on the impact parameter b for the body to hit the planet's surface.

(ii) If the body barely avoids the collision, what is its scattering angle?

3.25. Calculate the differential and total cross-sections of the classical elastic scattering of small particles by a hard sphere of radius R.

3.26. The most famous[35] confirmation of Einstein's general relativity theory has come from the observation, by A. Eddington and his associates, of star light's deflection by the Sun, during the May 1919 solar eclipse. Considering light photons as classical particles propagating with the speed of light, $v_0 \to c \approx 3.00\times10^8$m/s, and using the astronomic data for the Sun's mass ($M_S \approx 1.99\times10^{30}$kg) and radius ($R_S \approx 6.96\times10^8$m), calculate the non-relativistic mechanics' prediction for the angular deflection of the light rays grazing the Sun's surface.

3.27. Generalize the expression for the small angle of scattering, obtained in the solution of the previous problem, to a spherically symmetric but otherwise arbitrary potential $U(r)$. Use the result to calculate the differential cross-section of small-angle scattering by the potential $U = C/r^n$, with integer $n > 0$.

Hint: You may like to use the following table integral: $\int_1^\infty \frac{d\xi}{\xi^{n+1}\left(\xi^2-1\right)^{1/2}} = \pi^{1/2}\frac{\Gamma\left(n/2+1/2\right)}{n\Gamma\left(n/2\right)}$.

[35] It was not the first confirmation, though. The first one came four years earlier from Albert Einstein himself, who showed that his theory may qualitatively explain the difference between the rate of Mercury orbit's precession, known from earlier observations, and the non-relativistic theory of that effect.

Chapter 4. Rigid Body Motion

This chapter discusses the motion of rigid bodies, with a heavy focus on its most nontrivial part: rotation. Some byproducts of this analysis enable a discussion, at the end of the chapter, of the motion of point particles as observed from non-inertial reference frames.

4.1. Translation and rotation

It is natural to start a discussion of many-particle systems from a (relatively :-) simple limit when the changes of distances $r_{kk'} \equiv |\mathbf{r}_k - \mathbf{r}_{k'}|$ between the particles are negligibly small. Such an abstraction is called the (*absolutely*) *rigid body*; it is a reasonable approximation in many practical problems, including the motion of solid samples. In other words, this model neglects *deformations* – which will be the subject of the next chapters. The rigid-body approximation reduces the number of degrees of freedom of the system of N particles from $3N$ to just six – for example, three Cartesian coordinates of one point (say, 0), and three angles of the system's rotation about three mutually perpendicular axes passing through this point – see Fig. 1.[1]

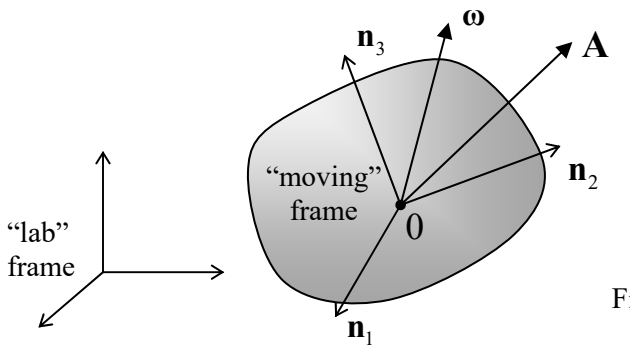

Fig. 4.1. Deriving Eq. (8).

As it follows from the discussion in Secs. 1.1-1.3, any purely *translational motion* of a rigid body, at which the velocity vectors $\mathbf{v}$ of all points are equal, is not more complex than that of a point particle. Indeed, according to Eqs. (1.8) and (1.30), in an inertial reference frame, such a body moves exactly as a point particle upon the effect of the net external force $\mathbf{F}^{(\text{ext})}$. However, the rotation is a bit more tricky.

Let us start by showing that an arbitrary elementary displacement of a rigid body may be always considered as a sum of the translational motion and of what is called a *pure rotation*. For that, consider a "moving" reference frame $\{\mathbf{n}_1, \mathbf{n}_2, \mathbf{n}_3\}$, firmly bound to the body, and an arbitrary vector $\mathbf{A}$ (Fig. 1). The vector may be represented by its Cartesian components A_j in that moving frame:

$$\mathbf{A} = \sum_{j=1}^{3} A_j \mathbf{n}_j \ . \tag{4.1}$$

[1] An alternative way to arrive at the same number six is to consider three points of the body, which uniquely define its position. If movable independently, the points would have nine degrees of freedom, but since three distances $r_{kk'}$ between them are now fixed, the resulting three constraints reduce the number of degrees of freedom to six.

Let us calculate the time derivative of this vector as observed from a different ("lab") frame, taking into account that if the body rotates relative to this frame, the directions of the unit vectors $\mathbf{n}_j$, as seen from the lab frame, change in time. Hence, in each product contributing to the sum (1), we have to differentiate both operands:

$$\frac{d\mathbf{A}}{dt}\Big|_{\text{in lab}} = \sum_{j=1}^{3} \frac{dA_j}{dt}\mathbf{n}_j + \sum_{j=1}^{3} A_j \frac{d\mathbf{n}_j}{dt}. \tag{4.2}$$

On the right-hand side of this equality, the first sum obviously describes the change of vector $\mathbf{A}$ as observed from the moving frame. In the second sum, each of the infinitesimal vectors $d\mathbf{n}_j$ may be represented by its Cartesian components:

$$d\mathbf{n}_j = \sum_{j'=1}^{3} d\varphi_{jj'}\mathbf{n}_{j'}, \tag{4.3}$$

where $d\varphi_{jj'}$ are some dimensionless scalar coefficients. To find out more about them, let us scalar-multiply each side of Eq. (3) by an arbitrary unit vector $\mathbf{n}_{j''}$, and take into account the obvious orthonormality condition:

$$\mathbf{n}_{j'} \cdot \mathbf{n}_{j''} = \delta_{j'j''}, \tag{4.4}$$

where $\delta_{j'j''}$ is the Kronecker delta symbol.[2] As a result, we get

$$d\mathbf{n}_j \cdot \mathbf{n}_{j''} = d\varphi_{jj''}. \tag{4.5}$$

Now let us use Eq. (5) to calculate the first differential of Eq. (4):

$$d\mathbf{n}_{j'} \cdot \mathbf{n}_{j''} + \mathbf{n}_{j'} \cdot d\mathbf{n}_{j''} \equiv d\varphi_{j'j''} + d\varphi_{j''j'} = 0; \qquad \text{in particular,} \quad 2d\mathbf{n}_j \cdot \mathbf{n}_j = 2d\varphi_{jj} = 0. \tag{4.6}$$

These relations, valid for any choice of indices j, j', and j'' of the set {1, 2, 3}, show that the matrix with elements $d\varphi_{jj'}$ is antisymmetric with respect to the swap of its indices; this means that there are not nine just three non-zero independent coefficients $d\varphi_{jj'}$, all with $j \neq j'$. Hence it is natural to renumber them in a simpler way: $d\varphi_{jj'} = -d\varphi_{j'j} \equiv d\varphi_{j''}$, where the indices j, j', and j'' follow in the "correct" order – either {1,2,3}, or {2,3,1}, or {3,1,2}. It is straightforward to verify (either just by a component-by-component comparison or by using the Levi-Civita permutation symbol[3]) that in this new notation, Eq. (3) may be represented just as a vector product:

$$\boxed{d\mathbf{n}_j = d\boldsymbol{\varphi} \times \mathbf{n}_j,} \tag{4.7}$$

Elementary rotation

where $d\boldsymbol{\varphi}$ is the infinitesimal vector defined by its Cartesian components $d\varphi_j$ in the rotating reference frame $\{\mathbf{n}_1, \mathbf{n}_2, \mathbf{n}_3\}$.

This relation is the basis of all rotation kinematics. Using it, Eq. (2) may be rewritten as

$$\boxed{\frac{d\mathbf{A}}{dt}\Big|_{\text{in lab}} = \frac{d\mathbf{A}}{dt}\Big|_{\text{in mov}} + \sum_{j=1}^{3} A_j \frac{d\boldsymbol{\varphi}}{dt} \times \mathbf{n}_j \equiv \frac{d\mathbf{A}}{dt}\Big|_{\text{in mov}} + \boldsymbol{\omega} \times \mathbf{A}, \quad \text{where } \boldsymbol{\omega} \equiv \frac{d\boldsymbol{\varphi}}{dt}.} \tag{4.8}$$

Vector's evolution in time

To reveal the physical sense of the vector $\boldsymbol{\omega}$, let us apply Eq. (8) to the particular case when $\mathbf{A}$ is the radius vector $\mathbf{r}$ of a point of the body, and the lab frame is selected in a special way: its origin has the

[2] See, e.g., MA Eq. (13.1).

[3] See, e.g., MA Eq. (13.2). Using this symbol, we may write $d\varphi_{jj'} = -d\varphi_{j'j} \equiv \varepsilon_{jj'j''}d\varphi_{j''}$ for *any* choice of j, j', and j''.

same position and moves with the same velocity as that of the moving frame, in the particular instant under consideration. In this case, the first term on the right-hand side of Eq. (8) is zero, and we get

$$\left.\frac{d\mathbf{r}}{dt}\right|_{\text{in special lab frame}} = \boldsymbol{\omega}\times\mathbf{r}, \tag{4.9}$$

were vector $\mathbf{r}$ itself is the same in both frames. According to the vector product definition, the particle velocity described by this formula has a direction perpendicular to the vectors $\boldsymbol{\omega}$ and $\mathbf{r}$ (Fig. 2), and magnitude $\omega r\sin\theta$. As Fig. 2 shows, the last expression may be rewritten as $\omega\rho$, where $\rho = r\sin\theta$ is the distance from the line that is parallel to the vector $\boldsymbol{\omega}$ and passes through point 0. This is of course just the *pure rotation* about that line (called the *instantaneous axis of rotation*), with the angular velocity ω. According to Eqs. (3) and (8), the *angular velocity vector* $\boldsymbol{\omega}$ is defined by the time evolution of the moving frame alone, so it is the same for all points $\mathbf{r}$, i.e. for the rigid body as a whole. Note that nothing in our calculations forbids not only the magnitude but also the direction of the vector $\boldsymbol{\omega}$, and thus of the instantaneous axis of rotation, to change in time; hence the name.

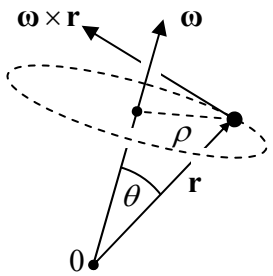

Fig. 4.2. The instantaneous axis and the angular velocity of rotation.

Now let us generalize our result a step further, considering two reference frames that do not rotate versus each other: one ("lab") frame is arbitrary, and another one is selected in the special way described above, so Eq. (9) is valid in it. Since the relative motion of these two reference frames is purely translational, we can use the simple velocity addition rule given by Eq. (1.6) to write

Body point's velocity

$$\boxed{\mathbf{v}\big|_{\text{in lab}} = \mathbf{v}_0\big|_{\text{in lab}} + \mathbf{v}\big|_{\text{in special lab frame}} = \mathbf{v}_0\big|_{\text{in lab}} + \boldsymbol{\omega}\times\mathbf{r},} \tag{4.10}$$

where $\mathbf{r}$ is the radius vector of a point is measured in the body-bound ("moving") frame 0.

4.2. Inertia tensor

Since the dynamics of each point of a rigid body is strongly constrained by the conditions $r_{kk'} = \text{const}$, this is one of the most important fields of application of the Lagrangian formalism discussed in Chapter 2. For using this approach, the first thing we need to calculate is the kinetic energy of the body in an inertial reference frame. Since it is just the sum of the kinetic energies (1.19) of all its points, we can use Eq. (10) to write:[4]

$$T \equiv \sum\frac{m}{2}\mathbf{v}^2 = \sum\frac{m}{2}\left(\mathbf{v}_0 + \boldsymbol{\omega}\times\mathbf{r}\right)^2 \equiv \sum\frac{m}{2}v_0^2 + \sum m\mathbf{v}_0\cdot(\boldsymbol{\omega}\times\mathbf{r}) + \sum\frac{m}{2}(\boldsymbol{\omega}\times\mathbf{r})^2. \tag{4.11}$$

[4] Actually, all symbols for particle masses, coordinates, and velocities should carry the particle's index, over which the summation is carried out. However, in this section, for the notation simplicity, this index is just implied.

Let us apply to the right-hand side of Eq. (11) two general vector analysis formulas listed in the Math Appendix: the so-called *operand rotation rule* MA Eq. (7.6) to the second term, and MA Eq. (7.7b) to the third term. The result is

$$T = \sum \frac{m}{2} v_0^2 + \sum m\mathbf{r} \cdot (\mathbf{v}_0 \times \boldsymbol{\omega}) + \sum \frac{m}{2} \left[\omega^2 r^2 - (\boldsymbol{\omega} \cdot \mathbf{r})^2 \right]. \tag{4.12}$$

This expression may be further simplified by making a specific choice of the point 0 (from which the radius vectors **r** of all particles are measured), namely by using for this point the *center of mass* of the body. As was already mentioned in Sec. 3.4 for the two-point case, the radius vector **R** of this point is defined as

$$M\mathbf{R} \equiv \sum m\mathbf{r}, \quad \text{with } M \equiv \sum m, \tag{4.13}$$

so M is the total mass of the body. In the reference frame centered at this point, we have **R** = 0, so that the second sum in Eq. (12) vanishes, and the kinetic energy is a sum of just two terms:

$$T = T_{\text{tran}} + T_{\text{rot}}, \quad T_{\text{tran}} \equiv \frac{M}{2} V^2, \quad T_{\text{rot}} \equiv \sum \frac{m}{2} \left[\omega^2 r^2 - (\boldsymbol{\omega} \cdot \mathbf{r})^2 \right], \tag{4.14}$$

where $\mathbf{V} \equiv d\mathbf{R}/dt$ is the center-of-mass velocity in our inertial reference frame, and all particle positions **r** are measured in the center-of-mass frame. Since the angular velocity vector **ω** is common for all points of a rigid body, it is more convenient to rewrite the rotational part of the energy in a form in that the summation over the components of this vector is separated from the summation over the points of the body:

$$T_{\text{rot}} = \frac{1}{2} \sum_{j,j'=1}^{3} I_{jj'} \omega_j \omega_{j'}, \tag{4.15}$$

Kinetic energy of rotation

where the 3×3 matrix with elements

$$I_{jj'} \equiv \sum m \left(r^2 \delta_{jj'} - r_j r_{j'} \right) \tag{4.16}$$

Inertia tensor

represents, in the selected reference frame, the *inertia tensor* of the body.[5]

Actually, the term "tensor" for the construct described by this matrix has to be justified, because in physics it implies a certain reference-frame-independent notion, whose matrix elements have to obey certain rules at the transfer between reference frames. To show that the matrix (16) indeed describes such a notion, let us calculate another key quantity, the total angular momentum **L** of the same body.[6] Summing up the angular momenta of each particle, defined by Eq. (1.31), and then using Eq. (10) again, in our inertial reference frame we get

$$\mathbf{L} \equiv \sum \mathbf{r} \times \mathbf{p} = \sum m\mathbf{r} \times \mathbf{v} = \sum m\mathbf{r} \times (\mathbf{v}_0 + \boldsymbol{\omega} \times \mathbf{r}) \equiv \sum m\mathbf{r} \times \mathbf{v}_0 + \sum m\mathbf{r} \times (\boldsymbol{\omega} \times \mathbf{r}). \tag{4.17}$$

We see that the momentum may be represented as a sum of two terms. The first one,

[5] While the ABCs of the rotational dynamics were developed by Leonhard Euler in 1765, an introduction of the inertia tensor's formalism had to wait very long – until the invention of the tensor analysis by Tullio Levi-Civita and Gregorio Ricci-Curbastro in 1900 – soon popularized by its use in Einstein's general relativity.

[6] Hopefully, there is very little chance of confusing the angular momentum **L** (a vector) and its Cartesian components L_j (scalars with an index) on one hand, and the Lagrangian function L (a scalar without an index) on the other hand.

$$\mathbf{L}_0 \equiv \sum m\mathbf{r}\times\mathbf{v}_0 = M\mathbf{R}\times\mathbf{v}_0, \tag{4.18}$$

describes the possible rotation of the center of mass about the inertial frame's origin. This term vanishes if the moving reference frame's origin 0 is positioned at the center of mass (where $\mathbf{R} = 0$). In this case, we are left with only the second term, which describes a pure rotation of the body about its center of mass:

$$\mathbf{L} = \mathbf{L}_{\rm rot} \equiv \sum m\mathbf{r}\times(\boldsymbol{\omega}\times\mathbf{r}). \tag{4.19}$$

Using one more vector algebra formula, the "bac minis cab" rule,[7] we may rewrite this expression as

$$\mathbf{L} = \sum m\left[\boldsymbol{\omega}r^2 - \mathbf{r}(\mathbf{r}\cdot\boldsymbol{\omega})\right]. \tag{4.20}$$

Let us spell out an arbitrary Cartesian component of this vector:

$$L_j = \sum m\left[\omega_j r^2 - r_j\sum_{j'=1}^{3} r_{j'}\omega_{j'}\right] \equiv \sum m\sum_{j'=1}^{3}\omega_{j'}\left(r^2\delta_{jj'} - r_j r_{j'}\right). \tag{4.21}$$

By changing the summation order and comparing the result with Eq. (16), the angular momentum may be conveniently expressed via the same matrix elements $I_{jj'}$ as the rotational kinetic energy:

Angular momentum

$$\boxed{L_j = \sum_{j'=1}^{3} I_{jj'}\omega_{j'}\,.} \tag{4.22}$$

Since $\mathbf{L}$ and $\boldsymbol{\omega}$ are both legitimate vectors (meaning that they describe physical vectors independent of the reference frame choice), the matrix of elements $I_{jj'}$ that relates them is a legitimate tensor. This fact, and the symmetry of the tensor ($I_{jj'} = I_{j'j}$), evident from its definition (16), allow the tensor to be further simplified. In particular, mathematics tells us that by a certain choice of the coordinate axes' orientations, any symmetric tensor may be reduced to a diagonal form

$$I_{jj'} = I_j\delta_{jj'}, \tag{4.23}$$

where in our case

Principal moments of inertia

$$\boxed{I_j = \sum m\left(r^2 - r_j^2\right) = \sum m\left(r_{j'}^2 + r_{j''}^2\right) \equiv \sum m\rho_j^2\,,} \tag{4.24}$$

ρ_j being the distance of the particle from the $j^{\rm th}$ axis, i.e. the length of the perpendicular dropped from the point to that axis. The axes of such a special coordinate system are called the *principal axes*, while the diagonal elements I_j given by Eq. (24), the *principal moments of inertia* of the body. In such a special reference frame, Eqs. (15) and (22) are reduced to very simple forms:

$T_{\rm rot}$ and $\mathbf{L}$ in principal-axes frame

$$\boxed{T_{\rm rot} = \sum_{j=1}^{3}\frac{I_j}{2}\omega_j^2\,,} \tag{4.25}$$

$$\boxed{L_j = I_j\omega_j.} \tag{4.26}$$

Both these results remind the corresponding relations for the translational motion, $T_{\rm tran} = MV^2/2$ and $\mathbf{P} = M\mathbf{V}$, with the angular velocity $\boldsymbol{\omega}$ replacing the linear velocity $\mathbf{V}$, and the tensor of inertia playing the role of scalar mass M. However, let me emphasize that even in the specially selected reference frame, with

[7] See, e.g., MA Eq. (7.5).

its axes pointing in principal directions, the analogy is incomplete, and rotation is generally more complex than translation, because the measures of inertia, I_j, are generally different for each principal axis.

Let me illustrate the last fact on a simple but instructive system of three similar massive particles fixed in the vertices of an equilateral triangle (Fig. 3).

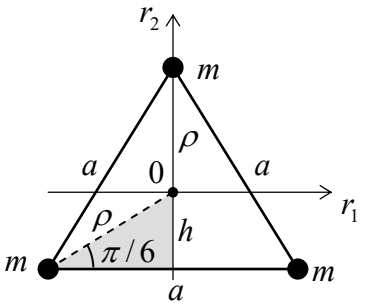

Fig. 4.3. Principal moments of inertia: a simple case study.

Due to the symmetry of the configuration, one of the principal axes has to pass through the center of mass 0 and be normal to the plane of the triangle. For the corresponding principal moment of inertia, Eq. (24) readily yields $I_3 = 3m\rho^2$. If we want to express this result in terms of the triangle's side a, we may notice that due to the system's symmetry, the angle marked in Fig. 3 equals $\pi/6$, and from the shaded right triangle, $a/2 = \rho\cos(\pi/6) \equiv \rho\sqrt{3}/2$, giving $\rho = a/\sqrt{3}$, so, finally, $I_3 = ma^2$.

Let me use this simple case to illustrate the following general *axis shift theorem*, which may be rather useful – especially for more complex systems. For that, let us relate the inertia tensor elements $I_{jj'}$ and $I'_{jj'}$, calculated in two reference frames – one with its origin at the center of mass 0, and another one (0') translated by a certain vector **d** (Fig. 4a), so for an arbitrary point, $\mathbf{r}' = \mathbf{r} + \mathbf{d}$. Plugging this relation into Eq. (16), we get

$$\begin{aligned} I'_{jj'} &= \sum m\left[(\mathbf{r}+\mathbf{d})^2\delta_{jj'} - (r_j + d_j)(r_{j'} + d_{j'})\right] \\ &= \sum m\left[(r^2 + 2\mathbf{r}\cdot\mathbf{d} + d^2)\delta_{jj'} - (r_j r_{j'} + r_j d_{j'} + r_{j'} d_j + d_j d_{j'})\right]. \end{aligned} \tag{4.27}$$

Since in the center-of-mass frame, all sums $\sum m r_j$ equal zero, we may use Eq. (16) to finally obtain

$$I'_{jj'} = I_{jj'} + M(\delta_{jj'} d^2 - d_j d_{j'}). \tag{4.28}$$

In particular, this equation shows that if the shift vector **d** is perpendicular to one (say, j^{th}) of the principal axes (Fig. 4b), i.e. $d_j = 0$, then Eq. (28) is reduced to a very simple formula:

$$\boxed{I'_j = I_j + Md^2.} \tag{4.29}$$

Principal axis' shift

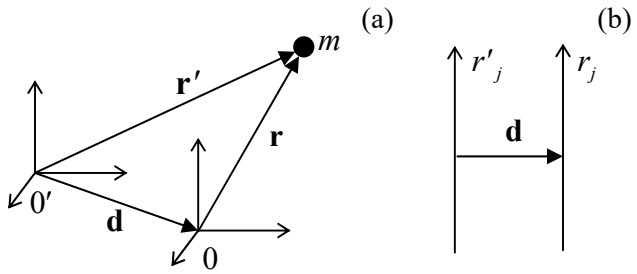

Fig. 4.4. (a) A general coordinate frame's shift from the center of mass, and (b) a shift perpendicular to one of the principal axes.

Now returning to the particular system shown in Fig. 3, let us perform such a shift to the new ("primed") axis passing through the location of one of the particles, still perpendicular to their common plane. Then the contribution of that particular mass to the primed moment of inertia vanishes, and $I'_3 = 2ma^2$. Now, returning to the center of mass and applying Eq. (29), we get $I_3 = I'_3 - M\rho^2 = 2ma^2 - (3m)(a/\sqrt{3})^2 = ma^2$, i.e. the same result as above.

The symmetry situation inside the triangle's plane is somewhat less obvious, so let us start by calculating the moments of inertia for the axes shown vertical and horizontal in Fig. 3. From Eq. (24), we readily get:

$$I_1 = 2mh^2 + m\rho^2 = m\left[2\left(\frac{a}{2\sqrt{3}}\right)^2 + \left(\frac{a}{\sqrt{3}}\right)^2\right] = \frac{ma^2}{2}, \qquad I_2 = 2m\left(\frac{a}{2}\right)^2 = \frac{ma^2}{2}, \tag{4.30}$$

where h is the distance from the center of mass and any side of the triangle: $h = \rho\sin(\pi/6) = \rho/2 = a/2\sqrt{3}$. We see that $I_1 = I_2$, and mathematics tells us that in this case, *any* in-plane axis (passing through the center-of-mass 0) may be considered as principal, and has the same moment of inertia. A rigid body with this property, $I_1 = I_2 \neq I_3$, is called the *symmetric top*. (The last direction is called the *main principal axis* of the system.)

Symmetric top: definition

Despite the symmetric top's name, the situation may be even more symmetric in the so-called *spherical tops*, i.e. highly symmetric systems whose principal moments of inertia are all equal,

Spherical top: definition

$$I_1 = I_2 = I_3 \equiv I, \tag{4.31}$$

Mathematics says that in this case, the moment of inertia for rotation about *any* axis (but still passing through the center of mass) is equal to the same I. Hence Eqs. (25) and (26) are further simplified for any direction of the vector $\boldsymbol{\omega}$:

Spherical top: properties

$$T_{\text{rot}} = \frac{I}{2}\omega^2, \qquad \mathbf{L} = I\boldsymbol{\omega}, \tag{4.32}$$

thus making the analogy of rotation and translation complete. (As will be discussed in the next section, this analogy is also complete if the rotation axis is fixed by external constraints.)

Evident examples of a spherical top are a uniform sphere and a uniform spherical shell; its less obvious example is a uniform cube – with masses either concentrated in vertices, or uniformly spread over the faces, or uniformly distributed over the volume. Again, in this case *any* axis passing through the center of mass is a principal one and has the same principal moment of inertia. For a sphere, this is natural; for a cube, rather surprising – but may be confirmed by a direct calculation.

4.3. Fixed-axis rotation

Now we are well equipped for a discussion of the rigid body's rotational dynamics. The general equation of this dynamics is given by Eq. (1.38), which is valid for dynamics of any system of particles – either rigidly connected or not:

$$\dot{\mathbf{L}} = \boldsymbol{\tau}, \tag{4.33}$$

where $\boldsymbol{\tau}$ is the net torque of external forces. Let us start exploring this equation from the simplest case when the axis of rotation, i.e. the direction of vector $\boldsymbol{\omega}$, is fixed by some external constraints. Directing

the z-axis along this vector, we have $\omega_x = \omega_y = 0$. According to Eq. (22), in this case, the z-component of the angular momentum,

$$L_z = I_{zz}\omega_z, \tag{4.34}$$

where I_{zz}, though not necessarily one of the principal moments of inertia. still may be calculated using Eq. (24):

$$I_{zz} = \sum m\rho_z^2 = \sum m\left(x^2 + y^2\right), \tag{4.35}$$

with ρ_z being the distance of each particle from the rotation axis z. According to Eq. (15), in this case the rotational kinetic energy is just

$$T_{\text{rot}} = \frac{I_{zz}}{2}\omega_z^2. \tag{4.36}$$

Moreover, it is straightforward to show that if the rotation axis is fixed, Eqs. (34)-(36) are valid even if the axis does not pass through the center of mass – provided that the distances ρ_z are now measured from that axis. (The proof is left for the reader's exercise.)

As a result, we may not care about other components of the vector **L**,[8] and use just one component of Eq. (33),

$$\dot{L}_z = \tau_z, \tag{4.37}$$

because it, when combined with Eq. (34), completely determines the dynamics of rotation:

$$I_{zz}\dot{\omega}_z = \tau_z, \qquad \text{i.e. } I_{zz}\ddot{\theta}_z = \tau_z, \tag{4.38}$$

where θ_z is the angle of rotation about the axis, so $\omega_z = \dot{\theta}$. The scalar relations (34), (36), and (38), describing rotation about a fixed axis, are completely similar to the corresponding formulas of 1D motion of a single particle, with ω_z corresponding to the usual ("linear") velocity, the angular momentum component L_z – to the linear momentum, and I_z – to the particle's mass.

The resulting motion about the axis is also frequently similar to that of a single particle. As a simple example, let us consider what is called the *physical* (or "compound") *pendulum* (Fig. 5) – a rigid body free to rotate about a fixed horizontal axis that does not pass through the center of mass 0, in a uniform gravity field **g**.

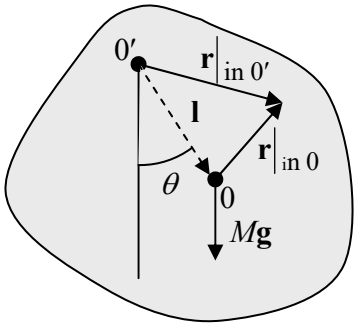

Fig. 4.5. Physical pendulum: a rigid body with a fixed (horizontal) rotation axis 0' that does not pass through the center of mass 0. (The plane of drawing is normal to that axis.)

[8] Note that according to Eq. (22), other Cartesian components of the angular momentum, L_x and L_y, may be different from zero, and even evolve in time. The corresponding torques τ_x and τ_y, which obey Eq. (33), are automatically provided by the external forces that keep the rotation axis fixed.

Let us drop the perpendicular from point 0 to the rotation axis, and call the oppositely directed vector **l** – see the dashed arrow in Fig. 5. Then the torque (relative to the rotation axis 0') of the forces keeping the axis fixed is zero, and the only contribution to the net torque is due to gravity alone:

$$\boldsymbol{\tau}\big|_{\text{in }0'} \equiv \sum \mathbf{r}\big|_{\text{in }0'} \times \mathbf{F} = \sum \left(\mathbf{l} + \mathbf{r}\big|_{\text{in }0}\right) \times m\mathbf{g} = \sum m(\mathbf{l} \times \mathbf{g}) + \sum m\mathbf{r}\big|_{\text{in }0} \times \mathbf{g} = M\mathbf{l} \times \mathbf{g}\,. \qquad (4.39)$$

(The last step used the facts that point 0 is the center of mass, so the second term on the right-hand side equals zero, and that the vectors **l** and **g** are the same for all particles of the body.)

This result shows that the torque is directed along the rotation axis, and its (only) component τ_z is equal to $-Mgl\sin\theta$, where θ is the angle between the vectors **l** and **g**, i.e. the angular deviation of the pendulum from the position of equilibrium – see Fig. 5 again. As a result, Eq. (38) takes the form,

$$I'\ddot{\theta} = -Mgl\sin\theta, \qquad (4.40)$$

where I' is the moment of inertia for rotation about the axis 0' rather than about the center of mass. This equation is identical to Eq. (1.18) for the point-mass (sometimes called "mathematical") pendulum, with small-oscillation frequency

Physical pendulum: frequency

$$\boxed{\Omega = \left(\frac{Mgl}{I'}\right)^{1/2} \equiv \left(\frac{g}{l_{\text{ef}}}\right)^{1/2}, \quad \text{with } l_{\text{ef}} \equiv \frac{I'}{Ml}.} \qquad (4.41)$$

As a sanity check, in the simplest case when the linear size of the body is much smaller than the suspension length l, Eq. (35) yields $I' = Ml^2$, i.e. $l_{\text{ef}} = l$, and Eq. (41) reduces to the well-familiar formula $\Omega = (g/l)^{1/2}$ for the point-mass pendulum.

Now let us discuss the situations when a rigid body not only rotates but also moves as a whole. As was mentioned in the introductory chapter, the total linear momentum of the body,

$$\mathbf{P} \equiv \sum m\mathbf{v} = \sum m\dot{\mathbf{r}} = \frac{d}{dt}\sum m\mathbf{r}\,, \qquad (4.42)$$

satisfies the 2nd Newton's law in the form (1.30). Using the definition (13) of the center of mass, the momentum may be represented as

$$\mathbf{P} = M\dot{\mathbf{R}} = M\mathbf{V}, \qquad (4.43)$$

so Eq. (1.30) may be rewritten as

C.o.m.: law of motion

$$\boxed{M\dot{\mathbf{V}} = \mathbf{F}\,,} \qquad (4.44)$$

where **F** is the vector sum of all external forces. This equation shows that the center of mass of the body moves exactly like a point particle of mass M, under the effect of the net force **F**. In many cases, this fact makes the translational dynamics of a rigid body absolutely similar to that of a point particle.

The situation becomes more complex if some of the forces contributing to the vector sum **F** depend on the rotation of the same body, i.e. if its rotational and translational motions are coupled. Analysis of such coupled motion is rather straightforward if the *direction* of the rotation axis does not change in time, and hence Eqs. (34)-(36) are still valid. Possibly the simplest example is a round cylinder (say, a wheel) rolling on a surface without slippage (Fig. 6). Here the no-slippage condition may be represented as the requirement to the net velocity of the particular wheel's point A that touches the surface to equal zero – in the reference frame bound to the surface. For the simplest case of plane

surface (Fig. 6a), this condition may be spelled out using Eq. (10), giving the following relation between the angular velocity ω of the wheel and the linear velocity V of its center:

$$V + r\omega = 0. \tag{4.45}$$

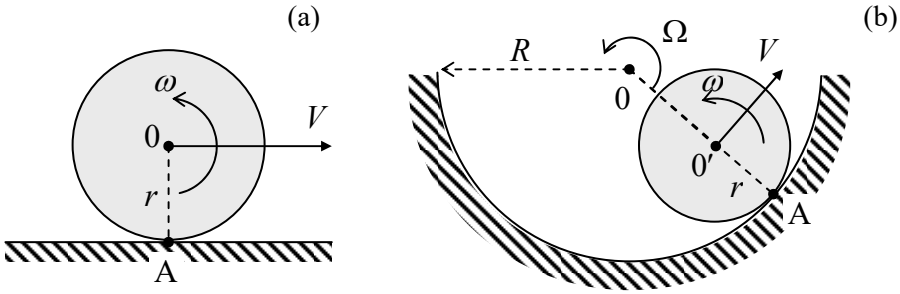

Fig. 4.6. Round cylinder rolling over (a) a plane surface and (b) a concave surface.

Such kinematic relations are essentially holonomic constraints, which reduce the number of degrees of freedom of the system. For example, without the no-slippage condition (45), the wheel on a plane surface has to be considered as a system with two degrees of freedom, making its total kinetic energy (14) a function of two independent generalized velocities, say V and ω:

$$T = T_{\text{tran}} + T_{\text{rot}} = \frac{M}{2}V^2 + \frac{I}{2}\omega^2. \tag{4.46}$$

Using Eq. (45) we may eliminate, for example, the linear velocity and reduce Eq. (46) to

$$T = \frac{M}{2}(\omega r)^2 + \frac{I}{2}\omega^2 \equiv \frac{I_{\text{ef}}}{2}\omega^2, \qquad \text{where } I_{\text{ef}} \equiv I + Mr^2. \tag{4.47}$$

This result may be interpreted as the kinetic energy of pure rotation of the wheel about the instantaneous rotation axis A, with I_{ef} being the moment of inertia about that axis, satisfying Eq. (29).

Kinematic relations are not always as simple as Eq. (45). For example, if a wheel is rolling on a concave surface (Fig. 6b), we need to relate the angular velocities of the wheel's rotation about its axis 0*'* (say, ω) and that (say, Ω) of its axis' rotation about the center 0 of curvature of the surface. A popular error here is to write $\Omega = -(r/R)\omega$ [WRONG!]. A prudent way to derive the correct relation is to note that Eq. (45) holds for this situation as well, and on the other hand, the same linear velocity of the wheel's center may be expressed as $V = (R - r)\,\Omega$. Combining these formulas, we get the correct relation

$$\Omega = -\frac{r}{R - r}\omega. \tag{4.48}$$

Another famous example of the relation between translational and rotational motion is given by the "sliding-ladder" problem (Fig. 7). Let us analyze it for the simplest case of negligible friction, and the ladder's thickness being small in comparison with its length l.

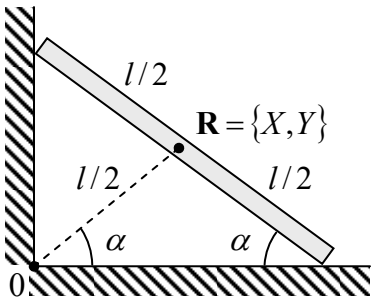

Fig. 4.7. The sliding-ladder problem.

To use the Lagrangian formalism, we may write the kinetic energy of the ladder as the sum (14) of its translational and rotational parts:

$$T = \frac{M}{2}\left(\dot{X}^2 + \dot{Y}^2\right) + \frac{I}{2}\dot{\alpha}^2, \tag{4.49}$$

where X and Y are the Cartesian coordinates of its center of mass in an inertial reference frame, and I is the moment of inertia for rotation about the z-axis passing through the center of mass. (For the uniformly distributed mass, an elementary integration of Eq. (35) yields $I = Ml^2/12$). In the reference frame with the center in the corner 0, both X and Y may be simply expressed via the angle α:

$$X = \frac{l}{2}\cos\alpha, \quad Y = \frac{l}{2}\sin\alpha. \tag{4.50}$$

(The easiest way to obtain these relations is to notice that the dashed line in Fig. 7 has length $l/2$, and the same slope α as the ladder.) Plugging these expressions into Eq. (49), we get

$$T = \frac{I_{\text{ef}}}{2}\dot{\alpha}^2, \qquad I_{\text{ef}} \equiv I + M\left(\frac{l}{2}\right)^2 = \frac{1}{3}Ml^2. \tag{4.51}$$

Since the potential energy of the ladder in the gravity field may be also expressed via the same angle,

$$U = MgY = Mg\frac{l}{2}\sin\alpha, \tag{4.52}$$

α may be conveniently used as the (only) generalized coordinate of the system. Even without writing the Lagrange equation of motion for that coordinate, we may notice that since the Lagrangian function $L \equiv T - U$ does not depend on time explicitly, and the kinetic energy (51) is a quadratic-homogeneous function of the generalized velocity $\dot{\alpha}$, the full mechanical energy,

$$E \equiv T + U = \frac{I_{\text{ef}}}{2}\dot{\alpha}^2 + Mg\frac{l}{2}\sin\alpha = \frac{Mgl}{2}\left(\frac{l\dot{\alpha}^2}{3g} + \sin\alpha\right), \tag{4.53}$$

is conserved, giving us the first integral of motion. Moreover, Eq. (53) shows that the system's energy (and hence dynamics) is identical to that of a physical pendulum with an unstable fixed point $\alpha_1 = \pi/2$, a stable fixed point at $\alpha_2 = -\pi/2$, and frequency

$$\Omega = \left(\frac{3g}{2l}\right)^{1/2} \tag{4.54}$$

of small oscillations near the latter point. (Of course, this fixed point cannot be reached in the simple geometry shown in Fig. 7, where the ladder's fall on the floor would change its equations of motion. Moreover, even before that, the left end of the ladder may detach from the wall. The analysis of this issue is left for the reader's exercise.)

4.4. Free rotation

Now let us proceed to more complex situations when the rotation axis is *not* fixed. A good illustration of the complexity arising in this case comes from the case of a rigid body left alone, i.e. not subjected to external forces and hence with its potential energy U constant. Since in this case, according

to Eq. (44), the center of mass (as observed from any inertial reference frame) moves with a constant velocity, we can always use a convenient inertial reference frame with the origin at that point. From the point of view of such a frame, the body's motion is a pure rotation, and $T_{tran} = 0$. Hence, the system's Lagrangian function is just its rotational energy (15), which is, first, a quadratic-homogeneous function of the components ω_j (which may be taken for generalized velocities), and, second, does not depend on time explicitly. As we know from Chapter 2, in this case the mechanical energy, here equal to T_{rot} alone, is conserved. According to Eq. (15), for the principal-axes components of the vector **ω,** this means

$$T_{rot} = \sum_{j=1}^{3} \frac{I_j}{2} \omega_j^2 = \text{const}. \tag{4.55}$$

Rotational energy's conservation

Next, as Eq. (33) shows, in the absence of external forces, the angular momentum **L** of the body is conserved as well. However, though we can certainly use Eq. (26) to represent this fact as

$$\mathbf{L} = \sum_{j=1}^{3} I_j \omega_j \mathbf{n}_j = \text{const}, \tag{4.56}$$

Angular momentum's conservation

where $\mathbf{n}_j$ are the principal axes, this does not mean that all components ω_j *a*re constant, because the principal axes are fixed relative to the rigid body, and hence may rotate with it.

Before exploring these complications, let us briefly mention two conceptually easy, but practically very important cases. The first is a spherical top ($I_1 = I_2 = I_3 = I$). In this case, Eqs. (55) and (56) imply that all components of the vector $\boldsymbol{\omega} = \mathbf{L}/I$, i.e. both the magnitude and the direction of the angular velocity are conserved, for any initial spin. In other words, the body conserves its rotation speed and axis direction, as measured in an inertial frame. The most obvious example is a spherical planet. For example, our Mother Earth, rotating about its axis with angular velocity $\omega = 2\pi/(1\text{ day}) \approx 7.3\times10^{-5}\text{ s}^{-1}$, keeps its axis at a nearly constant angle of 23°27' to the *ecliptic pole*, i.e. to the axis normal to the plane of its motion around the Sun. (In Sec. 6 below, we will discuss some very slow motions of this axis, due to gravity effects.)

Spherical tops are also used in the most accurate gyroscopes, usually with gas-jet or magnetic suspension in vacuum. If done carefully, such systems may have spectacular stability. For example, the gyroscope system of the Gravity Probe B satellite experiment, flown in 2004-2005, was based on quartz spheres – round with a precision of about 10 nm and covered with superconducting thin films (which enabled their magnetic suspension and monitoring). The whole system was stable enough to measure the so-called *geodetic effect* in general relativity (essentially, the space curving by the Earth's mass), resulting in the axis' precession by only 6.6 arc seconds per year, i.e. with an angular velocity of just $\sim10^{-11}\text{s}^{-1}$, with experimental results agreeing with theory with a record ~0.3% accuracy.[9]

The second simple case is that of the symmetric top ($I_1 = I_2 \neq I_3$) with the initial vector **L** aligned with the main principal axis. In this case, $\boldsymbol{\omega} = \mathbf{L}/I_3 = \text{const}$, so the rotation axis is conserved.[10] Such tops, typically in the shape of a *flywheel* (heavy, flat rotor), and supported by *gimbal systems* (also called the "Cardan suspensions") that allow for virtually torque-free rotation about three mutually perpendicular

[9] Still, the main goal of this rather expensive (~$750M) project, an accurate measurement of a more subtle relativistic effect, the so-called *frame-dragging drift* (also called "the Schiff precession"), predicted to be about 0.04 arc seconds per year, has not been achieved.

[10] This is also true for an asymmetric top, i.e. an arbitrary body (with, say, $I_1 < I_2 < I_3$), but in this case the alignment of the vector **L** with the axis $\mathbf{n}_2$ corresponding to the intermediate moment of inertia, is unstable.

axes,[11] are broadly used in more common gyroscopes. Invented by Léon Foucault in the 1850s and made practical later by H. Anschütz-Kaempfe, such gyroscopes have become core parts of automatic guidance systems, for example, in ships, airplanes, missiles, etc. Even if its support wobbles and/or drifts, the suspended gyroscope sustains its direction relative to an inertial reference frame.[12]

However, in the general case with no such special initial alignment, the dynamics of symmetric tops is more complicated. In this case, the vector **L** is still conserved, including its direction, but the vector **ω** is not. Indeed, let us direct the $\mathbf{n}_2$-axis normally to the common plane of the vector **L** and the current instantaneous direction $\mathbf{n}_3$ of the main principal axis (in Fig. 8 below, the plane of the drawing); then, in that particular instant, $L_2 = 0$. Now let us recall that in a symmetric top, the axis $\mathbf{n}_2$ is a principal one. According to Eq. (26) with $j = 2$, the corresponding component ω_2 has to be equal to L_2/I_2, so it is equal to zero. This means that in the particular instant we are considering, the vector **ω** lies in this plane (the common plane of vectors **L** and $\mathbf{n}_3$) as well – see Fig. 8a.

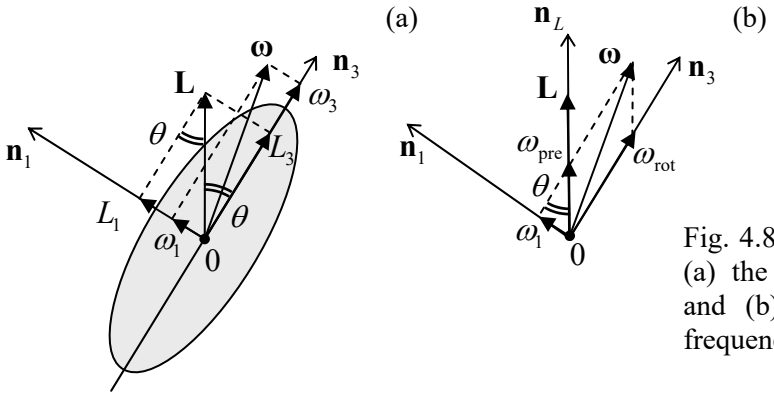

Fig. 4.8. Free rotation of a symmetric top: (a) the general configuration of vectors, and (b) calculating the free precession frequency.

Now consider some point located on the main principal axis $\mathbf{n}_3$, and hence on the plane [$\mathbf{n}_3$, **L**]. Since **ω** is the instantaneous axis of rotation, according to Eq. (9), the point's instantaneous velocity $\mathbf{v} = \boldsymbol{\omega}\times\mathbf{r}$ is directed normally to that plane. This is true for each point of the main axis (besides only one, with $\mathbf{r} = 0$, i.e. the center of mass, which does not move), so the axis as a whole has to move normally to the common plane of the vectors **L**, **ω**, and $\mathbf{n}_3$, while still passing through point 0. Since this conclusion is valid for any moment of time, it means that the vectors **ω** and $\mathbf{n}_3$ rotate about the space-fixed vector **L** together, with some angular velocity ω_{pre}, at each moment staying within one plane. This effect is called the *free* (or "torque-free", or "regular") *precession*, and has to be clearly distinguished it from the completely different effect of the *torque-induced precession*, which will be discussed in the next section.

To calculate ω_{pre}, let us represent the instant vector **ω** as a sum of not its Cartesian components (as in Fig. 8a), but rather of two non-orthogonal vectors directed along $\mathbf{n}_3$ and **L** (Fig. 8b):

$$\boldsymbol{\omega} = \omega_{\text{rot}}\mathbf{n}_3 + \omega_{\text{pre}}\mathbf{n}_L, \qquad \mathbf{n}_L \equiv \frac{\mathbf{L}}{L}. \tag{4.57}$$

[11] See, for example, a nice animation available online at http://en.wikipedia.org/wiki/Gimbal.

[12] Currently, optical gyroscopes are becoming more popular for all but the most precise applications. Much more compact but also much less accurate gyroscopes used, for example, in smartphones and tablet computers, are based on the effect of rotation on 2D mechanical oscillators (whose analysis is left for the reader's exercise), and are implemented as micro-electro-mechanical systems (MEMS) – see, e.g., Chapter 22 in V. Kaajakari, *Practical MEMS*, Small Gear Publishing, 2009.

Fig. 8b shows that ω_{rot} has the meaning of the angular velocity of rotation of the body about its main principal axis, while ω_{pre} is the angular velocity of rotation of that axis about the constant direction of the vector **L,** i.e. is exactly the frequency of precession that we are trying to find. Now ω_{pre} may be readily calculated from the comparison of two panels of Fig. 8, by noticing that the same angle θ between the vectors **L** and $\mathbf{n}_3$ participates in two relations:

$$\sin\theta = \frac{L_1}{L} = \frac{\omega_1}{\omega_{pre}}. \tag{4.58}$$

Since the $\mathbf{n}_1$-axis is a principal one, we may use Eq. (26) for $j = 1$, i.e. $L_1 = I_1\omega_1$, to eliminate ω_1 from Eq. (58), and get a very simple formula

$$\boxed{\omega_{pre} = \frac{L}{I_1}}. \tag{4.59}$$

Free precession: lab frame

This result shows that the precession *frequency* is constant and independent of the alignment of the vector **L** with the main principal axis $\mathbf{n}_3$, while its *amplitude* (characterized by the angle θ) does depend on the initial alignment, and vanishes if **L** is parallel to $\mathbf{n}_3$.[13] Note also that if all principal moments of inertia are of the same order, ω_{pre} is of the same order as the total angular speed $\omega \equiv |\boldsymbol{\omega}|$ of the rotation.

Now let us briefly discuss the free precession in the general case of an "asymmetric top", i.e. a body with arbitrary $I_1 \neq I_2 \neq I_3$. In this case, the effect is more complex because here not only the *direction* but also the *magnitude* of the instantaneous angular velocity $\boldsymbol{\omega}$ may evolve in time. If we are only interested in the relation between the instantaneous values of ω_j and L_j, i.e. the "trajectories" of the vectors $\boldsymbol{\omega}$ and **L** as observed from the reference frame $\{\mathbf{n}_1, \mathbf{n}_2, \mathbf{n}_3\}$ of the principal axes of the body, rather than in the explicit law of their time evolution, they may be found directly from the conservation laws. (Let me emphasize again that the vector **L**, being constant in an inertial reference frame, generally evolves in the frame rotating with the body.) Indeed, Eq. (55) may be understood as the equation of an ellipsoid in the Cartesian coordinates $\{\omega_1, \omega_2, \omega_3\}$, so for a free body, the vector $\boldsymbol{\omega}$ has to stay on the surface of that ellipsoid.[14] On the other hand, since the reference frame's rotation preserves the *length* of any vector, the *magnitude* (but not the direction!) of the vector **L** is also an integral of motion in the moving frame, and we can write

$$L^2 \equiv \sum_{j=1}^{3} L_j^2 = \sum_{j=1}^{3} I_j^2\omega_j^2 = \text{const}. \tag{4.60}$$

Hence the trajectory of the vector $\boldsymbol{\omega}$ follows the closed curve formed by the intersection of two ellipsoids, (55) and (60) – the so-called *Poinsot construction*. It is evident that this trajectory is generally "taco-edge-shaped", i.e. more complex than a planar circle, but never very complex either.[15]

The same argument may be repeated for the vector **L**, for whom the first form of Eq. (60) describes a sphere, and Eq. (55), another ellipsoid:

---

[13] For our Earth, free precession's amplitude is so small (corresponding to sub-10-m linear deviations of the symmetry axis from the vector **L** at the surface) that this effect is of the same order as other, more irregular motions of the axis, resulting from turbulent fluid flow effects in the planet's interior and its atmosphere.

[14] It is frequently called the *Poinsot's ellipsoid*, named after Louis Poinsot (1777-1859) who has made several important contributions to rigid body mechanics.

[15] Curiously, the "wobbling" motion along such trajectories was observed not only for macroscopic rigid bodies but also for heavy atomic nuclei – see, e.g., N. Sensharma *et al.*, *Phys. Rev. Lett.* **124**, 052501 (2020).

$$T_{\rm rot} = \sum_{j=1}^{3} \frac{1}{2I_j} L_j^2 = \text{const}. \tag{4.61}$$

On the other hand, if we are interested in the trajectory of the vector $\boldsymbol{\omega}$ as observed from an *inertial* frame (in which the vector $\mathbf{L}$ stays still), we may note that the general relation (15) for the same rotational energy $T_{\rm rot}$ may also be rewritten as

$$T_{\rm rot} = \frac{1}{2} \sum_{j=1}^{3} \omega_j \sum_{j'=1}^{3} I_{jj'} \omega_{j'}. \tag{4.62}$$

But according to the Eq. (22), the second sum on the right-hand side is nothing more than L_j, so

$$T_{\rm rot} = \frac{1}{2} \sum_{j=1}^{3} \omega_j L_j = \frac{1}{2} \boldsymbol{\omega} \cdot \mathbf{L}. \tag{4.63}$$

This equation shows that for a free body ($T_{\rm rot}$ = const, $\mathbf{L}$ = const), even if the vector $\boldsymbol{\omega}$ changes in time, its endpoint should stay on a plane normal to the angular momentum $\mathbf{L}$. Earlier, we have seen that for the particular case of the symmetric top – see Fig. 8b, but for an asymmetric top, the trajectory of the endpoint may not be circular.

If we are interested not only in the trajectory of the vector $\boldsymbol{\omega}$ but also in the law of its evolution in time, it may be calculated using the general Eq. (33) expressed in the principal components ω_j. For that, we have to recall that Eq. (33) is only valid in an inertial reference frame, while the frame $\{\mathbf{n}_1, \mathbf{n}_2, \mathbf{n}_3\}$ may rotate with the body and hence is generally not inertial. We may handle this problem by applying, to the vector $\mathbf{L}$, the general kinematic relation (8):

$$\left.\frac{d\mathbf{L}}{dt}\right|_{\text{in lab}} = \left.\frac{d\mathbf{L}}{dt}\right|_{\text{in mov}} + \boldsymbol{\omega} \times \mathbf{L}. \tag{4.64}$$

Combining it with Eq. (33), in the moving frame we get

$$\frac{d\mathbf{L}}{dt} + \boldsymbol{\omega} \times \mathbf{L} = \boldsymbol{\tau}, \tag{4.65}$$

where $\boldsymbol{\tau}$ is the external torque. In particular, for the principal-axis components L_j, related to the components ω_j by Eq. (26), the vector equation (65) is reduced to a set of three scalar *Euler equations*

Euler equations

$$I_j \dot{\omega}_j + (I_{j''} - I_{j'}) \omega_{j'} \omega_{j''} = \tau_j, \tag{4.66}$$

where the set of indices $\{j, j', j''\}$ has to follow the usual "right" order – e.g., {1, 2, 3}, etc.[16]

In order to get a feeling of how the Euler equations work, let us return to the particular case of a free symmetric top ($\tau_1 = \tau_2 = \tau_3 = 0$, $I_1 = I_2 \neq I_3$). In this case, $I_1 - I_2 = 0$, so Eq. (66) with $j = 3$ yields ω_3 = const, while the equations for $j = 1$ and $j = 2$ take the following simple form:

$$\dot{\omega}_1 = -\Omega_{\rm pre} \omega_2, \qquad \dot{\omega}_2 = \Omega_{\rm pre} \omega_1, \tag{4.67}$$

where $\Omega_{\rm pre}$ is a constant determined by both the system parameters and the initial conditions:

[16] These equations are of course valid in the simplest case of the fixed rotation axis as well. For example, if $\boldsymbol{\omega} = \mathbf{n}_z \omega$, i.e. $\omega_x = \omega_y = 0$, Eq. (66) is reduced to Eq. (38).

$$\Omega_{\rm pre} \equiv \omega_3 \frac{I_3 - I_1}{I_1}. \qquad (4.68)$$

Free precession: body frame

The system of two equations (67) has a sinusoidal solution with frequency $\Omega_{\rm pre}$, and describes a uniform rotation of the vector $\boldsymbol{\omega}$, with that frequency, about the main axis $\mathbf{n}_3$. This is just another representation of the free precession analyzed above, but this time as observed from the rotating body. Evidently, $\Omega_{\rm pre}$ is substantially different from the frequency $\omega_{\rm pre}$ (59) of the precession as observed from the lab frame; for example, $\Omega_{\rm pre}$ vanishes for the spherical top (with $I_1 = I_2 = I_3$), while $\omega_{\rm pre}$, in this case, is equal to the rotation frequency.[17]

Unfortunately, for the rotation of an asymmetric top (i.e., an arbitrary rigid body) the Euler equations (66) are substantially nonlinear even in the absence of external torque, and may be solved analytically only in just a few cases. One of them is a proof of the already mentioned fact: the free top's rotation about one of its principal axes is stable if the corresponding principal moment of inertia is either the largest or the smallest one of the three. (This proof is easy, and is left for the reader's exercise.)

4.5. Torque-induced precession

The dynamics of rotation becomes even more complex in the presence of external forces. Let us consider the most counter-intuitive effect of *torque-induced precession*, for the simplest case of an axially-symmetric body (which is a particular case of the symmetric top, $I_1 = I_2 \neq I_3$), supported at some point A of its symmetry axis, that does not coincide with the center of mass 0 – see Fig. 9.

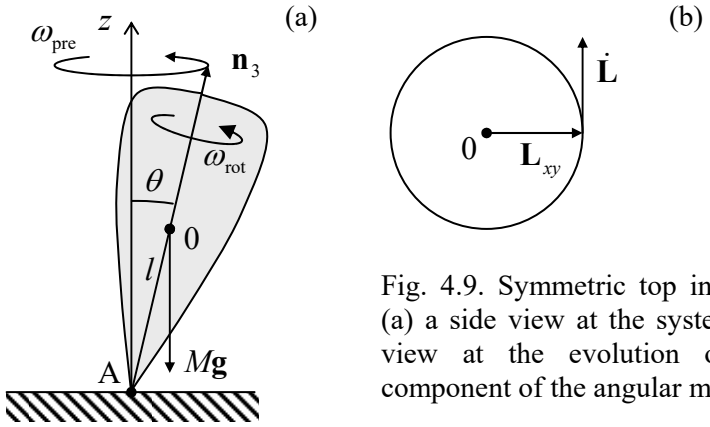

Fig. 4.9. Symmetric top in the gravity field: (a) a side view at the system and (b) the top view at the evolution of the horizontal component of the angular momentum vector.

The uniform gravity field $\mathbf{g}$ creates bulk-distributed forces that, as we know from the analysis of the physical pendulum in Sec. 3, are equivalent to a single force $M\mathbf{g}$ applied in the center of mass – in Fig. 9, point 0. The torque of this force relative to the support point A is

$$\boldsymbol{\tau} = \mathbf{r}_0\Big|_{\rm in\ A} \times M\mathbf{g} = Ml\mathbf{n}_3 \times \mathbf{g}. \qquad (4.69)$$

Hence the general equation (33) of the angular momentum evolution (valid in any inertial frame, for example the one with its origin at point A) becomes

[17] For our Earth with its *equatorial bulge* (see Sec. 6 below), the ratio $(I_3 - I_1)/I_1$ is ~1/300, so that $2\pi/\Omega_{\rm pre}$ is about 10 months. However, due to the fluid flow effects mentioned above, the observed precession is not very regular.

$$\dot{\mathbf{L}} = Ml\mathbf{n}_3 \times \mathbf{g}. \tag{4.70}$$

Despite the apparent simplicity of this (exact!) equation, its analysis is straightforward only in the limit when the top is spinning about its symmetry axis $\mathbf{n}_3$ with a very high angular velocity $\omega_{\rm rot}$. In this case, we may neglect the contribution to $\mathbf{L}$ due to a relatively small precession velocity $\omega_{\rm pre}$ (still to be calculated), and use Eq. (26) to write

$$\mathbf{L} = I_3\boldsymbol{\omega} = I_3\omega_{\rm rot}\mathbf{n}_3. \tag{4.71}$$

Then Eq. (70) shows that the vector $\dot{\mathbf{L}}$ is perpendicular to both $\mathbf{n}_3$ (and hence $\mathbf{L}$) and $\mathbf{g}$, i.e. lies within a horizontal plane and is perpendicular to the horizontal component $\mathbf{L}_{xy}$ of the vector $\mathbf{L}$ – see Fig. 9b. Since, according to Eq. (70), the magnitude of this vector is constant, $|\dot{\mathbf{L}}| = Mgl\sin\theta$, the vector $\mathbf{L}$ (and hence the body's main axis) rotates about the vertical axis with the following angular velocity:

Torque-induced precession: fast-rotation limit

$$\omega_{\rm pre} = \frac{|\dot{\mathbf{L}}|}{L_{xy}} = \frac{Mgl\sin\theta}{L\sin\theta} \equiv \frac{Mgl}{L} = \frac{Mgl}{I_3\omega_{\rm rot}}. \tag{4.72}$$

Thus, rather counter-intuitively, the fast-rotating top does not follow the external, vertical force and, in addition to fast spinning about the symmetry axis $\mathbf{n}_3$, performs a revolution, called the *torque-induced precession*, about the vertical axis.[18] Note that, similarly to the free-precession frequency (59), the torque-induced precession frequency (72) does not depend on the initial (and sustained) angle θ. However, the torque-induced precession frequency is inversely (rather than directly) proportional to $\omega_{\rm rot}$. This fact makes the above simple theory valid in many practical cases. Indeed, Eq. (71) is quantitatively valid if the contribution of the precession into $\mathbf{L}$ is relatively small: $I\omega_{\rm pre} << I_3\omega_{\rm rot}$, where I is a certain effective moment of inertia for the precession – to be calculated below. Using Eq. (72), this condition may be rewritten as

$$\omega_{\rm rot} >> \left(\frac{MglI}{I_3^2}\right)^{1/2}. \tag{4.73}$$

According to Eq. (16), for a body of not too extreme proportions, i.e. with all linear dimensions of the same length scale l, all inertia moments are of the order of Ml^2, so the right-hand side of Eq. (73) is of the order of $(g/l)^{1/2}$, i.e. comparable with the frequency of small oscillations of the same body as the physical pendulum at the absence of its fast rotation.

To develop a quantitative theory that would be valid beyond such approximate treatment, the Euler equations (66) may be used, but are not very convenient. A better approach, suggested by the same L. Euler, is to introduce a set of three independent angles between the principal axes $\{\mathbf{n}_1, \mathbf{n}_2, \mathbf{n}_3\}$ bound to the rigid body, and the axes $\{\mathbf{n}_x, \mathbf{n}_y, \mathbf{n}_z\}$ of an inertial reference frame (Fig. 10), and then express the basic equation (33) of rotation, via these angles. There are several possible options for the definition of such angles; Fig. 10 shows the set of *Euler angles*, most convenient for analyses of fast rotation.[19] As one can see, the first Euler angle, θ, is the usual polar angle measured from the $\mathbf{n}_z$-axis to the $\mathbf{n}_3$-axis. The second one is the azimuthal angle φ, measured from the $\mathbf{n}_x$-axis to the *line of nodes* formed by the intersection of planes $[\mathbf{n}_x, \mathbf{n}_y]$ and $[\mathbf{n}_1, \mathbf{n}_2]$. The last Euler angle, ψ, is measured within the

[18] A semi-quantitative interpretation of this effect is a very useful exercise, highly recommended to the reader.

[19] Of the several choices more convenient in the absence of fast rotation, the most common is the set of so-called *Tait-Brian angles* (called the *yaw*, *pitch*, and *roll*), which are broadly used for aircraft and maritime navigation.

Euler angles

plane [$\mathbf{n}_1$, $\mathbf{n}_2$], from the line of nodes to the $\mathbf{n}_1$-axis. For example, in the simple picture of slow force-induced precession of a symmetric top, that was discussed above, the angle θ is constant, the angle ψ changes rapidly, with the rotation velocity ω_{rot}, while the angle φ evolves with the precession frequency ω_{pre} (72).

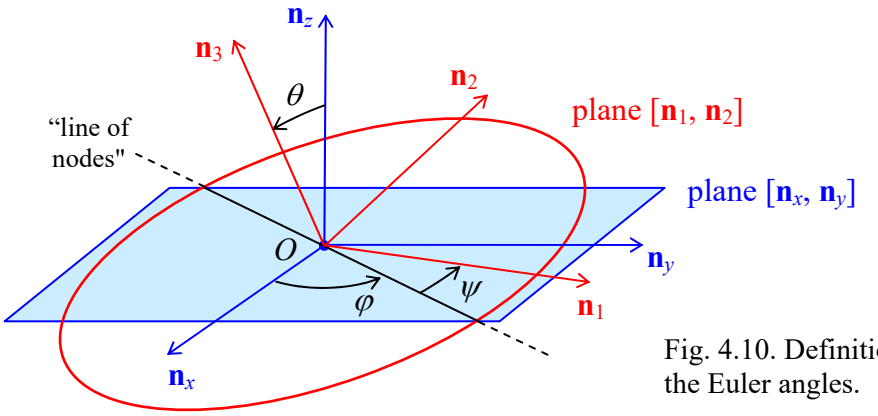

Fig. 4.10. Definition of the Euler angles.

Now we can express the principal-axes components of the instantaneous angular velocity vector, ω_1, ω_2, and ω_3, as measured in the lab reference frame, in terms of the Euler angles. This may be readily done by calculating, from Fig. 10, the contributions of the Euler angles' evolution to the rotation about each principal axis, and then adding them up:

$$\begin{aligned} \omega_1 &= \dot{\varphi}\sin\theta\sin\psi + \dot{\theta}\cos\psi, \\ \omega_2 &= \dot{\varphi}\sin\theta\cos\psi - \dot{\theta}\sin\psi, \\ \omega_3 &= \dot{\varphi}\cos\theta + \dot{\psi}. \end{aligned} \tag{4.74}$$

ω via Euler angles

These relations enable the expression of the kinetic energy of rotation (25) and the angular momentum components (26) via the generalized coordinates θ, φ, and ψ and their time derivatives (i.e. the corresponding generalized velocities), and then using the powerful Lagrangian formalism to derive their equations of motion. This is especially simple to do in the case of symmetric tops (with $I_1 = I_2$), because plugging Eqs. (74) into Eq. (25) we get an expression,

$$T_{\text{rot}} = \frac{I_1}{2}\left(\dot{\theta}^2 + \dot{\varphi}^2\sin^2\theta\right) + \frac{I_3}{2}\left(\dot{\varphi}\cos\theta + \dot{\psi}\right)^2, \tag{4.75}$$

which does not include explicitly either φ or ψ. (This reflects the fact that for a symmetric top we can always select the $\mathbf{n}_1$-axis to coincide with the line of nodes, and hence take $\psi = 0$ at the considered moment of time. Note that this trick does *not* mean we can take $\dot{\psi} = 0$, because the $\mathbf{n}_1$-axis, as observed from an inertial reference frame, moves!) Now we should not forget that at the torque-induced precession, the center of mass moves as well (see, e.g., Fig. 9), so according to Eq. (14), the total kinetic energy of the body is the sum of two terms,

$$T = T_{\text{rot}} + T_{\text{tran}}, \qquad T_{\text{tran}} = \frac{M}{2}V^2 = \frac{M}{2}l^2\left(\dot{\theta}^2 + \dot{\varphi}^2\sin^2\theta\right), \tag{4.76}$$

while its potential energy is just

$$U = Mgl\cos\theta + \text{const}. \tag{4.77}$$

Now we could readily use Eqs. (2.19) to write the Lagrange equations of motion for the Euler angles, but it is simpler to immediately notice that according to Eqs. (75)-(77), the Lagrangian function, $T - U$, does not depend explicitly on the "cyclic" coordinates φ and ψ, so the corresponding generalized momenta (2.31) are conserved:

$$p_\varphi \equiv \frac{\partial T}{\partial \dot{\varphi}} = I_A \dot{\varphi} \sin^2\theta + I_3(\dot{\varphi}\cos\theta + \dot{\psi})\cos\theta = \text{const}, \tag{4.78}$$

$$p_\psi \equiv \frac{\partial T}{\partial \dot{\psi}} = I_3(\dot{\varphi}\cos\theta + \dot{\psi}) = \text{const}, \tag{4.79}$$

where $I_A \equiv I_1 + Ml^2$. (According to Eq. (29), I_A is just the body's moment of inertia for rotation about a horizontal axis passing through the support point A.) According to the last of Eqs. (74), p_ψ is just L_3, i.e. the angular momentum's component along the *precessing* axis $\mathbf{n}_3$. On the other hand, by its very definition (78), p_φ is L_z, i.e. the same vector $\mathbf{L}$'s component along the *stationary* axis z. (Actually, we could foresee in advance the conservation of both these components of $\mathbf{L}$ for our system, because the vector (69) of the external torque is perpendicular to both $\mathbf{n}_3$ and $\mathbf{n}_z$.) Using this notation, and solving the simple system of two linear equations (78)-(79) for the angle derivatives, we get

$$\dot{\varphi} = \frac{L_z - L_3\cos\theta}{I_A \sin^2\theta}, \qquad \dot{\psi} = \frac{L_3}{I_3} - \frac{L_z - L_3\cos\theta}{I_A \sin^2\theta}\cos\theta\,. \tag{4.80}$$

One more conserved quantity in this problem is the full mechanical energy[20]

$$E \equiv T + U = \frac{I_A}{2}\left(\dot{\theta}^2 + \dot{\varphi}^2\sin^2\theta\right) + \frac{I_3}{2}\left(\dot{\varphi}\cos\theta + \dot{\psi}\right)^2 + Mgl\cos\theta. \tag{4.81}$$

Plugging Eqs. (80) into Eq. (81), we get a first-order differential equation for the angle θ, which may be represented in the following physically transparent form:

$$\frac{I_A}{2}\dot{\theta}^2 + U_{ef}(\theta) = E, \qquad U_{ef}(\theta) \equiv \frac{(L_z - L_3\cos\theta)^2}{2I_A\sin^2\theta} + \frac{L_3^2}{2I_3} + Mgl\cos\theta + \text{const}\,. \tag{4.82}$$

Thus, similarly to the planetary problems considered in Sec. 3.4, the torque-induced precession of a symmetric top has been reduced (without any approximations!) to a 1D problem of the motion of just one of its degrees of freedom, the polar angle θ, in the effective potential $U_{ef}(\theta)$. According to Eq. (82), very similar to Eq. (3.44) for the planetary problem, this potential is the sum of the actual potential energy U given by Eq. (77), and a contribution from the kinetic energy of motion along two other angles. In the absence of rotation about the axes $\mathbf{n}_z$ and $\mathbf{n}_3$ (i.e., $L_z = L_3 = 0$), Eq. (82) is reduced to the first integral of the equation (40) of motion of a physical pendulum, with $I' = I_A$. If the rotation is present, then (besides the case of very special initial conditions when $\theta(0) = 0$ *and* $L_z = L_3$),[21] the first contribution to $U_{ef}(\theta)$ diverges at $\theta \to 0$ and π, so the effective potential energy has a minimum at some non-zero value θ_0 of the polar angle θ – see Fig. 11.

[20] Indeed, since the Lagrangian does not depend on time explicitly, H = const, and since the full kinetic energy T (75)-(76) is a quadratic-homogeneous function of the generalized velocities, we have $E = H$.

[21] In that simple case, the body continues to rotate about the vertical symmetry axis: $\theta(t) = 0$. Note, however, that such motion is stable only if the spinning speed is sufficiently high – see Eq. (85) below.

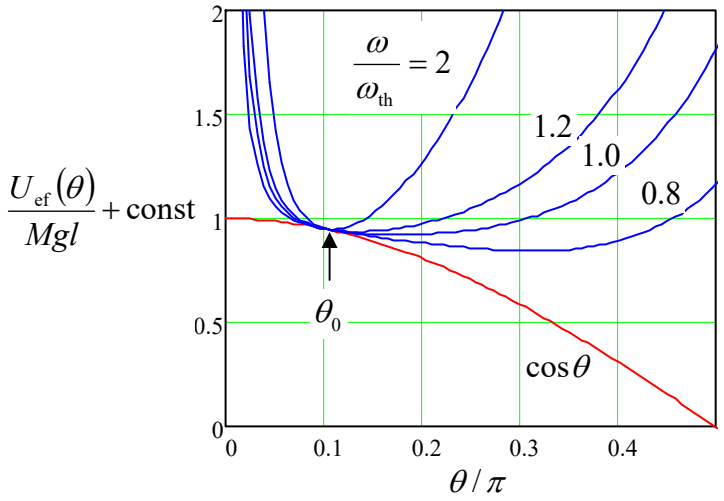

Fig. 4.11. The effective potential energy U_{ef} of the symmetric top, given by Eq. (82), as a function of the polar angle θ, for a particular value (0.95) of the ratio $r \equiv L_z/L_3$ (so that at $\omega_{rot} >> \omega_{th}$, $\theta_0 = \cos^{-1} r \approx 0.1011\pi$), and several values of the ratio ω_{rot}/ω_{th} – see Eq. (85).

If the initial angle $\theta(0)$ is equal to this value θ_0, i.e. if the initial effective energy is equal to its minimum value $U_{ef}(\theta_0)$, the polar angle remains constant through the motion: $\theta(t) = \theta_0$. This corresponds to the pure torque-induced precession whose angular velocity is given by the first of Eqs. (80):

$$\omega_{pre} \equiv \dot{\varphi} = \frac{L_z - L_3 \cos\theta_0}{I_A \sin^2\theta_0}. \tag{4.83}$$

The condition for finding θ_0, $dU_{ef}/d\theta = 0$, is a transcendental algebraic equation that cannot be solved analytically for arbitrary parameters. However, in the high spinning speed limit (73), this is possible. Indeed, in this limit the Mgl-proportional contribution to U_{ef} is small, and we may analyze its effect by successive approximations. In the 0^{th} approximation, i.e. at $Mgl = 0$, the minimum of U_{ef} is evidently achieved at $\cos\theta_0 = L_z/L_3$, turning the precession frequency (83) to zero. In the next, 1^{st} approximation, we may require that at $\theta = \theta_0$, the derivative of the first term of Eq. (82) for U_{ef} over $\cos\theta$, equal to $-L_z(L_z - L_3\cos\theta)/I_A\sin^2\theta$,[22] is canceled with that of the gravity-induced term, equal to Mgl. This immediately yields $\omega_{pre} = (L_z - L_3\cos\theta_0)/I_A\sin^2\theta_0 = Mgl/L_3$, so by identifying ω_{rot} with $\omega_3 \equiv L_3/I_3$ (see Fig. 8), we recover the simple expression (72).

The second important result that may be readily obtained from Eq. (82) is the exact expression for the threshold value of the spinning speed for a vertically rotating top ($\theta = 0$, $L_z = L_3$). Indeed, in the limit $\theta \to 0$ this expression may be readily simplified:

$$U_{ef}(\theta) \approx \text{const} + \left(\frac{L_3^2}{8I_A} - \frac{Mgl}{2}\right)\theta^2. \tag{4.84}$$

This formula shows that if $\omega_{rot} \equiv L_3/I_3$ is higher than the following threshold value,

$$\omega_{th} \equiv 2\left(\frac{MglI_A}{I_3^2}\right)^{1/2}, \tag{4.85}$$

Threshold rotation speed

[22] Indeed, the derivative of the fraction $1/2I_A\sin^2\theta$, taken at the point $\cos\theta = L_z/L_3$, is multiplied by the numerator, $(L_z - L_3\cos\theta)^2$, which turns to zero at this point.

then the coefficient at θ^2 in Eq. (84) is positive, so U_{ef} has a stable minimum at $\theta_0 = 0$. On the other hand, if ω_3 is decreased below ω_{th}, the fixed point becomes unstable, so the top falls. As the plots in Fig. 11 show, Eq. (85) for the threshold frequency works very well even for non-zero but small values of the precession angle θ_0. Note that if we take $I = I_A$ in the condition (73) of the approximate treatment, it acquires a very simple sense: $\omega_{rot} >> \omega_{th}$.

Finally, Eqs. (82) give a natural description of one more phenomenon. If the initial energy is larger than $U_{ef}(\theta_0)$, the angle θ oscillates between two classical turning points on both sides of the fixed point θ_0 – see Fig. 11 again. The law and frequency of these oscillations may be found exactly as in Sec. 3.3 – see Eqs. (3.27) and (3.28). At $\omega_3 >> \omega_{th}$, this motion is a fast rotation of the body's symmetry axis $\mathbf{n}_3$ about its average position performing the slow torque-induced precession. Historically, these oscillations are called *nutations*, but their physics is similar to that of the free precession that was analyzed in the previous section, and the order of magnitude of their frequency is given by Eq. (59).

It may be proved that small friction (not taken into account in the above analysis) leads first to a decay of these nutations, then to a slower drift of the precession angle θ_0 to zero, and finally, to a gradual decay of the spinning speed ω_{rot} until it reaches the threshold (85) and the top falls.

4.6. Non-inertial reference frames

Now let us use the results of our analysis of the rotation kinematics in Sec. 1 to complete the discussion of the transfer between two reference frames, which was started in the introductory Chapter 1. As Fig. 12 (which reproduces Fig. 1.2 in a more convenient notation) shows, even if the "moving" frame 0 rotates relative to the "lab" frame 0*'*, the radius vectors observed from these two frames are still related, at any moment of time, by the simple Eq. (1.5). In our new notation:

$$\mathbf{r}' = \mathbf{r}_0 + \mathbf{r}\,. \tag{4.86}$$

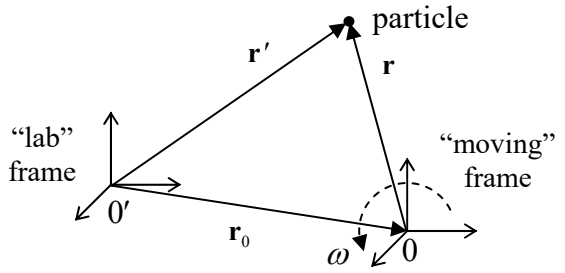

Fig. 4.12. The general case of transfer between two reference frames.

However, as was mentioned in Sec. 1, the general addition rule for velocities is already more complex. To find it, let us differentiate Eq. (86) over time:

$$\frac{d}{dt}\mathbf{r}' = \frac{d}{dt}\mathbf{r}_0 + \frac{d}{dt}\mathbf{r}. \tag{4.87}$$

The left-hand side of this relation is evidently the particle's velocity as measured in the lab frame, and the first term on the right-hand side is the velocity $\mathbf{v}_0$ of point 0, as measured in the same lab frame. The last term is more complex: due to the possible mutual rotation of the frames 0 and 0*'*, that term may not vanish even if the particle does not move relative to the rotating frame 0 – see Fig. 12.

Fortunately, we have already derived the general Eq. (8) to analyze situations exactly like this one. Taking $\mathbf{A} = \mathbf{r}$ in it, we may apply the result to the last term of Eq. (87), to get

$$\mathbf{v}\big|_{\text{in lab}} = \mathbf{v}_0\big|_{\text{in lab}} + (\mathbf{v} + \boldsymbol{\omega} \times \mathbf{r}), \tag{4.88}$$

Trans-formation of velocity

where $\boldsymbol{\omega}$ is the instantaneous angular velocity of an imaginary rigid body connected to the moving reference frame (or we may say, of this frame as such), as measured in the *lab* frame 0', while $\mathbf{v}$ is $d\mathbf{r}/dt$ as measured in the *moving* frame 0. The relation (88), on one hand, is a natural generalization of Eq. (10) for $\mathbf{v} \neq 0$; on the other hand, if $\boldsymbol{\omega} = 0$, it is reduced to simple Eq. (1.8) for the translational motion of the frame 0.

To calculate the particle's acceleration, we may just repeat the same trick: differentiate Eq. (88) over time, and then use Eq. (8) again, now for the vector $\mathbf{A} = \mathbf{v} + \boldsymbol{\omega} \times \mathbf{r}$. The result is

$$\mathbf{a}\big|_{\text{in lab}} \equiv \mathbf{a}_0\big|_{\text{in lab}} + \frac{d}{dt}(\mathbf{v} + \boldsymbol{\omega} \times \mathbf{r}) + \boldsymbol{\omega} \times (\mathbf{v} + \boldsymbol{\omega} \times \mathbf{r}). \tag{4.89}$$

Carrying out the differentiation in the second term, we finally get the goal relation,

$$\mathbf{a}\big|_{\text{in lab}} \equiv \mathbf{a}_0\big|_{\text{in lab}} + \mathbf{a} + \dot{\boldsymbol{\omega}} \times \mathbf{r} + 2\boldsymbol{\omega} \times \mathbf{v} + \boldsymbol{\omega} \times (\boldsymbol{\omega} \times \mathbf{r}), \tag{4.90}$$

Trans-formation of acceleration

where $\mathbf{a}$ is the particle's acceleration as measured in the moving frame. This result is a natural generalization of the simple Eq. (1.9) to the rotating frame case.

Now let the lab frame 0' be inertial; then the 2nd Newton's law for a particle of mass m is

$$m\mathbf{a}\big|_{\text{in lab}} = \mathbf{F}, \tag{4.91}$$

where $\mathbf{F}$ is the vector sum of all forces exerted on the particle. This is simple and clear; however, in many cases it is much more convenient to work in a non-inertial reference frame. For example, when describing most phenomena on the Earth's surface, it is rather inconvenient to use a reference frame bound to the Sun (or to the galactic center, etc.). In order to understand what we should pay for the convenience of using a moving frame, we may combine Eqs. (90) and (91) to write

$$m\mathbf{a} = \mathbf{F} - m\mathbf{a}_0\big|_{\text{in lab}} - m\boldsymbol{\omega} \times (\boldsymbol{\omega} \times \mathbf{r}) - 2m\boldsymbol{\omega} \times \mathbf{v} - m\dot{\boldsymbol{\omega}} \times \mathbf{r}. \tag{4.92}$$

Inertial "forces"

This result means that if we want to use an analog of the 2nd Newton's law in a non-inertial reference frame, we have to add, to the actual net force $\mathbf{F}$ exerted on a particle, four pseudo-force terms, called *inertial forces*, all proportional to the particle's mass. Let us analyze them one by one, always remembering that these are just mathematical terms, not actual physical forces. (In particular, it would be futile to seek a 3rd-Newton's-law counterpart for any inertial force.)

The first term, $-m\mathbf{a}_0|_{\text{in lab}}$, is the only one not related to rotation and is well known from undergraduate mechanics. (Let me hope the reader remembers all these weight-in-the-accelerating-elevator problems.) However, despite its simplicity, this term has more subtle consequences. As an example, let us consider, semi-qualitatively, the motion of a planet, such as our Earth, orbiting a star and also rotating about its own axis – see Fig. 13. The bulk-distributed gravity forces, acting on a planet from its star, are not quite uniform, because they obey the $1/r^2$ gravity law (1.15), and hence are equivalent to a single force applied to a point A slightly offset from the planet's center of mass 0, toward

the star. For a spherically symmetric planet, the direction from 0 to A would be exactly aligned with the direction toward the star. However, real planets are not absolutely rigid, so due to the centrifugal "force" (to be discussed momentarily), the rotation about their own axis makes them slightly ellipsoidal – see Fig. 13. (For our Earth, this equatorial bulge is about 10 km.) As a result, the net gravity force is slightly offset from the direction toward the center of mass 0. On the other hand, repeating all the arguments of this section for a body (rather than a point), we may see that, in the reference frame moving with the planet, the inertial force $-M\mathbf{a}_0$ (with the magnitude of the total gravity force, but directed *from* the star) is applied exactly to the center of mass. As a result, this pair of forces creates a torque $\boldsymbol{\tau}$ perpendicular to both the direction toward the star and the vector 0A. (In Fig. 13, the torque vector is perpendicular to the plane of the drawing). If the angle δ between the planet's "polar" axis of rotation and the direction towards the star was fixed, then, as we have seen in the previous section, this torque would induce a slow axis precession about that direction.

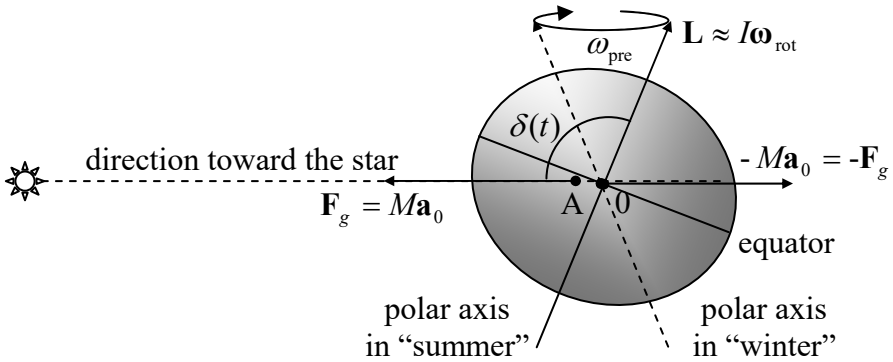

Fig. 4.13. The axial precession of a planet (with the equatorial bulge and the 0A-offset strongly exaggerated).

However, as a result of the orbital motion, the angle δ oscillates in time much faster (once a year) between values $(\pi/2 + \varepsilon)$ and $(\pi/2 - \varepsilon)$, where ε is the axis tilt, i.e. angle between the polar axis (the direction of vectors $\mathbf{L}$ and $\boldsymbol{\omega}_{\rm rot}$) and the normal to the *ecliptic plane* of the planet's orbit. (For the Earth, $\varepsilon \approx 23.4°$.) A straightforward averaging over these fast oscillations[23] shows that the torque leads to the polar axis' precession about the axis *perpendicular* to the ecliptic plane, keeping ε constant – see Fig. 13. For the Earth, the period $T_{\rm pre} = 2\pi/\omega_{\rm pre}$ of this *precession of the equinoxes*, corrected for a substantial effect of the Moon's gravity, is close to 26,000 years.[24]

Returning to Eq. (92), the direction of the second term of its right-hand side,

Centrifugal "force"

$$\mathbf{F}_{\rm cf} \equiv -m\boldsymbol{\omega}\times(\boldsymbol{\omega}\times\mathbf{r}), \tag{4.93}$$

called the *centrifugal force*, is always perpendicular to, and directed out of the instantaneous rotation axis – see Fig. 14. Indeed, the vector $\boldsymbol{\omega}\times\mathbf{r}$ is perpendicular to both $\boldsymbol{\omega}$ and $\mathbf{r}$ (in Fig. 14, normal to the drawing plane and directed from the reader) and has the magnitude $\omega r\sin\theta = \omega\rho$, where ρ is the distance of the particle from the rotation axis. Hence the outer vector product, with the account of the minus sign, is normal to the rotation axis $\boldsymbol{\omega}$, directed from this axis, and is equal to $\omega^2 r\sin\theta = \omega^2\rho$. The centrifugal "force" is of course just the result of the fact that the centripetal acceleration $\omega^2\rho$, explicit in the inertial reference frame, disappears in the rotating frame. For a typical location of the Earth ($\rho \sim R_{\rm E} \approx 6\times10^6$ m),

[23] Details of this calculation may be found, e.g., in Sec. 5.8 of the textbook by H. Goldstein *et al.*, *Classical Mechanics*, 3rd ed., Addison Wesley, 2002.

[24] This effect is known from antiquity, apparently discovered by Hipparchus of Rhodes (190-120 BC).

with its angular velocity $\omega_E \approx 10^{-4}$ s^{-1}, the acceleration is rather considerable, of the order of 3 cm/s^2, i.e. ~0.003 g, and is responsible, in particular, for the largest part of the equatorial bulge mentioned above.

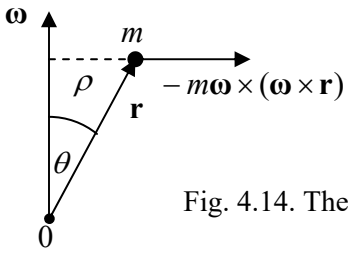

Fig. 4.14. The centrifugal force.

As an example of using the centrifugal force concept, let us return again to our "testbed" problem on the bead sliding along a rotating ring – see Fig. 2.1. In the non-inertial reference frame attached to the ring, we have to add, to the actual forces $m\mathbf{g}$ and $\mathbf{N}$ exerted on the bead, the horizontal centrifugal force[25] directed from the rotation axis, with the magnitude $m\omega^2\rho$. Its component tangential to the ring equals $(m\omega^2\rho)\cos\theta = m\omega^2 R\sin\theta\cos\theta$, and hence the component of Eq. (92) along this direction is $ma = -mg\sin\theta + m\omega^2 R\sin\theta\cos\theta$. With $a = R\ddot{\theta}$, this gives us an equation of motion equivalent to Eq. (2.25), which had been derived in Sec. 2.2 (in the inertial frame) using the Lagrangian formalism.

The third term on the right-hand side of Eq. (92),

$$\mathbf{F}_C \equiv -2m\boldsymbol{\omega}\times\mathbf{v}, \tag{4.94}$$

Coriolis "force"

is the so-called *Coriolis force*,[26] which is different from zero only if the particle moves in a rotating reference frame. Its physical sense may be understood by considering a projectile fired horizontally, say from the North Pole – see Fig. 15.

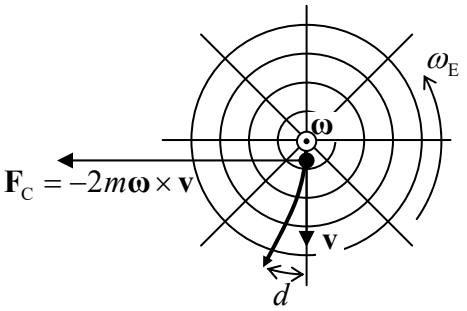

Fig. 4.15. The trajectory of a projectile fired horizontally from the North Pole, from the point of view of an Earth-bound observer looking down. The circles show parallels, while the straight lines mark meridians.

From the point of view of an Earth-based observer, the projectile will be affected by an additional Coriolis force (94), directed westward, with the magnitude $2m\omega_E v$, where $\mathbf{v}$ is the main, southward component of the velocity. This force would cause the westward acceleration $a = 2\omega_E v$, and hence the westward deviation growing with time as $d = at^2/2 = \omega_E v t^2$. (This formula is exact only if d is much smaller than the distance $r = vt$ passed by the projectile.) On the other hand, from the point of

[25] For this problem, all other inertial "forces", besides the Coriolis force (see below) vanish, while the latter force is directed normally to the ring and does not affect the bead's motion along it.

[26] Named after G.-G. de Coriolis (already reverently mentioned in Chapter 1) who described its theory and applications in detail in 1835, though the first semi-quantitative analyses of this effect were given by Giovanni Battista Riccioli and Claude François Dechales already in the mid-1600s, and all basic components of the Coriolis theory may be traced to a 1749 work by Leonard Euler.

view of an inertial-frame observer, the projectile's trajectory in the horizontal plane is a straight line. However, during the flight time t, the Earth's surface slips eastward from under the trajectory by the distance $d = r\varphi = (vt)(\omega_E t) = \omega_E v t^2$, where $\varphi = \omega_E t$ is the azimuthal angle of the Earth's rotation during the flight). Thus, both approaches give the same result – as they should.

Hence, the Coriolis "force" is just a fancy (but frequently very convenient!) way of describing a purely geometric effect pertinent to the rotation, from the point of view of the observer participating in it. This force is responsible, in particular, for the higher right banks of rivers in the Northern hemisphere, regardless of the direction of their flow – see Fig. 16. Despite the smallness of the Coriolis force (for a typical velocity of the water in a river, $v \sim 1$ m/s, it is equivalent to acceleration $a_C \sim 10^{-2}$ cm/s^2 $\sim 10^{-5}$ g), its multi-century effects may be rather prominent.[27]

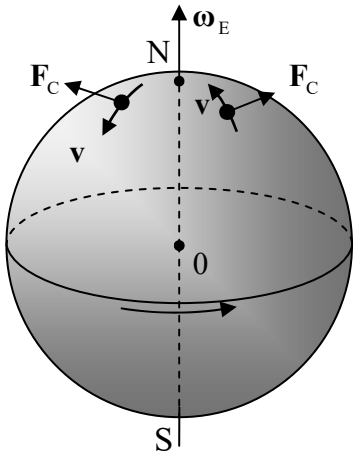

Fig. 4.16. Coriolis forces due to the Earth's rotation, in the Northern hemisphere.

Finally, the last, fourth term of Eq. (92), $-m\dot{\boldsymbol{\omega}} \times \mathbf{r}$, exists only when the rotation frequency changes in time, and may be interpreted as a local-position-specific addition to the first term.

The key relation (92), derived above from Newton's equation (91), may be alternatively obtained from the Lagrangian approach. Indeed, let us use Eq. (88) to represent the kinetic energy of the particle in an inertial "lab" frame in terms of $\mathbf{v}$ and $\mathbf{r}$ measured in a *rotating* frame:

$$T = \frac{m}{2}\left[\mathbf{v}_0\big|_{\text{in lab}} + (\mathbf{v} + \boldsymbol{\omega} \times \mathbf{r})\right]^2, \tag{4.95}$$

and use this expression to calculate the Lagrangian function. For the relatively simple case of a particle's motion in the field of potential forces, measured from a reference frame that performs a pure rotation (so $\mathbf{v}_0|_{\text{in lab}} = 0$)[28] with a constant angular velocity $\boldsymbol{\omega}$, we get

$$L \equiv T - U = \frac{m}{2}v^2 + m\mathbf{v}\cdot(\boldsymbol{\omega}\times\mathbf{r}) + \frac{m}{2}(\boldsymbol{\omega}\times\mathbf{r})^2 - U \equiv \frac{m}{2}v^2 + m\mathbf{v}\cdot(\boldsymbol{\omega}\times\mathbf{r}) - U_{\text{ef}}, \tag{4.96a}$$

where the effective potential energy,[29]

[27] The same force causes the counterclockwise circulation in the "Nor'easter" storms on the US East Coast, with the radial component of the air velocity directed toward the cyclone's center, due to lower pressure in its middle.

[28] A similar analysis of the cases with $\mathbf{v}_0|_{\text{in lab}} \neq 0$, for example, of a translational relative motion of the reference frames, is left for the reader's exercise.

$$U_{\rm ef} \equiv U + U_{\rm cf}, \qquad \text{with } U_{\rm cf} \equiv -\frac{m}{2}(\boldsymbol{\omega}\times\mathbf{r})^2, \tag{4.96b}$$

is just the sum of the actual potential energy U of the particle and the so-called *centrifugal potential energy*, associated with the centrifugal "force" (93):

$$\mathbf{F}_{\rm cf} = -\nabla U_{\rm cf} = -\nabla\left[-\frac{m}{2}(\boldsymbol{\omega}\times\mathbf{r})^2\right] = -m\boldsymbol{\omega}\times(\boldsymbol{\omega}\times\mathbf{r}). \tag{4.97}$$

It is straightforward to verify that the Lagrange equations (2.19), derived from Eqs. (96) considering the Cartesian components of $\mathbf{r}$ and $\mathbf{v}$ as generalized coordinates and velocities, coincide with Eq. (92) (with $\mathbf{a}_0|_{\text{in lab}} = 0$, $\dot{\boldsymbol{\omega}} = 0$, and $\mathbf{F} = -\nabla U$).

Now it is very informative to have a look at a by-product of this calculation, the generalized momentum (2.31) corresponding to the particle's coordinate $\mathbf{r}$ as measured in the rotating reference frame,[30]

$$\boldsymbol{\mathcal{p}} \equiv \frac{\partial L}{\partial \mathbf{v}} = m(\mathbf{v} + \boldsymbol{\omega}\times\mathbf{r}). \tag{4.98}$$

Canonical momentum at rotation

According to Eq. (88) with $\mathbf{v}_0|_{\text{in lab}} = 0$, the expression in the parentheses is just $\mathbf{v}|_{\text{in lab}}$. However, from the point of view of the moving frame, i.e. not knowing about the simple physical sense of the vector $\boldsymbol{\mathcal{p}}$, we would have a reason to speak about two different linear momenta of the same particle, the so-called *kinetic momentum* $\mathbf{p} = m\mathbf{v}$ and the *canonical momentum* $\boldsymbol{\mathcal{p}} = \mathbf{p} + m\boldsymbol{\omega}\times\mathbf{r}$.[31] Let us calculate the Hamiltonian function H defined by Eq. (2.32), and the energy E as functions of the same moving-frame variables:

$$H \equiv \sum_{j=1}^{3}\frac{\partial L}{\partial v_j}v_j - L = \boldsymbol{\mathcal{p}}\cdot\mathbf{v} - L = m(\mathbf{v}+\boldsymbol{\omega}\times\mathbf{r})\cdot\mathbf{v} - \left[\frac{m}{2}v^2 + m\mathbf{v}\cdot(\boldsymbol{\omega}\times\mathbf{r}) - U_{\rm ef}\right] = \frac{mv^2}{2} + U_{\rm ef}, \tag{4.99}$$

$$E \equiv T + U = \frac{m}{2}v^2 + m\mathbf{v}\cdot(\boldsymbol{\omega}\times\mathbf{r}) + \frac{m}{2}(\boldsymbol{\omega}\times\mathbf{r})^2 + U = \frac{m}{2}v^2 + U_{\rm ef} + m\mathbf{v}\cdot(\boldsymbol{\omega}\times\mathbf{r}) + m(\boldsymbol{\omega}\times\mathbf{r})^2. \tag{4.100}$$

These expressions clearly show that E and H are *not* equal.[32] In hindsight, this is not surprising, because the kinetic energy (95), expressed in the moving-frame variables, includes a term linear in $\mathbf{v}$, and hence

---

[29] For the attentive reader who has noticed the difference between the negative sign in the expression for $U_{\rm cf}$, and the positive sign before the similar second term in Eq. (3.44): as was already discussed in Chapter 3, it is due to the difference of assumptions. In the planetary problem, even though the angular momentum $\mathbf{L}$ and hence its component L_z are fixed, the corresponding angular velocity $\dot{\varphi}$ is not. On the opposite, in our current discussion, the angular velocity $\boldsymbol{\omega}$ of the reference frame is assumed to be fixed, i.e. is independent of $\mathbf{r}$ and $\mathbf{v}$.

[30] Here $\partial L/\partial\mathbf{v}$ is just a shorthand for a vector with Cartesian components $\partial L/\partial v_j$. In a more formal language, this is the gradient of the scalar function L in the velocity space.

[31] A very similar situation arises at the motion of a particle with electric charge q in magnetic field $\mathcal{B}$. In that case, the role of the additional term $\boldsymbol{\mathcal{p}} - \mathbf{p} = m\boldsymbol{\omega}\times\mathbf{r}$ is played by the product $q\mathcal{A}$, where $\mathcal{A}$ is the vector potential of the field $\mathcal{B} = \nabla\times\mathcal{A}$ – see, e.g., EM Sec. 9.7, and in particular Eqs. (9.183) and (9.192).

[32] Please note the last form of Eq. (99), which shows the physical sense of the Hamiltonian function of a particle in the rotating frame very clearly, as the sum of its kinetic energy (as measured in the moving frame), and the effective potential energy (96b), including that of the centrifugal "force".

is not a quadratic-homogeneous function of this generalized velocity. The difference between these functions may be represented as

$$E - H = m\mathbf{v}\cdot(\boldsymbol{\omega}\times\mathbf{r}) + m(\boldsymbol{\omega}\times\mathbf{r})^2 \equiv m(\mathbf{v}+\boldsymbol{\omega}\times\mathbf{r})\cdot(\boldsymbol{\omega}\times\mathbf{r}) = m\mathbf{v}\big|_{\text{in lab}}\cdot(\boldsymbol{\omega}\times\mathbf{r}). \tag{4.101}$$

Now using the operand rotation rule again, we may transform this expression into a simpler form:[33]

E – H at rotation

$$\boxed{E - H = \boldsymbol{\omega}\cdot\left(\mathbf{r}\times m\mathbf{v}\big|_{\text{in lab}}\right) = \boldsymbol{\omega}\cdot\left(\mathbf{r}\times\mathbf{p}\right) = \boldsymbol{\omega}\cdot\mathbf{L}\big|_{\text{in lab}}}. \tag{4.102}$$

As a sanity check, let us apply this general expression to the particular case of our testbed problem – see Fig. 2.1. In this case, the vector $\boldsymbol{\omega}$ is aligned with the z-axis, so that of all Cartesian components of the vector $\mathbf{L}$, only the component L_z is important for the scalar product in Eq. (102). This component evidently equals $\omega I_z = \omega m\rho^2 = \omega m(R\sin\theta)^2$, so that

$$E - H = m\omega^2 R^2 \sin^2\theta, \tag{4.103}$$

i.e. the same result that follows from the subtraction of Eqs. (2.40) and (2.41).

4.7. Exercise problems

4.1. Calculate the principal moments of inertia for the following uniform rigid bodies:

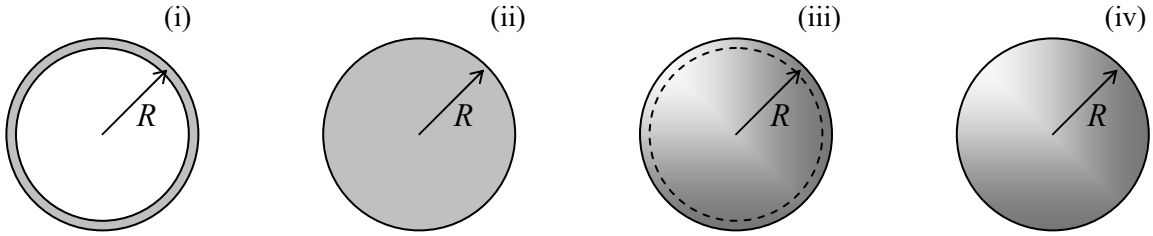

(i) a thin, planar, round hoop, (ii) a flat round disk, (iii) a thin spherical shell, and (iv) a solid sphere.

Compare the results, assuming that all the bodies have the same radius R and mass M, and give an interpretation of their difference.

4.2. Calculate the principal moments of inertia for the rigid bodies shown in the figure below:

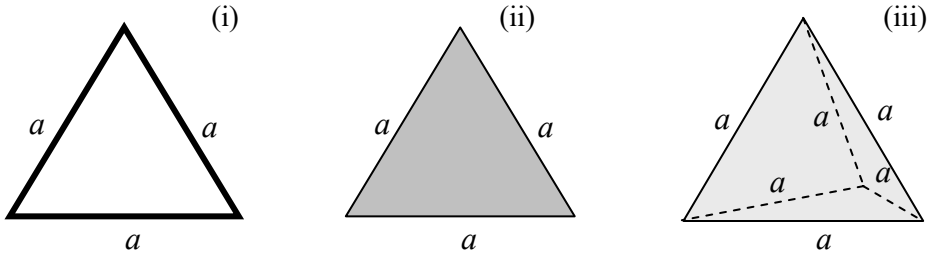

(i) an equilateral triangle made of thin rods with a constant linear mass density μ,
(ii) a thin plate in the shape of an equilateral triangle, with a constant areal mass density σ, and
(iii) a tetrahedron with a constant bulk mass density ρ.

[33] Note that by the definition (1.36), the angular momenta $\mathbf{L}$ of particles merely add up. As a result, the final form of Eq. (102) is valid for an arbitrary system of particles.

Assuming that the total mass of the three bodies is the same, compare the results and give an interpretation of their difference.

4.3. Calculate the principal moments of inertia of a thin uniform plate cut in the form of a right triangle with two $\pi/4$ angles.

4.4. Prove that Eqs. (34)-(36) are valid for the rotation of a rigid body about the fixed z-axis, even if it does not pass through its center of mass.

4.5. Calculate the kinetic energy of a right circular cone with height H, base radius R, and a constant mass density ρ, that rolls over a horizontal surface without slippage, making f turns per second about the vertical axis – see the figure on the right.

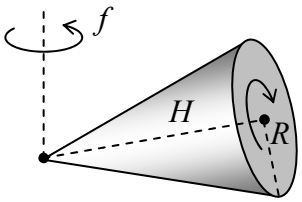

4.6. External forces exerted on a rigid body rotating with an angular velocity $\boldsymbol{\omega}$, have zero vector sum but a non-vanishing net torque $\boldsymbol{\tau}$ about its center of mass.

(i) Calculate the work of the forces on the body per unit time, i.e. their instantaneous power.

(ii) Prove that the same result is valid for a body rotating about a fixed axis and the torque's component along this axis.

(iii) Use the last result to prove that at negligible friction, the gear assembly shown in the figure on the right distributes the external torque, applied to its satellite-carrier axis to rotate it about the common axis of two axle shafts, equally to both shafts, even if they rotate with different angular velocities.

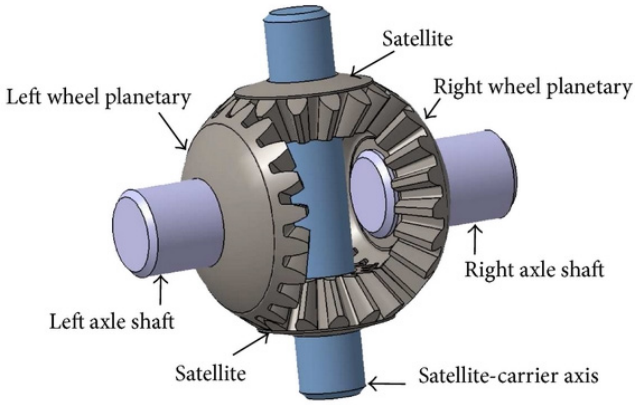

Figure from G. Antoni, *Sci. World J.*, **2014**, 523281 (2014), adapted with permission. Both satellite gears may rotate freely about their common carrier axis.

4.7. The end of a uniform thin rod of length $2l$ and mass m, initially at rest, is hit by a bullet of mass m', flying with a velocity $\mathbf{v}_0$ perpendicular to the rod (see the figure on the right), which gets stuck in it. Use two different approaches to calculate the velocity of the opposite end of the rod right after the collision.

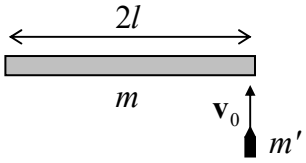

4.8. A ball of radius R, initially at rest on a horizontal surface, is hit with a billiard cue in the horizontal direction, at height h above the table – see the figure on the right. Using the Coulomb approximation for the kinetic friction force between the ball and the surface ($|F_f| = \mu N$), calculate the final linear velocity of the rolling ball as a function of h. Would it matter if the hit point is shifted horizontally (normally to the plane of the drawing)?

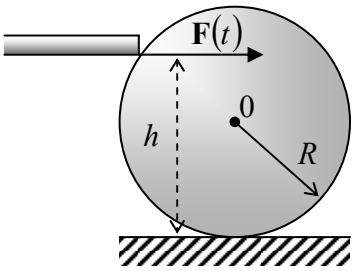

Hint: As in most solid body collision problems, during the short

time of the cue hit, all other forces exerted on the ball may be considered negligibly small.

4.9. A round cylinder of radius R and mass M may roll, without slippage, over a horizontal surface. The mass density distribution inside the cylinder is not uniform, so its center of mass is at some distance $l \neq 0$ from its geometrical axis, and the moment of inertia I (for rotation about the axis parallel to the symmetry axis but passing through the center of mass) is different from $MR^2/2$, where M is the cylinder's mass. Derive the equation of motion of the cylinder under the effect of the uniform vertical gravity field, and use it to calculate the frequency of small oscillations of the cylinder near its stable equilibrium position.

4.10. A body may rotate about a fixed horizontal axis – see Fig. 5. Find the frequency of its small oscillations in a uniform gravity field, as a function of the distance l of the axis from the body's center of mass 0, and analyze the result.

4.11. Calculate the frequency, and sketch the mode of oscillations[34] of a round uniform cylinder of radius R and the mass M, that may roll, without slippage, on a horizontal surface of a block of mass M'. The block, in turn, may move in the same direction, without friction, on an immobile horizontal surface, being connected to it with an elastic spring – see the figure on the right.

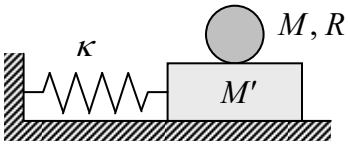

4.12. A thin uniform bar of mass M and length l is hung on a light thread of length l' (like a "chime" bell – see the figure on the right). Derive the equations of the system's motion within a vertical plane passing through the suspension point.

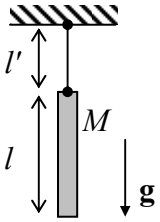

4.13. A uniform round solid cylinder of mass M can roll, without slippage, over a concave round cylindrical surface of a block of mass M', in a uniform gravity field – see the figure on the right. The block can slide without friction on a horizontal surface. Using the Lagrangian formalism,

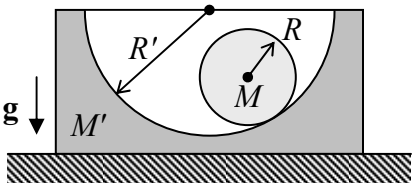

(i) find the frequency of small oscillations of the system near the equilibrium, and
(ii) sketch the oscillation mode for the particular case $M' = M$, $R' = 2R$.

4.14. A uniform solid hemisphere of radius R and mass M is placed on a horizontal surface – see the figure on the right. Find the frequency of its small oscillations within a vertical plane, for two ultimate cases:

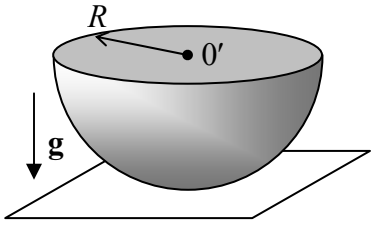

(i) there is *no friction* between the sphere and the horizontal surface;
(ii) the static friction between them is so strong that there is *no slippage*.

[34] The term *mode* usually refers to the spatial pattern of oscillations; it will be much discussed in later chapters.

4.15. For the "sliding ladder" problem started in Sec. 3 (see Fig. 7), find the critical value α_c of the angle α at that the ladder loses its contact with the vertical wall, assuming that it starts sliding from the vertical position, with a negligible initial velocity.

4.16. Six similar, uniform rods of length l and mass m are connected by light joints so that they may rotate, without friction, versus each other, forming a planar polygon. Initially, the polygon was at rest, and had the correct hexagon shape – see the figure on the right. Suddenly, an external force **F** is applied to the middle of one rod, in the direction of the hexagon's symmetry center. Calculate the accelerations: of the rod to which the force is applied (a), and of the opposite rod (a'), immediately after the application of the force.

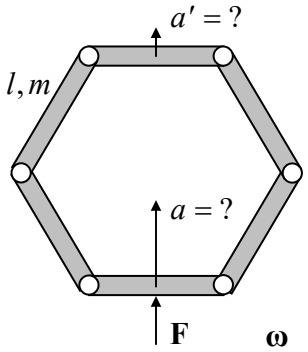

4.17. A rectangular cuboid (parallelepiped) with sides a_1, a_2, and a_3, made of a material with a constant mass density ρ, is rotated with a constant angular velocity ω about one of its space diagonals – see the figure on the right. Calculate the torque τ necessary to sustain this rotation.

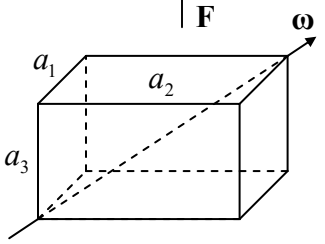

4.18. A uniform round ball rolls, without slippage, over a "turntable": a horizontal plane rotated about a vertical axis with a time-independent angular velocity Ω. Derive a self-consistent equation of motion of the ball's center, and discuss its solutions.

4.19. Calculate the free precession frequency of a uniform thin round disk rotating with an angular velocity ω about a direction very close to its symmetry axis, from the point of view of:

(i) an observer rotating with the disk, and
(ii) a lab-based observer.

4.20. Use the Euler equations to prove the fact mentioned in Sec. 4: free rotation of an arbitrary body ("asymmetric top") about its principal axes with the smallest and largest moments of inertia is stable, while that about the intermediate-I_j axis is not. Illustrate the same fact using the Poinsot construction.

4.21. Give an interpretation of the torque-induced precession, that would explain its direction, by using a simple system exhibiting this effect, as a model.

4.22. One end of a light shaft of length l is firmly attached to the center of a thin uniform solid disk of radius R and mass M, whose plane is perpendicular to the shaft. Another end of the shaft is attached to a vertical axis (see the figure on the right) so that the shaft may rotate about the axis without friction. The disk rolls, without slippage, over a horizontal surface so that the whole system rotates about the vertical axis with a constant angular velocity ω. Calculate the (vertical) supporting force N exerted on the disk by the surface.

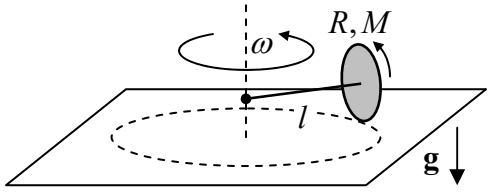

4.23. A coin of radius r is rolled over a horizontal surface, without slippage. Due to its tilt θ, it rolls around a circle of radius R – see the figure on the right. Modeling the coin as a very thin round disk, calculate the time period of its motion around the circle.

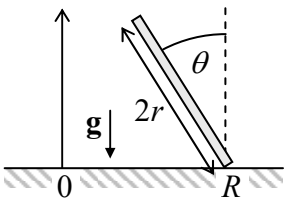

4.24. Solve the previous problem in the limit when the coin tilt angle θ and the ratio r/R are small, by simpler means, using

(i) an inertial ("lab") reference frame, and

(ii) the non-inertial reference frame moving with the coin's center but not rotating with it.

4.25. A symmetric top on a point support (as shown see, e.g., Fig. 9), rotating around its symmetry axis with a high angular velocity ω_{rot}, is subjected to not only its weight $M\mathbf{g}$ but also an additional force also applied to the top's center of mass, with its vector rotating in the horizontal plane with a constant angular velocity $\omega << \omega_{rot}$. Derive the system of equations describing the top's motion. Analyze their solution for the simplest case when ω is exactly equal to the frequency (72) of the torque-induced precession in the gravity field alone.

4.26. Analyze the effect of small friction on a fast rotation of a symmetric top around its axis, using a simple model in that the lower end of the body is a right cylinder of radius R.

4.27. An air-filled balloon is placed inside a water-filled container, which moves by inertia in free space, at negligible gravity. Suddenly, force $\mathbf{F}$ is applied to the container, pointing in a certain direction. What direction does the balloon move relative to the container?

4.28. Two planets are in a circular orbit around their common center of mass. Calculate the effective potential energy of a much lighter body (say, a spacecraft) rotating with the same angular velocity, on the line connecting the planets. Sketch the radial dependence of U_{ef} and find out the number of so-called *Lagrange points* in which the potential energy has local maxima. Calculate their position explicitly in the limit when one of the planets is much more massive than the other one.

4.29. Besides the three Lagrange points L_1, L_2, and L_3 discussed in the previous problem, which are located on the line connecting two planets on circular orbits about their mutual center of mass, there are two off-line points L_4 and L_5 – both within the plane of the planets' rotation. Calculate their positions.

4.30. The following simple problem may give additional clarity to the physics of the Coriolis "force". A bead of mass m may slide, without friction, along a straight rod that is rotated within a horizontal plane with a constant angular velocity ω – see the figure on the right. Calculate the bead's acceleration and the force $\mathbf{N}$ exerted on it by the rod, in:

(i) an inertial ("lab") reference frame, and

(ii) the non-inertial reference frame rotating with the rod (but not moving with the bead),

and compare the results.

4.31. Analyze the dynamics of the famous *Foucault pendulum* used for spectacular demonstrations of the Earth's rotation. In particular, calculate the angular velocity of the rotation of its

oscillation plane relative to the Earth's surface, at a location with a polar angle ("colatitude") Θ. Assume that the pendulum oscillation amplitude is small enough to neglect nonlinear effects and that its oscillation period is much shorter than 24 hours.

4.32. A small body is dropped down to the surface of Earth from a height $h << R_E$, without initial velocity. Calculate the magnitude and direction of its deviation from the vertical, due to the Earth's rotation. Estimate the effect's magnitude for a body dropped from the Empire State Building.

4.33. Calculate the height of solar tides on a large ocean, using the following simplifying assumptions: the tide period (½ of the Earth's day) is much longer than the period of all ocean waves, the Earth (of mass M_E) is a sphere of radius R_E, and its distance r_S from the Sun (of mass M_S) is constant and much larger than R_E.

4.34. A satellite is on a circular orbit of radius R, around the Earth. Neglecting the gravity field of the satellite,

(i) write the equations of motion of a small body as observed from the satellite and simplify them for the case when the motion is limited to the satellite's close vicinity;

(ii) use these equations to prove that a body may be placed on an elliptical trajectory around the satellite's center of mass, within its plane of rotation around the Earth. Calculate the ellipse's orientation and eccentricity.

4.35. A non-spherical shape of an artificial satellite may ensure its stable angular orientation relative to the Earth's surface, advantageous for many practical goals. By modeling a satellite as a strongly elongated, axially-symmetric body moving around the Earth on a circular orbit of radius R, find its stable orientation.

4.36. A rigid, straight, uniform rod of length l, with the lower end on a pivot, falls in a uniform gravity field – see the figure on the right. Neglecting friction, calculate the distribution of the bending torque τ along its length, and analyze the result.

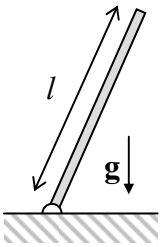

Hint: As will be discussed in detail in Sec. 7.5 of the lecture notes, the bending torque's gradient along the rod's length is equal to the rod-normal ("shear") component of the total force between two parts of the rod, mentally separated by its cross-section.

4.37. Let **r** be the radius vector of a particle, as measured in a possibly non-inertial but certainly non-rotating reference frame. Taking its Cartesian components for the generalized coordinates, calculate the corresponding generalized momentum $\boldsymbol{p}$ of the particle and its Hamiltonian function H. Compare $\boldsymbol{p}$ with $m\mathbf{v}$, and H with the particle's energy E. Derive the Lagrangian equation of motion in this approach, and compare it with Eq. (92).

Chapter 5. Oscillations

In this course, oscillations and waves are discussed in detail, because of their importance for fundamental and applied physics. This chapter starts with a discussion of the harmonic oscillator, whose differential equation of motion is linear and hence allows the full analytical solution, and then proceeds to so-called "nonlinear" and "parametric" systems whose dynamics may be only explored by either approximate analytical or numerical methods.

5.1. Free and forced oscillations

In Sec. 3.2 we briefly discussed oscillations in a keystone Hamiltonian system – a 1D *harmonic oscillator* described by a very simple Lagrangian[1]

$$L \equiv T(\dot{q}) - U(q) = \frac{m}{2}\dot{q}^2 - \frac{\kappa}{2}q^2, \tag{5.1}$$

whose Lagrange equation of motion,[2]

Harmonic oscillator: equation

$$m\ddot{q} + \kappa q = 0, \qquad \text{i.e. } \ddot{q} + \omega_0^2 q = 0, \qquad \text{with } \omega_0^2 \equiv \frac{\kappa}{m} \geq 0, \tag{5.2}$$

is a *linear homogeneous* differential equation. Its general solution is given by Eq. (3.16), which is frequently recast into another, amplitude-phase form:

Harmonic oscillator: motion

$$q(t) = u\cos\omega_0 t + v\sin\omega_0 t \equiv A\cos(\omega_0 t - \varphi), \tag{5.3a}$$

where A is the *amplitude* and φ is the *phase* of the oscillations, which are determined by the initial conditions. Mathematically, it is frequently easier to work with sinusoidal functions as complex exponents, by rewriting the last form of Eq. (3a) in one more form:[3]

$$q(t) = \mathrm{Re}\left[Ae^{-i(\omega_0 t - \varphi)}\right] = \mathrm{Re}\left[ae^{-i\omega_0 t}\right], \tag{5.3b}$$

Real and complex amplitudes

where a is the *complex amplitude* of the oscillations:

$$a \equiv Ae^{i\varphi}, \qquad |a| = A, \qquad \mathrm{Re}\,a = A\cos\varphi = u, \qquad \mathrm{Im}\,a = A\sin\varphi = v. \tag{5.4}$$

For an autonomous, Hamiltonian oscillator, Eqs. (3) give the full classical description of its dynamics. However, it is important to understand that this *free-oscillation* solution, with a constant amplitude A,

[1] For the notation brevity, in this chapter, I will drop indices "ef" in the energy components T and U, and in parameters like m, κ, etc. However, the reader should still remember that T and U do not necessarily coincide with the actual kinetic and potential energies (even if those energies may be uniquely identified) – see Sec. 3.1.

[2] ω_0 is usually called the *own frequency* of the oscillator. In quantum mechanics, the Germanized version of the same term, *eigenfrequency*, is used more. In this series, I will use either of the terms, depending on the context.

[3] Note that this is the so-called *physics convention*. Most engineering texts use the opposite sign in the imaginary exponent, $\exp\{-i\omega t\} \to \exp\{i\omega t\}$, with the corresponding sign implications for intermediate formulas but identical final results for real variables.

© K. Likharev

means the conservation of the energy $E \equiv T + U = \kappa A^2/2$ of the oscillator. If its energy changes for any reason, the description needs to be generalized.

First of all, if the energy leaks out of the oscillator to its environment (the effect usually called *energy dissipation*), the free oscillations decay with time. The simplest model of this effect is represented by an additional *linear drag* (or "kinematic friction") *force*, proportional to the generalized velocity and directed opposite to it:

$$F_v = -\eta \dot{q}\,, \tag{5.5}$$

where constant η is called the *drag coefficient*.[4] The inclusion of this force modifies the equation of motion (2) to become

$$m\ddot{q} + \eta\dot{q} + \kappa q = 0\,. \tag{5.6a}$$

This equation is frequently rewritten in the form

$$\ddot{q} + 2\delta\dot{q} + \omega_0^2 q = 0, \qquad \text{with } \delta \equiv \frac{\eta}{2m}, \tag{5.6b}$$

Free oscillator with damping

where the parameter δ is called the *damping coefficient* (or just "damping"). Note that Eq. (6) is still a linear homogeneous second-order differential equation, and its general solution still has the form of the sum (3.13) of two exponents of the type $\exp\{\lambda t\}$, with arbitrary pre-exponential coefficients. Plugging such an exponent into Eq. (6), we get the following algebraic characteristic equation for λ:

$$\lambda^2 + 2\delta\lambda + \omega_0^2 = 0. \tag{5.7}$$

Solving this quadratic equation, we get

$$\lambda_\pm = -\delta \pm i\omega_0', \qquad \text{where } \omega_0' \equiv \left(\omega_0^2 - \delta^2\right)^{1/2}, \tag{5.8}$$

so for not very high damping ($\delta < \omega_0$) we get the following generalization of Eq. (3):[5]

$$q_{\text{free}}(t) = c_+ e^{\lambda_+ t} + c_- e^{\lambda_- t} = \left(u_0 \cos\omega_0' t + v_0 \sin\omega_0' t\right) e^{-\delta t} = A_0 e^{-\delta t}\cos\left(\omega_0' t - \varphi_0\right). \tag{5.9}$$

The result shows that, besides a certain correction to the free oscillation frequency (which is very small in the most interesting *low damping limit*, $\delta << \omega_0$), the energy dissipation leads to an exponential decay of oscillation amplitude with the time constant $\tau = 1/\delta$:

---

[4] Here Eq. (5) is treated as a phenomenological model, but in statistical mechanics, such dissipative term may be *derived* as an average force exerted upon a system by its environment, at very general assumptions. As will be discussed in detail later in this series (QM Chapter 7 and SM Chapter 5), due to the numerous degrees of freedom of a typical environment (think about the molecules of air surrounding a macroscopic pendulum), its force also has a random component; as a result, the *dissipation* is fundamentally related to *fluctuations*. The latter effect may be neglected (as it is in this course) only if the oscillator's energy E is much higher than the energy scale of its random fluctuations – in the thermal equilibrium at temperature T, the larger of $k_B T$ and $\hbar\omega_0/2$.

[5] Systems with high damping ($\delta > \omega_0$) can hardly be called oscillators, and though they are used in engineering and physical experiment (e.g., for shock and sound isolation), due to the lack of time/space, for their detailed discussion I have to refer the interested reader to special literature – see, e.g., C. Harris and A. Piersol, *Shock and Vibration Handbook*, 5th ed., McGraw Hill, 2002. Let me only note that according to Eq. (8), the dynamics of systems with very high damping ($\delta >> \omega_0$) has two very different time scales: a relatively short "momentum relaxation time" $1/|\lambda_-| \approx 1/2\delta = m/\eta$, and a much longer "coordinate relaxation time" $1/|\lambda_+| \approx 2\delta/\omega_0^2 = \eta/\kappa$.

Decaying free oscillations

$$A = A_0 e^{-t/\tau}, \quad \text{where } \tau \equiv \frac{1}{\delta} = \frac{2m}{\eta}. \tag{5.10}$$

A very popular dimensionless measure of damping is the so-called *quality factor* Q (or just the *Q-factor*) which is defined as $\omega_0/2\delta$, and may be rewritten in several other useful forms:

$$Q \equiv \frac{\omega_0}{2\delta} = \frac{m\omega_0}{\eta} = \frac{(m\kappa)^{1/2}}{\eta} = \pi\frac{\tau}{\mathcal{T}} = \frac{\omega_0\tau}{2}, \tag{5.11}$$

where $\mathcal{T} \equiv 2\pi/\omega_0$ is the oscillation period in the absence of damping – see Eq. (3.29). Since the oscillation energy E is proportional to A^2, i.e. decays as $\exp\{-2t/\tau\}$, i.e. with the time constant $\tau/2$, the last form of Eq. (11) may be used to rewrite the Q-factor in one more form:

$$Q = \omega_0 \frac{E}{(-\dot{E})} \equiv \omega_0 \frac{E}{\mathcal{P}}, \tag{5.12}$$

where $\mathcal{P}$ is the energy dissipation rate. (Other practical ways to measure Q will be discussed below.) The range of Q-factors of mechanical oscillators is very broad, from $Q \sim 10$ for a human leg (with relaxed muscles), to $Q \sim 10^4$ of the quartz crystals used in electronic clocks and watches, and all the way up to $Q > 10^{10}$ for nanoparticles suspended (by electrostatic forces) in high vacuum.

In contrast to the decaying free oscillations, *forced oscillations* induced by an external force $F(t)$, may maintain their amplitude (and hence energy) infinitely, even at non-zero damping. This process may be described using a still linear but now *inhomogeneous* differential equation

$$m\ddot{q} + \eta\dot{q} + \kappa q = F(t), \tag{5.13a}$$

or, more usually, the following generalization of Eq. (6b):

Forced oscillator with damping

$$\ddot{q} + 2\delta\dot{q} + \omega_0^2 q = f(t), \quad \text{where } f(t) \equiv F(t)/m. \tag{5.13b}$$

For a mechanical linear, dissipative 1D oscillator (6), under the effect of an additional external force $F(t)$, Eq. (13a) is just an expression of the 2nd Newton law. However, according to Eq. (1.41), Eq. (13) is valid for any dissipative, *linear*[6] 1D system whose Gibbs potential energy (1.39) has the form $U_G(q, t) = \kappa q^2/2 - F(t)q$.

The forced-oscillation solutions to Eq. (13) may be analyzed by two mathematically equivalent methods whose relative convenience depends on the character of function $f(t)$.

(i) *Frequency domain.* Representing the function $f(t)$ as a Fourier sum of sinusoidal harmonics:[7]

$$f(t) = \sum_{\omega} f_\omega e^{-i\omega t}, \tag{5.14}$$

and using the linearity of Eq. (13), we may represent its general solution as a sum of the decaying free oscillations (9) with the frequency ω_0', that are independent of the function $f(t)$, and forced oscillations due to each of the Fourier components of the force:[8]

[6] This is a very unfortunate, but common jargon, meaning "the system described by linear equations of motion".

[7] Here, in contrast to Eq. (3b), we may drop the operator Re, assuming that $f_{-\omega} = f_\omega^*$, so that the imaginary components of the sum compensate for each other.

$$q(t) = q_{\text{free}}(t) + q_{\text{forced}}(t), \quad q_{\text{forced}}(t) = \sum_{\omega} a_{\omega} e^{-i\omega t}. \tag{5.15}$$

General solution of Eq. (13)

Plugging Eq. (15) into Eq. (13), and requiring the factors before each $e^{-i\omega t}$ on both sides to be equal, we get

$$a_{\omega} = f_{\omega}\chi(\omega), \tag{5.16}$$

where the complex function $\chi(\omega)$, in our particular case equal to

$$\chi(\omega) = \frac{1}{\left(\omega_0^2 - \omega^2\right) - 2i\omega\delta}, \tag{5.17}$$

is called either the *response function* or (especially for non-mechanical oscillators) the *generalized susceptibility*. From here, and Eq. (4), the amplitude of the oscillations under the effect of a sinusoidal force is

$$A_{\omega} \equiv |a_{\omega}| = |f_{\omega}||\chi(\omega)|, \qquad \text{with } |\chi(\omega)| = \frac{1}{\left[(\omega_0^2 - \omega^2)^2 + (2\omega\delta)^2\right]^{1/2}}. \tag{5.18}$$

Forced oscillations

This formula describes, in particular, an increase of the oscillation amplitude A_{ω} at $\omega \to \omega_0$ – see the left panel of Fig. 1. In particular, at the exact equality of these two frequencies,

$$|\chi(\omega)|_{\omega=\omega_0} = \frac{1}{2\omega_0\delta}, \tag{5.19}$$

so, according to Eq. (11), the ratio of the response magnitudes at $\omega = \omega_0$ and $\omega = 0$ ($|\chi(\omega)|_{\omega=0} = 1/\omega_0^2$) is exactly equal to the Q-factor of the oscillator. Thus, the response increase is especially strong in the low-damping limit ($\delta << \omega_0$, i.e. $Q >> 1$); moreover, at $Q \to \infty$ and $\omega \to \omega_0$, the response diverges. (This mathematical fact is very useful for the methods to be discussed later in this section.) This is the classical description of the famous phenomenon of *resonance*, so ubiquitous in physics.

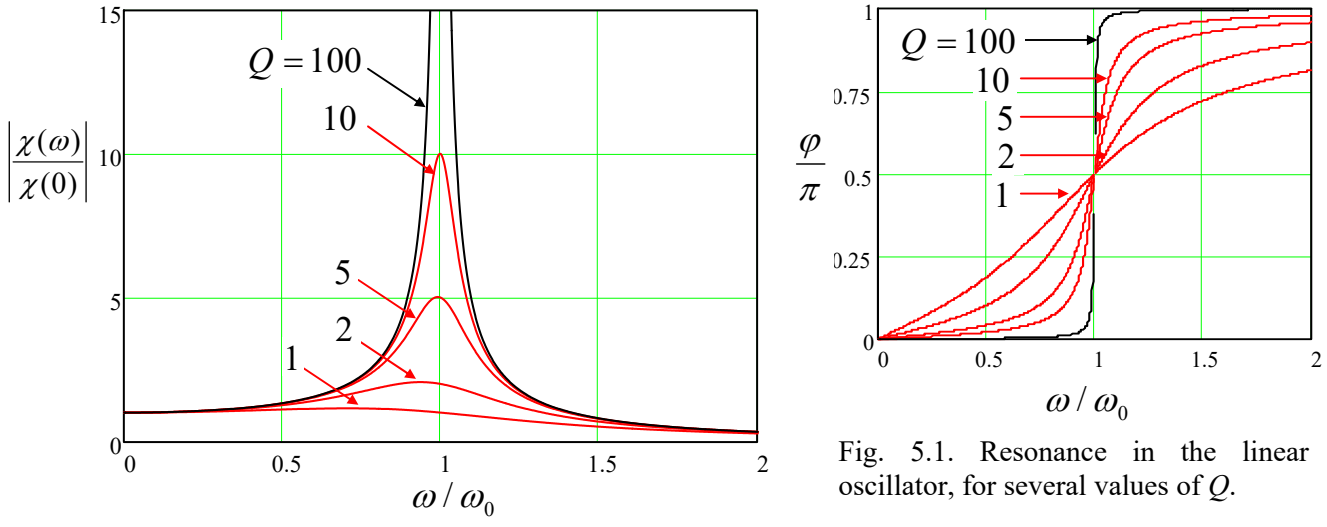

Fig. 5.1. Resonance in the linear oscillator, for several values of Q.

[8] In physics, this mathematical property of linear equations is frequently called the *linear superposition principle*.

Due to the increase of the resonance peak height, its width is inversely proportional to Q. Quantitatively, in the most interesting low-damping limit, i.e. at $Q >> 1$, the reciprocal Q-factor gives the normalized value of the so-called *full-width at half-maximum* (FWHM) of the resonance curve:[9]

$$\frac{\Delta\omega}{\omega_0} = \frac{1}{Q}. \tag{5.20}$$

Indeed, this $\Delta\omega$ is defined as the difference $(\omega_+ - \omega_-)$ between such two values of ω at that the modulus squared of the oscillator response function, $|\chi(\omega)|^2$ (which is proportional to the oscillation energy), equals a half of its resonance value (19). In the low damping limit, these points are very close to ω_0, so in the linear approximation in $|\omega - \omega_0| << \omega_0$, we may write $(\omega_0^2 - \omega^2) \equiv -(\omega+\omega_0)(\omega - \omega_0) \approx -2\omega\xi \approx -2\omega_0\xi$, where

$$\xi \equiv \omega - \omega_0 \tag{5.21}$$

is a convenient parameter called *detuning*, which will be repeatedly used later in this chapter, and beyond it. In this approximation, the second of Eqs. (18) is reduced to[10]

$$|\chi(\omega)|^2 = \frac{1}{4\omega_0^2\left(\delta^2 + \xi^2\right)}. \tag{5.22}$$

As a result, the points $\omega_\pm$ correspond to $\xi^2 = \delta^2$, i.e. $\omega_\pm = \omega_0 \pm \delta = \omega_0(1 \pm 1/2Q)$, so $\Delta\omega \equiv \omega_+ - \omega_- = \omega_0/Q$, thus proving Eq. (20).

(ii) *Time domain.* Returning to an arbitrary external force $f(t)$, one may argue that Eqs. (9), (15)-(17) provide a full solution of the forced oscillation problem even in this general case. This is formally correct, but this solution may be very inconvenient if the external force is far from a sinusoidal function of time, especially if it is not periodic at all. In this case, we should first calculate the complex amplitudes f_ω participating in the Fourier sum (14). In the general case of a non-periodic $f(t)$, this is actually the Fourier integral,[11]

$$f(t) = \int_{-\infty}^{+\infty} f_\omega e^{-i\omega t}\, dt, \tag{5.23}$$

so f_ω should be calculated using the reciprocal Fourier transform,

$$f_\omega = \frac{1}{2\pi}\int_{-\infty}^{+\infty} f(t')e^{i\omega t'}\, dt'. \tag{5.24}$$

Now we may use Eq. (16) for each Fourier component of the resulting forced oscillations, and rewrite the last of Eqs. (15) as

[9] Note that the phase shift $\varphi \equiv \arg[\chi(\omega)]$ between the oscillations and the external force (see the right panel in Fig. 1) makes its steepest change, by $\pi/2$, within the same frequency interval $\Delta\omega$.

[10] Such function of frequency may be met in many branches of science, frequently under special names, including the "Cauchy distribution", "the Lorentz function" (or "Lorentzian line", or "Lorentzian distribution"), "the Breit-Wigner function" (or "the Breit-Wigner distribution"), etc.

[11] Let me hope that the reader knows that Eq. (23) may be used for periodic functions as well; in such a case, f_ω is a set of equidistant delta functions. (A reminder of the basic properties of the Dirac δ-function may be found, for example, in MA Sec. 14.)

$$q_{\text{forced}}(t) = \int_{-\infty}^{+\infty} a_\omega e^{-i\omega t} d\omega = \int_{-\infty}^{+\infty} \chi(\omega) f_\omega e^{-i\omega t} d\omega = \int_{-\infty}^{+\infty} d\omega\, \chi(\omega) \frac{1}{2\pi} \int_{-\infty}^{+\infty} dt'\, f(t') e^{i\omega(t'-t)}$$
$$\equiv \int_{-\infty}^{+\infty} dt'\, f(t') \left[\frac{1}{2\pi} \int_{-\infty}^{+\infty} d\omega\, \chi(\omega) e^{i\omega(t'-t)} \right], \tag{5.25}$$

with the response function $\chi(\omega)$ given, in our case, by Eq. (17). Besides requiring two integrations, Eq. (25) is conceptually uncomforting: it seems to indicate that the oscillator's coordinate at time t depends not only on the external force exerted at earlier times $t' < t$, but also at future times. This would contradict one of the most fundamental principles of physics (and indeed, science as a whole), *causality*: no effect may precede its cause.

Fortunately, a straightforward calculation (left for the reader's exercise) shows that the response function (17) satisfies the following rule:[12]

$$\int_{-\infty}^{+\infty} \chi(\omega) e^{-i\omega\tau} d\omega = 0, \qquad \text{for } \tau < 0. \tag{5.26}$$

This fact allows the last form of Eq. (25) to be rewritten in either of the following equivalent forms:

$$q_{\text{forced}}(t) = \int_{-\infty}^{t} f(t') G(t-t') dt' \equiv \int_{0}^{\infty} f(t-\tau) G(\tau) d\tau, \tag{5.27}$$

Linear system's response

where $G(\tau)$, defined as the Fourier transform of the response function,

$$G(\tau) \equiv \frac{1}{2\pi} \int_{-\infty}^{+\infty} \chi(\omega) e^{-i\omega\tau} d\omega, \tag{5.28}$$

Temporal Green's function

is called the (*temporal*) *Green's function* of the system. According to Eq. (26), $G(\tau) = 0$ for all $\tau < 0$.

While the second form of Eq. (27) is frequently more convenient for calculations, its first form is more suitable for physical interpretation of the Green's function. Indeed, let us consider the particular case when the force is a delta function

$$f(t) = \delta(t-t'), \qquad \text{with } t' < t, \ \text{ i.e. } \tau \equiv t - t' > 0, \tag{5.29}$$

representing an ultimately short pulse at the moment t', with unit "area" $\int f(t)dt$. Substituting Eq. (29a) into Eq. (27),[13] we get

$$q(t) = G(t-t'). \tag{5.30}$$

Thus Green's function $G(t - t')$ is just the oscillator's response, as measured at time t, to a short force pulse of unit "area", exerted at time t'. Hence Eq. (27) expresses the linear superposition principle in the time domain: the full effect of the force $f(t)$ on a linear system is a sum of the effects of short pulses of duration dt' and magnitude $f(t')$, each with its own "weight" $G(t - t')$ – see Fig. 2.

[12] Eq. (26) is true for any linear physical system in which $f(t)$ represents a cause, and $q(t)$ its effect. Following tradition, I discuss the frequency-domain expression of this causality relation (called the *Kramers-Kronig relations*) in the *Classical Electrodynamics* part of this lecture series – see EM Sec. 7.2.

[13] Technically, for this integration, t' in Eq. (27) should be temporarily replaced with another letter, say t''.

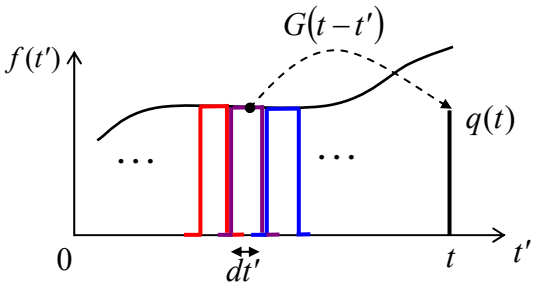

Fig. 5.2. A schematic, finite-interval representation of a force $f(t)$ as a sum of short pulses at all times $t' < t$, and their contributions to the linear system's response $q(t)$, as given by Eq. (27).

This picture may be used for the calculation of Green's function for our particular system. Indeed, Eqs. (29)-(30) mean that $G(\tau)$ is just the solution of the differential equation of motion of the system, in our case, Eq. (13), with the replacement $t \to \tau$, and a δ-functional right-hand side:

$$\frac{d^2G(\tau)}{d\tau^2} + 2\delta\frac{dG(\tau)}{d\tau} + \omega_0^2 G(\tau) = \delta(\tau). \tag{5.31}$$

Since Eqs. (27) describes only the second term in Eq. (15), i.e. only the forced, rather than free oscillations, we have to exclude the latter by solving Eq. (31) with zero initial conditions:

$$G(-0) = \frac{dG}{d\tau}(-0) = 0, \tag{5.32}$$

where $\tau = -0$ means the instant immediately preceding $\tau = 0$.

This problem may be simplified even further. Let us integrate both sides of Eq. (31) over an infinitesimal interval including the origin, e.g. $[-d\tau/2, +d\tau/2]$, and then follow the limit $d\tau \to 0$. Since Green's function has to be continuous because of its physical sense as the (generalized) coordinate, all terms on the left-hand side but the first one vanish, while the first term yields $dG/d\tau\big|_{+0} - dG/d\tau\big|_{-0}$. Due to the second of Eqs. (32), the last of these two derivatives has to equal zero, while the right-hand side of Eq. (31) yields 1 upon the integration. Thus, the function $G(\tau)$ may be calculated for $\tau > 0$ (i.e. for all times when it is different from zero) by solving the *homogeneous* version of the system's equation of motion for $\tau > 0$, with the following special initial conditions:

$$G(0) = 0, \qquad \frac{dG}{d\tau}(0) = 1. \tag{5.33}$$

This approach gives us a convenient way for the calculation of Green's functions of linear systems. In particular for the oscillator with not very high damping ($\delta < \omega_0$, i.e. $Q > ½$), imposing the boundary conditions (33) on the homogeneous equation's solution (9), we immediately get

Oscillator's Green's function

$$G(\tau) = \frac{1}{\omega_0'} e^{-\delta\tau} \sin \omega_0' \tau. \tag{5.34}$$

(The same result may be obtained directly from Eq. (28) with the response function $\chi(\omega)$ given by Eq. (19). This way is, however, a little bit more cumbersome, and is left for the reader's exercise.)

Relations (27) and (34) provide a very convenient recipe for solving many forced oscillations problems. As a very simple example, let us calculate the transient process in an oscillator under the effect of a constant force being turned on at $t = 0$, i.e. proportional to the Heaviside step function:

$$f(t) = f_0\theta(t) \equiv \begin{cases} 0, & \text{for } t < 0, \\ f_0, & \text{for } t > 0, \end{cases} \tag{5.35}$$

provided that at $t < 0$ the oscillator was at rest, so in Eq. (15), $q_{\text{free}}(t) \equiv 0$. Then the second form of Eq. (27), together with Eq. (34), yield

$$q(t) = \int_0^\infty f(t-\tau)\,G(\tau)\,d\tau = f_0 \int_0^t \frac{1}{\omega_0'} e^{-\delta\tau} \sin\omega_0'\tau \; d\tau. \tag{5.36}$$

The simplest way to work out such integrals is to represent the sine function under it as the imaginary part of $\exp\{i\omega_0't\}$, and merge the two exponents, getting

$$q(t) = f_0 \frac{1}{\omega_0'} \mathrm{Im}\left[\frac{1}{-\delta + i\omega_0'} e^{-\delta\tau + i\omega_0'\tau}\right]_0^t = \frac{F_0}{k}\left[1 - e^{-\delta t}\left(\cos\omega_0't + \frac{\delta}{\omega_0'}\sin\omega_0't\right)\right]. \tag{5.37}$$

This result, plotted in Fig. 3, is rather natural: it describes nothing more than the transient from the initial position $q = 0$ to the new equilibrium position $q_0 = f_0/\omega_0^2 = F_0/\kappa$, accompanied by decaying oscillations. For this particular simple function $f(t)$, the same result might be also obtained by introducing a new variable $\tilde{q}(t) \equiv q(t) - q_0$ and solving the resulting *homogeneous* equation for $\tilde{q}$ (with appropriate initial condition $\tilde{q}(0) = -q_0$). However, for more complicated functions $f(t)$, Green's function approach is irreplaceable.

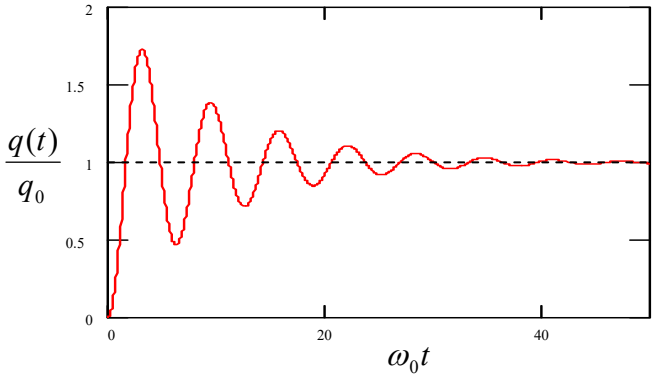

Fig. 5.3. The transient process in a linear oscillator, induced by a step-like force $f(t)$, for the particular case $\delta/\omega_0 = 0.1$ (i.e., $Q = 5$).

Note that for any particular linear system, its Green's function should be calculated only once, and then may be repeatedly used in Eq. (27) to calculate the system response to various external forces – either analytically or numerically. This property makes Green's function approach very popular in many other fields of physics – with the corresponding generalization or re-definition of the function.[14]

5.2. Weakly nonlinear oscillations

In comparison with systems discussed in the last section, which are described by linear differential equations with constant coefficients and thus allow a complete and exact analytical solution, oscillations in nonlinear systems (very unfortunately but commonly called *nonlinear oscillations*) present a complex and, generally, analytically intractable problem. However, much insight into possible

[14] See, e.g., Sec. 6.6, and also EM Sec. 2.7 and QM Sec. 2.2.

processes in such systems may be gained from a discussion of an important case of *weakly nonlinear* systems, which may be explored analytically. An important example of such systems is given by an *anharmonic oscillator* – a 1D system whose higher terms in the potential's expansion (3.10) cannot be neglected, but are small and may be accounted for approximately. If, in addition, damping is low (or negligible), and the external harmonic force exerted on the system is not too large, the equation of motion is a slightly modified version of Eq. (13):

Weakly nonlinear oscillator

$$\ddot{q} + \omega^2 q = f(t, q, \dot{q}, ...), \tag{5.38}$$

where $\omega \approx \omega_0$ is the anticipated frequency of oscillations (whose choice may be to a certain extent arbitrary – see below), and the right-hand side f is small (say, scales as some small dimensionless parameter $\varepsilon << 1$), and may be considered as a small *perturbation*.

Since at $\varepsilon = 0$, this equation has the sinusoidal solution given by Eq. (3), one might naïvely think that at a nonzero but small ε, the approximate solution to Eq. (38) should be sought in the form

Perturbative solution

$$q(t) = q^{(0)} + q^{(1)} + q^{(2)} + ..., \quad \text{where } q^{(n)} \propto \varepsilon^n, \tag{5.39}$$

with $q^{(0)} = A\cos(\omega_0 t - \varphi) \propto \varepsilon^0$. This is a good example of apparently impeccable mathematical reasoning that would lead to a very inefficient procedure. Indeed, let us apply it to the problem we already know the exact solution for, namely free oscillations in a linear but damped oscillator, for this occasion assuming the damping to be very low, $\delta/\omega_0 \sim \varepsilon << 1$. The corresponding equation of motion, Eq. (6), may be represented in form (38) if we take $\omega = \omega_0$ and

$$f = -2\delta\dot{q}, \qquad \text{with } \delta \propto \varepsilon. \tag{5.40}$$

The naïve perturbation theory based on Eq. (39) would allow us to find *small* corrections, of the order of δ, to the free, non-decaying oscillations $A\cos(\omega_0 t - \varphi)$. However, we already know from Eq. (9) that the main effect of damping is a gradual decrease of the free oscillation amplitude to zero, i.e. a very *large* change of the amplitude, though at low damping, $\delta << \omega_0$, this decay takes large time $t \sim \tau >> 1/\omega_0$. Hence, if we want our approximate method to be productive (i.e. to work at all time scales, in particular for forced oscillations with stationary amplitude and phase), we need to account for the fact that even a *small* right-hand side of Eq. (38) may eventually lead to *large* changes of oscillation's amplitude A (and sometimes, as we will see below, also of oscillation's phase φ) at large times, because of the *slowly accumulating* effects of the small perturbation.[15]

This goal may be achieved[16] by the account of these slow changes already in the "0th approximation", i.e. the basic part of the solution in the expansion (39):

[15] The same flexible approach is necessary for approximations used in quantum mechanics. The method discussed here is closer in spirit (though not completely identical) to the *WKB approximation* (see, e.g., QM Sec. 2.4) rather than most perturbative approaches (QM Ch. 6).

[16] This approach has a long history and, unfortunately, does not have a commonly accepted name. It had been gradually developed in celestial mechanics, but its application to 1D systems (on which I am focusing) was clearly spelled out only in 1926 by Balthasar van der Pol. So, I will follow several authors who call it the *van der Pol method*. Note, however, that in optics and quantum mechanics, this method is commonly called the *Rotating Wave Approximation* (RWA). In math-oriented texts, this approach, and especially its extensions to higher approximations, is usually called either the *small parameter method* or the *asymptotic method*. The list of other

$$q^{(0)} = A(t)\cos[\omega t - \varphi(t)], \qquad \text{with } \dot{A}, \dot{\varphi} \to 0 \text{ at } \varepsilon \to 0. \tag{5.41}$$

0th approximation

(It is evident that Eq. (9) is a particular case of this form.) Let me discuss this approach using a simple but representative example of a dissipative (but high-Q) pendulum driven by a weak sinusoidal external force with a nearly resonant frequency:

$$\ddot{q} + 2\delta\dot{q} + \omega_0^2 \sin q = f_0 \cos \omega t, \tag{5.42}$$

with $|\omega - \omega_0|$, $\delta << \omega_0$, and the force amplitude f_0 so small that $|q| << 1$ at all times. From what we know about the forced oscillations from Sec. 1, in this case, it is natural to identify ω on the left-hand side of Eq. (38) with the force's frequency. Expanding $\sin q$ into the Taylor series in small q, keeping only the first two terms of this expansion, and moving all small terms to the right-hand side, we can rewrite Eq. (42) in the following popular form (38):[17]

$$\ddot{q} + \omega^2 q = -2\delta\dot{q} + 2\xi\omega q + \alpha q^3 + f_0 \cos \omega t \equiv f(t, q, \dot{q}). \tag{5.43}$$

Duffing equation

Here $\alpha = \omega_0^2/6$ in the case of the pendulum (though the calculations below will be valid for any α), and the second term on the right-hand side was obtained using the approximation already employed in Sec. 1: $(\omega^2 - \omega_0^2)\, q \approx 2\omega(\omega - \omega_0)\, q = 2\omega\xi q$, where $\xi \equiv \omega - \omega_0$ is the detuning parameter that was already used earlier – see Eq. (21).

Now, following the general recipe expressed by Eqs. (39) and (41), in the 1st approximation in $f \propto \varepsilon$ we may look for the solution to Eq. (43) in the following form:

$$q(t) = A\cos\Psi + q^{(1)}(t), \quad \text{where } \Psi \equiv \omega t - \varphi, \qquad q^{(1)} \sim \varepsilon. \tag{5.44}$$

Let us plug this solution into both parts of Eq. (43), keeping only the terms of the first order in ε. Thanks to our (smart :-) choice of ω on the left-hand side of that equation, the two zero-order terms in that part cancel each other. Moreover, since each term on the right-hand side of Eq. (43) is already of the order of ε, we may drop $q^{(1)} \propto \varepsilon$ from the substitution into that part at all, because this would give us only terms $O(\varepsilon^2)$ or higher. As a result, we get the following approximate equation:

$$\ddot{q}^{(1)} + \omega^2 q^{(1)} = f^{(0)}(t) \equiv -2\delta\frac{d}{dt}(A\cos\Psi) + 2\xi\omega(A\cos\Psi) + \alpha(A\cos\Psi)^3 + f_0\cos\omega t. \tag{5.45}$$

According to Eq. (41), generally, A and φ should be considered (slow) functions of time. However, let us leave the analyses of the transient process and system's stability until the next section, and use Eq. (45) to find stationary oscillations in the system, that are established after an initial transient process. For that limited task, we may take A = const, φ = const, so $q^{(0)}$ represents sinusoidal oscillations of frequency ω. Sorting the terms on the right-hand side according to their time dependence,[18] we see that it has terms with frequencies ω and 3ω:

---

scientists credited for the development of this method, its variations, and extensions includes, most notably, N. Krylov, N. Bogolyubov, and Yu. Mitroplolsky.

[17] This equation is frequently called the *Duffing equation* (or the equation of the *Duffing oscillator*), after Georg Duffing who carried out its first (rather incomplete) analysis in 1918.

[18] Using the second of Eqs. (44), $\cos\omega t$ may be rewritten as $\cos(\Psi + \varphi) \equiv \cos\Psi\cos\varphi - \sin\Psi\sin\varphi$. Then using the identity given, for example, by MA Eq. (3.4): $\cos^3\Psi = (3/4)\cos\Psi + (1/4)\cos 3\Psi$, we get Eq. (46).

$$f^{(0)} = \left(2\xi\omega A + \frac{3}{4}\alpha A^3 + f_0\cos\varphi\right)\cos\Psi + \left(2\delta\omega A - f_0\sin\varphi\right)\sin\Psi + \frac{1}{4}\alpha A^3\cos 3\Psi. \qquad (5.46)$$

Now comes the main punch of the van der Pol approach: mathematically, Eq. (45) may be viewed as the equation of oscillations in a linear, *dissipation-free* harmonic oscillator of own frequency ω (not ω_0!) under the action of an external force $f^{(0)}(t)$. In our particular case, this force is given by Eq. (46) and has three terms: two "quadrature" components with that very frequency ω, and the third one with frequency 3ω. As we know from our analysis of this problem in Sec. 1, if any of the first two components is not equal to zero, $q^{(1)}$ grows to infinity – see Eq. (19) with $\delta = 0$. At the same time, by the very structure of the van der Pol approximation, $q^{(1)}$ has to be finite – moreover, small! The only way to avoid these infinitely growing (so-called *secular*) terms is to require that the amplitudes of both quadrature components of $f^{(0)}$ with frequency ω are equal to zero:

$$2\xi\omega A + \frac{3}{4}\alpha A^3 + f_0\cos\varphi = 0, \qquad 2\delta\omega A - f_0\sin\varphi = 0. \qquad (5.47)$$

These two *harmonic balance equations* enable us to find both parameters of the forced oscillations: their amplitude A and phase φ. The phase may be readily eliminated from this system (most easily, by expressing $\sin\varphi$ and $\cos\varphi$ from Eqs. (47) and then requiring the sum $\sin^2\varphi + \cos^2\varphi$ to equal 1), and the solution for A recast in the following implicit but convenient form:

$$A^2 = \frac{f_0^2}{4\omega^2}\frac{1}{\xi^2(A) + \delta^2}, \qquad \text{where } \xi(A) \equiv \xi + \frac{3}{8}\frac{\alpha A^2}{\omega} = \omega - \left(\omega_0 - \frac{3}{8}\frac{\alpha A^2}{\omega}\right). \qquad (5.48)$$

This expression differs from Eq. (22) for the linear resonance in the low-damping limit only by the replacement of the detuning ξ with its effective amplitude-dependent value $\xi(A)$ – or, equivalently, the replacement of the frequency ω_0 of the oscillator with its effective, amplitude-dependent value

$$\omega_0(A) = \omega_0 - \frac{3}{8}\frac{\alpha A^2}{\omega}. \qquad (5.49)$$

The physical meaning of $\omega_0(A)$ is simple: this is just the frequency of free oscillations of amplitude A in a similar nonlinear system but with zero damping.[19] Indeed, for $\delta = 0$ and $f_0 = 0$, we could repeat our calculations, assuming that ω is an amplitude-dependent eigenfrequency $\omega_0(A)$. Then the second of Eqs. (47) is trivially satisfied, while the second of them gives Eq. (49). The implicit relation (48) enables us to draw the curves of this *nonlinear resonance* just by bending the linear resonance plots (Fig. 1) according to the so-called *skeleton curve* expressed by Eq. (49). Figure 4 shows the result of this procedure. Note that at small amplitude, $\omega(A) \to \omega_0$, i.e. we return to the usual, "linear" resonance (22).

To bring our solution to its logical completion, we should still find the first perturbation $q^{(1)}(t)$ from what is left of Eq. (45). Since the structure of this equation is identical to Eq. (13) with zero damping and the force of frequency 3ω, we may use Eqs. (16)-(17) to obtain

[19] The effect of the pendulum's frequency dependence on its oscillation amplitude was observed as early as 1673 by Christiaan Huygens – who by the way had invented the pendulum clock, increasing the timekeeping accuracy by about three orders of magnitude. (He also discovered the largest of Saturn's moons, Titan).

$$q^{(1)}(t) = -\frac{1}{32\omega^2}\alpha A^3 \cos 3(\omega t - \varphi). \qquad (5.50)$$

Adding this perturbation (note the negative sign!) to the sinusoidal oscillation (41), we see that as the amplitude A of oscillations in a system with $\alpha > 0$ (e.g., a pendulum) grows, their waveform becomes a bit more "blunt" near the largest deviations from the equilibrium.

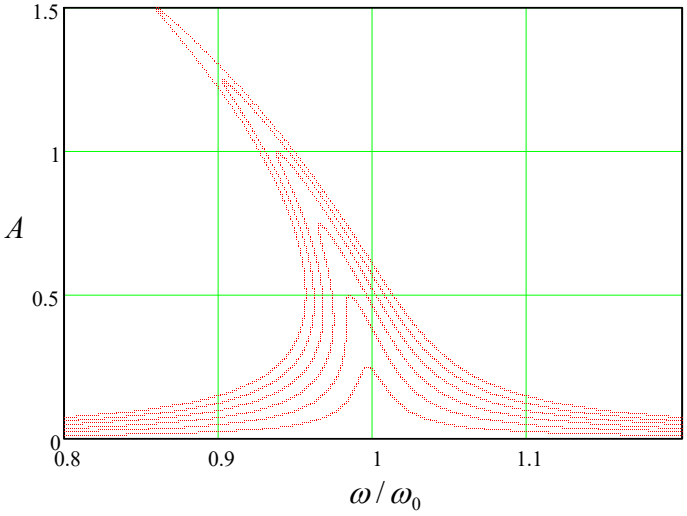

Fig. 5.4. The nonlinear resonance in the Duffing oscillator, as described by Eq. (48), for the particular case $\alpha = \omega_0^2/6$, $\delta/\omega = 0.01$ (i.e. $Q = 50$), and several values of the parameter f_0/ω_0^2, increased by equal steps of 0.005 from 0 to 0.03.

The same Eq. (50) also enables an estimate of the range of validity of our first approximation: since it has been based on the assumption $|q^{(1)}| << |q^{(0)}| \le A$, for this particular problem we have to require $\alpha A^2/32\omega^2 << 1$. For a pendulum (i.e. for $\alpha = \omega_0^2/6$), this condition becomes $A^2 << 192$. Though numerical coefficients in such strong inequalities should be taken with a grain of salt, the large magnitude of this particular coefficient gives a good hint that the method may give very accurate results even for relatively large oscillations with $A \sim 1$. In Sec. 7 below, we will see that this is indeed the case.

From the mathematical viewpoint, the next step would be to write the next approximation as

$$q(t) = A\cos\Psi + q^{(1)}(t) + q^{(2)}(t), \qquad q^{(2)} \sim \varepsilon^2, \qquad (5.51)$$

and plug it into the Duffing equation (43), which (thanks to our special choice of $q^{(0)}$ and $q^{(1)}$) would retain only the sum $\ddot{q}^{(2)} + \omega^2 q^{(2)}$ on its left-hand side. Again, requiring the amplitudes of two quadrature components of the frequency ω on the right-hand side to vanish, we may get second-order corrections to the values of A and φ. Then we may use the remaining part of the equation to calculate $q^{(2)}$, and then go after the third-order terms, etc. [20] However, for most purposes, the sum $q^{(0)} + q^{(1)}$, and sometimes even the crudest approximation of $q^{(0)}$ alone, are completely sufficient. For example, according to Eq. (50), in the case of a simple pendulum swinging as much as between the opposite horizontal positions ($A = \pi/2$), the 1st order correction $q^{(1)}$ is of the order of 0.5%. (Soon beyond this value, completely new dynamic phenomena start – see Sec. 7 below – but they cannot be described by these successive approximations

[20] For a mathematically rigorous treatment of higher approximations, see, e.g., Yu. Mitropolsky and N. Dao, *Applied Asymptotic Methods in Nonlinear Oscillations*, Springer, 2004. A more layman (and, by today's standards, somewhat verbose) discussion of various oscillatory phenomena may be found in the classical text A. Andronov, A. Vitt, and S. Khaikin, *Theory of Oscillators*, first published in the 1960s and still available online as Dover's republication in 2011.

at all.) Due to such reasons, for the analysis of particular systems, higher approximations are rarely pursued.

5.3. Reduced equations

A much more important issue is the stability of the solutions described by Eq. (48). Indeed, Fig. 4 shows that within a certain range of parameters, these equations give three different values for the oscillation amplitude (and phase), and it is important to understand which of them are stable. Since these solutions are not the fixed points in the sense discussed in Sec. 3.2 (each point in Fig. 4 represents a nearly-sinusoidal oscillation), their stability analysis needs a more general approach that would be valid for oscillations with amplitude and phase slowly evolving in time. This approach will also enable the analysis of non-stationary (especially the initial transient) processes, which are of importance for some dynamic systems.

First of all, let us formalize the way the harmonic balance equations, such as Eqs. (47), should be obtained for the general case (38) – rather than for the particular Eq. (43) considered in the last section. After plugging in the 0^{th} approximation (41) into the right-hand side of equation (38) we have to require the amplitudes of both quadrature components of frequency ω to vanish. From the standard Fourier analysis, we know that these requirements may be represented as

Harmonic balance equations

$$\boxed{\overline{f^{(0)}\sin\Psi}=0,\quad \overline{f^{(0)}\cos\Psi}=0,} \tag{5.52}$$

where the top bar means the time averaging – in our current case, over the period $2\pi/\omega$ of the right-hand side of Eq. (52), with the arguments calculated in the 0^{th} approximation:

$$f^{(0)}\equiv f(t,q^{(0)},\dot{q}^{(0)},...)\equiv f\left(t,A\cos\Psi,-A\omega\sin\Psi,...\right),\qquad \text{with } \Psi=\omega t-\varphi\,. \tag{5.53}$$

Now, for a transient process the contribution of $q^{(0)}$ to the left-hand side of Eq. (38) is not zero any longer, because its amplitude and phase may be both slow functions of time – see Eq. (41). Let us calculate this contribution. The exact result would be

$$\begin{aligned}\ddot{q}^{(0)}+\omega^2 q^{(0)}&\equiv\left(\frac{d^2}{dt^2}+\omega^2\right)A\cos(\omega t-\varphi)\\&=\left(\ddot{A}+2\dot{\varphi}\omega A-\dot{\varphi}^2A\right)\cos(\omega t-\varphi)-2\dot{A}(\omega-\dot{\varphi})\sin(\omega t-\varphi).\end{aligned} \tag{5.54}$$

However, in the first approximation in ε, we may neglect the second derivative of A, and also the squares and products of the first derivatives of A and φ (which are all of the second order in ε), so Eq. (54) is reduced to

$$\ddot{q}^{(0)}+\omega^2 q^{(0)}\approx 2A\dot{\varphi}\omega\cos(\omega t-\varphi)-2\dot{A}\omega\sin(\omega t-\varphi)\,. \tag{5.55}$$

On the right-hand side of Eq. (53), we can neglect the time derivatives of the amplitude and phase at all, because this part is already proportional to the small parameter. Hence, in the first order in ε, Eq. (38) becomes

$$\ddot{q}^{(1)}+\omega^2 q^{(1)}=f_{\text{ef}}^{(0)}\equiv f^{(0)}-\left(2A\dot{\varphi}\omega\cos\Psi-2\dot{A}\omega\sin\Psi\right). \tag{5.56}$$

Now, applying Eqs. (52) to the function $f_{ef}^{(0)}$, and taking into account that the time averages of $\sin^2\Psi$ and $\cos^2\Psi$ are both equal to ½, while the time average of the product $\sin\Psi\cos\Psi$ vanishes, we get a pair of so-called *reduced equations* (alternatively called either "truncated", or "RWA", or "van der Pol" equations) for the time evolution of the amplitude and phase:

$$\dot{A} = -\frac{1}{\omega}\overline{f^{(0)}\sin\Psi}, \qquad \dot{\varphi} = \frac{1}{\omega A}\overline{f^{(0)}\cos\Psi}. \tag{5.57a}$$

Reduced (RWA) equations

Extending the definition (4) of the complex amplitude of oscillations to their slow evolution in time, $a(t) \equiv A(t)\exp\{i\varphi(t)\}$, and differentiating this relation, the two equations (57a) may be also rewritten in the form of either one equation for a:

$$\dot{a} = \frac{i}{\omega}\overline{f^{(0)}e^{i(\Psi+\varphi)}} \equiv \frac{i}{\omega}\overline{f^{(0)}e^{i\omega t}}, \tag{5.57b}$$

Reduced equations: alternative forms

or two equations for the real and imaginary parts of $a(t) = u(t) + iv(t)$:

$$\dot{u} = -\frac{1}{\omega}\overline{f^{(0)}\sin\omega t}, \qquad \dot{v} = \frac{1}{\omega}\overline{f^{(0)}\cos\omega t}. \tag{5.57c}$$

The first-order harmonic balance equations (52) are evidently just the particular case of the reduced equations (57) for stationary oscillations ($\dot{A} = \dot{\varphi} = 0$).[21]

Superficially, the system (57a) of two coupled, first-order differential equations may look more complex than the initial, second-order differential equation (38), but actually, it is usually much simpler. For example, let us spell them out for the easy case of free oscillations a linear oscillator with damping. For that, we may reuse the ready Eq. (46) by taking $\alpha = f_0 = 0$, and thus turning Eqs. (57a) into

$$\dot{A} = -\frac{1}{\omega}\overline{f^{(0)}\sin\Psi} \equiv -\frac{1}{\omega}\overline{(2\xi\omega A\cos\Psi + 2\delta\omega A\sin\Psi)\sin\Psi} \equiv -\delta A, \tag{5.58a}$$

$$\dot{\varphi} = \frac{1}{\omega A}\overline{f^{(0)}\cos\Psi} \equiv \frac{1}{\omega A}\overline{(2\xi\omega A\cos\Psi + 2\delta\omega A\sin\Psi)\cos\Psi} \equiv \xi. \tag{5.58b}$$

The solution of Eq. (58a) gives us the same "envelope" law $A(t) = A(0)e^{-\delta t}$ as the exact solution (10) of the initial differential equation, while the elementary integration of Eq. (58b) yields $\varphi(t) = \xi t + \varphi(0) \equiv \omega t - \omega_0 t + \varphi(0)$. This means that our approximate solution,

$$q^{(0)}(t) = A(t)\cos[\omega t - \varphi(t)] = A(0)e^{-\delta t}\cos[\omega_0 t - \varphi(0)], \tag{5.59}$$

agrees with the exact Eq. (9), and misses only the correction (8) of the oscillation frequency. (This correction is of the second order in δ, i.e. of the order of ε^2, and hence is beyond the accuracy of our first approximation.) It is remarkable how nicely do the reduced equations recover the proper frequency of free oscillations in this autonomous system – in which the very notion of ω is ambiguous.

[21] One may ask why we cannot stick to just one, most compact, complex–amplitude form (57b) of the reduced equations. The main reason is that when the function $f(q,\dot{q},t)$ is nonlinear, we cannot replace its real arguments, such as $q = A\cos(\omega t - \varphi)$, with their complex-function representations like $a\exp\{-i\omega t\}$ (as could be done in the linear problems considered in Sec. 5.1), and need to use real variables, such as either $\{A, \varphi\}$ or $\{u, v\}$, anyway.

The result is different at forced oscillations. For example, for the (generally, nonlinear) Duffing oscillator described by Eq. (43) with $f_0 \neq 0$, Eqs. (57a) yield the reduced equations,

$$\dot{A} = -\delta A + \frac{f_0}{2\omega}\sin\varphi, \qquad A\dot{\varphi} = \xi(A)\,A + \frac{f_0}{2\omega}\cos\varphi, \tag{5.60}$$

which are valid for an arbitrary function $\xi(A)$, provided that this nonlinear detuning remains much smaller than the oscillation frequency. Here (after a transient), the amplitude and phase tend to the stationary states described by Eqs. (47). This means that φ becomes a constant, so $q^{(0)} \to A\cos(\omega t -$ const), i.e. the reduced equations again automatically recover the correct frequency of the solution, in this case, equal to the external force frequency.

Note that each stationary oscillation regime, with certain amplitude and phase, corresponds to a fixed point of the reduced equations, so the stability of those fixed points determines that of the oscillations. In the next three sections, we will carry out such analyses for several simple systems of key importance for physics and engineering.

5.4. Self-oscillations and phase locking

B. van der Pol's motivation for developing his method was the analysis of one more oscillatory motion type: the so-called *self-oscillations*. Several systems, e.g., electronic rf amplifiers with positive feedback and optical media with quantum-level population inversion, provide convenient means for the compensation and even over-compensation of the intrinsic energy losses in oscillators. Phenomenologically, this effect may be described as the change of sign of the coefficient δ from positive to negative. Since for small oscillations, the equation of motion is still linear, we may use Eq. (9) to describe its general solution. This equation shows that at $\delta < 0$, even infinitesimal deviations from equilibrium (say, due to unavoidable fluctuations) lead to oscillations with exponentially growing amplitude. Of course, in any real system such growth cannot persist infinitely, and shall be limited by this or that effect – e.g., in the above examples, respectively, by the amplifier's saturation and the quantum level population's exhaustion.

In many cases, the amplitude limitation may be described reasonably well by making the following replacement:

$$2\delta\dot{q} \to 2\delta\dot{q} + \beta\dot{q}^3, \tag{5.61}$$

with $\beta > 0$. Let us analyze the effects of such *nonlinear damping*, applying the van der Pol's approach[22] to the corresponding differential equation:

$$\ddot{q} + 2\delta\dot{q} + \beta\dot{q}^3 + \omega_0^2 q = 0. \tag{5.62}$$

Carrying out the dissipative and detuning terms to the right-hand side, and taking them for f in the canonical Eq. (38), we can easily calculate the right-hand sides of the reduced equations (57a), getting[23]

$$\dot{A} = -\delta(A)\,A, \qquad \text{where } \delta(A) \equiv \delta + \frac{3}{8}\beta\omega^2 A^2, \tag{5.63a}$$

[22] In his original work, B. van der Pol considered a very similar equation (frequently called the van *der Pol oscillator*) that differs from Eq. (62) only by the nonlinear term: $\dot{q}^3 \to q^2\dot{q}$, and has very similar properties.

[23] For that, one needs to use the trigonometric identity $\sin^3\Psi = (3/4)\sin\Psi - (1/4)\sin 3\Psi$ – see, e.g., MA Eq. (3.4).

$$A\dot{\varphi} = \xi A\,. \tag{5.63b}$$

The last of these equations has exactly the same form as Eq. (58b) for the case of decaying oscillations and hence shows that the self-oscillations (if they happen, i.e. if $A \neq 0$) have the own frequency ω_0 of the oscillator – cf. Eq. (59). However, Eq. (63a) is more substantive. If the initial damping δ is positive, it has only the trivial fixed point, $A_0 = 0$ (that describes the oscillator at rest), but if δ is negative, there is also another fixed point,

$$A_1 = \frac{2}{\sqrt{3}} q_0, \quad \text{where } q_0 \equiv \left(\frac{2|\delta|}{\beta\omega^2} \right)^{1/2}, \qquad \text{for } \delta < 0\,, \tag{5.64}$$

which describes steady self-oscillations with a non-zero amplitude A_1.

To understand which of these points is stable, let us apply the general approach discussed in Sec. 3.2, the linearization of equations of motion, to Eq. (63a). For the trivial fixed point $A_0 = 0$, its linearization is reduced to discarding the nonlinear term in the definition of the amplitude-dependent damping $\delta(A)$. The resulting linear equation evidently shows that the system's equilibrium point, $A = A_0 = 0$, is stable at $\delta > 0$ and unstable at $\delta < 0$. (This *self-excitation condition* was already discussed above.) On the other hand, the linearization of near the non-trivial fixed point A_1 requires a bit more math: in the first order in $\tilde{A} \equiv A - A_1 \to 0$, we get

$$\dot{\tilde{A}} \equiv \dot{A} = -\delta(A_1 + \tilde{A}) - \frac{3}{8}\beta\omega^2 (A_1 + \tilde{A})^3 \approx -\delta\,\tilde{A} - \frac{3}{8}\beta\omega^2 3A_1^2 \tilde{A} = \left(-\delta + 3\delta\right)\tilde{A} = 2\delta\tilde{A}\,, \tag{5.65}$$

where Eq. (64) has been used to eliminate A_1. We see that the fixed point A_1 (and hence the self-oscillation process) is stable as soon as it exists ($\delta < 0$) – similarly to the situation in our "testbed problem" (Fig. 2.1), besides that in our current, dissipative system, the stability is "actual" rather than "orbital" – see Sec. 6 for more on this issue.

Now let us consider another important problem: the effect of an external oscillating force on a self-excited oscillator. If the force is sufficiently small, its effects on the self-excitation condition and the oscillation amplitude are negligible. However, if the frequency ω of such a weak force is close to the own frequency ω_0 of the oscillator, it may lead to *phase locking*[24] – also called "synchronization", though the latter term also has a much broader meaning. At this effect, the oscillation frequency deviates from ω_0, and becomes exactly equal to the external force's frequency ω, within a certain range

$$-\Delta \le \omega - \omega_0 < +\Delta\,. \tag{5.66}$$

To prove this fact, and also to calculate the phase-locking range width 2Δ, we may repeat the calculation of the right-hand sides of the reduced equations (57a), adding the term $f_0 \cos\omega t$ to the right-hand side of Eq. (62) – cf. Eqs. (42)-(43). This addition modifies Eqs. (63) as follows:[25]

$$\dot{A} = -\delta(A)\,A + \frac{f_0}{2\omega}\sin\varphi, \tag{5.67a}$$

$$A\dot{\varphi} = \xi A + \frac{f_0}{2\omega}\cos\varphi. \tag{5.67b}$$

[24] Apparently, the phase locking was first noticed by the same C. Huygens for pendulum clocks.

[25] Actually, this result should be evident, even without calculations, from the comparison of Eqs. (60) and (63).

If the system is self-excited, and the external force is weak, its effect on the oscillation amplitude is small, and in the first approximation in f_0 we can take A to be constant and equal to the value A_1 given by Eq. (64). Plugging this approximation into Eq. (67b), we get a very simple equation[26]

Phase locking equation

$$\dot{\varphi} = \xi + \Delta\cos\varphi, \tag{5.68}$$

where in our current case

$$\Delta \equiv \frac{f_0}{2\omega A_1}. \tag{5.69}$$

Within the range $-|\Delta| < \xi < +|\Delta|$, Eq. (68) has two fixed points on each 2π-segment of the variable φ:

$$\varphi_\pm = \pm\cos^{-1}\left(-\frac{\xi}{\Delta}\right) + 2\pi n. \tag{5.70}$$

It is easy to linearize Eq. (68) near each point to analyze their stability in our usual way; however, let me use this case to demonstrate another convenient way to do this in 1D systems, using the *phase plane* $[\varphi, \dot{\varphi}]$ – see Fig. 5, where the red line shows the right-hand side of Eq. (68).

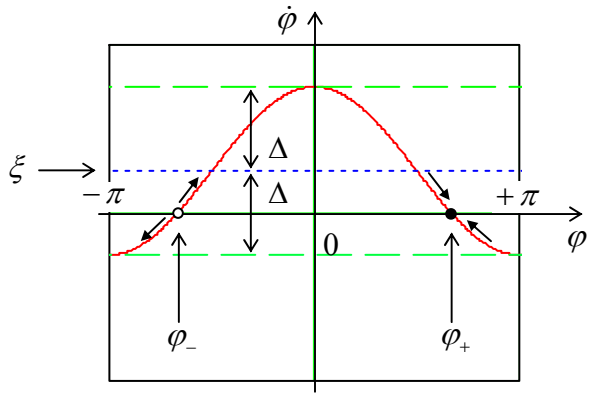

Fig. 5.5. The phase plane of a phase-locked oscillator, for the particular case $\xi = \Delta/2$, $f_0 > 0$.

Since according to Eq. (68), positive values of the plotted function correspond to the growth of phase φ in time and vice versa, we may draw the arrows showing the direction of phase evolution. From this graphics, it is clear that one of these fixed points (for $f_0 > 0$, φ_+) is stable, while its counterpart (in this case, φ_-) is unstable. Hence the magnitude of Δ given by Eq. (69) is indeed the phase-locking range (or rather its half) that we wanted to find. Note that the range is proportional to the phase-locking signal's amplitude – perhaps the most important quantitative feature of this effect.

To complete our simple analysis, based on the assumption of fixed oscillation amplitude, we need to find the condition of its validity. For that, we may linearize Eq. (67a), for the stationary case, near the value A_1, just as we have done in Eq. (65) for the transient process. The stationary result,

$$\tilde{A} \equiv A - A_1 = \frac{1}{2|\delta|}\frac{f_0}{2\omega}\sin\varphi_\pm \approx A_1\left|\frac{\Delta}{2\delta}\right|\sin\varphi_\pm, \tag{5.71}$$

shows that our assumption, $|\tilde{A}| << A_1$, and hence the final result (69), are valid if the calculated phase-locking range 2Δ is much smaller than $4|\delta|$.

[26] This equation is ubiquitous in phase-locking system descriptions, including even some digital electronic circuits used for that purpose – at the proper re-definition of the phase difference φ.

5.5. Parametric excitation

In both problems solved in the last section, the stability analysis was easy because it could be carried out for just one slow variable, *either* amplitude *or* phase. More generally, such an analysis of the reduced equations involves both of these variables. A classical example of such a situation is provided by one important physical effect – the *parametric excitation* of oscillations. A simple example of such excitation is given by a pendulum with a variable parameter, for example, the suspension length $l(t)$ – see Fig. 6. Experiments[27] and numerical simulations show that if the length is changed periodically (*modulated*) with some frequency 2ω that is close to $2\omega_0$, and a sufficiently large depth Δl, the equilibrium position of the pendulum becomes unstable, and it starts oscillating with frequency ω equal *exactly* to the half of the modulation frequency – and hence only *approximately* equal to the average frequency ω_0 of the oscillator.

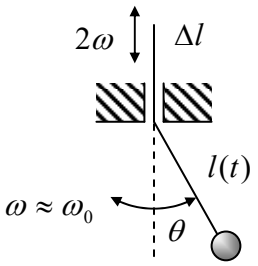

Fig. 5.6. Parametric excitation of a pendulum.

For an elementary analysis of this effect, we may consider the simplest case when the oscillations are small. At the lowest point ($\theta = 0$), where the pendulum moves with the highest velocity v_{max}, the suspension string's tension $\mathcal{T}$ is *higher* than mg by the centripetal force: $\mathcal{T}_{max} = mg + mv_{max}^2/l$. On the contrary, at the maximum deviation of the pendulum from the equilibrium, the force is *lower* than mg, because of the string's tilt: $\mathcal{T}_{min} = mg\cos\theta_{max}$. Using the energy conservation, $E = mv_{max}^2/2 = mgl(1 - \cos\theta_{max})$, we may express these values as $\mathcal{T}_{max} = mg + 2E/l$ and $\mathcal{T}_{min} = mg - E/l$. Now, if during each oscillation period, the string is pulled up slightly by Δl (with $|\Delta l| << l$) at each of its two passages through the lowest point, and is let to go down by the same amount at each of two points of the maximum deviation, the net work of the external force per period is positive:

$$\mathcal{W} \approx 2(\mathcal{T}_{max} - \mathcal{T}_{min})\Delta l \approx 6\frac{\Delta l}{l}E, \tag{5.72}$$

and hence increases the oscillator's energy. If the parameter modulation depth Δl is sufficient, this increase may overcompensate the energy drained out by damping during the same period. Quantitatively, Eq. (10) shows that low damping ($\delta << \omega_0$) leads to the following energy decrease,

$$\Delta E \approx -4\pi\frac{\delta}{\omega_0}E, \tag{5.73}$$

per oscillation period. Comparing Eqs. (72) and (73), we see that the net energy flow into the oscillations is positive, $\mathcal{W} + \Delta E > 0$, i.e. oscillation amplitude has to grow if[28]

[27] The simplest experiments of this kind may be done with the usual playground swings, where moving your body up and down moves the system's c.o.m. position, and hence the effective length l_{ef} of the support – see Eq. (4.41).

[28] Modulation of the pendulum's mass (say, by periodic pumping water in and out of a suspended bottle) gives a qualitatively similar result. Note, however, that parametric oscillations cannot be excited by modulating *every*

$$\frac{\Delta l}{l} > \frac{2\pi\delta}{3\omega_0} \equiv \frac{\pi}{3Q}. \tag{5.74}$$

Since this result is independent of the oscillation energy E, the growth of energy and amplitude is exponential (until E becomes so large that some of our assumptions fail), so Eq. (74) is the parametric excitation's condition – in this simple model.

However, this result does not account for a possible difference between the oscillation frequency ω and the eigenfrequency ω_0, and also does not clarify whether the best phase shift between the oscillations and parameter modulation, assumed in the above calculation, may be sustained automatically. To address these issues, we may apply the van der Pol approach to a simple but reasonable model:

$$\ddot{q} + 2\delta\dot{q} + \omega_0^2(1 + \mu\cos 2\omega t)q = 0, \tag{5.75}$$

describing the parametric excitation in a linear oscillator with a sinusoidal modulation of the parameter $\omega_0^2(t)$. Rewriting this equation in the canonical form (38),

$$\ddot{q} + \omega^2 q = f(t, q, \dot{q}) \equiv -2\delta\dot{q} + 2\xi\omega q - \mu\omega_0^2 q\cos 2\omega t, \tag{5.76}$$

and assuming that the dimensionless ratios δ/ω and $|\xi|/\omega$, and the modulation depth μ are all much less than 1, we may use general Eqs. (57a) to get the following reduced equations:

$$\begin{aligned} \dot{A} &= -\delta A - \frac{\mu\omega}{4} A\sin 2\varphi, \\ A\dot{\varphi} &= A\xi - \frac{\mu\omega}{4} A\cos 2\varphi. \end{aligned} \tag{5.77}$$

These equations evidently have a fixed point, with $A_0 = 0$, but its stability analysis (though possible) is not absolutely straightforward, because the phase φ of oscillations is undetermined at that point. In order to avoid this (technical rather than conceptual) difficulty, we may use, instead of the real amplitude and phase of oscillations, either their complex amplitude $a = A\exp\{i\varphi\}$, or its components u and v – see Eqs. (4). Indeed, for our function f, Eq. (57b) gives

$$\dot{a} = (-\delta + i\xi)a - i\frac{\mu\omega}{4}a^*, \tag{5.78}$$

while Eqs. (57c) yield

$$\begin{aligned} \dot{u} &= -\delta u - \xi v - \frac{\mu\omega}{4} v, \\ \dot{v} &= -\delta v + \xi u - \frac{\mu\omega}{4} u. \end{aligned} \tag{5.79}$$

We see that in contrast to Eqs. (77), in the "Cartesian coordinates" $\{u, v\}$ the trivial fixed point $A_0 = 0$ (i.e. $u_0 = v_0 = 0$) is absolutely regular. Moreover, equations (78)-(79) are already linear, so they do not require any additional linearization. Thus we may use the same approach as was already used in Secs. 3.2 and 5.1, i.e. look for the solution of Eqs. (79) in the exponential form $\exp\{\lambda t\}$. However, now

oscillator's parameter – for example, the oscillator's damping coefficient (at least if it stays positive at all times), because this does not change the system's energy, just the energy drain rate.

we are dealing with two variables and should allow them to have, for each value of λ, a certain ratio u/v. For that, we may take the partial solution in the form

$$u = c_u e^{\lambda t}, \quad v = c_v e^{\lambda t}. \tag{5.80}$$

where the constants c_u and c_v are frequently called the *distribution coefficients*. Plugging this solution into Eqs. (79), we get from them the following system of two linear algebraic equations:

$$\begin{aligned} \left(-\delta - \lambda\right)c_u + \left(-\xi - \frac{\mu\omega}{4}\right)c_v = 0, \\ \left(+\xi - \frac{\mu\omega}{4}\right)c_u + \left(-\delta - \lambda\right)c_v = 0. \end{aligned} \tag{5.81}$$

The characteristic equation of this system, i.e. the condition of compatibility of Eqs. (81),

$$\begin{vmatrix} -\delta - \lambda & -\xi - \frac{\mu\omega}{4} \\ \xi - \frac{\mu\omega}{4} & -\delta - \lambda \end{vmatrix} \equiv \lambda^2 + 2\delta\lambda + \delta^2 + \xi^2 - \left(\frac{\mu\omega}{4}\right)^2 = 0, \tag{5.82}$$

has two roots:

$$\lambda_{\pm} = -\delta \pm \left[\left(\frac{\mu\omega}{4}\right)^2 - \xi^2\right]^{1/2}. \tag{5.83}$$

Requiring the fixed point to be unstable, $\mathrm{Re}\lambda_+ > 0$, we get the parametric excitation condition

$$\frac{\mu\omega}{4} > \left(\delta^2 + \xi^2\right)^{1/2}. \tag{5.84}$$

Thus the parametric excitation may indeed happen without any external phase control: the arising oscillations self-adjust their phase to pick up energy from the external source responsible for the periodic parameter variation.

Our key result (84) may be compared with two other calculations. First, in the case of negligible damping ($\delta = 0$), Eq. (84) turns into the condition $\mu\omega/4 > |\xi|$. This result may be compared with the well-developed theory of the so-called *Mathieu equation*, whose canonical form is

$$\frac{d^2y}{dv^2} + \left(a - 2b\cos 2v\right)y = 0. \tag{5.85}$$

With the substitutions $y \to q$, $v \to \omega t$, $a \to (\omega_0/\omega)^2$, and $b/a \to -\mu/2$, this equation is just a particular case of Eq. (75) for $\delta = 0$. In terms of Eq. (85), our result (84) may be rewritten just as $b > |a - 1|$, and is supposed to be valid for $b << 1$. The boundaries given by this condition are shown with dashed lines in Fig. 7 together with the numerically calculated[29] stability boundaries for the Mathieu equation. One can see that the van der Pol approximation works just fine within its applicability limit (and a bit beyond :-), though it fails to predict some other important features of the Mathieu equation, such as the existence of higher, more narrow regions of parametric excitation (at $a \approx n^2$, i.e. $\omega_0 \approx \omega/n$, for all integer n), and some

[29] Such calculations are substantially simplified by the use of the so-called *Floquet theorem*, which is also the mathematical basis for the discussion of wave propagation in periodic media – see the next chapter.

spill-over of the stability region into the lower half-plane $a < 0$.[30] The reason for these failures is the fact that, as can be seen in Fig. 7, these phenomena do not appear in the first approximation in the parameter modulation amplitude $\mu \propto b$, which is the realm of the reduced equations (79).

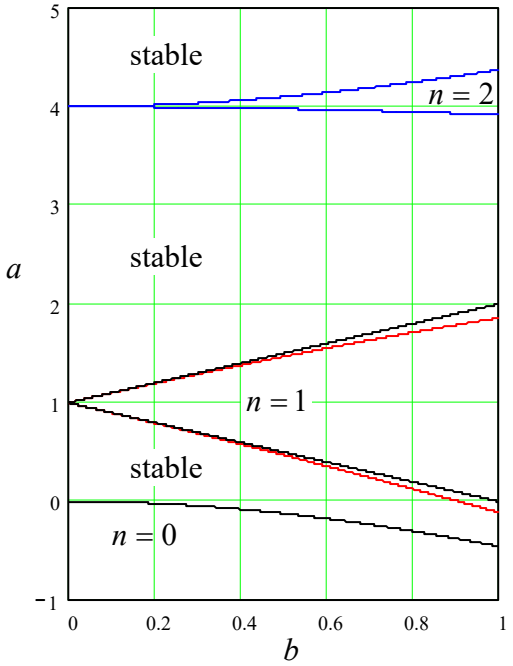

Fig. 5.7. Stability boundaries of the Mathieu equation (85), as calculated: numerically (solid curves) and using the reduced equations (79) (dashed straight lines). In the regions numbered by various n, the trivial solution $y = 0$ of the equation is unstable, i.e. its general solution $y(v)$ includes an exponentially growing term.

In the opposite case of non-zero damping but exact tuning ($\xi = 0$, $\omega \approx \omega_0$), Eq. (84) becomes

$$\mu > \frac{4\delta}{\omega_0} \equiv \frac{2}{Q}. \tag{5.86}$$

This condition may be compared with Eq. (74) by taking $\Delta l/l = 2\mu$. The comparison shows that while the structure of these conditions is similar, the numerical coefficients are different by a factor close to 2. The first reason for this difference is that the instant parameter change at optimal moments of time is more efficient than the smooth, sinusoidal variation described by (75). Even more significantly, the change of the pendulum's length modulates not only its frequency $\omega_0 \equiv (g/l)^{1/2}$ as Eq. (75) implies but also its *mechanical impedance* $Z \equiv (gl)^{1/2}$ – the notion to be discussed in detail in the next chapter. (The analysis of the general case of the simultaneous modulation of ω_0 and Z is left for the reader's exercise.)

To conclude this section, let me summarize the most important differences between the excitation of parametric and forced oscillations:

(i) Parametric oscillations completely disappear outside of their excitation range, while the forced oscillations have a non-zero amplitude for any frequency and amplitude of the external force – see Eq. (18).

(ii) While the parametric excitation may be described by linear equations such as Eq. (75), such equations cannot predict a finite oscillation amplitude within the excitation range, even at finite

[30] This region (for $b << 1$, $-b^2/2 < a < 0$) describes, in particular, the counter-intuitive stability of the so-called *Kapitza pendulum* – an inverted pendulum with the suspension point oscillated fast in the vertical direction – the effect first observed by Andrew Stephenson in 1908.

damping. In order to describe stationary parametric oscillations, some nonlinear effects have to be taken into account. (I am leaving analyses of such effects for the reader's exercise.)

One more important feature of parametric oscillations will be discussed in the next section.

5.6. Fixed point classification

The reduced equations (79) give us a good pretext for a brief discussion of an important general topic of dynamics: classification and stability of the fixed points of a system described by two time-independent, first-order differential equations with time-independent coefficients.[31] After their linearization near a fixed point, the equations for deviations can always be expressed in a form similar to Eq. (79):

$$\begin{aligned} \dot{\tilde{q}}_1 &= M_{11}\tilde{q}_1 + M_{12}\tilde{q}_2, \\ \dot{\tilde{q}}_2 &= M_{21}\tilde{q}_1 + M_{22}\tilde{q}_2, \end{aligned} \tag{5.87}$$

where $M_{jj'}$ (with $j,j' = 1, 2$) are some real scalars, which may be viewed as the elements of a 2×2 matrix M. Looking for an exponential solution of the type (80),

$$\tilde{q}_1 = c_1 e^{\lambda t}, \quad \tilde{q}_2 = c_2 e^{\lambda t}, \tag{5.88}$$

we get a general system of two linear equations for the distribution coefficients $c_{1,2}$:

$$\begin{aligned} (M_{11} - \lambda)c_1 + M_{12}c_2 &= 0, \\ M_{21}c_1 + (M_{22} - \lambda)c_2 &= 0. \end{aligned} \tag{5.89}$$

These equations are consistent if

$$\begin{vmatrix} M_{11} - \lambda & M_{12} \\ M_{21} & M_{22} - \lambda \end{vmatrix} = 0, \tag{5.90}$$

giving us a quadratic characteristic equation:

$$\lambda^2 - \lambda(M_{11} + M_{22}) + (M_{11}M_{22} - M_{12}M_{21}) = 0. \tag{5.91}$$

Its solution,[32]

$$\lambda_\pm = \frac{1}{2}(M_{11} + M_{22}) \pm \frac{1}{2}\left[(M_{11} - M_{22})^2 + 4M_{12}M_{21}\right]^{1/2}, \tag{5.92}$$

shows that the following situations are possible:

A. The expression under the square root, $(M_{11} - M_{22})^2 + 4M_{12}M_{21}$, is positive. In this case, both characteristic exponents $\lambda_\pm$ are real, and we can distinguish three sub-cases:

---

[31] Autonomous systems described by a single, second-order homogeneous differential equation, say $F(q, \dot{q}, \ddot{q}) = 0$, also belong to this class, because we may always treat the generalized velocity $\dot{q} \equiv v$ as a new variable, and use this definition as one first-order differential equation, while the initial equation, in the form $F(q, v, \dot{v}) = 0$, as the second first-order equation.

[32] In the language of linear algebra, $\lambda_\pm$ are the *eigenvalues*, and the corresponding sets of the distribution coefficients $[c_1, c_2]_\pm$ are the *eigenvectors* of the matrix M with elements $M_{jj'}$.

(i) Both λ_+ and λ_- are negative. As Eqs. (88) show, in this case the deviations $\tilde{q}$ tend to zero at $t \to \infty$, i.e. the fixed point is stable. Because of generally different magnitudes of the exponents $\lambda_\pm$, the process represented on the phase plane $[\tilde{q}_1, \tilde{q}_2]$ (see Fig. 8a, with the solid arrows, for an example) may be seen as consisting of two stages: first, a faster (with the rate $|\lambda_-| > |\lambda_+|$) relaxation to a linear *asymptote*,[33] and then a slower decline, with the rate $|\lambda_+|$, along this line, i.e. at a virtually fixed ratio of the variables. Such a fixed point is called the *stable node*.

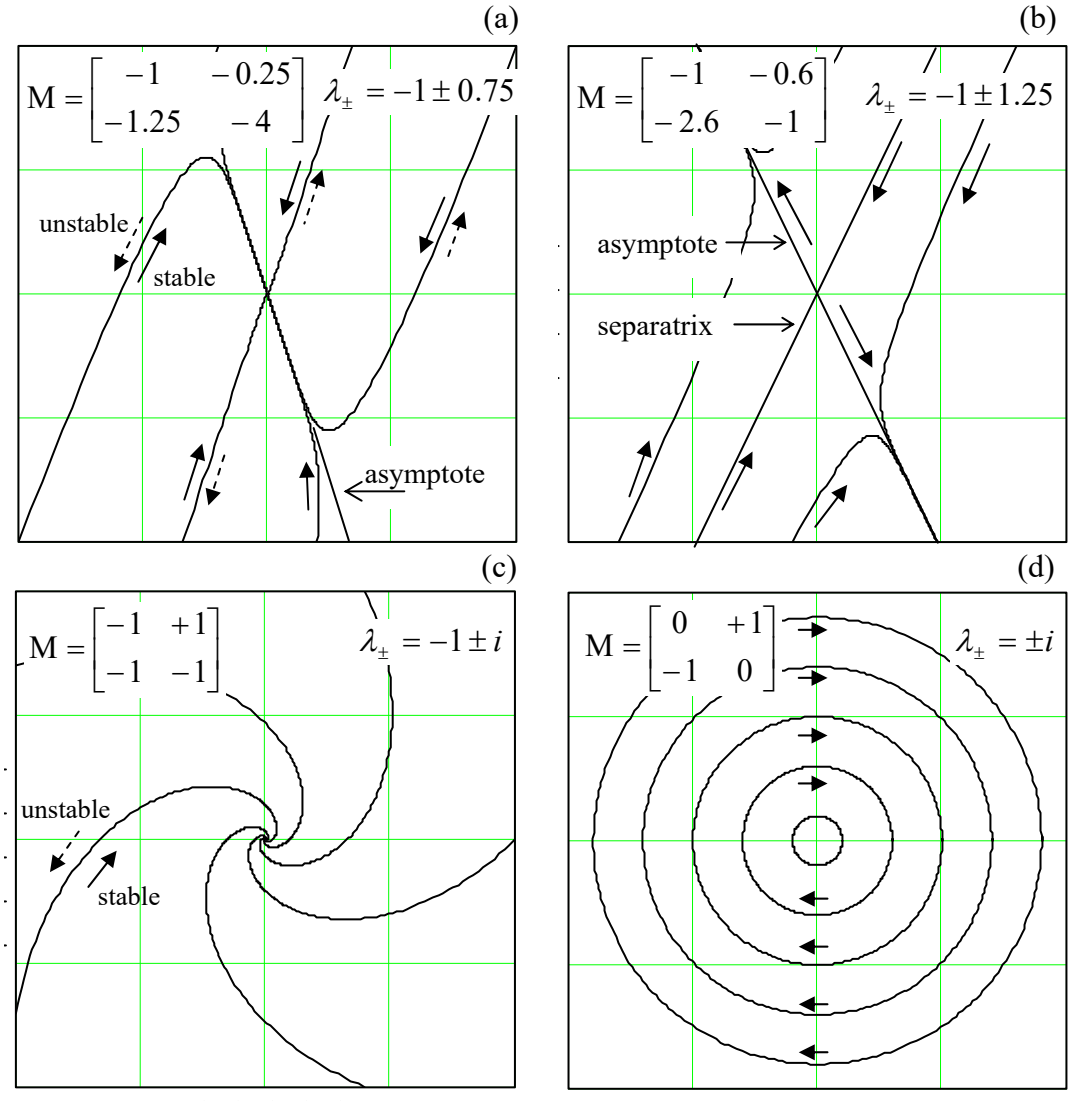

Fig. 5.8. Typical trajectories on the phase plane $[\tilde{q}_1, \tilde{q}_2]$ near fixed points of different types: (a) node, (b) saddle, (c) focus, and (d) center. The particular matrices M used for the first three panels correspond to Eqs. (81) for the parametric excitation, with $\xi = \delta$ and three different values of the ratio $\mu\omega/4\delta$: (a) 1.25, (b) 1.6, and (c) 0.

[33] The asymptote direction may be found by plugging the value λ_+ back into Eq. (89) and finding the corresponding ratio c_1/c_2. Note that the separation of the system's evolution into the two stages is conditional, being most vivid in the case of a large difference between the exponents λ_+ and λ_-.

(ii) Both λ_+ and λ_- are positive. This case of an *unstable node* differs from the previous one only by the direction of motion along the phase plane trajectories – see the dashed arrows in Fig. 8a. Here the variable ratio is also approaching a constant soon, now the one corresponding to $\lambda_+ > \lambda_-$.

(iii) Finally, in the case of a *saddle* ($\lambda_+ > 0$, $\lambda_- < 0$), the system's dynamics is different (Fig. 8b): after the rate-$|\lambda_-|$ relaxation to an asymptote, with the perturbation starts to grow, with the rate λ_+, along one of two opposite directions. (The direction is determined on which side of another straight line, called the *separatrix*, the system has been initially.) So the saddle[34] is an unstable fixed point.

B. The expression under the square root in Eq. (92), $(M_{11} - M_{22})^2 + 4M_{12}M_{21}$, is negative. In this case, the square root is imaginary, making the real parts of both roots equal, $\mathrm{Re}\lambda_\pm = (M_{11} + M_{22})/2$, and their imaginary parts equal but opposite. As a result, here there can be just two types of fixed points:

(i) *Stable focus*, at $(M_{11} + M_{22}) < 0$. The phase plane trajectories are spirals going to the origin (i.e. toward the fixed point) – see Fig. 8c with the solid arrow.

(ii) *Unstable focus*, taking place at $(M_{11} + M_{22}) > 0$, differs from the stable one only by the direction of motion along the phase trajectories – see the dashed arrow in the same Fig. 8c.

C. Frequently, the border case, $M_{11} + M_{22} = 0$, corresponding to the orbital ("indifferent") stability already discussed in Sec. 3.2, is also distinguished, and the corresponding fixed point is referred to as the *center* (Fig. 8d). Considering centers as a separate category makes sense because such fixed points are typical for Hamiltonian systems, whose first integral of motion may be frequently represented as the distance of the representing point from a certain center. For example, by introducing new variables $\tilde{q}_1 \equiv \tilde{q}$ and $\tilde{q}_2 \equiv m\dot{\tilde{q}}_1$, we may rewrite Eq. (3.12) of a harmonic oscillator without dissipation (again, with indices "ef" dropped for brevity), as a system of two first-order differential equations:

$$\dot{\tilde{q}}_1 = \frac{1}{m}\tilde{q}_2, \qquad \dot{\tilde{q}}_2 = -\kappa\tilde{q}_1, \tag{5.93}$$

i.e. as a particular case of Eq. (87), with $M_{11} = M_{22} = 0$, and $M_{12}M_{21} = -\kappa/m \equiv -\omega_0^2 < 0$, and hence $(M_{11} - M_{22})^2 + 4M_{12}M_{21} = -4\omega_0^2 < 0$, and $M_{11} + M_{22} = 0$. On the symmetrized phase plane $[\tilde{q}_1, \tilde{q}_2/Z]$, where the parameter $Z \equiv (\kappa m)^{1/2} \equiv m\omega_0$ is the oscillator's impedance, the sinusoidal oscillations of amplitude A are represented by a circle of radius A about the center-type fixed point $A = 0$. In the case when $\tilde{q}_1 \equiv \tilde{q}$ is the linear coordinate q of an actual mechanical oscillator, so $\tilde{q}_2 \equiv m\dot{\tilde{q}}_1$ is its linear momentum $p = m\dot{q}$, such a circular trajectory corresponds to the conservation of the oscillator's energy

$$E \equiv T + U \equiv \frac{p^2}{2m} + \frac{\kappa q^2}{2} \equiv \frac{\kappa}{2}\left[\tilde{q}_1^2 + \left(\frac{\tilde{q}_2}{Z}\right)^2\right] = \frac{\kappa A^2}{2} = \text{const}. \tag{5.94}$$

This is a convenient moment for a brief discussion of the so-called *Poincaré* (or "slow-variable", or "stroboscopic") *plane*.[35] From the point of view of the basic Eq. (41), the sinusoidal oscillations $q(t)$

[34] The term "saddle" is due to the fact that in this case, the system's dynamics is qualitatively similar to that of a heavily damped motion in a 2D potential $U(\tilde{q}_1, \tilde{q}_2)$ having the shape of a horse saddle (or a mountain pass).

[35] Named after Jules Henri Poincaré (1854-1912), who is credited, among many other achievements in physics and mathematics, for his contributions to special relativity (see, e.g., EM Chapter 9), and the basic idea of unstable trajectories responsible for the deterministic chaos – to be discussed in Chapter 9 of this course.

$= A\cos(\omega t - \varphi)$, described by a circular trajectory on the actual (symmetrized) phase plane, correspond to a fixed point $\{A, \varphi\}$, which may be conveniently represented by a stationary geometric point on the plane with these polar coordinates – see Fig. 9a. (As follows from Eq. (4), the point's Cartesian coordinates on that plane are just the variables $u \equiv A\cos\varphi$ and $v \equiv A\cos\varphi$ that were used, in particular, in the last section.) The quasi-sinusoidal process (41), with slowly changing A and φ, may be represented by slow motion of that point on this Poincaré plane.

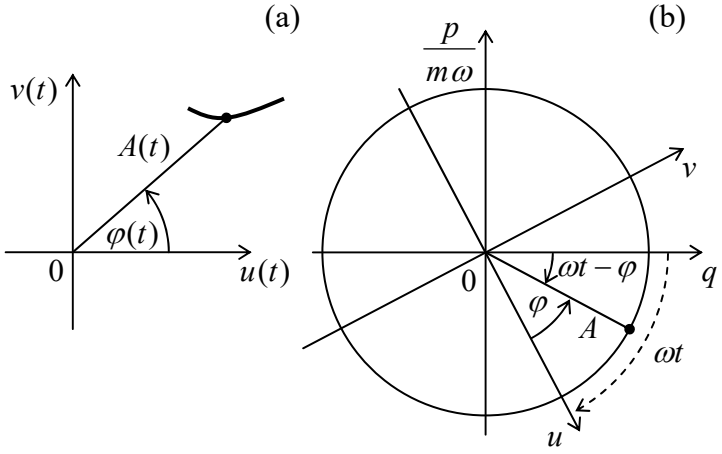

Fig. 5.9. (a) Representation of a sinusoidal oscillation (point) and a slow transient process (line) on the Poincaré plane, and (b) the relation between the usual ("fast") phase plane and the "slow" (Poincaré) plane.

Figure 9b shows a convenient way to visualize the relation between the actual phase plane of an oscillator, with the "fast" symmetrized coordinates q and $p/m\omega$, and the Poincaré plane with the "slow" coordinates u and v: the latter plane rotates relative to the former one, about the origin, clockwise, with the angular velocity ω.[36] Another, "stroboscopic" way to generate the Poincaré plane pattern is to have a fast glance at the "real" phase plane just once during the oscillation period $\mathcal{T} = 2\pi/\omega$.

In many cases, the representation on the Poincaré plane is more convenient than that on the "real" phase plane. In particular, we have already seen that the reduced equations for such important phenomena as phase locking and parametric oscillations, whose original differential equations include time explicitly, are time-independent – cf., e.g., Eqs. (75) and (79) describing the latter effect. This simplification brings the equations into the category considered earlier in this section and enables an easy classification of their fixed points, which may shed additional light on their dynamic properties.

In particular, Fig. 10 shows the classification of the only (trivial) fixed point $A_1 = 0$ on the Poincaré plane of the parametric oscillator, which follows from Eq. (83). As the parameter modulation depth μ is increased, the type of this fixed point changes from a stable focus (pertinent to a simple oscillator with damping) to a stable node and then to a saddle describing the parametric excitation. In the last case, the two directions of the perturbation growth, so prominently featured in Fig. 8b, correspond to the two possible values of the oscillation phase φ, with the phase choice determined by initial conditions.

This double degeneracy of the parametric oscillation's phase could already be noticed from Eqs. (77), because they are evidently invariant with respect to the replacement $\varphi \to \varphi + \pi$. Moreover, the degeneracy is not an artifact of the van der Pol approximation, because the initial equation (75) is already invariant with respect to the corresponding replacement $q(t) \to q(t - \pi/\omega)$. This invariance

[36] This notion of phase plane rotation is the origin of the term "Rotating Wave Approximation", mentioned above. (The word "wave" is an artifact of this method's wide application in classical and quantum optics.)

means that all other characteristics (including the amplitude) of the parametric oscillations excited with either of the two phases are *exactly* similar. At the dawn of the computer age (in the late 1950s and early 1960s), there were substantial attempts, especially in Japan, to use this property for storage and processing digital information coded in the binary-phase form. Though these attempts have not survived the competition with simpler approaches based on binary-voltage coding, some current trends in the development of prospective reversible and quantum computers may be traced back to that idea.

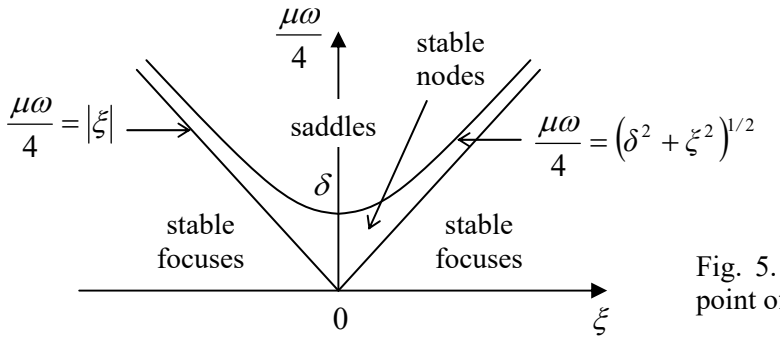

Fig. 5.10. Types of the trivial fixed point of a parametric oscillator.

5.7. Numerical approaches

If the amplitude of oscillations, for whatever reason, becomes so large that nonlinear terms in the equation describing an oscillator become comparable with its linear terms, numerical methods are virtually the only avenue available for their theoretical studies. In Hamiltonian 1D systems, such methods may be applied directly to Eq. (3.26), but dissipative and/or parametric systems typically lack such first integrals of motion, so the initial differential equation has to be solved.

Let us discuss the general idea of such methods on the example of what mathematicians call the *Cauchy problem* (finding the solution for all moments of time, starting from the known initial conditions) for the first-order differential equation

$$\dot{q} = f(t,q). \tag{5.95}$$

(The generalization to a system of several such equations is straightforward.) Breaking the time axis into small equal steps h (Fig. 11) we can reduce the equation integration problem to finding the function's value at the next time point, $q_{n+1} \equiv q(t_{n+1}) \equiv q(t_n + h)$ from the previously found value $q_n = q(t_n)$ – and, if necessary, the values of q at other previous time steps.

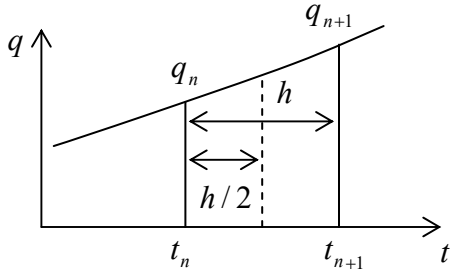

Fig. 5.11. The basic notions used at numerical integration of ordinary differential equations.

In the simplest approach (called the *Euler method*), q_{n+1} is found using the following formula:

$$\begin{aligned} q_{n+1} &= q_n + k, \\ k &\equiv h\, f(t_n, q_n). \end{aligned} \tag{5.96}$$

This approximation is equivalent to the replacement of the genuine function $q(t)$, on the segment $[t_n, t_{n+1}]$, with the two first terms of its Taylor expansion in point t_n:

$$q(t_n + h) \approx q(t_n) + \dot{q}(t_n)h \equiv q(t_n) + hf(t_n, q_n). \tag{5.97}$$

This approximation has an error proportional to h^2. One could argue that by making the step h sufficiently small, the Euler method's error might be made arbitrarily small, but even with all the number-crunching power of modern computer platforms, the CPU time necessary to reach sufficient accuracy may be too large for big problems.[37] Besides that, the increase of the number of time steps, which is necessary at $h \to 0$ at a fixed total time interval, increases the total rounding errors and eventually may cause an increase, rather than the reduction of the overall error of the computed result.

A more efficient way is to modify Eq. (96) to include the terms of the second order in h. There are several ways to do this, for example using the *2nd-order Runge-Kutta* method:

$$\begin{aligned} &q_{n+1} = q_n + k_2, \\ &k_2 \equiv h f\left(t_n + \frac{h}{2}, q_n + \frac{k_1}{2}\right), \quad k_1 \equiv h f(t_n, q_n). \end{aligned} \tag{5.98}$$

One can readily check that this method gives the exact result if the function $q(t)$ is a quadratic polynomial, and hence in the general case its errors are of the order of h^3. We see that the main idea here is to first break the segment $[t_n, t_{n+1}]$ in half (see Fig. 11 again), evaluate the right-hand side of the differential equation (95) at the point intermediate (in both t and q) between the points number n and $(n + 1)$, and then use this information to evaluate q_{n+1}.

The advantage of the Runge-Kutta approach over other second-order methods is that it may be readily extended to the 4th order, without an additional breakup of the interval $[t_n, t_{n+1}]$:

$$\begin{aligned} &q_{n+1} = q_n + \frac{1}{6}(k_1 + 2k_2 + 2k_3 + k_4), \\ &k_4 \equiv h f(t_n + h, q_n + k_3), \ k_3 \equiv h f\left(t_n + \frac{h}{2}, q_n + \frac{k_2}{2}\right), \ k_2 \equiv h f\left(t_n + \frac{h}{2}, q_n + \frac{k_1}{2}\right), \ k_1 \equiv h f(t_n, q_n). \end{aligned} \tag{5.99}$$

This method has a much lower error, $O(h^5)$, without being too cumbersome. These features have made the 4th-order Runge-Kutta the default method in most numerical libraries. Its extension to higher orders is possible, but requires more complex formulas, and is justified only for some special cases, e.g., very abrupt functions $q(t)$.[38] The most frequent enhancement of the method is an automatic adjustment of the step h to reach the pre-specified accuracy, but not make more calculations than necessary.

Figure 12 shows a typical example of an application of that method to the very simple problem of a damped linear oscillator, for two values of the fixed time step h – expressed in terms of the number (N) of such steps per oscillation period. The black straight lines connect the adjacent points obtained by

[37] In addition, the Euler method is not time-reversible. This handicap that may be essential for Hamiltonian systems described by systems of second-order differential equations. However, this drawback may be partly overcome by the so-called *leapfrogging* – the overlap of time steps h for a generalized coordinate and the corresponding generalized velocity.

[38] The most popular approaches in such cases are the *Richardson extrapolation*, the *Bulirsch-Stoer algorithm*, and a set of so-called *prediction-correction techniques*, e.g. the *Adams-Bashforth-Moulton method* – see the literature recommended in MA Sec. 16(iii).

the 4th-order Runge-Kutta method, while the points connected with the green straight lines represent the exact analytical solution (22). The plots show that a-few-percent errors start to appear only at as few as ~10 time steps per period, so the method is indeed very efficient.

Let me hope that the discussion in the next section will make the conveniences and the handicaps of the numerical approach to problems of nonlinear dynamics very clear.

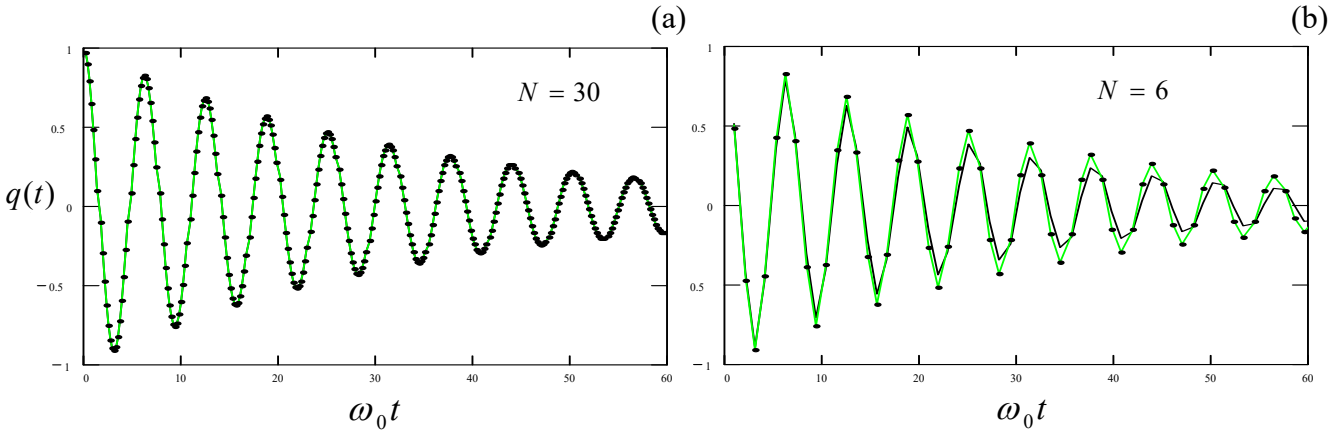

Fig. 5.12. Results of the Runge-Kutta solution of Eq. (6) (with $\delta/\omega_0 = 0.03$) for: (a) 30 and (b) 6 points per oscillation period. The results are shown by points; the black and green lines are only the guides for the eye.

5.8. Higher-harmonic and subharmonic oscillations

Figure 13 shows the numerically calculated[39] transient process and stationary oscillations in a linear oscillator and a very representative nonlinear system, the pendulum described by Eq. (42), both with the same ω_0. Both systems are driven by a sinusoidal external force of the same amplitude and frequency – in this illustration, equal to the own small-oscillation frequency ω_0 of both systems. The plots show that despite a very substantial amplitude of the pendulum oscillations (the angle amplitude of about one radian), their waveform remains almost exactly sinusoidal.[40] On the other hand, the nonlinearity affects the oscillation amplitude very substantially. These results imply that the corresponding reduced equations (60), which are based on the assumption (41), may work very well far beyond its formal restriction $|q| << 1$.

Still, the waveform of oscillations in a nonlinear system always differs from that of the applied force – in our case, from the sine function of frequency ω. This fact is frequently formulated as the generation, by the system, of *higher harmonics*. Indeed, the Fourier theorem tells us that any non-sinusoidal periodic function of time may be represented as a sum of its basic harmonic of frequency ω, plus higher harmonics with frequencies $n\omega$, with integer $n > 1$.

Note that an effective generation of higher harmonics is only possible with adequate nonlinearity of the system. For example, consider the nonlinear term αq^3 used in the equations explored in Secs. 2

[39] All numerical results shown in this section have been obtained by the 4th-order Runge-Kutta method with the automatic step adjustment that guarantees the relative error of the order of 10^{-4} – much smaller than the pixel size in the shown plots.

[40] In this particular case, the higher harmonic content is about 0.5%, dominated by the 3rd harmonic, whose amplitude and phase are in very good agreement with Eq. (50).

and 3. If the waveform $q(t)$ is sinusoidal, such term will have only the basic (1st) and the 3rd harmonics – see, e.g., Eq. (50). As another example, the "pendulum nonlinearity" sin$q$ cannot produce, without a time-independent component ("bias") in $q(t)$, any even harmonic, including the 2nd one. The most efficient generation of harmonics may be achieved using systems with the sharpest nonlinearities – e.g., semiconductor diodes whose current may follow an exponential dependence on the applied voltage through several orders of magnitude. [41]

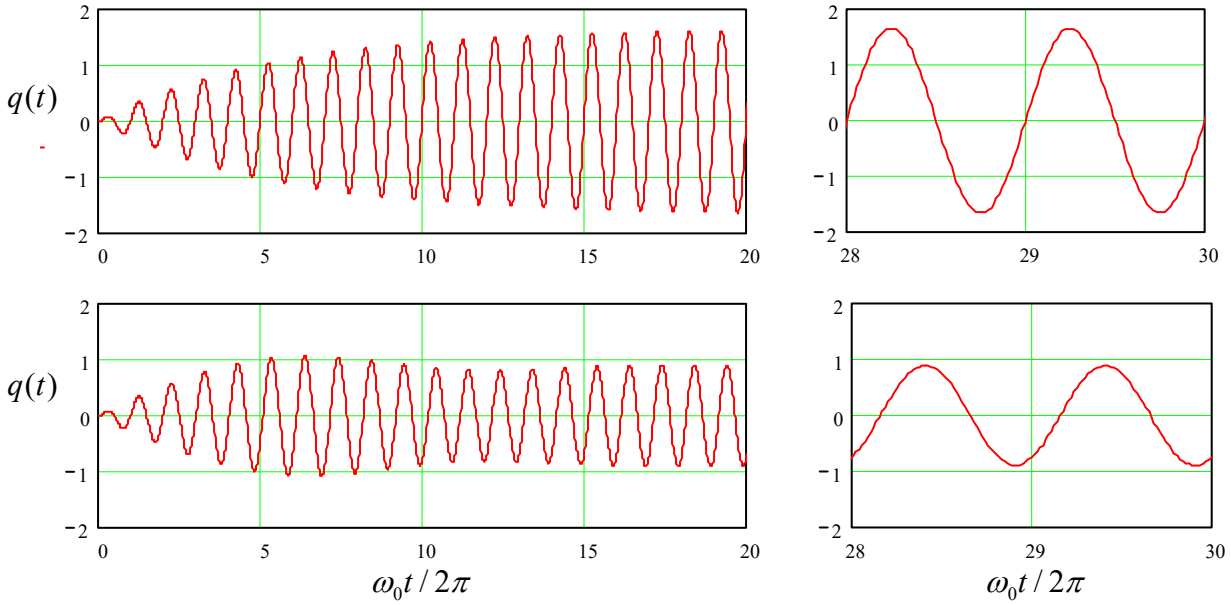

Fig. 5.13. The oscillations induced by a similar sinusoidal external force (turned on at $t = 0$) in two systems with the same small-oscillation frequency ω_0 and low damping: a linear oscillator (two top panels) and a pendulum (two bottom panels). In all cases, $\delta/\omega_0 = 0.03$, $f_0 = 0.1$, and $\omega = \omega_0$.

Another way to increase the contents of an n^{th} higher harmonic in a nonlinear oscillator is to reduce the excitation frequency ω to $\sim\omega_0/n$, so the oscillator resonated at the frequency $n\omega \approx \omega_0$ of the desired harmonic. For example, Fig. 14a shows the oscillations in a pendulum described by the same Eq. (42), but driven at frequency $\omega = \omega_0/3$. One can see that the 3rd harmonic amplitude may be comparable with that of the basic harmonic, especially if the external frequency is additionally lowered (Fig. 14b) to accommodate for the deviation of the effective frequency $\omega_0(A)$ of own oscillations from its small-oscillation value ω_0 – see Eq. (49), Fig. 4, and their discussion in Sec. 2 above.

However, numerical modeling of nonlinear oscillators, as well as experiments with their physical implementations, bring more surprises. For example, the bottom panels of Fig. 15 show oscillations in a pendulum under the effect of a strong sinusoidal force with a frequency ω close to $3\omega_0$. One can see that at some parameter values and initial conditions, the system's oscillation spectrum is heavily contributed (almost dominated) by the 3rd *sub*harmonic, i.e. the Fourier component of frequency $\omega/3 \approx \omega_0$.

This counter-intuitive phenomenon of such *subharmonic generation* may be explained as follows. Let us assume that subharmonic oscillations of frequency $\omega/3 \approx \omega_0$ have somehow appeared, and coexist with the forced oscillations of frequency 3ω:

[41] This method is used in practice, for example, for the generation of electromagnetic waves with frequencies in the terahertz range (10^{12}-10^{13} Hz), which is still in wait for efficient electronic self-oscillators.

$$q(t) \approx A\cos\Psi + A_{\text{sub}}\cos\Psi_{\text{sub}}, \qquad \text{where } \Psi \equiv \omega t - \varphi, \quad \Psi_{\text{sub}} \equiv \frac{\omega t}{3} - \varphi_{\text{sub}}. \tag{5.100}$$

Then the leading nonlinear term, αq^3, of the Taylor expansion of the pendulum's nonlinearity $\sin q$, is proportional to

$$\begin{aligned} q^3 &= (A\cos\Psi + A_{\text{sub}}\cos\Psi_{\text{sub}})^3 \\ &\equiv A^3\cos^3\Psi + 3A^2A_{\text{sub}}\cos^2\Psi\cos\Psi_{\text{sub}} + 3AA_{\text{sub}}^2\cos\Psi\cos^2\Psi_{\text{sub}} + A_{\text{sub}}^3\cos^3\Psi_{\text{sub}}. \end{aligned} \tag{5.101}$$

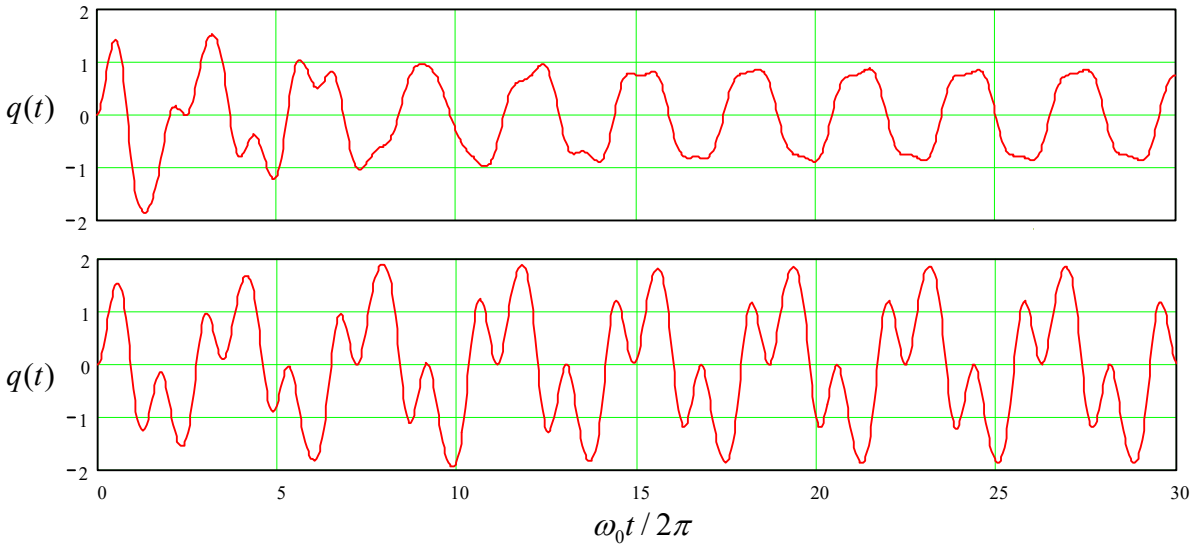

Fig. 5.14. The oscillations induced in a pendulum, with damping $\delta/\omega_0 = 0.03$, by a sinusoidal external force of amplitude $f_0 = 0.75$, and frequencies $\omega_0/3$ (top panel) and $0.8\times\omega_0/3$ (bottom panel).

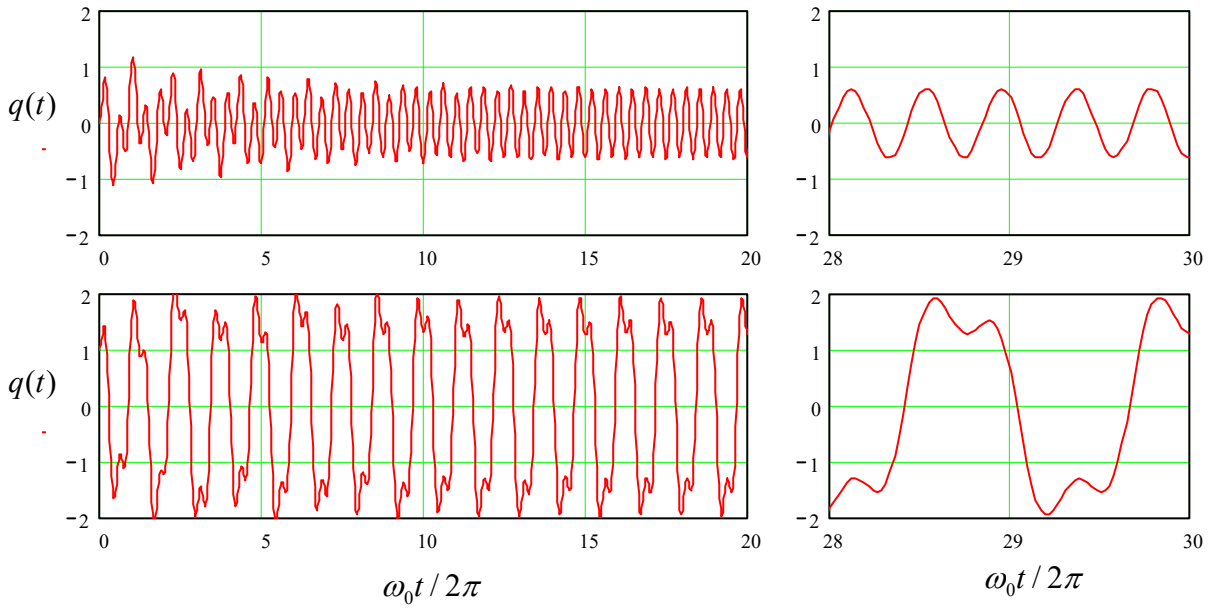

Fig. 5.15. The oscillations of a pendulum with $\delta/\omega_0 = 0.03$, driven by a sinusoidal external force of amplitude $f_0 = 3$ and frequency $0.8\times3\omega_0$, at initial conditions $q(0) = 0$ (the top panels) and $q(0) = 1$ (the bottom panels), with $dq/dt\ (0) = 0$ in both cases.

While the first and the last terms of the last expression depend only on the amplitudes of the individual components of oscillations, the two middle terms are more interesting, because they produce so-called *combinational frequencies* of the two components. In our case, the third term,

$$3A\,A_{\rm sub}^2\cos\Psi\cos^2\Psi_{\rm sub}=\frac{3}{4}AA_{\rm sub}^2\cos(\Psi-2\Psi_{\rm sub})+\ldots, \tag{5.102}$$

is of special importance, because it produces (besides other combinational frequencies) the subharmonic component with the total phase

$$\Psi-2\Psi_{\rm sub}=\frac{\omega t}{3}-\varphi+2\varphi_{\rm sub}. \tag{5.103}$$

Thus, this nonlinear contribution is synchronous with the subharmonic oscillations, and describes the interaction that can, within a certain range of the mutual phase shift between the Fourier components, deliver to them energy from the external force, so that the oscillations may be sustained. Note, however, that the amplitude of the term describing this energy exchange is proportional to the square of $A_{\rm sub}$, and vanishes at the linearization of the equations of motion near the trivial fixed point. This means that the point is always stable, i.e., the 3rd subharmonic cannot be self-excited and always needs an initial "kick-off" – compare the two panels of Fig. 15. The same is true for higher-order subharmonics.

Only the second subharmonic is a special case. Indeed, let us make a calculation similar to Eq. (102), by replacing Eq. (101) with

$$q(t)\approx A\cos\Psi+A_{\rm sub}\cos\Psi_{\rm sub},\qquad \text{where } \Psi\equiv\omega t-\varphi,\quad \Psi_{\rm sub}\equiv\frac{\omega t}{2}-\varphi_{\rm sub}, \tag{5.104}$$

for a nonlinear term proportional to q^2:

$$q^2=(A\cos\Psi+A_{\rm sub}\cos\Psi_{\rm sub})^2=A^2\cos^2\Psi+2AA_{\rm sub}\cos\Psi\cos\Psi_{\rm sub}+A_{\rm sub}^2\cos^2\Psi_{\rm sub}. \tag{5.105}$$

Here the combinational-frequency term capable of supporting the 2nd subharmonic,

$$2AA_{\rm sub}\cos\Psi\cos\Psi_{\rm sub}=AA_{\rm sub}\cos\left(\Psi-\Psi_{\rm sub}\right)=AA_{\rm sub}\cos\left(\omega t-\varphi+\varphi_{\rm sub}\right)+\ldots, \tag{5.106}$$

is *linear* in the subharmonic's amplitude, i.e. survives the linearization near the trivial fixed point. This means that the second subharmonic may arise spontaneously, from infinitesimal fluctuations.

Moreover, such excitation of the second subharmonic is very similar to the parametric excitation that was discussed in detail in Sec. 5, and this similarity is not coincidental. Indeed, let us redo the expansion (106) making a somewhat different assumption – that the oscillations are a sum of the forced oscillations at the external force's frequency ω and an *arbitrary but weak* perturbation:

$$q(t)=A\cos(\omega t-\varphi)+\tilde{q}(t),\qquad \text{with } \left|\tilde{q}\right|<<A. \tag{5.107}$$

Then, neglecting the small term proportional to $\tilde{q}^2$, we get

$$q^2\approx A^2\cos^2(\omega t-\varphi)+2\tilde{q}(t)A\cos(\omega t-\varphi). \tag{5.108}$$

Besides the inconsequential phase shift φ, the second term in the last formula is *exactly* similar to the term describing the parametric effects in Eq. (75). This fact means that for a weak perturbation, a system with a quadratic nonlinearity in the presence of a strong "pumping" signal of frequency ω is equivalent to a system with parameters changing in time with frequency ω. This fact is broadly used for the

parametric excitation at high (e.g., optical) frequencies, where the mechanical means of parameter modulation (see, e.g., Fig. 5) are not practicable. The necessary quadratic nonlinearity at optical frequencies may be provided by a *non-centrosymmetric nonlinear crystal*, e.g., the β-phase barium borate (BaB_2O_4).

Before finishing this section, let me elaborate a bit on a general topic: the relation between the numerical and analytical approaches to problems of dynamics – and to physics as a whole. We have just seen that sometimes numerical solutions, like those shown in Fig. 15b, may give vital clues for previously unanticipated phenomena such as the excitation of subharmonics. (The phenomenon of deterministic chaos, which will be discussed in Chapter 9 below, presents another example of such "numerical discoveries".) One might also argue that for problems without exact analytical solutions, the numerical simulation may be an equally productive theoretical tool. These hopes are, however, muted by the general problem that is frequently called the *curse of dimensionality*,[42] in which the last word refers to the number of parameters of the problem to be solved.[43]

Indeed, let us have one more look at Fig. 15. OK, we have been lucky to find a new phenomenon, the 3rd subharmonic generation, for a particular set of parameters – in that case, five of them: $\delta/\omega_0 = 0.03$, $\omega/\omega_0 = 2.4$, $f_0 = 3$, $q(0) = 1$, and $dq/dt\ (0) = 0$. Could we tell anything about how common this effect is? Are subharmonics with different n possible in this system? The only way to address these questions computationally is to carry out similar numerical simulations at many points of the d-dimensional (in this case, $d = 5$) space of parameters. Say, we have decided that breaking the reasonable range of each parameter to $N = 100$ points is sufficient. (For many problems, even more points are necessary – see, e.g., Sec. 9.1.) Then the total number of numerical experiments to carry out is $N^d = (10^2)^5 = 10^{10}$ – not a simple task even for the powerful modern computing facilities. (Besides the pure number of required CPU cycles, consider the storage and analysis of the results.) For many important problems of nonlinear dynamics, e.g., turbulence, the parameter dimensionality d is substantially larger, and the computer resources necessary even for one numerical experiment, are much greater.

In view of the curse of dimensionality, approximate analytical considerations, like those outlined above for the subharmonic excitation, are invaluable. More generally, physics used to stand on two legs: experiment and analytical theory. The enormous progress of computer performance during the few last decades has provided it with one more support point (a tail? :-) – numerical simulation. This does not mean we can afford to discard any of the legs we are standing on.

5.9. Relaxation oscillations

Such synthesis of the analytical and numerical approaches is also beneficial for the discussion of the last subject of this chapter: nonlinear oscillators with high damping. Perhaps the most interesting effect in such systems is the so-called *relaxation oscillations*, a type of self-oscillations with highly non-sinusoidal waveforms. Let me demonstrate them using our old friend, Eq. (62) with $\delta < 0$, whose

[42] This term had been coined in 1957 by Richard Bellman in the context of the optimal control theory (where the dimensionality means the number of parameters affecting the system under control) but gradually has spread all over quantitative sciences using numerical methods.

[43] In EM Sec. 1.2, I discuss the implications of this "curse" for a different case, when both analytical and numerical solutions to the same problem are possible.

properties at $|\delta| << \omega_0$ were discussed in Sec. 4, because it will enable us to follow the crossover from the harmonic oscillations to the relaxation ones.

Figure 16 shows the results of the numerical solution of this equation for three characteristic values of its only substantial parameter[44]

$$\mathcal{D} \equiv \frac{2|\delta|}{\omega_0} > 0. \qquad (5.109)$$

(Indeed, if we introduce the natural dimensionless variables: time $\tau \equiv \omega_0 t$, displacement $x \equiv q/q_0$, where q_0 is the scale defined in Eq. (64), and velocity $y \equiv dx/d\tau$, then the second-order differential equation (62) may be rewritten as the following system of two first-order equations:[45]

$$\frac{dx}{d\tau} = y, \qquad \frac{dy}{d\tau} = \mathcal{D}\left(1 - y^2\right)y - x, \qquad (5.110)$$

with $\mathcal{D}$ being its only parameter.) The left panels show phase planes $[x, dx/d\tau]$ of the oscillator, with their axes swapped[46] for the comparison with the right panels showing the displacement x as a function of time.

If the damping is low (top two panels), the system, launched from any initial state, gradually approaches the "limit cycle" of nearly sinusoidal oscillations. Note that even for this, not extremely small value $\mathcal{D} = 0.2$, deviations of the waveform $x(\tau)$ from a purely sinusoidal function of time are

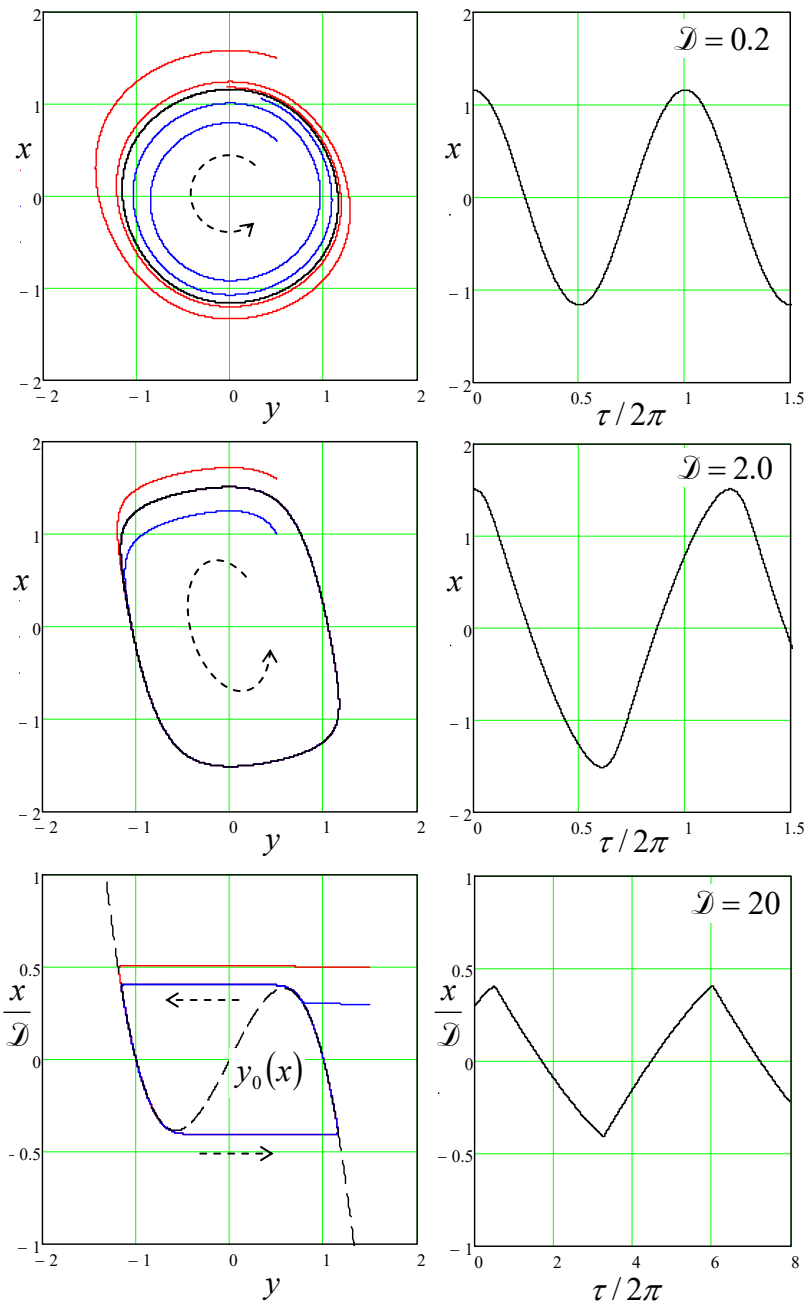

Fig. 5.16. The phase plane and time evolution of the self-oscillator described by Eqs. (62) and (110), for three values of the normalized damping (109). The red and blue lines show the system's dynamics for two representative initial conditions, while the black lines, its asymptotic behavior (the "limit cycles").

[44] As Eq. (11) shows, for positive damping, this parameter is just the reciprocal Q-factor.

[45] A somewhat different equation used in 1926 by B. van der Pol to trace the harmonic-to-relaxation-oscillation crossover for the first time may be also reduced to Eq. (110) by using the so-called *Liénard's transformation*.

[46] Note that while on the usual phase plane, the free-oscillation process corresponds to a clockwise rotation of the representation point (see, e.g., Fig. 9), the axes' swap in Fig. 16 makes the rotation counterclockwise.

very small, its period (in the normalized time τ) is very close to the small-oscillation value 2π, and its amplitude is also very close to the value $2/\sqrt{3} \approx 1.15$ predicted by the van der Pol method – see Eq. (64).

As the damping is increased to $\mathcal{D} = 2$ (middle panels), the limit cycle's deviations from the circle, and hence the deviations of the waveform $x(\tau)$ from a sinusoidal function become obvious. Note also that while the oscillation period becomes somewhat *longer* than its small-oscillation value, the transient processes of approaching the limit cycle become *faster*.

The trend of these changes becomes evident on the bottom panels, showing case $\mathcal{D} = 20$. (The further increase of the damping does not change the results noticeably, only rescaling the displacements as $x \propto \mathcal{D}$ – note the vertical scale of the bottom panels of Fig. 16.) It shows that the oscillation period is dominated by two similar parts, of equal duration. During these two intervals of relatively slow evolution, the limit cycle closely follows the declining branches of the function

$$x = \mathcal{D}\left(1 - y_0^2\right) y_0, \tag{5.111}$$

corresponding to the zero value of the first (and nominally, the largest) term in the second equation of the system (110) – see the dashed line on the left bottom panel. During these intervals, the displacement x grows in accordance with the first of these equations, with its right-hand part virtually equal to the y_0 corresponding to Eq. (111). Even without solving the resulting differential equation exactly,[47] we see that at these brunches, with $y_0 \approx \pm 1$, $x(\tau)$ changes with a speed of the order of $\mathcal{D}$, and hence the path from the initial and final points of each branch, of a length $\Delta x \sim \mathcal{D}$, takes a time interval $\Delta\tau$ of the order of 1 – exactly as the right panel shows.

As soon as the system reaches the branch's endpoint $x = \pm(2/3\sqrt{3})\mathcal{D} \approx \pm 0.385\mathcal{D}$, where the derivative dy_0/dx diverges, the balance of the terms on the right-hand part of the second Eq. (110) is not more possible, and its magnitude abruptly becomes of the order of $\mathcal{D} >> 1$. As a result, the system jumps from this point to the opposite branch of the curve (111) very rapidly, during a time interval $\Delta\tau \sim \Delta y_0/\mathcal{D} \sim 1/\mathcal{D} << 1$, insufficient for x to change much. (The initial transient processes, i.e. the approaches to the limit cycle from almost arbitrary initial conditions, are equally fast, also with $x \approx$ const.) Upon reaching the new branch, the system "relaxes" to a relatively slow evolution in the opposite direction (hence the term "relaxation oscillations"), and the process repeats again and again.

Such oscillations take place in a large number of practical mechanical systems and electronic devices, ranging from bowed string musical instruments (including those of the violin family), to usual mechanical clocks, to car light blinkers. Many of them allow for simple analyses; to save time/space, let me leave a couple of problems of this type for the reader's exercise.

5.10. Exercise problems

5.1. A body of mass m is connected to its support not only with an elastic spring but also with a *damper* (say, an air brake) that provides a drag force obeying Eq. (5) – see the figure on the right.

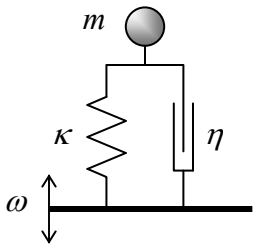

[47] Its integration leads to an elementary function for $\tau(y)$, but transcendental equations for $y(\tau)$ and $x(\tau)$.

(i) How to select the constants κ and η to minimize the body's vibrations caused by vertical oscillations of its support with frequency ω?

(ii)* What if the oscillations are random?

5.2. For a system with the response function given by Eq. (17):

(i) prove Eq. (26), and

(ii) use an approach different from the one used in Sec. 1, to derive Eq. (34).

Hint: You may like to use the *Cauchy integral theorem* and the *Cauchy integral formula* for analytical functions of a complex variable.[48]

5.3. A square-wave pulse of force (see the figure on the right) is exerted on a damping-free linear oscillator of frequency ω_0, initially at rest. Calculate the law of motion $q(t)$, sketch it, and interpret the result.

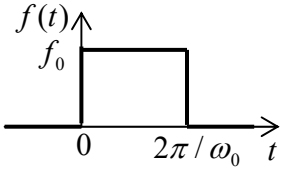

5.4. A linear oscillator with frequency ω_0 and damping δ was at rest at $t \le 0$. At $t = 0$, an external force $F(t) = F_0 \cos \omega t$ starts to be exerted on it.

(i) Derive the general expression for the time evolution of the oscillator's displacement, and interpret the result.

(ii) Spell out the result for the exact resonance ($\omega = \omega_0$) in a system with low damping ($\delta << \omega_0$) and explore the limit $\delta \to 0$.

5.5. A pulse of external force $F(t)$, with a finite duration $\mathcal{T}$, is exerted on a linear oscillator with negligible damping, initially at rest in its equilibrium position. Use two different approaches to calculate the resulting change of the oscillator's energy.

5.6. A bead may slide, without friction, in a vertical plane along a parabolic curve $y = \alpha x^2/2$, in a uniform gravity field $\mathbf{g} = -g\mathbf{n}_y$. Calculate the change its free oscillations' frequency as a function of their amplitude A, in the first nonvanishing approximation in $A \to 0$, by using two different approaches.

5.7. For a system with the Lagrangian function

$$L = \frac{m}{2}\dot{q}^2 - \frac{\kappa}{2}q^2 + \varepsilon \dot{q}^4,$$

with small parameter ε, use the harmonic balance method to find the frequency of free oscillations as a function of their amplitude.

5.8. Use a different approach to derive Eq. (49) for the frequency of free oscillations of the system described by the Duffing equation (43) with $\delta = 0$, in the first nonvanishing approximation in the small parameter $\alpha A^2/\omega_0^2 << 1$.

5.9. On the plane $[a_1, a_2]$ of two real parameters a_1 and a_2, find the regions in which the fixed point of the following system of equations,

[48] See, e.g., MA Eq. (15.1).

$$\dot{q}_1 = a_1(q_2 - q_1),$$
$$\dot{q}_2 = a_2 q_1 - q_2,$$

is unstable, and sketch the regions of each fixed point type – stable and unstable nodes, focuses, etc.

5.10. Solve Problem 4(ii) by using the reduced equations (57), and compare the result with the exact solution.

5.11. Use the reduced equations to analyze forced oscillations in an oscillator with weak nonlinear damping, described by the following equation:

$$\ddot{q} + 2\delta\dot{q} + \omega_0^2 q + \beta\dot{q}^3 = f_0 \cos\omega t,$$

with $\omega \approx \omega_0$; $\beta, \delta > 0$; and $\beta\omega A^2 << 1$. In particular, find the stationary amplitude of the forced oscillations and analyze their stability. Discuss the effect(s) of the nonlinear term on the resonance.

5.12. Within the approach discussed in Sec. 4, calculate the average frequency of a self-oscillator outside of the range of its phase locking by a weak sinusoidal force.

5.13.* Use the reduced equations to analyze the stability of the forced nonlinear oscillations described by the Duffing equation (43). Relate the result to the slope of the resonance curves (Fig. 4).

5.14. Use the van der Pol method to find the condition of parametric excitation of an oscillator described by the following equation:

$$\ddot{q} + 2\delta\dot{q} + \omega_0^2(t) q = 0,$$

where $\omega_0^2(t)$ is the square-wave function shown in the figure on the right, with $\omega \approx \omega_0$.

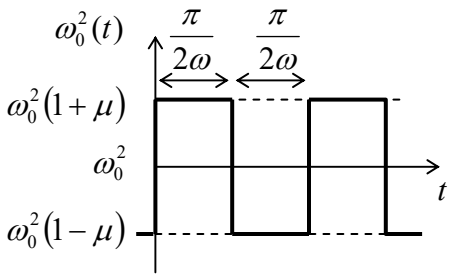

5.15. Use the van der Pol method to analyze the parametric excitation of an oscillator with weak nonlinear damping, described by the following equation:

$$\ddot{q} + 2\delta\dot{q} + \beta\dot{q}^3 + \omega_0^2(1 + \mu\cos 2\omega t)q = 0,$$

with $\omega \approx \omega_0$; $\beta, \delta > 0$; and $\mu, \beta\omega A^2 << 1$. In particular, find the amplitude of stationary oscillations and analyze their stability.

5.16. Upon adding the nonlinear term αq^3 to the left-hand side of Eq. (75),

(i) find the corresponding addition to the reduced equations,
(ii) calculate the stationary amplitude A of the parametric oscillations,
(iii) find the type and stability of each fixed point of the reduced equations,
(iv) sketch the Poincaré phase plane of the system in major parameter regions.

5.17. Use the van der Pol method to find the condition of parametric excitation of a linear oscillator with simultaneous weak modulation of the effective mass $m(t) = m_0(1 + \mu_m\cos 2\omega t)$ and the effective spring constant $\kappa(t) = \kappa_0[1 + \mu_\kappa\cos(2\omega t - \psi)]$, with the same frequency $2\omega \approx 2\omega_0$, for arbitrary

modulation depths ratio μ_m/μ_κ and phase shift ψ. Interpret the result in terms of modulation of the oscillator's instantaneous frequency $\omega(t) \equiv [\kappa(t)/m(t)]^{1/2}$ and impedance $Z(t) \equiv [\kappa(t)m(t)]^{1/2}$.

5.18.* Find the condition of parametric excitation of a nonlinear oscillator described by the following equation:

$$\ddot{q} + 2\delta\dot{q} + \omega_0^2 q + \gamma q^2 = f_0 \cos 2\omega t,$$

with sufficiently small δ, γ, f_0, and $\xi \equiv \omega - \omega_0$.

5.19. Find the condition of stability of the equilibrium point $q = 0$ of a parametric oscillator described by Eq. (75), in the limit when $\delta << |\omega_0| << \omega$ and $\mu << 1$. Use the result to analyze the stability of the Kapitza pendulum mentioned in Sec. 5.

5.20.* Use numerical simulation to explore phase-plane trajectories $[q, \dot{q}]$ of an autonomous pendulum described by Eq. (42) with $f_0 = 0$, for both low and high damping, and discuss their most significant features.

5.21. Analyze relaxation oscillations of the system shown in the figure on the right. Here an elastic spring prevents a block of mass m from being carried away by a horizontal conveyor belt moving with a constant velocity u. Assume that the coefficient μ_k of the kinematic friction between the block and the belt is lower than the static friction coefficient μ_s.

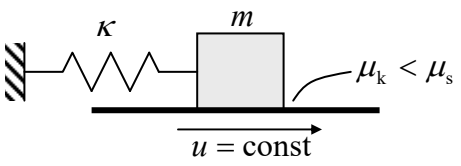

5.22. The figure on the right shows the circuit of the simplest electronic relaxation oscillator. N is a bistable circuit element that switches very rapidly from its very-high-resistance state to a very-low-resistance state as the voltage across it is increased beyond some value V_t, and switches back as the voltage is decreased below another value $V_t' < V_t$.[49] Calculate the waveform and the time period of voltage oscillations in the circuit.

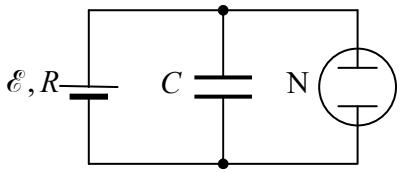

Hint: The solution of this problem requires a very basic understanding of electric circuits, including such notions as the e.m.f. $\mathscr{E}$ and the internal resistance R of a dc current source – e.g., of an electric battery.

[49] This is a reasonable model for many two-terminal gas-discharge devices (such as *glow lamps*), whose effective resistance may drop by up to 5 orders of magnitude when the discharge has been ignited by voltage $V > V_t$. In usual neon glow lamps, the discharge stops at a voltage V_t' that is about 30% lower than V_t.

This page is intentionally left blank

Chapter 6. From Oscillations to Waves

In this chapter, the discussion of oscillations is extended to systems with two and more degrees of freedom. This extension naturally leads to another key notion of physics – waves, so far in simple, mostly 1D systems. (In the next chapter, this discussion will be extended to more complex elastic continua.) However, even the limited scope of the models analyzed in this chapter will still enable us to discuss such important general aspects of waves as their dispersion, phase and group velocities, impedance, reflection, and attenuation.

6.1. Two coupled oscillators

Let us discuss oscillations in systems with several degrees of freedom, starting from the simplest case of two linear (harmonic), dissipation-free, 1D oscillators. If the oscillators are independent of each other, the Lagrangian function of their system may be expressed as a sum of two independent terms of the type (5.1):

$$L = L_1 + L_2, \quad L_{1,2} = T_{1,2} - U_{1,2} = \frac{m_{1,2}}{2}\dot{q}_{1,2}^2 - \frac{\kappa_{1,2}}{2}q_{1,2}^2. \tag{6.1}$$

Correspondingly, Eqs. (2.19) for $q_j = q_{1,2}$ yields two independent equations of motion of the oscillators, each one being similar to Eq. (5.2):

$$m_{1,2}\ddot{q}_{1,2} + m_{1,2}\Omega_{1,2}^2 q_{1,2} = 0, \qquad \text{where } \Omega_{1,2}^2 = \frac{\kappa_{1,2}}{m_{1,2}}. \tag{6.2}$$

(In the context of what follows, $\Omega_{1,2}$ are sometimes called the *partial frequencies*.) This means that in this simplest case, an arbitrary motion of the system is just a sum of independent sinusoidal oscillations at two frequencies equal to the partial frequencies (2).

However, as soon as the oscillators are *coupled* (i.e. interact), the full Lagrangian L contains an additional *mixed* term L_{int} depending on both generalized coordinates q_1 and q_2 and/or generalized velocities. As a simple example, consider the system shown in Fig. 1, where two small masses $m_{1,2}$ are constrained to move in only one direction (shown horizontal), and are kept between two stiff walls with three springs.

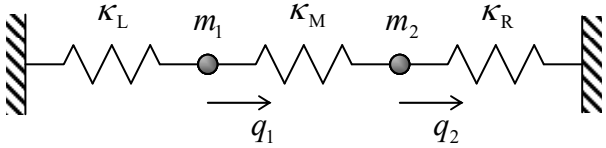

Fig. 6.1. A simple system of two coupled linear oscillators.

In this case, the kinetic energy is still separable, $T = T_1 + T_2$, but the total potential energy, consisting of the elastic energies of three springs, is not:

$$U = \frac{\kappa_L}{2}q_1^2 + \frac{\kappa_M}{2}(q_1 - q_2)^2 + \frac{\kappa_R}{2}q_2^2, \tag{6.3a}$$

where $q_{1.2}$ are the horizontal displacements of the particles from their equilibrium positions. It is convenient to rewrite this expression as

$$U = \frac{\kappa_1}{2} q_1^2 + \frac{\kappa_2}{2} q_2^2 - \kappa q_1 q_2, \qquad \text{where } \kappa_1 \equiv \kappa_L + \kappa_M, \quad \kappa_2 \equiv \kappa_R + \kappa_M, \quad \kappa \equiv \kappa_M. \tag{6.3b}$$

This formula shows that the Lagrangian function $L = T - U$ of this system contains, besides the partial terms (1), a *bilinear* interaction term:

$$L = L_1 + L_2 + L_{\text{int}}, \quad L_{\text{int}} = \kappa q_1 q_2. \tag{6.4}$$

The resulting Lagrange equations of motion are as follows:

$$\boxed{\begin{aligned} m_1 \ddot{q}_1 + m_1 \Omega_1^2 q_1 &= \kappa q_2, \\ m_2 \ddot{q}_2 + m_2 \Omega_2^2 q_2 &= \kappa q_1. \end{aligned}} \tag{6.5}$$

Linearly coupled oscillators

Thus the interaction leads to an effective generalized force κq_2 exerted on subsystem 1 by subsystem 2, and the reciprocal effective force κq_1.

Please note two important aspects of this (otherwise rather simple) system of equations. First, in contrast to the *actual* physical interaction forces (such as $F_{12} = -F_{21} = \kappa_M(q_2 - q_1)$ for our system[1]) the *effective* forces on the right-hand sides of Eqs. (5) do not obey the 3rd Newton law. Second, the forces are proportional to the same coefficient κ; this feature is a result of the general bilinear structure (4) of the interaction energy, rather than of any special symmetry.

From our prior discussions, we already know how to solve Eqs. (5), because it is still a system of linear and homogeneous differential equations, so its general solution is a sum of particular solutions of the form similar to Eqs. (5.88),

$$q_1 = c_1 e^{\lambda t}, \qquad q_2 = c_2 e^{\lambda t}, \tag{6.6}$$

with all possible values of λ. These values may be found by plugging Eq. (6) into Eqs. (5), and requiring the resulting system of two linear, homogeneous algebraic equations for the distribution coefficients $c_{1,2}$,

$$\begin{aligned} m_1 \lambda^2 c_1 + m_1 \Omega_1^2 c_1 &= \kappa c_2, \\ m_2 \lambda^2 c_2 + m_2 \Omega_2^2 c_2 &= \kappa c_1, \end{aligned} \tag{6.7}$$

to be self-consistent. In our particular case, we get a characteristic equation,

$$\begin{vmatrix} m_1(\lambda^2 + \Omega_1^2) & -\kappa \\ -\kappa & m_2(\lambda^2 + \Omega_2^2) \end{vmatrix} = 0, \tag{6.8}$$

that is quadratic in λ^2, and thus has a simple analytical solution:

$$\begin{aligned} (\lambda^2)_\pm &= -\frac{1}{2}(\Omega_1^2 + \Omega_2^2) \mp \left[\frac{1}{4}(\Omega_1^2 + \Omega_2^2)^2 - \Omega_1^2 \Omega_2^2 + \frac{\kappa^2}{m_1 m_2} \right]^{1/2} \\ &\equiv -\frac{1}{2}(\Omega_1^2 + \Omega_2^2) \mp \left[\frac{1}{4}(\Omega_1^2 - \Omega_2^2)^2 + \frac{\kappa^2}{m_1 m_2} \right]^{1/2}. \end{aligned} \tag{6.9}$$

[1] Using these expressions, Eqs. (5) may be readily obtained from the Newton laws, but the Lagrangian approach used above will make their generalization, in the next section, more straightforward.

According to Eqs. (2) and (3b), for any positive spring constants, the product $\Omega_1\Omega_2 = (\kappa_L + \kappa_M)(\kappa_R + \kappa_M)/(m_1m_2)^{1/2}$ is always larger than $\kappa/(m_1m_2)^{1/2} = \kappa_M/(m_1m_2)^{1/2}$, so the square root in Eq. (9) is always smaller than $(\Omega_1^2+\Omega_2^2)/2$. As a result, both values of λ^2 are negative, i.e. the general solution to Eq. (5) is a sum of four terms, each proportional to $\exp\{\pm i\omega_\pm t\}$, where both *normal frequencies* (also called "own frequencies", or "natural frequencies", or "eigenfrequencies") $\omega_\pm \equiv i\lambda_\pm$ are real:

Anticrossing: example

$$\omega_\pm^2 \equiv -\lambda_\pm^2 = \frac{1}{2}\left(\Omega_1^2 + \Omega_2^2\right) \pm \left[\frac{1}{4}\left(\Omega_1^2 - \Omega_2^2\right)^2 + \frac{\kappa^2}{m_1m_2}\right]^{1/2}. \tag{6.10}$$

A plot of these frequencies as a function of one of the partial frequencies (say, Ω_1), with the other partial frequency fixed, gives us the famous *anticrossing* (also called the "avoided crossing" or "non-crossing") *diagram* – see Fig. 2. One can see that at weak coupling, the normal frequencies $\omega_\pm$ are close to the partial frequencies $\Omega_{1,2}$ everywhere besides a narrow range near the anticrossing point $\Omega_1 = \Omega_2$. Most remarkably, at passing through this region, ω_+ smoothly "switches" from following Ω_2 to following Ω_1 and vice versa.

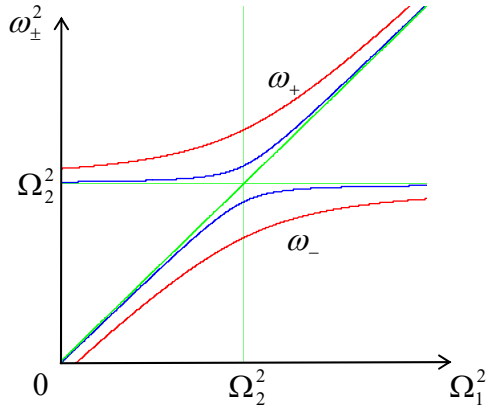

Fig. 6.2. The anticrossing diagram for two values of the normalized coupling strength $\kappa/(m_1m_2)^{1/2}\Omega_2^2$: 0.3 (red lines) and 0.1 (blue lines). In this plot, Ω_1 is assumed to be changed by varying κ_1 rather than m_1, but in the opposite case, the diagram is qualitatively similar.

The reason for this counterintuitive behavior may be found by examining the distribution coefficients $c_{1,2}$ corresponding to each branch of the diagram, which may be obtained by plugging the corresponding value of $\lambda_\pm = -i\omega_\pm$ back into Eqs. (7). For example, at the anticrossing point $\Omega_1 = \Omega_2 \equiv \Omega$, Eq. (10) is reduced to

$$\omega_\pm^2 = \Omega^2 \pm \frac{\kappa}{(m_1m_2)^{1/2}} = \Omega^2\left(1 \pm \frac{\kappa}{(\kappa_1\kappa_2)^{1/2}}\right). \tag{6.11}$$

Plugging this expression back into any of Eqs. (7), we see that for the two branches of the anticrossing diagram, the distribution coefficient ratio is the same by magnitude but opposite by sign:

$$\left(\frac{c_1}{c_2}\right)_\pm = \mp\left(\frac{m_2}{m_1}\right)^{1/2}, \quad \text{at } \Omega_1 = \Omega_2. \tag{6.12}$$

In particular, if the system is symmetric ($m_1 = m_2$, $\kappa_L = \kappa_R$), then at the upper branch, corresponding to $\omega_+ > \omega_-$, we get $c_1 = -c_2$. This means that in this so-called *hard mode*,[2] masses oscillate

[2] In physics, the term "mode" (or "normal mode") is typically used to describe the distribution of a variable in space, at its oscillations with a single frequency. In our current case, when the notion of space is reduced to two oscillator numbers, each mode is fully specified by the corresponding ratio of two distribution coefficients $c_{1,2}$.

in anti-phase: $q_1(t) \equiv -q_2(t)$. The resulting substantial extension/compression of the middle spring (see Fig. 1 again) yields additional returning force which increases the oscillation frequency. On the contrary, at the lower branch, corresponding to ω_-, the particle oscillations are in phase: $c_1 = c_2$, i.e. $q_1(t) \equiv q_2(t)$, so the middle spring is neither stretched nor compressed at all. As a result, in this *soft mode*, the normal frequency ω_- is lower than ω_+, and does not depend on κ_M:

$$\omega_-^2 = \Omega^2 - \frac{\kappa}{m} = \frac{\kappa_L}{m} = \frac{\kappa_R}{m} . \tag{6.13}$$

Note that for both modes, the oscillations equally engage both particles.

Far from the anticrossing point, the situation is completely different. Indeed, a similar calculation of $c_{1,2}$ shows that on each branch of the diagram, the magnitude of one of the distribution coefficients is much larger than that of its counterpart. Hence, in this limit, any particular mode of oscillations involves virtually only one particle. A slow change of system parameters, bringing it through the anticrossing, leads, first, to a maximal delocalization of each mode at $\Omega_1 = \Omega_2$, and then to a restoration of the localization, but in a different partial degree of freedom.

We could readily carry out similar calculations for the case when the systems are coupled via their velocities, $L_{int} = m\dot{q}_1\dot{q}_2$, where m is a coupling coefficient – not necessarily a certain physical mass.[3] The results are generally similar to those discussed above, again with the maximum level splitting at $\Omega_1 = \Omega_2 \equiv \Omega$:

$$\omega_\pm^2 = \frac{\Omega^2}{1 \mp |m|/(m_1 m_2)^{1/2}} \approx \Omega^2 \left[1 \pm \frac{|m|}{(m_1 m_2)^{1/2}} \right], \tag{6.14}$$

the last relation being valid for weak coupling. The generalization to the case of simultaneous coordinate and velocity coupling is also straightforward – see the next section.[4]

One more property of weakly coupled oscillators is a periodic slow transfer of energy between them, especially strong at or near the anticrossing point $\Omega_1 = \Omega_2$. Let me leave an analysis of such transfer for the reader's exercise. (Due to the importance of this effect for quantum mechanics, it will be discussed in detail in the QM part of this series.)

6.2. *N* coupled oscillators

The calculations of the previous section may be readily generalized to the case of an arbitrary number (say, N) of coupled harmonic oscillators, with an arbitrary type of coupling. It is obvious that in this case Eq. (4) should be replaced with

[3] In mechanics, with $q_{1,2}$ standing for the actual displacements of particles, such coupling is not very natural, but there are many dynamic systems of non-mechanical nature in which such coupling is the most natural one. The simplest example is the system of two LC ("tank") circuits, with either capacitive or inductive coupling. Indeed, as was discussed in Sec. 2.2, for such a system, the very notions of the potential and kinetic energies are conditional and interchangeable.

[4] Note that the anticrossing diagram shown in Fig. 2, is even more ubiquitous in quantum mechanics, because, due to the time-oscillatory character of the Schrödinger equation solutions, a weak coupling of any two quantum states leads to qualitatively similar behavior of the eigenfrequencies $\omega_\pm$ of the system, and hence of its *eigenenergies* ("*energy levels*") $E_\pm = \hbar\omega_\pm$ of the system.

$$L = \sum_{j=1}^{N} L_j + \sum_{j,j'=1}^{N} L_{jj'}. \tag{6.15}$$

Moreover, we can generalize the above expression for the mixed terms $L_{jj'}$, taking into account their possible dependence not only on the generalized coordinates but also on the generalized velocities, in a bilinear form similar to Eq. (4). The resulting Lagrangian may be represented in a compact form,

$$L = \sum_{j,j'=1}^{N} \left(\frac{m_{jj'}}{2} \dot{q}_j \dot{q}_{j'} - \frac{\kappa_{jj'}}{2} q_j q_{j'} \right), \tag{6.16}$$

where the off-diagonal terms are index-symmetric: $m_{jj'} = m_{j'j}$, $\kappa_{jj'} = \kappa_{j'j}$, and the factors ½ compensate for the double-counting of each term with $j \neq j'$, at the summation over two independently running indices. One may argue that Eq. (16) is quite general if we still want to keep the equations of motion linear – as they always are if the oscillations are small enough.

Plugging Eq. (16) into the general form (2.19) of the Lagrange equation, we get N equations of motion of the system, one for each value of the index $j' = 1, 2, \ldots, N$:

$$\sum_{j=1}^{N} \left(m_{jj'} \ddot{q}_j + \kappa_{jj'} q_j \right) = 0. \tag{6.17}$$

Just as in the previous section, let us look for a particular solution to this system in the form

$$q_j = c_j e^{\lambda t}. \tag{6.18}$$

As a result, we are getting a system of N linear, homogeneous algebraic equations,

$$\sum_{j=1}^{N} \left(m_{jj'} \lambda^2 + \kappa_{jj'} \right) c_j = 0, \tag{6.19}$$

for the set of N distribution coefficients c_j. The condition that this system is self-consistent is that the determinant of its matrix equals zero:

$$\mathrm{Det}\left(m_{jj'} \lambda^2 + \kappa_{jj'} \right) = 0. \tag{6.20}$$

This characteristic equation is an algebraic equation of degree N for λ^2, and so has N roots $(\lambda^2)_n$. For any Hamiltonian system with stable equilibrium, the matrices $m_{jj'}$ and $\kappa_{jj'}$ ensure that all these roots are real and negative. As a result, the general solution to Eq. (17) is the sum of $2N$ terms proportional to $\exp\{\pm i\omega_n t\}$, $n = 1, 2, \ldots, N$, where all N normal frequencies ω_n are real.

Plugging each of these $2N$ values of $\lambda = \pm i\omega_n$ back into a particular set of linear equations (17), one can find the corresponding sets of distribution coefficients $c_{j\pm}$. Generally, the coefficients are complex, but to keep $q_j(t)$ real, the coefficients c_{j+} corresponding to $\lambda = +i\omega_n$, and c_{j-} corresponding to $\lambda = -i\omega_n$ have to be complex-conjugate of each other. Since the sets of the distribution coefficients may be different for each λ_n, they should be marked with two indices, j and n. Thus, at general initial conditions, the time evolution of the j^{th} generalized coordinate may be represented as

$$q_j = \frac{1}{2} \sum_{n=1}^{N} \left(c_{jn} \exp\{+i\omega_n t\} + c_{jn}^* \exp\{-i\omega_n t\} \right) \equiv \mathrm{Re} \sum_{n=1}^{N} c_{jn} \exp\{i\omega_n t\}. \tag{6.21}$$

This formula shows very clearly again the physical sense of the distribution coefficients c_{jn}: a set of these coefficients, with different values of index j but the same mode number n, gives the complex amplitudes of oscillations of the coordinates in this mode, i.e. for the special initial conditions that ensure purely sinusoidal motion of all the system, with frequency ω_n.

The calculation of the normal frequencies and the corresponding modes (distribution coefficient sets) of a particular coupled system with many degrees of freedom from Eqs. (19)–(20) is a task that frequently may be only done numerically.[5] Let us discuss just two particular but very important cases. First, let all the coupling coefficients be small in the following sense: $|m_{jj'}| << m_j \equiv m_{jj}$ and $|\kappa_{jj'}| << \kappa_j \equiv \kappa_{jj}$, for all $j \neq j$, and all partial frequencies $\Omega_j \equiv (\kappa_j/m_j)^{1/2}$ be not too close to each other:

$$\frac{\left|\Omega_j^2 - \Omega_{j'}^2\right|}{\Omega_j^2} >> \frac{\left|\kappa_{jj'}\right|}{\kappa_j}, \frac{\left|m_{jj'}\right|}{m_j}, \quad \text{for all } j \neq j'. \tag{6.22}$$

(Such a situation frequently happens if parameters of the system are "random" in the sense that they do not follow any special, simple rule – for example, the one resulting from some simple symmetry of the system.) Results of the previous section imply that in this case, the coupling does not produce a noticeable change in the normal frequencies: $\{\omega_n\} \approx \{\Omega_j\}$. In this situation, oscillations at each frequency ω_n are nearly concentrated in one degree of freedom, i.e. in each set of the distribution coefficients c_{jn} (for a given n), one coefficient's magnitude is much larger than all others.

Now let the conditions (22) be valid for all but one pair of partial frequencies, say Ω_1 and Ω_2, while these two frequencies are so close that the coupling of the corresponding partial oscillators becomes essential. In this case, the approximation $\{\omega_n\} \approx \{\Omega_j\}$ is still valid for all other degrees of freedom, and the corresponding terms may be neglected in Eqs. (19) for $j = 1$ and 2. As a result, we return to Eqs. (7) (perhaps generalized for velocity coupling) and hence to the anticrossing diagram (Fig. 2) discussed in the previous section. As a result, an extended change of only one partial frequency (say, Ω_1) of a weakly coupled system produces a sequence of frequency anticrossings – see Fig. 3.

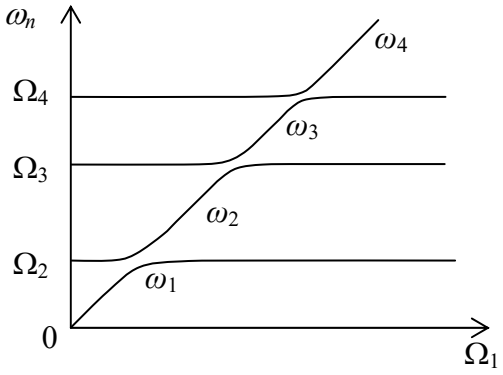

Fig. 6.3. The level anticrossing in a system of N weakly coupled oscillators – schematically.

6.3. 1D waves

The second case when the general results of the last section may be simplified are coupled systems with a considerable degree of symmetry. Perhaps the most important of them are uniform

[5] Fortunately, very effective algorithms have been developed for this *matrix diagonalization* task – see, e.g., references in MA Sec. 16(iii)-(iv). For example, the popular MATLAB software package was initially created exactly for this purpose. ("MAT" in its name stood for "matrix" rather than "mathematics".)

systems that may sustain traveling and standing *waves*. Figure 4a shows a simple example of such a system – a long uniform chain of particles, of mass m, connected with light, elastic springs, pre-stretched with the tension force $\mathcal{T}$ to have equal lengths d. (This system may be understood as a natural generalization of the two-particle system considered in Sec. 1 – cf. Fig. 1.)

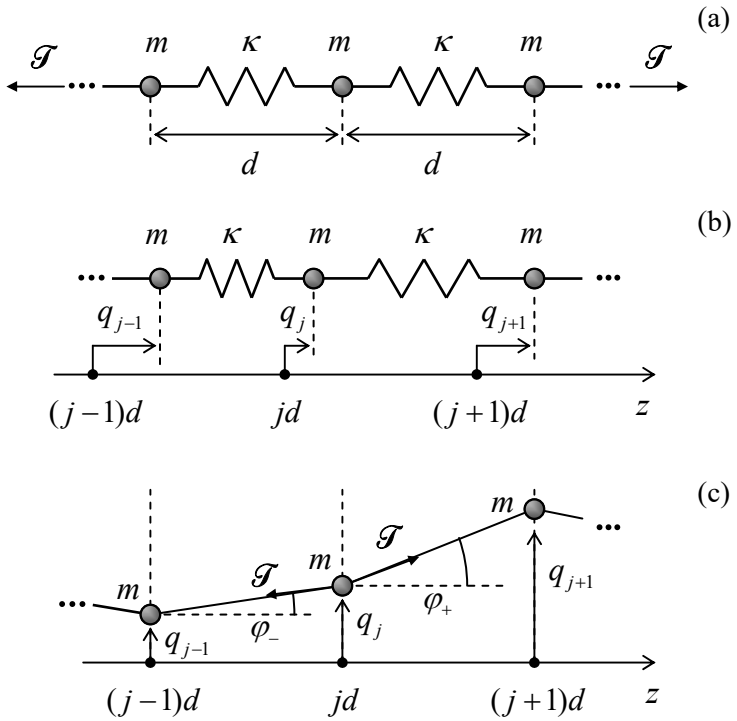

Fig. 6.4. (a) A uniform 1D chain of elastically coupled particles, and their small (b) longitudinal and (c) transverse displacements (much exaggerated for clarity).

The spring's pre-stretch does not affect small *longitudinal* oscillations q_j of the particles about their equilibrium positions $z_j = jd$ (where the integer j numbers the particles sequentially) – see Fig. 4b.[6] Indeed, in the 2nd Newton law for such a longitudinal motion of the j^{th} particle, the forces $\mathcal{T}$ and $(-\mathcal{T})$ exerted by the springs on the right and the left of it, cancel. However, the elastic additions, $\kappa\Delta q$, to these forces are generally different:

$$m\ddot{q}_j = \kappa(q_{j+1} - q_j) - \kappa(q_j - q_{j-1}). \tag{6.23}$$

On the contrary, for *transverse* oscillations within one plane (Fig. 4c), the net transverse component of the pre-stretch force exerted on the j^{th} particle, $\mathcal{T}_t = \mathcal{T}(\sin\varphi_+ - \sin\varphi_-)$, where $\varphi_\pm$ are the force direction angles, does not vanish. As a result, direct contributions to this force from small longitudinal oscillations, with $|q_j| << d$, $\mathcal{T}/\kappa$, are negligible. Also, due to the first of these strong conditions, the angles $\varphi_\pm$ are small, and hence may be approximated, respectively, as $\varphi_+ \approx (q_{j+1} - q_j)/d$ and $\varphi_- \approx (q_j - q_{j-1})/d$. Plugging these expressions into a similar approximation, $\mathcal{T}_t \approx \mathcal{T}(\varphi_+ - \varphi_-)$ for the transverse force, we see that it may be expressed as $\mathcal{T}(q_{j+1} - q_j)/d - \mathcal{T}(q_j - q_{j-1})/d$, i.e. is absolutely similar

[6] Note the need for a clear distinction between *the equilibrium position* z_j of the j^{th} point and its *deviation* q_j from it. Such distinction has to be sustained in the continuous limit (see below), where it is frequently called the *Eulerian description* – named after L. Euler, even though it was introduced to mechanics by J. d'Alembert. In this course, the distinction is emphasized by using different letters – respectively, z and q (in the 3D case, $\mathbf{r}$ and $\mathbf{q}$).

to that in the longitudinal case, just with the replacement $\kappa \to \mathcal{T}/d$. As a result, we may write the equation of motion of the j^{th} particle for these two cases in the same form:

$$m\ddot{q}_j = \kappa_{\text{ef}}(q_{j+1} - q_j) - \kappa_{\text{ef}}(q_j - q_{j-1}), \tag{6.24}$$

where κ_{ef} is the "effective spring constant", equal to κ for the longitudinal oscillations, and to $\mathcal{T}/d$ for the transverse oscillations.[7]

Apart from the (formally) infinite size of the system, Eq. (24) is just a particular case of Eq. (17), and thus its particular solution may be looked for in the form (18), where, in light of our previous experience, we may immediately take $\lambda^2 \equiv -\omega^2$. With this substitution, Eq. (24) gives the following simple form of the general system of equations (19) for the distribution coefficients c_j:

$$\left(-m\omega^2 + 2\kappa_{\text{ef}}\right)c_j - \kappa_{\text{ef}}c_{j+1} - \kappa_{\text{ef}}c_{j-1} = 0. \tag{6.25}$$

Now comes the most important conceptual step toward the wave theory. The *translational symmetry* of Eq. (25), i.e. its invariance with respect to the replacement $j \to j + 1$, allows it to have particular solutions of the following form:

$$c_j = ae^{i\alpha j}, \tag{6.26}$$

where the coefficient α may depend on ω (and system's parameters), but not on the particle number j. Indeed, plugging Eq. (26) into Eq. (25) and canceling the common factor $e^{i\alpha j}$, we see that this *differential* equation is indeed identically satisfied, provided that α obeys the following *algebraic* characteristic equation:

$$\left(-m\omega^2 + 2\kappa_{\text{ef}}\right) - \kappa_{\text{ef}}e^{+i\alpha} - \kappa_{\text{ef}}e^{-i\alpha} = 0. \tag{6.27}$$

The physical sense of the solution (26) becomes clear if we use it and Eq. (18) with $\lambda = \mp i\omega$, to write

$$q_j(t) = \text{Re}\left[a\exp\left\{i(kz_j \mp \omega t)\right\}\right] = \text{Re}\left[a\exp\left\{ik(z_j \mp v_{\text{ph}}t)\right\}\right], \tag{6.28}$$

1D traveling wave

where the *wave number* k is defined as $k \equiv \alpha/d$. Eq. (28) describes a *sinusoidal*[8] *traveling wave* of particle displacements, which propagates, depending on the sign before v_{ph}, to the right or the left along the particle chain, with the so-called *phase velocity*

$$v_{\text{ph}} \equiv \frac{\omega}{k}. \tag{6.29}$$

Phase velocity

Perhaps the most important characteristic of a wave system is the so-called *dispersion relation*, i.e. the relation between the wave's frequency ω and its wave number k – one may say, between the temporal and spatial frequencies of the wave. For our current system, this relation is given by Eq. (27) with $\alpha \equiv kd$. Taking into account that $(2 - e^{+i\alpha} - e^{-i\alpha}) \equiv 2(1 - \cos\alpha) \equiv 4\sin^2(\alpha/2)$, the dispersion relation may be rewritten in a simpler form:

[7] The re-derivation of Eq. (24) from the Lagrangian formalism, with the simultaneous strict proof that the small oscillations in the longitudinal direction and the two mutually perpendicular transverse directions are all independent of each other, is a very good exercise, left for the reader.

[8] In optics and quantum mechanics, such waves are usually called *monochromatic*; I will try to avoid this term until the corresponding parts (EM and QM) of my series.

$$\omega = \pm\omega_{\max}\sin\frac{\alpha}{2} \equiv \pm\omega_{\max}\sin\frac{kd}{2}, \qquad \text{where } \omega_{\max} \equiv 2\left(\frac{\kappa_{\text{ef}}}{m}\right)^{1/2}. \tag{6.30}$$

This result, sketched in Fig. 5, is rather remarkable in several aspects. I will discuss them in some detail, because most of these features are typical for waves of any type (including even the "de Broglie waves", i.e. wavefunctions, in quantum mechanics), propagating in periodic structures.

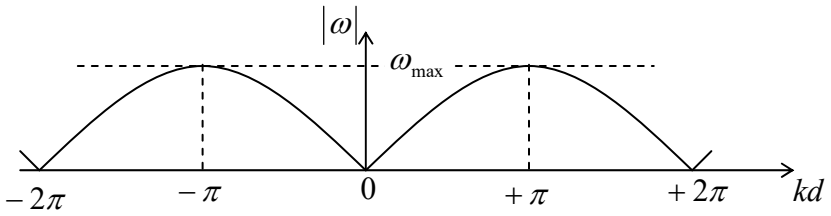

Fig. 6.5. The dispersion relation (30).

First, at low frequencies, $\omega << \omega_{\max}$, the dispersion relation (31) is linear:

$$\omega = \pm vk, \qquad \text{where } v \equiv \left|\frac{d\omega}{dk}\right|_{k=0} = \frac{\omega_{\max} d}{2} = \left(\frac{\kappa_{\text{ef}}}{m}\right)^{1/2} d\,. \tag{6.31}$$

Plugging Eq. (31) into Eq. (29), we see that the constant v plays, in the low-frequency limit, the role of the phase velocity for waves of any frequency. Due to its importance, this *acoustic wave*[9] limit will with be the subject of the special next section.

Second, when the wave frequency *is* comparable with $\omega_{\max}$, the dispersion relation is *not* linear, and the system is *dispersive*. This means that as a wave, whose Fourier spectrum has several essential components with frequencies of the order of $\omega_{\max}$, travels along the structure, its *waveform* (which may be defined as the shape of the line connecting all points $q_j(z)$, at the same time) changes.[10] This effect may be analyzed by representing the general solution of Eq. (24) as the sum (more generally, an integral) of the components (28) with different complex amplitudes a:

1D wave packet

$$q_j(t) = \text{Re}\int_{-\infty}^{+\infty} a_k \exp\left\{i\left[kz_j - \omega(k)t\right]\right\}dk\,. \tag{6.32}$$

This notation emphasizes the possible dependence of the component wave amplitudes a_k and frequencies ω on the wave number k. While the latter dependence is given by the dispersion relation, in our current case by Eq. (30), the function a_k is determined by the initial conditions. For applications, the case when a_k is substantially different from zero only in a narrow interval, of a width $\Delta k << k_0$ around some central value k_0, is of special importance. The Fourier transform reciprocal to Eq. (32) shows that this is true, in particular, for the so-called *wave packet* – a sinusoidal ("carrier") wave modulated by a spatial *envelope* function of a large width $\Delta z \sim 1/\Delta k >> 1/k_0$ – see, e.g., Fig. 6.

[9] This term is purely historical. Though the usual sound waves in air, which are the subject of acoustics, belong to this class, the waves we are discussing may have frequencies both well below and well above the human ear's sensitivity range.

[10] The waveform's deformation due to *dispersion* (which we are considering now) should be clearly distinguished from its possible change due to *attenuation* due to energy dissipation – which is *not* taken into account is our current energy-conserving model – cf. Sec. 6 below.

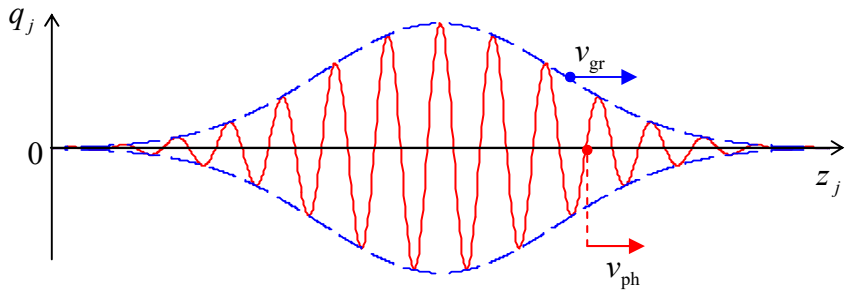

Fig. 6.6. The phase and group velocities of a wave packet.

Using the strong inequality $\Delta k \ll k_0$, the wave packet's propagation may be analyzed by expending the dispersion relation $\omega(k)$ into the Taylor series at point k_0, and, in the first approximation in $\Delta k/k_0$, restricting the expansion to its first two terms:

$$\omega(k) \approx \omega_0 + \left.\frac{d\omega}{dk}\right|_{k=k_0} \tilde{k}, \qquad \text{where } \omega_0 \equiv \omega(k_0), \text{ and } \tilde{k} \equiv k - k_0. \tag{6.33}$$

In this approximation, Eq. (32) yields

$$\begin{aligned} q_j(t) &\approx \mathrm{Re} \int_{-\infty}^{+\infty} a_k \exp\left\{ i\left[\left(k_0 + \tilde{k}\right) z_j - \left(\omega_0 + \left.\frac{d\omega}{dk}\right|_{k=k_0} \tilde{k} \right) t \right] \right\} dk \\ &\equiv \mathrm{Re}\left[\exp\left\{ i\left(k_0 z_j - \omega_0 t\right) \right\} \int_{-\infty}^{+\infty} a_k \exp\left\{ i\tilde{k}\left(z_j - \left.\frac{d\omega}{dk}\right|_{k=k_0} t \right) \right\} dk \right]. \end{aligned} \tag{6.34}$$

Comparing the last expression with the initial form of the wave packet,

$$q_j(0) = \mathrm{Re} \int_{-\infty}^{+\infty} a_k e^{ikz_j} dk \equiv \mathrm{Re}\left[\exp\left\{ ik_0 z_j \right\} \int_{-\infty}^{+\infty} a_k \exp\left\{ i\tilde{k} z_j \right\} dk \right], \tag{6.35}$$

and taking into account that the phase factors before the integrals in the last forms of Eqs. (34) and (35) do not affect its envelope, we see that in this approximation, the envelope sustains its initial form and propagates along the system with the so-called *group velocity*

$$\boxed{v_{gr} \equiv \left.\frac{d\omega}{dk}\right|_{k=k_0}}. \tag{6.36}$$

Group velocity

Except for the acoustic wave limit (31), this velocity, which characterizes the propagation of the waveform's envelope, is different from the phase velocity (29), which describes the propagation of the carrier wave, e.g., the spatial position of one of its zeros – see the red and blue arrows in Fig. 6.[11]

Next, for our particular dispersion relation (30), the difference between v_{ph} and v_{gr} increases as ω approaches ω_{max}, with the group velocity (36) tending to zero, while the phase velocity stays almost constant. The physics of such a maximum frequency available for the wave propagation may be readily understood by noticing that according to Eq. (30), at $\omega = \omega_{max}$, the wave number k equals $n\pi/d$, where n

[11] Taking into account the next term in the Taylor expansion of the function $\omega(q)$, proportional to $d^2\omega/dq^2$, we would find that the dispersion leads to a gradual change of the envelope's form. Such changes play an important role in quantum mechanics, so they are discussed in detail in the QM part of these lecture notes.

is an odd integer, and hence the phase shift $\alpha \equiv kd$ is an odd multiple of π. Plugging this value into Eq. (28), we see that at $\omega = \omega_{max}$, the oscillations of two adjacent particles are in anti-phase, for example:

$$q_0(t) = \mathrm{Re}\left[a \exp\{-i\omega t\}\right], \qquad q_1(t) = \mathrm{Re}\left[a \exp\{i\pi - i\omega t\}\right] = -q_0(t). \tag{6.37}$$

It is clear, especially from Fig. 4b for longitudinal oscillations, that at such a phase shift, all the springs are maximally stretched/compressed (just as in the hard mode of the two coupled oscillators analyzed in Sec. 1), so it is natural that this mode has the highest possible frequency.

This fact invites a natural question: what happens with the system if it is agitated at a frequency $\omega > \omega_{max}$, say by an external force exerted on its boundary? Reviewing the calculations that have led to the dispersion relation (30), we see that they are all valid not only for real but also for any complex values of k. In particular, at $\omega > \omega_{max}$ it gives

$$k = \frac{(2n-1)\pi}{d} \pm \frac{i}{\Lambda}, \qquad \text{where } n = 1, 2, 3, ..., \quad \Lambda \equiv \frac{d}{2\cosh^{-1}(\omega/\omega_{max})}. \tag{6.38}$$

Plugging this relation into Eq. (28), we see that the wave's amplitude becomes an exponential function of the particle's position:

$$\left|q_j\right| = \left|a\right| e^{\pm j \,\mathrm{Im}\, kd} \propto \exp\left\{\pm z_j / \Lambda\right\}. \tag{6.39}$$

Physically this means that penetrating into the structure, the wave decays exponentially (from the excitation point), dropping by a factor of $e \approx 3$ at the so-called *penetration depth* Λ. (According to Eq. (38), at $\omega \sim \omega_{max}$ this depth is of the order of the distance d between the adjacent particles, and decreases but rather slowly as the frequency is increased beyond ω_{max}.) Such a limited penetration is a very common property of waves, including electromagnetic waves penetrating into various plasmas and superconductors, and the quantum-mechanical de Broglie waves penetrating into classically forbidden regions of space. Note that this effect of "wave expulsion" from the medium's bulk does not require any energy dissipation.

Finally, one more fascinating feature of the dispersion relation (30) is its periodicity: if the relation is satisfied with some wave number $k_0(\omega)$, it is also satisfied with any $k_n(\omega) = k_0(\omega) + 2\pi n/d$, where n is an integer. This property is independent of the particular dynamics of the system and is a common property of all systems that are d-periodic in the usual ("direct") space. It has especially important implications for the quantum de Broglie waves in periodic systems – for example, crystals – leading, in particular, to the famous band/gap structure of their energy spectrum.[12]

6.4. Acoustic waves

Now let us return to the limit of low-frequency, dispersion-free *acoustic waves*, with $|\omega| << \omega_0$, propagating with the frequency-independent velocity (31). Such waves are the general property of *any* elastic continuous medium and obey a simple (and very important) partial differential equation. To derive it, let us note that in the acoustic wave limit, $|kd| << 1$,[13] the phase shift $\alpha \equiv kd$ is very close to

[12] For more detail see, e.g., QM Sec. 2.5.

[13] Strictly speaking, per the discussion at the end of the previous section, in this reasoning, k means the distance of the wave number from the closest point $2\pi n/d$ – see Fig. 5 again.

$2\pi n$. This means that the differences $q_{j+1}(t) - q_j(t)$ and $q_j(t) - q_{j-1}(t)$, participating in Eq. (24), are relatively small and may be approximated with $\partial q/\partial j \equiv \partial q/\partial(z/d) \equiv d(\partial q/\partial z)$, with the derivatives taken at middle points between the particles: respectively, $z_+ \equiv (z_{j+1} - z_j)/2$ and $z_- \equiv (z_j - z_{j-1})/2$. Let us now consider z as a continuous argument, and introduce the particle displacement $q(z, t)$ – a continuous function of space and time, satisfying the requirement $q(z_j, t) = q_j(t)$. In this notation, in the limit $kd \to 0$, the sum of the last two terms of Eq. (24) becomes $-\kappa d\,[\partial q/\partial z(z_+) - \partial q/\partial z(z_-)]$, and hence may be approximated as $-\kappa d^2(\partial^2 q/\partial z^2)$, with the second derivative taken at point $(z_+ - z_-)/2 \equiv z_j$, i.e. exactly at the same point as the time derivative. As a result, the whole set of *ordinary* differential equations (24), for different j, is reduced to just *one partial* differential equation

$$m\frac{\partial^2 q}{\partial t^2} - \kappa_{ef} d^2 \frac{\partial^2 q}{\partial z^2} = 0\,. \tag{6.40a}$$

Using Eq. (31), we may rewrite this *1D wave equation* in a more general form

$$\left(\frac{1}{v^2}\frac{\partial^2}{\partial t^2} - \frac{\partial^2}{\partial z^2}\right) q(z,t) = 0\,. \tag{6.40b}$$

1D wave equation

The most important property of the wave equation (40), which may be verified by an elementary substitution, is that it is satisfied by either of two *traveling wave* solutions (or their linear superposition):

$$q_+(z,t) = f_+(t - z/v), \qquad q_-(z,t) = f_-(t + z/v), \tag{6.41}$$

where $f_\pm$ are *any* smooth functions of one argument. The physical sense of these solutions may be revealed by noticing that the displacements $q_\pm$ do not change at the addition of an arbitrary change Δt to their time argument, provided that it is accompanied by an addition of the proportional addition of $\mp v\Delta t$ to their space argument. This means that with time, the waveforms just move (respectively, to the left or the right), with the constant speed v, retaining their form – see Fig. 7. [14]

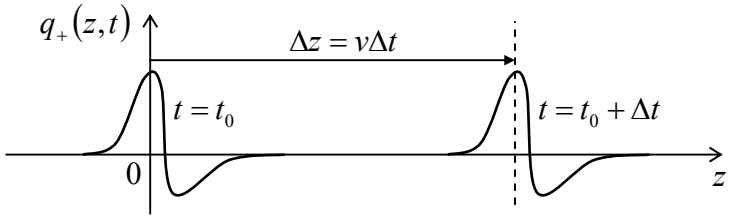

Fig. 6.7. Propagation of a traveling wave in a dispersion-free 1D system.

Returning to the simple model shown in Fig. 4, let me emphasize that the acoustic-wave velocity v is different for the waves of two types: for the longitudinal waves (with $\kappa_{ef} = \kappa$, see Fig. 4b),

$$v = v_l \equiv \left(\frac{\kappa}{m}\right)^{1/2} d\,, \tag{6.42}$$

while for the transverse waves (with $\kappa_{ef} = \mathcal{T}/d$, see Fig. 4c):

[14] From the point of view of Eq. (40), the only requirement to the "smoothness" of the functions $f_\pm$ is to be doubly differentiable. However, we should not forget that in our case the wave equation is only an approximation of the discrete Eq. (24), so according to Eq. (30), the traveling waveform conservation is limited by the acoustic wave limit condition $\omega << \omega_{max}$, which should be fulfilled for all Fourier components of these functions.

$$v = v_t = \left(\frac{\mathcal{T}}{md}\right)^{1/2} d \equiv \left(\frac{\mathcal{T}d}{m}\right)^{1/2} \equiv \left(\frac{\mathcal{T}}{\mu}\right)^{1/2}, \tag{6.43}$$

where the constant $\mu \equiv m/d$ has a simple physical sense of the particle chain's mass per unit length. Evidently, these velocities, in the same system, may be rather different.

The wave equation (40), with its only parameter v, may conceal the fact that any wave-supporting system is characterized by one more key parameter. In our current model (Fig. 4), this parameter may be revealed by calculating the forces $F_\pm(z, t)$ accompanying any of the traveling waves (41) of particle displacements. For example, in the acoustic wave limit $kd \to 0$ we are considering now, the force exerted by the j^{th} particle on its right neighbor may be approximated as

$$F(z_j, t) \equiv \kappa_{\text{ef}}\left[q_j(t) - q_{j+1}(t)\right] \approx -\kappa_{\text{ef}} \left.\frac{\partial q}{\partial z}\right|_{z=z_j} d, \tag{6.44}$$

where, as was discussed above, κ_{ef} is equal to κ for the longitudinal waves, and to $\mathcal{T}/d$ for the transverse waves. But for the traveling waves (41), the partial derivatives $\partial q_\pm/\partial z$ are equal to $\mp \dot{f}_\pm / v$ (where the dot means the differentiation over the full arguments of the functions $f_\pm$), so the corresponding forces are equal to

$$F_\pm = \mp \frac{\kappa_{\text{ef}} d}{v} \dot{f}_\pm, \tag{6.45}$$

i.e. are proportional to the particle's velocities $u = \partial q/\partial t$ in these waves,[15] $u_\pm = \dot{f}_\pm$, for the same z and t. This means that the ratio

$$\frac{F_\pm(z,t)}{u_\pm(z,t)} = -\kappa_{\text{ef}} d \frac{\partial q_\pm / \partial z}{\partial q_\pm / \partial t} = -\kappa_{\text{ef}} d \frac{\left(\mp \dot{f}_\pm\right)/v}{\dot{f}_\pm} \equiv \pm \frac{\kappa_{\text{ef}} d}{v}, \tag{6.46}$$

depends only on the wave propagation direction, but is independent of z and t, and also of the propagating waveform. Its magnitude,

Wave impedance

$$Z \equiv \left|\frac{F_\pm(z,t)}{u_\pm(z,t)}\right| = \frac{\kappa_{\text{ef}} d}{v} = \left(\kappa_{\text{ef}} m\right)^{1/2}, \tag{6.47}$$

characterizing the dynamic "stiffness" of the system for the propagating waves, is called the *wave impedance*.[16] Note that the impedance is determined by the *product* of the system's generic parameters κ_{ef} and m, while the wave velocity (31) is proportional to their *ratio*, so these two parameters are completely independent, and both are important. According to Eq. (47), the wave impedance, just as the wave velocity, is also different for the longitudinal and transverse waves:

$$Z_l = \frac{\kappa d}{v_l} \equiv \left(\kappa m\right)^{1/2}, \qquad Z_t = \frac{\mathcal{T}}{v_t} \equiv \left(\mathcal{T}\mu\right)^{1/2}. \tag{6.48}$$

[15] Of course, the *particle's* velocity u (which is proportional to the wave amplitude) should not be confused with the *wave's* velocity v (which is independent of this amplitude).

[16] This notion is regretfully missing from many physics (but not engineering!) textbooks.

(Note that the first of these expressions for Z coincides with the one used for a single oscillator in Sec. 5.6. In that case, Z may be also recast in a form similar to Eq. (46), namely, as the ratio of the force and velocity amplitudes at free oscillations.)

One of the wave impedance's key functions is to scale the power carried by a traveling wave:

$$\mathscr{P}_{\pm} \equiv F_{\pm}(z,t)u_{\pm}(z,t) = -\kappa_{\text{ef}} d \frac{\partial q_{\pm}}{\partial z}\frac{\partial q_{\pm}}{\partial t} = \pm\frac{\kappa_{\text{ef}} d}{v}\dot{f}_{\pm}^2 \equiv \pm Z\dot{f}_{\pm}^2 . \qquad (6.49)$$

Traveling wave's power

Two remarks about this important result. First, the sign of $\mathscr{P}$ depends only on the direction of the wave propagation, but not on the waveform. Second, the instant value of the power does not change if we move with the wave in question, i.e. measure $\mathscr{P}$ at points with $z \pm vt = \text{const}$. This is natural because in the Hamiltonian system we are considering, the wave energy is conserved. Hence, the wave impedance Z characterizes the energy *transfer* along the system rather than its *dissipation*.

Another important function of the wave impedance notion becomes clear when we consider waves in nonuniform systems. Indeed, our previous analysis assumed that the 1D system supporting the waves (Fig. 4) is exactly periodic, i.e. macroscopically uniform, and extends all the way from –∞ to +∞. Now let us examine what happens when this is not true. The simplest and very important example of such nonuniform systems is a *sharp interface*, i.e. a point (say, $z = 0$) at which system parameters experience a jump while remaining constant on each side of the interface – see Fig. 8.

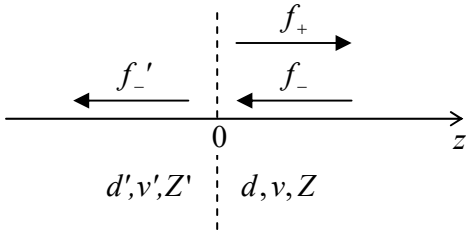

Fig. 6.8. Partial reflection of a wave from a sharp interface.

In this case, the wave equation (40) and its partial solutions (41) are is still valid for $z < 0$ and $z > 0$ – in the former case, with primed parameters. However, the jump of parameters at the interface leads to a partial *reflection* of the incident wave from the interface, so at least on the side of the incidence (in the case shown in Fig. 8, for $z \geq 0$) we need to use two such terms, one describing the incident wave and another one, the reflected wave:

$$q(z,t) = \begin{cases} f_-'(t + z/v'), & \text{for } z \leq 0, \\ f_-(t + z/v) + f_+(t - z/v), & \text{for } z \geq 0. \end{cases} \qquad (6.50)$$

To find the relations between the functions f_-, f_+, and f_-' (of which the first one, describing the incident wave, may be considered known), we may use two boundary conditions at $z = 0$. First, the displacement $q_0(t)$ of the particle at the interface has to be the same whether it is considered a part of the left or right sub-system, and it participates in Eqs. (50) for both $z \leq 0$ and $z \geq 0$. This gives us the first boundary condition:

$$f_-'(t) = f_-(t) + f_+(t). \qquad (6.51)$$

On the other hand, the forces exerted on the interface from the left and the right should also have equal magnitude, because the interface may be considered as an object with a vanishing mass, and any

nonzero net force would give it an infinite (and hence unphysical) acceleration. Together with Eqs. (45) and (47), this gives us the second boundary condition:

$$Z' \dot{f}_-'(t) = Z\left[\dot{f}_-(t) - \dot{f}_+(t)\right]. \tag{6.52}$$

Integrating both parts of this equation over time, and neglecting the integration constant (which describes a common displacement of all particles rather than their oscillations), we get

$$Z' f_-'(t) = Z\left[f_-(t) - f_+(t)\right]. \tag{6.53}$$

Now solving the system of two linear equations (51) and (53) for $f_+(t)$ and $f_+'(t)$, we see that both these functions are proportional to the incident waveform:

$$f_+(t) = \mathcal{R} f_-(t), \qquad f_-'(t) = \mathcal{T} f_-(t), \tag{6.54}$$

with the following *reflection* ($\mathcal{R}$) and *transmission* ($\mathcal{T}$) *coefficients*:

Reflection and transmission coefficients

$$\boxed{\mathcal{R} = \frac{Z - Z'}{Z + Z'}, \qquad \mathcal{T} = \frac{2Z}{Z + Z'}.} \tag{6.55}$$

Later in this series, we will see that with the appropriate re-definition of the impedance, these relations are also valid for waves of other physical nature (including the de Broglie waves in quantum mechanics) propagating in 1D continuous structures, and also in continua of higher dimensions, at the normal wave incidence upon the interface.[17] Note that the coefficients $\mathcal{R}$ and $\mathcal{T}$ give the ratios of wave *amplitudes*, rather than their *powers*. Combining Eqs. (49) and (55), we get the following relations for the powers – either at the interface or at the corresponding points of the reflected and transmitted waves:

$$\mathcal{P}_+ = \left(\frac{Z - Z'}{Z + Z'}\right)^2 \mathcal{P}_-, \qquad \mathcal{P}_-' = \frac{4ZZ'}{(Z + Z')^2} \mathcal{P}_-. \tag{6.56}$$

Note that $\mathcal{P}_- + \mathcal{P}_+ = \mathcal{P}_-'$, again reflecting the wave energy conservation.

Perhaps the most important corollary of Eqs. (55)–(56) is that the reflected wave completely vanishes, i.e. the incident wave is completely transmitted through the interface ($\mathcal{P}_+' = \mathcal{P}_+$), if the so-called *impedance matching condition* $Z' = Z$ is satisfied, even if the wave velocities v (32) are different on the left and the right sides of it. On the contrary, the equality of the acoustic velocities in the two continua does *not* guarantee the full transmission of their interface. Again, this is a very general result.

Finally, let us note that for the important particular case of a sinusoidal incident wave:[18]

$$f_-(t) = \mathrm{Re}\left[a e^{-i\omega t}\right], \qquad \text{so that} \quad f_+(t) = \mathrm{Re}\left[\mathcal{R} a e^{-i\omega t}\right], \tag{6.57}$$

where a is its complex amplitude, the total wave (50) on the right of the interface is

[17] See, e.g. the corresponding parts of this series: QM Sec. 2.3 and EM Sec. 7.3.

[18] In the acoustic wave limit, when the impedances Z and Z', and hence the reflection coefficient $\mathcal{R}$, are real, the factors $\mathcal{R}$ and Z may be taken out from under the Re operators in Eqs. (57)-(59). However, in the current, more general form of these relations, they are also valid for the case of arbitrary frequencies, $\omega \sim \omega_{\max}$, when these factors may be complex.

$$q(z,t) = \mathrm{Re}\left[a\, e^{-i\omega\left(t + z/v\right)} + \mathcal{R}\, a\, e^{-i\omega\left(t - z/v\right)} \right] \equiv \mathrm{Re}\left[a \left(e^{-ikz} + \mathcal{R}\, e^{+ikz} \right) e^{-i\omega t} \right], \quad \text{for } z \geq 0, \quad (6.58)$$

while according to Eq. (45), the corresponding force distribution is

$$F(z,t) = F_{-}(z,t) + F_{+}(z,t) = -Z\dot{f}_{-}\left(t - z/v\right) + Z\dot{f}_{+}\left(t - z/v\right) = \mathrm{Re}\left[i\omega Z a \left(e^{-ikz} - \mathcal{R}\, e^{+ikz} \right) e^{-i\omega t} \right]. \quad (6.59)$$

These expressions will be used in the next section.

6.5. Standing waves

Now let us consider the two limits in which Eqs. (55) predicts a *total wave reflection* ($\mathcal{T} = 0$): $Z'/Z \to \infty$ (when $\mathcal{R} = -1$) and $Z'/Z \to 0$ (when $\mathcal{R} = +1$). According to Eq. (53), the former limit corresponds to $f_{-}(t) + f_{+}(t) \equiv q(0, t) = 0$, i.e. to vanishing oscillations at the interface. This means that this particular limit describes a perfectly *rigid boundary*, not allowing the system's end to oscillate at all. In this case, Eqs. (58)-(59) yield

$$q(z,t) = \mathrm{Re}\left[a \left(e^{-ikz} - e^{+ikz} \right) e^{-i\omega t} \right] \equiv -2\,\mathrm{Re}\left[a\, e^{-i\omega t} \right] \sin kz, \quad (6.60)$$

$$F(z,t) = \mathrm{Re}\left[i\omega Z a \left(e^{-ikz} + e^{+ikz} \right) e^{-i\omega t} \right] \equiv 2\omega Z\, \mathrm{Re}\left[a\, e^{-i\left(\omega t - \pi/2\right)} \right] \cos kz. \quad (6.61)$$

These equalities mean that we may interpret the process on the right of the interface using two mathematically equivalent, but physically different languages: either as the sum of two *traveling waves* (the incident one and the reflected one, propagating in opposite directions), or as a single *standing wave*. Note that in contrast with the traveling wave (Fig. 9a, cf. Fig. 7), in the standing sinusoidal wave (Fig. 9b) all particles oscillate in time with the same phase.

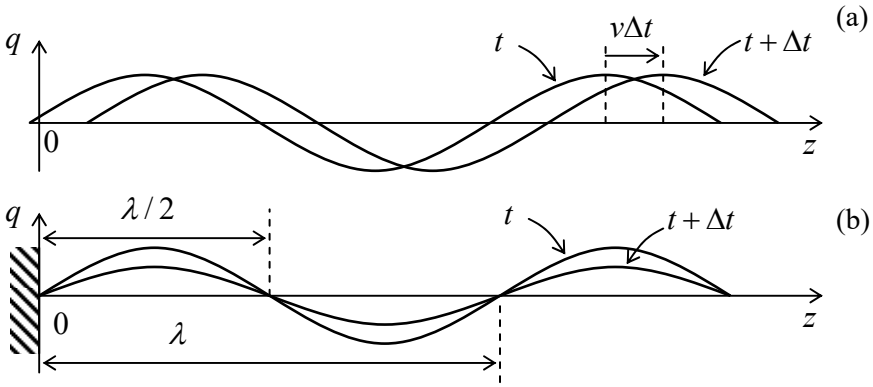

Fig. 6.9. The time evolution of (a) a traveling sinusoidal wave, and (b) a standing sinusoidal wave at a rigid boundary.

Note also that the phase of the force oscillations (61) is shifted, both in space and in time, by $\pi/2$ relative to the particle displacement oscillations. (In particular, at the rigid boundary the force amplitude reaches its maximum.) As a result, the average power flow vanishes, so the *average* energy of the standing wave does not change, though its *instant* energy still oscillates, at each spatial point, between its kinetic and potential components – just as at the usual harmonic oscillations of one particle. A similar standing wave, but with a maximum of the displacement q, and with a zero ("node") of the force F, is formed at the open boundary, with $Z'/Z \to 0$, and hence $\mathcal{R} = +1$.

Now I have to explain why I have used the sinusoidal waveform for the wave reflection analysis. Let us consider a 1D wave system, which obeys Eq. (40), of a finite length l, limited by two rigid walls (located, say, at $z = 0$ and $z = l$), which impose the corresponding boundary conditions,

$$q(0,t) = q(l,t) = 0, \tag{6.62}$$

on its motion. Naturally, a sinusoidal traveling wave, induced in the system, will be reflected from both ends, forming the standing wave patterns of the type (60) near each of them. These two patterns are compatible if l is exactly equal to an integer number (say, n) of $\lambda/2$, where $\lambda \equiv 2\pi/k$ is the wavelength:

$$l = n\frac{\lambda}{2} \equiv n\frac{\pi}{k}. \tag{6.63}$$

This requirement yields the following spectrum of possible wave numbers:

$$k_n = n\frac{\pi}{l}, \tag{6.64}$$

where the list of possible integers n may be limited to non-negative values: $n = 1, 2, 3,\ldots$ (Indeed, negative values give absolutely similar waves (60), while $n = 0$ yields $k_n = 0$, and the corresponding wave vanishes at all points: $\sin(0\cdot z) \equiv 0$.) In the acoustic wave limit we are discussing, Eq. (31), $\omega = \pm vk$, may be used to translate this wave-number spectrum into an equally simple spectrum of possible standing-wave frequencies:[19]

$$\omega_n = vk_n = n\frac{\pi v}{l}, \qquad \text{with } n = 1,2,3,... \tag{6.65}$$

Now let us notice that this spectrum, and the corresponding standing-wave patterns, [20]

$$q^{(n)}(z,t) = 2\,\mathrm{Re}\left[a_n \exp\{-i\omega_n t\}\right] \sin k_n z, \qquad \text{for } 0 \le z \le l, \tag{6.66}$$

may be calculated in a different way, by a direct solution of the wave equation (41) with the boundary conditions (62). Indeed, let us look for the general solution of this partial differential equation in the so-called *variable-separated* form[21]

$$q(z,t) = \sum_n Z_n(z)T_n(t), \tag{6.67}$$

where each partial product $Z_n(z)T_n(t)$ is supposed to satisfy the equation on its own. Plugging this partial solution into Eq. (40), and then dividing all its terms by the same product, Z_nT_n, we may rewrite the result as

$$\frac{1}{v^2}\frac{1}{T_n}\frac{d^2T_n}{dt^2} = \frac{1}{Z_n}\frac{d^2Z_n}{dz^2}. \tag{6.68}$$

Here comes the punch line of the variable separation method: since the left-hand side of the equation may depend only on t, while its right-hand side, only on z, Eq. (68) may be valid only if both sides are constant. Denoting this constant as $-k_n^2$, we get two similar ordinary differential equations,[22]

[19] Again, negative values of ω may be dropped, because they give similar real functions $q(z, t)$.

[20] They describe, in particular, the well-known transverse standing waves on a guitar string.

[21] This *variable separation method* is very general and is discussed in all parts of this series, especially in EM Chapter 2.

[22] The first of them is the 1D form of what is frequently called the *Helmholtz equation*.

$$\frac{d^2Z_n}{dz^2} + k_n^2 Z_n = 0, \qquad \frac{d^2T_n}{dt^2} + \omega_n^2 T_n = 0, \qquad \text{where } \omega_n^2 \equiv v^2 k_n^2, \tag{6.69}$$

with well-known (and similar) sinusoidal solutions

$$Z_n = c_n \cos k_n z + s_n \sin k_n z, \qquad T_n = u_n \cos \omega_n t + v_n \sin \omega_n z \equiv \mathrm{Re}\left[a_n \exp\{-i\omega_n t\}\right], \tag{6.70}$$

where c_n, v_n, u_n, and v_n (or, alternatively, $a_n \equiv u_n + iv_n$) are constants. The first of these relations, with all k_n different, may satisfy the boundary conditions only if for all n, $c_n = 0$, and $\sin k_n l = 0$, giving the same wave number spectrum (64) and hence the normal frequency spectrum (65), so the general solution (67) of the so-called *boundary problem*, given by Eqs. (40) and (62), takes the form

$$q(z,t) = \mathrm{Re}\sum_n a_n \exp\{-i\omega_n t\} \sin k_n z, \tag{6.71}$$

where the complex amplitudes a_n are determined by the initial conditions.

Hence such sinusoidal standing waves (Fig. 10a) are not just an assumption, but a natural property of the 1D wave equation. It is also easy to verify that the result (71) is valid for the same system with different boundary conditions, though with a modified wave number spectrum. For example, if the rigid boundary condition ($q = 0$) is implemented at $z = 0$, and the so-called *open* boundary condition ($F = 0$, i.e. $\partial q/\partial z = 0$) is imposed at $z = l$, the spectrum becomes

$$k_n = \left(n - \frac{1}{2}\right)\frac{\pi}{l}, \qquad \text{with } n = 1, 2, 3, ..., \tag{6.72}$$

so the lowest standing waves look like Fig. 10b shows.[23]

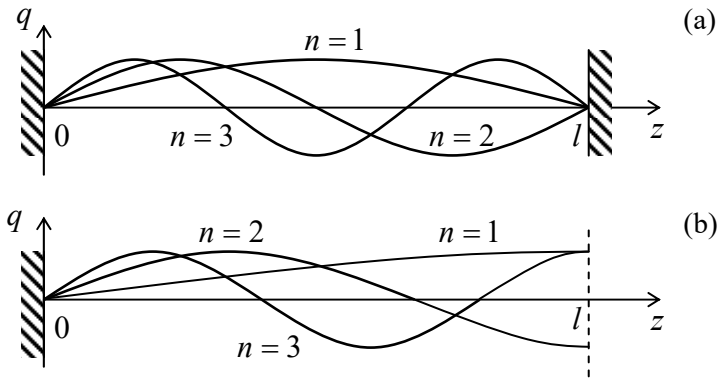

Fig. 6.10. The lowest standing wave modes for the 1D systems with (a) two rigid boundaries, and (b) one rigid and one open boundary.

Note that the difference between the sequential values of k_n is still a constant:

$$k_{n+1} - k_n = \frac{\pi}{l}, \tag{6.73}$$

the same one as for the spectrum (64). This is natural because in both cases the transfer from the n^{th} mode to the $(n + 1)^{\text{th}}$ mode corresponds just to an addition of one more half-wave – see Fig. 10. (This conclusion is valid for any combination of rigid and free boundary conditions.) As was discussed above, for the discrete-particle chain we have started with (Fig. 4), the wave equation (40), and hence the above

[23] The lowest standing wave of the system, with the smallest k_n and ω_n, is usually called its *fundamental mode*.

derivation of Eq. (71), are only valid in the acoustic wave limit, i.e. when the distance d between the particles is much less than the wavelengths $\lambda_n \equiv 2\pi/k_n$ of the mode under analysis. For a chain of length l, this means that the number of particles, $N \sim l/d$, has to be much larger than 1. However, a remarkable property of Eq. (71) is that it remains valid, with the same wave number spectrum (64), not only in the acoustic limit but also for arbitrary $N > 0$. Indeed, since $\sin k_n z \equiv (\exp\{+ik_n z\} - \exp\{-ik_n z\})/2$, each n^{th} term of Eq. (71) may be represented as a sum of two traveling waves with equal but opposite wave vectors. As was discussed in Sec. 3, such a wave is a solution of equation (24) describing the discrete-particle system for *any* k_n, with the only condition that its frequency obeys the general dispersion relation (30), rather than its acoustic limit (65).

Moreover, the expressions for k_n (with appropriate boundary conditions), such as Eq. (64) or Eq. (72), also survive the transition to arbitrary N, because their derivation above was based only on the sinusoidal form of the standing wave. The only new factor arising in the case of arbitrary N is that due to the equidistant property (73) of the wave number spectrum, as soon as n exceeds N, the waveforms (71), at particle locations $z_j = jd$, start to repeat. For example,

$$\sin k_{n+N} z_j = \sin\left(k_n + N\Delta k\right) jd = \sin\left(k_n + N\frac{\pi}{d}\right) jd = \sin\left(k_n z_j + \pi j N\right) \equiv \pm \sin k_n z_j . \tag{6.74}$$

Hence the system has only N different (linearly-independent) modes. But this result is in full compliance with the general conclusion made in Sec. 2, that *any* system of N coupled oscillators has exactly N normal frequencies and corresponding oscillation modes. So, our analysis of a particular system shown in Fig. 4, just exemplifies this general conclusion. Fig. 11 below illustrates this result for a particular finite value of N; the curve connecting the points shows exactly the same dispersion relation as was shown in Fig. 5, but now it is just a guide for the eye, because for a system with a finite length l, the wave number spectrum is discrete, and the intermediate values of k and ω do not have an immediate physical sense.[24] Note that the normal frequencies of the system are generally not equidistant, while the wave numbers are.

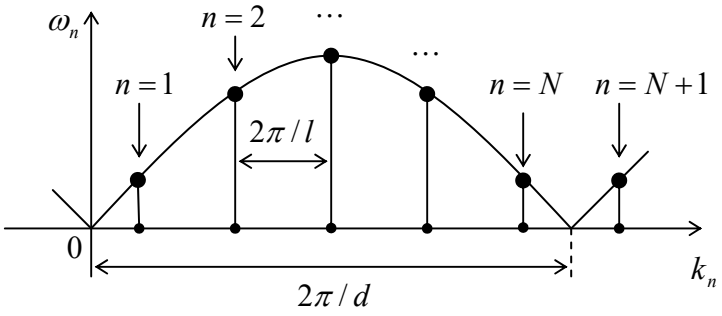

Fig. 6.11. The wave numbers and normal frequencies of a chain of a finite number N of particles in a chain with one rigid and one open boundary – schematically.

This insensitivity of the spacing (73) between the adjacent wave numbers to the particular physics of a macroscopically uniform system is a very general fact, common for waves of any nature, and is broadly used for analyses of systems with a very large number of particles (such as human-size crystals, with $N \sim 10^{23}$). For N so large, the effect of the boundary conditions, e.g., the difference

[24] Note that Fig. 11 shows the case of one rigid and one open boundary (see Fig. 10b), where $l = Nd$; for a conceptually simpler system with two rigid boundaries (Fig. 10a) we would need to take $l = (N + 1)d$ because neither of the end points can oscillate.

between the spectra (64) and (72) is negligible, and they may be summarized as the following rule for the number of different standing waves within some interval $\Delta k >> \pi/l$:

$$\Delta N \equiv \frac{\Delta k\big|_{\text{standing}}}{k_{n+1} - k_n} = \frac{l}{\pi}\Delta k\big|_{\text{standing}} . \tag{6.75a}$$

For such analyses, it is frequently more convenient to work with traveling waves rather than standing ones. In this case, we have to take into account that (as was just discussed above) each standing wave (66) may be decomposed into two traveling waves with wave numbers $\pm k_n$, so the interval Δk doubles, and Eq. (75a) becomes[25]

$$\boxed{\Delta N = \frac{l}{2\pi}\Delta k\big|_{\text{traveling}} .} \tag{6.75b}$$

Traveling wave number

Note that this counting rule is valid for waves of just one type. As was discussed above, for the model system we have studied (Fig. 4), there are 3 types of such waves – one longitudinal and two transverse, so if we need to count them all, ΔN should be multiplied by 3.

6.6. Wave decay and attenuation

Now let us discuss the effects of energy dissipation on the 1D waves, on the example of the same uniform system shown in Fig. 4. The simplest description of this effect is the linear drag that may be described, as it was done for a single oscillator in Sec. 5.1, by adding the term $\eta dq_j/dt$, to Eq. (24) for each particle:

$$m\ddot{q}_j + \eta\dot{q}_j - \kappa_{\text{ef}}(q_{j+1} - q_j) + \kappa_{\text{ef}}(q_j - q_{j-1}) = 0 . \tag{6.76}$$

(In a uniform system, the drag coefficient η should be similar for all particles, though it may be different for the longitudinal and transverse oscillations.)

To analyze the dissipation effect on the *standing* waves, we may again use the variable separation method, i.e. look for the solution of Eq. (76) in the form similar to Eq. (67), naturally re-adjusting it for our current discrete case:

$$q(z_j, t) = \sum_n Z_n(z_j)T_n(t) . \tag{6.77}$$

After dividing all terms by $mZ_n(z_j)T_n(t)$ and separating the time-dependent and space-dependent terms, we get

$$\frac{\ddot{T}_n}{T_n} + \frac{\eta}{m}\frac{\dot{T}_n}{T_n} = \frac{\kappa_{\text{ef}}}{m}\left[\frac{Z_n(z_{j+1})}{Z_n(z_j)} + \frac{Z_n(z_{j+1})}{Z_n(z_j)} - 2\right] = \text{const} . \tag{6.78}$$

As we know from the previous section, the resulting equation for the function $Z_n(z_j)$ is satisfied if the variable separation constant is equal to $-\omega_n^2$, where ω_n obeys the dispersion relation (30) for the wave number k_n, properly calculated for the *dissipation-free* system, with the account of the given boundary

[25] Note that this simple, but very important relation is frequently derived using the so-called *Born-Carman boundary condition* $q_0(t) \equiv q_N(t)$, which implies bending the system of interest into a closed loop. For a 1D system with $N >> 1$, such mental exercise may be somehow justified, but for systems of higher dimension, it is hardly physically plausible – and is unnecessary.

conditions – see, e.g. Eqs. (62) and (72). Hence for the function $T_n(t)$, we are getting the following ordinary differential equation:

$$\ddot{T}_n + 2\delta\dot{T}_n + \omega_n^2 T_n = 0, \qquad \text{with } \delta \equiv \frac{\eta}{2m}, \tag{6.79}$$

which is absolutely similar to Eq. (5.6b) for a single linear oscillator, which was studied in Sec. 5.1. As we already know, it has the solution (5.9) describing the free oscillation decay with the relaxation time given by (5.10), $\tau = 1/\delta$, and hence similar for all modes.[26]

Hence, the above analysis of the dissipation effect on *free* standing waves has not brought any surprises, but it gives us a hint of how their *forced* oscillations, induced by some external forces $F_j(t)$ exerted on the particles, may be analyzed. Indeed, representing each of the forces as a sum over the system's modes (spatial harmonics),

$$f(z_j,t) \equiv \frac{F_j(t)}{m} = \sum_n f_n(t) Z_n(z_j), \tag{6.80}$$

and using the variable separation (77), we arrive at the natural generalization of Eq. (79):

$$\ddot{T}_n + 2\delta\dot{T}_n + \omega_n^2 T_n = f_n(t), \tag{6.81}$$

which is identical to Eq. (5.13b) for a single oscillator. This fact enables us to use Eq. (5.27), with $G(\tau) \to G_n(\tau)$, for the calculation of each $T_n(t)$. Now finding the functions $f_n(t)$ from Eq. (80) by the usual reciprocal Fourier transform, and plugging these results into Eq. (77), we get the following generalization of Eq. (5.27):

$$q(z_j,t) = \sum_{j'=1}^{N} \int_0^\infty f(z_{j'}, t-\tau)\mathcal{G}(z_j, z_{j'}, \tau)\, d\tau, \quad \text{where } \mathcal{G}(z_j, z_{j'}, \tau) \equiv \sum_n G_n(\tau) Z_n(z_j) Z_n(z_{j'}). \tag{6.82}$$

(Here the mutually orthogonal functions $Z_n(z_j)$ are assumed to be normalized, i.e. the sums of their squares over $j = 1, 2, \ldots, N$ to equal 1.) Such function $\mathcal{G}(z_j, z_{j'}, \tau)$ is called the *spatial-temporal Green's function* of the system – in our current case, of a discrete 1D set of N particles located at points $z_j = jd$. The reader is challenged to spell out this function for at least one of the particular cases discussed above and use it to solve at least one forced-oscillation problem.

Now let us discuss the dissipation effects on the *traveling* waves, where they may take a completely different form of *attenuation*. Let us discuss it on a simple example when one end (located at $z = 0$) of a very long chain ($l \to \infty$) is externally forced to perform sinusoidal oscillations of a certain frequency ω and a fixed amplitude A_0. In this case, it is natural to look for a particular solution to Eq. (76) in a form very different from Eq. (77):

$$q(z_j,t) = \mathrm{Re}\left[c_j e^{-i\omega t} \right], \tag{6.83}$$

[26] Even an elementary experience with acoustic guitars shows that for their strings, this conclusion of our theory is not valid: higher modes ("overtones") decay substantially faster, leaving the fundamental mode oscillations for a slower decay. This is a result of another important energy dissipation (i.e. the wave decay) mechanism, not taken into account in Eq. (76) – the radiation of the sound into the guitar's body through the string supports, mostly through the bridge. Such radiation may be described by a proper modification of the boundary conditions (62), in terms of the ratio of the wave impedance (47) of the string and those of the supports.

with time-independent but generally complex amplitudes c_j. As our discussion of a single oscillator in Sec. 5.1 implies, this is not the general, but rather a partial solution, which describes the forced oscillations in the system, to that it settles after some initial transient process. (At non-zero damping, we may be sure that free oscillations fade after a finite time, and thus may be ignored for most purposes.)

Plugging Eq. (83) into Eq. (76), we reduce it to an equation for the amplitudes c_j,

$$\left(-m\omega^2 - i\omega\eta + 2\kappa_{\text{ef}}\right)c_j - \kappa_{\text{ef}}c_{j+1} - \kappa_{\text{ef}}c_{j-1} = 0, \tag{6.84}$$

which is a natural generalization of Eq. (25). As a result, partial solutions of the set of these equations (for $j = 0, 1, 2,\ldots$) may be looked for in the form (26) again, but now, because of the new, imaginary term in Eq. (84), we should be ready to get a complex phase shift α, and hence a complex wave number $k \equiv \alpha/d$.[27] Indeed, the resulting characteristic equation for k,

$$\sin^2\frac{kd}{2} = \frac{\omega^2}{\omega_{\max}^2} + i\frac{2\omega\delta}{\omega_{\max}^2} \tag{6.85}$$

(where $\omega_{\max}$ is defined by Eq. (30), and the damping coefficient is defined just as in a single oscillator, $\delta \equiv \eta/2m$), does not have a real solution even at $\omega < \omega_{\max}$. Using the well-known expressions for the sine function of a complex argument,[28] Eq. (85) may be readily solved in the most important low-damping limit $\delta << \omega$. In the linear approximation in δ, it does not affect the real part of k, but makes its imaginary part different from zero:

$$k = \pm\frac{2}{d}\left(\sin^{-1}\frac{\omega}{\omega_{\max}} + i\frac{\delta}{\omega_{\max}}\right) \equiv \pm\left(\frac{2}{d}\sin^{-1}\frac{\omega}{\omega_{\max}} + i\frac{\delta}{v}\right), \qquad \text{for } -\pi \le \text{Re}\,k \le \pi, \tag{6.86}$$

with a periodic extension to other periods – see Fig. 5. Just as was done in Eq. (28), due to two values of the wave number, generally we have to take c_j in the form of not a single wave (26), but of a linear superposition of two partial solutions:

$$c_j = \sum_{\pm} c_{\pm}\exp\left\{\pm i\,\text{Re}\,kz_j \mp \frac{\delta}{v}z_j\right\}, \tag{6.87}$$

where the constants $c_{\pm}$ should be found from the boundary conditions. In our particular case, when $|c_0| = A_0$ and $c_\infty = 0$, only one of these two waves, namely the wave exponentially decaying at its penetration into the system, is different from zero: $|c_+| = A_0$, $c_- = 0$. Hence our solution describes a single wave, with the real amplitude and the oscillation energy decreasing as

$$A_j \equiv |c_j| = A_0\exp\left\{-\frac{\delta}{v}z_j\right\}, \qquad E_j \propto A_j^2 \propto \exp\left\{-\alpha z_j\right\}, \qquad \text{with } \alpha = \frac{2\delta}{v}, \tag{6.88}$$

Wave attenuation

i.e. with a frequency-independent *attenuation constant* $\alpha = 2\delta/v$,[29] so the spatial scale of wave penetration into a dissipative system is given by $l_d \equiv 1/\alpha$. Certainly, our simple solution (88) is only valid for a system of length $l >> l_d$; otherwise, we would need the second term in the sum (87) to describe the wave reflected from its opposite end.

[27] As a reminder, we have already met such a situation in the absence of damping, but at $\omega > \omega_{\max}$ – see Eq. (38).

[28] See, e.g., MA Eq. (3.5).

[29] I am sorry to use for the attenuation the same letter α as for the phase shift in Eq. (26) and a few of its corollaries, but both notations are traditional.

6.7. Nonlinear and parametric effects

Now let me discuss (because of the lack of time, very briefly, and on a semi-quantitative level), the new nonlinear and parametric phenomena that appear in oscillatory systems with more than one degree of freedom – cf. Secs. 5.4-5.8. One important new effect here is the *mutual phase locking* of (two or more) weakly coupled self-excited oscillators with close frequencies: if the normal frequencies of the oscillators are sufficiently close, their oscillation frequencies "stick together" to become exactly equal. Though the dynamics of this process is very close to that of the phase locking of a single oscillator by an external signal, which was discussed in Sec. 5.4, it is rather counter-intuitive in view of the results discussed in Sec. 1, and in particular, the anticrossing diagram shown in Fig. 2. The analysis of the effect using the van der Pol method (which is left for the reader's exercise) shows that the origin of the difference is the oscillators' nonlinearity, which makes the oscillation amplitudes virtually independent of the phase evolution – see Eq. (5.68) and its discussion.

One more new effect is the so-called *non-degenerate parametric excitation*. It may be illustrated on the example of just two coupled oscillators – see Sec. 1 above. Let us assume that the coupling constant κ participating in Eqs. (5) is not constant, but oscillates in time – say with some frequency ω_p. In this case, the forces acting on each oscillator from its counterpart, described by the right-hand sides of Eqs. (5), will be proportional to $\kappa q_{2,1}(1 + \mu \cos\omega_p t)$. Assuming that the oscillations of q_1 and q_2 are close to sinusoidal ones, with certain frequencies $\omega_{1,2}$, we see that the force exerted on each oscillator contains the so-called *combinational frequencies*

$$\omega_p \pm \omega_{2,1}. \tag{6.89}$$

If one of these frequencies is close to the normal oscillation frequency of the oscillator, we can expect a substantial parametric interaction between the oscillators (on top of the constant coupling effects discussed in Sec. 1). According to Eq. (89), this may happen in two cases:

Parametric interaction conditions

$$\omega_p = \omega_1 + \omega_2, \tag{6.90a}$$

$$\omega_p = \omega_1 - \omega_2. \tag{6.90b}$$

The quantitative analysis (also highly recommended to the reader) shows that in the case (90a), the parameter modulation indeed leads to energy "pumping" into the oscillations.[30] As a result, a sufficiently large μ, at sufficiently small damping coefficients $\delta_{1,2}$ and the effective detuning

$$\xi \equiv \omega_p - (\Omega_1 + \Omega_2), \tag{6.91}$$

may lead to a simultaneous self-excitation of two frequency components $\omega_{1,2}$. These frequencies, while being approximately equal to the corresponding normal frequencies $\Omega_{1,2}$ of the system, are related to the *pumping frequency* ω_p by the exact relation (90a), but otherwise are arbitrary, e.g., may be incommensurate (Fig. 12a), thus justifying the term *non-degenerate* parametric excitation.[31] (The parametric excitation of a single oscillator, which was analyzed in Sec. 5.5, is a particular, *degenerate* case of such excitation, with $\omega_1 = \omega_2 = \omega_p/2$.) On the other hand, for the case described by Eq. (90b), the parameter modulation always extracts energy *from* the oscillations, effectively increasing the system's damping.

[30] Hence the common name of ω_p – the pumping frequency.

[31] Note that in some publications, the term *parametric down-conversion* (PDC) is used instead.

Somewhat counterintuitively, this difference between the two cases (90) may be interpreted more simply by using the basic notions of quantum mechanics. Namely, the equality $\omega_p = \omega_1 + \omega_2$ enables a decay of an external photon of energy $\hbar\omega_p$ into two photons of energies $\hbar\omega_1$ and $\hbar\omega_2$ of the oscillators. On the contrary, the complementary relation (90b), meaning that $\omega_1 = \omega_p + \omega_2$, results in a pumping-induced decay of photons of frequency ω_1.

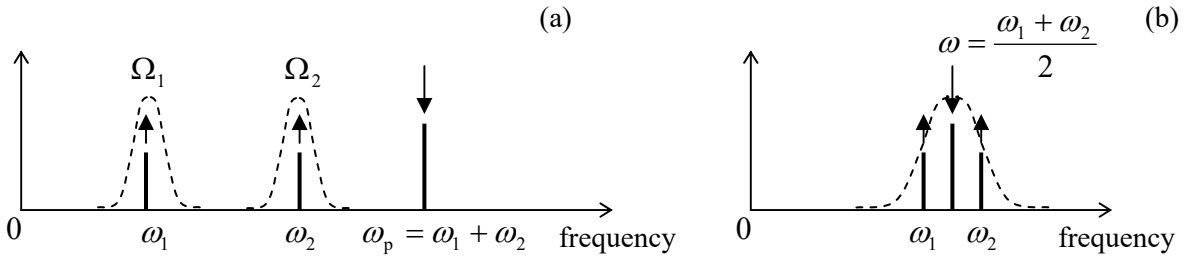

Fig. 6.12. Spectra of oscillations at (a) the non-degenerate parametric excitation, and (b) the four-wave mixing. The arrow directions symbolize the energy flows into and out of the system.

Note that even if the frequencies ω_1 and ω_2 of the parametrically excited oscillations are incommensurate, the oscillations are highly correlated. Indeed, the quantum-mechanical theory of this effect[32] shows that the generated photons are *entangled*. This fact makes the parametric excitation very popular for a broad class of experiments in several currently active fields including quantum computation and encryption, and the Bell inequality/local reality studies.[33]

Proceeding to nonlinear phenomena, let us note, first of all, that the simple reasoning that accompanied Eq. (5.108) in Sec. 5.8, is also valid in the case when oscillations consist of two (or more) sinusoidal components with incommensurate frequencies. Replacing the notation 2ω with ω_p, we see that the non-degenerate parametric excitation of the type (90a) is possible in a system of two coupled oscillators with a quadratic nonlinearity (of the type γq^2), "pumped" by an intensive external signal at frequency $\omega_p \approx \Omega_1 + \Omega_2$. In optics, it is often more convenient to have all three of these frequencies within the same, relatively narrow range. A simple calculation, similar to the one made in Eqs. (5.107)-(5.108), shows that this may be done using the cubic nonlinearity[34] of the type αq^3, which allows a similar parametric energy exchange at the frequency relation shown in Fig. 12b:

$$2\omega = \omega_1 + \omega_2, \qquad \text{with } \omega \approx \omega_1 \approx \omega_2 . \tag{6.92a}$$

Four-wave mixing

This process is often called the *four-wave mixing*, because it may be interpreted quantum-mechanically as the transformation of *two* externally-delivered photons, each with energy $\hbar\omega$, into two other photons of energies $\hbar\omega_1$ and $\hbar\omega_2$. The word "wave" in this term stems from the fact that at optical frequencies, it is hard to couple a sufficient volume of a nonlinear medium with lumped-type resonators. It is much easier to implement the parametric excitation (as well as other nonlinear phenomena such as the higher harmonic generation) of light in *distributed systems* of a linear size much larger than the involved wavelengths. In such systems, the energy transfer from the incoming wave of frequency ω to

[32] Which is, surprisingly, not much more complex than the classical theory – see, e.g., QM Sec.5.5.
[33] See, e.g., QM Secs. 8.5 and 10.3, respectively.
[34] In optics, such nonlinearity is implemented using transparent crystals such as lithium niobate ($LiNbO_3$), with the cubic-nonlinear dependence of the electric polarization on the applied electric field: $\mathscr{P} \propto \mathscr{E} + \alpha\mathscr{E}^3$.

generated waves of frequencies ω_1 and ω_2 is gradually accumulated at their joint propagation along the system. From the analogy between Eq. (85) (describing the evolution of the wave's amplitude *in space*), and the usual equation of the linear oscillator (describing its evolution *in time*), it is clear that this energy transfer accumulation requires not only the frequencies ω but also the wave numbers k be in similar relations. For example, the four-wave mixing requires not only the frequency balance (92a) but also a similar relation

$$2k = k_1 + k_2, \tag{6.92b}$$

to be fulfilled. Since all three frequencies are close, this relation is easy to arrange. Unfortunately, due to the lack of time/space, for more discussion of this very interesting subject, called *nonlinear optics*, I have to refer the reader to special literature.[35]

It may look like a dispersion-free media, with $\omega/k = v = \text{const}$, is the perfect solution for arranging the nonlinear/parametric interaction of waves, because in such media, for example, Eq. (92b) automatically follows from Eq. (92a). However, in such a medium, not only the desirable three parametrically interacting waves but also all their harmonics, have the same velocity. At these conditions, the energy transfer rates between all harmonics are of the same order. Perhaps the most important result of such a multi-harmonic interaction is that intensive incident traveling waves, interacting with a nonlinear medium, may develop sharply non-sinusoidal waveforms, in particular those with an almost instant change of the field at a certain moment. Such *shock waves*, especially the mechanical ones, are of large interest for certain applications – some of them not quite innocent, e.g., the dynamics of explosion in the usual (chemical) and nuclear bombs.[36]

To conclude this chapter, let me note that the above discussion of 1D acoustic waves will be extended, in Sec. 7.7, to elastic 3D media. There we will see that generally, the waves obey a more complex equation than the apparently natural generalization of Eq. (40):

$$\left(\frac{1}{v^2} \frac{\partial^2}{\partial t^2} - \nabla^2 \right) q(\mathbf{r}, t) = 0, \tag{6.93}$$

where ∇^2 is the 3D Laplace operator. This fact adds to the complexity of traveling-wave and standing-wave phenomena in higher dimensions. Moreover, in multi-dimensional systems, including such pseudo-1D systems as thin rods and pseudo-2D systems such as thin membranes, even static elastic deformations may be very nontrivial. An introduction to the general theory of small deformations, with a focus on elastic continua, will be the subject of the next chapter.

6.8. Exercise problems

For each of the systems specified in Problems 1-6:

(i) introduce convenient generalized coordinates q_j of the system,

[35] See, e.g., N. Bloembergen, *Nonlinear Optics*, 4th ed., World Scientific, 1996, or a more modern treatment by R. Boyd, *Nonlinear Optics*, 3rd ed., Academic Press, 2008. This field is currently very active. As just a single example, let me mention the recent experiments with parametric amplification of ultrashort (~20-fs) optical pulses to peak power as high as $\sim 5\times10^{12}$ W – see X. Zeng *et al*., *Optics Lett*. **42**, 2014 (2017).

[36] The classical (and perhaps still the best) monograph on the subject is Ya. Zeldovich, *Physics of Shock Waves and High-Temperature Phenomena,* Dover, 2002.

(ii) calculate the frequencies of its small harmonic oscillations near the equilibrium,
(iii) calculate the corresponding distribution coefficients, and
(iv) sketch the oscillation modes.

6.1. Two elastically coupled pendula confined to the vertical plane that contains both suspension points, with the parameters shown in the figure on the right (see also Problems 1.8 and 2.9).

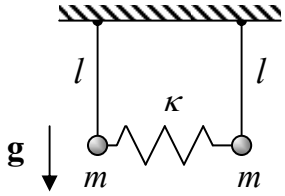

6.2. The double pendulum confined to the vertical plane containing the support point (which was the subject of Problem 2.1), with $m' = m$ and $l = l'$ – see the figure on the right.

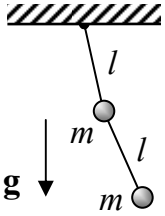

6.3 The chime bell considered in Problem 4.12 (see the figure on the right), for the particular case $l = l'$.

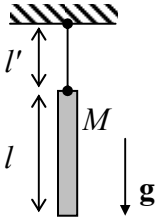

6.4. The triple pendulum shown in the figure on the right, with the motion confined to a vertical plane containing the support point.

Hint: You may use any (e.g., numerical) method to calculate the characteristic equation's roots.

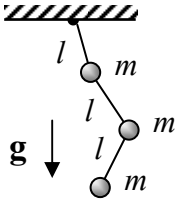

6.5. The symmetric three-particle system shown in the figure on the right, where the connections between the particles not only act as usual elastic springs (giving potential energies $U = \kappa(\Delta l)^2/2$) but also resist bending, giving additional potential energy $U' = \kappa'(l\theta)^2/2$, where θ is the (small) bending angle.[37]

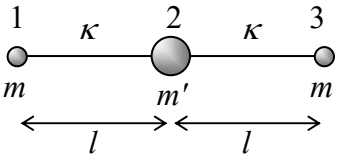

6.6. Three similar beads of mass m, which may slide along a round ring of radius R without friction, connected with similar springs with elastic constants κ and equilibrium lengths l_0 (not necessarily equal to $\sqrt{3}R$) – see the figure on the right.

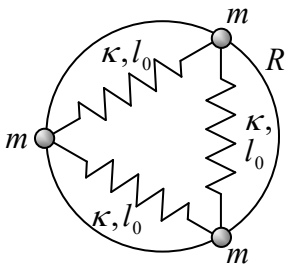

[37] This is a reasonable model for small oscillations of linear molecules such as the now-infamous CO_2.

6.7. On the example of the model considered in Problem 1, explore free oscillations in a system of two similar and weakly coupled linear oscillators.

6.8. A small body is held by four similar elastic springs as shown in the figure on the right. Analyze the effect of rotation of the system as a whole about the axis normal to its plane, on the body's small oscillations within this plane. Assume that the oscillation frequency is much higher than the angular velocity ω of the rotation. Discuss the physical sense of your results and possible ways of using such systems for measurement of the rotation.

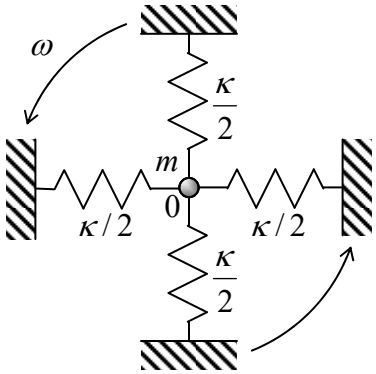

6.9. An external longitudinal force $F(t)$ is applied to the right particle of the system shown in Fig. 1, with $\kappa_L = \kappa_R = \kappa'$ and $m_1 = m_2 \equiv m$ (see the figure on the right), and the response $q_1(t)$ of the left particle to this force is being measured.

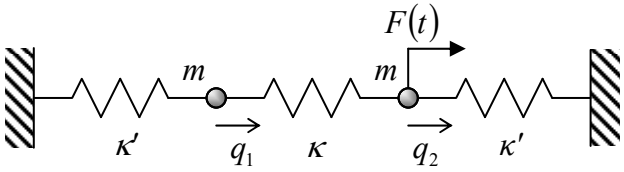

(i) Calculate the temporal Green's function for this response.

(ii) Use this function to calculate the response to the following force:

$$F(t) = \begin{cases} 0, & \text{for } t < 0, \\ F_0 \sin \omega t, & \text{for } 0 \le t, \end{cases}$$

with constant amplitude F_0 and frequency ω.

6.10. Use the Lagrangian formalism to re-derive Eqs. (24) for both the longitudinal and the transverse oscillations in the system shown in Fig. 4a.

6.11. Calculate the energy (per unit length) of a sinusoidal traveling wave propagating in the 1D system shown in Fig. 4a. Use your result to calculate the average power flow created by the wave, and compare it with Eq. (49) in the acoustic wave limit.

6.12. Calculate spatial distributions of the kinetic and potential energies in a standing sinusoidal 1D acoustic wave and analyze their evolution in time.

6.13. The midpoint of a guitar string of length l has been slowly pulled off sideways by a distance $h << l$ from its equilibrium position, and then let go. Neglecting energy dissipation, use two different approaches to calculate the midpoint's displacement as a function of time.

Hint: You may like to use the following series: $\sum_{m=1}^{\infty} \frac{\cos(2m-1)\xi}{(2m-1)^2} = \frac{\pi^2}{8}\left(1 - \frac{\xi}{\pi/2}\right)$, for $0 \le \xi \le \pi$.

6.14. Spell out the spatial-temporal Green's function (82) for waves in a uniform 1D system of N points, with rigid boundary conditions (62). Explore the acoustic limit of your result.

6.15. Calculate the dispersion law $\omega(k)$ and the highest and lowest frequencies of small longitudinal waves in a long chain of similar, spring-coupled pendula – see the figure on the right.

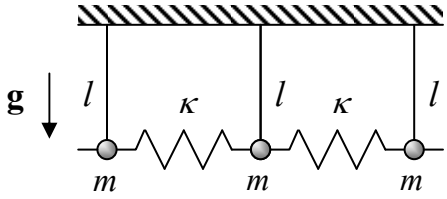

6.16. Calculate and analyze the dispersion relation $\omega(k)$ for small waves in a long chain of elastically coupled particles with alternating masses – see the figure on the right. In particular, discuss the dispersion relation's period Δk, and its evolution at $m' \to m$.

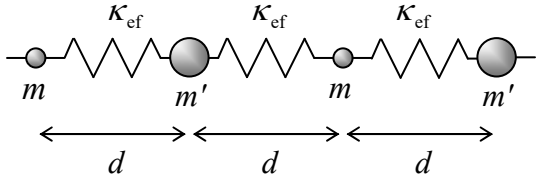

6.17. Analyze the traveling wave's reflection from a "point inhomogeneity": a single particle with a different mass $m_0 \neq m$, in an otherwise uniform 1D chain – see the figure on the right.

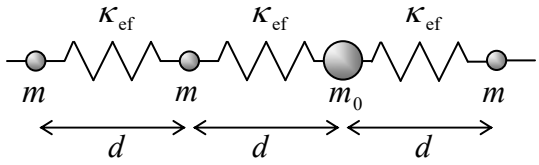

6.18.*

(i) Explore an approximate way to analyze small waves in a continuous 1D system with parameters slowly varying along its length.

(ii) Apply this method to calculate the frequencies of transverse standing waves on a freely hanging heavy rope of length l, with a constant mass μ per unit length – see the figure on the right.

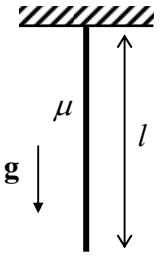

(iii) For the three lowest standing wave modes, compare the results with those obtained in the solution of Problem 4 for the triple pendulum.

Hint: The reader familiar with the WKB approximation in quantum mechanics (see, e.g., QM Sec. 2.4) is welcome to adapt it for this classical application. Another possible starting point is the van der Pol approximation discussed in Sec. 5.3, which should be translated from the time domain to the space domain.

6.19. A particle of mass m is attached to an infinite string, of mass μ per unit length, stretched with tension $\mathcal{T}$. The particle is confined to move along the x-axis perpendicular to the string (see the figure below), in an additional smooth potential $U(x)$ with a minimum at $x = 0$. Assuming that the waves on the string are excited only by the motion of the particle (rather than any external source), reduce the system of equations describing the system to an ordinary differential equation for small oscillations $x(t)$, and calculate their Q-factor of due to the drag caused by the string.

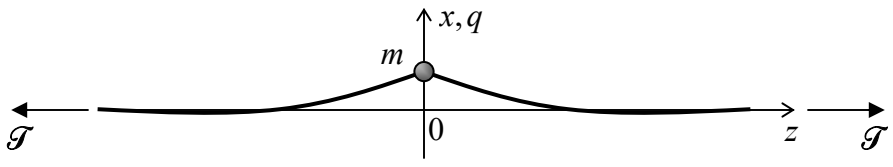

6.20.* Use the van der Pol method to analyze the mutual phase locking of two weakly coupled self-oscillators with the dissipative nonlinearity, for the cases of:

(i) the direct coordinate coupling described by Eq. (5), and
(ii) a bilinear but otherwise arbitrary coupling of two similar oscillators.

Hint: In Task (ii), describe the coupling by an arbitrary linear operator, and express the result via its Fourier image.

6.21.* Extend Task (ii) of the previous problem to the mutual phase locking of N similar self-oscillators. In particular, explore the in-phase mode's stability for the case of so-called *global coupling* via a single force F contributed equally by all oscillators.

6.22.* Find the condition of non-degenerate parametric excitation in a system of two coupled oscillators described by Eqs. (5), but with time-dependent coupling: $\kappa \to \kappa(1 + \mu\cos\omega_p t)$, with $\omega_p \approx \Omega_1 + \Omega_2$.

Hint: Use the van der Pol method, assuming the modulation depth μ, the static coupling coefficient κ, and the detuning $\xi \equiv \omega_p - (\Omega_1 + \Omega_2)$ are all sufficiently small.

6.23. Show that the cubic nonlinearity of the type αq^3 indeed enables the parametric interaction ("four-wave mixing") of oscillations with incommensurate frequencies related by Eq. (92a).

6.24. In the first nonvanishing approximation in small oscillation amplitudes, calculate their effect on the frequencies of the double-pendulum system that was the subject of Problem 1.

6.25. Calculate the velocity of small transverse waves propagating on a thin, planar, elastic membrane, with a constant mass m per unit area, pre-stretched with force τ per unit width.

6.26. A membrane discussed in the previous problem is stretched on a thin but firm plane frame of area $a \times a$.

(i) Calculate the frequency spectrum of small transverse standing waves in the system; sketch a few lowest wave modes.

(ii) Compare the results with those for a discrete-point analog of this system, with four particles of equal masses m, connected with light flexible strings that are stretched, with equal tensions $\mathcal{T}$, on a similar frame – see the figure on the right.

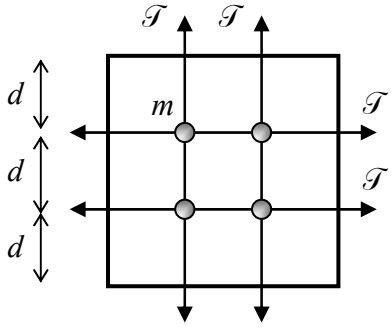

Hint: The frames do not allow the membrane edges/string ends to deviate from their planes.

This page is intentionally left blank

Chapter 7. Deformations and Elasticity

The objective of this chapter is a discussion of small deformations of 3D continua, with a focus on the elastic properties of solids. The reader will see that such deformations are nontrivial even in the absence of their evolution in time, so several key problems of statics will need to be discussed before proceeding to such dynamic phenomena as elastic waves in infinite media and thin rods.

7.1. Strain

As was already discussed in Chapters 4-6, in a *continuum*, i.e. a system of particles so close to each other that the system discreteness may be neglected, particle displacements **q** may be considered as a continuous function of not only time but also space. In this chapter, we will consider only *small* deviations from the rigid-body approximation discussed in Chapter 4, i.e. small *deformations*. The deformation smallness allows us to consider the displacement vector **q** as a function of the *initial* (pre-deformation) position of the particle, **r**, and time t – just as was done in Chapter 6 for 1D waves.

The first task of the deformation theory is to exclude from consideration the types of motion considered in Chapter 4, namely the body's translation and rotation, unrelated to deformations. This means, first of all, that the variables describing deformations should not depend on the displacement's part that is independent of the position **r** (i.e. is common for the whole media), because that part corresponds to a translational shift rather than to a deformation (Fig. 1a). Moreover, even certain non-uniform displacements do not contribute to deformation. For example, Eq. (4.9) (with $d\mathbf{r}$ replaced with $d\mathbf{q}$ to comply with our current notation) shows that a small displacement of the type

$$d\mathbf{q}|_{\text{rotation}} = d\boldsymbol{\varphi}\times\mathbf{r}, \tag{7.1}$$

where $d\boldsymbol{\varphi} = \boldsymbol{\omega}dt$ is an infinitesimal vector common for the whole continuum, corresponds to its elementary rotation of the body about the direction of that vector, and has nothing to do with its deformation (Fig. 1b).

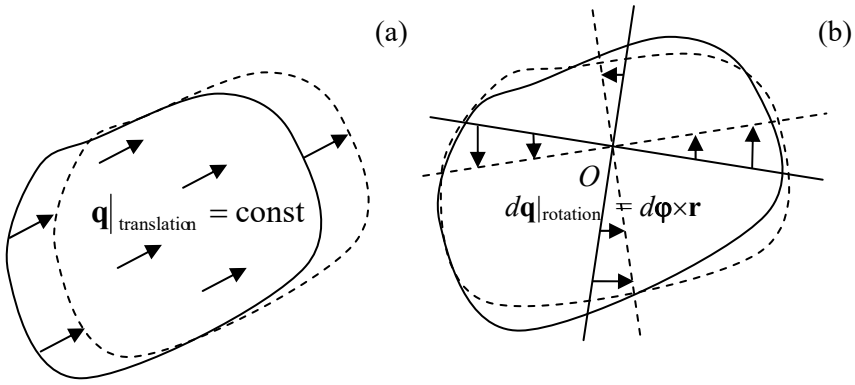

Fig. 7.1. Two types of displacement vector distributions that are unrelated to deformation: (a) translation and (b) rotation.

This is why to develop an adequate quantitative characterization of deformation, so far for fixed t, we should start with finding suitable functions of the spatial distribution of displacements, $\mathbf{q}(\mathbf{r})$, that exist only due to deformations. One such measure is the change of the distance $dl \equiv |d\mathbf{r}|$ between two close points:

© K. Likharev

$$(dl)^2\big|_{\text{after deformation}} - (dl)^2\big|_{\text{before deformation}} = \sum_{j=1}^{3}(dr_j + dq_j)^2 - \sum_{j=1}^{3}(dr_j)^2 \ , \tag{7.2}$$

where dq_j is the j^{th} Cartesian component of the difference $d\mathbf{q}$ between the displacements $\mathbf{q}$ of these close points. If the deformation is small in the sense $|d\mathbf{q}| << dl$, we may keep, in this expression, only the terms proportional to the first power of the infinitesimal vector $d\mathbf{q}$:

$$(dl)^2\big|_{\text{after deformation}} - (dl)^2\big|_{\text{before deformation}} = \sum_{j=1}^{3}\left[2dr_j dq_j + (dq_j)^2\right] \approx 2\sum_{j=1}^{3} dr_j dq_j \ . \tag{7.3}$$

Since q_j is a function of three independent scalar arguments r_j, its full differential (at fixed time) may be represented as

$$dq_j = \sum_{j'=1}^{3}\frac{\partial q_j}{\partial r_{j'}} dr_{j'}. \tag{7.4}$$

The coefficients $\partial q_j/\partial r_{j'}$ may be considered as elements of a tensor providing a linear relation between the vectors d$\mathbf{r}$ and d$\mathbf{q}$.[1] Plugging Eq. (4) into Eq. (2), we get

$$(dl)^2\big|_{\text{after deformation}} - (dl)^2{}_{|\text{before deformation}} = 2\sum_{j,j'=1}^{3}\frac{\partial q_j}{\partial r_{j'}} dr_j dr_{j'} \ . \tag{7.5}$$

The convenience of the tensor $\partial q_j/\partial r_{j'}$ for characterizing deformations is that it automatically excludes the translation displacement (Fig. 1a), which is independent of r_j. Its drawback is that its particular elements are still affected by the rotation of the body – even though the sum (5) is not. Indeed, according to the vector product's definition, Eq. (1) may be represented in Cartesian coordinates as

$$dq_j\big|_{\text{rotation}} = \left(d\varphi_{j'} r_{j''} - d\varphi_{j''} r_{j'}\right)\varepsilon_{jj'j''}, \tag{7.6}$$

where $\varepsilon_{jj'j''}$ is the Levi-Civita symbol. Differentiating Eq. (6) over a particular Cartesian coordinate of vector $\mathbf{r}$, and taking into account that this partial differentiation (∂) is independent of (and hence may be swapped with) the differentiation (d) over the common rotation angle φ, we get the amounts

$$d\left(\frac{\partial q_j}{\partial r_{j'}}\right)_{\text{rotation}} = -\varepsilon_{jj'j''} d\varphi_{j''} \quad \text{and} \quad d\left(\frac{\partial q_{j'}}{\partial r_j}\right)_{\text{rotation}} = -\varepsilon_{j'jj''} d\varphi_{j''} = \varepsilon_{jj'j''} d\varphi_{j''}, \tag{7.7}$$

which may differ from 0. However, notice that the *sum* of these two differentials equals zero for any $d\boldsymbol{\varphi}$, which is possible only if[2]

$$\left(\frac{\partial q_{j'}}{\partial r_j} + \frac{\partial q_j}{\partial r_{j'}}\right)_{\text{rotation}} = 0, \qquad \text{for } j \neq j'. \tag{7.8}$$

This is why it is convenient to rewrite Eq. (5) in a mathematically equivalent form,

[1] Since both $d\mathbf{q}$ and $d\mathbf{r}$ are legitimate physical vectors (whose Cartesian components are properly transformed as the transfer between reference frames), the 3×3 matrix with elements $\partial q_j/\partial r_{j'}$ is indeed a legitimate physical tensor – see the discussion in Sec. 4.2.

[2] As a result, the full sum (5), which includes three partial sums (8), is not affected by rotation – as we already know.

$$(dl)^2\Big|_{\text{after deformation}} - (dl)^2\Big|_{\text{before deformation}} = 2\sum_{j,j'=1}^{3} s_{jj'}\,dr_j\,dr_{j'}, \tag{7.9a}$$

where $s_{jj'}$ are the elements of the so-called *symmetrized strain tensor*, defined as

Strain tensor

$$s_{jj'} \equiv \frac{1}{2}\left(\frac{\partial q_j}{\partial r_{j'}} + \frac{\partial q_{j'}}{\partial r_j}\right). \tag{7.9b}$$

(Note that this modification does not affect the diagonal elements $s_{jj} = \partial q_j/\partial r_j$.) So, the advantage of the symmetrized tensor (9b) over the initial tensor with elements $\partial q_j/\partial r_{j'}$ is that according to Eq. (8), at pure rotation, all elements of the symmetrized strain tensor vanish.

Now let us discuss the physical meaning of this tensor. As was already mentioned in Sec. 4.2, any symmetric tensor may be diagonalized by an appropriate selection of the reference frame axes. In such principal axes, $s_{jj'} = s_{jj}\delta_{jj'}$, so Eq. (4) takes a simple form:

$$dq_j = \frac{\partial q_j}{\partial r_j}\,dr_j = s_{jj}\,dr_j. \tag{7.10}$$

We may use this expression to calculate the change of each side of an elementary cuboid (parallelepiped) with its sides dq_j parallel to the principal axes:

$$dr_j\Big|_{\text{after deformation}} - dr_j\Big|_{\text{before deformation}} \equiv dq_j = s_{jj}\,dr_j\ , \tag{7.11}$$

and of the cuboid's volume $dV = dr_1 dr_2 dr_3$:

$$dV\Big|_{\text{after deformation}} - dV\Big|_{\text{before deformation}} = \prod_{j=1}^{3}(dr_j + s_{jj}\,dr_j) - \prod_{j=1}^{3} dr_j = dV\left[\prod_{j=1}^{3}\left(1 + s_{jj}\right) - 1\right], \tag{7.12}$$

Since all our analysis is only valid in the linear approximation in small $s_{jj'}$, Eq. (12) is reduced to

$$dV\Big|_{\text{after deformation}} - dV\Big|_{\text{before deformation}} \approx dV\sum_{j=1}^{3} s_{jj} \equiv dV\,\mathrm{Tr}(\mathrm{s}), \tag{7.13}$$

where Tr (*trace*)[3] of any matrix (in particular, any tensor) is the sum of its diagonal elements; in our current case

$$\mathrm{Tr}\,(\mathrm{s}) \equiv \sum_{j=1}^{3} s_{jj}\ . \tag{7.14}$$

The tensor theory shows that the trace does not depend on the particular choice of the coordinate axes; so, the diagonal elements of the strain tensor characterize the medium's compression/extension.

Next, what is the meaning of its off-diagonal elements? It may be illustrated by the simplest example of a purely *shear deformation* shown in Fig. 2. (The geometry means to be uniform along the z-axis normal to the plane of the drawing.) In this case, all displacements (assumed small) have just one Cartesian component – in Fig. 2, along the x-axis: $\mathbf{q} = \mathbf{n}_x \alpha y$ (with $\alpha << 1$), so the only nonzero element of the initial strain tensor $\partial q_j/\partial r_{j'}$ is $\partial q_x/\partial y = \alpha$, and the symmetrized tensor (9b) is

[3] The traditional European notation for Tr is Sp (from the German *Spur* meaning "trace" or "track").

$$\mathrm{s} = \begin{pmatrix} 0 & \alpha/2 & 0 \\ \alpha/2 & 0 & 0 \\ 0 & 0 & 0 \end{pmatrix}. \tag{7.15}$$

Evidently, the change of volume, given by Eq. (13), vanishes in this case. Thus, off-diagonal elements of the tensor s characterize shear deformations.

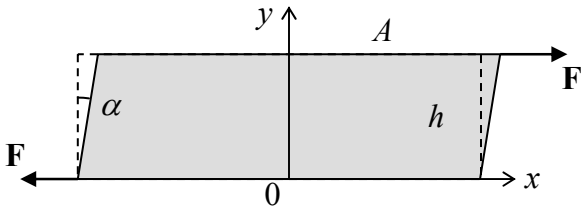

Fig. 7.2. An example of pure shear.

To conclude this section, let me note that Eq. (9) is only valid in Cartesian coordinates. For the solution of some important problems with the axial or spherical symmetry, it is frequently convenient to express six different elements of the symmetric strain tensor in either cylindrical or spherical coordinates via three components of the displacement vector **q** in the same coordinates. A straightforward differentiation of the definitions of these curvilinear coordinates, similar to that used to derive the well-known expressions for spatial derivatives of arbitrary functions,[4] yields, in particular, the following formulas for the diagonal elements of the tensor:

(i) in the cylindrical coordinates:

$$s_{\rho\rho} = \frac{\partial q_\rho}{\partial \rho}, \qquad s_{\varphi\varphi} = \frac{1}{\rho}\left(q_\rho + \frac{\partial q_\varphi}{\partial \varphi}\right), \qquad s_{zz} = \frac{\partial q_z}{\partial z}. \tag{7.16}$$

(ii) in the spherical coordinates:

$$s_{rr} = \frac{\partial q_r}{\partial r}, \qquad s_{\theta\theta} = \frac{1}{r}\left(q_r + \frac{\partial q_\theta}{\partial \theta}\right), \qquad s_{\varphi\varphi} = \frac{1}{r}\left(q_r + q_\theta \frac{\cos\theta}{\sin\theta} + \frac{1}{\sin\theta}\frac{\partial q_\varphi}{\partial \varphi}\right). \tag{7.17}$$

These expressions, which will be used below for the solution of some problems for symmetrical geometries, may be a bit counter-intuitive. Indeed, Eq. (16) shows that even for a purely radial, axially-symmetric deformation, $\mathbf{q} = q(\rho)\mathbf{n}_\rho$, the angular element of the strain tensor does not vanish: $s_{\varphi\varphi} = q/\rho$. (According to Eq. (17), in the spherical coordinates, both angular elements of the tensor exhibit the same property.) Note, however, that this relation describes a simple geometric fact: the change of the lateral distance $\rho d\varphi << \rho$ between two close points at the same distance from the symmetry axis, at a small change of ρ that keeps the angle $d\varphi$ between the directions towards these two points intact.

7.2. Stress

Now let us discuss the forces that cause the strain – or, from a legitimate alternative point of view, are caused by the strain. Internal forces acting inside (i.e. between arbitrarily defined parts of) a

[4] See, e.g., MA Eqs. (10.1)-(10.12).

continuum may be also characterized by a tensor. This *stress tensor,*[5] with elements $\sigma_{jj'}$, relates the Cartesian components of the vector $d\mathbf{F}$ of the force acting on an elementary area dA of an (in most cases, just imagined) interface between two parts of a continuum, to the components of the elementary vector $d\mathbf{A} = \mathbf{n}dA$ normal to the area – see Fig. 3:

Stress tensor

$$dF_j = \sum_{j'=1}^{3} \sigma_{jj'}\, dA_{j'} \,. \tag{7.18}$$

The usual sign convention here is to take the *outer* normal $d\mathbf{n}$, i.e. to direct $d\mathbf{A}$ out of "our" part of the continuum, i.e. the part on which the calculated force $d\mathbf{F}$ is exerted – by the complementary part.

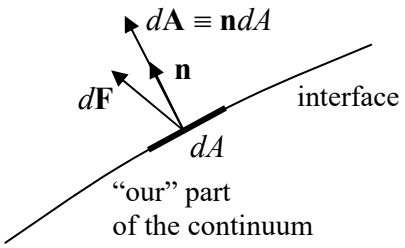

Fig. 7.3. The definition of vectors $d\mathbf{A}$ and $d\mathbf{F}$.

In some cases, the stress tensor's structure is very simple. For example, as will be discussed in detail in the next chapter, static and ideal *fluids* (i.e. liquids and gases) may only provide forces normal to any interface and usually are directed toward "our" part of the body, so

Pressure

$$d\mathbf{F} = -\mathcal{P}d\mathbf{A}, \qquad \text{i.e.}\ \sigma_{jj'} = -\mathcal{P}\delta_{jj'}, \tag{7.19}$$

where the scalar $\mathcal{P}$ (in most cases positive) is called *pressure*, and generally may depend on both the spatial position and time. This type of stress, with $\mathcal{P} > 0$, is frequently called *hydrostatic compression* – even if it takes place in solids, as it may.

However, in the general case, the stress tensor also has off-diagonal terms, which characterize the shear stress. For example, if the shear strain in Fig. 2 is caused by the shown pair of forces $\pm\mathbf{F}$, they create internal forces $F_x\mathbf{n}_x$, with $F_x > 0$ if we speak about the force acting upon a part of the sample below the imaginary horizontal interface we are discussing. To avoid a horizontal acceleration of each horizontal slice of the sample, the forces should not depend on y, i.e. $F_x = \text{const} = F$. Superficially, it may look that in this case, the only nonzero element of the stress tensor is $dF_x/dA_y = F/A = \text{const}$, so tensor is asymmetric, in contrast to the strain tensor (15) of the same system. Note, however, that the displayed pair of forces $\pm\mathbf{F}$ creates not only the shear stress but also a nonzero rotating torque $\boldsymbol{\tau} = -Fh\mathbf{n}_z = -(dF_x/dA_y)Ah\mathbf{n}_z = -(dF_x/dA_y)V\mathbf{n}_z$, where $V = Ah$ is the sample's volume. So, if we want to perform a static stress experiment, i.e. avoid the sample's rotation, we need to apply some other forces, e.g., a pair of vertical forces creating an equal and opposite torque $\boldsymbol{\tau}' = (dF_y/dA_x)V\mathbf{n}_z$, implying that $dF_y/dA_x = dF_x/dA_y = F/A$. As a result, the stress tensor becomes symmetric, and similar in structure to the symmetrized strain tensor (15):

[5] It is frequently called the *Cauchy stress tensor*, partly to honor Augustin-Louis Cauchy who introduced this notion (and is responsible for the development, mostly in the 1820s, much of the theory described in this chapter), and partly to distinguish it from other possible definitions of the stress tensor, including the *1st* and *2nd Piola-Kirchhoff tensors*. For the small deformations discussed in this course, all these notions coincide.

$$\sigma = \begin{pmatrix} 0 & F/A & 0 \\ F/A & 0 & 0 \\ 0 & 0 & 0 \end{pmatrix}. \tag{7.20}$$

In many situations, the body may be stressed not only by forces applied to their surfaces but also by some volume-distributed (*bulk*) forces $d\mathbf{F} = \mathbf{f}dV$, whose certain effective *bulk density* $\mathbf{f}$. (The most evident example of such forces is gravity. If its field is uniform as described by Eq. (1.16), then $\mathbf{f} = \rho\mathbf{g}$, where ρ is the mass density.) Let us derive the key formula describing the summation of the interface and bulk forces. For that, consider again an elementary cuboid with sides dr_j parallel to the corresponding coordinate axes $\mathbf{n}_j$ (Fig. 4) – now not necessarily the principal axes of the stress tensor.

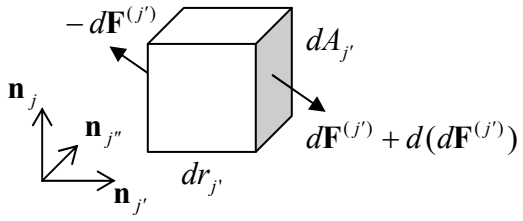

Fig. 7.4. Deriving Eq. (23).

If elements $\sigma_{jj'}$ of the tensor do not depend on position, the force $d\mathbf{F}^{(j')}$ acting on the j'^{th} face of the cuboid is exactly balanced by the equal and opposite force acting on its opposite face, because the vectors $d\mathbf{A}^{(j')}$ at these faces are equal and opposite. However, if $\sigma_{jj'}$ is a function of $\mathbf{r}$, then the net force $d(d\mathbf{F}^{(j')})$ does not vanish. (In this expression, the first differential sign refers to the elementary shift $dr_{j'}$, while the second one, to the elementary area $dA_{j'}$.) Using the expression $\sigma_{jj'}dA_{j'}$ for the j'^{th} contribution to the sum (18), in the first order in $d\mathbf{r}$ the j^{th} components of the vector $d(d\mathbf{F}^{(j')})$ is

$$d(dF_j^{(j')}) = d\left(\sigma_{jj'}dA_{j'}\right) = \frac{\partial\sigma_{jj'}}{\partial r_{j'}}dr_{j'}dA_{j'} \equiv \frac{\partial\sigma_{jj'}}{\partial r_{j'}}dV, \tag{7.21}$$

where the cuboid's volume $dV = dr_{j'}dA_{j'}$ evidently does not depend on the index j'. The addition of these force components for all three pairs of cuboid faces, i.e. the summation of Eqs. (21) over all three values of the upper index j', yields the following relation for the j^{th} Cartesian component of the net force exerted on the cuboid:

$$d(dF_j) = \sum_{j'=1}^{3} d(dF_j^{(j')}) = \sum_{j'=1}^{3} \frac{\partial\sigma_{jj'}}{\partial r_{j'}}dV \ . \tag{7.22}$$

Since any volume may be broken into such infinitesimal cuboids, Eq. (22) shows that the space-varying stress is equivalent to a volume-distributed force $d\mathbf{F}_{\text{ef}} = \mathbf{f}_{\text{ef}}dV$, whose *effective* (not real!) bulk density $\mathbf{f}_{\text{ef}}$ has the following Cartesian components

$$\left(f_{\text{ef}}\right)_j = \sum_{j'=1}^{3} \frac{\partial\sigma_{jj'}}{\partial r_{j'}}, \tag{7.23}$$

Euler-Cauchy principle

so in the presence of genuinely bulk forces $d\mathbf{F} = \mathbf{f}dV$, the densities $\mathbf{f}_{\text{ef}}$ and $\mathbf{f}$ just add up. This is the so-called *Euler-Cauchy stress principle*.

Let us use this addition rule to spell out the 2nd Newton law for a unit volume of a continuum:

$$\rho \frac{\partial^2 \mathbf{q}}{\partial t^2} = \mathbf{f}_{\text{ef}} + \mathbf{f}. \tag{7.24}$$

Using Eq. (23), the j^{th} Cartesian component of Eq. (24) may be represented as

Continuum dynamics: equation

$$\rho \frac{\partial^2 q_j}{\partial t^2} = \sum_{j'=1}^{3} \frac{\partial \sigma_{jj'}}{\partial r_{j'}} + f_j. \tag{7.25}$$

This is the key equation of the continuum's dynamics (and statics), which will be repeatedly used below.

For the solution of some problems, it is also convenient to have a general expression for the work $\delta\mathcal{W}$ of the stress forces at a virtual deformation $\delta\mathbf{q}$ – understood in the same variational sense as the virtual displacements $\delta\mathbf{r}$ in Sec. 2.1. Using the Euler-Cauchy principle (23), for any volume V of a medium not affected by volume-distributed forces, we may write[6]

$$\delta\mathcal{W} = -\int_V \mathbf{f}_{\text{ef}} \cdot \delta\mathbf{q}\, d^3r = -\sum_{j=1}^{3} \int_V (f_{\text{ef}})_j \delta q_j\, d^3r = -\sum_{j,j'=1}^{3} \int_V \frac{\partial \sigma_{jj'}}{\partial r_{j'}} \delta q_j\, d^3r. \tag{7.26}$$

Let us work out this integral by parts for a volume so large that the deformations δq_j on its surface are negligible. Then, swapping the operations of the variation and the spatial differentiation (just like it was done with the time differentiation in Sec. 2.1), we get

$$\delta\mathcal{W} = \sum_{j,j'=1}^{3} \int_V \sigma_{jj'} \delta \frac{\partial q_j}{\partial r_{j'}} d^3r. \tag{7.27}$$

Assuming that the tensor $\sigma_{jj'}$ is symmetric, we may rewrite this expression as

$$\delta\mathcal{W} = \frac{1}{2} \sum_{j,j'=1}^{3} \int_V \left(\sigma_{jj'} \delta \frac{\partial q_j}{\partial r_{j'}} + \sigma_{j'j} \delta \frac{\partial q_j}{\partial r_{j'}} \right) d^3r. \tag{7.28}$$

Now, swapping indices j and j' in the second expression, we finally get

$$\delta\mathcal{W} = \frac{1}{2} \sum_{j,j'=1}^{3} \int_V \delta \left(\frac{\partial q_j}{\partial r_{j'}} \sigma_{jj'} + \frac{\partial q_{j'}}{\partial r_j} \sigma_{jj'} \right) d^3r = -\sum_{j,j'=1}^{3} \int_V \sigma_{jj'} \delta s_{jj'} d^3r, \tag{7.29}$$

where $s_{jj'}$ are the elements of the strain tensor (9b). It is natural to rewrite this important formula as

Work of stress forces

$$\delta\mathcal{W} = \int_V \delta w(\mathbf{r}) d^3r, \qquad \text{where } \delta w(\mathbf{r}) \equiv \sum_{j,j'=1}^{3} \sigma_{jj'} \delta s_{j'j}, \tag{7.30}$$

and interpret the locally-defined scalar function $\delta w(\mathbf{r})$ as the work of the stress forces per unit volume, at a small variation of the deformation.

As a sanity check, for the pure pressure (19), Eq. (30) is reduced to the obviously correct result $\delta\mathcal{W} = -\mathcal{P}\delta V$, where V is the volume of the "our" part of the continuum.

[6] Here the sign corresponds to the work of the "external" stress force $d\mathbf{F}$ exerted on "our" part of the continuum by its counterpart – see Fig. 3. Note that some texts make the opposite definition of $\delta\mathcal{W}$, leading to its opposite sign.

7.3. Hooke's law

In order to form a complete system of equations describing the continuum's dynamics, one needs to complement Eq. (25) with an appropriate *constitutive equation* describing the relation between the forces described by the stress tensor $\sigma_{jj'}$, and the deformations **q** described (in the small deformation limit) by the strain tensor $s_{jj'}$. This relation depends on the medium, and generally may be rather complicated. Even leaving alone various anisotropic solids (e.g., crystals) and macroscopically-inhomogeneous materials (like ceramics or sand), strain typically depends not only on the current value of stress (possibly in a nonlinear way) but also on the previous history of stress application. Indeed, if strain exceeds a certain *plasticity threshold*, atoms (or nanocrystals) may slip to their new positions and never come back even if the strain is reduced. As a result, deformations become irreversible – see Fig. 5.

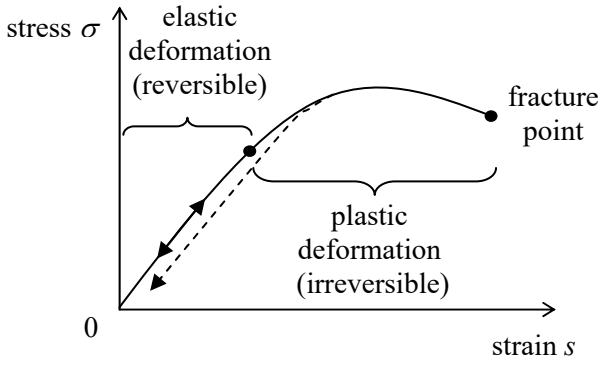

Fig. 7.5. A typical relation between the stress and strain in solids (schematically).

Only below the thresholds of nonlinearity and plasticity (which are typically close to each other), the strain is nearly proportional to stress, i.e. obeys the famous *Hooke's law*.[7] However, even in this *elastic range*, the law is not quite simple, and even for an isotropic medium is described not by one but by two constants, called the *elastic moduli*. The reason for that is that most elastic materials resist the strain accompanied by a volume change (say, the hydrostatic compression) differently from how they resist a shear deformation.

To describe this difference, let us first represent the symmetrized strain tensor (9b) in the following mathematically equivalent form:

$$s_{jj'} = \left(s_{jj'} - \frac{1}{3}\delta_{jj'}\mathrm{Tr}\,(\mathrm{s}) \right) + \left(\frac{1}{3}\delta_{jj'}\mathrm{Tr}\,(\mathrm{s}) \right). \tag{7.31}$$

According to Eq. (13), the *traceless tensor* in the first parentheses does not give any contribution to the volume change, e.g., may be used to characterize a purely shear deformation, while the second term describes the hydrostatic compression alone. Hence we may expect that the stress tensor may be represented (again, within the elastic deformation range only!) as

$$\sigma_{jj'} = 2\mu\left(s_{jj'} - \frac{1}{3}\mathrm{Tr}\,(\mathrm{s})\delta_{jj'} \right) + 3K\left(\frac{1}{3}\mathrm{Tr}\,(\mathrm{s})\delta_{jj'} \right), \tag{7.32}$$

Hooke's law via μ and K

where K and μ are constants. (The inclusion of coefficients 2 and 3 into Eq. (32) is justified by the simplicity of some of its corollaries – see, e.g., Eqs. (36) and (41) below.) Indeed, experiments show that

[7] Named after Robert Hooke (1635-1703), the polymath who was the first to describe the law in its simplest, 1D version.

Hooke's law in this form is followed, at small strain, by all isotropic materials. In accordance with the above discussion, the constant μ (in some texts, denoted as G) is called the *shear modulus*, while the constant K (sometimes denoted B), the *bulk modulus*. The two left columns of Table 1 show the approximate values of these moduli for typical representatives of several major classes of materials.[8]

Table 7.1. Elastic moduli, density, and sound velocities of a few representative materials (approximate values)

Material	K (GPa)	μ (GPa)	E (GPa)	ν	ρ (kg/m^3)	v_l (m/s)	v_t (m/s)
Diamond[(a)]	600	450	1,100	0.20	3,500	1,830	1,200
Hardened steel	170	75	200	0.30	7,800	5,870	3,180
Water[(b)]	2.1	0	0	0.5	1,000	1,480	0
Air[(b)]	0.00010	0	0	0.5	1.2	332	0

[(a)] Averages over crystallographic directions (~10% anisotropy).
[(b)] At the so-called *ambient conditions* (T = 20°C, $\mathcal{P}$ = 1 bar ≡ 10^5 Pa).

To better appreciate these values, let us first discuss the quantitative meaning of K and μ, using two simple examples of elastic deformation. However, in preparation for that, let us first solve the set of nine (or rather six different) linear equations (32) for $s_{jj'}$. This is easy to do, due to the simple structure of these equations: they relate the elements $\sigma_{jj'}$ and $s_{jj'}$ with the same indices, but the tensor's trace effect. This slight complication may be readily overcome by noticing that according to Eq. (32),

$$\mathrm{Tr}(\sigma) \equiv \sum_{j=1}^{3} \sigma_{jj} = 3K\,\mathrm{Tr}(s), \qquad \text{so that } \mathrm{Tr}(s) = \frac{1}{3K}\mathrm{Tr}(\sigma). \tag{7.33}$$

Plugging this result into Eq. (32) and solving it for $s_{jj'}$, we readily get the reciprocal relation, which may be represented in a similar form:

$$s_{jj'} = \frac{1}{2\mu}\left(\sigma_{jj'} - \frac{1}{3}\mathrm{Tr}(\sigma)\delta_{jj'}\right) + \frac{1}{3K}\left(\frac{1}{3}\mathrm{Tr}(\sigma)\delta_{jj'}\right). \tag{7.34}$$

Now let us apply Hooke's law, in the form of Eqs. (32) or (34), to two simple situations in which the strain and stress tensors may be found without using the full differential equation of the elasticity theory and boundary conditions for them. (That will be the subject of the next section.) The first situation is the hydrostatic compression when the stress tensor is diagonal, and all its diagonal elements are equal – see Eq. (19).[9] For this case, Eq. (34) yields

$$s_{jj'} = -\frac{\mathcal{P}}{3K}\delta_{jj'}, \tag{7.35}$$

[8] Since the strain tensor elements, defined by Eq. (9), are dimensionless, while the strain, defined by Eq. (18), has a dimensionality similar to pressure (of force per unit area), so do the elastic moduli K and μ.
[9] It may be proved that such a situation may be implemented not only in a fluid with pressure $\mathcal{P}$ but also in a solid sample of an *arbitrary* shape, for example by placing it into a compressed fluid.

i.e. regardless of the shear modulus, the strain tensor is also diagonal, with all diagonal elements equal. According to Eqs. (11) and (13), this means that all linear dimensions of the body are reduced by a similar factor, so its shape is preserved, while the volume is reduced by

$$\frac{\Delta V}{V} = \sum_{j=1}^{3} s_{jj} = -\frac{\mathcal{P}}{K}. \tag{7.36}$$

This formula clearly shows the physical sense of the bulk modulus K as the *reciprocal compressibility*. As Table 1 shows, the values of K may be dramatically different for various materials, and even for such "soft stuff" as water, this modulus is actually rather high. For example, even at the bottom of the deepest, 10-km ocean well ($\mathcal{P} \approx 10^3$ bar ≈ 0.1 GPa), the water's density increases by just about 5%. As a result, in most human-scale experiments, water may be treated as an *incompressible fluid* – the approximation that will be widely used in the next chapter. Many solids are even much less compressible – see, for example, the first two rows of Table 1.

Quite naturally, the most compressible media are gases. For a portion of gas, a certain background pressure $\mathcal{P}$ is necessary just for containing it within its volume V, so Eq. (36) is only valid for small increments of pressure, $\Delta\mathcal{P}$:

$$\frac{\Delta V}{V} = -\frac{\Delta \mathcal{P}}{K}. \tag{7.37}$$

Moreover, the compression of gases also depends on thermodynamic conditions. (In contrast, for most condensed media, the temperature effects are very small.) For example, at ambient conditions, most gases are reasonably well described by the equation of state called the *ideal classical gas*:

$$\mathcal{P}V = Nk_{\rm B}T, \qquad \text{i.e. } \mathcal{P} = \frac{Nk_{\rm B}T}{V}. \tag{7.38}$$

where N is the number of molecules in volume V, and $k_{\rm B} \approx 1.38\times10^{-23}$ J/K is the Boltzmann constant.[10] For a small volume change ΔV at a constant temperature T, this equation gives

$$\Delta\mathcal{P}\Big|_{T=\text{const}} = -\frac{Nk_{\rm B}T}{V^2}\Delta V = -\frac{\mathcal{P}}{V}\Delta V, \qquad \text{i.e. } \frac{\Delta V}{V}\Big|_{T=\text{const}} = -\frac{\Delta\mathcal{P}}{P}. \tag{7.39}$$

Comparing this expression with Eq. (36), we get a remarkably simple result for the isothermal compression of gases,

$$K\Big|_{T=\text{const}} = \mathcal{P}, \tag{7.40}$$

which means in particular that the bulk modulus listed in Table 1 is actually valid, at the ambient conditions, for almost any gas. Note, however, that the change of thermodynamic conditions (say, from isothermal to adiabatic[11]) may affect the compressibility of the gas..

Now let us consider the second, rather different, fundamental experiment: a purely shear deformation shown in Fig. 2. Since the traces of the matrices (15) and (20), which describe this situation, are equal to 0, for their off-diagonal elements, Eq. (32) gives merely $\sigma_{jj'} = 2\mu s_{jj'}$, so the deformation angle α (see Fig. 2) is just

[10] For the derivation and a detailed discussion of Eq. (37), see, e.g., SM Sec. 3.1.
[11] See, e.g., SM Sec. 1.3.

$$\alpha = \frac{1}{\mu}\frac{F}{A}. \tag{7.41}$$

Note that the angle does not depend on the thickness h of the sample, though of course the maximal linear deformation $q_x = \alpha h$ is proportional to the thickness. Naturally, as Table 1 shows, $\mu = 0$ for all fluids because they do not resist static shear stress.

However, not all situations, even apparently simple ones, involve just either K or μ. Let us consider stretching a long and thin elastic rod of a uniform cross-section of area A – the so-called *tensile stress experiment* shown in Fig. 6.[12]

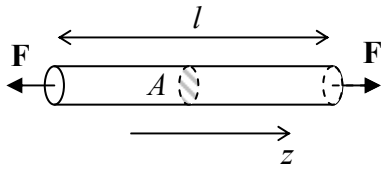

Fig. 7.6. The tensile stress experiment.

Though the deformation of the rod near its clamped ends depends on the exact way forces **F** are applied (we will discuss this issue later on), we may expect that over most of its length, the tension forces are directed virtually along the rod, $d\mathbf{F} = F_z\mathbf{n}_z$, and hence, with the coordinate choice shown in Fig. 6, $\sigma_{xj} = \sigma_{yj} = 0$ for all j, including the diagonal elements σ_{xx} and σ_{yy}. Moreover, due to the open lateral surfaces, on which, evidently, $dF_x = dF_y = 0$, there cannot be an internal stress force of *any* direction, acting on any elementary internal boundary parallel to these surfaces. This means that $\sigma_{zx} = \sigma_{zy} = 0$. So, of all elements of the stress tensor only one, σ_{zz}, is not equal to zero, and for a uniform sample, $\sigma_{zz} = \text{const} = F/A$. For this case, Eq. (34) shows that the strain tensor is also diagonal, but with different diagonal elements:

$$s_{zz} = \left(\frac{1}{9K} + \frac{1}{3\mu}\right)\sigma_{zz}, \tag{7.42}$$

$$s_{xx} = s_{yy} = \left(\frac{1}{9K} - \frac{1}{6\mu}\right)\sigma_{zz}. \tag{7.43}$$

Since tensile stress is most common in engineering practice (including physical experiment design), both combinations of the elastic moduli participating in these two relations have earned their own names. In particular, the constant in Eq. (42) is usually denoted as $1/E$ (but in many texts, as $1/Y$), where E is called *Young's modulus*:[13]

Young's modulus

$$\frac{1}{E} \equiv \frac{1}{9K} + \frac{1}{3\mu}, \qquad \text{i.e. } E \equiv \frac{9K\mu}{3K+\mu}. \tag{7.44}$$

[12] Though the analysis of compression in this situation gives similar results, in practical experiments a strong compression of a long sample may lead to the loss of the horizontal stability – the so-called *buckling* – of the rod.

[13] Named after another polymath, Thomas Young (1773-1829) – somewhat unfairly, because his work on elasticity was predated by a theoretical analysis by L. Euler in 1727 and detailed experiments by Giordano Riccati in 1782.

As Fig. 6 shows, in the tensile stress geometry $s_{zz} \equiv \partial q_z/\partial z = \Delta l/l$, so Young's modulus scales the linear relation between the relative extension of the rod and the force applied per unit area:[14]

$$\frac{\Delta l}{l} = \frac{1}{E}\frac{F}{A}. \tag{7.45}$$

The third column of Table 1 above shows the values of this modulus for two well-known solids: diamond (with the highest known value of E of all bulk materials[15]) and the steels (solid solutions of ~10% of carbon in iron) used in construction. Again, for all fluids, Young's modulus equals zero – as it follows from Eq. (44) for $\mu = 0$.

I am confident that most readers of these notes have been familiar with Eq. (42), in the form of Eq. (45), from their undergraduate studies. However, this can hardly be said about its counterpart, Eq. (43), which shows that at the tensile stress, the rod's cross-section dimensions also change. This effect is usually characterized by the following dimensionless *Poisson's ratio*:[16]

$$\nu \equiv -\frac{s_{xx}}{s_{zz}} = -\frac{s_{yy}}{s_{zz}} = -\left(\frac{1}{9K} - \frac{1}{6\mu}\right)\Bigg/\left(\frac{1}{9K} + \frac{1}{3\mu}\right) \equiv \frac{1}{2}\frac{3K - 2\mu}{3K + \mu}. \tag{7.46}$$

Poisson ratio

According to this formula, for realistic materials with $K > 0$, $\mu \geq 0$, ν may vary from (-1) to (+½), but for the vast majority of materials,[17] its values are between 0 and ½ – see the corresponding column of Table 1. The lower limit of this range is reached in porous materials like cork, whose *lateral dimensions* almost do not change at the tensile stress. Some soft materials such as natural and synthetic rubbers present the opposite case: $\nu \approx$ ½.[18] Since according to Eqs. (13) and (42), the volume change is

$$\frac{\Delta V}{V} = s_{xx} + s_{yy} + s_{zz} = \frac{1}{E}\frac{F}{A}(1 - 2\nu) \equiv (1 - 2\nu)\frac{\Delta l}{l}, \tag{7.47}$$

such materials virtually do not change their *volume* at the tensile stress. The ultimate limit of this trend, $\Delta V/V = 0$, is provided by fluids and gases, because, as it follows from Eq. (46) with $\mu = 0$, their Poisson's ratio ν is exactly ½. However, for most practicable construction materials such as various steels (see Table 1) the relative volume change (47) is as high as ~40% of that of the length.

Due to the tensile stress dominance in practice, the coefficients E and ν are frequently used as a pair of independent elastic moduli, instead of K and μ. Solving Eqs. (44) and (46) for them, we get

$$K = \frac{E}{3(1 - 2\nu)}, \qquad \mu = \frac{E}{2(1 + \nu)}. \tag{7.48}$$

[14] According to Eq. (47), E may be thought of as the force (per unit area) that would double the initial sample's length, if only Hooke's law was valid for deformations that large – as it typically isn't.

[15] E is probably somewhat higher (up to 2,000 GPa) in such nanostructures as carbon nanotubes and monatomic sheets (*graphene*), though there is still substantial uncertainty in experimentally measured elastic moduli of these structures – for a review see, e.g., G. Dimitrios *et al.*, *Prog. Mater. Sci.* **90**, 75 (2017).

[16] In some older texts, the Poisson's ratio is denoted σ, but its notation as ν dominates modern literature.

[17] The only known exceptions are certain exotic solids with very specific internal microstructure – see, e.g., R. Lakes, *Science* **235**, 1038 (1987) and references therein.

[18] For example, *silicone rubbers* (synthetic polymers broadly used in engineering and physics experiment design) have, depending on their particular composition, synthesis, and thermal curing, $\nu = 0.47 \div 0.49$, and as a result, combine respectable bulk moduli $K = (1.5 \div 2)$ GPa with very low Young's moduli: $E = (0.0001 \div 0.05)$ GPa.

Using these formulas, the two (equivalent) formulations of Hooke's law, expressed by Eqs. (32) and (34), may be rewritten as

Hooke's law via E and ν

$$\sigma_{jj'} = \frac{E}{1+\nu}\left(s_{jj'} + \frac{\nu}{1-2\nu}\mathrm{Tr}\,(\mathrm{s})\delta_{jj'} \right), \tag{7.49a}$$

$$s_{jj'} = \frac{1+\nu}{E}\left(\sigma_{jj'} - \frac{\nu}{1+\nu}\mathrm{Tr}\,(\sigma)\delta_{jj'} \right). \tag{7.49b}$$

The linear relation between the strain and stress tensor in elastic continua enables one more step in our calculation of the potential energy U due to deformation, which was started at the end of Sec. 2. Indeed, to each infinitesimal part of this strain increase, we may apply Eq. (30), with the elementary work $\delta\mathcal{W}$ of the surface forces increasing the potential energy of "our" part of the body by the equal amount δU. Let us slowly increase the deformation from a completely unstrained state (in which we may take $U = 0$) to a certain strained state, in the absence of bulk forces $\mathbf{f}$, keeping the deformation type, i.e. the relation between the elements of the stress tensor, intact. In this case, all elements of the tensor $\sigma_{jj'}$ are proportional to the same single parameter characterizing the stress (say, the total applied force), and according to Hooke's law, all elements of the tensor $s_{j'j}$ are proportional to that parameter as well. In this case, integration of Eq. (30) through the variation yields the following final value:[19]

Elastic deformation energy

$$U = \int_V u(\mathbf{r})d^3r, \qquad u(\mathbf{r}) = \frac{1}{2}\sum_{j,j'=1}^{3}\sigma_{jj'}s_{j'j}\,. \tag{7.50}$$

Evidently, this $u(\mathbf{r})$ may be interpreted as the volumic density of the potential energy of the elastic deformation.

7.4. Equilibrium

Now we are fully equipped to discuss the elastic deformation dynamics, but let us start with statics. The static (equilibrium) state may be described by requiring the right-hand side of Eq. (25) to vanish. To find the elastic deformation, we need to plug $\sigma_{jj'}$ from Hooke's law (49a), and then express the elements $s_{jj'}$ via the displacement distribution – see Eq. (9). For a uniform material, the result is[20]

$$\frac{E}{2(1+\nu)}\sum_{j'=1}^{3}\frac{\partial^2 q_j}{\partial r_{j'}^2} + \frac{E}{2(1+\nu)(1-2\nu)}\sum_{j'=1}^{3}\frac{\partial^2 q_{j'}}{\partial r_j \partial r_{j'}} + f_j = 0. \tag{7.51}$$

Taking into account that the first sum is just the j^{th} component of $\nabla^2\mathbf{q}$, while the second sum is the j^{th} component of $\nabla(\nabla\cdot\mathbf{q})$, we see that all three equations (51) for three Cartesian components (j = 1, 2, and 3) of the deformation vector $\mathbf{q}$, may be conveniently merged into one vector equation

Elastic continuum: equilibrium

$$\frac{E}{2(1+\nu)}\nabla^2\mathbf{q} + \frac{E}{2(1+\nu)(1-2\nu)}\nabla(\nabla\cdot\mathbf{q}) + \mathbf{f} = 0. \tag{7.52}$$

[19] To give additional clarity to the arising factor ½, let me spell out this integration for the simple case of a 1D spring. In this case, Eq. (30) is reduced to $\delta U = \delta\mathcal{W} = F\delta x$, and if the spring's force is elastic, $F = \kappa x$, the integration over x from 0 to its final value yields $U = \kappa x^2/2 \equiv Fx/2$.

[20] As it follows from Eqs. (48), the coefficient before the first sum in Eq. (51) is just the shear modulus μ, while that before the second sum is equal to $(K + \mu/3)$.

For some applications, it is more convenient to recast this equation into a different form, using the well-known vector identity[21] $\nabla^2\mathbf{q} = \nabla(\nabla\cdot\mathbf{q}) - \nabla\times(\nabla\times\mathbf{q})$. The result is

$$\frac{E(1-\nu)}{(1+\nu)(1-2\nu)}\nabla(\nabla\cdot\mathbf{q}) - \frac{E}{2(1+\nu)}\nabla\times(\nabla\times\mathbf{q}) + \mathbf{f} = 0. \tag{7.53}$$

It is interesting that in problems without volume-distributed forces ($\mathbf{f} = 0$), Young's modulus E cancels out. Even more fascinating, in this case, the equation may be re-written in a form not involving Poisson's ratio ν either. Indeed, calculating the divergence of the remaining terms of Eq. (53), taking into account MA Eqs. (9.2) and (11.2), we get a surprisingly simple equation

$$\nabla^2(\nabla\cdot\mathbf{q}) = 0. \tag{7.54}$$

A natural question here is how the elastic moduli affect the deformation distribution if they do not participate in the differential equation describing it. The answer is different in the following two cases. If what is fixed at the body's boundary are deformations, then the moduli are irrelevant, because the deformation distribution through the body does not depend on them. On the other hand, if the boundary conditions describe fixed stress (or a combination of stress and strain), then the elastic constants creep into the solution via the recalculation of these conditions into the strain. As a simple but representative example, let us calculate the deformation distribution in a (generally, thick) spherical shell under the effect of pressures inside and outside it – see Fig. 7a.

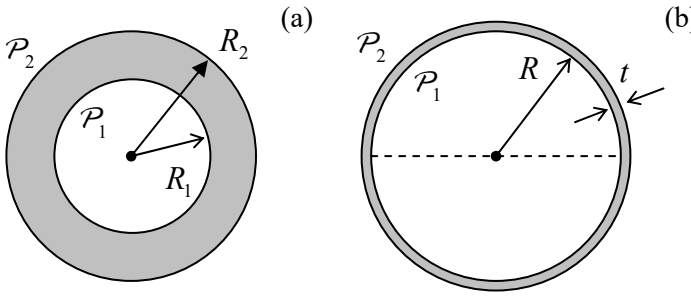

Fig. 7.7. The spherical shell problem: (a) the general case, and (b) the thin shell limit.

Due to the spherical symmetry of the problem, the deformation is obviously spherically symmetric and radial, $\mathbf{q}(\mathbf{r}) = q(r)\mathbf{n}_r$, i.e. is completely described by one scalar function $q(r)$. Since the curl of such a radial vector field is zero,[22] Eq. (53) is reduced to

$$\nabla(\nabla\cdot\mathbf{q}) = 0, \tag{7.55}$$

This means that the divergence of the function $q(r)$ is constant within the shell. In the spherical coordinates:[23]

$$\frac{1}{r^2}\frac{d}{dr}\left(r^2 q\right) = \text{const}. \tag{7.56}$$

Naming this constant $3a$ (with the numerical factor chosen just for the later notation's convenience), and integrating Eq. (56) over r, we get its solution,

[21] See, e.g., MA Eq. (11.3).
[22] If this is not immediately evident, please have a look at MA Eq. (10.11) with $\mathbf{f} = f_r(r)\mathbf{n}_r$.
[23] See, e.g., MA Eq. (10.10) with $\mathbf{f} = q(r)\mathbf{n}_r$

$$q(r) = ar + \frac{b}{r^2}, \tag{7.57}$$

which also includes another integration constant, b. The constants a and b may be determined from the boundary conditions. Indeed, according to Eq. (19),

$$\sigma_{rr} = \begin{cases} -\mathcal{P}_1, & \text{at } r = R_1, \\ -\mathcal{P}_2, & \text{at } r = R_2. \end{cases} \tag{7.58}$$

In order to relate this stress to strain, let us use Hooke's law, but for that, we first need to calculate the strain tensor components for the deformation distribution (57). Using Eqs. (17), we get

$$s_{rr} = \frac{\partial q}{\partial r} = a - 2\frac{b}{r^3}, \qquad s_{\theta\theta} = s_{\varphi\varphi} = \frac{q}{r} = a + \frac{b}{r^3}, \tag{7.59}$$

so Tr (s) = 3a. Plugging these relations into Eq. (49a) for σ_{rr}, we obtain

$$\sigma_{rr} = \frac{E}{1+\nu}\left[\left(a - 2\frac{b}{r^3}\right) + \frac{\nu}{1-2\nu}3a\right]. \tag{7.60}$$

Now plugging this relation into Eqs. (58), we get a system of two linear equations for the coefficients a and b. An easy solution to this system yields

$$a = \frac{1-2\nu}{E}\frac{\mathcal{P}_1 R_1^3 - \mathcal{P}_2 R_2^3}{R_2^3 - R_1^3}, \qquad b = \frac{1+\nu}{2E}\frac{(\mathcal{P}_1 - \mathcal{P}_2)R_1^3 R_2^3}{R_2^3 - R_1^3}. \tag{7.61}$$

Formulas (57) and (61) give a complete solution to our problem. (Note that the elastic moduli are back, as was promised.) This solution is rich in physical content and deserves at least some analysis. First of all, note that according to Eq. (48), the coefficient $(1 - 2\nu)/E$ in the expression for a is just $1/3K$, so the first term in Eq. (57) for the net deformation describes the hydrostatic compression. Now note that the second of Eqs. (61) yields $b = 0$ if $R_1 = 0$. Thus for a solid sphere, we have only the hydrostatic compression that was discussed in the previous section. Perhaps less intuitively, making two pressures equal also gives $b = 0$, i.e. the purely hydrostatic compression, for arbitrary $R_2 > R_1$.

However, in the general case, $b \neq 0$, so the second term in the deformation distribution (57), which describes the shear deformation,[24] is also substantial. In particular, let us consider the important thin-shell limit, when $R_2 - R_1 \equiv t << R_{1,2} \equiv R$ – see Fig. 7b. In this case, $q(R_1) \approx q(R_2)$ is just the change of the shell radius R, for which Eqs. (57) and (61) (with ${R_2}^3 - {R_1}^3 \approx 3R^2 t$) give

$$\Delta R \equiv q(R) \approx aR + \frac{b}{R^2} \approx \frac{(\mathcal{P}_1 - \mathcal{P}_2)R^2}{3t}\left(\frac{1-2\nu}{E} + \frac{1+\nu}{2E}\right) = (\mathcal{P}_1 - \mathcal{P}_2)\frac{R^2}{t}\frac{1-\nu}{2E}. \tag{7.62}$$

Naively, one could think that at least in this limit the problem could be analyzed by elementary means. For example, the total force exerted by the pressure difference $(\mathcal{P}_1 - \mathcal{P}_2)$ on the diametrical cross-section of the shell (see, e.g., the dashed line in Fig. 7b) is $F = \pi R^2(\mathcal{P}_1 - \mathcal{P}_2)$, giving the stress,

[24] Indeed, according to Eq. (48), the material-dependent factor in the second of Eqs. (61) is just $1/4\mu$.

$$\sigma = \frac{F}{A} = \frac{\pi R^2 (\mathcal{P}_1 - \mathcal{P}_2)}{2\pi R t} = (\mathcal{P}_1 - \mathcal{P}_2)\frac{R}{2t}, \tag{7.63}$$

directed along the shell's walls. One can check that this simple formula may be indeed obtained, in this limit, from the strict expressions for $\sigma_{\theta\theta}$ and $\sigma_{\varphi\varphi}$, following from the general treatment carried out above. However, if we now tried to continue this approach by using the simple relation (45) to find the small change Rs_{rr} of the sphere's radius, we would arrive at a result with the general structure of Eq. (62), but without the factor $(1 - \nu) < 1$ in the numerator. The reason for this error (which may be as significant as ~30% for typical construction materials – see Table 1) is that Eq. (45), while being valid for *thin rods* of arbitrary cross-section, is invalid for *thin but broad sheets*, and in particular the thin shell in our problem. Indeed, while at the tensile stress, both lateral dimensions of a thin rod may contract freely, in our last problem all dimensions of the shell are under stress – actually, under much more tangential stress than the radial one.[25]

7.5. Rod bending

The general approach to the static deformation analysis, outlined at the beginning of the previous section, may be simplified not only for symmetric geometries but also for uniform thin structures such as *thin plates* (also called "membranes" or "thin sheets") and *thin rods*. Due to the shortage of time, in this course, I will demonstrate typical approaches to such systems only on the example of thin rods. (The theory of thin plates and shells is conceptually similar but mathematically more involved.[26])

Besides the tensile stress analyzed in Sec. 3, the two other major types of rod deformation are *bending* and *torsion*. Let us start from a "local" analysis of bending caused by a pair of equal and opposite external torques $\boldsymbol{\tau} = \pm \mathbf{n}_y \tau_y$ perpendicular to the rod axis z (Fig. 8), assuming that the rod is "quasi-uniform", i.e. that on the scale of this analysis (comparable with the linear scale a of the cross-section) its material parameters and the cross-section A do not change substantially.

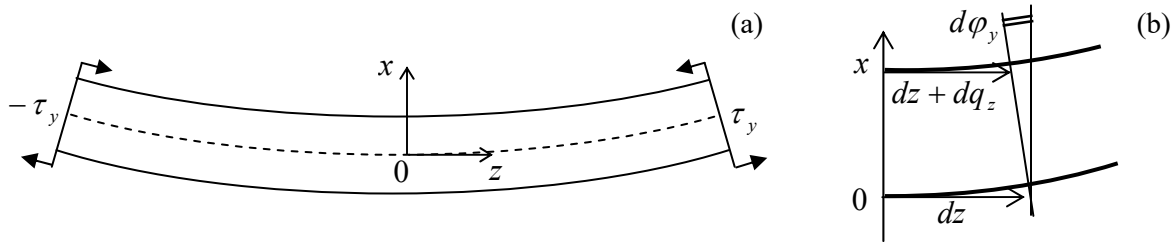

Fig. 7.8. Rod bending, in a local reference frame (specific for each cross-section). The bold arrows show the simplest way to create the two opposite torques τ_y: a couple of opposite forces for each torque.

Just as in the tensile stress experiment (Fig. 6), the components of the stress forces $d\mathbf{F}$, normal to the rod's length, have to equal zero on the surface of the rod. Repeating the arguments made for the tensile stress discussion, we have to conclude that only one diagonal element of the tensor (in Fig. 8, σ_{zz}) may differ from zero:

[25] Strictly speaking, this is only true if the pressure difference is not too small, namely, if $|\mathcal{P}_1 - \mathcal{P}_2| >> \mathcal{P}_{1,2} t/R$.

[26] For its review see, e.g., Secs. 11-15 in L. Landau and E. Lifshitz, *Theory of Elasticity*, 3rd ed., Butterworth-Heinemann, 1986.

$$\sigma_{jj'} = \delta_{jz}\sigma_{zz}. \tag{7.64}$$

However, in contrast to the tensile stress, at pure static bending, the net force directed along the rod has to vanish:

$$F_z = \int_S \sigma_{zz} d^2r = 0, \tag{7.65}$$

where S is the rod's cross-section, so σ_{zz} has to change its sign at some point of the x-axis, selected to lie in the plane of the bent rod. Thus, the bending deformation may be viewed as a combination of a stretch of some layers of the rod (bottom layers in Fig. 8) with compression of other (top) layers.

Since it is hard to make more conclusions about the stress distribution immediately, let us turn over to strain, assuming that the rod's cross-section is virtually constant over the length of our local analysis. From the above representation of bending as a combination of stretching and compression, it is evident that the longitudinal deformation q_z has to vanish along some *neutral line* on the rod's cross-section – in Fig. 8, represented by the dashed line.[27] Selecting the origin of the x-coordinate on this line, and expanding the relative deformation in the Taylor series in x, due to the cross-section smallness we may keep just the first, linear term of the expansion:

$$s_{zz} \equiv \frac{dq_z}{dz} = -\frac{x}{R}. \tag{7.66}$$

The constant R has the sense of the *curvature radius* of the bent rod. Indeed, on a small segment dz, the cross-section turns by a small angle $d\varphi_y = -dq_z/x$ (Fig. 8b). Using Eq. (66), we get $d\varphi_y = dz/R$, which is the usual definition of the curvature radius R in the differential geometry, for our special choice of the coordinate axes.[28]

Expressions for other elements of the strain tensor are harder to guess (like at the tensile stress, not all of them are equal to zero!), but what we already know about σ_{zz} and s_{zz} is sufficient to start formal calculations. Indeed, plugging Eq. (64) into Hooke's law in the form (49b), and comparing the result for s_{zz} with Eq. (66), we find

$$\sigma_{zz} = -E\frac{x}{R}. \tag{7.67}$$

From the same Eq. (49b), we could also find the transverse elements of the strain tensor, and conclude that they are related to s_{zz} exactly as at the tensile stress:

$$s_{xx} = s_{yy} = -\nu s_{zz}, \tag{7.68}$$

and then, integrating these relations along the cross-section of the rod, find the deformation of the cross-section's shape. More important for us, however, is to calculate the relation between the rod's curvature and the net torque acting on a given cross-section S (taking $dA_z > 0$):

$$\tau_y \equiv \int_S (\mathbf{r}\times d\mathbf{F})_y = -\int_S x\sigma_{zz} d^2r = \frac{E}{R}\int_S x^2 d^2r \equiv \frac{EI_y}{R}, \tag{7.69}$$

[27] Strictly speaking, that dashed line is the intersection of the *neutral surface* (the continuous set of such neutral lines for all cross-sections of the rod) with the plane of the drawing.

[28] Indeed, for $(dx/dz)^2 << 1$, the general formula MA Eq. (4.3) for the curvature (with the appropriate replacements $f \to x$ and $x \to z$) is reduced to $1/R = d^2x/dz^2 = d(dx/dz)/dz = d(\tan\varphi_y)/dz \approx d\varphi_y/dz$.

where I_y is a geometric constant defined as

$$I_y \equiv \int_S x^2 dxdy\,. \tag{7.70}$$

Note that this factor, defining the bending rigidity of the rod, grows as fast as a^4 with the linear scale a of the cross-section.[29]

In these expressions, x has to be measured from the neutral line. Let us see where exactly this line passes through the rod's cross-section. Plugging the result (67) into Eq. (65), we get the condition defining the neutral line:

$$\int_S x dxdy = 0. \tag{7.71}$$

This condition allows for a simple interpretation. Imagine a thin sheet of some material, with a constant mass density σ per unit area, cut in the form of the rod's cross-section. If we place a reference frame into its center of mass, then, by its definition,

$$\sigma \int_S \mathbf{r} dxdy = 0. \tag{7.72}$$

Comparing this condition with Eq. (71), we see that one of the neutral lines has to pass through the center of mass of the sheet, which may be called the "center of mass of the cross-section". Using the same analogy, we see that the integral I_y given by Eq. (72) may be interpreted as the moment of inertia of the same imaginary sheet of material, with σ formally equal to 1, for its rotation about the neutral line – cf. Eq. (4.24). This analogy is so convenient that the integral is usually called the *moment of inertia of the cross-section* and denoted similarly – just as has been done above. So, our basic result (69) may be rewritten as

$$\boxed{\frac{1}{R} = \frac{\tau_y}{EI_y}}\,. \tag{7.73}$$

Rod bending: curvature vs. torque

This relation is only valid if the deformation is small in the sense $R >> a$. Still, since the deviations of the rod from its unstrained shape may accumulate along its length, Eq. (73) may be used for calculations of large "global" deviations of the rod from equilibrium, on a length scale much larger than a. To describe such deformations, Eq. (73) has to be complemented by conditions of the balance of the bending forces and torques. Unfortunately, a general analysis of such deformations requires a bit more differential geometry than I have time for, so I will only discuss this procedure for the simplest case of relatively small transverse deviations $q \equiv q_x$ of an initially horizontal rod from its straight shape that will be used for the z-axis (Fig. 9a), by some forces, possibly including bulk-distributed forces $\mathbf{f} = \mathbf{n}_x f_x(z)$. (Again, the simplest example is a uniform gravity field, for which $f_x = -\rho g = \text{const}$.) Note that in the forthcoming discussion, the reference frame will be global, i.e. common for the whole rod, rather than local (pertaining to each cross-section) as it was in the previous analysis – cf. Fig. 8.

First of all, we may write a static relation for the total vertical force $\mathbf{F} = \mathbf{n}_x F_x(z)$ exerted on the part of the rod to the left of the considered cross-section – located at point z. The differential form of this relation expresses the balance of vertical forces exerted on a small fragment dz of the rod (Fig. 9a), necessary for the absence of its *linear* acceleration: $F_x(z + dz) - F_x(z) + f_x(z)A dz = 0$, giving

[29] In particular, this is the reason why the usual electric wires are made not of a solid copper core, but rather a twisted set of thinner sub-wires, which may slip relative to each other, increasing the wire flexibility.

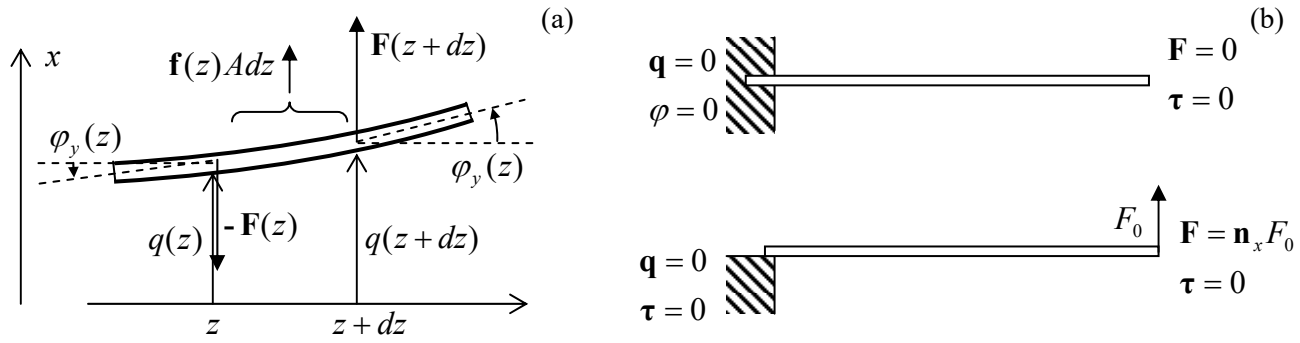

Fig. 7.9. A global picture of rod bending: (a) the forces acting on a small fragment of a rod, and (b) two bending problem examples, each with two typical but different boundary conditions.

$$\frac{dF_x}{dz} = -f_x A, \tag{7.74}$$

where A is the cross-section's area. Note that this vertical component of the internal forces has been neglected in our derivation of Eq. (73), and hence our final results will be valid only if the ratio F_x/A is much smaller than the magnitude of σ_{zz} described by Eq. (67). However, in reality, these are exactly the forces that create the very torque $\boldsymbol{\tau} = \mathbf{n}_y \tau_y$ that in turn causes the bending, and thus have to be taken into account in the analysis of the global picture.

Such an account may be made by writing the balance of the components of the elementary torque exerted on the same rod fragment of length dz, necessary for the absence of its *angular* acceleration: $d\tau_y + F_x dz = 0$, so

$$\frac{d\tau_y}{dz} = -F_x. \tag{7.75}$$

These two equations should be complemented by two geometric relations. The first of them is $d\varphi_y/dz = 1/R$, which has already been discussed above. We may immediately combine it with the basic result (73) of our local analysis, getting:

$$\frac{d\varphi_y}{dz} = \frac{\tau_y}{EI_y}. \tag{7.76}$$

The final equation is the geometric relation evident from Fig. 9a:

$$\frac{dq_x}{dz} = \varphi_y, \tag{7.77}$$

which is (as all expressions of our simple analysis) only valid for small bending angles, $|\varphi_y| << 1$.

The four differential equations (74)-(77) are sufficient for the full solution of the weak-bending problem, if complemented by appropriate boundary conditions. Figure 9b shows the conditions most frequently met in practice. Let us solve, for example, the problem shown on the top panel of Fig. 9b: bending of a rod, "clamped" at one end (say, immersed into a rigid wall), under its own weight. As should be clear from their derivation, Eqs. (74)-(77) are valid for any distribution of parameters A, E, I_y, and ρ over the rod's length, provided that the rod is *quasi-uniform*, i.e. its parameters' changes are so slow that the local relation (76) is still valid at any point. However, just for simplicity, let us consider a

uniform rod. The simple structure of Eqs. (74)-(77) allows for their integration one by one, each time using the appropriate boundary conditions. To start, Eq. (74) with $f_x = -\rho g = \text{const}$ yields

$$F_x = \rho g A z + \text{const} = \rho g A (z - l), \tag{7.78}$$

where the integration constant has been selected to satisfy the right-end boundary condition: $F_x = 0$ at $z = l$. As a sanity check, at the left wall ($z = 0$), $F_x = -\rho g A l = -mg$, meaning that the whole weight of the rod is exerted on the supporting wall – fine.

Next, by plugging Eq. (78) into Eq. (75) and integrating, we get

$$\tau_y = -\frac{\rho g A}{2}\left(z^2 - 2lz\right) + \text{const} = -\frac{\rho g A}{2}\left(z^2 - 2lz + l^2\right) \equiv -\frac{\rho g A}{2}(z - l)^2, \tag{7.79}$$

where the integration constant's choice ensures the second right-boundary condition: $\tau_y = 0$ at $z = l$ – see Fig. 9b again. Now proceeding in the same fashion to Eq. (76), we get

$$\varphi_y = -\frac{\rho g A}{2EI_y}\frac{(z - l)^3}{3} + \text{const} = -\frac{\rho g A}{6EI_y}\left[(z - l)^3 + l^3\right], \tag{7.80}$$

where the integration constant is selected to satisfy the *clamping condition* at the left end of the rod: $\varphi_y = 0$ at $z = 0$. (Note that this is different from the *support condition* illustrated on the lower panel of Fig. 9b, which allows the *angle* φ_y to be different from zero at $z = 0$, but requires the *torque* to vanish at that point.) Finally, integrating Eq. (77) with φ_y given by Eq. (80), we get the rod's global deformation law,

$$q_x(z) = -\frac{\rho g A}{6EI_y}\left[\frac{(z - l)^4}{4} + l^3 z + \text{const}\right] = -\frac{\rho g A}{6EI_y}\left[\frac{(z - l)^4}{4} + l^3 z - \frac{l^4}{4}\right], \tag{7.81}$$

where the integration constant is selected to satisfy the second left-boundary condition: $q = 0$ at $z = 0$. So, the bending law is sort of complicated even in this very simple problem. It is also remarkable how fast the end's displacement grows with the increase of the rod's length:

$$q_x(l) = -\frac{\rho g A l^4}{8EI_y}. \tag{7.82}$$

To conclude this solution, let us discuss the validity of this result. First, the geometric relation (77) is only valid if $|\varphi_y(l)| << 1$, and hence if $|q_x(l)| << l$. Next, the local formula Eq. (76) is valid if $1/R = \tau(l)/EI_y << 1/a \sim A^{-1/2}$. Using the results (79) and (82), we see that the latter condition is equivalent to $|q_x(l)| << l^2/a$, i.e. is weaker than the former one, because all our analysis has been based on the assumption $l >> a$. Another point of concern may be that the off-diagonal stress element $\sigma_{xz} \sim F_x/A$, which is created by the vertical gravity forces, has been ignored in our local analysis. For that approximation to be valid, this element must be much smaller than the diagonal element $\sigma_{zz} \sim aE/R = a\tau/I_y$ taken into account in that analysis. Using Eqs. (78) and (80), we are getting the following estimates: $\sigma_{xz} \sim \rho g l$, $\sigma_{zz} \sim a\rho g A l^2/I_y \sim a^3 \rho g l^2/I_y$. According to its definition (70), I_y may be crudely estimated as a^4, so we finally get the simple condition $a << l$, which has been assumed from the very beginning of our solution.

7.6. Rod torsion

One more class of analytically solvable elasticity problems is the torsion of quasi-uniform, straight rods by a couple of axially-oriented torques $\boldsymbol{\tau} = \pm\mathbf{n}_z\tau_z$ – see Fig. 10.

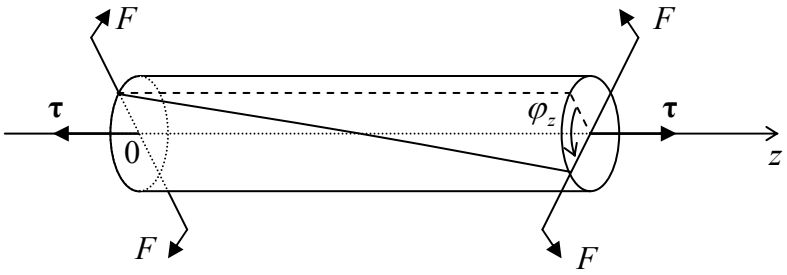

Fig. 7.10. Rod torsion. Just as in Fig. 8, the couples of forces **F** are just vivid representations of the opposite torques $\pm\boldsymbol{\tau}$.

This problem is simpler than the bending in the sense that due to its longitudinal uniformity, $d\varphi_z/dz = \text{const}$, it is sufficient to relate the torque τ_z to the so-called *torsion parameter*

$$\kappa \equiv \frac{d\varphi_z}{dz}. \tag{7.83}$$

If the deformation is elastic and small (in the sense $\kappa a << 1$, where a is again the characteristic size of the rod's cross-section), κ is proportional to τ_z. Hence our task is to calculate their ratio,

Torsional rigidity: definition

$$C \equiv \frac{\tau_z}{\kappa} \equiv \frac{\tau_z}{d\varphi_z/dz}, \tag{7.84}$$

called the *torsional rigidity* of the rod.

As the first guess (as we will see below, of a limited validity), one may assume that the torsion does not change either the shape or size of the rod's cross-sections, but leads just to their mutual rotation about a certain central line. Using a reference frame with the origin on that line, this assumption immediately enables the calculation of Cartesian components of the displacement vector $d\mathbf{q}$, by using Eq. (6) with $d\boldsymbol{\varphi} = \mathbf{n}_z d\varphi_z$:

$$dq_x = -y\,d\varphi_z = -\kappa y\,dz, \qquad dq_y = x\,d\varphi_z = \kappa x\,dz, \qquad dq_z = 0. \tag{7.85}$$

From here, we can calculate all Cartesian elements (9) of the symmetrized strain tensor:

$$s_{xx} = s_{yy} = s_{zz} = 0, \quad s_{xy} = s_{yx} = 0, \quad s_{xz} = s_{zx} = -\frac{\kappa}{2}y, \quad s_{yz} = s_{zy} = \frac{\kappa}{2}x. \tag{7.86}$$

The first of these equalities means that the elementary volume does not change, i.e. we are dealing with purely shear deformation. As a result, all nonzero elements of the stress tensor, calculated from Eqs. (32), are proportional to the shear modulus alone:[30]

$$\sigma_{xx} = \sigma_{yy} = \sigma_{zz} = 0, \qquad \sigma_{xy} = \sigma_{yx} = 0, \qquad \sigma_{xz} = \sigma_{zx} = -\mu\kappa y, \qquad \sigma_{yz} = \sigma_{zy} = \mu\kappa x. \tag{7.87}$$

[30] Note that for this problem, with a purely shear deformation, using the alternative elastic moduli E and ν would be rather unnatural. If needed, we may always use the second of Eqs. (48): $\mu = E/2(1 + \nu)$.

Now it is straightforward to use this result to calculate the full torque as an integral over the cross-section's area A:

$$\tau_z \equiv \int_A (\mathbf{r} \times d\mathbf{F})_z = \int_A (x dF_y - y dF_x) = \int_A (x\sigma_{yz} - y\sigma_{xz}) dx dy. \tag{7.88}$$

Using Eq. (87), we get $\tau_z = \mu\kappa I_z$, i.e.

$$C = \mu I_z, \quad \text{where} \quad I_z \equiv \int_A (x^2 + y^2) dx dy\,. \tag{7.89}$$

C at axial symmetry

Again, just as in the case of thin rod bending, we have got an integral, in this case I_z, similar to a moment of inertia, this time for the rotation about the z-axis passing through a certain point of the cross-section. For any axially symmetric cross-section, this has to be its central point. Then, for example, for the practically important case of a uniform round pipe with internal radius R_1 and external radius R_2, Eq. (89) yields

$$C = \mu\, 2\pi \int_{R_1}^{R_2} \rho^3 d\rho = \frac{\pi}{2} \mu\left(R_2^4 - R_1^4\right). \tag{7.90}$$

In particular, for the solid rod of radius R (which may be treated as a pipe with $R_1 = 0$ and $R_2 = R$), this result gives the following torsional rigidity

$$C = \frac{\pi}{2} \mu R^4, \tag{7.91a}$$

while for a hollow pipe of small thickness $t \ll R$, Eq. (90) is reduced to

$$C = 2\pi\mu R^3 t\,. \tag{7.91b}$$

Note that per unit cross-section area A (and hence per unit mass of the rod) the thin pipe's rigidity is twice higher than that of a solid rod:

$$\frac{C}{A}\Big|_{\text{thin round pipe}} = \mu R^2 > \frac{C}{A}\Big|_{\text{solid round rod}} = \frac{1}{2}\mu R^2\,. \tag{7.92}$$

This fact is one reason for the broad use of thin pipes in engineering and physical experiment design.

However, for rods with axially asymmetric cross-sections, Eq. (89) gives *wrong* results. For example, for a narrow rectangle of area $A = w \times t$ with $t \ll w$, it yields the expression $C = \mu t w^3/12$ [WRONG!], which is even functionally different from the correct result – cf. Eq. (104) below. The reason for this error is that the above analysis does not describe possible bending $q_z(x, y)$ of the rod's cross-section in the direction *along* the rod. (For axially-symmetric rods, such bending is evidently forbidden by the symmetry, so Eq. (89) is valid, and the results (90)-(92) are absolutely correct.)

Let us describe[31] this counter-intuitive effect by taking

$$q_z = \kappa\psi(x, y), \tag{7.93}$$

[31] I would not be terribly shocked if the reader skipped the balance of this section at the first reading. Though the calculation described in it is very elegant, instructive, and typical for the theory of elasticity (and for good physics as a whole!), its results will not be used in other chapters of this course or other parts of this series.

(where ψ is some function to be determined), but still keeping Eq. (87) for two other components of the displacement vector. The addition of ψ does not perturb the equality to zero of the diagonal elements of the strain tensor, as well as of s_{xy} and s_{yx}, but contributes to other off-diagonal elements:

$$s_{xz} = s_{zx} = \frac{\kappa}{2}\left(-y + \frac{\partial \psi}{\partial x}\right), \qquad s_{yz} = s_{zy} = \frac{\kappa}{2}\left(x + \frac{\partial \psi}{\partial y}\right), \tag{7.94}$$

and hence to the corresponding elements of the stress tensor:

$$\sigma_{xz} = \sigma_{zx} = \mu\kappa\left(-y + \frac{\partial \psi}{\partial x}\right), \qquad \sigma_{yz} = \sigma_{zy} = \mu\kappa\left(x + \frac{\partial \psi}{\partial y}\right). \tag{7.95}$$

Now let us find the requirement imposed on the function $\psi(x,y)$ by the fact that the stress force component parallel to the rod's axis,

$$dF_z = \sigma_{zx} dA_x + \sigma_{zy} dA_y = \mu\kappa dA\left[\left(-y + \frac{\partial \psi}{\partial x}\right)\frac{dA_x}{dA} + \left(x + \frac{\partial \psi}{\partial y}\right)\frac{dA_y}{dA}\right], \tag{7.96}$$

has to vanish at the rod's surface(s), i.e. at a cross-section's border. The coordinates $\{x, y\}$ of any point at the border may be considered as unique functions, $x(l)$ and $y(l)$, of the arc l of that line – see Fig. 11.

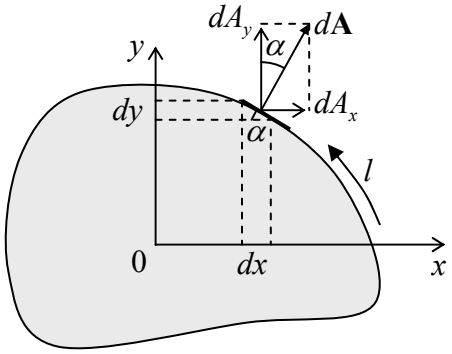

Fig. 7.11. Deriving Eq. (99).

As this sketch shows, the elementary area ratios participating in Eq. (96) may be readily expressed via the derivatives of these functions: $dA_x/dA = \sin\alpha = dy/dl$, $dA_y/dA = \cos\alpha = -dx/dl$, so we may write

$$\left[\left(-y + \frac{\partial \psi}{\partial x}\right)\left(\frac{dy}{dl}\right) + \left(x + \frac{\partial \psi}{\partial y}\right)\left(-\frac{dx}{dl}\right)\right]_{\text{border}} = 0. \tag{7.97}$$

Introducing, instead of ψ, a new function $\chi(x,y)$, defined by its derivatives as

$$\frac{\partial \chi}{\partial x} \equiv \frac{1}{2}\left(-x - \frac{\partial \psi}{\partial y}\right), \qquad \frac{\partial \chi}{\partial y} \equiv \frac{1}{2}\left(-y + \frac{\partial \psi}{\partial x}\right), \tag{7.98}$$

we may rewrite Eq. (97) as

$$2\left(\frac{\partial \chi}{\partial y}\frac{dy}{dl} + \frac{\partial \chi}{\partial x}\frac{dx}{dl}\right)_{\text{border}} \equiv 2\frac{d\chi}{dl}\Big|_{\text{border}} = 0, \tag{7.99}$$

so the function χ has to be constant at each border of the cross-section.

In particular, for a singly-connected cross-section, limited to just one continuous border line (as in Fig. 11), this constant is arbitrary, because according to Eqs. (98), its choice does not affect the longitudinal deformation function $\psi(x,y)$ and hence the deformation as a whole. Now let us use the definition (98) of $\chi(x, y)$ to calculate the 2D Laplace operator of this function:

$$\nabla_{x,y}^2 \chi \equiv \frac{\partial^2 \chi}{\partial^2 x} + \frac{\partial^2 \chi}{\partial^2 y} = \frac{1}{2}\frac{\partial}{\partial x}\left(-x - \frac{\partial \psi}{\partial y}\right) + \frac{1}{2}\frac{\partial}{\partial y}\left(-y + \frac{\partial \psi}{\partial y}\right) \equiv -1. \tag{7.100}$$

This is a 2D *Poisson equation* (frequently met, for example, in electrostatics), but with a very simple, constant right-hand side. Plugging Eqs. (98) into Eqs. (95), and those into Eq. (88), we may express the torque τ_z, and hence the torsional rigidity C, via the same function:

$$C \equiv \frac{\tau_z}{\kappa} = -2\mu \int_A \left(x\frac{\partial \chi}{\partial x} + y\frac{\partial \chi}{\partial y} \right) dxdy. \tag{7.101a}$$

C for arbitrary cross-section

Sometimes, it is easier to use this result in either of its two different forms. The first of them may be readily obtained from Eq. (101a) using the integration by parts:

$$\begin{aligned} C &= -2\mu\left(\int dy \int x d\chi + \int dx \int y d\chi\right) = -2\mu\left[\int dy\left(x\chi_{\text{border}} - \int \chi dx\right) + \int dx\left(y\chi_{\text{border}} - \int \chi dy\right)\right] \\ &= 4\mu\left[\int_A \chi\, dxdy - \chi_{\text{border}} \int_A dxdy\right], \end{aligned} \tag{7.101b}$$

while the proof of one more form,

$$C = 4\mu \int_A \left(\nabla_{x,y}\chi\right)^2 dxdy, \tag{7.101c}$$

is left for the reader's exercise. Thus, if we need to know the rod's rigidity alone, it is sufficient to calculate the function $\chi(x, y)$ from Eq. (100) with the boundary condition $\chi|_{\text{border}} = \text{const}$, and then plug it into any of Eqs. (101). Only if we are also curious about the longitudinal deformation (93) of the cross-section, we may continue by using Eq. (98) to find the function $\psi(x,y)$ describing this deformation.

Let us see how this recipe works for the two examples discussed above. For the round cross-section of radius R, both the Poisson equation (100) and the boundary condition, $\chi = \text{const}$ at $x^2 + y^2 = R^2$, are evidently satisfied by the following axially symmetric function:

$$\chi = -\frac{1}{4}(x^2 + y^2) + \text{const}. \tag{7.102}$$

For this case, Eq. (101a) yields

$$C = 4\mu \int_A \left[\left(-\frac{1}{2}x\right)^2 + \left(-\frac{1}{2}y\right)^2\right] dxdy = \mu \int_A \left(x^2 + y^2\right) d^2 r, \tag{7.103}$$

i.e. the same result (89) that we had for $\psi = 0$. Indeed, plugging Eq. (102) into Eqs. (98), we see that in this case $\partial\psi/\partial x = \partial\psi/\partial y = 0$, so $\psi(x,y) = \text{const}$, i.e. the cross-section is not bent. (As was discussed in Sec. 1, a uniform translation $dq_z = \kappa\psi = \text{const}$ does not constitute a deformation.)

Now, turning to a rod with a narrow rectangular cross-section $A = w \times t$ with $t \ll w$, we may use this strong inequality to solve the Poisson equation (100) approximately, neglecting the second

derivative of χ along the wider dimension (say, y). The remaining 1D differential equation $d^2\chi/d^2x = -1$, with boundary conditions $\chi|_{x=+t/2} = \chi|_{x=-t/2}$, has an obvious solution: $\chi = -x^2/2 + \text{const}$. Plugging this expression into any form of Eq. (101), we get the following (correct!) result for the torsional rigidity:

$$C = \frac{1}{3}\mu w t^3. \tag{7.104}$$

Now let us have a look at the cross-section bending law (93) for this particular case. Using Eqs. (98), we get

$$\frac{\partial \psi}{\partial y} = -x - 2\frac{\partial \chi}{\partial x} = x, \qquad \frac{\partial \psi}{\partial x} = y + 2\frac{\partial \chi}{\partial y} = y. \tag{7.105}$$

Integrating these differential equations over the cross-section, and taking the integration constant (again, not contributing to the deformation) for zero, we get a beautifully simple result:

$$\psi = xy, \qquad \text{i.e. } q_z = \kappa xy\,. \tag{7.106}$$

It means that the longitudinal deformation of the rod has a "propeller bending" form: while the regions near the opposite corners (on the same diagonal) of the cross-section bend toward one direction of the z-axis, the corners on the other diagonal bend in the opposite direction. (This qualitative conclusion remains valid for rectangular cross-sections with any "aspect ratio" t/w.)

For rods with several surfaces, i.e. with cross-sections limited by several boundaries (say, hollow pipes), finding the function $\chi(x, y)$ requires a bit more care and Eq. (103b) has to be modified because the function may be equal to a different constant at each boundary. Let me leave the calculation of the torsional rigidity for this case for the reader's exercise.

7.7. 3D acoustic waves

Now moving from the statics to dynamics, we may start with Eq. (24), which may be transformed into the vector form exactly as this was done for the static case at the beginning of Sec. 4. Comparing Eqs. (24) and (52), we immediately see that the result may be represented as

Elastic continuum: dynamics

$$\rho\frac{\partial^2 \mathbf{q}}{\partial t^2} = \frac{E}{2(1+\nu)}\nabla^2\mathbf{q} + \frac{E}{2(1+\nu)(1-2\nu)}\nabla(\nabla\cdot\mathbf{q}) + \mathbf{f}(\mathbf{r},t)\,. \tag{7.107}$$

Let us use this general equation for the analysis of the perhaps most important type of time-dependent deformations: *acoustic waves*. First, let us consider the simplest case of a virtually infinite, uniform elastic medium, with no external forces: $\mathbf{f} = 0$. In this case, due to the linearity and homogeneity of the equation of motion, and taking clues from the analysis of the simple 1D model (see Fig. 6.4a) in Secs. 6.3-6.5,[32] we may look for a particular time-dependent solution in the form of a sinusoidal, *linearly polarized*, *plane traveling wave*

Plane, sinusoidal wave

$$\mathbf{q}(\mathbf{r},t) = \mathrm{Re}\left[\mathbf{a}e^{i\left(\mathbf{k}\cdot\mathbf{r} - \omega t\right)}\right], \tag{7.108}$$

[32] Note though that Eq. (107) is more complex than the simple wave equation (6.40).

where **a** is the constant complex amplitude of a wave (now a vector!), and **k** is the *wave vector*, whose magnitude is equal to the wave number k. The direction of these two vectors should be clearly distinguished: while **a** determines the wave's *polarization*, i.e. the direction of particle displacements, the vector **k** is directed along the spatial gradient of the full phase of the wave

$$\Psi \equiv \mathbf{k}\cdot\mathbf{r} - \omega t + \arg a\,, \tag{7.109}$$

i.e. along the direction of the wave front propagation.

The importance of the angle between these two vectors may be readily seen from the following simple calculation. Let us point the z-axis of an (inertial) reference frame along the direction of vector **k,** and the x-axis in such direction that the vector **q**, and hence **a**, lie within the $\{x, z\}$ plane. In this case, all variables may change only along the z-axis, i.e. $\nabla = \mathbf{n}_z(\partial/\partial z)$, and the amplitude vector may be represented as the sum of just two Cartesian components:

$$\mathbf{a} = a_x\mathbf{n}_x + a_z\mathbf{n}_z\,. \tag{7.110}$$

Let us first consider a *longitudinal* wave, with the particle motion along the wave direction: $a_x = 0$, $a_z = a$. Then the vector **q** in Eq. (107) describing this wave, has only one (z-) component, so $\nabla\cdot\mathbf{q} = \partial q_z/\partial z$ and $\nabla(\nabla\cdot\mathbf{q}) = \mathbf{n}_z(\partial^2\mathbf{q}/\partial z^2)$, and the Laplace operator gives the same expression: $\nabla^2\mathbf{q} = \mathbf{n}_z(\partial^2\mathbf{q}/\partial z^2)$. As a result, Eq. (107), with $\mathbf{f} = 0$, is reduced to a 1D wave equation

$$\rho\frac{\partial^2 q_z}{\partial t^2} = \left[\frac{E}{2(1+\nu)} + \frac{E}{2(1+\nu)(1-2\nu)}\right]\frac{\partial^2 q_z}{\partial z^2} \equiv \frac{E(1-\nu)}{(1+\nu)(1-2\nu)}\frac{\partial^2 q_z}{\partial z^2}\,, \tag{7.111}$$

similar to Eq. (6.40). As we already know from Sec. 6.4, this equation is indeed satisfied with the solution (108), provided that ω and k obey a linear dispersion relation, $\omega = v_l k$, with the following longitudinal wave velocity:

$$\boxed{v_l^2 = \frac{E(1-\nu)}{(1+\nu)(1-2\nu)\rho} \equiv \frac{K + (4/3)\mu}{\rho}.} \tag{7.112}$$

Longitudinal waves: velocity

The last expression allows for a simple interpretation. Let us consider a static experiment, similar to the tensile test experiment shown in Fig. 6, but with a sample much wider than l in both directions perpendicular to the force. Then the lateral contraction is impossible ($s_{xx} = s_{yy} = 0$), and we can calculate the only finite stress element, σ_{zz}, directly from Eq. (34) with Tr (s) = s_{zz}:

$$\sigma_{zz} = 2\mu\left(s_{zz} - \frac{1}{3}s_{zz}\right) + 3K\left(\frac{1}{3}s_{zz}\right) \equiv \left(K + \frac{4}{3}\mu\right)s_{zz}\,. \tag{7.113}$$

We see that the numerator in Eq. (112) is nothing more than the static elastic modulus for such a uniaxial deformation, and it is recalculated into the velocity exactly as the spring constant in the 1D waves considered in Secs. 6.3-6.4 – cf. Eq. (6.42).

Formula (114) becomes especially simple in fluids, where $\mu = 0$, and the wave velocity is described by the well-known expression

$$\boxed{v_l = \left(\frac{K}{\rho}\right)^{1/2}.} \tag{7.114}$$

Longitudinal waves: velocity in fluids

Note, however, that for gases, with their high compressibility and temperature sensitivity, the value of K participating in this formula may differ, at high frequencies, from that given by Eq. (40), because fast compressions/extensions of gas are usually adiabatic rather than isothermal. This difference is noticeable in Table 1, one of whose columns lists the values of v_l for representative materials.

Now let us consider an opposite case of *transverse* waves with $a_x = a$, $a_z = 0$. In such a wave, the displacement vector is perpendicular to $\mathbf{n}_z$, so $\nabla\cdot\mathbf{q} = 0$, and the second term on the right-hand side of Eq. (107) vanishes. On the contrary, the Laplace operator acting on such vector still gives the same non-zero contribution $\nabla^2\mathbf{q} = n_z(\partial^2\mathbf{q}/\partial z^2)$ to Eq. (107), so the equation yields

$$\rho\frac{\partial^2 q_x}{\partial t^2} = \frac{E}{2(1+\nu)}\frac{\partial^2 q_x}{\partial z^2}, \tag{7.115}$$

and we again get the linear dispersion relation, $\omega = v_t k$, but with a different velocity: [33]

Transverse waves: velocity

$$v_t^2 = \frac{E}{2(1+\nu)\rho} = \frac{\mu}{\rho}. \tag{7.116}$$

We see that the speed of the transverse waves depends exclusively on the shear modulus μ of the medium.[34] This is also very natural: in such waves, the particle displacements $\mathbf{q} = \mathbf{n}_x q$ are perpendicular to the elastic forces $d\mathbf{F} = \mathbf{n}_z dF$, so only one element σ_{xz} of the stress tensor is involved. Also, the strain tensor $s_{jj'}$ has no diagonal elements, Tr (s) = 0, so μ is the only elastic modulus actively participating in Hooke's law (32). In particular, fluids cannot carry transverse waves at all (formally, their velocity (116) vanishes), because they do not resist shear deformations. For all other materials, the longitudinal waves are faster than the transverse ones.[35] Indeed, for all known natural materials' Poisson's ratio is positive so the velocity ratio that follows from Eqs. (112) and (116),

$$\frac{v_l}{v_t} = \left(\frac{2-2\nu}{1-2\nu}\right)^{1/2}, \tag{7.117}$$

is above $\sqrt{2} \approx 1.4$. For the most popular construction materials, with $\nu \approx 0.3$, Poisson's ratio is about 2 – see Table 1.

Let me emphasize again that for both the longitudinal and the transverse waves, the dispersion relation between the wave number and frequency is linear: $\omega = vk$. As was already discussed in Chapter 6, in this case of *acoustic waves* (or just "sound"), the phase and group velocities are equal, and waves of more complex form, consisting of several (or many) Fourier components of the type (108), preserve

[33] Just as in Chapter 6, let me emphasize that the *wave* velocities we are discussing in this section and Sec. 8 below have nothing to do with *particle* velocities $\partial\mathbf{q}/\partial t$. For example, in the transverse wave we are discussing now, v_t is the velocity in the z-direction, while the particles of the medium move across it, in the x-direction. Also, v_l and v_t do not depend on the wave amplitudes, while the particle velocities are proportional to them.

[34] Because of that, one can frequently meet the term *shear waves*. Note also that in contrast to the transverse waves in the simple 1D model analyzed in Chapter 6 (see Fig. 6.4a), those in a 3D continuum do not need a pre-stretch tension $\mathcal{T}$. We will return to the effect of tension in the next section.

[35] Because of this difference between v_l and v_t, in geophysics, the longitudinal waves are known as *P-waves* (with the letter P standing for "primary") because they arrive at the detection site, say from an earthquake, first – before the transverse waves, called the *S-waves*, with S standing for "secondary". (An alternative, also quite logical, decoding of these abbreviations is "pressure waves" and "shear waves".)

their form during propagation. This means that both Eqs. (111) and (115) are satisfied by solutions of the type (6.41):

$$q_{\pm}(z,t) = f_{\pm}\left(t \mp \frac{z}{v}\right), \tag{7.118}$$

where the functions $f_{\pm}$ describe the propagating waveforms. (However, if the initial wave is a mixture, of the type (110), of the longitudinal and transverse components, then these components, propagating with different velocities, will "run from each other".) As one may infer from the analysis of a periodic system model in Chapter 6, the wave dispersion becomes essential at very high (*hypersound*) frequencies where the wave number k becomes close to the reciprocal distance d between the particles of the medium (e.g., atoms or molecules), and hence the approximation of the medium as a continuum, used through this chapter, becomes invalid.

As we already know from Chapter 6, besides the velocity, the waves of each type are characterized by one more important parameter, the wave impedance Z – for acoustic waves frequently called the *acoustic impedance* of the medium. Generalizing Eq. (6.46) to the 3D case, we may define the impedance as the ratio of the force *per unit area* (i.e. the corresponding element of the stress tensor) exerted by the wave, and the particles' velocity. For the longitudinal waves,

$$Z_{\mathrm{l}} \equiv \left|\frac{\sigma_{zz}}{\partial q_z/\partial t}\right| = \left|\frac{\sigma_{zz}}{s_{zz}}\frac{s_{zz}}{\partial q_z/\partial t}\right| = \left|\frac{\sigma_{zz}}{s_{zz}}\frac{\partial q_z/\partial z}{\partial q_z/\partial t}\right|. \tag{7.119}$$

Plugging in Eqs. (108), (112), and (113), we get

$$\boxed{Z_{\mathrm{l}} = \left[(K + 4\mu/3)\rho\right]^{1/2},} \tag{7.120}$$

Longitudinal waves: impedance

in a clear analogy with the first of Eqs. (6.48). Similarly, for the transverse waves, the appropriately modified definition, $Z_{\mathrm{t}} \equiv |\sigma_{xz}/(\partial q_x/\partial z)|$, yields

$$\boxed{Z_{\mathrm{t}} = (\mu\rho)^{1/2}.} \tag{7.121}$$

Transverse waves: impedance

Just like in the 1D models studied in Chapter 6, one role of the wave impedance is to scale the power $\mathcal{P}$ carried by the wave. For plane 3D waves in infinite media, with their infinite wave front area, it is more appropriate to speak about the *power density*, i.e. power $\mathcal{P} = d\mathcal{P}/dA$ per unit area of the front, and characterize it by not only its magnitude,

$$\mathcal{P} = \frac{d\mathbf{F}}{dA}\cdot\frac{\partial \mathbf{q}}{\partial t}, \tag{7.122}$$

but also the direction of the energy propagation, that (for a plane acoustic wave in an isotropic medium) coincides with the direction of the wave vector: $\boldsymbol{\mathcal{P}} \equiv \mathcal{P}\mathbf{n}_{\mathbf{k}}$. Using the definition (18) of the stress tensor, the Cartesian components of this *Umov vector*[36] may be expressed as

[36] Named after N. A. Umov, who introduced this concept in 1874 – ten years before a similar notion for electromagnetic waves (see, e.g., EM Sec. 6.4) was suggested by J. Poynting. In a dissipation-free elastic medium, the Umov vector obeys the continuity equation $\partial(\rho v^2/2 + u)/\partial t + \nabla\cdot\boldsymbol{\mathcal{P}} = 0$, with u given by Eq. (52), which expresses the conservation of the total (kinetic plus potential) energy of the elastic deformation.

$$\mathscr{p}_j = \sum_{j'} \sigma_{jj'} \frac{\partial q_{j'}}{\partial t}. \tag{7.123}$$

Returning to plane waves propagating along axis z, and acting exactly like in Sec. 6.4, for both the longitudinal and transverse waves we again arrive at Eq. (6.49), but for $\mathscr{p}$ rather than $\mathscr{P}$ (due to a different definition of the wave impedance – per unit area rather than per particle chain). For the sinusoidal waves of the type (108), it yields

$$\mathscr{p}_z = \frac{\omega^2 Z}{2} aa^*, \tag{7.124}$$

with Z being the corresponding impedance – either Z_l or Z_t.

Just as in the 1D case, one more important effect, in which the notion of impedance is crucial, is the partial *wave reflection* from at an interface between two media. The two boundary conditions, necessary for the analysis of the reflection, may be obtained from the continuity of the vectors **q** and $d\mathbf{F}$. (The former condition is evident, while the latter one may be obtained by applying the 2nd Newton law to any infinitesimal volume $dV = dAdz$, where the segment dz straddles the interface.) Let us start from the simplest case of the *normal incidence* on a plane interface between two uniform media, each with its own elastic moduli and mass density. Due to the symmetry of the system, it is obvious that the longitudinal/transverse incident wave may only excite similarly polarized reflected and transferred waves. As a result, we may literally repeat the calculations of Sec. 6.4, again arriving at the fundamental relations (6.55) and (6.56), with the replacement of Z and Z' with the corresponding values of either Z_l (120) or Z_t (121). Thus, at the normal incidence, the wave reflection is determined solely by the acoustic *impedances* of the media, while the sound *velocities* are not involved.

The situation, however, becomes more complicated at a nonzero incidence angle $\theta^{(i)}$ (Fig. 12), where the transmitted wave is generally also *refracted*, i.e. propagates under a different angle, $\theta' \neq \theta^{(i)}$, beyond the interface. Moreover, at $\theta^{(i)} \neq 0$ the directions of particle motion (vector **q**) and of the stress forces (vector $d\mathbf{F}$) in the incident wave are neither exactly parallel nor exactly perpendicular to the interface, and thus this wave may serve as an actuator for the reflected and refracted waves of both polarizations – see Fig. 12, drawn for the particular case when the incident wave is transverse. The corresponding four angles, $\theta_t^{(r)}$, $\theta_t^{(r)}$, θ'_l, θ'_t, may be readily related to $\theta_t^{(i)}$ by the "kinematic" condition that the incident wave, as well as the reflected and refracted waves of both types, must have the same spatial distribution along the interface plane, i.e. for the interface particles participating in all five waves. According to Eq. (108), the necessary boundary condition is the equality of the tangential components (in Fig. 12, k_x), of all five wave vectors:

$$k_t \sin\theta_t^{(r)} = k_l \sin\theta_l^{(r)} = k_l' \sin\theta_l' = k_t' \sin\theta_t' = k_x \equiv k_t \sin\theta_t^{(i)}. \tag{7.125}$$

Since the acoustic wave vector magnitudes k, at fixed frequency ω, are inversely proportional to the corresponding wave velocities, we immediately get the following relations:

$$\theta_t^{(r)} = \theta_t^{(i)}, \quad \frac{\sin\theta_l^{(r)}}{v_l} = \frac{\sin\theta_l'}{v_l'} = \frac{\sin\theta_t'}{v_t'} = \frac{\sin\theta_t^{(i)}}{v_t}, \tag{7.126}$$

so generally all four angles are different. (This is of course an analog of the well-known *Snell law* in optics – where, however, only transverse waves are possible.) These relations show that, just like in optics, the direction of a wave propagating into a medium with lower velocity is closer to the normal (in

Fig. 12, to the z-axis). In particular, this means that if $v' > v$, the acoustic waves, at larger angles of incidence, may exhibit the effect of total internal reflection, so well known from optics[37], when the *refracted* wave vanishes. In addition, Eqs. (126) show that in acoustics, the *reflected* longitudinal wave, with velocity $v_l > v_t$, may vanish at sufficiently large angles of the transverse wave incidence.

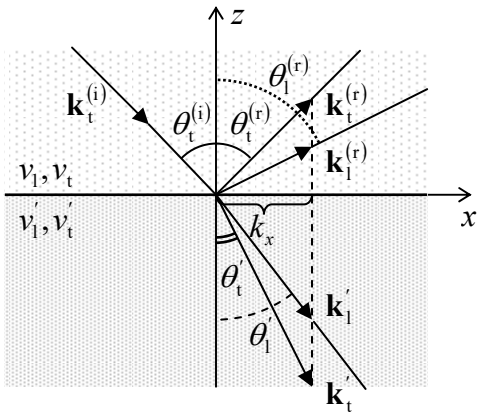

Fig. 7.12. Deriving the "kinematic" conditions (126) of the acoustic wave reflection and refraction (for the case of a transverse incident wave).

All these facts automatically follow from general expressions for amplitudes of the reflected and refracted waves via the amplitude of the incident wave. These relations are straightforward to derive (again, from the continuity of the vectors $\mathbf{q}$ and $d\mathbf{F}$), but since they are much bulkier than those in the electromagnetic wave theory (where they are called the *Fresnel formulas*[38]), I would not have time/space to spell out and discuss them. Let me only note that, in contrast to the case of normal incidence, these relations involve eight media parameters: the impedances Z, Z', and the velocities v, v' on both sides of the interface, and for both the longitudinal and transverse waves.

There are other interface effects as well. Within certain frequency ranges, interfaces and surfaces of elastic solids may sustain so-called *surface acoustic waves* (SAW), in particular, the *Rayleigh waves* and the *Love waves*.[39] The main feature that distinguishes such waves from their *bulk* (longitudinal and transverse) counterparts discussed above, is that the displacement amplitudes are largest at the interface and decay exponentially into the bulk of both adjacent media, so the waves cannot be plane in the usual sense of being independent of two Cartesian coordinates.

For an analysis of such waves, it is important that in a uniform medium, even non-plane elastic waves may be always separated into independent longitudinal and transverse components. Indeed, it is straightforward (and hence left for the reader) to prove that Eq. (107) may be satisfied by a vector sum $\mathbf{q}(\mathbf{r}, t) = \mathbf{q}_l(\mathbf{r}, t) + \mathbf{q}_t(\mathbf{r}, t)$, with the former component having zero curl ($\nabla\times\mathbf{q}_l = 0$) and propagating with the velocity (112), and the latter component having zero divergence ($\nabla\cdot\mathbf{q}_t = 0$) and propagating with the velocity (116). The plane waves $q_l\mathbf{n}_z$ and $q_t\mathbf{n}_x$ analyzed above certainly fall into these two categories, but in more general waves, there may be no clear association between the longitudinal and transverse components and their polarization.

This is true, in particular, in the Rayleigh waves, where the particle displacement vector $\mathbf{q}$ may be represented as the sum $\mathbf{q}_l + \mathbf{q}_t$, each of the vectors having more than one Cartesian component. In

[37] See, e.g., EM Sec. 7.5.

[38] Their discussion may be also found in EM Sec. 7.5.

[39] Named, respectively, after Lord Rayleigh (born J. Strutt, 1842-1919) who has theoretically predicted the very existence of surface acoustic waves, and A. Love (1863-1940).

contrast to the bulk waves, the longitudinal and transverse components are coupled via their interaction with the interface, and as a result, propagate with a single velocity v_R. A straightforward analysis of the Rayleigh waves on the *surface* of an elastic solid (i.e. its interface with free space) yields the following equation for v_R:

$$\left(1-\frac{v_R^2}{2v_t^2}\right)^4=\left(1-\frac{v_R^2}{v_t^2}\right)\left(1-\frac{v_R^2}{v_l^2}\right). \tag{7.127}$$

According to this formula, and Eqs. (112) and (116), for realistic materials with the Poisson index between 0 and ½, the Rayleigh waves are slightly (by 4 to 13%) slower than the bulk transverse waves – and hence substantially slower than the bulk longitudinal waves.

In the simplest case a "1D-plane" Rayleigh wave, independent of one Cartesian coordinate, the net vector **q** has just two Cartesian components (each contributed by $\mathbf{q}_l$ and $\mathbf{q}_t$): one parallel to the propagation direction and hence to the interface, and another one normal to it. As a result, the trajectory of each particle in the wave is an ellipse in the plane normal to the interface. In contrast, the Love waves are purely transverse, with **q** oriented parallel to the interface. However, the interaction of these waves with the interface reduces their velocity v_L in comparison with that (v_t) of the bulk transverse waves, keeping it within the narrow interval between v_t and v_R:

$$v_R < v_L < v_t < v_l . \tag{7.128}$$

The practical importance of surface acoustic waves is that their amplitude decays very slowly with distance r from their point-like source: $a \propto 1/r^{1/2}$, while any bulk waves decay much faster, as $a \propto 1/r$. (Indeed, in the latter case the power $\mathscr{P} \propto a^2$, emitted by such source, is distributed over a spherical surface area proportional to r^2, while in the former case all the power goes into a thin surface circle whose length scales as r.) At least two areas of applications of the surface acoustic waves have to be mentioned: geophysics (for earthquake detection and the Earth crust seismology), and electronics (for signal processing, with a focus on frequency filtering). Unfortunately, I cannot dwell on these interesting topics and I have to refer the reader to special literature.[40]

7.8. Elastic waves in restricted geometries

From what was discussed at the end of the last section, it should be pretty clear that generally, the propagation of acoustic waves in elastic bodies of finite size is rather complicated. There is, however, one important limit in which several important simple results may be readily obtained. This is the limit of (relatively) low frequencies, where the corresponding wavelength is much larger than at least one dimension of the system.

Let us consider, for example, various waves that may propagate along thin rods, in this case "thin" meaning that the characteristic size a of the rod's cross-section is much smaller than not only the length of the rod but also the wavelength $\lambda = 2\pi/k$. In this case, there is a considerable range Δz of distances along the rod,

$$a << \Delta z << \lambda , \tag{7.129}$$

[40] See, for example, K. Aki and P. Richards, *Quantitative Seismology*, 2nd ed., University Science Books, 2002; and D. Morgan, *Surface Acoustic Waves*, 2nd ed., Academic Press, 2007.

in that we can neglect the material's inertia, and apply the results of our earlier static analyses. For example, for a *longitudinal* wave of stress, which is essentially a wave of periodic tensile extensions and compressions of the rod, within the range (129) we may use the static relation (42):

$$\sigma_{zz} = E s_{zz}. \tag{7.130}$$

In this simple case, it is easier to use the general equation of elastic dynamics not in its vector form (107), but rather in the precursor, Cartesian-component form (25), with $f_j = 0$. For the plane waves of stress, propagating along the z-axis, only one component (with $j' \to z$) of the sum on the right-hand side of that equation is not equal to zero, and it is reduced to

$$\rho \frac{\partial^2 q_j}{\partial^2 t^2} = \frac{\partial \sigma_{jz}}{\partial z}. \tag{7.131}$$

In our current case of longitudinal waves, all components of the stress tensor but σ_{zz} are equal to zero. With σ_{zz} from Eq. (130), and using the definition $s_{zz} = \partial q_z/\partial z$, Eq. (131) is reduced to a simple 1D wave equation,

$$\rho \frac{\partial^2 q_z}{\partial^2 t^2} = E \frac{\partial^2 q_z}{\partial z^2}, \tag{7.132}$$

which shows that the velocity of such *tensile waves* is

$$v = \left(\frac{E}{\rho} \right)^{1/2}. \tag{7.133}$$

Tensile waves: velocity

Comparing this result with Eq. (112), we see that the tensile wave velocity, for any realistic material with a positive Poisson's ratio, is lower than the velocity v_l of longitudinal waves in the bulk of the same material. The reason for this difference is simple: in thin rods, the cross-section is free to oscillate (e.g., shrink in the longitudinal extension phase of the passing wave),[41] so the effective force resisting the longitudinal deformation is smaller than in a border-free space. Since (as it is clearly visible from the wave equation), the scale of the force determines that of v^2, this difference translates into slower waves in rods. Of course, as the wave frequency is increased to $ka \sim 1$, there is a (rather complicated and cross-section-depending) crossover from Eq. (133) to Eq. (112).

Proceeding to *transverse* waves on rods, let us first have a look at long *bending waves* for which the condition (129) is satisfied, so the vector $\mathbf{q} = \mathbf{n}_x q_x$ (with the x-axis being the bending direction – see Fig. 8) is virtually constant in the whole cross-section. In this case, the only element of the stress tensor contributing to the net transverse force F_x is σ_{xz}, so the integral of Eq. (131) over the cross-section is

$$\rho A \frac{\partial^2 q_x}{\partial t^2} = \frac{\partial F_x}{\partial z}, \qquad \text{with } F_x = \int_A \sigma_{xz} d^2 r. \tag{7.134}$$

Now, if Eq. (129) is satisfied, we again may use the static local relations (75)-(77), with all derivatives d/dz duly replaced with their partial form $\partial/\partial z$, to express the force F_x via the bending deformation q_x. Plugging these relations into each other one by one, we arrive at a rather unusual differential equation

[41] For this reason, the tensile waves can be called longitudinal only in a limited sense: while the stress wave is purely longitudinal: $\sigma_{xx} = \sigma_{yy} = 0$, the strain wave is not: $s_{xx} = s_{yy} = -\sigma s_{zz} \neq 0$, i.e. $\mathbf{q}(\mathbf{r}, t) \neq \mathbf{n}_z q_z$.

$$\rho A \frac{\partial^2 q_x}{\partial t^2} = -EI_y \frac{\partial^4 q_x}{\partial z^4}. \tag{7.135}$$

Looking for its solution in the form of a sinusoidal wave (108), we get the following dispersion relation:[42]

Bending waves: dispersion relation

$$\boxed{\omega^2 = \frac{EI_y}{\rho A} k^4}. \tag{7.136}$$

This relation means that the bending waves are not acoustic at *any* frequency, and cannot be characterized by a single velocity that would be valid for all wave numbers k, i.e. for all spatial Fourier components of a waveform. According to our discussion in Sec. 6.3, such *strongly dispersive* systems cannot pass non-sinusoidal waveforms too far without changing their waveform rather considerably.

This situation changes, however, if the rod is pre-stretched with a tension force $\mathcal{T}$ – just as in the discrete 1D model that was analyzed in Sec. 6.3. The calculation of the effect of this force is essentially similar; let us repeat it for the continuous case, for a minute neglecting the bending stress – see Fig. 13.

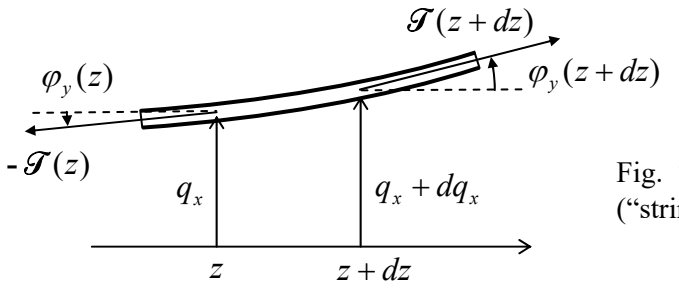

Fig. 7.13. Additional forces in a thin rod ("string"), due to the background tension $\mathcal{T}$.

Still sticking to the limit of small angles φ, the additional vertical component $d\mathcal{T}_x$ of the net force acting on a small rod fragment of length dz is $\mathcal{T}_x(z - dz) - \mathcal{T}_x(z) = \mathcal{T}\,\varphi_y(z + dz) - \mathcal{T}\varphi_y(z) \approx \mathcal{T}\,(\partial\varphi_y/\partial z)dz$, so $\partial F_x/\partial z = \mathcal{T}\,(\partial\varphi_y/\partial z)$. With the geometric relation (77) in its partial-derivative form $\partial q_x/\partial z = \varphi_y$, this additional term becomes $\mathcal{T}\,(\partial^2 q_x/\partial z^2)$. Now adding it to the right-hand side of Eq. (135), we get the following dispersion relation

$$\omega^2 = \frac{1}{\rho A}\left(EI_y k^4 + \mathcal{T}k^2\right). \tag{7.137}$$

Since the product ρA in the denominator of this expression is just the rod's mass per unit length (which was denoted μ in Chapter 6), at low k (and hence low frequencies), this expression is reduced to the linear dispersion law, with the velocity given by Eq. (6.43):

$$v = \left(\frac{\mathcal{T}}{\rho A}\right)^{1/2}. \tag{7.138}$$

So Eq. (137) describes a smooth crossover from the "guitar-string" acoustic waves to the highly dispersive bending waves (136).

[42] Note that since the "moment of inertia" I_y, defined by Eq. (70), may depend on the bending direction (unless the cross-section is sufficiently symmetric), the dispersion relation (136) may give different results for different directions of the bending wave polarization.

Now let us consider another type of transverse waves in thin rods – the so-called *torsional waves*, which are essentially the dynamic propagation of the torsional deformation discussed in Sec. 6. The easiest way to describe these waves, again within the limits (129), is to write the equation of rotation of a small segment dz of the rod about the z-axis, passing through the "center of mass" of its cross-section, under the difference of torques $\boldsymbol{\tau} = \mathbf{n}_z \tau_z$ applied on its ends – see Fig. 10:

$$\rho I_z dz \frac{\partial^2 \varphi_z}{\partial t^2} = d\tau_z, \tag{7.139}$$

where I_z is the "moment of inertia" defined by Eq. (91), which now, after its multiplication by ρdz, i.e. by the mass per unit area, has turned into the genuine moment of inertia of a dz-thick slice of the rod. Dividing both sides of Eq. (139) by dz, and using the static local relation (84), $\tau_z = C\kappa = C(\partial\varphi_z/\partial z)$, we get the following differential equation

$$\rho I_z \frac{\partial^2 \varphi_z}{\partial t^2} = C \frac{\partial^2 \varphi_z}{\partial z^2}. \tag{7.140}$$

Just as Eqs. (111), (115), and (132), this equation describes an acoustic (dispersion-free) wave, which propagates with the following frequency-independent velocity

$$v = \left(\frac{C}{\rho I_z} \right)^{1/2}. \tag{7.141}$$

Torsional waves: velocity

As we have seen in Sec. 6, for rods with axially-symmetric cross-sections, the torsional rigidity C is described by the simple relation (89), $C = \mu I_z$, so Eq. (141) is reduced to Eq. (116) for the transverse waves in infinite media. The reason for this similarity is straightforward: in a torsional wave, particles oscillate along small arcs (Fig. 14a), so if the rod's cross-section is round, its surface is stress-free, and does not perturb or modify the motion in any way, and hence does not affect the transverse velocity.

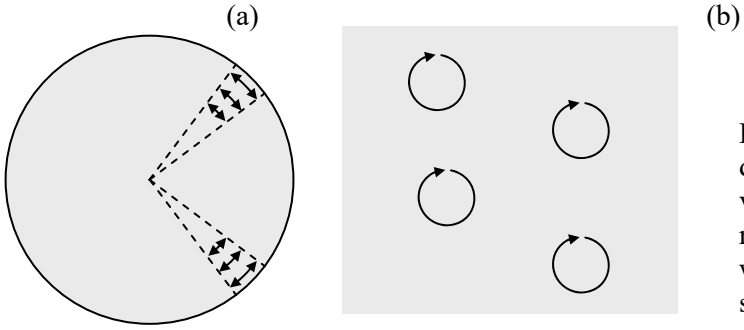

Fig. 7.14. Particle trajectories in two different transverse waves with the same velocity: (a) torsional waves in a thin round rod and (b) circularly polarized waves in an infinite (or very broad) sample.

This fact raises an interesting issue of the relation between the torsional and *circularly polarized* waves. Indeed, in Sec. 7, I have not emphasized enough that Eq. (116) is valid for a transverse wave polarized in any direction perpendicular to the wave vector $\mathbf{k}$ (in our notation, directed along the z-axis). In particular, this means that such waves are doubly degenerate: any isotropic elastic continuum can carry simultaneously two non-interacting transverse waves propagating in the same direction with the same velocity (116), with two mutually perpendicular linear polarizations (directions of the vector $\mathbf{a}$),

for example, directed along the x- and y-axes.[43] If both waves are sinusoidal (108), with the same frequency, each point of the medium participates in two simultaneous sinusoidal motions within the [x, y] plane:

$$q_x = \mathrm{Re}\left[a_x e^{i(kz-\omega t)}\right] = A_x \cos\Psi, \qquad q_y = \mathrm{Re}\left[a_y e^{i(kz-\omega t)}\right] = A_y \cos(\Psi+\varphi), \tag{7.142}$$

where $\Psi \equiv kz - \omega t + \varphi_x$, and $\varphi \equiv \varphi_y - \varphi_x$. Basic geometry tells us that the trajectory of such a motion on the [x, y] plane is an ellipse (Fig. 15), so such waves are called *elliptically polarized*. The most important particular cases of such polarization are:

(i) $\varphi = 0$ or π: a *linearly-polarized* wave, with the displacement vector **a** is directed at angle $\theta = \tan^{-1}(A_y/A_x)$ to the x-axis; and

(ii) $\varphi = \pm \pi/2$ and $A_x = A_y$: two possible *circularly-polarized* waves, with the *right* or *left* polarization, respectively.[44]

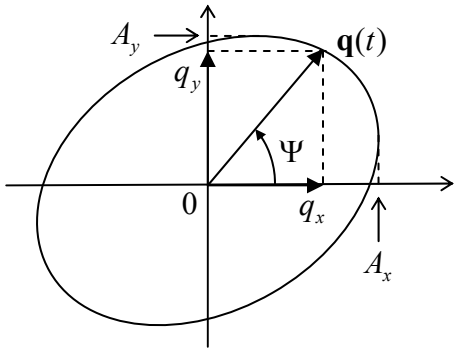

Fig. 7.15. The trajectory of a particle in an elliptically polarized transverse wave, within the plane perpendicular to the direction of wave propagation.

Now comparing the trajectories of particles in the torsional wave in a thin round rod (or pipe) and the circularly polarized wave in a broad sample (Fig. 14), we see that, despite the same wave propagation velocity, these transverse waves are rather different. In the former case (Fig. 14a) each particle moves back and forth along an arc, with the arc's length different for different particles (and vanishing at the rod's center), so the waves are *not* plane. On the other hand, in a circularly polarized wave, all particles move along similar, circular trajectories, so such a wave *is* plane.

To conclude this chapter, let me briefly mention the opposite limit when the size of the body, from whose boundary the waves are completely reflected,[45] is much larger than the wavelength. In this case, the waves propagate almost as in an infinite 3D continuum (which was analyzed in Sec. 7), and the most important new effect is the finite number of wave modes in the body. Repeating the 1D analysis at the end of Sec. 6.5, for each dimension of a 3D cuboid of volume $V = l_1 l_2 l_3$, and taking into account that the numbers k_n in each of the three dimensions are independent, we get the following generalization of

[43] As was discussed in Sec. 6.3, this is also true in the simple 1D model shown in Fig. 6.4a.

[44] The circularly polarized waves play an important role in quantum mechanics, where they may be most naturally quantized, with their elementary excitations (in the case of mechanical waves we are discussing, called *phonons*) having either positive or negative angular momentum $L_z = \pm\hbar$.

[45] For acoustic waves, such a condition is easy to implement. Indeed, from Sec. 7 we already know that the strong inequality of the wave impedances Z is sufficient for such reflection. The numbers in Table 1 show that, for example, the impedance of a longitudinal wave in a typical metal (say, steel) is almost two orders of magnitude higher than that in air, ensuring their virtually full reflection from the surface.

Eq. (6.75) for the number ΔN of different traveling waves with wave vectors within a relatively small volume d^3k of the wave vector space:

$$dN = g\frac{V}{(2\pi)^3}d^3k >> 1, \qquad \text{for } \frac{1}{V} << d^3k << k^3, \tag{7.143}$$

3D density of modes

where $k >>> 1/l_{1,2,3}$ is the center of this volume, and g is the number of different possible wave modes with the same wave vector $\mathbf{k}$. For the mechanical waves analyzed above, with one longitudinal mode, and two transverse modes with different polarizations, $g = 3$.

Note that since the derivation of Eqs. (6.75) and (143) does not use other properties of the waves (in particular, their dispersion relations), this mode counting rule is ubiquitous in physics, being valid, in particular, for electromagnetic waves (where $g = 2$) and quantum "de Broglie waves" (i.e. wavefunctions), whose degeneracy factor g is usually determined by the particle's spin.[46]

7.9. Exercise problems

7.1. Derive Eqs. (16).

Hint: Besides basic calculus and the definition of the cylindrical coordinates, you may like to use Eq. (4.7) with $d\boldsymbol{\varphi} = (d\varphi)\mathbf{n}_z$.

7.2. A uniform thin sheet of an isotropic elastic material, of thickness t and area $A >> t^2$, is compressed by two plane, parallel, broad, rigid surfaces – see the figure on the right. Assuming that there is no slippage between the sheet and the surfaces, calculate the relative compression $(-\Delta t/t)$ as a function of the compressing force. Compare the result with that for the tensile stress calculated in Sec. 3.

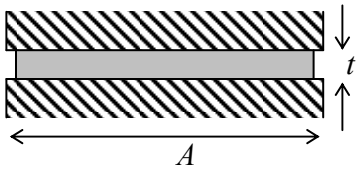

7.3. Two opposite edges of a thin but wide sheet of an isotropic elastic material are clamped in two rigid, plane, parallel walls that are pulled apart with force F, along the sheet's length l. Find the relative extension $\Delta l/l$ of the sheet in the direction of the force and its relative compression $\Delta t/t$ in the perpendicular direction, and compare the results with Eqs. (45)-(46) for the tensile stress and with the solution of the previous problem.

7.4. Calculate the radial extension ΔR of a thin, long, round cylindrical pipe due to its rotation with a constant angular velocity ω about its symmetry axis (see the figure on the right), in terms of the elastic moduli E and ν.

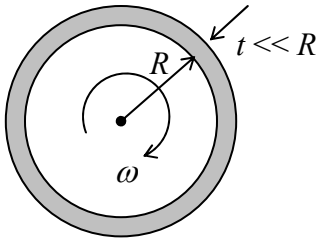

7.5.* A static force $\mathbf{F}$ is exerted on an inner point of a uniform and isotropic elastic body. Calculate the spatial distribution of the deformation created by the force, assuming that far from the point of its application and the points we are interested in, the body's position is kept fixed.

[46] See, e.g., EM Secs. 7.8 and QM Sec. 1.7.

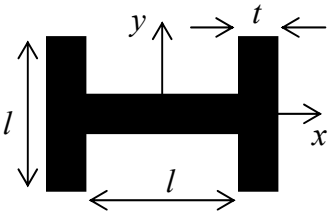

7.6. A long uniform rail with the cross-section shown in the figure on the right is being bent with the same (small) torque twice: first within the *xz*-plane and then within the *yz*-plane. Assuming that $t << l$, find the ratio of the bending deformations in these two cases.

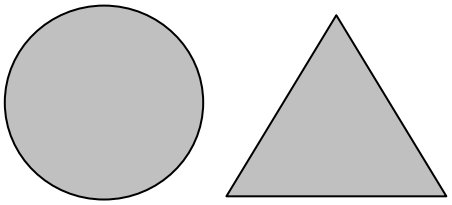

7.7. Two thin rods of the same length and mass are made of the same isotropic and elastic material. The cross-section of one of them is a circle, while the other one is an equilateral triangle – see the figure on the right. Which of the rods is stiffer for bending along its length? Quantify the relation. Does the result depend on the bending plane's orientation?

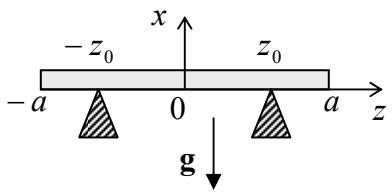

7.8. A thin, uniform, initially straight elastic beam is placed on two point supports at the same height – see the figure on the right. . Calculate the support placements that:

(i) ensure that the beam ends are horizontal, and

(ii) minimize the largest deflection of the beam from the horizontal baseline.

Hint: For Task (ii), an approximate answer (with an accuracy better than 1%) is acceptable.

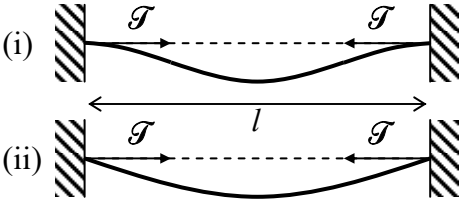

7.9. Calculate the largest longitudinal compression force $\mathcal{T}$ that may be withstood by a thin, straight, elastic rod without buckling (see the figure on the right) for each of the shown cases:

(i) the rod's ends are clamped, and

(ii) the rod is free to turn about the support points.

7.10. A thin elastic pole with a square cross-section of area $A = a \times a$ is firmly dug into the ground in the vertical position, sticking out by height $h >> a$.

(i) What largest compact mass M may be placed straight on the top of a light pole without stability loss?

(ii) In the absence of such an additional mass, how massive a uniform pole may be to retain its stability?

Hint: For Task (ii), you may use the same WKB approximation as in Problem 6.18.

7.11. Calculate the potential energy of a small and slowly changing, but otherwise arbitrary bending deformation of a uniform, initially straight elastic rod. Can the result be used to derive the dispersion relation (136)?

7.12. Calculate the torsional rigidity of a long uniform rod whose cross-section is an ellipse with semi-axes a and b.

7.13. Calculate the potential energy of a small but otherwise arbitrary torsional deformation $\varphi_z(z)$ of a uniform and straight elastic rod.

7.14. Calculate the spring constant $\kappa \equiv dF/dl$ of a coil made of a uniform elastic wire with a circular cross-section of diameter d, wound as a dense round spiral of $N >> 1$ turns of radius $R >> d$ – see the figure on the right.

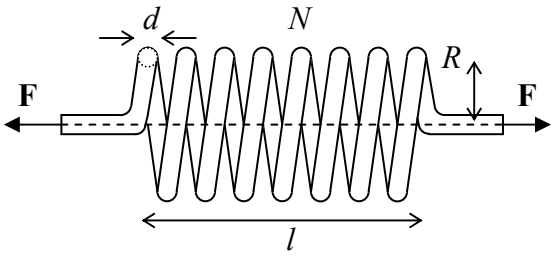

7.15. The coil studied in the previous problem is now used as what is sometimes called the *torsion spring* – see the figure on the right. Find the corresponding spring constant $d\tau/d\varphi$, where τ is the torque of the external forces **F** relative to the center of the coil (point 0).

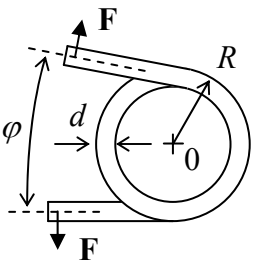

7.16. Use Eqs. (99) and (100) to recast Eq. (101b) for the torsional rigidity C of a thin rod into the form given by Eq. (101c).

7.17.* Generalize Eq. (101b) to the case of rods with more than one cross-section's boundary. Use the result to calculate the torsional rigidity of a thin round pipe, and compare it with Eq. (91).

7.18. Prove that in a uniform isotropic medium, an arbitrary (not necessarily plane) elastic wave may be decomposed into a longitudinal wave with $\nabla \times \mathbf{q}_l = 0$ and a transverse wave with $\nabla \cdot \mathbf{q}_t = 0$, and find the equations satisfied by these functions.

7.19.* Use the wave equations derived in the solution of the previous problem and the semi-quantitative description of the Rayleigh surface waves given in Sec. 7 of the lecture notes, to calculate the structure of the waves and to derive Eq. (127).

7.20.* Calculate the modes and frequencies of free radial oscillations of a sphere of radius R, made of a uniform elastic material.

7.21. A long steel wire has a circular cross-section with a 3-mm diameter and is pre-stretched with a constant force of 10 N. Which of the longitudinal and transverse waves with frequency 1 kHz has the largest group velocity in the wire? Accept the following parameters for the steel (see Table 1): E = 170 GPa, $\nu = 0.30$, $\rho = 7.8$ g/cm^3.

7.22. Define and calculate the wave impedances for (i) tensile and (ii) torsional waves in a thin rod, that are appropriate in the long-wave limit. Use the results to calculate the fraction of each wave's power $\mathscr{P}$ reflected from a firm connection of a long rod with a round cross-section to a similar rod with a twice smaller diameter – see the figure on the right.

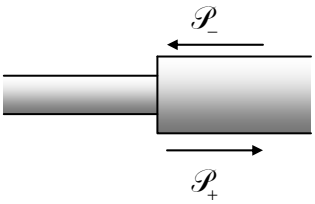

7.23. Calculate the fundamental frequency of small transverse standing waves on a free uniform thin rod, and the position of displacement nodes in this mode.

Hint: A numerical solution of the final transcendental equation is acceptable.

Chapter 8. Fluid Mechanics

This chapter describes the basic notions of fluid mechanics, discusses a few core problems of statics and dynamics of ideal and viscous fluids, and gives a very brief review of such a complicated phenomenon as turbulence. In addition, the viscous fluid flow discussion is used as a platform for an elementary introduction to numerical methods of the partial differential equation solution – whose importance extends well beyond this particular field.

8.1. Hydrostatics

The mechanics of *fluids* (defined as the materials that cannot keep their geometric form on their own, and include both liquids and gases) is both more simple and more complex than that of elastic solids, with the simplifications mostly in *statics*.[1] Indeed, fluids, by definition, cannot resist static shear deformations. There are two ways to express this fact. First, we can formally take the shear modulus μ, describing this resistance, to equal zero. Then Hooke's law (7.32) shows that the stress tensor is diagonal:

$$\sigma_{jj'} = \sigma_{jj}\delta_{jj'}. \tag{8.1}$$

Alternatively, the same conclusion may be reached just by looking at the stress tensor definition (7.19) and/or Fig. 7.3, and saying that in the absence of shear stress, the elementary interface $d\mathbf{F}$ has to be normal to the area element dA, i.e. parallel to the vector $d\mathbf{A}$.

Moreover, in fluids at equilibrium, all three diagonal elements σ_{jj} of the stress tensor have to be equal at each point. To prove that, it is sufficient to single out (mentally rather than physically), from a static fluid, a small volume in the shape of a right prism, with mutually perpendicular faces normal to the two directions we are interested in – in Fig. 1, along the x- and y-axes.

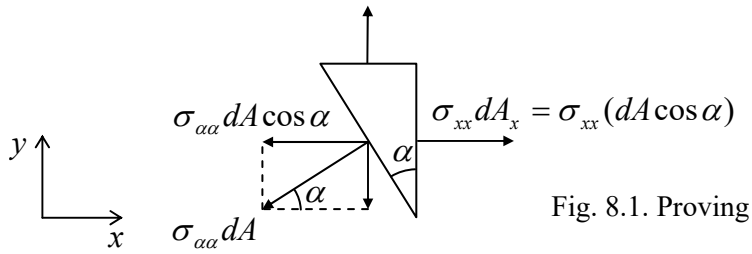

Fig. 8.1. Proving the pressure isotropy.

The prism is in equilibrium if each Cartesian component of the vector of the total force exerted on all its faces equals zero. For the x-component, this balance may be expressed as $\sigma_{xx}dA_x - (\sigma_{\alpha\alpha}dA)\cos\alpha = 0$. However, from the geometry (Fig. 1), $dA_x = dA\cos\alpha$, so the above expression yields $\sigma_{\alpha\alpha} = \sigma_{xx}$. A similar argument for the y-component gives $\sigma_{\alpha\alpha} = \sigma_{yy}$, so $\sigma_{xx} = \sigma_{yy}$. Changing the orientation of the prism, we can get such equalities for any pair of diagonal elements of the stress tensor, σ_{jj}, so all three of them have to be equal.

[1] It is often called *hydrostatics* because water has always been the most important liquid for the human race and hence for science and engineering.

This common diagonal element of the stress matrix is usually denoted as (-$\mathcal{P}$), because in the vast majority of cases, the parameter $\mathcal{P}$, called *pressure*, is positive. Thus we arrive at the key relation (which was already mentioned in Sec. 7.2):

$$\sigma_{jj'} = -\mathcal{P}\delta_{jj'}. \tag{8.2}$$

Pressure

In the absence of bulk forces, pressure should be constant through the volume of fluid, due to the translational symmetry. Let us see how this result is affected by bulk forces. With the simple stress tensor (2), the general condition of equilibrium of a continuous medium, expressed by Eq. (7.25) with the left-hand side equal to zero, becomes

$$-\frac{\partial \mathcal{P}}{\partial r_j} + f_j = 0, \tag{8.3}$$

and may be re-written in the following convenient vector form:

$$-\nabla \mathcal{P} + \mathbf{f} = 0. \tag{8.4}$$

In the simplest case of a heavy fluid with mass density ρ, in a uniform gravity field $\mathbf{f} = \rho\mathbf{g}$, the equation of equilibrium becomes,

$$-\nabla \mathcal{P} + \rho\mathbf{g} = 0, \tag{8.5}$$

with only one nonzero component – near the Earth's surface, the vertical one. If, in addition, the fluid may be considered *incompressible,* with its density ρ constant,[2] this equation may be readily integrated over the vertical coordinate (say, y) to give the so-called *Pascal equation*:[3]

$$\mathcal{P} + \rho g y = \text{const}, \tag{8.6}$$

Pascal equation

where the direction of the y-axis is taken opposite to that of vector $\mathbf{g}$.

Two manifestations of this key equation are well known. The first one is the fact that in interconnected vessels filled with a fluid, its pressure is equal at all points at the same height (y), regardless of the vessel shape, provided that the fluid is in equilibrium.[4] In particular, if a heavy liquid has an open surface, then in equilibrium, it has to be horizontal – at least, not too close to the retaining walls (see Sec. 2).

The second manifestation of Eq. (6) is the *buoyant force* $\mathbf{F}_b$ exerted by a liquid on a (possibly, partly) submerged body, i.e. the vector sum of the elementary pressure forces $d\mathbf{F} = \mathcal{P}d\mathbf{A}$ exerted on all elementary areas dA of the submerged part of the body's surface – see Fig. 2. According to Eq. (6), with the constant equal to zero (corresponding to zero pressure at the liquid's surface taken for $y = 0$, see Fig. 2a), the vertical component of this elementary force is

[2] As was discussed in Sec. 7.3 in the context of Table 7.1, this is an excellent approximation, for example, for human-scale experiments with water.

[3] The equation, and the SI unit of pressure 1 Pa ≡ 1N/m^2, are named after Blaise Pascal (1623-1662) who not only pioneered hydrostatics, but also invented the first mechanical calculator, and made several other important contributions to mathematics – and to Christian philosophy!

[4] This simple fact opens wide opportunities for the engineering field of *hydraulics*, in particular enabling a very simple and efficient way to magnify forces, using interconnected *hydraulic cylinders* of different diameters.

$$dF_y = dF\cos\varphi = \mathcal{P}dA\cos\varphi = -\rho g y\cos\varphi dA = -\rho g y dA_h\,. \tag{8.7}$$

where $dA_h = \cos\varphi dA$ is the horizontal footprint (say, $dxdz$) of the elementary area dA. Now integrating this relation over all the surface, we get the total vertical buoyant force:[5]

Archimedes principle

$$F_b = \rho g\int_S (-y)dA_h \equiv \rho g V, \tag{8.8}$$

where V is the volume of the *submerged* part of the body's volume, while ρ is the liquid's density, so by magnitude, F_b equals the weight of the liquid that *would* fill the submerged volume.

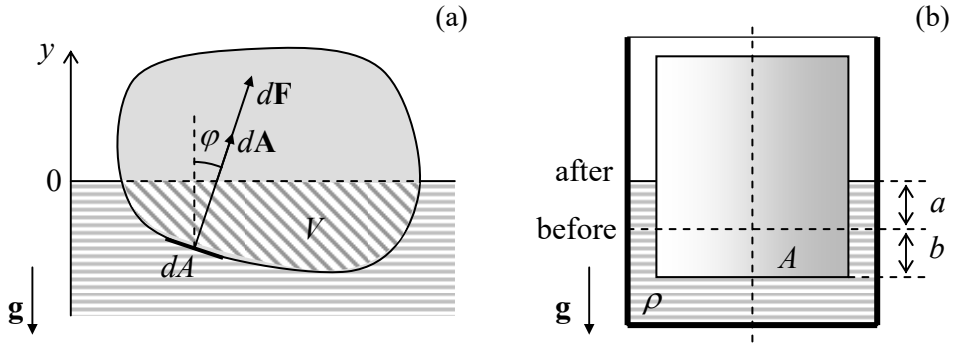

Fig. 8.2. Calculating the buoyant force.

This well-known *Archimedes principle* may be proved even more simply using the following argument: the liquid's pressure forces, and hence the resulting buoyant force, cannot depend on what is inside the body's volume. Hence F_b would be the same if we filled the volume V in question with a liquid similar to the surrounding one. But in this case, the liquid should be still in equilibrium even if the surface is completely flexible, so both forces acting on its inner part, the buoyant force $\mathbf{F}_b$ and the inner liquid's weight $m\mathbf{g} = \rho V\mathbf{g}$, have to be equal and opposite, thus proving Eq. (8) again.

Despite the simplicity of the Archimedes principle, its erroneous formulations, such as "*The buoyant force's magnitude is equal to the weight of the displaced liquid*" [WRONG!] creep from one undergraduate textbook to another, leading to application errors. A typical example is shown in Fig. 2b, where a solid vertical cylinder with the base area A is pressed into a liquid inside a container of comparable size, pushing the liquid's level up by distance a. The correct answer for the buoyant force, following from Eq. (8), is

$$F_b = \rho g V = \rho g A(a+b), \tag{8.9a}$$

because the volume V of the *submerged* part of the cylinder is evidently $A(a + b)$. But the wrong formulation cited above, using the term *displaced liquid*, would give a different answer:

$$F_b = \rho g V_{\text{displaced}} = \rho g A b\,. \quad \text{[WRONG!]} \tag{8.9b}$$

(The latter result is correct only asymptotically, in the limit $b/a \to \infty$.)

Another frequent error in hydrostatics concerns the angular stability of a freely floating body – the problem of vital importance for the boat/ship design. It is sometimes claimed that the body is stable

[5] The force is vertical, because the horizontal components of the elementary forces $d\mathbf{F}$ exerted on opposite elementary areas dA, at the same height y, cancel.

only if the so-called *buoyancy center*, the effective point of buoyant force application (in Fig, 3, point B),[6] is *above* the center of mass (C) of the floating body. However, as Fig. 3 shows, this is unnecessary; indeed in the shown case, point B remains *below* point C, even at a small tilt. Still, in this case, the torque created by the pair of forces $\mathbf{F}_b$ and $m\mathbf{g}$ tries to return the body to the equilibrium position, which is therefore stable. As Fig. 3 shows, the actual condition of the angular stability may be expressed as the requirement for point M (in shipbuilding, called the *metacenter* of the ship's hull) to be above the ship's center of mass C.[7]

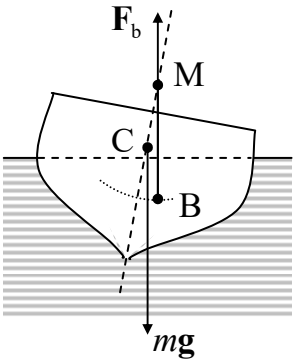

Fig. 8.3. Angular stability of a floating body.

To conclude this section, let me note that the integration of Eq. (4) may be more complex in the case if the bulk forces $\mathbf{f}$ depend on position,[8] and/or if the fluid is substantially compressible. In the latter case, Eq. (4) has to be solved together with the medium-specific *equation of state* $\rho = \rho(\mathcal{P})$ describing its compressibility law – whose example is given by Eq. (7.38) for ideal gases: $\rho \equiv mN/V = m\mathcal{P}/k_B T$, where m is the mass of one gas molecule.

8.2. Surface tension effects

Besides the bulk (volume-distributed) forces, one more possible source of pressure is *surface tension*. This effect results from the difference between the potential energy of atomic interactions on the interface between two different fluids and that in their bulks, and thus may be described by an additional potential energy

$$U_i = \gamma A, \tag{8.10}$$

Surface tension

where A is the interface area, and γ is called the *surface tension constant* – or just the "surface tension". For a stable interface of any two fluids, γ is always positive.[9] For surfaces of typical liquids (or their interfaces with air), at room temperature, the surface tension equals a few 10^{-2} J/m^2,[10] corresponding to

[6] A simple calculation, similar to the one resulting in Eq. (8), but for the total torque rather than the total force, shows that B is just the center of mass of the submerged volume V filled with any uniform material.

[7] It is easy (and hence is left for the reader) to prove that a small tilt of the body leads to a small lateral displacement of point B, but does not affect the position of the metacenter M.

[8] A simple example of such a problem is given by the fluid equilibrium in a container rotating with a constant angular velocity $\boldsymbol{\omega}$. If we solve such a problem in a reference frame rotating together with the container, the real bulk forces should be complemented by the centrifugal "force" (4.93), depending on $\mathbf{r}$.

[9] Indeed, if the γ of the interface of certain two fluids is negative, it self-reconfigures to decrease U_i, i.e. to increase $|U_i|$, by increasing the interface area, i.e. fragments the system into a macroscopically uniform solution.

[10] For a better feeling of this number, one should remember that 1 J/m^2 ≡ 1 N/m.

the potential energy U_i of a few 10^{-2} eV per surface molecule – i.e. just a fraction of the full *binding* (or "cohesive") *energy* of the same liquid, which is typically of the order of 10^{-1} eV per molecule.

In the absence of other forces, the surface tension makes a liquid drop spherical to minimize its surface area A at a fixed volume. For the analysis of the surface tension effects for more complex geometries, and in the presence of other forces, it is convenient to reduce them to a certain additional effective pressure drop $\Delta\mathcal{P}_{ef}$ at the interface. To calculate $\Delta\mathcal{P}_{ef}$, let us consider the condition of equilibrium of a small part dA of a smooth interface between two fluids (Fig. 2), in the absence of bulk forces.

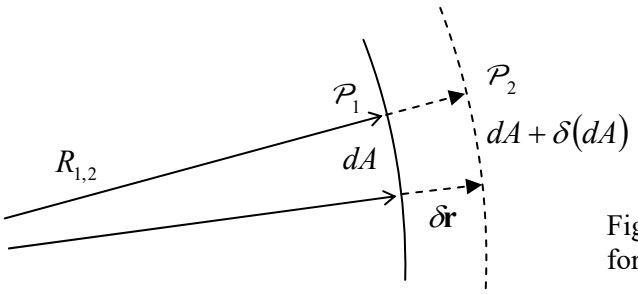

Fig. 8.4. Deriving the Young-Laplace formula (13).

If the pressures $\mathcal{P}_{1,2}$ on the two sides of the interface are different, the work of stress forces on fluid 1 at a small virtual displacement $\delta\mathbf{r} = \mathbf{n}\delta r$ of the interface (where $\mathbf{n} = d\mathbf{A}/dA$ is the unit vector normal to the interface) equals[11]

$$\delta\mathcal{W} = dA\delta r\left(\mathcal{P}_1 - \mathcal{P}_2\right). \tag{8.11}$$

For equilibrium, this work has to be compensated by an equal change of the interface energy, $\delta U_i = \gamma\delta(dA)$. Differential geometry tells us that in the linear approximation in δr, the relative change of the elementary surface area, corresponding to a fixed solid angle $d\Omega$, may be expressed as

$$\frac{\delta(dA)}{dA} = \frac{\delta r}{R_1} + \frac{\delta r}{R_2}, \tag{8.12}$$

where $R_{1,2}$ are the so-called *principal radii* of the interface curvature.[12] Combining Eqs. (10)-(12), we get the following *Young-Laplace formula*:[13]

Young-Laplace formula

$$\mathcal{P}_1 - \mathcal{P}_2 = \Delta\mathcal{P}_{ef} \equiv \gamma\left(\frac{1}{R_1} + \frac{1}{R_2}\right). \tag{8.13}$$

[11] This equality follows from the general relation (7.30), with the stress tensor elements expressed by Eq. (2), but in this simple case of the net stress force $d\mathbf{F} = (\mathcal{P}_1 - \mathcal{P}_2)d\mathbf{A}$ parallel to the interface element vector $d\mathbf{A}$, it may be even more simply obtained just from the definition of work: $\delta\mathcal{W} = d\mathbf{F}\cdot\delta\mathbf{r}$ at the virtual displacement $\delta\mathbf{r} = \mathbf{n}\delta r$.

[12] This general formula may be readily verified for a sphere of radius r (for which $R_1 = R_2 = r$ and $dA = r^2 d\Omega$, so $\delta(dA)/dA = \delta(r^2)/r^2 = 2\delta r/r$), and for a round cylindrical interface of radius R (for which $R_1 = r$, $R_2 = \infty$, and $dA = rd\varphi dz$, so $\delta(dA)/dA = \delta r/r$). For more on curvature, see, for example, M. do Camo, *Differential Geometry of Curves and Surfaces*, 2nd ed., Dover, 2016.

[13] This result (not to be confused with Eq. (15), called *Young's equation*) was derived in 1806 by Pierre-Simon Laplace (of the Laplace operator/equation fame) on the basis of the first analysis of the surface tension effects by Thomas Young (yes, the same Young who performed the famous two-slit experiment with light!) a year earlier.

In particular, this formula shows that the additional pressure created by surface tension inside a spherical drop of a liquid, of radius R, equals $2\gamma/R$, i.e. decreases with R. In contrast, according to Eqs. (5)-(6), the pressure effects of bulk forces, for example gravity, grow as $\rho g R$. The comparison of these two pressure components shows that if the drop radius (or more generally, the characteristic linear size of a liquid's sample) is much larger than the so-called *capillary length*

$$a_c \equiv \left(\frac{2\gamma}{\rho g}\right)^{1/2}, \tag{8.14}$$

Capillary length

the surface tension may be safely ignored – as will be done in all following sections of this chapter, besides a brief discussion at the end of Sec. 4. For the water surface, or more exactly its interface with air at ambient conditions, $\gamma \approx 0.073$ J/m^2, while $\rho \approx 1{,}000$ kg/m^3, so $a_c \approx 4$ mm.

On the other hand, in very narrow tubes, such as blood capillary vessels with radius $a \sim 1$ μm, i.e. $a << a_c$, the surface tension effects are very important. The key notion for the analysis of these effects is the *contact angle* θ_c (also called the "wetting angle") at an equilibrium edge of a liquid wetting a solid – see Fig. 5.

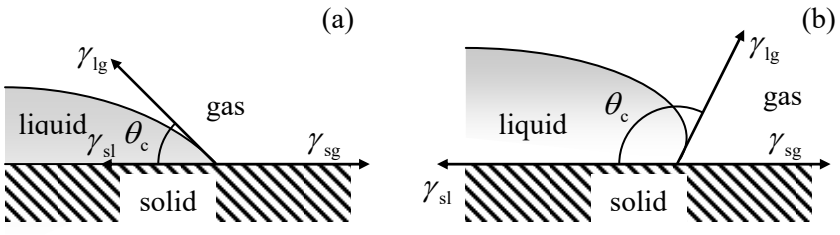

Fig. 8.5. Contact angles for (a) hydrophilic and (b) hydrophobic surfaces.

According to its definition (10), the constant γ may be interpreted as a force (per unit length of the interface boundary) directed normally to the boundary, and "trying" to reduce the interface area. As a result, the balance of horizontal components of the three such forces, shown in Fig. 5a, immediately yields the *Young's equation*

$$\gamma_{sl} + \gamma_{lg}\cos\theta_c = \gamma_{sg}, \tag{8.15}$$

Young's equation

where the indices of the three constants γ correspond to three possible interfaces between the liquid, solid, and gas. For the so-called *hydrophilic* surfaces that "like to be wet" by a particular liquid (not necessarily water), meaning that $\gamma_{sl} < \gamma_{sg}$, this relation yields $\cos\theta_c > 0$, i.e. $\theta_c < \pi/2$ – the situation shown in Fig. 5a. On the other hand, for *hydrophobic* surfaces with $\gamma_{sl} > \gamma_{sg}$, Eq. (15) yields larger contact angles, $\theta_c > \pi/2$ – see Fig. 5b.

Let us use this notion to solve the simplest and perhaps the most practically important problem of this field – find the height h of the fluid column lifted by the surface tension forces in a narrow vertical tube made of a hydrophilic material, assuming its internal surface to be a round cylinder of radius a – see Fig. 6. Inside an incompressible fluid, pressure drops with height according to the Pascal equation (6), so just below the surface, $\mathcal{P} \approx \mathcal{P}_0 - \rho g h$, where $\mathcal{P}_0$ is the background (e.g., atmospheric) pressure. This means that at $a << h$, the pressure variation along the concave surface (called the *meniscus*) of the liquid is negligible, so according to the Young-Poisson equation (13), the sum $(1/R_1 + 1/R_2)$ has to be virtually constant along the surface. Due to the axial symmetry of the problem, this means that the surface has to be a part of a sphere. From the contact angle definition, the radius R of the

sphere is equal to $a/\cos\theta_c$ – see Fig. 6. Plugging this relation into Eq. (3) with $\mathcal{P}_1 - \mathcal{P}_2 = \rho g h$, we get the following result for h:

$$\rho g h = \frac{2\gamma \cos\theta_c}{a}. \tag{8.16a}$$

In hindsight, this result might be obtained more directly – by requiring the total weight $\rho g V = \rho g(\pi a^2 h)$ of the lifted liquid's column to be equal to the vertical component $F\cos\theta_c$ of the full surface tension force $F = \gamma p$, acting on the perimeter $p = 2\pi a$ of the meniscus. Using the definition (11) of the capillary length a_c, Eq. (16a) may be represented as the so-called *Jurin rule:*

Jurin rule

$$h = \frac{a_c^2}{a}\cos\theta_c \le \frac{a_c^2}{a}; \tag{8.16b}$$

according to our initial assumption $h >> a$, Eq. (16) is only valid for narrow tubes, with radius $a << a_c$.

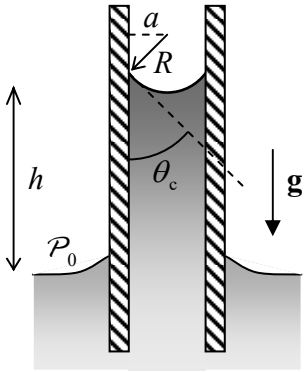

Fig. 8.6. Liquid's rise in a vertical capillary tube.

This capillary rise is the basic mechanism of lifting water with nutrients from roots to the branches and leaves of plants, so the tallest tree heights correspond to the Jurin rule (16), with $\cos\theta_c \approx 1$, and the pore radius a limited from below by a few microns, because of the viscosity effects restricting the fluid discharge – see Sec. 5 below.

8.3. Kinematics

In contrast to the stress tensor, which is frequently very simple – see Eq. (2), the strain tensor is *not* a very useful notion in fluid mechanics. Indeed, besides a very few situations,[14] typical problems of this field involve fluid *flow*, i.e. a state when the velocity of fluid particles has some nonzero time average. This means that the trajectory of each particle is a long line, and the very notion of its displacement $\mathbf{q}$ from the initial position becomes impracticable. However, the particle's velocity $\mathbf{v} \equiv d\mathbf{q}/dt$ remains a very useful notion, especially if it is considered as a function of the *observation point* $\mathbf{r}$ and (generally) time t. In an important class of fluid dynamics problems, the so-called *stationary* (or "steady", or "static") *flow,* the velocity defined in this way does not depend on time, $\mathbf{v} = \mathbf{v}(\mathbf{r})$.

[14] One of them is sound propagation, where the particle displacements $\mathbf{q}$ are typically small, so the results of Sec. 7.7 are applicable. As a reminder, they show that in fluids, with $\mu = 0$, the transverse sound cannot propagate, while the longitudinal sound can – see Eq. (7.114).

There is, however, a price to pay for the convenience of this notion: namely, due to the difference between the vectors **q** and **r**, the particle's acceleration $\mathbf{a} = d^2\mathbf{q}/dt^2$ (that participates, in particular, in the 2nd Newton law) cannot be calculated just as the time derivative of the velocity $\mathbf{v}(\mathbf{r}, t)$. This fact is evident, for example, for the static flow case, in which the acceleration of individual fluid particles may be very significant even if $\mathbf{v}(\mathbf{r})$ does not depend on time – just think about the acceleration of a drop of water flowing over the Niagara Falls' rim, first accelerating fast and then virtually stopping below, while the water velocity **v** at every particular point, as measured from a bank-based reference frame, is nearly constant. Thus the primary task of fluid kinematics is to express **a** via **v**; let us do this.

Since each Cartesian component v_j of the velocity **v** has to be considered as a function of four *independent* scalar variables: three Cartesian components r_j of the vector **r** and time t, its full time derivative may be represented as

$$\frac{dv_j}{dt} = \frac{\partial v_j}{\partial t} + \sum_{j'=1}^{3} \frac{\partial v_j}{\partial r_{j'}} \frac{dr_{j'}}{dt}. \tag{8.17}$$

Let us apply this *general* relation to a *specific* set of infinitesimal changes $\{dr_1, dr_2, dr_3\}$ that follows a small displacement $d\mathbf{q}$ of a certain particle of the fluid: $d\mathbf{r} = d\mathbf{q} = \mathbf{v}dt$, i.e.

$$dr_j = v_j dt. \tag{8.18}$$

In this case, dv_j/dt is the j^{th} component a_j of the particle's acceleration **a**, so Eq. (17) yields the following key relation of fluid kinematics:

$$\boxed{a_j = \frac{\partial v_j}{\partial t} + \sum_{j'=1}^{3} v_{j'} \frac{\partial v_j}{\partial r_{j'}}.} \tag{8.19a}$$

Fluid particle's acceleration

Using the del operator ∇, this result may be rewritten in the following compact vector form:[15]

$$\boxed{\mathbf{a} = \frac{\partial \mathbf{v}}{\partial t} + (\mathbf{v}\cdot\nabla)\mathbf{v}.} \tag{8.19b}$$

This relation already signals the main technical problem of fluid dynamics: many equations involving the particle's acceleration are nonlinear in velocity, excluding such a powerful tool as the linear superposition principle (which was used so frequently in the previous chapters of this course) from the applicable mathematical arsenal.

One more basic relation of fluid kinematics is the so-called *continuity equation*, which is essentially just the differential version of the mass conservation law. Let us mark, inside a fluid flow, an arbitrary volume V limited by a stationary (time-independent) surface S. The total mass of the fluid inside the volume may change only due to its flow through the boundary:

$$\frac{dM}{dt} \equiv \frac{d}{dt}\int_V \rho\, d^3r = -\int_S \rho v_n d^2r \equiv -\int_S \rho\, \mathbf{v}\cdot d\mathbf{A}, \tag{8.20a}$$

[15] Note that the operator relation $d/dt = \partial/\partial t + (\mathbf{v}\cdot\nabla)$ is applicable to an arbitrary (scalar or vector) function; it is frequently called the *convective derivative*. (Alternative adjectives, such as "Lagrangian", "substantial", or "Stokes", are sometimes used for this derivative as well.) The relation has numerous applications well beyond the fluid dynamics – see, e.g., EM Chapter 9 and QM Chapter 1.

where the elementary area vector $d\mathbf{A}$ is defined just as in Sec. 7.2 – see Fig. 7.

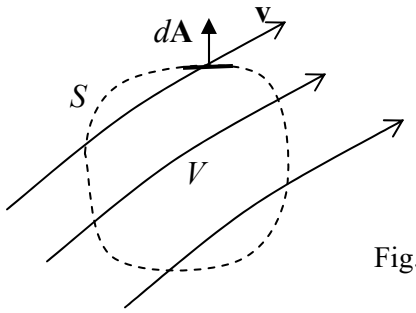

Fig. 8.7. Deriving the continuity equation.

Now using the same divergence theorem that has been used several times in this course,[16] the surface integral in Eq. (20a) may be transformed into the integral of $\nabla(\rho\mathbf{v})$ over the volume V, so the relation may be rewritten as

$$\int_V \left(\frac{\partial \rho}{\partial t} + \nabla \cdot \mathbf{j} \right) d^3 r = 0 , \tag{8.20b}$$

where the vector $\mathbf{j} \equiv \rho\mathbf{v}$ is called either the *mass flux density* (or the "mass current"). Since Eq. (20b) is valid for an arbitrary stationary volume V, the function under the integral has to vanish at any point:

Continuity equation

$$\boxed{\frac{\partial \rho}{\partial t} + \nabla \cdot \mathbf{j} = 0 .} \tag{8.21}$$

Note that similar continuity equations are valid not only for mass but also for other conserved physics quantities (e.g., the electric charge, probability, etc.), with the proper re-definitions of ρ and $\mathbf{j}$.[17]

8.4. Dynamics: Ideal fluids

Let us start our discussion of fluid dynamics from the simplest case when the stress tensor obeys Eq. (2) even in motion. Physically, this means that the fluid viscosity effects, leading to mechanical energy loss, are negligible. (The conditions of this assumption will be discussed in the next section.) Then the equation of motion of such an *ideal fluid* (essentially the 2nd Newton law for its unit volume) may be obtained from Eq. (7.25) using the simplifications of its right-hand side, discussed in Sec. 1:

$$\rho\mathbf{a} = -\nabla\mathcal{P} + \mathbf{f} . \tag{8.22}$$

Now using the basic kinematic relation (19), we arrive at the following *Euler equation*:[18]

Euler equation

$$\boxed{\rho \frac{\partial \mathbf{v}}{\partial t} + \rho(\mathbf{v} \cdot \nabla)\mathbf{v} = -\nabla\mathcal{P} + \mathbf{f} .} \tag{8.23}$$

Generally, this equation has to be solved together with the continuity equation (21) and the equation of state of the particular fluid, $\rho = \rho(\mathcal{P})$. However, as we have already discussed, in many

[16] If the reader still needs a reminder, see MA Eq. (12.1).
[17] See, e.g., EM Sec. 4.1, QM Sec. 1.4, and SM Sec. 5.6.
[18] It was derived in 1755 by the same Leonhard Euler whose name has already been (reverently) mentioned several times in this course.

situations, the compressibility of water and other important liquids is very low and may be ignored, so ρ may be treated as a given constant. Moreover, in many cases, the bulk forces $\mathbf{f}$ are conservative and may be represented as a gradient of a certain potential function $u(\mathbf{r})$ – the potential energy per unit volume:

$$\mathbf{f} = -\nabla u\,; \tag{8.24}$$

for example, for a uniform, vertical gravity field, $u(\mathbf{r}) = \rho g y$, where y is measured from some (arbitrary) horizontal level. In this case, the right-hand side of Eq. (23) becomes $-\nabla(\mathcal{P} + u)$. For these cases, it is beneficial to recast the left-hand of that equation as well, using the following well-known identity of vector algebra[19]

$$(\mathbf{v}\cdot\nabla)\mathbf{v} = \nabla\left(\frac{v^2}{2}\right) - \mathbf{v}\times(\nabla\times\mathbf{v}). \tag{8.25}$$

As a result, the Euler equation takes the following form:

$$\rho\frac{\partial\mathbf{v}}{\partial t} - \rho\mathbf{v}\times(\nabla\times\mathbf{v}) + \nabla\left(\mathcal{P} + u + \rho\frac{v^2}{2}\right) = 0. \tag{8.26}$$

In a stationary flow, the first term of this equation vanishes. If the second term, describing fluid's *vorticity*, is zero as well, then Eq. (26) has the first integral of motion,

$$\boxed{\mathcal{P} + u + \frac{\rho}{2}v^2 = \text{const}\,,} \tag{8.27}$$

Bernoulli equation

called the *Bernoulli equation*.[20] Numerous examples of the application of Eq. (27) to simple problems of stationary flow in pipes, both with and without the Earth gravity field, should be well known to the readers from their undergraduate courses, so I hope I can skip their discussion without much harm.

In the general case, an ideal fluid may have vorticity, so Eq. (27) is not always valid. Moreover, due to the absence of viscosity in an ideal fluid, the vorticity, once created, does not decrease along the so-called *streamline* – the fluid particle's trajectory, to which the velocity is tangential at every point.[21] Mathematically, this fact[22] is expressed by the following *Kelvin theorem*: $(\nabla\times\mathbf{v})\cdot d\mathbf{A}$ = const along any small contiguous group of streamlines crossing an elementary area dA.[23]

However, in many important cases, the vorticity is negligible. For example, even if the vorticity exists in some part of the fluid volume (say, induced by local turbulence, see Sec. 6 below), it may decay due to the fluid's viscosity, to be discussed in Sec. 5, well before it reaches the region of our interest. (If this viscosity is sufficiently small, its effects on the fluid's flow in the region of interest are

[19] It readily follows, for example, from MA Eq. (11.6) with $\mathbf{g} = \mathbf{f} = \mathbf{v}$.

[20] Named after Daniel Bernoulli (1700-1782), not to be confused with Jacob Bernoulli or one of several Johanns of the same famous Bernoulli family, which gave the world so many famous mathematicians and scientists.

[21] Perhaps the most spectacular manifestation of the vorticity conservation is the famous *toroidal vortex rings* (see, e.g., a nice photo and a movie at https://en.wikipedia.org/wiki/Vortex_ring), predicted in 1858 by H. von Helmholtz, and then demonstrated by P. Tait in a series of spectacular experiments with smoke in the air. The persistence of such a ring, once created, is only limited by the fluid's viscosity – see the next section.

[22] This theorem was first formulated (verbally) by Hermann von Helmholtz.

[23] Its proof may be found, e.g., in Sec. 8 of L. Landau and E. Lifshitz, *Fluid Mechanics*, 2nd ed., Butterworth-Heinemann, 1987.

negligible, i.e. the ideal-fluid approximation is still acceptable.) Another important case is when a solid body of an arbitrary shape is embedded into an ideal fluid whose flow is uniform (meaning, by definition, that $\mathbf{v}(\mathbf{r},t) = \mathbf{v}_0 = \text{const}$) at large distances,[24] its vorticity is zero everywhere. Indeed, since $\nabla\times\mathbf{v} = 0$ at the uniform flow, the vorticity is zero at distant points of any streamline, and according to the Kelvin theorem, should equal zero everywhere.

In such cases, the velocity distribution, as any curl-free vector field, may be represented as a gradient of some effective potential function,

$$\mathbf{v} = -\nabla\phi. \tag{8.28}$$

Such *potential flow* may be described by a simple differential equation. Indeed, the continuity equation (21) for a steady flow of an incompressible fluid is reduced to $\nabla\cdot\mathbf{v} = 0$. Plugging Eq. (28) into this relation, we get the scalar Laplace equation,

$$\nabla^2\phi = 0, \tag{8.29}$$

which should be solved with appropriate boundary conditions. For example, the fluid flow may be limited by solid bodies, inside which the fluid cannot penetrate. Then the fluid velocity $\mathbf{v}$ at the solid body boundaries should not have a normal component; according to Eq. (28), this means

$$\frac{\partial\phi}{\partial n}\Big|_{\text{surfaces}} = 0. \tag{8.30}$$

On the other hand, if at large distances the fluid flow is known, e.g., uniform, then:

$$\nabla\phi = -\mathbf{v}_0 = \text{const}, \quad \text{at } r \to \infty. \tag{8.31}$$

As the reader may already know (for example, from a course on electrodynamics[25]), the Laplace equation (29) is analytically solvable in several simple (symmetric) but important situations. Let us consider, for example, the case of a round cylinder, with radius R, immersed into a flow with the initial velocity $\mathbf{v}_0$ perpendicular to the cylinder's axis (Fig. 8). For this problem, it is natural to use the cylindrical coordinates, with the z-axis coinciding with the cylinder's axis. In this case, the velocity distribution is obviously independent of z, so we may simplify the general expression of the Laplace operator in cylindrical coordinates[26] by taking $\partial/\partial z = 0$. As a result, Eq. (29) is reduced to[27]

$$\frac{1}{\rho}\frac{\partial}{\partial\rho}\left(\rho\frac{\partial\phi}{\partial\rho}\right) + \frac{1}{\rho^2}\frac{\partial^2\phi}{\partial\theta^2} = 0, \quad \text{at } \rho \ge R. \tag{8.32}$$

The general solution of this equation may be obtained using the variable separation method, similar to that used in Sec. 6.5 – see Eq. (6.67). The result is[28]

[24] This case is very important, because the motion of a solid body, with a constant velocity $\mathbf{u}$, in the otherwise stationary fluid, gives exactly the same problem (with $\mathbf{v}_0 = -\mathbf{u}$), in a reference frame bound to the body.

[25] See, e.g., EM Secs. 2.3-2.8.

[26] See, e.g., MA Eq. (10.3).

[27] Let me hope that the letter ρ, used here to denote the magnitude of the 2D radius vector $\boldsymbol{\rho} = \{x, y\}$, will not be confused with the fluid's density ρ – which does not participate in this boundary problem.

[28] See, e.g., EM Eq. (2.112). Note that the most general solution of Eq. (32) also includes a term proportional to φ, but in our geometry, this term should be zero for such a single-valued function as the velocity potential.

$$\phi = a_0 + b_0 \ln\rho + \sum_{n=1}^{\infty} \left(c_n \cos n\varphi + s_n \sin n\varphi\right)\left(a_n \rho^n + b_n \rho^{-n}\right), \tag{8.33}$$

where the coefficients a_n and b_n have to be found from the boundary conditions (30) and (31). Choosing the x-axis to be parallel to the vector $\mathbf{v}_0$ (Fig. 8a), so $x = \rho\cos\varphi$, we may spell out these conditions in the following form:

$$\frac{\partial\phi}{\partial\rho} = 0, \quad \text{at } \rho = R, \tag{8.34}$$

$$\phi \to -v_0 \rho\cos\varphi + \phi_0, \quad \text{at } \rho >> R, \tag{8.35}$$

where ϕ_0 is an arbitrary constant, which does not affect the velocity distribution and may be taken for zero. The condition (35) is incompatible with any term of the sum (33) except the term with $n = 1$ (with $s_1 = 0$ and $c_1 a_1 = -v_0$), so Eq. (33) is reduced to

$$\phi = \left(-v_0\rho + \frac{c_1 b_1}{\rho}\right)\cos\varphi. \tag{8.36}$$

Now, plugging this solution into Eq. (34), we get $c_1 b_1 = -v_0 R^2$, so, finally,

$$\phi = -v_0\left(\rho + \frac{R^2}{\rho}\right)\cos\varphi. \tag{8.37a}$$

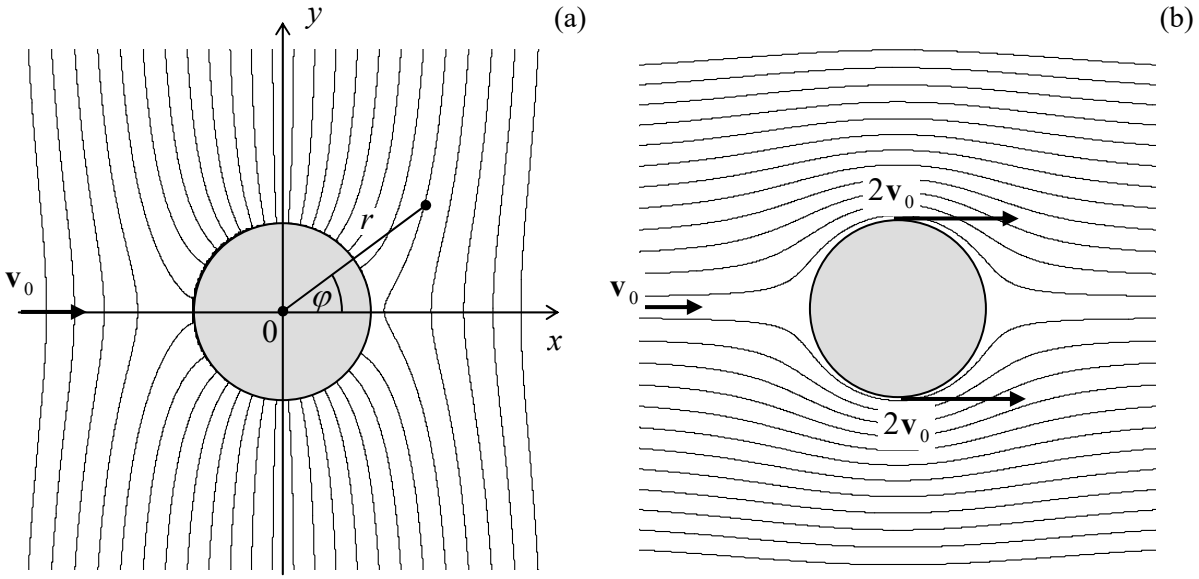

Fig. 8.8. The flow of an ideal, incompressible fluid around a cylinder: (a) equipotential surfaces and (b) streamlines.

Figure 8a shows the surfaces of constant velocity potential ϕ given by Eq. (37a). To find the fluid velocity, it is easier to rewrite that result in the Cartesian coordinates $x = \rho\cos\varphi$, $y = \rho\sin\varphi$:

$$\phi = -v_0 x\left(1 + \frac{R^2}{\rho^2}\right) = -v_0 x\left(1 + \frac{R^2}{x^2 + y^2}\right). \tag{8.37b}$$

From here, we may readily calculate the Cartesian components of the fluid's velocity: [29]

$$v_x = -\frac{\partial \phi}{\partial x} = v_0\left[1 + R^2\frac{y^2 - x^2}{\left(x^2 + y^2\right)^2}\right] \equiv v_0\left(1 + \frac{R^2}{\rho^2}\cos 2\varphi\right),$$
$$v_y = -\frac{\partial \phi}{\partial y} = -v_0 R^2\frac{2xy}{\left(x^2 + y^2\right)^2} \equiv -v_0\frac{R^2}{\rho^2}\sin 2\varphi. \qquad (8.38)$$

These expressions show that the maximum fluid's speed is achieved at the transverse diameter's ends ($\rho = R$, $\varphi = \pm \pi/2$), where $v = 2v_0$, while at the longitudinal diameter's ends ($\rho = R$, $\varphi = 0, \pm\pi$), the velocity vanishes – the so-called *stagnation points*.

Now the pressure distribution may be calculated by plugging Eqs. (38) into the Bernoulli equation (27) with $u(\mathbf{r}) = 0$. The result shows that the pressure reaches its maximum at the stagnation points, while at the ends of the transverse diameter $x = 0$, where the velocity is largest, it is lower by $2\rho v_0^2$. Note that the distributions of both the velocity and the pressure are symmetric with respect to the transverse axis $x = 0$, so the fluid flow does not create any net drag force in its direction. It may be shown that this result, which stems from the conservation of the mechanical energy of an ideal fluid, remains valid for a solid body of arbitrary shape moving inside an infinite volume of an ideal fluid – the so-called *D'Alembert paradox*. However, if a body moves near an ideal fluid's surface, its energy may be transformed into that of the surface waves, and the drag becomes possible.

Speaking about the *surface waves*: the description of such waves in a gravity field[30] is one more classical problem of the ideal fluid dynamics.[31] Let us consider an open surface of an ideal liquid of density ρ in a uniform gravity field $\mathbf{f} = \rho\mathbf{g} = -\rho g\mathbf{n}_y$ – see Fig. 9.

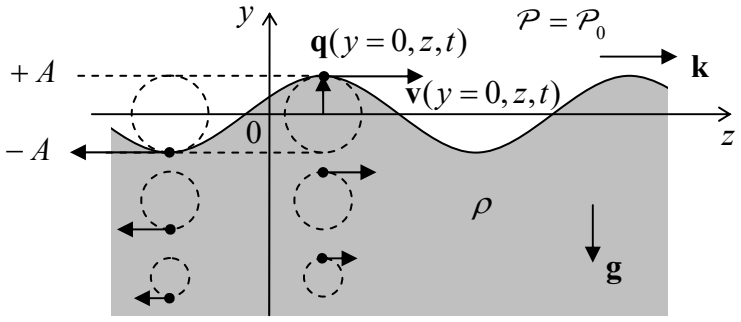

Fig. 8.9. Small surface wave on a deep heavy liquid. Dashed lines show particle trajectories. (For clarity, the displacement amplitude A is strongly exaggerated.)

If the wave amplitude A is sufficiently small, we may neglect the nonlinear term $(\mathbf{v}\cdot\nabla)\mathbf{v} \propto A^2$ in the Euler equation (23) in comparison with the first term, $\partial\mathbf{v}/\partial t$, which is linear in A. For a wave with

[29] Figure 8b shows the flow streamlines. They may be found by the integration of the obvious equation $dy/dx = v_y(x, y)/v_x(x, y)$. For our simple problem, this may be done analytically, giving $y(1 - R^2/\rho^2) = \text{const}$, where the constant is specific for each streamline.

[30] The alternative, historical term "gravity waves" for this phenomenon may nowadays lead to confusion with the relativistic effect of gravity waves – which may propagate in free space.

[31] It was solved by Sir George Biddell Airy (1801-19892), of the Airy functions' fame. (He was also a prominent astronomer and, in particular, established Greenwich as the prime meridian.)

frequency ω and wave number k, the particle's velocity $\mathbf{v} = d\mathbf{q}/dt$ is of the order of ωA, so this approximation is legitimate if $\omega^2 A >> k(\omega A)^2$, i.e. when

$$kA << 1, \tag{8.39}$$

i.e. when the wave's amplitude A is much smaller than its wavelength $\lambda = 2\pi/k$. Due to this assumption, we may neglect the liquid vorticity effects, and (for an incompressible fluid) again use the Laplace equation (29) for the wave's analysis. Looking for its solution in the natural form of a sinusoidal wave, uniform in one of the horizontal directions (x),

$$\phi = \mathrm{Re}\left[\Phi(y)e^{i(kz-\omega t)}\right], \tag{8.40}$$

we get a very simple equation

$$\frac{d^2\Phi}{dy^2} - k^2\Phi = 0, \tag{8.41}$$

with an exponential solution (properly decaying at $y \to -\infty$), $\Phi = \Phi_A \exp\{ky\}$, so Eq. (40) becomes

$$\phi = \mathrm{Re}\left[\Phi_A e^{ky} e^{i(kz-\omega t)}\right] = \Phi_A e^{ky}\cos(kz-\omega t), \tag{8.42}$$

where the last form is valid if Φ_A is real – which may be always arranged by a proper selection of the origins of z and/or t. Note that the rate k of the wave's decay in the vertical direction is exactly equal to the wave number of its propagation in the horizontal direction – along the fluid's surface. Because of that, the trajectories of fluid particles are exactly circular – see Fig. 9. Indeed, using Eqs. (28) and (42) to calculate velocity components,

$$v_x = 0, \qquad v_y = -\frac{\partial\phi}{\partial y} = -k\Phi_A e^{ky}\cos(kz-\omega t), \qquad v_z = -\frac{\partial\phi}{\partial z} = k\Phi_A e^{ky}\sin(kz-\omega t), \tag{8.43}$$

we see that v_y and v_z, at the same height y, have equal real amplitudes, and are phase-shifted by $\pi/2$. This result becomes even more clear if we use the velocity definition $\mathbf{v} = d\mathbf{q}/dt$ to integrate Eqs. (43) over time to recover the particle displacement law $\mathbf{q}(t)$. Due to the strong inequality (39), the integration may be done at fixed y and z:

$$q_y = q_A e^{ky}\sin(kz-\omega t), \qquad q_z = q_A e^{ky}\cos(kz-\omega t), \qquad \text{with } q_A \equiv \frac{k}{\omega}\Phi_A. \tag{8.44}$$

Note that the phase of oscillations of v_z coincides with that of q_y. This means, in particular, that at the wave's "crest", particles are moving in the direction of the wave's propagation – see arrows in Fig. 9.

It is remarkable that all this picture follows from the Laplace equation alone! The "only" remaining feature to calculate is the dispersion law $\omega(k)$, and for that, we need to combine Eq. (42) with what remains, in our linear approximation, of the Euler equation (23). In this approximation, and with the bulk force potential $u = \rho g y$, the equation is reduced to

$$\nabla\left(-\rho\frac{\partial\phi}{\partial t} + \mathcal{P} + \rho g y\right) = 0. \tag{8.45}$$

This equality means that the function in the parentheses is constant in space; at the surface, and at negligible surface tension, it should be equal to the pressure $\mathcal{P}_0$ above the surface (say, the atmospheric pressure), which we assume to be constant. This means that on the surface, the contributions to $\mathcal{P}$ that come from the first and the third terms in Eq. (45) have to compensate for each other. Let us take the average surface position for $y = 0$; then the surface with waves is described by the relation $y(z, t) = q_y(y, z, t)$ – see Fig. 9. Due to the strong relation (39), we can use Eqs. (42) and (44) with $y = 0$, so the above compensation condition yields

$$-\rho\omega\Phi_A \sin(kz-\omega t)+\rho g\frac{k}{\omega}\Phi_A \sin(kz-\omega t)=0\,. \tag{8.46}$$

This condition is identically satisfied on the whole surface (and for any Φ_A) as soon as

Surface waves' dispersion

$$\boxed{\omega^2 = gk\,,} \tag{8.47}$$

This equality is the dispersion relation we were looking for. Looking at this very simple result (which includes just one constant, g), note, first of all, that it does not involve the fluid's density. This is not too surprising, because due to the weak equivalence principle, particle masses always drop out from the solutions of problems involving gravitational forces alone. Second, the dispersion law (47) is strongly nonlinear, and in particular, does not have an acoustic wave limit at all. This means that the surface wave propagation is strongly dispersive, with both the phase velocity $u_{\rm ph} \equiv \omega/k = g/\omega$ and the group velocity $u_{\rm gr} \equiv d\omega/dk = g/2\omega \equiv u_{\rm ph}/2$ diverging at $\omega \to 0$.[32]

This divergence is an artifact of our assumption of the infinitely deep liquid. A rather straightforward generalization of the above calculations to a layer of a finite thickness h, using the additional boundary condition $v_y|_{y=-h} = 0$, yields a more general dispersion relation:[33]

$$\omega^2 = gk\tanh kh\,. \tag{8.48}$$

It shows that relatively long waves, with $\lambda >> h$, i.e. with $kh << 1$, propagate without dispersion (i.e. have $\omega/k = \text{const} \equiv u$), with the following velocity:

$$u = (gh)^{1/2}\,. \tag{8.49}$$

For the Earth's oceans, this velocity is rather high, close to 250 m/s (!) for the average ocean depth $h \approx 5$ km. This result explains, in particular, the very fast propagation of tsunami waves.

In the opposite limit of very short waves (large k), Eq. (47) also does not give a good description of typical experimental data, due to surface tension effects – see Sec. 2 above. Using Eq. (13), it is easy (and hence also left for the reader's exercise) to show that their account leads (at $kh >> 1$) to the following modification of Eq. (47):

$$\omega^2 = gk + \frac{\gamma k^3}{\rho}\,. \tag{8.50}$$

[32] Here, unlike in Chapters 6 and 7, the wave velocity is denoted by the letter u to avoid any chance of confusion with the velocity $\mathbf{v}$ (43) of the liquid's particles.

[33] This calculation (left for the reader's exercise), shows also that at finite h, the particle trajectories are elliptical rather than circular, becoming more and more stretched in the wave propagation direction near the bottom of the layer.

According to this formula, the surface tension is important at wavelengths smaller than the capillary constant a_c given by Eq. (14). Much shorter waves, for that Eq. (50) yields $\omega \propto k^{3/2}$, are called the *capillary waves* – or just "ripples".

8.5. Dynamics: Viscous fluids

The viscosity of many fluids, at not overly high velocities, may be described surprisingly well by adding, to the static stress tensor (2), additional elements proportional to the velocity $\mathbf{v} \equiv d\mathbf{q}/dt$:

$$\sigma_{jj'} = -\mathcal{P}\delta_{jj'} + \tilde{\sigma}_{jj'}(\mathbf{v}) . \tag{8.51}$$

In view of our experience with Hooke's law (7.32) expressing a stress tensor proportional to particle displacements $\mathbf{q}$, we may expect a similar expression with the replacement $\mathbf{q} \to \mathbf{v} = d\mathbf{q}/dt$:

$$\tilde{\sigma}_{jj'} = 2\eta\left(e_{jj'} - \frac{1}{3}\delta_{jj'}\mathrm{Tr}(\mathrm{e})\right) + 3\zeta\left(\frac{1}{3}\delta_{jj'}\mathrm{Tr}(\mathrm{e})\right), \tag{8.52a}$$

where $e_{jj'}$ are the elements of the symmetrized strain derivative tensor:

$$e_{jj'} \equiv \frac{ds_{jj'}}{dt} = \frac{1}{2}\left(\frac{\partial v_j}{\partial r_{j'}} + \frac{\partial v_{j'}}{\partial r_j}\right). \tag{8.52b}$$

Experiment confirms that Eq. (52) gives a good description of the viscosity effects in a broad range of isotropic fluids. The coefficient η is called either the *shear viscosity,* or the *dynamic viscosity,* or just *viscosity*, while ζ is called the *second* (or *bulk*) viscosity.

In the most frequent case of virtually incompressible fluids, $\mathrm{Tr}(\mathrm{e}) = d[\mathrm{Tr}(\mathrm{s})]/dt = (dV/dt)/V = 0$, so the term proportional to ζ vanishes, and η is the only important viscosity parameter.[34] Table 1 shows the approximate values of the viscosity, together with the mass density ρ, for several representative fluids.

Table 8.1. Important parameters of several representative fluids (approximate values)

Fluid (all at 300 K, until indicated otherwise)	η (mPa·s)	ρ (kg/m^3)
Glasses	10^{21}–10^{24}	2,200–2,500
Earth magmas (at 800 to 1,400 K)	10^{4}–10^{14}	2,200–2,800
Machine oils (SAE 10W – 40 W)	65-320	900
Water	0.89	1,000
Mercury	1.53	13,530
Liquid helium 4 (at 4.2K, 10^5 Pa)	0.019	130
Air (at 10^5 Pa)	0.018	1.3

[34] Probably the most important effect we miss by neglecting ζ is the attenuation of the (longitudinal) acoustic waves, into which the second viscosity makes a major contribution – whose (rather straightforward) analysis is left for the reader's exercise.

One can see that η may vary in very broad limits; the extreme cases of fluids are glasses (which, somewhat counter-intuitively, are not stable solids even at room temperature, but rather may "flow", though extremely slowly, until they eventually crystallize) and liquid helium (whose viscosity is of the order of that of gases,[35] despite its much higher density).

Incorporating the additional elements of $\sigma_{jj'}$ to the equation (23) of fluid motion, absolutely similar to how it was done at the derivation of Eq. (7.107) of the elasticity theory, and with the account of Eq. (19), we arrive at the famous *Navier-Stokes equation*:[36]

Navier-Stokes equation

$$\rho\frac{\partial \mathbf{v}}{\partial t}+\rho(\mathbf{v}\cdot\nabla)\mathbf{v}=-\nabla\mathcal{P}+\mathbf{f}+\eta\nabla^2\mathbf{v}+\left(\zeta+\frac{\eta}{3}\right)\nabla(\nabla\cdot\mathbf{v}). \tag{8.53}$$

The apparent simplicity of this equation should not mask a big range of phenomena that are described by it (notably turbulence – see the next section), and the enormous complexity of some solutions even for some simple geometries. In most problems interesting for practice, the only option is to use numerical methods, but due to a large number of parameters (ρ, η, ζ, plus geometrical parameters of the involved bodies, plus the distribution of bulk forces **f,** plus boundary conditions), this way is strongly plagued by the *curse of dimensionality* that was discussed in the end of Sec. 5.8.

Let us see how the Navier-Stokes equation works, on several simple examples. As the simplest case, let us consider the so-called *Couette flow* of an incompressible fluid layer between two wide, horizontal plates (Fig. 10), caused by their mutual sliding with a constant relative velocity $\mathbf{v}_0$.

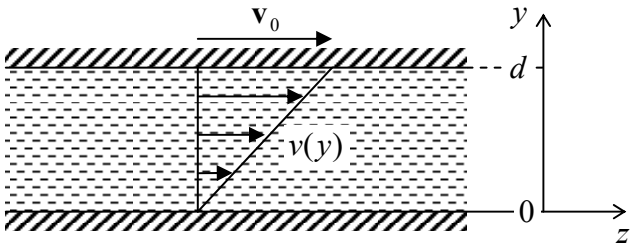

Fig. 8.10. The simplest problem of the viscous fluid flow.

Let us assume a *laminar* (vorticity-free) fluid flow. (As will be discussed in the next section, this assumption is only valid within certain limits.) Then we may use the evident symmetry of the problem, to take, in the coordinate frame shown in Fig. 10, $\mathbf{v} = \mathbf{n}_z v(y)$. Let the bulk forces be vertical, $\mathbf{f} = \mathbf{n}_y f$, so they do not give an additional drive to the fluid flow. Then for the stationary flow ($\partial\mathbf{v}/\partial t = 0$), the vertical, y-component of the Navier-Stokes equation is reduced to the static Pascal equation (6), showing that the pressure distribution is not affected by the plate (and fluid) motion. In the horizontal, z-component of the equation, only one term, $\nabla^2 v$, survives, so for the only Cartesian component of the fluid's velocity we get the 1D Laplace equation

$$\frac{d^2v}{dy^2}=0. \tag{8.54}$$

[35] Actually, at even lower temperatures (for He 4, at $T < T_\lambda \approx 2.17$ K), helium becomes a *superfluid*, i.e. loses its viscosity completely, as a result of the Bose-Einstein condensation – see, e.g., SM Sec. 3.4.

[36] Named after Claude-Louis Navier (1785-1836) who had suggested the equation, and Sir George Gabriel Stokes (1819-1903) who has demonstrated its relevance by solving the equation for several key situations.

In contrast to the ideal fluid (see, e.g., Fig. 8b), the relative velocity of a viscous fluid and a solid wall it flows by should approach zero at the wall,[37] so Eq. (54) should be solved with boundary conditions

$$v = \begin{cases} 0, & \text{at } y = 0, \\ v_0, & \text{at } y = d. \end{cases} \tag{8.55}$$

Using the evident solution to this boundary problem, $v(y) = (y/d)v_0$, illustrated by the arrows in Fig. 10, we can now calculate the horizontal *drag force* acting on a unit area of each plate. For the bottom plate,

$$\frac{F_z}{A_y} = \sigma_{zy}\Big|_{y=0} = \eta \frac{\partial v}{\partial y}\Big|_{y=0} = \eta \frac{v_0}{d}. \tag{8.56}$$

(For the top plate, the derivative $\partial v/\partial y$ has the same value, but the sign of dA_y has to be changed to reflect the direction of the outer normal to the solid surface, so we get a similar force but with the negative sign.) The well-known result (56) is often used, in undergraduate physics courses, for a definition of the dynamic viscosity η, and indeed shows its meaning very well.[38]

As the next, slightly less trivial example let us consider the so-called *Poiseuille problem*:[39] finding the relation between the constant external pressure gradient $\chi \equiv -\partial \mathcal{P}/\partial z$ applied along a round pipe with internal radius R (Fig. 11) and the so-called *discharge* Q – defined as the mass of fluid flowing through the pipe's cross-section in unit time.

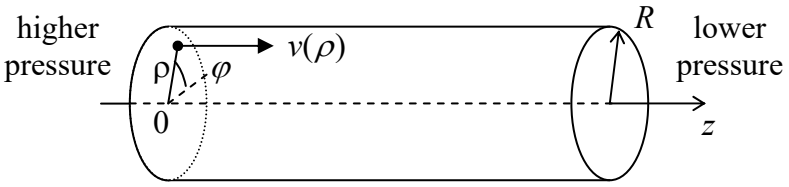

Fig. 8.11. The Poiseuille problem.

Again assuming a laminar flow, we can involve the problem's uniformity along the z-axis and its axial symmetry to infer that $\mathbf{v} = \mathbf{n}_z v(\rho)$, and $\mathcal{P} = -\chi z + f(\rho, \varphi) + \text{const}$ (where $\boldsymbol{\rho} = \{\rho, \varphi\}$ is again the 2D radius vector rather than the fluid density), so the Navier-Stokes equation (53) for an incompressible fluid (with $\nabla \cdot \mathbf{v} = 0$) is reduced to the following 2D Poisson equation:

$$\eta \nabla_2^2 v = -\chi\,. \tag{8.57}$$

After spelling out the 2D Laplace operator in polar coordinates for our axially-symmetric case $\partial/\partial\varphi = 0$, Eq. (57) becomes a simple ordinary differential equation,

[37] This is essentially an additional experimental fact, which that may be understood as follows. The tangential component of the velocity should be continuous at the interface between two viscous fluids, in order to avoid infinite stress – see Eq. (52), and solid may be considered as an ultimate case of fluid, with infinite viscosity.

[38] The very notion of viscosity η was introduced (by nobody other than the same Sir Isaac Newton) via a formula similar to Eq. (56), so any effect resulting in a drag force proportional to velocity is frequently called *Newtonian viscosity*.

[39] It was solved by G. Stokes in 1845 to explain the experimental results obtained by Gotthilf Hagen in 1839 and (independently) by Jean Poiseuille in 1840-41.

$$\eta \frac{1}{\rho}\frac{d}{d\rho}\left(\rho \frac{dv}{d\rho}\right) = -\chi, \tag{8.58}$$

which has to be solved on the segment $0 \le \rho \le R$, with the following boundary conditions:

$$\begin{aligned} v &= 0, \quad \text{at } \rho = R, \\ \frac{dv}{d\rho} &= 0, \quad \text{at } \rho = 0. \end{aligned} \tag{8.59}$$

(The latter condition is required by the axial symmetry.) A straightforward double integration yields:

$$v = \frac{\chi}{4\eta}\left(R^2 - \rho^2\right), \tag{8.60}$$

so the (easy) integration of the mass flow density over the cross-section of the pipe,

$$Q \equiv \int_A \rho v d^2 r = 2\pi\rho \frac{\chi}{4\eta}\int_0^R (R^2 - \rho^2)\rho d\rho, \tag{8.61}$$

immediately gives us the so-called *Poiseuille* (or "Hagen-Poiseuille") *law* for the fluid's discharge:

Poiseuille law

$$\boxed{Q = \frac{\pi}{8}\rho\frac{\chi}{\eta}R^4.} \tag{8.62}$$

The most prominent (and practically important) feature of this result is a very strong dependence of the discharge on the pipe's radius.

Of course, the 2D Poisson equation (57) is so readily solvable not for each cross-section shape. For example, consider a very simple, square-shaped cross-section with side a (Fig. 12).

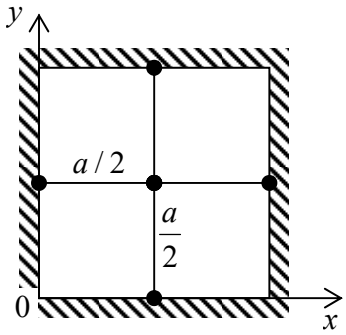

Fig. 8.12. Application of the finite-difference method with a very coarse mesh (with step $h = a/2$) to the problem of viscous fluid flow in a pipe with a square cross-section.

In this case, it is natural to use the Cartesian coordinates aligned with the cross-section's sides, so Eq. (57) becomes

$$\frac{\partial^2 v}{\partial x^2} + \frac{\partial^2 v}{\partial y^2} = -\frac{\chi}{\eta} = \text{const}, \quad \text{for } 0 \le x, y \le a, \tag{8.63}$$

and has to be solved with boundary conditions

$$v = 0, \quad \text{at } x, y = 0, a. \tag{8.64}$$

For this boundary problem, analytical methods such as the variable separation lead to answers in the form of infinite sums (series), which ultimately require computers anyway – at least for their plotting

and comprehension. Let me use this pretext to discuss how explicitly numerical methods may be used for such problems – or for any partial differential equations involving the Laplace operator. The simplest of them is the *finite-difference* method[40] in which the function to be calculated, $f(\mathbf{r})$, is represented by its values $f(\mathbf{r}_1)$, $f(\mathbf{r}_2)$, … in discrete points of a rectangular grid (frequently called *mesh*) of the corresponding dimensionality – Fig. 13.

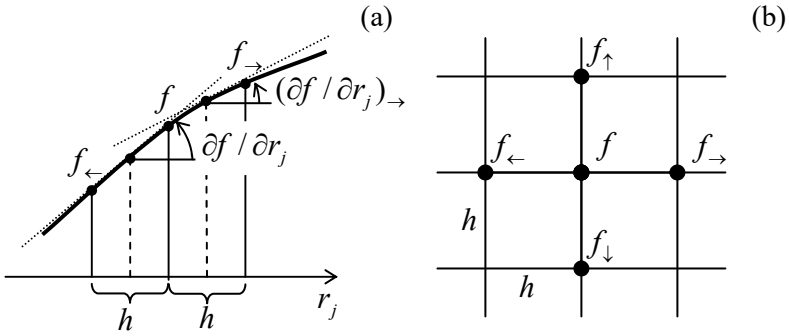

Fig. 8.13. The idea of the finite-difference method in (a) one and (b) two dimensions.

In Sec. 5.7, we have already discussed how to use such a grid to approximate the first derivative of the function – see Eq. (5.97). Its extension to the second derivative is straightforward – see Fig. 13a:[41]

$$\frac{\partial^2 f}{\partial r_j^2} \equiv \frac{\partial}{\partial r_j}\left(\frac{\partial f}{\partial r_j}\right) \approx \frac{1}{h}\left(\frac{\partial f}{\partial r_j}\Big|_\rightarrow - \frac{\partial f}{\partial r_j}\Big|_\leftarrow\right) \approx \frac{1}{h}\left[\frac{f_\rightarrow - f}{h} - \frac{f - f_\leftarrow}{h}\right] \equiv \frac{f_\rightarrow + f_\leftarrow - 2f}{h^2}. \qquad (8.65)$$

The relative error of this approximation is of the order of $h^2\partial^4 f/\partial r_j^4$, quite acceptable in many cases. As a result, the left-hand side of Eq. (63), treated on a square mesh with step h (Fig. 13b), may be approximated with the so-called *five-point scheme*:

$$\frac{\partial^2 v}{\partial x^2} + \frac{\partial^2 v}{\partial y^2} \approx \frac{v_\rightarrow + v_\leftarrow - 2v}{h^2} + \frac{v_\uparrow + v_\downarrow - 2v}{h^2} = \frac{v_\rightarrow + v_\leftarrow + v_\uparrow + v_\downarrow - 4v}{h^2}. \qquad (8.66)$$

(The generalization to the *seven-point scheme*, appropriate for 3D problems, is straightforward.) Let us apply this scheme to the tube with the square cross-section, using an extremely coarse mesh with step $h = a/2$, shown in Fig. 12. In this case, the fluid velocity v should equal zero at the walls, i.e. at all points of the five-point scheme except for the central point (in which the velocity obviously reaches its maximum), so Eqs. (63) and (66) yield[42]

$$\frac{0+0+0+0-4v_{\max}}{(a/2)^2} \approx -\frac{\chi}{\eta}, \qquad \text{i.e. } v_{\max} \approx \frac{1}{16}\frac{\chi a^2}{\eta} \qquad (8.67)$$

[40] For more details see, e.g., R. Leveque, *Finite Difference Methods for Ordinary and Partial Differential Equations*, SIAM, 2007.

[41] As a reminder, at the beginning of Sec. 6.4 we have already discussed the reciprocal transition – from a similar sum to the second derivative in the continuous limit ($h \to 0$).

[42] Note that the value (67) of $v_{\max}$ is exactly the same as given by the analytical formula (60) for the round cross-section with the radius $R = a/2$. This is not an occasional coincidence. The velocity distribution given by (60) is a quadratic function of both x and y. For such functions, with all derivatives higher than $\partial^2 f/\partial r_j^2$ equal to zero, equation (66) is exact rather than approximate.

This result for the maximal velocity is only ~20% different from the exact value. Using a slightly finer mesh with $h = a/4$, which gives a readily solvable system of three linear equations for three different velocity values (the exercise left for the reader), brings us within just a couple of percent from the exact result. So numerical methods may be practically more efficient than the "analytical" ones, even if the only available tool is a calculator app on your smartphone rather than an advanced computer.

Of course, many practical problems of fluid dynamics do require high-performance computing, especially in conditions of turbulence with its complex, irregular spatial-temporal structure – see the next section). In such cases, the finite-difference approach discussed above may become unsatisfactory, because it implies the same accuracy of the derivative approximation through the whole area of interest. A more powerful (but also much more complex for implementation) approach is the *finite-element method* in which the discrete-point mesh is based on triangles with unequal sides and is (in most cases, automatically) generated from the system geometry, giving more mesh points at the location(s) of the higher gradients of the calculated function (Fig. 14), and hence a better calculation accuracy for the same total number of points. Unfortunately, I do not have time/space to go into the details of that method, so the interested reader is referred to the special literature on this subject.[43]

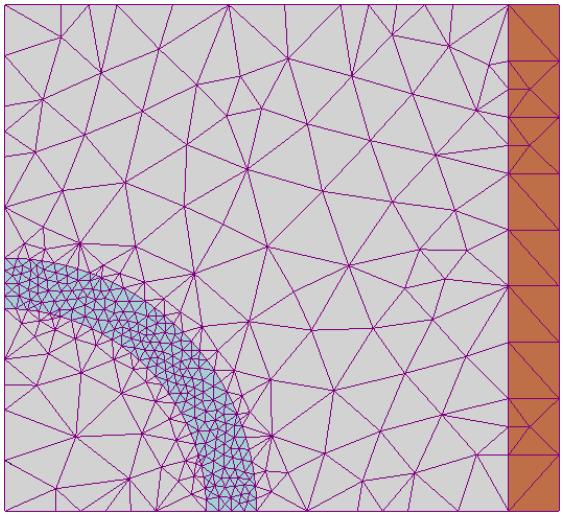

Fig. 8.14. A typical finite-element mesh generated automatically for a system with relatively complex geometry – a round cylindrical shell inside another one, with mutually perpendicular axes. (Adapted from the original by I. Zureks, https://commons.wikimedia.org/w/index.php?curid=2358783, under the CC license BY-SA 3.0.)

Before proceeding to our next topic, let me mention one more important problem that is analytically solvable using the Navier-Stokes equation: a slow motion of a solid sphere of radius R, with a constant velocity $\mathbf{v}_0$, through an incompressible viscous fluid – or equivalently, a slow flow of the fluid (uniform at large distances) around an immobile sphere. In the limit $\nu \to 0$, the second term on the left-hand side of Eq. (53) is negligible (just as at the surface wave analysis in Sec. 3), the equation takes the form

$$-\nabla \mathcal{P} + \eta \nabla^2 \mathbf{v} = 0, \qquad \text{for } R \le r < \infty, \tag{8.68}$$

and should be complemented with the incompressibility condition $\nabla \cdot \mathbf{v} = 0$ and the boundary conditions

[43] I can recommend, e.g., C. Johnson, *Numerical Solution of Partial Differential Equations by the Finite Element Method*, Dover, 2009, or T. Hughes, *The Finite Element Method*, Dover, 2000.

$$\begin{aligned} \mathbf{v} &= 0, \quad \text{at } r = R, \\ \mathbf{v} &\to \mathbf{v}_0, \text{ at } r \to \infty. \end{aligned} \tag{8.69}$$

In spherical coordinates, with the polar axis directed along the vector $\mathbf{v}_0$, this boundary problem has axial symmetry (so $\partial\mathbf{v}/\partial\varphi = 0$ and $v_\varphi = 0$), and allows the following analytical solution:

$$v_r = v_0 \cos\theta\left(1 - \frac{3R}{2r} + \frac{R^3}{2r^2}\right), \quad v_\theta = -v_0 \sin\theta\left(1 - \frac{3R}{4r} - \frac{R^3}{4r^2}\right), \quad \mathcal{P} = -\frac{3\eta v_0 R}{2r^2}\cos\theta\,. \tag{8.70}$$

Now calculating the tensor elements (52b) at $r = R$, using them to find the stress tensor elements from Eq. (52a), and integrating the elementary forces (7.18) over the surface of the sphere, it is straightforward to obtain the famous *Stokes formula* for the drag force acting on the sphere:[44]

$$F = 6\pi\eta R v_0. \tag{8.71}$$

Stokes formula

For water drops with a 1-micron diameter, usually taken for the border between *aerosols* and *droplets*, descending in the ambient-condition air under their own weight, it predicts an equilibrium velocity v of close to 0.1 meters per hour, with the further scaling $v \propto R^2$.[45] (Note, however, that at R below ~10 μm, corrections due to air molecule discreteness become noticeable.)

For what follows in the next section, it is convenient to recast this result into the following form:

$$C_d = \frac{24}{Re}, \tag{8.72}$$

where C_d is the *drag coefficient* defined as

$$C_d \equiv \frac{F}{\rho v_0^2 A/2}, \tag{8.73}$$

with $A \equiv \pi R^2$ being the sphere's cross-section "as seen by the incident fluid flow", and Re is the so-called *Reynolds number*.[46] In the general case, the number is defined as

$$Re \equiv \frac{\rho v l}{\eta}, \tag{8.74}$$

Reynolds number

where l is the linear-size scale of the problem, and v is its velocity scale. (In the particular case of Eq. (72) for the sphere, l is identified with the sphere's diameter $D = 2R$, and v with v_0). The physical sense of these two definitions will be discussed in the next section.

---

[44] This formula played an important role in the first precise (better than 1%) calculation of the fundamental electric charge e by R. Millikan and H. Fletcher from their famous oil drop experiments in 1909-1913.

[45] These numbers are of key importance not only for the recent heated discussions of contagious disease transmission, but also for many other fields including atmospheric physics. For example, for an average water droplet in clouds, with $R \sim 10$ μm, Eq. (71) (even with a due account of a slightly lower air viscosity at typical cloud heights) yields the descent velocity of the order of 10 m/hr, substantiating the correct answer to the popular high-school question, "Why clouds do not fall?" (The answer is: water droplets do descend, but so slowly that they has ample time to evaporate near the lower surface of the cloud, so the cloud as a whole may maintain its height.)

[46] This notion was introduced in 1851 by the same G. Stokes but eventually named after O. Reynolds who popularized it three decades later.

8.6. Turbulence

As Fig. 15 shows, the Stokes result (71)-(72) is only valid at $Re << 1$, while for larger values of the Reynolds number, i.e. at higher velocities v_0, the drag force is larger. This very fact is not quite surprising, because at the derivation of the Stokes' result, the nonlinear term $(\mathbf{v}\cdot\nabla)\mathbf{v}$ in the Navier-Stokes equation (53), which scales as v^2, was neglected in comparison with the linear terms, scaling as v. What is more surprising is that the function $C_d(Re)$ exhibits such a complicated behavior over many orders of the velocity's magnitude, giving a hint that the fluid flow at large Reynolds numbers should be also very complicated. Indeed, the reason for this complexity is a gradual development of very intricate, time-dependent fluid patterns, called *turbulence*, rich with vortices – for example, see Fig. 16. These vortices are especially pronounced in the region behind the moving body (the so-called *wake*), while the region before the body remains almost unperturbed. As Fig. 15 indicates, the turbulence exhibits rather different behaviors at various velocities (i.e. values of *Re*), and sometimes changes rather abruptly – see, for example, the significant drag's drop at $Re \approx 5\times10^5$.

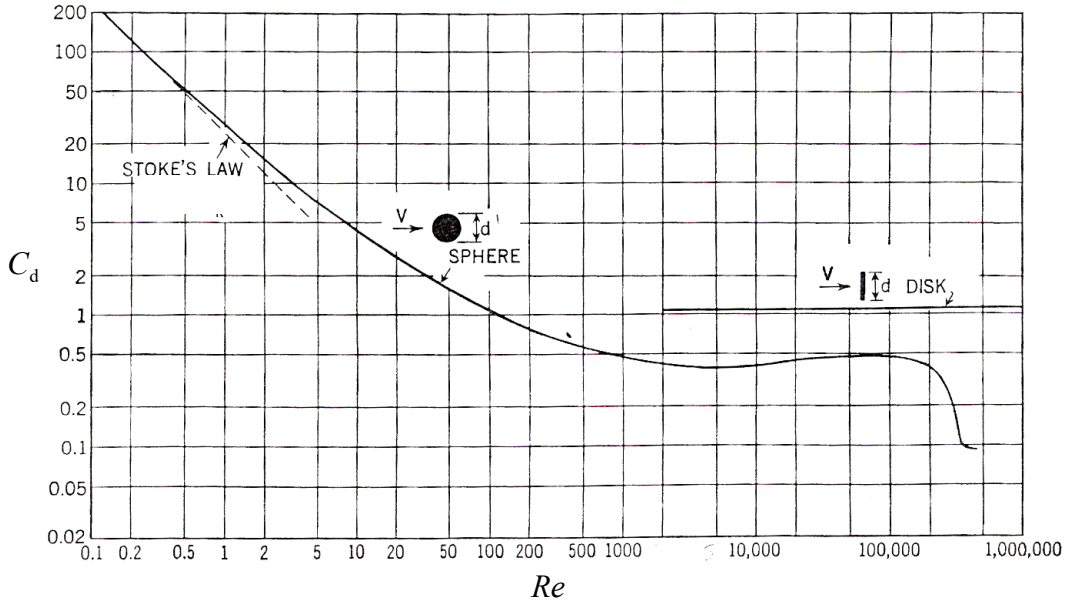

Fig. 8.15. The drag coefficient for a sphere and a thin round disk as functions of the Reynolds number. Adapted from F. Eisner, *Das Widerstandsproblem*, Proc. 3rd Int. Cong. on Appl. Mech., Stockholm, 1931.

In order to understand the conditions of this phenomenon, let us estimate the scale of various terms of the Navier-Stokes equation (53) for a generic body with characteristic size l, moving in an otherwise static incompressible fluid, with velocity v. In this case, the time scale of possible non-stationary phenomena is given by the ratio l/v,[47] so we arrive at the following estimates:

[47] The time scale of phenomena in externally-driven systems may be different; for example, for forced oscillations with frequency ω, it may be the oscillation period $\mathcal{T} \equiv 2\pi/\omega$. For such problems, the ratio $S \equiv (l/v)/\mathcal{T}$, commonly called either the *Strouhal number* or the *reduced frequency*, serves as another dimensionless constant.

$$\begin{array}{lcccc} \text{Equation term:} & \rho\dfrac{\partial \mathbf{v}}{\partial t} & \rho(\mathbf{v}\cdot\nabla)\mathbf{v} & \mathbf{f} & \eta\nabla^2\mathbf{v} \\ \text{Order of magnitude:} & \rho\dfrac{v^2}{l} & \rho\dfrac{v^2}{l} & \rho g & \eta\dfrac{v}{l^2} \end{array} \tag{8.75}$$

(I have skipped the term $\nabla\mathcal{P}$ because as we have seen in the previous section, in typical fluid flow problems, it balances the viscosity term, and hence is of the same order of magnitude.)

Fig. 8.16. A snapshot of the turbulent tail (*wake*) behind a sphere moving in a fluid with a high Reynolds number, showing the so-called *von Kármán vortex street*. Adapted from the original (actually, a very nice animation, http://www.mcef.ep.usp.br/staff/jmeneg/cesareo/vort2.gif) by Cesareo de La Rosa Siqueira, as a copyright-free material, available at https://commons.wikimedia.org/w/index.php?curid=87351.

Estimates (75) show that the relative importance of the terms may be characterized by two dimensionless ratios.[48] The first of them is the so-called *Froude number*[49]

$$F \equiv \frac{\rho v^2/l}{\rho g} \equiv \frac{v^2}{lg}, \tag{8.76}$$

which characterizes the relative importance of the gravity – or, upon appropriate modification, of other bulk forces. In most practical problems (with the important exception of surface waves, see Sec. 4 above), $F >> 1$ so the gravity effects may be neglected.

Much more important is another ratio, the Reynolds number (74), which may be rewritten as

$$Re \equiv \frac{\rho v l}{\eta} \equiv \frac{\rho v^2/l}{\eta v/l^2}, \tag{8.77}$$

and hence is a measure of the relative importance of the fluid particle's inertia in comparison with the viscosity effects.[50] So again, it is natural that for a sphere, the role of the vorticity-creating term $(\mathbf{v}\cdot\nabla)\mathbf{v}$

[48] For substantially compressible fluids (e.g., gases), the most important additional dimensionless parameter is the *Mach number* $M \equiv v/v_l$, where $v_l = (K/\rho)^{1/2}$ is the velocity of the longitudinal sound – which is, as we already know from Chapter 7, the only wave mode possible in an infinite fluid. Especially significant for practice are *supersonic effects* (including the shock wave in the form of the famous *Mach cone* with half-angle $\theta_M = \sin^{-1}M^{-1}$) that arise at $M > 1$. For a more thorough discussion of these issues, I have to refer the reader to more specialized texts – either Chapter IX of the Landau-Lifshitz volume cited above or Chapter 15 in I. Cohen and P. Kundu, *Fluid Mechanics*, 4th ed., Academic Press, 2007 – which is generally a good book on the subject.

[49] Named after William Froude (1810-1879), one of the applied hydrodynamics pioneers.

[50] Note that the "dynamic" viscosity η participates in this number (and many other problems of fluid dynamics) only in the combination η/ρ, which thereby has deserved a special name of *kinematic viscosity*.

becomes noticeable already at $Re \sim 1$ – see Fig. 15. What is very counter-intuitive is the onset of turbulence in systems where the laminar (turbulence-free) flow is formally an exact solution to the Navier-Stokes equation for any Re. For example, at $Re > Re_t \approx 2{,}100$ (with $l \equiv 2R$ and $v \equiv v_{max}$) the laminar flow in a round pipe, described by Eq. (60), becomes unstable, and the resulting turbulence decreases the fluid discharge Q in comparison with the Poiseuille law (62). Even more strikingly, the critical value of Re is rather insensitive to the pipe wall roughness and does not diverge even in the limit of perfectly smooth walls.

Since $Re >> 1$ in many real-life situations, turbulence is very important for practice. (Indeed, the values of η and ρ for water listed in Table 1 imply that even for a few-meter-sized object, such as a human body or a small boat, $Re > 1{,}000$ at any speed above just ~1 mm/s.) However, despite nearly a century of intensive research, there is no general, quantitative analytical theory of this phenomenon, and most results are still obtained either by rather approximate analytical treatments, or by the numerical solution of the Navier-Stokes equations using the approaches discussed in the previous section, or in experiments (e.g., on scaled models[51] in *wind tunnels*). A rare exception is the relatively recent theoretical result by S. Orszag (1971) for the turbulence threshold in a flow of an incompressible fluid through a gap of thickness t between two parallel plane walls (see Fig. 10): $Re_t \approx 5{,}772$ (for $l \equiv t/2$ and $v \equiv v_{max}$). However, even for this simplest geometry, the analytical theory still cannot predict the turbulence patterns at $Re > Re_t$. Only certain general, semi-quantitative features of turbulence may be understood from simple arguments.

For example, Fig. 15 shows that within a very broad range of Reynolds numbers, from $\sim 10^2$ to $\sim 3\times 10^5$, C_d of a thin round disk perpendicular to the incident flow, C_d is very close to 1.1 for any $Re > 10^3$, and that of a sphere is not too far away. The approximate equality $C_d \approx 1$, meaning that the drag force F is close to $\rho v_0^2 A/2$, may be understood (in the picture where the object is moved by an external force F with the velocity v_0 through a fluid that was initially at rest) as the equality of the force-delivered power Fv_0 and the fluid's kinetic energy $(\rho v_0^2/2)V$ created in volume $V = v_0 A$ in unit time. This relation would be exact if the object gave its velocity v_0 to each and every fluid particle its cross-section runs into, for example by dragging all such particles behind itself. In reality, much of this kinetic energy goes into vortices, where the particle velocity may differ from v_0, so the equality $C_d \approx 1$ is only approximate.

Another important general effect is that at very high values of Re, fluid flow at the leading surface of solid objects forms a thin, highly turbulent *boundary layer* that matches the zero relative velocity of the fluid at the surface with its substantial velocity in the outer region, which is almost free of turbulence and many cases, of other viscosity effects. This fact, clearly visible in Fig. 16, enables semi-quantitative analyses of several effects, for example, the so-called *Magnus lift force*[52] $\mathbf{F}_l$ exerted (on top of the usual drag force $\mathbf{F}_d$) on rotating objects, and directed across the fluid flow – see Fig. 17.

An even more important application of this concept is an approximate analysis of the forces exerted on non-rotating *airfoils* (such as aircraft wings) with special cross-sections forming sharp angles at their back ends. Such a shape minimizes the airfoil's contacts with the vortex street it creates in its

[51] The crucial condition of correct modeling is the equality of the Reynolds numbers (74) (and if relevant, also of the Froude numbers and/or the Mach numbers) of the object of interest and its model.

[52] Named after G. Magnus, who studied this effect in detail in 1852, though it had been described much earlier (in 1672) by I. Newton, and by B. Robins after him (in 1742).

wake, and allows the thin boundary layer to extend over virtually all of its surface, enhancing the lift force.

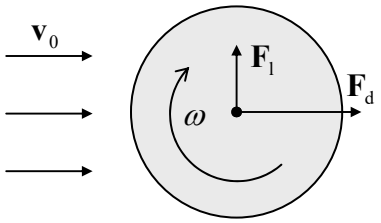

Fig. 8.17. The Magnus effect.

Unfortunately, due to the time/space restrictions, for a more detailed discussion of these results I have to refer the reader to more specialized literature,[53] and will conclude this chapter with a brief discussion of just one issue: can turbulence be explained by a single mechanism? (In other words, can it be reduced, at least on a semi-quantitative level, to a set of simpler phenomena that are commonly considered "well understood"?) Apparently, the answer is *no*,[54] though nonlinear dynamics of simpler systems may provide some useful insights.

In the middle of the last century, the most popular qualitative explanation of turbulence had been the formation of an "energy cascade" that would transfer the energy from the regular fluid flow to a hierarchy of vortices of various sizes.[55] With our background, it is easier to retell that story in the time-domain language (with the velocity v serving as the conversion factor), using the fact that in a rotating vortex, each Cartesian component of a particle's radius vector oscillates in time, so to some extent the vortex plays the role of an oscillatory motion mode.

Let us consider the passage of a solid body between two, initially close, small parts of the fluid. The body pushes them apart, but after its passage, these partial volumes are free to return to their initial positions. However, the dominance of inertia effects at motion with $Re >> 1$ means that the volumes continue to oscillate for a while about those equilibrium positions. (Since elementary volumes of an incompressible fluid cannot merge, these oscillations take the form of rotating vortices – see Fig. 16 again.)

Now, from Sec. 5.8 we know that intensive oscillations in a system with the quadratic nonlinearity, in this case, provided by the convective term $(\mathbf{v}\cdot\nabla)\mathbf{v}$, are equivalent, for small perturbations, to the oscillation of the system's parameters at the corresponding frequency. On the other hand, as was briefly discussed in Sec. 6.7, in a system with two oscillatory degrees of freedom, a periodic parameter change with frequency ω_p may lead to the non-degenerate parametric excitation ("down-conversion") of oscillations with frequencies $\omega_{1,2}$ satisfying the relation $\omega_1 + \omega_2 = \omega_p$. Moreover, the spectrum of oscillations in such a system also has higher combinational frequencies such as $(\omega_p + \omega_1)$, thus pushing the oscillation energy up the frequency scale ("up-conversion"). In the presence of other oscillatory modes, these oscillations may in turn produce, via the same nonlinearity, even higher frequencies, etc. In a fluid, the spectrum of these "oscillatory modes" (actually, vortex

[53] See, e.g., P. Davidson, *Turbulence*, Oxford U. Press, 2004.

[54] The following famous quote is attributed to Werner Heisenberg on his deathbed: "When I meet God, I will ask him two questions: Why relativity? And why turbulence? I think he will have an answer for the first question." Though probably inaccurate, this story reflects rather well the frustration of the fundamental physics community, renowned for their reductionist mentality, with the enormous complexity of phenomena that obey simple (e.g., the Navier-Stokes) equations, i.e. from the reductionist point of view, do not describe any new physics.

[55] This picture was suggested in 1922 by Lewis F. Richardson.

structures) is essentially continuous, so the above arguments make very plausible a sequential transfer of the energy from the moving body to a broad range of oscillatory modes – whose frequency spectrum is limited from above by the energy dissipation due to the fluid's viscosity. When excited, these modes interact (in particular, mutually phase-lock) via the system's nonlinearity, creating the complex motion we call turbulence.

Though not having much quantitative predictive power, such handwaving explanations, which are essentially based on the excitation of a *large* number of effective degrees of freedom, had been dominating the turbulence reviews until the mid-1960s. At that point, the discovery (or rather re-discovery) of quasi-random motions in classical dynamic systems with just *a few* degrees of freedom altered the discussion substantially. Since this phenomenon, called *deterministic chaos*, extends well beyond the fluid dynamics, I will devote to it a separate (albeit short) next chapter, and in its end will briefly return to the discussion of turbulence.

8.7. Exercise problems

8.1. For a mirror-symmetric but otherwise arbitrary shape of a ship's hull, derive an explicit expression for the height of its metacenter M – see Fig. 3. Spell out this expression for a rectangular hull.

8.2. Neglecting surface tension, find the stationary shape of the open surface of an incompressible heavy fluid in a container rotated about its vertical axis with a constant angular velocity ω – see the figure on the right.

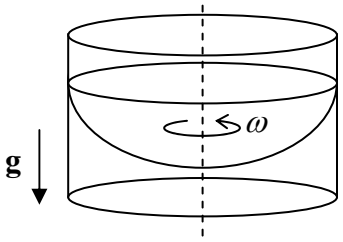

8.3. In the first order in the so-called *flattening* $f \equiv (R_e - R_p)/R_p << 1$ of the Earth (where R_e and R_p are, respectively, its equatorial and polar radii), calculate it within a simple model in that our planet is a uniformly-rotating nearly-spherical fluid ball, whose gravity field is dominated by a relatively small spherical core. Compare your result with the experimental value of f, and discuss the difference.

Hint: You may use experimental values $R_e \approx 6{,}378$ km, $R_p \approx 6{,}357$ km, and $g \approx 9.807$ m/s^2.

8.4.* Use two different approaches to calculate the stationary shape of the surface of an incompressible liquid of density ρ near a vertical plane wall, in a uniform gravity field – see the figure on the right. In particular, find the height h of the liquid's rise at the wall surface as a function of the contact angle θ_c.

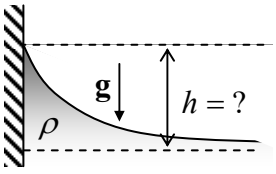

8.5.* A soap film with surface tension γ is stretched between two similar, coaxial, thin, round rings of radius R – see the figure on the right. Neglecting gravity, calculate the equilibrium shape of the film, and the external force needed for keeping the rings at distance d.

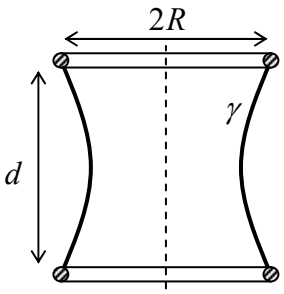

8.6. A solid sphere of radius R has been placed into a vorticity-free steady flow, with velocity v_0, of an ideal incompressible fluid. Find the spatial distribution of the fluid's velocity and pressure, and in particular their extreme values. Compare the results with those obtained in Sec. 4 for a round cylinder.

8.7.* Solve the same problem for a long and thin solid strip of width $2w$, with its plane normal to the unperturbed fluid flow.

Hint: You may like to use the so-called *elliptic coordinates* $\{\mu, \eta\}$ defined by their relations with the Cartesian coordinates $\{x, y\}$:

$$x = C\cosh\mu\cos\nu, \quad y = C\sinh\mu\sin\nu, \qquad \text{with } 0 \le \mu < \infty, \quad -\pi \le \nu < +\pi,$$

where C is a constant; in these coordinates,

$$\nabla^2 = \frac{1}{C^2(\cosh^2\mu - \cos^2\nu)}\left(\frac{\partial^2}{\partial\mu^2} + \frac{\partial^2}{\partial\nu^2}\right).$$

8.8. A small source, located at distance d from a plane wall of a container filled with an ideal incompressible fluid of density ρ, injects additional fluid isotropically, with a time-independent mass current ("discharge") $Q \equiv dM/dt$ – see the figure on the right. Calculate the fluid's velocity distribution and its pressure on the wall, created by the flow.

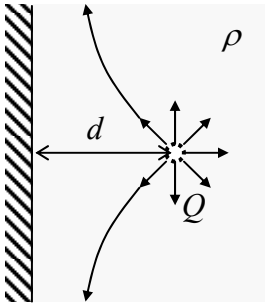

Hint: Recall the charge image method in electrostatics,[56] and contemplate its possible analog.

8.9. Calculate the average kinetic, potential, and full energies (per unit area) of a traveling sinusoidal wave, of a small amplitude q_A, on the surface of an ideal, incompressible, deep liquid of density ρ, in a uniform gravity field $\mathbf{g}$.

8.10. Calculate the average power carried by the surface wave discussed in the previous problem (per unit width of its front), and relate the result to the wave's energy.

8.11. Derive Eq. (48) for the surface waves on a finite-thickness layer of an incompressible ideal liquid.

8.12. The utmost simplicity of Eq. (49) for the velocity of waves on a relatively shallow ($h << \lambda$) layer of an ideal incompressible liquid implies that they may be described using a very simple physical picture. Develop such a picture, and verify that it yields the same expression for the velocity.

8.13. Extend the solution of the previous problem to calculate the energy and power of the shallow-layer waves, and use the result to explain the high tides on some ocean shores, for two models:

(i) the water depth h decreases gradually toward the shore, and

(ii) h decreases sharply, at some distance l from the shore – as it does on the ocean shelf border.

[56] See, e.g., EM Secs. 2.9, 3.3, and 4.3.

8.14.* Derive the differential equation describing 2D propagation of relatively long ($\lambda >> h$) surface waves in a plane layer of thickness h, of an ideal incompressible liquid. Use this equation to calculate the longest standing wave modes in a layer covering a spherical planet of radius $R >> h$, and their frequencies.

Hint: The second task requires some familiarity with the basic properties of spherical harmonics.[57]

8.15. Calculate the velocity distribution and the dispersion relation of the waves propagating along the horizontal interface of two ideal, incompressible liquids of different densities.

8.16. Derive Eq. (50) for the capillary waves ("ripples").

8.17. Use the finite-difference approximation for the Laplace operator, with the mesh step $h = a/4$, to find the maximum velocity and the total discharge Q of an incompressible viscous fluid's flow through a long tube with a square-shaped cross-section of side a. Compare the results with those described in Sec. 5 for the same problem with the mesh step $h = a/2$ and for a pipe with a circular cross-section of the same area.

8.18. A layer, of thickness h, of a heavy, viscous, incompressible liquid flows down a long and wide inclined plane, under its own weight – see the figure on the right. Calculate the liquid's stationary velocity distribution profile and its discharge per unit width.

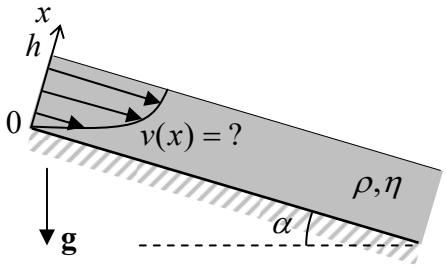

8.19. An external force moves two coaxial round disks of radius R, with an incompressible viscous fluid in the gap between them, toward each other with a constant velocity u. Calculate the applied force in the limit when the gap's thickness t is already much smaller than R.

8.20. Calculate the drag torque exerted on a unit length of a solid round cylinder of radius R that rotates about its axis with an angular velocity ω, inside an incompressible fluid with viscosity η, kept static far from the cylinder.

8.21. Solve a similar problem for a sphere of radius R, rotating about one of its principal axes.

Hint: You may like to use the following expression for the relevant element of the strain derivative tensor $e_{jj'}$ in spherical coordinates:

$$e_{r\varphi} = \frac{1}{2}\left(\frac{\partial v_\varphi}{\partial r} - \frac{v_\varphi}{r} \right).$$

8.22. Calculate the tangential force (per unit area) exerted by an incompressible fluid, with density ρ and viscosity η, on a broad solid plane placed over its surface and forced to oscillate along it with amplitude a and frequency ω.

[57] See, e.g., EM Sec. 2.8 and/or QM Sec. 3.6.

8.23. Calculate the frequency and the damping factor of longitudinal oscillations of a mercury column, of the total length l, in a U-shaped mercury manometer (see the figure on the right), assuming that its tube has a round cross-section with a relatively small radius R. Formulate the quantitative conditions of validity of your result and check whether they are fulfilled for the following parameters: $l = 1$ m and $R = 0.25$ mm.

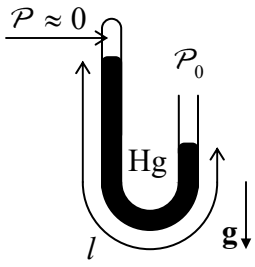

8.24. A barge, with a flat bottom of area A, floats in shallow water, with clearance $h << A^{1/2}$ – see the figure on the right. Analyze the time dependence of the barge's velocity $V(t)$, and the water's velocity profile, after the barge's engine has been turned off. Discuss the limits of large and small values of the dimensionless parameter $M/\rho Ah$.

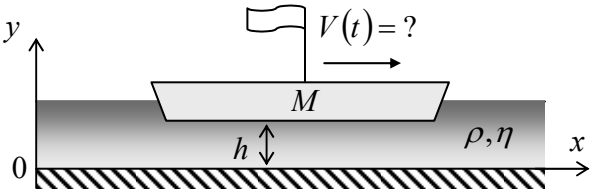

8.25.* Derive a general expression for mechanical energy loss rate in an incompressible fluid that obeys the Navier-Stokes equation, and use this expression to calculate the attenuation coefficient of the surface waves, assuming that the viscosity is small. (Quantify this condition).

8.26. Use the Navier-Stokes equation to calculate the coefficient of attenuation of a sinusoidal plane acoustic wave.

8.27.* Use two different approaches for a semi-quantitative calculation of the Magnus lift force $\mathbf{F}_l$ exerted by an incompressible fluid of density ρ on a round cylinder of radius R, with its axis normal to the fluid's velocity $\mathbf{v}_0$, which rotates about the axis with an angular velocity ω – see Fig. 17. Discuss the relation of the results.

Chapter 9. Deterministic Chaos

This chapter gives a very brief review of chaotic phenomena in deterministic maps and dynamic systems with and without dissipation, and an even shorter discussion of the possible role of chaos in fluid turbulence.

9.1. Chaos in maps

The possibility of quasi-random dynamics of deterministic systems with a few degrees of freedom (nowadays called *deterministic chaos* – or just "chaos") had been noticed before the 20th century,[1] but became broadly recognized only after the publication of a 1963 paper by theoretical meteorologist Edward Lorenz. In that work, he examined numerical solutions of the following system of three nonlinear, ordinary differential equations,

Lorenz system

$$\begin{aligned} \dot{q}_1 &= a_1(q_2 - q_1), \\ \dot{q}_2 &= a_2 q_1 - q_2 - q_1 q_3, \\ \dot{q}_3 &= q_1 q_2 - a_3 q_3, \end{aligned} \tag{9.1}$$

as a rudimentary model of heat transfer through a horizontal layer of fluid separating two solid plates. (Experiment shows that if the bottom plate is kept hotter than the top one, the fluid may exhibit turbulent convection.) He has found that within a certain range of the constants $a_{1,2,3}$, the solution to Eq. (1) follows complex, unpredictable, non-repeating trajectories in the 3D q-space. Moreover, the functions $q_j(t)$ (where j = 1, 2,3) are so sensitive to initial conditions $q_j(0)$ that at sufficiently large times t, solutions corresponding to slightly different initial conditions become completely different.

Very soon it was realized that such behavior is typical for even simpler mathematical objects called *maps*, so I will start my discussion of chaos from these objects. A 1D map is essentially a rule for finding the next number q_{n+1} of a discrete sequence numbered by the integer index n, in the simplest cases using only its last known value q_n. The most famous example is the so-called *logistic map*:[2]

Logistic map

$$q_{n+1} = f(q_n) \equiv r q_n (1 - q_n). \tag{9.2}$$

The basic properties of this map may be understood using its (hopefully, self-explanatory) graphical representation shown in Fig. 1.[3] One can readily see that at $r < 1$ (Fig. 1a) the logistic map sequence rapidly converges to the trivial fixed point $q^{(0)} = 0$ because each next value of q is less than the previous one. However, if r is increased above 1 (as in the example shown in Fig. 1b), the fixed point

[1] It may be traced back at least to an 1892 paper by the same Jules Henri Poincaré who was already reverently mentioned in Chapter 5. Citing it: "*...it may happen that small differences in the initial conditions produce very great ones in the final phenomena*. […] *Prediction becomes impossible*."

[2] Its chaotic properties were first discussed in 1976 by Robert May, though the map itself is one of the simple ecological models repeatedly discussed much earlier and may be traced back at least to the 1838 work by Pierre François Verhulst.

[3] Since the maximum value of the function $f(q)$, achieved at q = ½, equals r/4, the mapping may be limited to segment x = [0, 1], if the parameter r is between 0 and 4. Since all interesting properties of the map, including chaos, may be found within these limits, I will discuss only this range of r.

© K. Likharev

$q^{(0)}$ becomes unstable. Indeed, at $q_n << 1$, the map yields $q_{n+1} \approx rq_n$, so at $r > 1$, the values q_n grow with each iteration. Instead of the unstable point $q^{(0)} = 0$, in the range $1 < r < r_1$, where $r_1 \equiv 3$, the map has a stable fixed point $q^{(1)}$ that may be found by plugging this value into both parts of Eq. (2):

$$q^{(1)} = f\left(q^{(1)}\right) \equiv rq^{(1)}(1-q^{(1)}), \tag{9.3}$$

giving $q^{(1)} = 1 - 1/r$ – see the leftmost branch of the plot shown in Fig. 2.

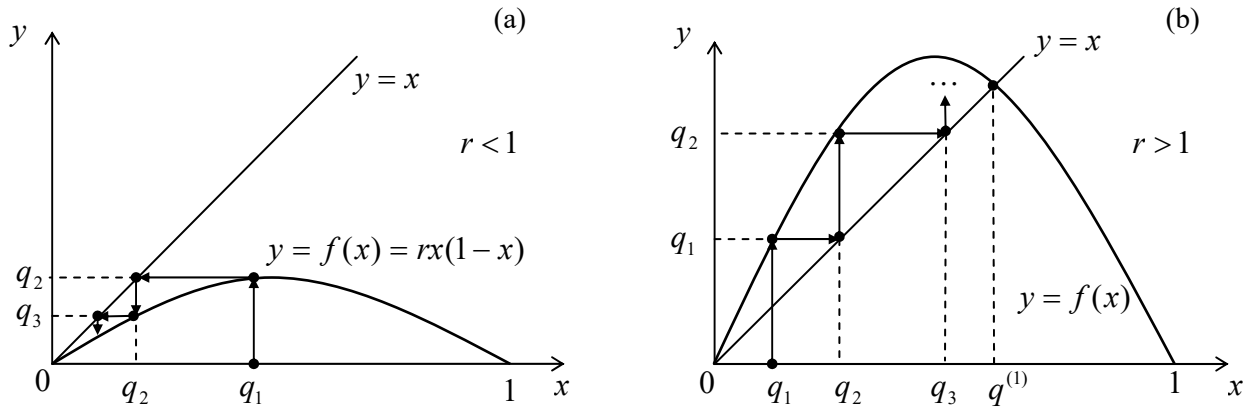

Fig. 9.1. Graphical analysis of the logistic map for: (a) $r < 1$ and (b) $r > 1$.

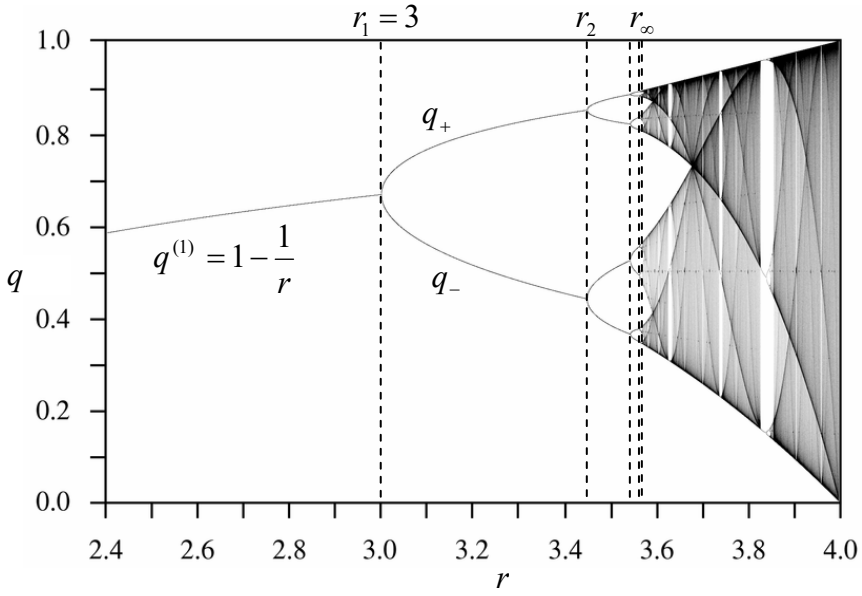

Fig. 9.2. The fixed points and chaotic regions of the logistic map. Adapted, under the CCO 1.0 Universal Public Domain Dedication, from the original by Jordan Pierce, available at http://en.wikipedia.org/wiki/Logistic_map. (A very nice live simulation of the map is also available on this website.)

However, at $r > r_1 = 3$, the fixed point $q^{(1)}$ also becomes unstable. To prove that, let us take $q_n \equiv q^{(1)} + \tilde{q}_n$, assume that the deviation $\tilde{q}_n$ from the fixed point $q^{(1)}$ is small, and linearize the map (2) in $\tilde{q}_n$ – just as we repeatedly did for differential equations earlier in this course. The result is

$$\tilde{q}_{n+1} = \left.\frac{df}{dq}\right|_{q=q^{(1)}} \tilde{q}_n = r(1-2q^{(1)})\tilde{q}_n \equiv (2-r)\tilde{q}_n . \tag{9.4}$$

It shows that at $0 < 2 - r < 1$, i.e. at $1 < r < 2$, the deviations $\tilde{q}_n$ decrease monotonically. At $-1 < 2 - r < 0$, i.e. in the range $2 < r < 3$, the deviations' sign alternates, but their magnitude still decreases – as in a stable focus, see Sec. 5.6. However, at $-1 < 2 - r$, i.e. $r > r_1 \equiv 3$, the deviations grow by magnitude, while still changing their sign, at each step. Since Eq. (2) has no other fixed points, this means that at $n \to \infty$, the values q_n do not converge to one point; rather, within the range $r_1 < r < r_2$, they approach a *limit cycle* of alternation of two points, q_+ and q_-, that satisfy the following system of algebraic equations:

$$q_+ = f(q_-), \qquad q_- = f(q_+). \tag{9.5}$$

These points are also plotted in Fig. 2, as functions of the parameter r. What has happened at the point $r_1 = 3$ is called the *period-doubling bifurcation*.

The story repeats at $r = r_2 \equiv 1 + \sqrt{6} \approx 3.45$, where the system goes from the 2-point limit cycle to a 4-point cycle, then at $r = r_3 \approx 3.54$, where the limit cycle begins to consist of 8 alternating points, etc. Most remarkably, the period-doubling bifurcation points r_n, at that the number of points in the limit cycle doubles from 2^{n-1} points to 2^n points, become closer and closer to each other. Numerical simulations show that at $n \to \infty$, these points obey the following asymptotic behavior:

Feigenbaum bifurcation sequence

$$r_n \to r_\infty - \frac{C}{\delta^n}, \quad \text{where } r_\infty = 3.5699..., \quad \delta = 4.6692... \tag{9.6}$$

The parameter δ is called the *Feigenbaum constant*; for other maps, and some dynamic systems (see the next section), period-doubling sequences follow a similar law, but with different values of δ.

More important for us, however, is what happens at $r > r_\infty$. Numerous numerical experiments, repeated with increasing precision,[4] have confirmed that here the system is disordered, with no reproducible limit cycle, though (as Fig. 2 shows) at $r \approx r_\infty$, all sequential values q_n are still confined to a few narrow regions.[5] However, as parameter r is increased well beyond r_∞, these regions broaden and merge. This is the so-called *deep chaos*, with no apparent order at all.[6]

The most important feature of the chaos (in this and any other system) is the *exponential divergence of trajectories*. For a 1D map, this means that even if the initial conditions q_1 in two map implementations differ by a very small amount Δq_1, the difference Δq_n between the corresponding sequences q_n is growing, on average, exponentially with n. Such exponents may be used to characterize chaos. Indeed, an evident generalization of the linearized Eq. (4) to an arbitrary point q_n is

$$\Delta q_{n+1} = e_n \Delta q_n, \qquad e_n \equiv \left. \frac{df}{dq} \right|_{q=q_n}. \tag{9.7}$$

[4] The reader should remember that just like the usual ("nature") experiments, numerical experiments also have limited accuracy, due to unavoidable rounding errors.

[5] The geometry of these regions is essentially *fractal*, i.e. has a dimensionality intermediate between 0 (which any final set of geometric points would have) and 1 (pertinent to a 1D continuum). An extensive discussion of fractal geometries and their relation to deterministic chaos may be found, for example, in the book by B. Mandelbrot, *The Fractal Geometry of Nature*, W. H. Freeman, 1983.

[6] This does not mean that chaos depth is always a monotonic function of r. As Fig. 2 shows, within certain intervals of this parameter, the chaotic behavior suddenly disappears, being replaced, typically, with a few-point limit cycle, just to resume on the other side of the interval. Sometimes (but not always!) the "route to chaos" on the borders of these intervals follows the same Feigenbaum sequence of period-doubling bifurcations.

Let us assume that Δq_1 is so small that N first values q_n are relatively close to each other. Then using Eq. (7) iteratively for these steps, we get

$$\Delta q_N = \Delta q_1 \prod_{n=1}^{N} e_n, \qquad \text{so that} \quad \ln\left|\frac{\Delta q_N}{\Delta q_1}\right| = \sum_{n=1}^{N} \ln|e_n|. \tag{9.8}$$

Numerical experiments show that in most chaotic regimes, at $N \to \infty$ such a sum fluctuates about an average, which grows as λN, with the parameter

$$\lambda \equiv \lim_{\Delta q_1 \to 0} \lim_{N \to \infty} \frac{1}{N} \sum_{n=1}^{N} \ln|e_n|, \tag{9.9}$$

Lyapunov exponent

called the *Lyapunov exponent*,[7] being independent of the initial conditions. The bottom panel in Fig. 3 shows λ as a function of the parameter r for the logistic map (2). (Its top panel shows the same pattern as Fig. 2, which is reproduced here just for the sake of comparison.)

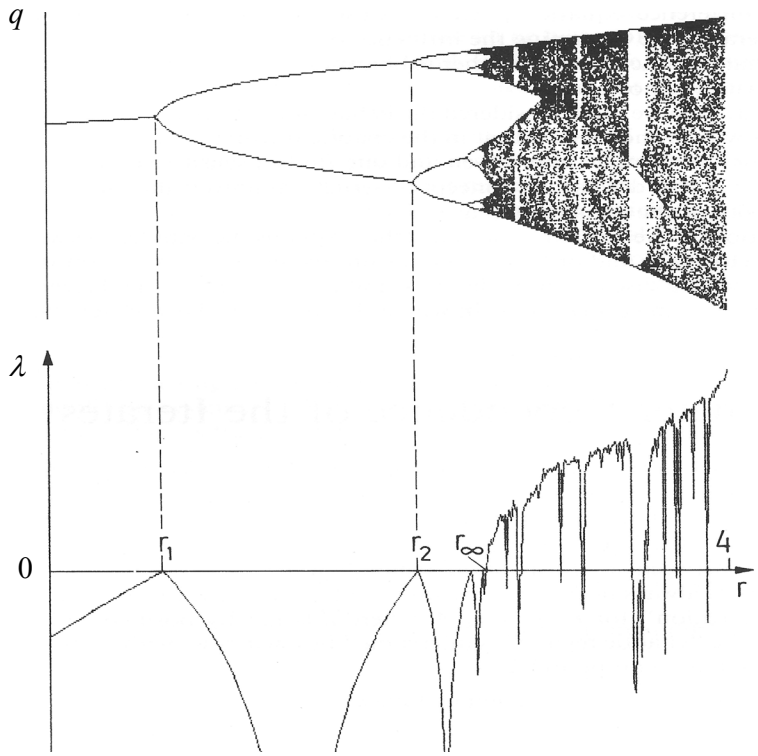

Fig. 9.3. The Lyapunov exponent for the logistic map. Adapted, with permission, from the monograph by Schuster and Just (cited below). © Wiley-VCH Verlag GmbH & Co. KGaA.

Note that at $r < r_\infty$, λ is negative, indicating the sequence's stability, besides the points r_1, r_2, … where λ would become positive if the limit cycle changes (bifurcations) had not brought it back into the negative territory. However, at $r > r_\infty$, λ becomes positive, returning to negative values only in limited intervals of stable limit cycles. It is evident that in numerical experiments (which dominate the studies of deterministic chaos) the Lyapunov exponent may be used as a good measure of the chaos' depth.[8]

[7] After Alexandr Mikhailovich Lyapunov (1857-1918), famous for his studies of the stability of dynamic systems.

[8] N-dimensional maps that relate N-dimensional vectors rather than scalars, may be characterized by N Lyapunov exponents rather than one. For chaotic behavior, it is sufficient for just one of them to become positive. For such systems, another measure of chaos, the *Kolmogorov entropy,* may be more relevant. This measure and its relation with the Lyapunov exponents are discussed, for example, in SM Sec. 2.2.

Despite the abundance of results published for particular maps,[9] and several interesting observations (like the already discussed existence of the Feigenbaum bifurcation sequences), to the best of my knowledge, nobody can yet predict the patterns like those shown in Fig. 2 and 3 by just studying the mapping rule itself, i.e. without carrying out actual numerical experiments. Unfortunately, the understanding of deterministic chaos in other systems is not much better.

9.2. Chaos in dynamic systems

Proceeding to the discussion of chaos in dynamic systems, it is more natural, with our background, to illustrate this discussion not with the Lorenz equations, but with the system of equations describing a dissipative pendulum driven by a sinusoidal external force, which was repeatedly discussed in Chapter 5. Introducing two new variables, the normalized momentum $p \equiv (dq/dt)/\omega_0$, and the external force's full phase $\psi \equiv \omega t$, we may rewrite Eq. (5.42), describing the pendulum, in a form similar to Eq. (1), i.e. as a system of three first-order ordinary differential equations:

$$\begin{aligned} \dot{q} &= \omega_0 p, \\ \dot{p} &= -\omega_0 \sin q - 2\delta p + (f_0/\omega_0)\cos\psi, \\ \dot{\psi} &= \omega. \end{aligned} \tag{9.10}$$

Figure 4 shows several results of a numerical solution of Eq. (10).[10] In all cases, parameters δ, ω_0, and f_0 are fixed, while the external frequency ω is gradually changed. For the case shown on the top two panels, the system still tends to a stable periodic solution, with very low contents of higher harmonics. If the external force frequency is reduced by a just few percent, the 3rd subharmonic may be excited. (This effect has already been discussed in Sec. 5.8 – see, e.g., Fig. 5.15.) The next row shows that just a small further reduction of the frequency ω leads to a new tripling of the period, i.e. the generation of a complex waveform with the 9th subharmonic. Finally (see the bottom panels of Fig. 4), even a minor further change of ω leads to oscillations without any visible period, e.g., to the chaos.

In order to trace this transition, a direct inspection of the oscillation waveforms $q(t)$ is not very convenient, and trajectories on the phase plane $[q, p]$ also become messy if plotted for many periods of the external frequency. In situations like this, the Poincaré (or "stroboscopic") plane, already discussed in Sec. 5.6, is much more useful. As a reminder, this is essentially just the phase plane $[q, p]$, but with the points highlighted only once a period, e.g., at $\psi = 2\pi n$, with $n = 1, 2, \ldots$ On this plane, periodic oscillations of frequency ω are represented just as one fixed point – see, e.g. the top panel in the right column of Fig. 4. The 3rd subharmonic generation, shown on the next panel, means the oscillation period's tripling and is represented as the splitting of the fixed point into three. It is evident that this transition is similar to the period-doubling bifurcation in the logistic map, besides the fact (already discussed in Sec. 5.8) that in systems with an antisymmetric nonlinearity, such as the pendulum (10), the 3rd subharmonic is easier to excite. From this point, the 9th harmonic generation (shown on the 3rd panel of Fig. 4), i.e. one more splitting of the points on the Poincaré plane, may be understood as one more step on the Feigenbaum-like route to chaos – see the bottom panel of that figure.

---

[9] See, e.g., Chapters 2-4 in H. Schuster and W. Just, *Deterministic Chaos*, 4th ed., Wiley-VCH, 2005, or Chapters 8-9 in J. Thompson and H. Stewart, *Nonlinear Dynamics and Chaos*, 2nd ed., Wiley, 2002.

[10] In the actual simulation, a small term εq, with $\varepsilon << 1$, has been added to the left-hand side of this equation. This term slightly tames the trend of the solution to spread along the q-axis, and makes the presentation of results easier, without affecting the system's dynamics too much.

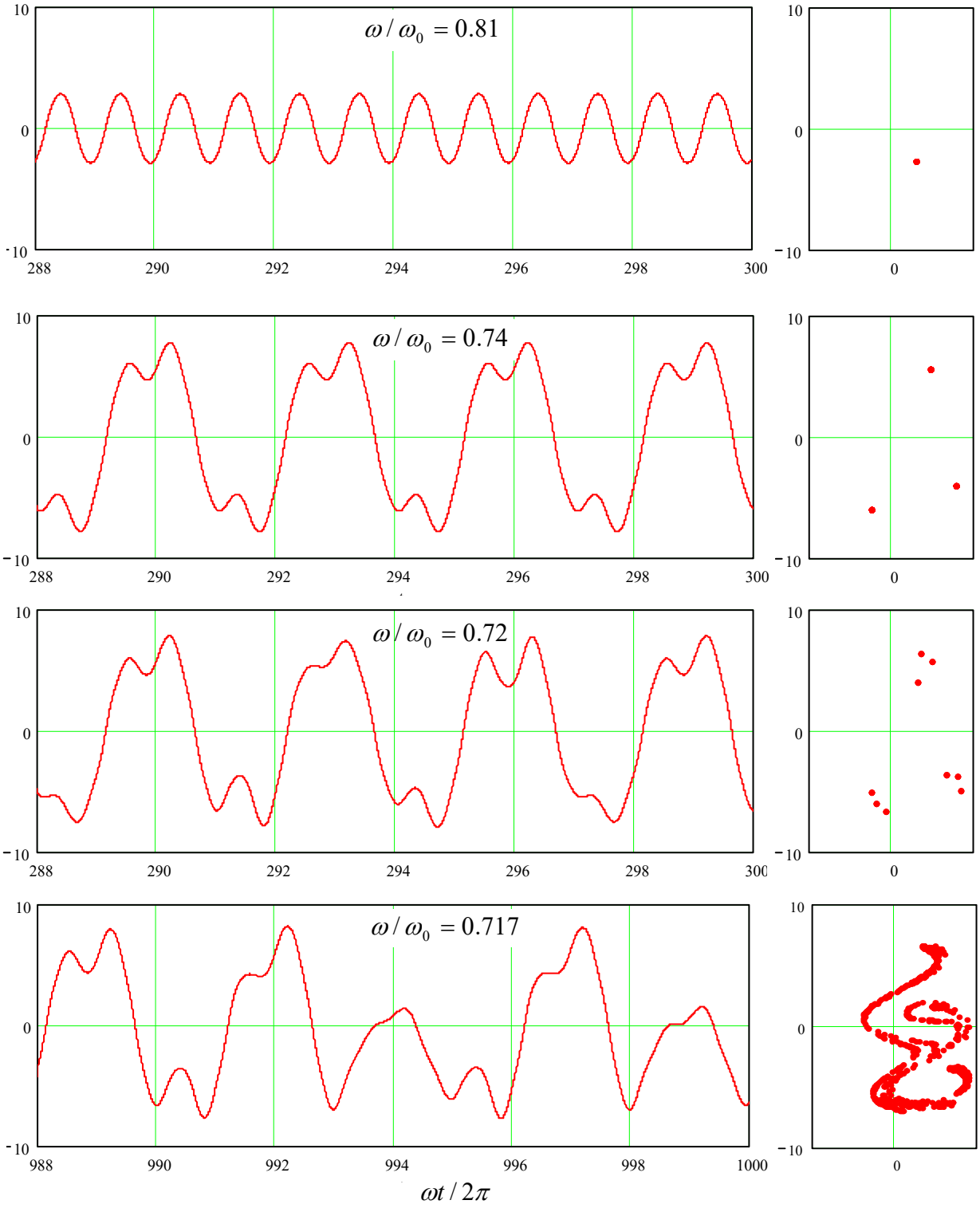

Fig. 9.4. Oscillations in a pendulum with weak damping, $\delta/\omega_0 = 0.1$, driven by a sinusoidal external force with a fixed effective amplitude $f_0/\omega_0^2 = 1$, and several close values of the frequency ω (listed on the panels). Left panel column: the oscillation waveforms $q(t)$ recorded after certain initial transient intervals. Right column: representations of the same processes on the Poincaré plane of the variables $[q, p]$, with the q-axis turned vertically, for the convenience of comparison with the left panels.

So, the transition to chaos in dynamic systems may be at least qualitatively similar to that in 1D maps, with a law similar to Eq. (6) for the critical values of some parameter of the system (in Fig. 4, frequency ω), though with a system-specific value of the coefficient δ. Moreover, we may consider the first two differential equations of the system (10) as a 2D map that relates the vector $\{q_{n+1}, p_{n+1}\}$ of the coordinate and momentum, measured at $\psi = 2\pi(n + 1)$, with the previous value $\{q_n, p_n\}$ of that vector, reached at $\psi = 2\pi n$.

Unfortunately, this similarity also implies that the deterministic chaos in dynamic systems is at least as complex, and is as little understood, as in maps. For example, Fig. 5 shows (a part of) the phase diagram of the externally-driven pendulum, with the red bar marking the route to chaos traced in Fig. 4, and shading/hatching styles marking different oscillation regimes. One can see that the pattern is at least as complex as that shown in Figs. 2 and 3, and, besides a few features,[11] is equally unpredictable from the form of the equation.

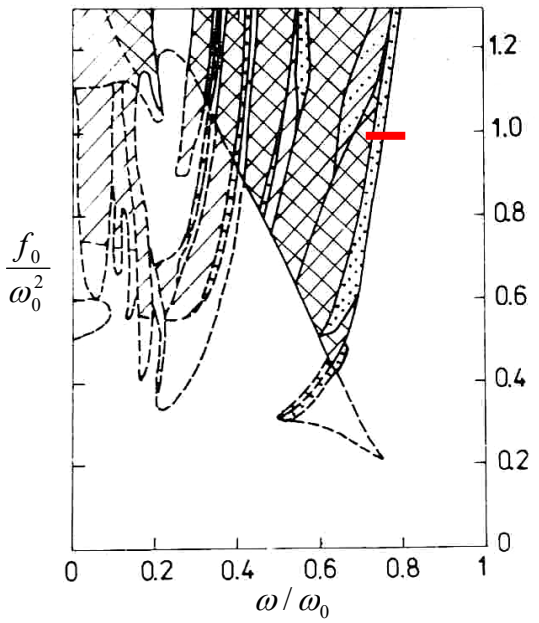

Fig. 9.5. The phase diagram of an externally driven pendulum with weak damping ($\delta/\omega_0 = 0.1$). The regions of oscillations with the basic period are not shaded; the notation for other regions is as follows. Doted: subharmonic generation; cross-hatched: chaos; hatched: either chaos or the basic period (depending on the initial conditions); hatch-dotted: either the basic period or subharmonics. Solid lines show the boundaries of single-regime regions, while dashed lines are the boundaries of the regions where several types of motion are possible. (Figure courtesy by V. Kornev.)

Are there any valuable general results concerning the deterministic chaos in dynamic systems? The most important (though an almost evident) result is that this phenomenon is impossible in any system described by one or two first-order differential equations with time-independent right-hand sides. Indeed, let us start with a single equation

$$\dot{q} = f(q), \tag{9.11}$$

where $f(q)$ is any single-valued function. This equation may be directly integrated to give

$$t = \int^{q} \frac{dq'}{f(q')} + \text{const}, \tag{9.12}$$

showing that the relation between q and t is unique and hence does not leave any place for chaos.

[11] In some cases, it is possible to predict a parameter region where chaos *cannot* happen, due to the lack of any instability-amplification mechanism. Unfortunately, typically the analytically predicted boundaries of such a region form a rather loose envelope of the actual (numerically simulated) chaotic regions.

Next, let us explore a system of two such equations:

$$\begin{aligned} \dot{q}_1 &= f_1(q_1, q_2), \\ \dot{q}_2 &= f_2(q_1, q_2). \end{aligned} \tag{9.13}$$

Consider its phase plane shown schematically in Fig. 6. In a "usual" system, the trajectories approach either some fixed point (Fig. 6a) describing static equilibrium, or a limit cycle (Fig. 6b) describing periodic oscillations. (Both notions are united by the term *attractor* because they "attract" trajectories launched from various initial conditions.) On the other hand, phase plane trajectories of a chaotic system of equations that describe physical variables (which cannot be infinite), should be confined to a limited phase plane area, and simultaneously cannot start repeating each other. (This topology is frequently called the *strange attractor*.) For that, the 2D trajectories need to cross – see, e.g., point A in Fig. 6c.

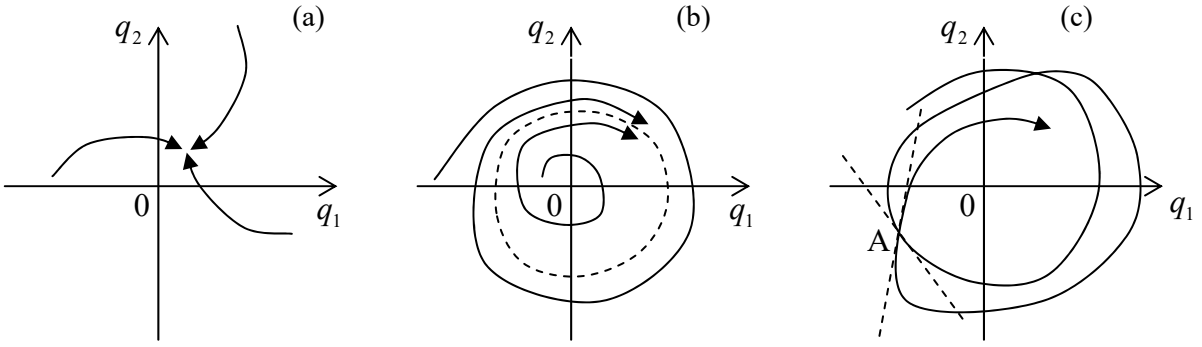

Fig. 9.6. Attractors in dynamical systems: (a) a fixed point, (b) a limit cycle, and (c) a strange attractor.

However, in the case described by Eqs. (13), such a crossing is clearly impossible, because according to these equations, the tangent of a phase plane trajectory is a unique function of the coordinates $\{q_1, q_2\}$:

$$\frac{dq_1}{dq_2} = \frac{f_1(q_1, q_2)}{f_2(q_1, q_2)}. \tag{9.14}$$

Thus, in this case, the deterministic chaos is impossible.[12] It becomes, however, readily possible if the right-hand sides of a system similar to Eq. (13) depend either on other variables of the system or time. For example, if we consider the first two differential equations of the system (10), in the case $f_0 = 0$ they have the structure of the system (13), and hence the chaos is impossible – even at $\delta < 0$ when (as we know from Sec. 5.4) the system allows self-excitation of oscillations, leading to a limit-cycle attractor. However, if $f_0 \neq 0$, this argument does not work any longer, and (as we have already seen) the system may have a strange attractor – which is, for dynamic systems, a synonym for the deterministic chaos.

Thus, chaos is only possible in autonomous dynamic systems described by three or more differential equations of the first order.[13]

[12] A mathematically strict formulation of this statement is called the *Poincaré-Bendixon theorem*, which was proved by Ivar Bendixon in 1901.

[13] Since a typical dynamic system with one degree of freedom is described by two such equations, the number of first-order equations describing a dynamic system is sometimes called the number of its *half-degrees of freedom.* This notion is very useful and popular in statistical mechanics – see, e.g., SM Sec. 2.2 and on.

9.3. Chaos in Hamiltonian systems

The last conclusion is of course valid for Hamiltonian systems, which are just a particular type of dynamic systems. However, one may wonder whether these systems, which feature at least one first integral of motion, H = const, and hence are more "ordered" than the systems discussed above, can exhibit chaos at all. The answer is *yes* because such systems still can have mechanisms for the exponential growth of a small initial perturbation.

As the simplest way to show it, let us consider the so-called *mathematical billiard*, i.e. system with a ballistic particle (a "ball") moving freely by inertia on a horizontal plane surface ("table") limited by rigid walls. In this idealized model of the usual game of billiards, the ball's velocity $\mathbf{v}$ is conserved when it moves on the table, and when it runs into a wall, the ball is elastically reflected from it as from a mirror,[14] with the reversal of the sign of the normal velocity v_n, and the conservation of the tangential velocity v_τ, and hence without any loss of its kinetic (and hence the full) energy

$$E = H = T = \frac{m}{2}v^2 = \frac{m}{2}\left(v_n^2 + v_\tau^2\right). \tag{9.15}$$

This model, while being a legitimate 2D dynamic system,[15] allows geometric analyses for several simple table shapes. The simplest of them is a rectangular billiard of area $a \times b$ (Fig. 7), whose analysis may be readily carried out just by the replacement of each *ball* reflection event with the mirror reflection of the *table* in that wall – see the dashed lines on panel (a).

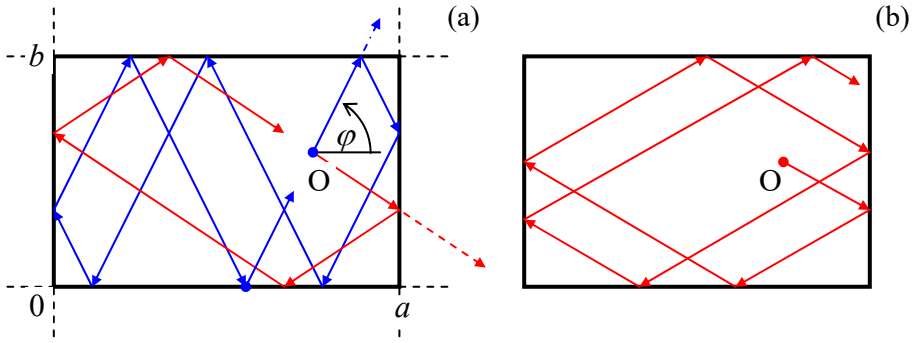

Fig. 9.7. Ball motion on a rectangular billiard at (a) a commensurate, and (b) an incommensurate launch angle.

Such analysis (left for the reader's pleasure :-) shows that if the tangent of the ball launching angle φ is commensurate with the side length ratio:

$$\tan\varphi = \pm\frac{m}{n}\frac{b}{a}, \tag{9.16}$$

where n and m are non-negative integers without common integer multipliers, the ball returns exactly to the launch point O, after bouncing m times from each wall of length a, and n times from each wall of length b. (Red lines in Fig. 7a show an example of such a trajectory for $n = m = 1$, while blue lines, for $m = 3$, $n = 1$.) The larger is the sum $(m + n)$, the more complex is such a closed "orbit".

[14] A more scientific-sounding name for such a reflection is *specular* – from the Latin word "speculum" meaning a metallic mirror.

[15] Indeed, it is fully described by the following Lagrangian function: $L = mv^2/2 - U(\boldsymbol{\rho})$, with $U(\boldsymbol{\rho}) = 0$ for the 2D radius vectors $\boldsymbol{\rho}$ belonging to the table area, and $U(\boldsymbol{\rho}) = +\infty$ outside the area.

Finally, if $(n + m) \to \infty$, i.e. $\tan\varphi$ and b/a are incommensurate (meaning that their ratio is an irrational number), the trajectory covers all of the table area, and the ball never returns exactly to the launch point. Still, this is not genuine chaos. Indeed, a small shift of the launch point O shifts all the trajectory fragments by the same displacement. Moreover, at any time t, each of Cartesian components $v_j(t)$ of the ball's velocity (with coordinate axes parallel to the table sides) may take only two values, $\pm v_j(0)$, and hence may vary only as much as the initial velocity is being changed.

In 1963, i.e. well before E. Lorenz's work, Yakov Sinai showed that the situation changes completely if an additional wall, in the shape of a circle, is inserted into the rectangular billiard (Fig. 8). For most initial conditions, the ball's trajectory eventually runs into the circle (see the red line on panel (a) as an example), and the further trajectory becomes essentially chaotic. Indeed, let us consider the ball's reflection from a circle-shaped wall – Fig. 8b. Due to the conservation of the tangential velocity, and the sign change of the normal velocity component, the reflection obeys a simple law: $\theta_r = \theta_i$. Figure 8b shows that as the result, the magnitude of a small difference $\delta\varphi$ between the angles of two close trajectories (as measured in the lab system), doubles at each reflection from the curved wall. This means that the small deviation grows along the ball trajectory as

$$\left|\delta\varphi(N)\right| \sim \left|\delta\varphi(0)\right| \times 2^N \equiv \left|\delta\varphi(0)\right| e^{N \ln 2}, \tag{9.17}$$

where N is the number of reflections from the convex wall.[16] As we already know, such exponential divergence of trajectories, with a positive Lyapunov exponent, is the main feature of deterministic chaos.[17]

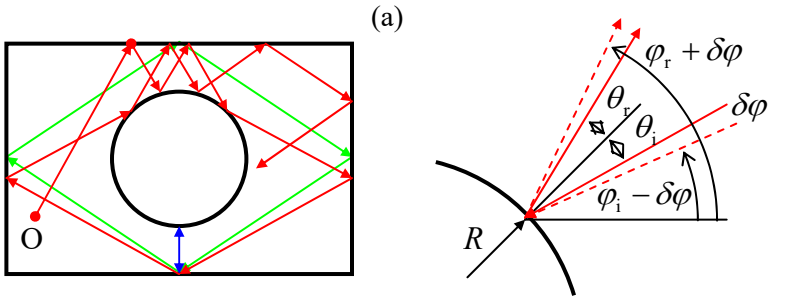

Fig. 9.8. (a) Motion on a Sinai billiard table, and (b) the mechanism of the exponential divergence of close trajectories.

The most important new feature of the dynamic chaos in Hamiltonian systems is its dependence on initial conditions. (In the systems discussed in the previous two sections, that lack the integrals of motion, the initial conditions are rapidly "forgotten", and the chaos is usually characterized after an initial transient period – see, e.g., Fig. 4.) Indeed, even a Sinai billiard allows periodic motion, along closed orbits, under certain initial conditions – see the blue and green lines in Fig. 8a as examples. Thus

[16] Superficially, Eq. (17) is also valid for a plane wall, but as was discussed above, a billiard with such walls features a full correlation between sequential reflections, so angle φ always returns to its initial value. In a Sinai billiard, such correlation disappears. Concave walls may also make a billiard chaotic; a famous example is the *stadium billiard*, suggested by Leonid Bunimovich in 1974, with two straight, parallel walls connecting two semi-circular, concave walls. Another example, which allows a straightforward analysis (first carried out by Martin Gutzwiller in the 1980s), is the so-called *Hadamard billiard*: an infinite (or rectangular) table with a non-horizontal surface of negative curvature.

[17] Curved-wall billiards are also a convenient platform for studies of quantum properties of classically chaotic systems (for their conceptual discussion, see QM Sec. 3.5), in particular, the features called "quantum scars" – see, e.g., the spectacular numerical simulation results by E. Heller, *Phys. Rev. Lett.* **53**, 1515 (1984).

the chaos "depth" in such systems may be characterized by the "fraction"[18] of the phase space of initial parameters (for a 2D billiard, of the 3D space of the initial values of x, y, and φ) resulting in chaotic trajectories.

This conclusion is also valid for Hamiltonian systems that are met in physics much more frequently than exotic billiards, for example, coupled nonlinear oscillators without damping. Perhaps the earliest and the most popular example is the so-called *Hénon-Heiles* system,[19] which may be described by the following Lagrangian function:

$$L = \frac{m_1}{2}\left(\dot{q}_1^2 - \omega_1^2 q_1^2\right) + \frac{m_2}{2}\left(\dot{q}_2^2 - \omega_2^2 q_2^2\right) - \varepsilon\left(q_1^2 - \frac{1}{3}q_2^2\right)q_2 . \tag{9.18}$$

Hénon-Heiles system

It is straightforward to use this function to derive the corresponding Lagrange equations of motion,

$$\begin{aligned} m_1\left(\ddot{q}_1 + \omega_1^2 q_1\right) &= -2\varepsilon q_1 q_2 , \\ m_2\left(\ddot{q}_2 + \omega_2^2 q_2\right) &= -\varepsilon\left(q_1^2 - q_2^2\right), \end{aligned} \tag{9.19}$$

and find their first integral of motion (physically, the energy conservation law):

$$H = E = \frac{m_1}{2}\left(\dot{q}_1^2 + \omega_1^2 q_1^2\right) + \frac{m_2}{2}\left(\dot{q}_2^2 + \omega_2^2 q_2^2\right) + \varepsilon\left(q_1^2 - \frac{1}{3}q_2^2\right)q_2 = \text{const} . \tag{9.20}$$

In the context of our discussions in Chapters 5 and 6, Eqs. (19) may be readily interpreted as those describing two oscillators, with small-oscillation frequencies ω_1 and ω_2, coupled only by the quadratic terms on the right-hand sides of the equations. This means that as the oscillation amplitudes $A_{1,2}$, and hence the total energy E of the system, are close to zero, the oscillator subsystems are virtually independent, each performing sinusoidal oscillations at its own frequency. This observation suggests a convenient way to depict the system's motion.[20] Let us consider a Poincaré plane for one of the oscillators (say, with coordinate q_2), similar to that discussed in Sec. 2 above, with the only difference is that (because of the absence of an explicit function of time in the system's equations), the trajectory on the phase plane $[q_2, \dot{q}_2]$ is highlighted at the moments when $q_1 = 0$.

Let us start from the limit $A_{1,2} \to 0$ when the oscillations of q_2 are virtually sinusoidal. As we already know (see Fig. 5.9 and its discussion), if the representation point highlighting was perfectly synchronous with frequency ω_2 of the oscillations, there would be only one point on the Poincaré plane – see, e.g. the right top panel of Fig. 4. However, at the q_1 – initiated highlighting, there is no such synchronism, so each period, a different point of the elliptical (at the proper scaling of the velocity,

[18] Actually, quantitative characterization of the fraction is not trivial, because it may have *fractal dimensionality*. Unfortunately, due to lack of time I have to refer the reader interested in this issue to special literature, e.g., the monograph by B. Mandelbrot (cited above) and references therein.

[19] It was first studied in 1964 by M. Hénon and C. Heiles as a simple model of star rotation about a galactic center. Most studies of this equation have been carried out for the following particular case: $m_2 = 2m_1$, $m_1\omega_1^2 = m_2\omega_2^2$. In this case, by introducing new variables $x \equiv \varepsilon q_1$, $y \equiv \varepsilon q_2$, and $\tau \equiv \omega_1 t$, it is possible to rewrite Eqs. (19) in a parameter-free form. All the results shown in Fig. 9 below are for this case.

[20] Generally, the system has a trajectory in 4D space, e.g., that of coordinates $q_{1,2}$ and their time derivatives, although the first integral of motion (20) means that for each fixed energy E, the motion is limited to a 3D subspace. Still, this is one dimension too many for a convenient representation of the motion.

circular) trajectory is highlighted, so the resulting points, for certain initial conditions, reside on a circle of radius A_2. If we now vary the initial conditions, i.e. redistribute the initial energy between the oscillators, but keep the total energy E constant, on the Poincaré plane we get a set of ellipses.

Now, if the initial energy is increased, the nonlinear interaction of the oscillations starts to deform these ellipses, causing also their crossings – see, e.g., the top left panel of Fig. 9. Still, below a certain threshold value of E, all Poincaré points belonging to a certain initial condition sit on a single closed contour. Moreover, these contours may be calculated approximately, but with pretty good accuracy, using a straightforward generalization of the method discussed in Sec. 5.2.[21]

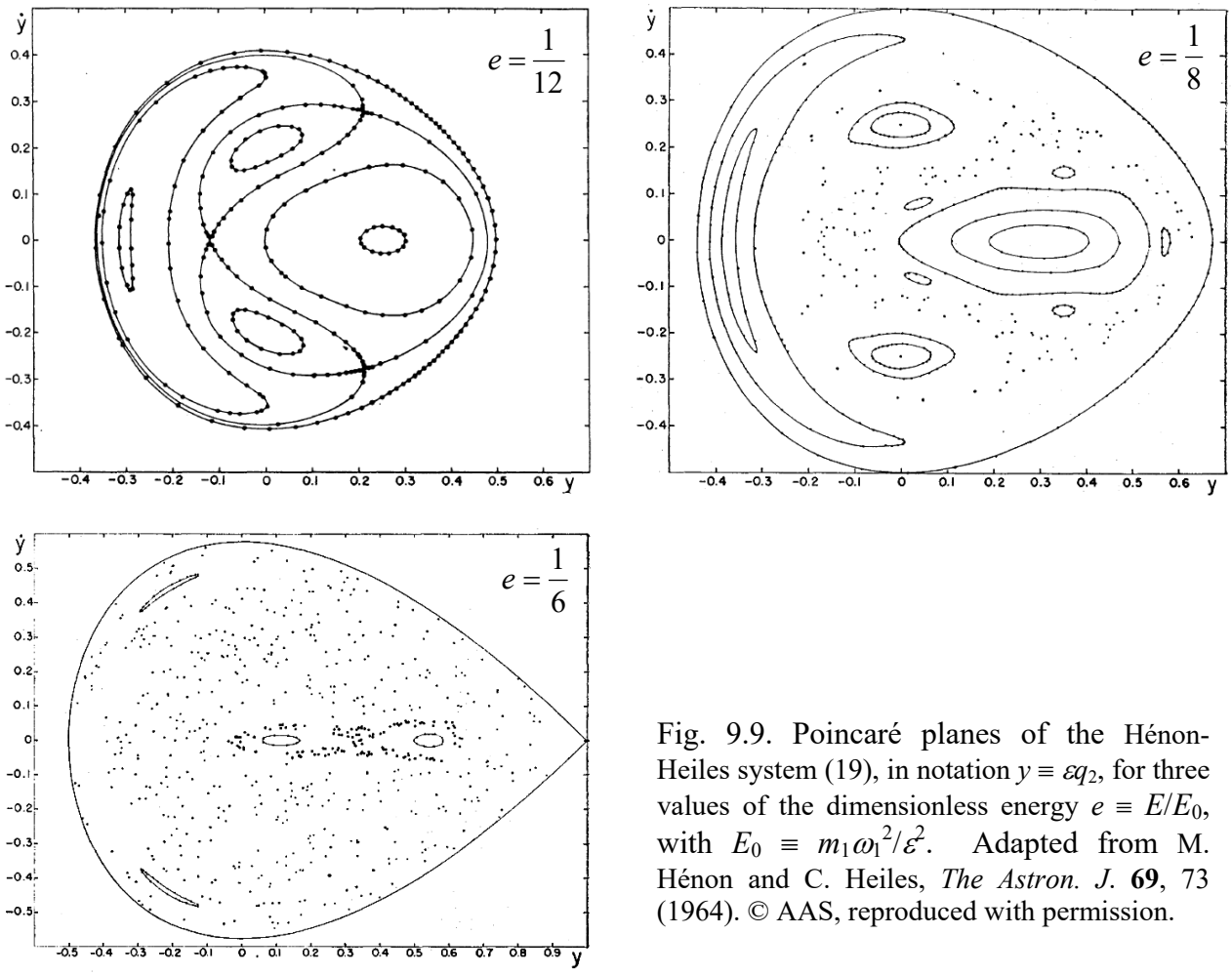

Fig. 9.9. Poincaré planes of the Hénon-Heiles system (19), in notation $y \equiv \varepsilon q_2$, for three values of the dimensionless energy $e \equiv E/E_0$, with $E_0 \equiv m_1\omega_1^2/\varepsilon^2$. Adapted from M. Hénon and C. Heiles, *The Astron. J.* **69**, 73 (1964). © AAS, reproduced with permission.

However, starting from some value of energy, certain initial conditions lead to sequences of points scattered over parts of the Poincaré plane, with a nonzero area – see the top right panel of Fig. 9. This means that the corresponding oscillations $q_2(t)$ do not repeat from one (quasi-) period to the next one – cf. Fig. 4 for the dissipative, forced pendulum. This is chaos.[22] Still, some other initial conditions

[21] See, e.g., M. Berry, in: S. Jorna (ed.), *Topics in Nonlinear Dynamics*, AIP Conf. Proc. No. 46, AIP, 1978, pp. 16-120.

[22] This fact complies with the necessary condition of chaos, discussed at the end of Sec. 2, because Eqs. (19) may be rewritten as a system of *four* differential equations of the first order.

lead to closed contours. This feature is similar to that in Sinai billiards and is typical for Hamiltonian systems. As the energy is increased, larger and larger parts of the Poincaré plane correspond to the chaotic motion, signifying deeper and deeper chaos – see the bottom panel of Fig. 9.

9.4. Chaos and turbulence

This extremely short section consists of essentially just one statement, extending the discussion in Sec. 8.5. The (re-) discovery of the deterministic chaos in systems with just a few degrees of freedom in the 1960s has changed the tone of the debates concerning turbulence origins, very considerably. At first, an extreme point of view that equated the notions of chaos and turbulence, became the debate's favorite.[23] However, after the initial excitement, a significant role of the Richardson-style energy-cascade mechanisms, involving many degrees of freedom, were rediscovered and could not be ignored any longer. To the best knowledge of this author, who is a distant albeit interested observer of that field, most experimental and numerical-simulation data carry features of both mechanisms, so the debate continues.[24] Due to the age difference, most readers of these notes have much better chances than the author to see where this discussion eventually leads.[25]

9.5. Exercise problems

9.1. Generalize the reasoning of Sec. 1 to an arbitrary 1D map $q_{n+1} = f(q_n)$, with the function $f(q)$ differentiable at all points of interest. In particular, derive the condition of stability of an N-point limit cycle $q^{(1)} \to q^{(2)} \to \ldots \to q^{(N)} \to q^{(1)} \ldots$

9.2. Use the stability condition derived in the previous problem, to analyze the possibility of deterministic chaos in the so-called *tent map*, with

$$f(q) = \begin{cases} rq, & \text{for } 0 \le q \le ½, \\ r(1-q), & \text{for } ½ \le q \le 1, \end{cases} \qquad \text{with } 0 \le r \le 2.$$

9.3. Find the conditions of existence and stability of fixed points of the so-called *standard circle map*:

$$q_{n+1} = q_n + \Omega - \frac{K}{2\pi} \sin 2\pi q_n,$$

where q_n are real numbers defined modulo 1 (i.e. with $q_n + 1$ identified with q_n), while Ω and K are constant parameters. Discuss the relevance of the result for phase locking of self-oscillators – see, e.g., Sec. 5.4.

[23] An important milestone in that way was the work by S. Newhouse *et al., Comm. Math. Phys*. **64**, 35 (1978), who proved the existence of a strange attractor in a rather abstract model of fluid flow.

[24] See, e.g., U. Frisch, *Turbulence*: *The Legacy of A. N. Kolmogorov*, Cambridge U. Press, 1996.

[25] The reader interested in deterministic chaos as such may like to have a look at a very popular book by S. Strogatz, *Nonlinear Dynamics and Chaos*, Westview, 2001.

9.4. Find the conditions of existence and stability of fixed points of the so-called *Hénon map*:[26]

$$q_{n+1} = 1 - aq_n^2 + p_n,$$
$$p_{n+1} = bq_n, \quad \text{with } 0 < b < 1.$$

9.5. Is the deterministic chaos possible in our "testbed" problem shown in Fig. 2.1? What if an additional periodic external force is applied to the bead? Explain your answers.

[26] This map, first explored by M. Hénon in 1976 (for a particular set of constants a and b), has played an important historic role in the study of strange attractors.

Chapter 10. A Bit More of Analytical Mechanics

This concluding chapter reviews two alternative approaches to analytical mechanics, whose major value is a closer parallel to quantum mechanics in general and its quasiclassical (WKB) approximation in particular. One of them, the Hamiltonian formalism, is also convenient for the derivation of an important asymptotic result, the adiabatic invariance, for classical systems with slowly changing parameters.

10.1. Hamilton equations

Throughout this course, we have seen how analytical mechanics, in its Lagrangian form, is invaluable for solving various particular problems of classical mechanics. Now let us discuss several alternative formulations[1] that may not be much more useful for this purpose, but shed additional light on possible extensions of classical mechanics, most importantly to quantum mechanics.

As was already discussed in Sec. 2.3, the partial derivative $p_j \equiv \partial L/\partial \dot{q}_j$ participating in the Lagrange equation (2.19),

$$\frac{d}{dt}\frac{\partial L}{\partial \dot{q}_j} - \frac{\partial L}{\partial q_j} = 0, \tag{10.1}$$

may be considered as the generalized momentum corresponding to the generalized coordinate q_j, and the full set of these momenta may be used to define the Hamiltonian function (2.32):

$$H \equiv \sum_j p_j \dot{q}_j - L\,. \tag{10.2}$$

Now let us rewrite the full differential of this function[2] in the following form:

$$\begin{aligned} dH &= d\left(\sum_j p_j \dot{q}_j - L\right) = \sum_j \left[d(p_j)\dot{q}_j + p_j d(\dot{q}_j)\right] - dL \\ &= \sum_j \left[d(p_j)\dot{q}_j + p_j d(\dot{q}_j)\right] - \left[\frac{\partial L}{\partial t}dt + \sum_j \left(\frac{\partial L}{\partial q_j}d(q_j) + \frac{\partial L}{\partial \dot{q}_j}d(\dot{q}_j)\right)\right]. \end{aligned} \tag{10.3}$$

According to the definition of the generalized momentum, the second terms of each sum over j in the last expression cancel each other, while according to the Lagrange equation (1), the derivative $\partial L/\partial q_j$ is equal to $\dot{p}_j$, so

$$dH = -\frac{\partial L}{\partial t}dt + \sum_j \left(\dot{q}_j dp_j - \dot{p}_j dq_j\right). \tag{10.4}$$

So far, this is just a universal identity. Now comes the main trick of Hamilton's approach: let us consider H as a function of the following independent arguments: time t, the generalized coordinates q_j,

[1] Due to not only William Rowan Hamilton (1805-1865), but also Carl Gustav Jacob Jacobi (1804-1851).

[2] Actually, this differential was already spelled out (but partly and implicitly) in Sec. 2.3 – see Eqs. (2.33)-(2.35).

© K. Likharev

and the generalized *momenta* p_j – rather than generalized *velocities* $\dot{q}_j$ as in the Lagrangian formalism. With this new commitment, the general "chain rule" of differentiation of a function of several arguments gives

$$dH = \frac{\partial H}{\partial t}dt + \sum_j \left(\frac{\partial H}{\partial q_j}dq_j + \frac{\partial H}{\partial p_j}dp_j \right), \tag{10.5}$$

where dt, dq_j, and dp_j are independent differentials. Since Eq. (5) should be valid for any choice of these argument differentials, it should hold in particular if they correspond to the real law of motion, for which Eq. (4) is valid as well. The comparison of Eqs. (4) and (5) gives us three relations:

$$\frac{\partial H}{\partial t} = -\frac{\partial L}{\partial t}. \tag{10.6}$$

$$\boxed{\dot{q}_j = \frac{\partial H}{\partial p_j}, \qquad \dot{p}_j = -\frac{\partial H}{\partial q_j}.} \tag{10.7}$$

Hamilton equations

Comparing the first of them with Eq. (2.35), we see that

$$\frac{dH}{dt} = \frac{\partial H}{\partial t}, \tag{10.8}$$

meaning that the function $H(t, q_j, p_j)$ can change in time only via its explicit dependence on t. Two Eqs. (7) are even more substantial: provided that such function $H(t, q_j, p_j)$ has been calculated, they give us two first-order differential equations (called the *Hamilton equations*) for the time evolution of the generalized coordinate and generalized momentum of each degree of freedom of the system.[3]

Let us have a look at these equations for the simplest case of a system with one degree of freedom, with the Lagrangian function (3.3):

$$L = \frac{m_{\text{ef}}}{2}\dot{q}^2 - U_{\text{ef}}(q,t). \tag{10.9}$$

In this case, $p \equiv \partial L / \partial \dot{q} = m_{\text{ef}}\dot{q}$, and $H \equiv p\dot{q} - L = m_{\text{ef}}\dot{q}^2/2 + U_{\text{ef}}(q,t)$. To honor our new commitment, we need to express the Hamiltonian function explicitly via t, q, and p (rather than $\dot{q}$). From the above expression for p, we immediately have $\dot{q} = p/m_{\text{ef}}$; plugging this expression back to Eq. (9), we get

$$H = \frac{p^2}{2m_{\text{ef}}} + U_{\text{ef}}(q,t). \tag{10.10}$$

Now we can spell out Eqs. (7) for this particular case:

$$\dot{q} \equiv \frac{\partial H}{\partial p} = \frac{p}{m_{\text{ef}}}, \tag{10.11}$$

$$\dot{p} \equiv -\frac{\partial H}{\partial q} = -\frac{\partial U_{\text{ef}}}{\partial q}. \tag{10.12}$$

[3] Of course, the right-hand side of each equation (7) may include coordinates and momenta of other degrees of freedom as well, so the equations of motion for different j are generally coupled.

While the first of these equations just repeats the definition of the generalized momentum corresponding to the coordinate q, the second one gives the equation of momentum's change. Differentiating Eq. (11) over time, and plugging Eq. (12) into the result, we get:

$$\ddot{q} = \frac{\dot{p}}{m_{\rm ef}} = -\frac{1}{m_{\rm ef}}\frac{\partial U_{\rm ef}}{\partial q}. \tag{10.13}$$

So, we have returned to the same equation (3.4) that had been derived from the Lagrangian approach.[4]

Thus, Hamiltonian formalism does not give much help for the solution of this problem – and indeed most problems of classical mechanics. (This is why its discussion had been postponed until the very end of this course.) Moreover, since the Hamiltonian function $H(t, q_j, p_j)$ does not include generalized velocities explicitly, the phenomenological introduction of dissipation in this approach is less straightforward than that in the Lagrangian equations, whose precursor form (2.17) is valid for dissipative forces as well. However, the Hamilton equations (7), which treat the generalized coordinates and momenta in a manifestly symmetric way, are heuristically fruitful – besides being very appealing aesthetically. This is especially true in the cases where these arguments participate in H in a similar way. For example, in the very important case of a dissipation-free linear ("harmonic") oscillator, for which $U_{\rm ef} = \kappa_{\rm ef}q^2/2$, Eq. (10) gives the symmetric form

$$H = \frac{p^2}{2m_{\rm ef}} + \frac{\kappa_{\rm ef}x^2}{2} \equiv \frac{p^2}{2m_{\rm ef}} + \frac{m_{\rm ef}\omega_0^2 x^2}{2}, \qquad \text{where } \omega_0^2 \equiv \frac{\kappa_{\rm ef}}{m_{\rm ef}}. \tag{10.14}$$

The Hamilton equations (7) for this system preserve that symmetry, especially evident if we introduce the normalized momentum $\not{p} \equiv p/m_{\rm ef}\omega_0$ (already used in Secs. 5.6 and 9.2):

$$\frac{dq}{dt} = \omega_0 \not{p}, \qquad \frac{d\not{p}}{dt} = -\omega_0 q. \tag{10.15}$$

More practically, the Hamilton approach gives additional tools for the search for the integrals of motion. To see that, let us consider the full time derivative of an arbitrary function $f(t, q_j, p_j)$:

$$\frac{df}{dt} = \frac{\partial f}{\partial t} + \sum_j \left(\frac{\partial f}{\partial q_j}\dot{q}_j + \frac{\partial f}{\partial p_j}\dot{p}_j \right). \tag{10.16}$$

Plugging in $\dot{q}_j$ and $\dot{p}_j$ from the Hamilton equations (7), we get

Dynamics of arbitrary variable

$$\boxed{\frac{df}{dt} = \frac{\partial f}{\partial t} + \sum_j \left(\frac{\partial H}{\partial p_j}\frac{\partial f}{\partial q_j} - \frac{\partial H}{\partial q_j}\frac{\partial f}{\partial p_j} \right) \equiv \frac{\partial f}{\partial t} + \{H, f\}.} \tag{10.17}$$

The last term on the right-hand side of this expression is the so-called *Poisson bracket*,[5] and is defined, for two arbitrary functions $f(t, q_j, p_j)$ and $g(t, q_j, p_j)$, as

[4] The reader is strongly encouraged to perform a similar check for a few more problems, for example those listed at the end of the chapter, to get a better feeling of how the Hamiltonian formalism works.

[5] Named after Siméon Denis Poisson (1781-1840), of the Poisson equation and the Poisson statistical distribution fame.

$$\{g,f\} \equiv \sum_j \left(\frac{\partial g}{\partial p_j}\frac{\partial f}{\partial q_j} - \frac{\partial f}{\partial p_j}\frac{\partial g}{\partial q_j} \right). \tag{10.18}$$

Poisson bracket

From this definition, one can readily verify that besides evident relations $\{f,f\} = 0$ and $\{f, g\} = -\{g, f\}$, the Poisson brackets obey the following important *Jacobi identity*:

$$\{f,\{g,h\}\} + \{g,\{h,f\}\} + \{h,\{f,g\}\} = 0. \tag{10.19}$$

Now let us use these relations for a search for integrals of motion. First, Eq. (17) shows that if a function f does not depend on time explicitly, and

$$\{H,f\} = 0, \tag{10.20}$$

then $df/dt = 0$, i.e. that function is an integral of motion. Moreover, it turns out that if we already know two integrals of motion, say f and g, then the following function,

$$F \equiv \{f,g\}, \tag{10.21}$$

is also an integral of motion – the so-called *Poisson theorem*. In order to prove it, we may use the Jacobi identity (19) with $h = H$. Next, using Eq. (17) to express the Poisson brackets $\{g, H\}$, $\{H, g\}$, and $\{H,\{f, g\}\} = \{H, F\}$ via the full and partial time derivatives of the functions f, g, and F, we get

$$\left\{f, \frac{\partial g}{\partial t} - \frac{dg}{dt}\right\} + \left\{g, \frac{df}{dt} - \frac{\partial f}{\partial t}\right\} + \frac{dF}{dt} - \frac{\partial F}{\partial t} = 0, \tag{10.22}$$

so if f and g are indeed integrals of motion, i.e., $df/dt = dg/dt = 0$, then

$$\frac{dF}{dt} = \frac{\partial F}{\partial t} + \left\{g, \frac{\partial f}{\partial t}\right\} - \left\{f, \frac{\partial g}{\partial t}\right\} = \frac{\partial F}{\partial t} - \left[\left\{\frac{\partial f}{\partial t}, g\right\} + \left\{f, \frac{\partial g}{\partial t}\right\}\right]. \tag{10.23}$$

Plugging Eq. (21) into the first term of the right-hand side of this equation, and differentiating it by parts, we get $dF/dt = 0$, i.e. F is indeed an integral of motion as well.

Finally, one more important role of the Hamilton formalism is that it allows one to trace the close formal connection between classical and quantum mechanics. Indeed, using Eq. (18) to calculate the Poisson brackets of the generalized coordinates and momenta, we readily get

$$\{q_j, q_{j'}\} = 0, \quad \{p_j, p_{j'}\} = 0, \quad \{q_j, p_{j'}\} = -\delta_{jj'}. \tag{10.24}$$

In quantum mechanics, the operators of these variables ("observables") obey commutation relations[6]

$$\left[\hat{q}_j, \hat{q}_{j'}\right] = 0, \quad \left[\hat{p}_j, \hat{p}_{j'}\right] = 0, \quad \left[\hat{q}_j, \hat{p}_{j'}\right] = i\hbar\delta_{jj'}, \tag{10.25}$$

where the definition of the commutator, $\left[\hat{g}, \hat{f}\right] \equiv \hat{g}\,\hat{f} - \hat{f}\,\hat{g}$, is to a certain extent[7] similar to that (18) of the Poisson bracket. We see that the classical relations (24) are similar to the quantum-mechanical relations (25) if the following parallel has been made:

[6] See, e.g., QM Sec. 2.1.

CM ↔ QM relation

$$\{g, f\} \leftrightarrow \frac{i}{\hbar}\left[\hat{g}, \hat{f}\right]. \tag{10.26}$$

This analogy extends well beyond Eqs. (24)-(25). For example, by making the replacement (26) in Eq. (17), we get

$$\frac{d\hat{f}}{dt} = \frac{\partial \hat{f}}{\partial t} + \frac{i}{\hbar}\left[\hat{H}, \hat{f}\right], \qquad \text{i.e. } i\hbar\frac{d\hat{f}}{dt} = i\hbar\frac{\partial \hat{f}}{\partial t} + \left[\hat{f}, \hat{H}\right], \tag{10.27}$$

which is the correct equation of operator evolution in the Heisenberg picture of quantum mechanics.[8] The parallel (26) may give important clues in the search for the proper quantum-mechanical operator of a given observable – which is not always elementary.

10.2. Adiabatic invariance

One more application of the Hamiltonian formalism in classical mechanics is the solution of the following problem.[9] Earlier in the course, we already studied some effects of time variation of parameters of a single oscillator (Sec. 5.5) and coupled oscillators (Sec. 6.5). However, those discussions were focused on the case when the parameter variation speed is comparable with the own oscillation frequency (or frequencies) of the system. Another practically important case is when some system's parameter (let us call it λ) is changed much more slowly (*adiabatically*[10]),

$$\left|\frac{\dot{\lambda}}{\lambda}\right| << \frac{1}{\mathcal{T}}, \tag{10.28}$$

where $\mathcal{T}$ is a typical period of oscillations in the system. Let us consider a 1D system whose Hamiltonian $H(q, p, \lambda)$ depends on time only via such a slow evolution of such parameter $\lambda = \lambda(t)$, and whose initial energy restricts the system's motion to a finite coordinate interval – see, e.g., Fig. 3.2c.

Then, as we know from Sec. 3.3, if the parameter λ is constant, the system performs a periodic (though not necessarily sinusoidal) motion back and forth the q-axis, or, in a different language, along a closed trajectory on the phase plane $[q, p]$ – see Fig. 1.[11] According to Eq. (8), in this case, H is constant along the trajectory. (To distinguish this particular *value* of H from the Hamiltonian *function* as such, I will call it E, implying that this constant coincides with the full mechanical energy E – as does for the Hamiltonian (10), though this assumption is not necessary for the calculation made below.)

The oscillation period $\mathcal{T}$ may be calculated as a contour integral along this closed trajectory:

---

[7] There is, of course, a conceptual difference between the "usual" products of the function derivatives participating in the Poisson brackets, and the operator "products" (meaning their sequential action on a state vector) forming the commutator.

[8] See, e.g., QM Sec. 4.6.

[9] Various aspects of this problem and its quantum-mechanical extensions were first discussed by L. Le Cornu (1895), Lord Rayleigh (1902), H. Lorentz (1911), P. Ehrenfest (1916), and M. Born and V. Fock (1928).

[10] This term is also used in thermodynamics and statistical mechanics, where it implies not only a slow parameter variation (if any) but also thermal insulation of the system – see, e.g., SM Sec. 1.3. Evidently, the latter condition is irrelevant in our current context.

[11] As a reminder, we discussed such phase-plane representations in Chapter 5 – see, e.g., Figs. 5.5, 5.9, and 5.16.

$$\mathcal{T} \equiv \int_0^{\mathcal{T}} dt = \oint \frac{dt}{dq} dq \equiv \oint \frac{1}{\dot{q}} dq \,. \tag{10.29}$$

Using the first of the Hamilton equations (7), we may represent this integral as

$$\mathcal{T} = \oint \frac{1}{\partial H / \partial p} dq \,. \tag{10.30}$$

At each given point q, $H = E$ is a function of p alone, so we may flip the partial derivative in the denominator just as the full derivative, and rewrite Eq. (30) as

$$\mathcal{T} = \oint \frac{\partial p}{\partial E} dq \,. \tag{10.31}$$

For the particular Hamiltonian (10), this relation is immediately reduced to Eq. (3.27), now in the form of a contour integral:

$$\mathcal{T} = \left(\frac{m_{\text{ef}}}{2} \right)^{1/2} \oint \frac{1}{[E - U_{\text{ef}}(q)]^{1/2}} dq \,. \tag{10.32}$$

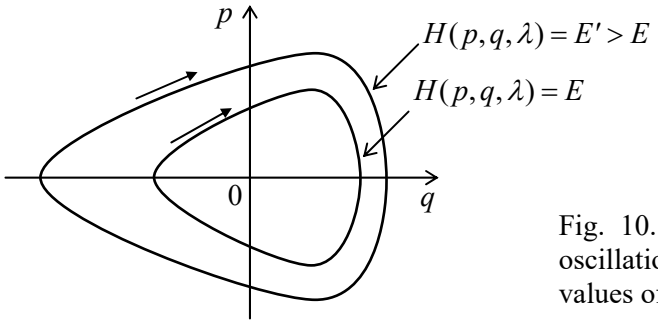

Fig. 10.1. Phase-plane representation of periodic oscillations of a 1D Hamiltonian system, for two values of energy (schematically).

Naively, it may look that these formulas may be also used to find the motion period's change when the parameter λ is being changed adiabatically, for example, by plugging the given functions $m_{\text{ef}}(\lambda)$ and $U_{\text{ef}}(q, \lambda)$ into Eq. (32). However, there is no guarantee that the energy E in that integral would stay constant as the parameter changes, and indeed we will see below that this is not necessarily the case. Even more interestingly, in the most important case of the harmonic oscillator ($U_{\text{ef}} = \kappa_{\text{ef}} q^2/2$), whose oscillation period $\mathcal{T}$ does not depend on E (see Eq. (3.29) and its discussion), its variation in the adiabatic limit (28) may be readily predicted: $\mathcal{T}(\lambda) = 2\pi/\omega_0(\lambda) = 2\pi[m_{\text{ef}}(\lambda)/\kappa_{\text{ef}}(\lambda)]^{1/2}$, but the dependence of the oscillation energy E (and hence of the oscillation amplitude) on λ is not immediately obvious.

In order to address this issue, let us use Eq. (8) (with $E = H$) to represent the rate of the energy change with $\lambda(t)$, i.e. in time, as

$$\frac{dE}{dt} = \frac{\partial H}{\partial t} = \frac{\partial H}{\partial \lambda} \frac{d\lambda}{dt} \,. \tag{10.33}$$

Since we are interested in a very slow (adiabatic) time evolution of energy, we can average Eq. (33) over fast oscillations in the system, for example over one oscillation period $\mathcal{T}$, treating $d\lambda/dt$ as a constant during this averaging. (This is the most critical point of this argumentation, because at any non-

vanishing rate of parameter change the oscillations are, strictly speaking, non-periodic.[12]) The averaging yields

$$\overline{\frac{dE}{dt}} = \frac{d\lambda}{dt}\overline{\frac{\partial H}{\partial \lambda}} \equiv \frac{d\lambda}{dt}\frac{1}{\mathcal{T}}\int_0^{\mathcal{T}} \frac{\partial H}{\partial \lambda}\, dt\,. \tag{10.34}$$

Transforming this time integral to the contour one, just as we did at the transition from Eq. (29) to Eq. (30), and then using Eq. (31) for $\mathcal{T}$, we get

$$\overline{\frac{dE}{dt}} = \frac{d\lambda}{dt}\frac{\oint \frac{\partial H/\partial \lambda}{\partial H/\partial p}\, dq}{\oint \frac{\partial p}{\partial E}\, dq}\,. \tag{10.35}$$

At each point q of the contour, H is a function of not only λ, but also of p, which may be also λ-dependent, so if E is fixed, the partial differentiation of the relation $E = H$ over λ yields

$$\frac{\partial H}{\partial \lambda} + \frac{\partial H}{\partial p}\frac{\partial p}{\partial \lambda} = 0, \quad \text{i.e.} \quad \frac{\partial H/\partial \lambda}{\partial H/\partial p} = -\frac{\partial p}{\partial \lambda}\,. \tag{10.36}$$

Plugging the last relation to Eq.(35), we get

$$\overline{\frac{dE}{dt}} = -\frac{d\lambda}{dt}\frac{\oint \frac{\partial p}{\partial \lambda}\, dq}{\oint \frac{\partial p}{\partial E}\, dq}\,. \tag{10.37}$$

Since the left-hand side of Eq. (37) and the derivative $d\lambda/dt$ do not depend on q, we may move them into the integrals over q as constants, and rewrite Eq. (37) as

$$\oint \left(\frac{\partial p}{\partial E}\overline{\frac{dE}{dt}} + \frac{\partial p}{\partial \lambda}\frac{d\lambda}{dt} \right) dq = 0. \tag{10.38}$$

Now let us consider the following integral over the same phase-plane contour,

Action variable

$$J \equiv \frac{1}{2\pi}\oint p\, dq\,, \tag{10.39}$$

called the *action variable*. Just to understand its physical sense, let us calculate J for a harmonic oscillator (14). As we know very well from Chapter 5, for such an oscillator, $q = A\cos\Psi$, $p = -m_{\text{ef}}\omega_0 A\sin\Psi$ (with $\Psi = \omega_0 t + \text{const}$), so J may be easily expressed either via the oscillations' amplitude A, or via their energy $E = H = m_{\text{ef}}\omega_0^2 A^2/2$:

$$J = \frac{1}{2\pi}\oint p\, dq = \frac{1}{2\pi}\int_{\Psi=0}^{\Psi=2\pi} \left(-m_{\text{ef}}\omega_0 A\sin\Psi\right) d\left(A\cos\Psi\right) = \frac{m_{\text{ef}}\omega_0}{2}A^2 = \frac{E}{\omega_0}. \tag{10.40}$$

[12] Because of the implied nature of this conjecture (which is very close to the assumptions made at the derivation of the reduced equations in Sec. 5.3), new, more strict (but also much more cumbersome) proofs of the final Eq. (42) are still being offered in literature – see, e.g., C. Wells and S. Siklos, *Eur. J. Phys.* **28**, 105 (2007) and/or A. Lobo *et al.*, *Eur. J. Phys*. **33**, 1063 (2012).

Returning to a general system with adiabatically changed parameter λ, let us use the definition of J, Eq. (39), to calculate its time derivative, again taking into account that at each point q of the trajectory, p is a function of E and λ:

$$\frac{dJ}{dt} = \frac{1}{2\pi}\oint \frac{dp}{dt}dq = \frac{1}{2\pi}\oint\left(\frac{\partial p}{\partial E}\frac{dE}{dt} + \frac{\partial p}{\partial \lambda}\frac{d\lambda}{dt}\right)dq\,. \tag{10.41}$$

Within the accuracy of our approximation, in which the contour integrals (38) and (41) are calculated along a closed trajectory, the factor dE/dt is indistinguishable from its time average, and these integrals coincide, so the result (38) is applicable to Eq. (41) as well. Hence, we have finally arrived at a very important result: at a slow parameter variation, $dJ/dt = 0$, i.e. the action variable remains constant:

$$\boxed{J = \text{const}\,.} \tag{10.42}$$

Adiabatic invariance

This is the famous *adiabatic invariance*.[13] In particular, according to Eq. (40), in a harmonic oscillator, the energy of oscillations changes proportionately to its own (slowly changed) frequency.

Before moving on, let me briefly note that the adiabatic invariance is not the only application of the action variable J. Since the initial choice of generalized coordinates and velocities (and hence the generalized momenta) in analytical mechanics is arbitrary (see Sec. 2.1), it is almost evident that J may be taken for a new generalized momentum corresponding to a certain new generalized coordinate Θ,[14] and that the pair $\{J, \Theta\}$ should satisfy the Hamilton equations (7), in particular,

$$\frac{d\Theta}{dt} = \frac{\partial H}{\partial J}. \tag{10.43}$$

Following the commitment of Sec. 1 (made there for the "old" arguments q_j, p_j), before the differentiation on the right-hand side of Eq. (43), H should be expressed as a function (besides t) of the "new" arguments J and Θ. For time-independent Hamiltonian systems, H is uniquely defined by J – see, e.g., Eq. (40). Hence in this case the right-hand side of Eq. (43) does not depend on either t or Θ, so according to that equation, Θ (called the *angle variable*) is a linear function of time:

$$\Theta = \frac{\partial H}{\partial J}t + \text{const}\,. \tag{10.44}$$

For a harmonic oscillator, according to Eq. (40), the derivative $\partial H/\partial J = \partial E/\partial J$ is just $\omega_0 \equiv 2\pi/\mathcal{T}$, so $\Theta = \omega_0 t$ + const, i.e. it is just the full phase Ψ that was repeatedly used in this course – especially in Chapter 5. It may be shown that a more general form of this relation,

$$\frac{\partial H}{\partial J} = \frac{2\pi}{\mathcal{T}}, \tag{10.45}$$

[13] For certain particular oscillators, e.g., a point pendulum, Eq. (42) may be also proved directly – an exercise highly recommended to the reader.

[14] This, again, is a plausible argument but not a strict proof. Indeed: though, according to its definition (39), J is nothing more than a sum of several (formally, the infinite number of) values of the momentum p, they are not independent, but have to be selected on the same closed trajectory on the phase plane. For more mathematical vigor, the reader is referred to Sec. 45 of *Mechanics* by Landau and Lifshitz (which was repeatedly cited above), which discusses the general rules of the so-called *canonical transformations* from one set of Hamiltonian arguments to another one – say from $\{p, q\}$ to $\{J, \Theta\}$.

is valid for an arbitrary system described by Eq. (10). Thus, Eq. (44) becomes

$$\Theta = 2\pi \frac{t}{\mathcal{T}} + \text{const} . \tag{10.46}$$

This means that for an arbitrary (nonlinear) 1D oscillator, the angle variable Θ is a convenient generalization of the full phase Ψ. Due to this reason, the variables J and Θ present a convenient tool for discussion of certain fine points of the dynamics of strongly nonlinear oscillators – for whose discussion I, unfortunately, do not have time/space.[15]

10.3. The Hamilton principle

Now let me show that the Lagrange equations of motion, which were derived in Sec. 2.1 from the Newton laws, may be also obtained from the so-called *Hamilton principle*,[16] namely the condition of a minimum (or rather an extremum) of the following integral called *action*:

Action

$$S \equiv \int_{t_{\text{ini}}}^{t_{\text{fin}}} L dt , \tag{10.47}$$

where t_{ini} and t_{fin} are, respectively, the initial and final moments of time, at which all generalized coordinates and velocities are considered fixed (not varied) – see Fig. 2.

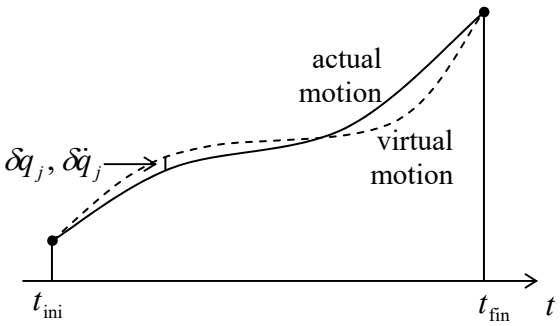

Fig. 10.2. Deriving the Hamilton principle.

The proof of that statement is rather simple. Considering, similarly to Sec. 2.1, a possible virtual variation of the motion, described by infinitesimal deviations $\{\delta q_j(t), \delta \dot{q}_j(t)\}$ from the real motion, the necessary condition for S to be minimal is

Hamilton principle

$$\delta S \equiv \int_{t_{\text{ini}}}^{t_{\text{fin}}} \delta L \, dt = 0 , \tag{10.48}$$

where δS and δL are the variations of the action and the Lagrange function, corresponding to the set $\{\delta q_j(t), \delta \dot{q}_j(t)\}$. As has been already discussed in Sec. 2.1, we can use the operation of variation just

[15] An interested reader may be referred, for example, to Chapter 6 in J. Jose and E. Saletan, *Classical Dynamics*, Cambridge U. Press, 1998.

[16] It is also called the "principle of least action". (This name may be fairer in the context of a long history of the development of the principle, starting from its simpler particular forms, which includes the names of P. de Fermat, P. Maupertuis, L. Euler, and J.-L. Lagrange.)

as the usual differentiation (but at a fixed time, see Fig. 2), swapping these two operations if needed – see Fig. 2.3 and its discussion. Thus, we may write

$$\delta L = \sum_j \left(\frac{\partial L}{\partial q_j} \delta q_j + \frac{\partial L}{\partial \dot{q}_j} \delta \dot{q}_j \right) = \sum_j \frac{\partial L}{\partial q_j} \delta q_j + \sum_j \frac{\partial L}{\partial \dot{q}_j} \frac{d}{dt} \delta q_j . \tag{10.49}$$

After plugging the last expression into Eq. (48), we can integrate the second term by parts:

$$\begin{aligned} \delta S &= \int_{t_{\rm ini}}^{t_{\rm fin}} \sum_j \frac{\partial L}{\partial q_j} \delta q_j dt + \sum_j \int_{t_{\rm ini}}^{t_{\rm fin}} \frac{\partial L}{\partial \dot{q}_j} \frac{d}{dt} \delta q_j dt \\ &= \int_{t_{\rm ini}}^{t_{\rm fin}} \sum_j \frac{\partial L}{\partial q_j} \delta q_j dt + \sum_j \left[\frac{\partial L}{\partial \dot{q}_j} \delta q_j \right]_{t_{\rm ini}}^{t_{\rm fin}} - \sum_j \int_{t_{\rm ini}}^{t_{\rm fin}} \delta q_j d\left(\frac{\partial L}{\partial \dot{q}_j} \right) = 0. \end{aligned} \tag{10.50}$$

Since the generalized coordinates in the initial and final points are considered fixed (not affected by the variation), all $\delta q_j(t_{\rm ini})$ and $\delta q_j(t_{\rm fin})$ vanish, so the second term in the last form of Eq. (50) vanishes as well. Now multiplying and dividing the last term of that expression by dt, we finally get

$$\delta S = \int_{t_{\rm ini}}^{t_{\rm fin}} \sum_j \frac{\partial L}{\partial q_j} \delta q_j dt - \sum_j \int_{t_{\rm ini}}^{t_{\rm fin}} \delta q_j \frac{d}{dt}\left(\frac{\partial L}{\partial \dot{q}_j} \right) dt = - \int_{t_{\rm ini}}^{t_{\rm fin}} \sum_j \left[\frac{d}{dt}\left(\frac{\partial L}{\partial \dot{q}_j} \right) - \frac{\partial L}{\partial q_j} \right] \delta q_j \, dt = 0. \tag{10.51}$$

This relation should hold for an arbitrary set of functions $\delta q_j(t)$, and for any time interval, and this is only possible if the expressions in the square brackets equal zero for all j, giving us the set of the Lagrange equations (2.19). So, the Hamilton principle indeed gives the Lagrange equations of motion.

It is fascinating to see how the Hamilton principle works for particular cases. As a very simple example, let us consider the usual 1D linear oscillator, with the Lagrangian function used so many times before in this course:

$$L = \frac{m}{2} \dot{q}^2 - \frac{m\omega_0^2}{2} q^2 . \tag{10.52}$$

As we know very well, the Lagrange equations of motion for this L are exactly satisfied by any sinusoidal function with the frequency ω_0, in particular by a symmetric function of time

$$q_{\rm e}(t) = A \cos \omega_0 t, \qquad \text{so that } \dot{q}_{\rm e}(t) = -A\omega_0 \sin \omega_0 t . \tag{10.53}$$

On a limited time interval, say $0 \le \omega_0 t \le +\pi/2$, this function is rather smooth and may be well approximated by another simple, reasonably selected functions of time, for example

$$q_{\rm a}(t) = A\left(1 - \lambda t^2\right), \qquad \text{so that } \dot{q}_{\rm a}(t) = -2A\lambda t , \tag{10.54}$$

provided that the parameter λ is also selected reasonably. Let us take $\lambda = (\pi/2\omega_0)^2$, so the approximate function $q_{\rm a}(t)$ coincides with the exact function $q_{\rm e}(t)$ at both ends of our time interval (Fig.3):

$$q_{\rm a}(t_{\rm ini}) = q_{\rm e}(t_{\rm ini}) = A, \quad q_{\rm a}(t_{\rm fin}) = q_{\rm e}(t_{\rm fin}) = 0, \qquad \text{where } t_{\rm ini} \equiv 0, \quad t_{\rm fin} \equiv \frac{\pi}{2\omega_0}, \tag{10.55}$$

and check which of them the Hamilton principle "prefers", i.e. which function gives the least action.

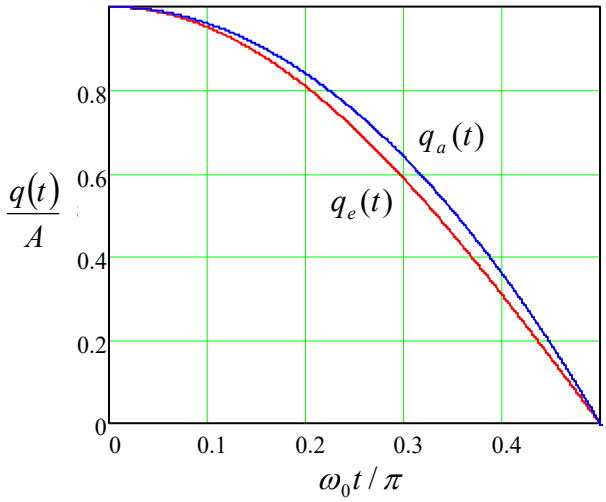

Fig. 10.3. Plots of the functions $q(t)$ given by Eqs. (53) and (54).

An elementary calculation of the action (47) corresponding to these two functions, yields

$$S_{\rm e} = \left(\frac{\pi}{8} - \frac{\pi}{8}\right) m\omega_0 A^2 = 0, \qquad S_{\rm a} = \left(\frac{4}{3\pi} - \frac{2\pi}{15}\right) m\omega_0 A^2 \approx (0.4244 - 0.4189) m\omega_0 A^2 > 0, \tag{10.56}$$

with the first terms in all the parentheses coming from the time integrals of the kinetic energy, and the second terms, from those of the potential energy.

This result shows, first, that the exact function of time, for which these two contributions *exactly* cancel,[17] is indeed "preferable" for minimizing the action. Second, for the approximate function, the two contributions to the action are rather close to the exact ones, and hence *almost* cancel each other, signaling that this approximation is very reasonable. It is evident that in some cases when the exact analytical solution of the equations of motion cannot be found, the minimization of S by adjusting one or more free parameters, incorporated into a guessed "trial" function, may be used to find a reasonable approximation for the actual law of motion.[18]

It is also very useful to make the notion of action S, defined by Eq. (47), more transparent by calculating it for the simple case of a single particle moving in a potential field that conserves its energy $E = T + U$. In this case, the Lagrangian function $L = T - U$ may be represented as

$$L = T - U = 2T - (T + U) = 2T - E = mv^2 - E, \tag{10.57}$$

with a time-independent E, so

$$S = \int L dt = \int mv^2 dt - Et + \text{const}. \tag{10.58}$$

Recasting the expression under the remaining integral as $m\mathbf{v}\cdot\mathbf{v}dt = \mathbf{p}\cdot(d\mathbf{r}/dt)dt = \mathbf{p}\cdot d\mathbf{r}$, we finally get

$$S = \int \mathbf{p}\cdot d\mathbf{r} - Et + \text{const} = S_0 - Et + \text{const}, \tag{10.59}$$

[17] Such cancellation, i.e. the equality $S = 0$, is of course not the general requirement; it is specific only for this particular example, with a specific choice of the arbitrary constant in the potential energy of the system.

[18] This is essentially a classical analog of the variational method of quantum mechanics – see, e.g., QM Sec. 2.9.

where the time-independent integral

$$S_0 \equiv \int \mathbf{p} \cdot d\mathbf{r} \tag{10.60}$$

is frequently called the *abbreviated action*.[19]

This expression may be used to establish one more important connection between classical and quantum mechanics – now in its Schrödinger picture. Indeed, in the quasiclassical (WKB) approximation of that picture[20] a particle of fixed energy E is described by a de Broglie wave

$$\Psi(\mathbf{r},t) \propto \exp\left\{i\left(\int \mathbf{k} \cdot d\mathbf{r} - \omega t + \text{const}\right)\right\}, \tag{10.61}$$

where the wave vector $\mathbf{k}$ is proportional to the particle's momentum (which is possibly a slow function of $\mathbf{r}$) and the frequency ω, to its energy:

$$\mathbf{k} = \frac{\mathbf{p}}{\hbar}, \quad \omega = \frac{E}{\hbar}. \tag{10.62}$$

Plugging these expressions into Eq. (61) and comparing the result with Eq. (59), we see that the WKB wavefunction may be represented as

$$\Psi \propto \exp\{iS/\hbar\}. \tag{10.63}$$

Hence the Hamilton principle (48) means that the total phase of the quasiclassical wavefunction should be minimal along the particle's real trajectory. But this is exactly the so-called *eikonal minimum principle* well known from the optics (though it is valid for any other waves as well), where it serves to define the ray paths in the geometric optics limit – similar to the WKB approximation. Thus, the ratio $S/\hbar$ may be considered just as the eikonal, i.e. the total phase accumulation, of the de Broglie waves.[21]

Now, comparing Eq. (60) with Eq. (39), we see that the action variable J is just the change of the abbreviated action S_0 along a single phase-plane contour, divided by 2π. This means, in particular, that in the WKB approximation, J is the number of de Broglie waves along the classical trajectory of a particle, i.e. an integer value of the corresponding quantum number. If the system's parameters are changed slowly, the quantum number has to stay integer, and hence J cannot change, giving a quantum-mechanical interpretation of the adiabatic invariance. The reader should agree that this is really fascinating: a fact of classical mechanics may be "derived" (or at least understood) more easily from the quantum mechanics' standpoint. (As a reminder, we have run into a similarly pleasant surprise at our discussion of the non-degenerate parametric excitation in Sec. 6.7.)

[19] Comparing Eq. (59) with the Hamilton principle (48), we see that if the variational trajectories are limited to those of only one (actual) energy E, the real motion corresponds to the minimum of not only S but S_0 as well. This fact is called the *Maupertuis principle*. (Historically, this result rather than Eq. (48), was called the "principle of least action", and some authors still use this terminology, so the reader's caution is advised.)

[20] See, e.g., QM Sec. 3.1.

[21] Indeed, Eq. (63) was the starting point for R. Feynman's development of his path-integral formulation of quantum mechanics – see, e.g., QM Sec. 5.3.

10.4. The Hamilton-Jacobi equation

The action S, defined by Eq. (47), may be used for one more analytical formulation of classical mechanics. For that, we need to make one more, different commitment: S has to be considered as a function of the following independent arguments: the final time point $t_{\rm fin}$ (which I will, for brevity, denote as t in this section), and the set of generalized coordinates (but not of the generalized velocities!) at that point:

Hamilton-Jacobi action

$$S \equiv \int_{t_{\rm ini}}^{t} L dt = S\left[t, q_j(t)\right]. \tag{10.64}$$

Let us calculate the variation of this (from the variational point of view, new!) function, resulting from an arbitrary combination of variations of the final values $q_j(t)$ of the coordinates while keeping t fixed. Formally this may be done by repeating the variational calculations described by Eqs. (49)-(51), besides that now the variations δq_j at the finite point (t) do not necessarily equal zero. As a result, we get

$$\delta S = \sum_j \frac{\partial L}{\partial \dot{q}_j} \delta q_j \Big|_t - \int_{t_{\rm ini}}^{t} dt \sum_j \left[\frac{d}{dt}\left(\frac{\partial L}{\partial \dot{q}_j} \right) - \frac{\partial L}{\partial q_j} \right] \delta q_j \,. \tag{10.65}$$

For the motion along the real trajectory, i.e. satisfying the Lagrange equations (2.19), the second term of this expression equals zero. Hence Eq. (65) shows that, for (any) fixed time t,

$$\frac{\partial S}{\partial q_j} = \frac{\partial L}{\partial \dot{q}_j}. \tag{10.66}$$

But the last derivative is nothing else than the generalized momentum p_j, so

$$\frac{\partial S}{\partial q_j} = p_j \,. \tag{10.67}$$

(As a reminder, both parts of this relation refer to the final moment t of the trajectory.) As a result, the full derivative of the action $S[t, q_j(t)]$ over time takes the form

$$\frac{dS}{dt} = \frac{\partial S}{\partial t} + \sum_j \frac{\partial S}{\partial q_j} \dot{q}_j = \frac{\partial S}{\partial t} + \sum_j p_j \dot{q}_j . \tag{10.68}$$

Now, by the definition of S, the full derivative dS/dt is nothing more than the Lagrangian function L, so Eq. (67) yields

$$\frac{\partial S}{\partial t} = L - \sum_j p_j \dot{q}_j . \tag{10.69}$$

However, according to the definition (2) of the Hamiltonian function H, the right-hand side of Eq. (69) is just ($-H$), and we get an extremely simply-looking *Hamilton-Jacobi equation*

Hamilton-Jacobi equation

$$\frac{\partial S}{\partial t} = -H. \tag{10.70}$$

This simplicity is, however, rather deceiving, because to use this equation for the calculation of the function $S(t, q_j)$ for any particular problem, the Hamiltonian function has to be first expressed as a function of time t, generalized coordinates q_j, and the generalized momenta p_j (which may be, according

to Eq. (67), represented just as the derivatives $\partial S/\partial q_j$). Let us see how this procedure works for the simplest case of a 1D system with the Hamiltonian function given by Eq. (10). In this case, the only generalized momentum is $p = \partial S/\partial q$, so

$$H = \frac{p^2}{2m_{\text{ef}}} + U_{\text{ef}}(q,t) = \frac{1}{2m_{\text{ef}}}\left(\frac{\partial S}{\partial q}\right)^2 + U_{\text{ef}}(q,t), \tag{10.71}$$

and Eq. (70) is reduced to the following partial differential equation,

$$\frac{\partial S}{\partial t} + \frac{1}{2m_{\text{ef}}}\left(\frac{\partial S}{\partial q}\right)^2 + U_{\text{ef}}(q,t) = 0\,. \tag{10.72}$$

Its solution may be readily found in the easiest case of time-independent potential energy $U_{\text{ef}} = U_{\text{ef}}(q)$. In this case, Eq. (72) is evidently satisfied by the following variable-separated solution:

$$S(t,q) = S_0(q) + \text{const} \times t\,. \tag{10.73}$$

Plugging this solution into Eq. (72), we see that since the sum of the two last terms on the left-hand side of that equation represents the full mechanical energy E, the constant in Eq. (73) is nothing but $(-E)$. Thus for the function $S_0(q)$ we get an ordinary differential equation

$$-E + \frac{1}{2m_{\text{ef}}}\left(\frac{dS_0}{dq}\right)^2 + U_{\text{ef}}(q) = 0. \tag{10.74}$$

Integrating it, we get

$$S_0 = \int \left\{2m_{\text{ef}}\left[E - U_{\text{ef}}(q)\right]\right\}^{1/2} dq + \text{const}, \tag{10.75}$$

so, finally, the action is equal to

$$S = \int \left\{2m_{\text{ef}}\left[E - U_{\text{ef}}(q)\right]\right\}^{1/2} dq - Et + \text{const}. \tag{10.76}$$

For the case of 1D motion of a single 1D particle, i.e. for $q = x$, $m_{\text{ef}} = m$, $U_{\text{ef}}(q) = U(x)$, this solution is just the 1D case of the more general Eqs. (59)-(60), which were obtained above in a much more simple way. (In particular, S_0 is just the abbreviated action.)

This particular example illustrates that the Hamilton-Jacobi equation is not the most efficient way for the solution of most practical problems of classical mechanics. However, it may be rather useful for studies of certain mathematical aspects of dynamics.[22] Moreover, in the early 1950s this approach was extended to a completely different field – the optimal control theory, in which the role of the action S is played by the so-called *cost function* – a certain functional of a system (understood in a very general sense of this term), that should be minimized by an optimal choice of a *control signal* – a function of time that affects the system's evolution in time. From the point of view of this theory, Eq. (70) is a particular case of a more general *Hamilton-Jacobi-Bellman* equation.[23]

[22] See, e.g., Chapters 6-9 in I. C. Percival and D. Richards, *Introduction to Dynamics*, Cambridge U. Press, 1983.

[23] See, e.g., T. Bertsekas, *Dynamic Programming and Optimal Control*, vols. 1 and 2, Aetna Scientific, 2005 and 2007. The reader should not be intimidated by the very unnatural term "dynamic programming", which was invented by the founding father of this field, Richard Bellman, to lure government bureaucrats into funding his research, deemed too theoretical at that time. (Presently, it has a broad range of important applications.)

10.5. Exercise problems

In each of Problems 1-3, for the given system:

(i) derive the Hamilton equations of motion, and

(ii) check whether these equations are equivalent to those derived from the Lagrangian formalism.

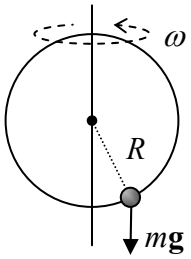

10.1. Our "testbed" system: a bead on a ring rotated, with a fixed angular velocity ω, about its vertical diameter – see Fig. 2.1, partly reproduced on the right.

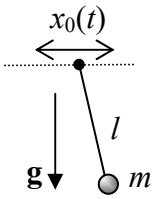

10.2. The system considered in Problem 2.3: a pendulum hanging from a point whose motion $x_0(t)$ in the horizontal direction is fixed – see the figure on the right. (No vertical-plane constraint.)

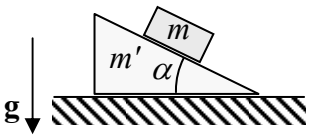

10.3. The system considered in Problem 2.8: a block of mass m that can slide, without friction, along the inclined surface of a heavy wedge of mass m'. The wedge is free to move, also without friction, along a horizontal surface – see the figure on the right. (Both motions are within the vertical plane containing the steepest slope line.)

10.4. Derive and solve the equations of motion of a particle with the following Hamiltonian function:

$$H = \frac{1}{2m}(\mathbf{p} + a\mathbf{r})^2,$$

where a is a constant scalar.

10.5. Let L be the Lagrangian function, and H the Hamiltonian function, of the same system. What three of the following four statements,

$$\text{(i)}\ \frac{dL}{dt} = 0, \qquad \text{(ii)}\ \frac{\partial L}{\partial t} = 0, \qquad \text{(iii)}\ \frac{dH}{dt} = 0, \qquad \text{(iv)}\ \frac{\partial H}{\partial t} = 0,$$

are equivalent? Give an example of when those three equalities hold, but the fourth one does not.

10.6. Calculate the Poisson brackets of a Cartesian component of the angular momentum $\mathbf{L}$ of a particle moving in a central force field and its Hamiltonian function H, and discuss the most evident implication of the result.

10.7. After small oscillations had been initiated in the point pendulum shown in Fig. on the right, the supporting string is being pulled up slowly, so that the pendulum's length l is being reduced. Neglecting dissipation,

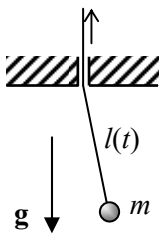

(i) prove by a direct calculation that the oscillation energy is indeed changing proportionately to the oscillation frequency, as it follows from the constancy of the corresponding adiabatic invariant (40); and

(ii) find the l-dependence of the amplitudes of the angular and linear deviations from the equilibrium.

10.8. The mass m of a small body that performs 1D oscillations in the potential well $U(x) = ax^{2n}$, with $n > 0$, is being changed slowly, without exerting any additional direct force. Calculate the oscillation energy E as a function of m.

10.9. A stiff ball is bouncing vertically from the floor of an elevator whose upward acceleration changes very slowly. Neglecting the energy dissipation, calculate how much the bounce height h changes during the acceleration's increase from 0 to g. Is your result valid for an equal but abrupt increase of the elevator's acceleration?

10.10.* A 1D particle of a constant mass m moves in a time-dependent potential $U(q, t) = m\omega^2(t)q^2/2$, where $\omega(t)$ is a slow function of time, with $|\dot{\omega}| << \omega^2$. Develop the approximate method for the solution of the corresponding equation of motion, similar to the WKB approximation used in quantum mechanics.[24] Use the approximation to confirm the conservation of the action variable (40) for this system.

Hint: You may like to look for the solution to the equation of motion in the form

$$q(t) = \exp\{\Lambda(t) + i\Psi(t)\},$$

where Λ and Ψ are some real functions of time, and then make proper approximations in the resulting equations for these functions.

[24] See, e.g., QM Sec. 2.4.